THE PETROCHEMISTRY OF

THE BRITISH OLD RED SANDSTONE

VOLCANIC PROVINCE

MATTHEW FRANCIS THIRLWALL B.A.

A Thesis submitted for the Degree of Doctor of

Philosophy

University of Edinburgh

October 1979

PAGE
NUMBERS
CUT OFF
IN
ORIGINAL

Text cut off in original

DECLARATION

I hereby declare that this thesis has been composed by myself, and that the work described herein is my own unless specifically acknowledged.

29/10/79

(M.F. Thirlwall)

This thesis is dedicated to

"Pippin"

ABSTRACT

The lavas and minor intrusions associated with the sediments of the Old Red Sandstone were extensively sampled over a broad area of Scotland, northern England and the north of Ireland. The main areas of outcrop are Lorne, Glencoe and Ben Nevis (the SW Highlands); the Sidlaw, Ochil and North Fife Hills (the North Midland Valley); Ayrshire and the Pentland Hills (the South Midland Valley); the Cheviot Hills; St. Abb's Head and Shetland. Most of the samples collected have been examined petrographically, and 597 have been analysed for 10 major and 17 trace elements. The phenocryst compositions of many of the lavas has also been investigated by microprobe. The large number of samples to be analysed required the development of a rapid and accurate system of analysis by X-ray fluorescence spectrometry, and a wide range of data processing and data handling computer programs, described in the Appendices.

In general, the rocks have strong affinities with modern calc-alkaline volcanic suites, although those from Shetland and from Straiton, Ayrshire, show some characteristics transitional to tholeiitic types. Although the rocks of each outcrop area are petrographically and chemically diverse, the variation is generally inexplicable by fractional crystallisation processes, except for Shetland and (possibly) the Cheviot Hills. Chemical variation in most areas can only be explained by complex contamination models.

Rocks with >100 ppm Ni are unusually abundant for calc-alkaline suites, and may be found in most outcrop areas. These rocks show pronounced geographical variation in their concentrations of Sr, P, light rare earth elements, Ba, K, Y and, to a lesser extent, Nb and Sc. All except Y and Sc show a marked increase in a traverse from the South Midland Valley to the SW Grampian Highlands, and a similar relationship also exists for rocks poorer in Ni. This geographical variation is similar to that seen in modern subduction-related calc-alkaline suites, and constitutes strong evidence that the rocks of the province were genetically related to a subduction zone. Little satisfactory evidence is available for the age of the Scottish Lower Old Red Sandstone, and it is believed that the rocks were deposited during the Silurian, rather than the Lower Devonian as has been

generally accepted, prior to final closure of the Iapetus Ocean. The rocks of the Cheviot Hills are thought to have been erupted a little later, after final closure. The bulk of the volcanic rocks were however probably directly related to the subduction responsible for closure.

In order to explain the geographical variation in concentrations of the above elements in terms of a single subduction zone, it is necessary to postulate a major change in strike of the zone from ENE in southern Scotland to nearly N in the North Sea. This strike change, in conjunction with almost east-west relative plate motion, can explain the contrast in end-Silurian deformation styles between Britain and Scandinavia. It is believed that motion was largely transcurrent on the British-Irish sector of the subduction zone.

The possible origins of the geographic variation in incompatible element concentrations are constrained by the failure of Rb and Zr to correlate with other incompatible elements, and by the decrease in Y with increasing depth to the inferred Benioff zone. These variations are best explained by a model involving
(i) generation of melts in the vicinity of the subducted lithosphere
(ii) their ascent through the mantle and the zone-refining of dispersed incompatible elements (but not those located in minor crystalline mantle phases such as phlogopite, ilmenite or apatite). The concentration of an incompatible element in a particular magma is then mainly a function of the path length to the surface and the distribution of minor phases along that path.

TABLE OF CONTENTS

List of tables vi
List of figures ix
Chapter 1 : Introduction 1
1.1 : Objectives of Research 4
1.2 : The Old Red Sandstone 4
1.3 : Age of the Scottish Old Red Sandstone 9
1.4 : The circa 400 Ma Plutonic Episode 12
1.5 : The Old Red Sandstone Volcanoes 13

Chapter 2 : Alteration 16
2.1 : Macroscopic Extent 16
2.2 : Mineralogical Effects 17
2.3 : Chemical Effects 22

Chapter 3 : Introduction to Petrochemistry 37
3.1 : Rock Nomenclature 37
3.2 : Mineral Analyses 39
3.3 : Variation Diagrams 39
3.4 : Geochemistry 40

Chapter 4 : Southwest Highlands 46
4.1 : Lorne Plateau 46
4.2 : Glencoe 74
4.3 : Ben Nevis 82
4.4 : SW Highlands - Conclusions 84

Chapter 5 : North Midland Valley 94
5.1 : Montrose Region 97
5.2 : The Sidlaw Hills 120
5.3 : The Western Ochil Hills 132
5.4 : North Fife Hills 142
5.5 : North Midland Valley : Conclusions 157

Chapter 6 : South Midland Valley 171
6.1 : The Pentland Hills 172
6.2 : Ayrshire 182
6.3 : South Midland Valley 191

Chapter 7 : The Cheviot Hills 195

Chapter 8 : Minor occurrences of O.R.S. Volcanics 214
8.1 : St. Abb's Head & Eyemouth 214
8.2 : Ireland 222
8.3 : Arran 226
8.4 : Huntly 228
8.5 : Shetland 229
8.6 : Orkney 249

Chapter 9 : Spatial Variation, Discussion and Conclusions 252
9.1 : Characteristics of the O.R.S. volcanic suite 252
9.2 : Spatial Variation in Modern Calc-alkaline suites . . 256
9.3 : Spatial Chemical Variation in O.R.S. mafic rocks 259
9.4 : Spatial Chemical Variation in less mafic rocks 268
9.5 : Subduction Direction 272
9.6 : The Siluro-Devonian Orogeny in Britain . . . 281
9.7 : Origin of Spatial Chemical Variation 288

Acknowledgements 305
References 306

Appendix A : Pre-analytical Procedures 315
A1 : Sample Collection 315
A2 : Selection of Samples for Analysis 315
A3 : Reduction of Samples to Powder 327

Appendix B : X-ray fluorescence analytical techniques . . 329
B1 : Introduction 329
B2 : Sample Preparation 329
B3 : Storage of Prepared Samples 333
B4 : Use of Monitor 333
B5 : Analytical Conditions 334
B6 : XRF Output 341
B7 : Standards 341
B8 : Matrix Corrections 347
B9 : Analytical Accuracy 368
B10 : Data Processing 369
B11 : Comparison with other XRF Methods 399

B12 : Future Improvements in Method 401

Appendix C : Electron Microprobe Techniques 437

C1 : Wavelength Dispersive System 437

C2 : Energy Dispersive System 437

Appendix D : Data Handling Computer Programs 455

D1 : ABSTRACT 455

D2 : MEANFILE 455

D3 : RATCALC 455

D4 : ANALTAB 455

D5 : ATOM 455

D6 : NORMS 456

D7 : VARPLOT 456

LIST OF TABLES

Table 2.1 p. 23
Relationship between Loss on Ignition and Petrographic Alteration State.

Table 4.1 p. 50
Average compositions of SW Highlands volcanic rocks.

Table 4.2 p. 75
Stratigraphic sequence of O.R.S. rocks of Glencoe.

Table 5.1 p. 95
Lower Old Red Sandstone stratigraphy of the north Midland Valley

Table 5.2 p. 104
Petrochemical characteristics of alumina-based subdivisions of the Ferryden Member, Montrose.

Table 5.3 p. 107
Enrichment factors for LIL and high field strength elements in the "trachyandesites" relative to high-alumina basic andesites, Montrose.

Table 5.4 p. 116
Chemical characteristics of the major lava groups of the Montrose Region.

Table 9.1 p. 266
Average analyses of samples with >100 ppm Ni.

Table 9.2 p. 267
Interquartile ranges for selected chemical parameters in samples with >100 ppm Ni.

Table A1 p. 315 - 327
List of samples analysed, localities and brief petrographies.

Table A2 p. 328
Comparison between analyses of powders of phenocryst-rich rocks crushed using different Tema mills on different occasions.

Table B1 p. 331
Reproducability of glass discs.

Table B2 p. 332
Trace element analyses of sample SA1 using 4g and 7g pellets.

Table B3 p. 332
Reproducability of trace element pressed powder pellets

Table B4 p. 334
Secular changes in major element calibration constants.

Table B5 p. 336
Interferences on X-ray analytical lines and backgrounds.

Table B6 p. 337
XRF analytical conditions

Table B7 p. 340
Analytical precision/repeatability data.

Table B8 p. 342
Specimen XRF output of major element program.

Table B9 p. 343
Specimen XRF output of Cr-tube trace element program.

Table B10 p. 344
Specimen XRF output of W-tube trace element program.

Table B11 p. 345
Standards used in trace element calibrations.

Table B12 p. 346
Major element composition of synthetic base glasses INTSG and INTSB

Table B13 p. 346
Trace element compounds used in spiking synthetic glasses.

Table B14 p. 348
Theoretical compositions of synthetic trace element standards.

Table B15 p. 367
Analytical accuracy.

Table B16 p. 368
Comparison between XRF and Isotope Dilution analyses for Rb and Sr

Table B17 pp. 402-436
Major and trace element analyses of the samples collected.

Table C1 p. 438
Analytical conditions used in wavelength dispersive electron microprobe analysis and approximate precision.

Table C2 pp. 439- 452
Average core compositions of O.R.S. phenocryst minerals.

Table C3 p. 453
Electron microprobe analyses of phenocryst minerals showing important zoning.

Table C4 p. 454
Average electron microprobe analyses for trace elements in O.R.S. phenocryst minerals.

Table D1 p. 457
"Phenocryst Assemblages" corresponding to numbers after the '@' symbol in rock names, and incorporated in program VARPLOT.

LIST OF FIGURES

Fig. 1.1 p. 6
Distribution of Lower and Middle O.R.S. sediments and volcanic rocks in northern Britain.

Fig. 2.1 p. 30
Spurious correlation between MgO and CaO at Lorne resulting from alteration.

Fig. 4.1 pp. 51-53
Variation diagrams for some 'incompatible' elements versus silica at Lorne.

Fig. 4.2 pp. 54-57
Variation diagrams for samples from Lorne.

Fig. 4.3 pp. 61-62
Relationships between high field strength elements at Lorne.

Fig. 4.4 pp. 64-65
Relationships between LIL elements at Lorne.

Fig. 4.5 p. 67
Relationship between Zr, Nb and Cr at Lorne.

Fig. 4.6 pp. 77-78
Variation diagrams, Glencoe and Ben Nevis.

Fig. 4.7 pp. 79-81
Variation diagrams, Glencoe and Ben Nevis.

Fig. 4.8 p. 86
Phenocryst chemistry of SW Highlands O.R.S. igneous rocks.

Fig. 4.9 p. 90
Variation diagrams for Lorne mafic samples.

Fig. 5.1 p. 96
Distribution of volcanic rocks in the Montrose Region.

Fig. 5.2 pp. 109-111
Variation diagrams, Montrose Region.

Fig. 5.3 p. 123
Harker variation diagrams for samples from the Sidlaw Hills.

Fig. 5.4 pp. 124-125
Variation diagrams, Sidlaw Hills.

Fig. 5.5 pp. 127-128
Variation diagrams, Sidlaw Hills.

Fig. 5.6 pp. 135-137
Variation diagrams, Western Ochil Hills.

Fig. 5.7 pp. 145-147
Variation diagrams, North Fife Hills.

Fig. 5.8 pp. 149-150
Variation diagrams, North Fife Hills.

Fig. 5.9 pp. 158-160
Phenocryst chemistry of North Midland Valley igneous rocks.

Fig. 5.10 pp. 167-170
Relationships between LIL elements, North Midland Valley.

Fig. 6.1 pp. 174-176
Variation diagrams, Pentland Hills.

Fig. 6.2 pp. 179-181
Variation diagrams, Pentland Hills.

Fig. 6.3 pp. 185-187
Variation diagrams, Ayrshire.

Fig. 6.4 pp. 188-190
Variation diagrams, Ayrshire.

Fig. 6.5 p. 192
Phenocryst chemistry of South Midland Valley O.R.S. igneous rocks.

Fig. 7.1 pp. 199-201
Variation diagrams, Cheviot Hills.

Fig. 7.2 pp. 202-204
Variation diagrams, Cheviot Hills.

Fig. 7.3 p. 209
Phenocryst chemistry of Cheviot igneous rocks.

Fig. 7.4 p. 211
Variation diagrams, Cheviot Hills.

Fig. 8.1 pp. 216-219
Variation diagrams, St. Abb's Head & Eyemouth.

Fig. 8.2a&b p. 227
Strontium and Barium variation in Arran and Ireland.

Fig. 8,2c p. 230
Distribution of O.R.S. rocks in Shetland.

Fig. 8.3 pp. 234-238
Variation diagrams, Shetland and Orkney.

Fig. 9.1 p. 253
K_2O : SiO_2 variation diagrams for the main outcrop areas.

Fig. 9.2 pp. 261-264
Relationships between LIL elements, and Ni and Cr, in rocks with more than 100 ppm Ni.

Fig. 9.3 p. 269
Sr : SiO_2 variation diagrams for the main outcrop areas.

Fig. 9.4 pp. 270-271
Regression lines for the variation of several parameters showing spatial variation with silica.

Fig. 9.5 p. 273
Ranges in Sr and La/Y versus distance from the suture of Phillips et al. (1976).

Fig. 9.6 p. 276
The anomalously high La/Y of the Cheviot lavas, relative to other rocks with between 60 and 65% SiO_2.

Fig. 9.7 p. 279
The suggested position of the surface trace of the late Silurian subduction zone.

Fig. 9.8 pp. 291-293
Spatial variation in Y, Rb, Zr and Nb.

Fig. B1 pp. 349-353
Major element calibration graphs.

Fig. B2 p. 355
Calibration graphs for Zr and Sc using the Anderman-Kemp matrix correction procedure.

Fig. B3 pp. 357-366
Trace element calibration graphs.

Fig. B4 p. 371
Flow diagram of computer processing of XRF data.

Fig. B5 pp. 372-373
Compiled listing of program RATMAJ

Fig. B6 p. 373
Example of a major element count ratio,file.

Fig. B7 pp. 374-377
Compiled listing of program MAJORS.

Fig. B8 p. 378
Part of file ANAL - major element standard data.

Fig. B9 p. 378
Example of file STDATA - major element calibration data.

Fig. B10 p. 378
Example of major element analysis file.

Fig. B11 p. 378
Example of norminput file.

Fig. B12 pp. 382-384
Compiled listing of program CRTRACE

Fig. B13 pp. 385-388
Compiled listing of program WTRACE

Fig. B14 pp. 389-398
Compiled listing of program TRACE

Fig. B15 p. 398
Part of file TRACANAL - trace element standard data.

Fig. B16 p. 400
Comparison of analyses of SM8-S52 from Table B17 and Gandy (1973a).

CHAPTER 1 : INTRODUCTION

The prolonged crustal instability of the British region during the Lower Palaeozoic, terminating in the Caledonian Orogeny, has provided a fertile source of material for research in all branches of geology. Most recent models for the tectonic development of the region are in accord in postulating an ocean, Iapetus, separating an Anglo-European continent from one comprising Scotland and America north of the Appalachians. Strong evidence, from faunal provincialism (e.g. Williams, 1972) and from palaeomagnetism (e.g. Briden et al., 1973), supports the existence of this ocean for much of Cambrian and Ordovician time, with final closure and continental suturing during the Silurian. The subduction necessary to produce closure has formed the basis of several interpretations of Lower Palaeozoic tectonomagmatic events; for example, those of Dewey (1969), Mitchell and McKerrow (1975) and Phillips et al. (1976).

Recent work in the Southern Uplands (McKerrow et al., 1977) has provided convincing evidence that the Ordovician to Silurian sedimentary successions of this area represent material deposited on the northern floor of Iapetus, and accreted onto the northern continental margin during subduction of the ocean floor, as suggested by Mitchell and McKerrow (1975). In contrast, Church and Gayer (1973) suggest termination of northward subduction in the late Caradoc. Evidence for southeastward subduction has been

presented by Fitton and Hughes (1970) for the Lake District and Wales, and for southeast Ireland by Stillman and Williams (1979). These authors have demonstrated the existence of spatial changes in the chemistry of the volcanic rocks in these regions, from tholeiitic or transitional rocks with flat chondrite-normalized rare earth element (REE) patterns in the north, to light REE enriched calc-alkaline rocks in the south, comparable with changes with increasing distance from the trench in many modern magmatic arcs (e.g. Jakes and White, 1972). The Iapetus suture at present erosion level must therefore pass along the Solway Firth: Phillips et al. (1976) list evidence for its extrapolation into Ireland.

Evidence from volcanic rocks for northward subduction is far less satisfactory, for the major pre-Carboniferous volcanic episode in the north is generally thought to be of Devonian age, and thus significantly younger than the Silurian date of closure inferred from the ending of marine sedimentation and the unification of the palaeomagnetic and faunal records of both sides of the orogen. Mitchell and McKerrow (1975) suggest that the Wrae volcanics of Peebleshire, and the andesite clasts in Upper Ordovician greywackes at the Rhinns of Galloway, are representatives of calc-alkaline volcanism associated with the accretion of sediment at the Southern Uplands subduction zone. These volcanic episodes are trivial relative to the later outburst, and the rocks at Wrae have recently been shown to be peralkaline rhyolites (Thirlwall, in preparation), and

thus most probably quite unrelated to subduction. Furthermore, the nature of the rocks of the Siluro-Devonian volcanic episode is not clear from the literature. While generally believed to be calc-alkaline (e.g. Taylor, 1972; Groome, 1972), alkali basalts have been described from Orkney (Kellock, 1969), a mugearite from Shetland (Mykura, 1976), trachyandesites in the Sidlaw and Ochil Hills (Harry, 1956; Francis et al., 1970) and trachytes in the Pentland and Cheviot Hills (Mykura, 1960; Carruthers et al., 1932). Gandy (1973a) proposed a petrogenetic model for the volcanic rocks of the Sidlaw Hills involving two-stage fractional crystallisation of olivine-tholeiite. The volcanic rocks of the Cheviot Hills lie across the suture line of Phillips et al. (1976) and can therefore not be related to the subduction models proposed therein.

Despite these uncertainties, Phillips et al. (1976) use calc-alkaline rocks from both sides of the suture as evidence for oblique collision between a west-striking northern subduction zone and a southwest-striking southern zone, followed by 560 miles (900 km) of dextral strike-slip. In the south, they interpret the younger age of the Siluro-Ordovician volcanic episode to the southwest as a result of later closure in this direction, but do not clearly demonstrate a similar phenomenon in the north. Here they use the Devonian age of the magmatism as evidence for dextral translation of the Devonian closing position in the north to become opposite to the Caradocian closing position in the south, despite faunal and palaeomagnetic evidence

suggesting Silurian closure.

1.1 : OBJECTIVES OF RESEARCH

It is clear from the preceeding discussion that most models for the Lower Palaeozoic development of the British Isles suffer difficulties in their postulation of post-Llanvirn northward subduction because of the lack of consistent and comprehensive petrochemical data for the post-Llanvirn pre-Carboniferous volcanic rocks of Scotland, Northumberland and northern Ireland. The research described in this thesis was designed to remedy this deficiency, to determine the petrochemical affinities of the rocks of the Siluro-Devonian volcanic episode, and to place restrictions on models for their petrogenesis.

1.2 : THE OLD RED SANDSTONE

With the exceptions of the aforementioned Wrae volcanics, the Caradocian alkaline complex of Bail Hill (M. McMurtry, pers. comm., 1979), the clasts at the Rhinns of Galloway, and spilitic volcanics in the Southern Uplands and Mayo Trough Ordovician, all post-Llanvirn, pre-Carboniferous volcanic rocks north of the suture of Phillips *et al.* (1976) are associated with the essentially untectonized continental sediments known throughout Britain and Scandinavia as the Old Red Sandstone (O.R.S.). The conglomerates, sandstones and shales of this large lithostratigraphic grouping are thought to have been

deposited in a number of intermontane and lacustrine basins. Their present outcrop, together with the locations of contemporaneous volcanism, is shown in Fig. 1.1. Only small pockets of O.R.S. conglomerates exist between the southernmost depositional basin of the Scottish Old Red Sandstone (Berwickshire - Northumberland) and the large depositional basin of the Anglo-Welsh cuvette, and it is probable that these basins were not linked for much of the duration of O.R.S, deposition. No volcanic rocks are associated with the O.R.S. sediments south of the suture of Phillips *et al.* (1976), and the same relationship is true further northeast, where volcanic rocks are present in the Old Red Sandstone of east Greenland, but are absent from the Norwegian Old Red Sandstone.

The Midland Valley basin has by far the thickest development of O.R.S. sediments and volcanic rocks (19000 ft, 6000m; Armstrong and Paterson, 1970), and its sedimentary history has been described by Bluck (1978) and Morton (1979). These authors have suggested progressive subsidence along the bounding faults and infilling from the edges by a succession of alluvial and debris flow fans, derived from the surrounding mountains. In the southeast there may have been some link with the Berwickshire-Cheviot area, although thicknesses of sediment here are not great. In the southwest, Morton (1979) postulates a link through Kintyre to the SW Grampian basin, which he considers to have been filled in by the Lorne Plateau lavas. There is some evidence that the SW Grampian basin may have been a tidal

Fig. 1.1 : Distribution of Lower and Middle Old Red Sandstone sediments and volcanic rocks in northern Britain

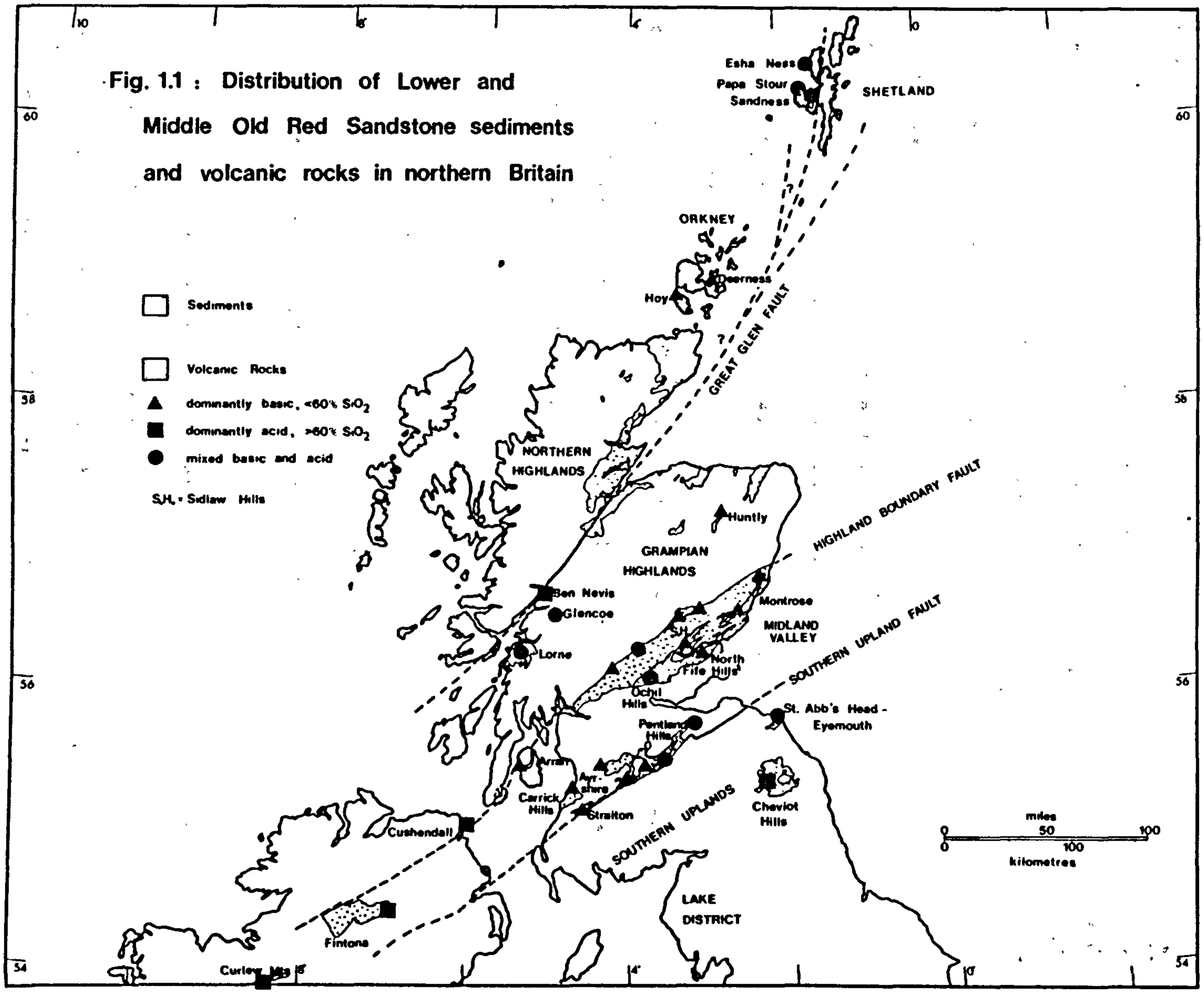

cuvette (Tarlo and Gurr, 1964).

In the northeast, sedimentation was dominated by the Orcadian Lake, which at its maximum extent may have covered the area between the Moray Firth and western Shetland, with marginal alluvial deposition in Sutherland, Cromarty and northern Aberdeenshire. Further north, in Shetland, three distinct sedimentary successions have been juxtaposed by faulting, of which the western (Melby) has most similarities with the Orcadian sequence (Mykura, 1976). The central area (Sandness and Walls Formations) is most unusual in that the Old Red Sandstone has suffered polyphase deformation, and the sediments were thought by Mykura and Phemister (1976) to be probably of deeper water facies than normal, although not marine. Recent re-interpretation by Melvin (1977) has confirmed their fluviatile nature. The southeastern succession was probably originally the most northerly, and in facies resembles the Orcadian sediments (Mykura, 1976, p.69).

It is difficult to judge how far the distribution shown in Fig. 1.1 is the product of the primary depositional pattern and the extent to which this has been modified by differential uplift and erosion. The high degree of rounding of quartzite clasts in fanglomerates on the northern margin of the Midland Valley suggests that they had been previously involved in alluvial processes, presumably in small Highland basins. Similarly, the abundance of volcanic clasts in these fanglomerates demonstrates that

volcanic rocks were more widespread in the Highlands than at present, and that the apparently close relation between location of volcanic rocks and major transcurrent faults is mainly the result of preservation of Old Red Sandstone near these faults.

Correlation of Old Red Sandstone strata between the several depositional basins is based on rare horizons with fish and arthropod faunas, together with some plants. Three divisions have been recognized using this palaeontological information, although unconformities provide the main mapping criteria. These are the Lower, Middle and Upper Old Red Sandstones. In many areas continental facies sedimentation began before deposition of the Lower, and continued after deposition of the Upper Old Red Sandstone: the terms have therefore acquired chronostratigraphic meanings.

In England, Wales and Scotland south of Aberdeen, rocks of the Middle division are absent, and the Upper division, resting unconformably on older rocks, is overlain conformably by the lowest Carboniferous strata. The Lower division appears to rest conformably on older rocks in Lanarkshire and Ayrshire, and in the Anglo-Welsh cuvette rests conformably on Ludlow strata with the intervening type Downtonian. In general, however, it rests unconformably on rocks ranging in age from Pre-Cambrian to Silurian. In northeast Scotland, rocks of the Lower division have only recently been recognized, and the succession is dominated by

strata belonging to the Middle division. Fossils are infrequent in the Irish Old Red Sandstone, and the stratigraphy is less well-established than in Britain.

1.3 : AGE OF THE SCOTTISH OLD RED SANDSTONE

It has been observed that the term Old Red Sandstone has acquired a chronostratigraphic meaning, so that it is often used as a synonym for the term Devonian. It is clear that the O.R.S. of the Anglo-Welsh cuvette is of Devonian age, and that Upper O.R.S. conformably overlain by Carboniferous strata is Devonian or younger, but neither of these have associated volcanic rocks. The only volcanic rocks assigned to the Upper Old Red Sandstone are the Hoy lavas (Fig. 1.1; Mykura, 1976, p.89), and some doubts are expressed about this assignation. The Devonian age of the remainder of the Scottish Old Red Sandstone rests on correlation of fish and arthropod faunas and on lithological similarities with the Welsh Border succession. Lithological correlation is clearly invalid, for Old Red Sandstone facies sediments are present in both Silurian and Carboniferous strata. Well preserved faunas have been collected from Shetland (Mykura and Phemister, 1976), Caithness and Orkney (Wilson et al., 1935), Lorne (Kynaston and Hill, 1908) and in the Stonehaven, Arbuthnott and Garvock groups of the northern Midland Valley (Armstrong and Paterson, 1970). Those from Caithness, Orkney and Shetland are not directly comparable with faunas from the Welsh Borderland, but are assigned to the Middle Old Red Sandstone. The fauna from

the Stonehaven Group has been assigned to the Downtonian (Westoll, 1945), but Lamont (1952) considers it to be earlier. The fauna from Lorne is similar to the Arbuthnott Group fauna, which was assigned to the Dittonian by Westoll (1951). It should be noted that the use of fish as accurate time markers in continental facies sediments must be suspect, for the spreading of newly evolved species will be very slow in the absence of direct freshwater links. Plant spores may prove to be better for chronostratigraphic correlation, but at present there is a lack of stratigraphic control.

A few radiometric age determinations have been made on volcanic members of the Old Red Sandstone. An Rb-Sr isochron age of 365±2 Ma (recalculated to $\lambda^{87}Rb = 1.42 \times 10^{-11}$ yr^{-1}) derived from three samples of the Grind of the Navir ignimbrite, Shetland, has been reported by Flinn et al. (1968). Samples SH5 and SH6 are representative of this formation, and it is unlikely that Rb and Sr were immobile under the alteration that these rocks have suffered. The possibility that the quoted age is an alteration age should be considered. A stepwise degassing $^{40}Ar/^{39}Ar$ age determination on two samples of the Hoy lavas has been reported by Halliday et al. (1977), giving 'plateau ages' of 368±8 and 353±7 Ma. This is a substantial difference between the two samples. Brown (1975) has reported results of Rb-Sr and K-Ar isotopic studies in the Lorne and Glencoe areas. The Lorne lavas, and rocks of the later Etive plutonic complex, fall on good isochrons giving ages between

410 and 420 Ma, the lava isochron giving an age of 415±7 Ma. Samples from Glencoe were thought by Brown (1975) not to form an isochron within error, but Groome (1972) has interpreted the same data as an isochron of age 480±20 Ma. The Lorne samples have recently been re-analysed with improved precision, but leading to only very minor change in the age (Brown, pers. comm., 1979).

With the exception of the age from Glencoe, these dates in general seem to confirm the vertebrate stratigraphy, although the most reliable isochron, that for the Lorne lavas, would be Upper Silurian on the timescale of Harland *et al.* (1964). However, a recent Rb-Sr isochron age of 421±3 Ma on the Ashgillian Stockdale Rhyolite, Lake District, has led to an important revision of the Palaeozoic time-scale (Gale *et al.*, 1979), with a shortening of the Silurian to 24 Ma. On this basis, the Lorne lavas are early Silurian in age, and the possibility that the vertebrate ages are sufficiently imprecise to encompass the whole of the Silurian must be seriously considered. It is notable that the youngest reliable age for rocks overlain by Old Red Sandstone north of the Southern Uplands Fault is an Upper Llandovery graptolite fauna in the Pentland Hills, although Wenlock graptolites occur close to the O.R.S unconformity in the Cheviot Hills.

There appears therefore to be little evidence for a Devonian age for most of the O.R.S volcanic sequences, and some evidence in favour of a Silurian age. Accordingly, the

terms Lower, Middle and Upper Old Red Sandstone are not used with any chronostratigraphic meaning in this thesis.

1.4 : THE CIRCA 400 MA PLUTONIC EPISODE

The restriction of Old Red Sandstone volcanic rocks to the northern side of the Iapetus suture is not paralleled in the distribution of plutonic rocks. Granitic bodies of batholithic proportions are found intrusive into Lower Palaeozoic and older rocks throughout Scotland, Ireland and northern England, with a number of smaller plutons in Wales and Leicestershire. Many of these have recently been the subjects of precise lead and strontium isotope studies, which have resulted in the recognition of a number of magmatic episodes, closely spaced in time. In England many plutons previously thought to be end-Silurian have been shown to be Ordovician (e.g. Rundle, 1979), and thus possibly related to the southeast directed subduction zone of Fitton and Hughes (1970). The few remaining plutons are distinctly younger than 400 Ma (e.g. Shap, 394±3 Ma; Wadge *et al.*, 1978). Distinkhorn, and the Southern Uplands plutons, show some similarities with the English plutons in their lack of inherited zircons (Pidgeon and Aftalion, 1978) but some appear to be slightly older (e.g. Loch Doon, 408±2 Ma; Halliday and Stephens, in press). Initial Sr isotope ratios are generally close to 0.707 for all these rocks, but higher values are found further south (Wensleydale, 0.721; Dunham, 1974).

Granitic plutons in the Highlands form two groups broadly corresponding to the forceful and permitted granites of Read (1961), the former generally earlier with high initial $^{87}Sr/^{86}Sr$ and chemistries similar to their country rocks, and the latter with low initial $^{87}Sr/^{86}Sr$ and incompatible element enriched chemistries. Brown (1979) interprets the first of these as the product of crustal melting associated with major tectonism, but suggests that the latter were intruded in a period of post-suturing crustal relaxation. The Donegal plutons appear to be anomalous in their low initial $^{87}Sr/^{86}Sr$ (Brown, 1979).

In addition to the plutonic rocks, large numbers of minor intrusions of around 400 Ma age are present in Britain, particularly in the Scottish Highlands. The hornblende-pyroxene rocks of the Appinite suite have been interpreted as feeders to the Lorne lavas (Groome and Hall, 1974), but in general there has been little work on these minor intrusions. The large numbers of Caledonian dykes are generally later than the volcanic rocks, and have a more restricted compositional range in the SW Highlands area (Groome, 1972).

1.5 : THE OLD RED SANDSTONE VOLCANOES

The continental facies of the associated sediments clearly implies that the O.R.S volcanic rocks were erupted in a continental environment. Pillow lavas are never seen, but the widespread sand-veining of lavas was taken by Geikie

(1902) to suggest fracturing of lava on eruption into small bodies of water. The volcanic rocks have all suffered to some extent from hydrothermal alteration (Chapter 2), most probably in an immediately post-eruptive, deuteric interaction with meteoric water, although some show evidence for contact metamorphism by later plutons (e.g. Glencoe). Tops and bases of flows are frequently autobrecciated and vesicular, these features often extending through the whole flow. Frequent reddening of flow tops is additional evidence for subaerial eruption.

Unlike modern subaerial andesite volcanoes, the volcanic products are almost entirely lava flows. Substantial accumulations of pyroclastic rocks are only found at the base of the volcanic sequence in the Ochil Hills (Francis et al., 1970) and at Lorne, where they have been interpreted as lahar deposits (Groome, 1972). The absence of pyroclastic material may imply that the magmas were less viscous or poorer in volatiles than modern andesitic magmas, but it is also possible that the high fluvial activity resulted in rapid erosion and transport of the pyroclastic rocks.

The lava flows have nowhere been shown to exhibit depositional dip as if on the flanks of major stratovolcanoes, and often have wide lateral extent. While this may again suggest low viscosity magmas, it is also possible that the preserved volcanics represent regions most remote from the central cones, and that eruption into a

rapidly subsiding intermontane basin destroys any resemblance to volcanic cone structures.

CHAPTER 2 : ALTERATION

The products of the Old Red Sandstone volcanoes have all been subjected to some degree of post-eruptive alteration, frequently resulting in the replacement of all the primary igneous minerals by a chlorite-sericite-haematite-calcite-quartz assemblage. Such alteration may lead to difficulty in the interpretation of petrography and chemistry, and is therefore reviewed prior to discussion of these subjects.

2.1 : MACROSCOPIC EXTENT

Fortunately, total replacement of primary minerals is not ubiquitous in any of the volcanic outcrop areas, and careful search will reveal almost unaltered samples. These may usually be distinguished in the field by the lustre of fresh groundmass feldspar, and are typically free from veins, amygdales, closely spaced joints and other fractures. Pyroclastic rocks and autobrecciated parts of lava flows are generally severely altered. The restriction of altered rocks to more permeable parts of the volcanic sequence suggests that hydrothermal fluids were of much greater importance in effecting alteration than any regional temperature rise due to plutonism, and the latter is probably only important in close proximity to major intrusions (e.g. the Cruachan Granite, Glencoe). The greater frequency of fresh samples in the north Midland Valley may be the result of the lack of intrusive activity

in this area, or may be due to mineralogical differences, in particular the paucity of phenocryst plagioclase in SW Highland rocks.

2.2 : MINERALOGICAL EFFECTS

Alteration of primary minerals frequently hinders their identification in thin section, particularly in the case of groundmass minerals or small numbers of poorly shaped phenocrysts. Groundmasses usually contain one or more chloritic minerals, probably mainly replacing glass, but sometimes also replacing groundmass olivine or pyroxenes. Lavas with more than 60% silica often have a very fine granular groundmass of quartz, feldspar, haematite and a chloritic mineral, which may be very difficult to resolve. It is not certain whether this is a primary texture or the result of devitrification or recrystallisation.

Over 95% of the rocks collected are porphyritic, and therefore the difficulty in groundmass phase recognition caused by alteration is not too important. Pseudomorphed phenocryst minerals may be identified by a combination of criteria: shape, alteration product, internal structure, and the presence in the same rock of other more easily recognized pseudomorphs or fresh minerals. The frequent association of olivine, orthopyroxene, calcic clinopyroxene and plagioclase as phenocrysts in mafic lavas allows the determination of their relative susceptibility to

alteration, and partially altered phenocrysts allow the identification of characteristic alteration products.

(a) Olivine

Olivine pseudomorphs may usually be recognized by their characteristic bipyramidal shape and by their internal fracture pattern, which is often marked by haematite. The latter feature allows the recognition of anhedral phenocrysts. Olivine was the mineral most prone to alteration, and is seen as fresh relicts in only five samples. Alteration/replacement products are varied, and range from serpentine and iddingsite through chloritic minerals and haematite to quartz or calcite. Distinction from orthopyroxene or hornblende is difficult in a few samples (e.g. L61), and it is not impossible that these minerals are present in association with olivine in a few rocks from which olivine alone has been recorded. The large number of hornblende-olivine-phyric basic rocks reported from Lorne by Groome (1972) contrasted with the small number noted in this study may in part be the result of this difficulty.

(b) Pyroxene

Fresh pyroxene phenocrysts are either diopsidic augite or orthopyroxene, of which the latter is much the more susceptible to alteration. Orthopyroxene is characteristically pseudomorphed by a pleochroic pale green

or brown chlorite, while clinopyroxene may be pseudomorphed by carbonate and some chlorite. When euhedral, the octagonal shape allows distinction from other minerals, and they may usually be distinguished from each other by their alteration products. It is possible, however, that small patches of carbonate may represent pseudomorphed clinopyroxene in some rocks from which it has not been reported. The former existence of pigeonite, pseudomorphed by a chlorite similar to that pseudomorphing orthopyroxene, has been inferred from exsolution relationships in some Shetland and Straiton pyroxenes. At Ben Nevis, clinopyroxene is pseudomorphed by tremolitic amphibole (e.g. analyses 6,8, Table C2), probably indicating higher temperature alteration than is usual. At Esha Ness, haematite-rich pseudomorphs of general pyroxene shape in the more siliceous rocks (SH1-3, 12, 13) may be the result of the alteration of more iron-rich augites.

(c) Feldspar

Plagioclase feldspars are less susceptible to alteration than calcic clinopyroxene in most of the province, contrasting with the behaviour of these minerals in the Lower Palaeozoic volcanic rocks of England and Wales (Fitton et al., in press), where alteration may have occurred at higher temperatures. Most of the Shetland lavas, however, and a few samples from elsewhere (e.g. PE18), show fresh augite coexisting with highly altered plagioclase. Plagioclase shows a range in

alteration products from very minor development of sericite to heavily sericitized, albitized, carbonated or rarely epidotized varieties, but is always easily distinguished from other phenocryst minerals. Some samples have both heavily altered and fresh feldspar, where the alteration is usually restricted to more calcic cores (e.g. OC88B). Alkali feldspar is rare as a phenocryst, and is usually partly kaolinized, when it may be difficult to distinguish from plagioclase.

(d) Amphibole

Amphibole, usually pargasitic, is probably slightly more susceptible to alteration than calcic clinopyroxene, although in samples from Ben Nevis fresh pargasitic amphibole coexists with the pale green tremolite after clinopyroxene. It may be altered to a variety of chloritic minerals, carbonate and sometimes quartz, and is characteristically surrounded by a wide opaque resorption rim. The latter, in conjunction with the 120° cleavage angle in basal sections, usually allows recognition of amphibole unless resorption has proceeded too far (resorption pseudomorphs). In some rocks (e.g. OC87A), the former cleavage planes of pseudomorphed amphibole may be picked out by haematite.

(e) Biotite

Biotite is not common in the rocks of the province,

but it is probably fairly resistant to alteration. Where alteration does occur, it usually takes the form of haematite grains along the cleavage planes, followed by replacement by a bright green chlorite (e.g. GC6, MT52). The hexagonal basal and rectangular prism sections usually allow recognition, but resorption may create difficulties in distinction from amphibole (e.g. L113).

(f) Oxide Minerals

Reflected light microscopy indicates that in altered rocks both magnetite and ilmenite show phase separation, either as lamellae or patches, probably leading eventually, with oxidation, to the formation of haematite and rutile respectively. The latter mineral has not been positively identified, but is suspected in some altered samples.

The only other phenocryst minerals, apatite, quartz and garnet, do not suffer alteration in any of the rocks collected.

In addition to the alteration of primary minerals, a number of new minerals have been introduced by precipitation from hydrothermal fluids in joints and vesicles. The requirement of a geographically widespread collection has made unavoidable the collection of a few samples showing such features; for example, the one *in situ* lava on Arran is almost net-veined by carbonate. Carbonate is the main mineral so introduced, but quartz, chalcedony, chlorite and

infrequent zeolites also occur.

Mineral alteration, while extensive, does not therefore present any major difficulty in interpretation of the phenocryst mineralogy of the samples collected, although groundmass mineralogy is frequently difficult to determine. The common association of olivine, 2 pyroxenes and plagioclase allows the placing of most rocks on a petrographic alteration scale (PAS) from 1 to 5, bounded in the first two grades by disappearance of fresh olivine and orthopyroxene respectively, in the third by one of augite or plagioclase, and in the fourth by the other. Table A1 lists the alteration state (PAS) of all rocks analysed in this study: it is not very satisfactory as a measure of alteration for it relies on the presence of these four minerals in each rock.

2.3 : CHEMICAL EFFECTS

(a) Volatiles

The mineral alteration previously described should in general lead to an increase in the H_2O^+ and CO_2 content of a rock with increasing intensity, the CO_2 content being particularly sensitive to the introduction of carbonate. It will also lead to an increase in the Fe_2O_3/FeO ratio. These three parameters are very sensitive to only slight alteration, and for this reason, and also because it is relatively time-consuming, measurement of these was not

undertaken. The quoted Loss on Ignition (LOI) is a composite function of these approximately equal to $H_2O^+ + CO_2 - 0.11 \times FeO$, the last term resulting from oxidation of FeO on ignition. Provided that $H_2O^+ + CO_2$ in the unaltered sample was relatively small, the LOI may be used as an independant measure of alteration. The relationship between PAS and LOI is given in Table 2.1: rocks with high PAS show a very diffuse LOI distribution, and lower PAS samples have lower modal LOI.

Table 2.1 : Relationship between LOI and PAS. The number of samples of each alteration state is given for a range in LOI.

	%LOI	<1	1-1.5	1.5-2	2-2.5	2.5-3	3-3.5	3.5-4	4-4.5	4.5-5	>5
	1		2	2			1				
	2	19	12	7	2	2	1	1			
	3	51	97	47	17	14	5	5			2
PAS	4	21	25	17	15	17	7	11	6	2	14
	5	19	26	24	25	20	16	16	11	7	17
	*	1	3	5	1	1	1	1			

*= samples with fresh glass in groundmass and PAS=2

The use of LOI as a measure of alteration has several advantages over the PAS numbers. It is an objective measurement for each sample, not greatly affected by original mineralogical variation between rocks. It is possibly a direct measure of the degree of interaction of a sample with the volatiles believed to have caused the alteration, and is very responsive to carbonate alteration.

A number of mineralogically altered samples have low LOI. Most of these are silica-rich, where silicification is

the main form of alteration, and there is a lack of mafic constituents suitable for the formation of secondary hydrous or carbonate minerals. The effect of alteration on rhyolitic rocks must therefore be treated slightly differently, and too few have been collected to allow detailed conclusions to be drawn. Other petrographically altered low LOI rocks are the few contact-metamorphosed samples in the collection: the low LOI merely indicates lack of major interaction with volatiles since metamorphism.

It is noteworthy that most samples with alteration state 2 and LOI>1.5% have fresh glass in the groundmass. All of these have a fresh 2 pyroxene-plagioclase phenocryst assemblage, and therefore the water implied by the high LOI must be present in the glass. This suggests that, despite its fresh appearance, the glass has interacted with meteoric water and should be regarded as altered. Further evidence for this will be presented in section (e).

(b) Chemical alteration and primary chemistry : criteria

Investigation of the chemical effect of alteration is necessarily dependant on the identification of pre-alteration chemistry. In ancient volcanic provinces this may cause a severe problem, but in the O.R.S. province the frequent occurrence of relatively fresh samples (PAS 1-3, LOI <2.5%) in most areas of volcanic outcrop makes this less difficult. The mineral alteration described in section 2.2 suggests that no element has remained immobile during

alteration of even these samples, for all elements are present in the olivine, orthopyroxene and interstitial glass which may here be altered. This will have no effect on the concentration of an element if the sample analysed has remained a closed system to that element. This will occur if there is no transporting medium available, if the rock is not permeable to the medium, or if the element is not readily transported. Under more intense alteration than experienced in this province, there is known to be considerable variation in the ease with which different elements may be transported (e.g. Smith and Smith, 1976), and it is likely that fresher samples would have remained closed to transportation of Al, Fe, Ti, Mn, P, Sc, V, Y, Zr, Nb, Cr and rare earth elements (REE). The hydrothermal fluids were probably silica-saturated, for chalcedony deposition is frequent in vesicles and joints. It is possible that the fluids were therefore unable to transport much silica from the fresher samples, and, in the absence of secondary silica, it is probable that these samples were also closed systems for Si.

It is most unlikely that alteration could produce systematic variation between concentrations of any pair of these elements. If systematic variation is observed, it is probable that it also existed between these and the more mobile elements (alkalis, alkaline earths, and possibly Cu, Zn, Ni and Th) prior to alteration. The effect of alteration may then be judged by the degree of scatter of this variation, and is only important if the more altered

samples show more scatter. Whole-rock variation diagrams in this thesis use 3 sizes of symbols, for LOI≤2%, 2<LOI≤3% and LOI>3%, with smallest symbols for the highest LOI, to facilitate the interpretation of alteration effects on each diagram. The effect of alteration on variation between two mobile elements is harder to interpret, unless their variation with less mobile elements is previously well-understood, and spurious correlation may result.

In samples containing relict fresh minerals, the pre-alteration chemistry may sometimes be inferred from whole rock - phenocryst distribution relationships for minor elements. Both this method and the use of variation diagrams only provide information when there is substantial alteration of primary chemistry, and minor alteration may not be detected.

Since the intensity of alteration is similar throughout the province, with perhaps the least in the north Midland Valley, it is possible to extrapolate from areas showing systematic variation in the less mobile elements to areas which do not, for it is reasonable to assume that the mobility of an element will remain fairly constant throughout the province. It is therefore possible to judge whether scatter on a variation diagram is primary or the result of alteration.

(c) The less mobile elements

The elements suggested to be less mobile in section (b) are, with the exception of Si, those which are not readily transported by hydrothermal fluids. Systematic variation between these and SiO_2 in the more altered outcrop areas is most unlikely to be produced by mobilization during alteration. Such variation may be demonstrated for Lorne (average LOI=2.85%, PAS=3.99), Glencoe (LOI=1.34, PAS=4.27), Cheviot (LOI=2.21, PAS=3.79) and St. Abbs (LOI=4.74, PAS=4.26) for Al, Fe, Ti, Mn, P, Sc and V (e.g. Figs. 4.2, 4.6, 7.1, 8.1). No correlation with LOI is observed, except in a few cases where the only samples of a particular rock type are highly altered (e.g. L87 and L91 for Sc and Fe). In these cases, it is thought that the unusual rock types had primary chemistries unrelated to the main variation, although this may not be conclusively demonstrated.

Variation diagrams of these elements for samples from the less altered areas e.g. the Sidlaw Hills (average LOI=1.28, PAS=3.08) and the North Fife Hills (LOI=1.45, PAS=3.11) show far more scatter (e.g. Figs. 5.3, 5.7) than diagrams for the more altered areas. Again, with the exception of some unusual rock types, no correlation exists between LOI and breadth of scatter, which, taken in conjunction with the lower average LOI and PAS, implies that the scatter is primary and not the result of alteration. In areas with more severe alteration e.g. the Pentland Hills (LOI=3.41, PAS=4.05), it is again true that the breadth of

scatter does not correlate with LOI (e.g. Fig. 6.1), and sufficient low LOI, low PAS samples are present to suggest that the scatter is primary.

The elements Cr, Zr, Y and Nb, together with Ti and P considered above, are thought to be among the least mobile elements (e.g. Pearce and Cann, 1973; Smith and Smith, 1976), and their concentrations have been accepted as primary in rocks considerably more altered than those of the O.R.S. province. Mobility of REE has been demonstrated in rocks showing metasomatic alteration (e.g. Hellman et al., 1977), but such intensely altered rocks are very rare in the O.R.S. province and it is thought that REE may have been fairly immobile. Since elements more mobile than these appear not to have been redistributed by alteration in the samples under study, it is improbable that alteration could have affected the concentrations of Cr, Y, Zr, Nb and REE. It is difficult to use the same criteria to establish this, however, for there are few unscattered variation diagrams against silica for these elements. Despite this, breadth of scatter is not correlated with LOI, unusual samples excepted, and variation between pairs of these elements e.g. Zr and Ce, is often systematic. In particular, the constancy of Zr/Nb for some rock groups (e.g. the opx-cpx-phyric and opx-cpx-pl-phyric rocks of Lorne, Fig. 4.3) is strong evidence for the immobility of these elements.

(d) Ca, Mg, Ni

The systematic variation for relatively immobile elements demonstrated at Lorne, Glencoe, St. Abb's Head and the Cheviot Hills suggests that, prior to alteration, a similar variation may have existed for Ca, Mg and Ni. Mg and Ni are liable to be greatly affected by alteration of phenocryst olivine and pyroxene, and both Ca and Mg may be easily transported in solution. Ca is readily introduced in the form of carbonate, which at Lorne may often replace olivine. If alteration is not closed system for Ca and Mg, then such rocks should show Mg loss and Ca gain. Similarly, sericitization or albitization of plagioclase may lead to Ca loss and alkali gain.

Figs. 4.2 and 7.1 demonstrate that samples from Lorne and Cheviot with LOI<2 (larger symbols) show systematic variation with silica for MgO and CaO. The scatter in Ni variation with silica is not correlated with LOI, and Ni variation with Cr is more systematic (Fig. 7.2). It is concluded that Ni behaves as a relatively immobile element. A number of high LOI samples from Lorne and the Cheviot Hills show Ca and Mg concentrations considerably outside the scatter of the main variation. Mg has probably been lost by a number of samples, but Ca shows both losses and gains. The alteration of olivine to carbonate at Lorne produces an inverse Ca-Mg correlation for basic rocks (Fig. 2.1), despite the lack of such correlation for less altered samples. This is an example of a spurious systematic

Fig. 2.1

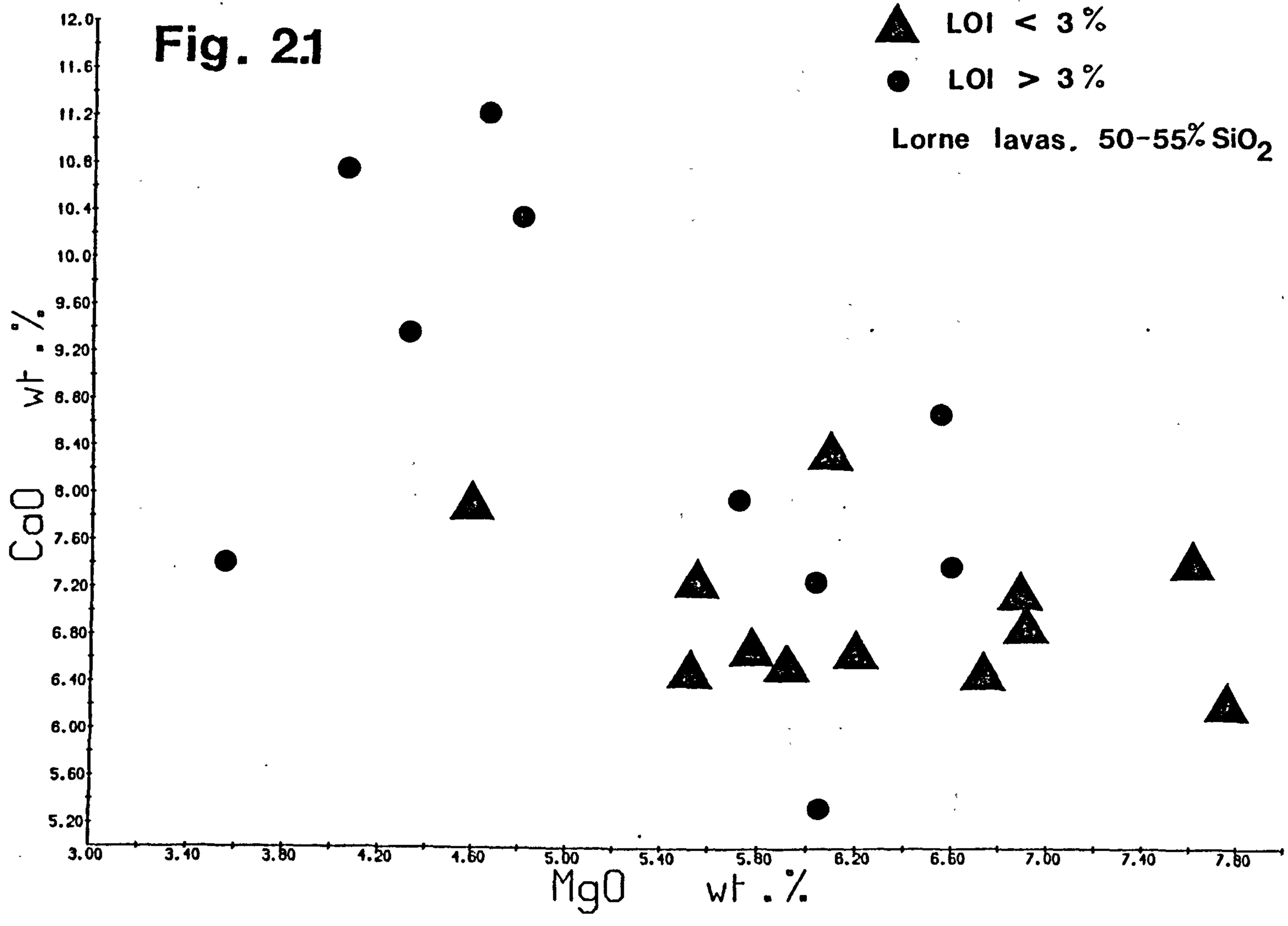

▲ LOI < 3 %

● LOI > 3 %

Lorne lavas. 50–55% SiO_2

relation between two more mobile elements resulting from alteration (section 2.3b). A number of low Ca, high LOI samples may be attributed to severe sericitization or albitization of feldspars (Fig. 7.1; C22, C34, C60).

The extension of these relationships to the Midland Valley samples is difficult because of the lack of systematic variation between immobile elements, but it is thought that the bulk of samples with low LOI retain primary Ca and Mg levels. An example of the effect of severe sericitization of plagioclase is provided by the three samples collected from the Dunnichen Member, MT6-8. These have very similar petrography except that MT6 and 7 are sericitized. Chemistries of the three samples are very similar, except that the sericitized samples show higher K and lower Ca and Sr.

(e) <u>The alkali metals, Ba, Sr</u>

These generally mobile elements (e.g. Smith and Smith, 1976) may be treated in the same fashion as Ca and Mg. Scatter on Na variation diagrams is in part produced by poor analytical precision, but more extreme values correlate with high LOI or petrographic alteration, and Na appears to be both lost and gained on alteration. K, Rb, Ba and Sr are probably more mobile, and while all four show systematic variation with silica for both Lorne and Cheviot samples (e.g. Figs. 9.1, 7.1), a large scatter is present which includes a number of low LOI samples. This could either be

due to mobilization of these elements in these low LOI samples, or to primary differences in concentrations of these elements unrelated to silica content.

At Lorne, the scattered low LOI samples are richer in these elements than the main variation trend with silica, and the bulk of the K-rich samples are also rich in Rb, Ba and Sr (Fig. 4.4). This is unlikely to be the result of alteration, for in low PAS rocks Sr is likely to be fixed in fresh groundmass plagioclase. Further, correlation with La/Y also exists (Fig. 4.4), and it may be concluded that much of the scatter of low LOI rocks at Lorne is primary.

In the Cheviot Hills, K and Rb are enriched and Sr is depleted in three high LOI, high PAS samples (C22, C34 and C35, Fig. 7.1), of which the first two have identical mineralogy to the 2 pyroxene-plagioclase-phyric andesites of the main trend. While it may not be proved that these compositions are the result of alteration, it is most unlikely that a K-rich mineral would not crystallise early from liquids with 7.5 and 5.8% K20 (C22 and C34 respectively). Four low LOI samples (C9, 15, 33 and 54) show depletion of K, Rb and enrichment of Sr, Na, and, in three samples, Ba. These again have the same phenocryst mineralogy as the main trend samples, but are unusual in being vitrophyric with a fresh glass groundmass. They are petrographically very fresh (PAS=2), but have a slightly higher LOI than most samples with PAS=2 (Table 2.1). Analyses of phenocryst plagioclase from these and from main

trend rocks show no differences in K or Sr content (Plagioclase analyses 71 and 74, Tables C2 and C4), and the Sr content of plagioclase in C33 would imply an unreasonable phenocryst/host rock distribution coefficient of only slightly more than 1 (Chapter 3). It is concluded that the fresh glass has exchanged water, alkalis, Sr and Ba with hydrothermal solutions, and that devitrified glasses retain better their primary composition. Similar vitrophyric samples from the north Midland Valley (e.g. OC98, OC123, MT15) also display anomalously low K and Rb, again probably resulting from glass-volatile interaction.

It may be concluded from regions showing simple systematic variation between silica and immobile elements that K, Ba and Sr are not seriously modified by alteration in samples with LOI<3, PAS 1-3, unless the samples contain fresh groundmass glass. Rb appears to be slightly more mobile than K: there are several Cheviot samples anomalously low in Rb. Despite the scatter on variation diagrams for many less mobile elements, previously interpreted as primary, variation diagrams against silica for K, Rb, Ba and Sr for the least altered Midland Valley areas are relatively unscattered (e.g. Figs. 9.1,9.3 for the Sidlaw Hills, North Fife Hills and coastal Ayrshire). This confirms that the scatter of the less mobile elements is not the result of alteration.

(f) Cu, Zn, Th

It is difficult to predict the behaviour of these elements under alteration. Systematic variation exists for all three in many areas, but in some cases a scatter exists which may neither be correlated with other elements nor with LOI. In the case of Cu and Zn this may have been caused by the mobility of sulphides, either in the magma or possibly during alteration. Zn removal during hydrothermal alteration has, however, been suggested for the Ordovician peralkaline rocks of Wrae (Thirlwall, in preparation). Th appears to be relatively immobile in the Cheviot lavas although there is some tendency towards lower Th in the samples with fresh glass. Scatter in areas such as Lorne may be partly caused by the low analytical precision, for there is no correlation with LOI.

(g) Conclusions

With the exception of the most acid lavas (>68% SiO_2) and some thermally metamorphosed samples, loss on ignition (LOI) is a good objective measure of alteration. Because of the lack of LOI correlated scatter, it is inferred that almost all the non-acid rocks analysed have retained their original concentrations of Si, Al, Fe, Ti, Mn, P, Ni, Th, Y, Zr, Nb, Cr, Sc, V and REE. Insufficient samples prevent the determination of the effects of alteration on the more acid rocks, but it may be unimportant for these elements, with the exception of silica. Silicification may explain the

bend at about 73% SiO_2 on many Glencoe variation diagrams (e.g. Fig. 4.6), although it should be noted that this is not present for MnO and Zn.

Concentrations of the more mobile elements Ca, Mg, Na, K, Rb, Sr and Ba have probably not been affected by alteration in samples with low LOI (<2.5%) and relatively fresh mineralogies (PAS=1-3), except for K, Rb, Ba and Sr in certain samples with a fresh glassy groundmass. Many more altered samples have probably remained closed to transport of these elements, but in areas where there is little control from fresher samples (e.g. St. Abb's Head), it may be very difficult to determine the primary variation of these elements. It is again not possible to determine the effect of alteration on concentrations of these elements in the more acid rocks, but it is thought that the few mineralogically fresh samples may have retained primary magmatic concentrations.

Despite the lack of any major chemical alteration in the fresher samples, it is considered advisable to have a measure of alteration, the LOI, incorporated into each variation diagram, and to consider the possible effect of alteration on any major deduction made from the chemistry. It is useful in variation diagrams if alteration is only allowed to change the position of a point in a horizontal or vertical direction, and it is therefore inadvisable to plot variation diagrams between pairs of mobile elements. It follows that it is unwise to use a mobile element as an

index of differentiation, for it is convenient to be able to compare the behaviour of every element against the index of differentiation. Alteration in particular rules out the use of Larsen or Thornton-Tuttle differentiation indices, for these are complex functions of several elements whose behaviour under alteration may differ considerably. For similar reasons, the effect of alteration on the norm of a rock is difficult to predict.

Finally, it is important to note that the criteria used in recognizing the chemical effect of alteration only respond to moderately large chemical changes. It is highly probable that mobile elements have suffered small changes in most rocks, and this in particular restricts their use as indices of variation.

CHAPTER 3 : INTRODUCTION TO PETROCHEMISTRY

In the following chapters, the stratigraphy, petrography and chemistry of the Old Red Sandstone volcanic rocks will be discussed, separated into the outcrop areas of Fig 1.1.

3.1 : ROCK NOMENCLATURE

Rocks of calc-alkaline suites usually show a wide range in silica content, and most workers have used nomenclatural divisions separated by silica content, of basalt, basic andesite, andesite, dacite and rhyolite. The bounding silica concentrations used by such authors lie in the ranges 52-54, 56-58, 62-65 and 68-70% silica respectively, but there is no concensus on the precise divisions which should be used. Many recent classifications have subdivided these groups into shoshonitic, high-K and low-K, based on the belief that K content has special genetic significance (e.g. Ewart, in press). Comparable classifications have been used by Gandy (1973a) and Taylor (1972) for rocks of the O.R.S. province, but it is thought that major divisions based on K content are inadvisable because of the ease with which K may be mobilized during alteration. The use of silica as the major criterion for nomenclature can be very misleading, for it is commonly assumed that basalt is a 'primitive' rock type, and andesite an 'evolved' rock type. The occurrence in the province of rocks with <53% silica (i.e. basalts) and <10 ppm Cr and of

others with 57% silica (i.e. andesites) and 370 ppm Cr means that the semantic equation of 'basalt' and 'primitive' can not be assumed if a silica based nomenclature is used.

In general, silica content is not a particularly good indicator of rock chemistry in the Old Red Sandstone volcanic province, and therefore no attempt has been made to use a rigid nomenclatural system. Instead, the terms basalt, andesite etc. have been used merely as indicators of silica concentration, and should not be taken to imply 'primitive' or 'evolved' character. Where nomenclatural systems of previous authors have included well-defined groups (e.g. the "trachyandesites" of the Ochil Hills, Francis et al., 1970; the "mica-felsites" of the Cheviot Hills, Carruthers et al., 1932) their names have been retained for convenience, but most rocks have been classified by their petrography, in particular by their phenocryst mineral association. While this may often have little genetic significance, the phenocryst associations given in Appendix D are useful in that they provide a wholly non-chemical method of rock classification on variation diagrams. The phenocryst association is designated by a number following the '@' symbol in a rock number (Appendix D), and is written as a name using the following abbreviations: ol=olivine, opx=orthopyroxene, cpx=calcic clinopyroxene, pl=plagioclase, hb=amphibole and bi=biotite. For example, S33@11 is an ol-pl-phyric basalt.

Rock analyses are given in Table B17.

3.2 : MINERAL ANALYSES

Mineral analyses referred to as numbers in the text are to be found in Tables C2-C4 of the Appendix. Table C2 quotes average core compositions for the phenocrysts of each rock; these are arranged by mineral type, and the numbers in the text refer to the analysis number for the particular mineral type. Table C3 lists selected core-rim pairs, and Table C4 lists the concentrations of some minor elements for some of the minerals in Table C2.

3.3 : VARIATION DIAGRAMS

About 1000 variation diagrams for rocks and minerals of the province have been produced using the computer program VARPLOT (Appendix D). A far larger number of diagrams than are presented here has therefore been considered in the course of this research, and it is believed that those not presented do not conflict with the petrogenetic hypotheses suggested in later chapters.

All variation diagrams for bulk rock compositions use smaller symbols for samples with higher Loss on Ignition (LOI), for the reasons given in Chapter 2. This is not the case on diagrams for mineral chemistry. Symbols usually refer to the phenocryst association or rock type as appropriate; the phenocryst associations may have quartz, apatite and opaque oxides additional to the phenocryst minerals quoted (see Appendix A for full list of phenocrysts

in each rock). Symbols on diagrams for mineral chemistry refer to the phenocryst association of the host rock. On variation diagrams involving mobile elements, more altered samples may on occasion be outside any relevant field boundaries given. This will occur if the anomalous composition of a rock is thought to be due to alteration.

3.4 : GEOCHEMISTRY

Much literature has accumulated concerning the geochemical behaviour of the elements analysed, and some items believed to be relevant to the petrochemistry of the O.R.S. province are summarized below.

(a) Silica is present in olivines, pyroxenes and feldspars in concentrations only slightly lower than that of an equilibrium basic liquid. Equilibration with these minerals can produce only minor silica enrichment in evolved liquids, and typical calc-alkaline trends of silica enrichment require equilibration with silica-poor phases such as garnet, amphibole, biotite or opaque oxides.

(b) Alumina is only likely to be reduced in evolved liquids by equilibration with assemblages rich in calcic plagioclase. Amphibole and some spinels may contain substantial alumina, but in general fractional crystallisation of plagioclase-free assemblages should lead to increase in alumina in evolved liquids.

(c) Iron. Lack of major iron enrichment relative to Mg in evolved rocks separates calc-alkaline from tholeiitic suites, and requires equilibration with a high Fe/Mg phase

such as garnet, amphibole or opaque oxides if a suite is thought to be genetically related.

(d) Magnesium will have lower concentrations in more evolved liquids unless plagioclase and opaque oxides constitute more than some 75% of the equilibrium crystal assemblage.

(e) Calcium will have lower concentrations in more evolved liquids unless these are in equilibrium with an assemblage rich in olivine, Ca-poor pyroxene, biotite or opaque oxide.

(f) Sodium will increase in more evolved liquids unless these are in equilibrium with an assemblage rich in socic feldspar or amphibole.

(g) Potassium will increase in more evolved liquids unless these are in equilibrium with an assemblage rich in potassic feldspar or biotite.

(h) Titanium crystal-liquid distribution coefficients have been given by Pearce and Norry (1979); they are >>1 for amphibole, biotite and opaque oxides, and <<1 for olivine and plagioclase. See also Table C2.

(i) Manganese distribution is probably mainly controlled by variations in oxygen fugacity, for it may show much variation in oxidation state. Plagioclase is the only common Mn-poor igneous phase, and increase in Mn with evolution probably implies equilibration with plagioclase-rich assemblages.

(j) Phosphorus is only present in any quantity in phosphate minerals, and will therefore increase in evolved liquids unless these are in equilibrium with phosphate phases. Apatite is the most common phosphate mineral, although the presence of whitlockite in mantle mineral assemblages has

been suggested by Beswick and Carmichael (1978).

(k) Nickel and Chromium have high distribution coefficients for all mafic and oxide mineral phases (Gill, 1978), with Cr in particular strongly concentrated in clinopyroxene and spinel. Olivine-liquid distribution coefficients for Ni increase rapidly with decreasing magmatic MgO (Hart and Davis, 1978). Ni and Cr can not both increase in evolved liquids unless these are in equilibrium with assemblages very poor in mafic and oxide mineral phases. Ni concentrations may sometimes be affected by equilibration with sulphides.

(l) Vanadium has very high distribution coefficients for amphibole, biotite and oxide minerals (Gill, 1978), and equilibration with assemblages rich in these minerals will lead to strong depletion in V in evolved liquids, as noted by Taylor et al. (1969). V distribution coefficients for garnet and pyroxenes are also high, and increase in V with evolution implies equilibration with olivine-plagioclase rich assemblages.

(m) Scandium has high distribution coefficients for garnet and clinopyroxene, and low for olivine and plagioclase. Equilibration with garnet-rich assemblages, in particular, would lead to strong Sc depletion in evolved liquids.

(n) Copper and Zinc distribution may be mainly controlled by sulphide phases, although zinc concentrations in excess of 1% ZnO have been observed in some phenocryst titanomagnetites (Table C2).

(o) Rubidium substitutes for K in most igneous minerals, and has lower distribution coefficients than K for most phases

except biotite (Gill, 1978). Only equilibration with biotite- (or phlogopite-) rich assemblages can prevent decrease in K/Rb with evolution, but this could also lead to decrease in K and Rb concentrations.

(p) Strontium distribution coefficients are only >1 for plagioclase and apatite (Gill, 1978), although amphibole may contain substantial Sr (Table C4). Only equilibration with plagioclase-rich (>c.40%) assemblages can prevent increase in Sr in evolved liquids.

(q) Barium distribution coefficients are high only for alkali feldspar and biotite, although plagioclase and amphibole may contain substantial Ba (Table C4). It has been suggested (Taylor, 1972) that equilibration with biotite/phlogopite could lead to K/Ba increase in residual liquids, but Ba content of micas is very variable (Table C4).

(r) Thorium distribution coefficients are not well-known, but they are probably <<1 for most igneous phases except zircon, thorite, allanite and phosphate minerals. There is a possibility of higher Th distribution coefficients for opaque oxide minerals.

(s) Zirconium and Niobium distribution coefficients have been given by Pearce and Norry (1979). High values are only quoted for amphibole, biotite+zircon and titanomagnetite in intermediate and acid liquids, but microprobe studies on phenocryst amphibole and titanomagnetite in intermediate rocks (e.g. GC29@16, Table C4, amphibole analysis 2 and spinel 9) suggest that, in both cases, the distribution coefficients for Zr are substantially less than 1. Only

phenocryst ilmenite has been found to contain significant Zr, but this is variable, giving phenocryst-whole rock distribution coefficients between 2 and 8, much greater than the value of 0.28 quoted by Pearce and Norry (1979). Coefficients given by Pearce and Norry (1979) for Nb are all greater than those for Zr, with the exception of zircon. This implies that Zr/Nb can not decrease with evolution. Analysis 5, Table C4, for Nb has confirmed that Zr/Nb is also lower in ilmenite than in host rock.

(t) Rare earth elements and Y distribution coefficients have been given by Schnetzler and Philpotts (1970) and many other workers for the REE, and by Pearce and Norry (1979) for Y. Y behaves geochemically as a heavy REE (Goldschmidt, 1954, p.310). Olivine, orthopyroxene and plagioclase have coefficients <<1 for all REE except Eu; heavier REE partition preferentially into clinopyroxene, amphibole and garnet, with coefficients just <1 in basic liquids for clinopyroxene and amphibole, and high HREE coefficients (4-50) for garnet. LREE coefficients of these three phases are <1 and therefore equilibration with assemblages rich in them will lead to LREE enrichment (higher La/Y) in evolved liquids. Garnet will be much the most effective at producing LREE enrichment. Apatite and zircon are the only common igneous minerals with high distribution coefficients for LREE (Nagasawa, 1970); apatite is slightly LREE enriched relative to the host rock (Table C2).

(u) Nomenclature

Throughout this thesis, the term 'large ion lithophile elements' (LILE) will be used for K, Rb, Ba, Sr, P and LREE;

and the term 'high field strength elements' (e.g. Pearce and Norry, 1979) will be used for Ti, Zr, Y and Nb. The term 'compatible trace element' will refer to Ni, Cr, Sc and V.

CHAPTER 4 : SOUTHWEST HIGHLANDS

The Old Red Sandstone successions of the southwest Grampian Highlands are dominated by volcanic rocks. There are three Lower O.R.S. outcrops, at Ben Nevis, Glencoe and the Lorne Plateau (Fig. 1.1). In this region the volcanic rocks are associated with a wide range of intrusive igneous rocks, including large granodioritic plutons, kentallenitic and appinitic stocks and a voluminous suite of NE-SW porphyritic microdiorite dykes.

4.1 : LORNE PLATEAU

The O.R.S. of the Lorne Plateau is a relatively thin (c. 2000 ft, 650 m; Kynaston and Hill, 1908) succession of lava flows, rare pyroclastic deposits and some sediments, disposed about a shallow SW-trending syncline and resting unconformably on Dalradian metasediments. The O.R.S. is cut by the NE-SW dyke swarm, and similar lavas (e.g. L82) form a highly altered screen in the plutonic Etive Complex. A few minor plugs and sills also cut the volcanics (Lee and Bailey, 1925), and are thought to be very closely related to the volcanism.

Detailed stratigraphic sequences have been given by Kynaston and Hill (1908) and Lee and Bailey (1925) for small areas near Oban, but the lack of marker horizons has prevented the erection of an accurate stratigraphy for the whole area. The lower part of the sequence appears to be

composed of andesites and basalts lacking phenocryst plagioclase, interbedded with sediments towards the base in the west. The sediments are rich in large lava clasts, and were considered by Groome (1972) to be the products of lahars. Central parts of the sequence are more varied and siliceous, with hornblende- and biotite-andesites and intermittent acid lavas and tuffs. The latter include several ignimbrites, correlated with those at Glencoe by Roberts (1966). The highest flows in the sequence have been described as hypersthene-andesites (Kynaston and Hill, 1908) and are rich in plagioclase phenocrysts.

The petrography of the volcanic rocks has been described by Kynaston and Hill (1908), Lee and Bailey (1925) and Groome (1972), who have all reported a wide variety of associations of the phenocryst minerals olivine, orthopyroxene ('hypersthene'), augite, hornblende, biotite, plagioclase, apatite, titanomagnetite and ilmenite. These occur in a variably textured feldspathic matrix, in which there is usually also augite and opaque material. Some of the groundmass feldspar is probably alkali feldspar (Bailey and Maufe, 1960, p.233) and biotite may also be a groundmass phase. Quartz crystals (up to 4mm) occur frequently in rocks without phenocryst plagioclase from western Lorne, and are usually rimmed by augite or its alteration products, or sometimes by biotite or hornblende (e.g. L21).

Groome (1972) has described the chemistry of some of the volcanic rocks from northern Lorne, and has shown that

the rocks are alkali-calcic (Peacock, 1931) and not high-alumina. He therefore described them as 'orogenic', on the basis of their relation to the Caledonian orogeny. He noted that the rocks are rich in Na, K, Cr, Ni and Sr and poor in Fe, Ca, Cu and Rb/K relative to rocks of most basalt-andesite-dacite-rhyolite associations.

The smooth variation between total iron and silica shown by the Lorne basalts and andesites led Groome and Hall (1974) to the conclusion that these rocks formed a closely related series, implying a common source. The acid lavas were thought to be derived from a different source, because of discontinuities on Harker diagrams for Fe, Sr, Ti and Li. Such discontinuities are not present when data from a wider area is considered (e.g. Fig. 4.2), although additional Li data is not available.

(a) <u>General chemical characteristics</u>

The chemical data reported here for samples from the Lorne Plateau confirm the general features of the Lorne rocks relative to most basalt-andesite associations. Additionally, the rocks have high concentrations of Zr, Nb, Th, P, LREE and relatively low concentrations of Y. The rocks therefore have a very highly fractionated REE pattern relative to chondrites.

The data presented here display the apparently smooth variation of element concentrations with silica described by

Groome and Hall (1974), and additionally, Sc and V decrease and Ba increases with increasing silica. Average analyses (Table 4.1) display the relative levels of each element with increasing silica.

Nb, Th, Y, Zr and LREE do not show the smooth variation with silica thought by Groome and Hall (1974) to be demonstrated by other elements in the basalts and andesites (Fig. 4.1). Scatter in the concentrations of these elements, with the possible exception of Th, is most unlikely to be the result of alteration (Chapter 2): at worst, this would result in translation of points parallel to the SiO2 axis, and could therefore not produce the scatter, particularly in Zr concentrations. Further confirmation that alteration is not important is provided by the high degree of scatter on the Zr-Ce distribution (Fig. 4.1). Analytical precision and accuracy are good (Appendix B9), and the analytical errors are trivial relative to the magnitude of the scatter.

The use of phenocryst association as a means of classification in Fig. 4.1 instead of the silica-based divisions used by Groome and Hall (1974) demonstrates that the scatter is not random. For example, it is clear that opx-cpx-phyric samples have lower Th, Y and Zr than opx-cpx-pl-phyric samples, despite having roughly the same Nb, Ce and SiO_2. Examination of other variation diagrams (e.g. Fig. 4.2) discloses that rocks of at least some phenocryst associations have distinctive chemistries for

TABLE 4.1 : Average analyses of SW Highlands volcanic rocks.

	1	2	3	4	5	6
SiO_2	54.23	55.91	60.14	62.03	64.03	64.53
Al_2O_3	16.68	16.30	16.58	16.67	16.54	16.53
Fe_2O_3	8.14	7.40	6.09	5.36	4.56	4.42
MgO	5.41	5.39	3.82	3.08	2.29	2.37
CaO	7.19	6.68	4.72	4.13	3.69	3.78
Na_2O	3.96	3.88	4.50	4.23	4.30	4.38
K_2O	2.14	2.44	2.51	3.11	3.23	3.01
TiO_2	1.40	1.18	0.94	0.88	0.71	0.61
MnO	0.11	0.09	0.08	0.07	0.07	0.07
P_2O_5	0.46	0.45	0.36	0.28	0.24	0.22
Total	99.72	99.72	99.74	99.84	99.66	99.92
LOI	3.05	2.38	2.14	2.77	1.51	0.62
Ni	151	145	77	49	36	35
Cr	293	270	154	83	69	60
V	158	144	111	112	78	79
Sc	22	19	15	14	10	10
Cu	32	27	24	23	17	18
Zn	82	74	70	66	65	62
Sr	1151	1154	1108	993	963	1048
Rb	34	43	39	68	70	59
Th	4	4	4	7	5	4
Zr	207	191	166	200	222	139
Nb	15	13	10	10	10	8
Ba	952	1123	1225	1215	1368	1386
La	36	37	34	35	35	28
Ce	80	80	71	74	72	57
Nd	37	37	33	34	31	26
Sm	7	8	7	4	5	4
Y	21	19	16	18	17	13
No.	23	10	9	10	9	11

1 = ol-phyric samples, 2 = ol-cpx-phyric samples, Lorne.

3 = opx-cpx-phyric and related samples, 4 = opx-cpx-pl-phyric samples, Lorne.

5 = Glencoe samples with $62 < SiO_2 < 67\%$.

6 = Ben Nevis samples.

Fig. 4.1 a & b : Bulk rock variation diagrams. Fields are:

1 = ol- and ol-cpx-phyric samples

2 = opx-cpx-phyric and related samples

3 = opx-cpx-pl-phyric samples

4 = cpx-hb-bi-phyric samples and related intrusions

Conventions as section 3.3

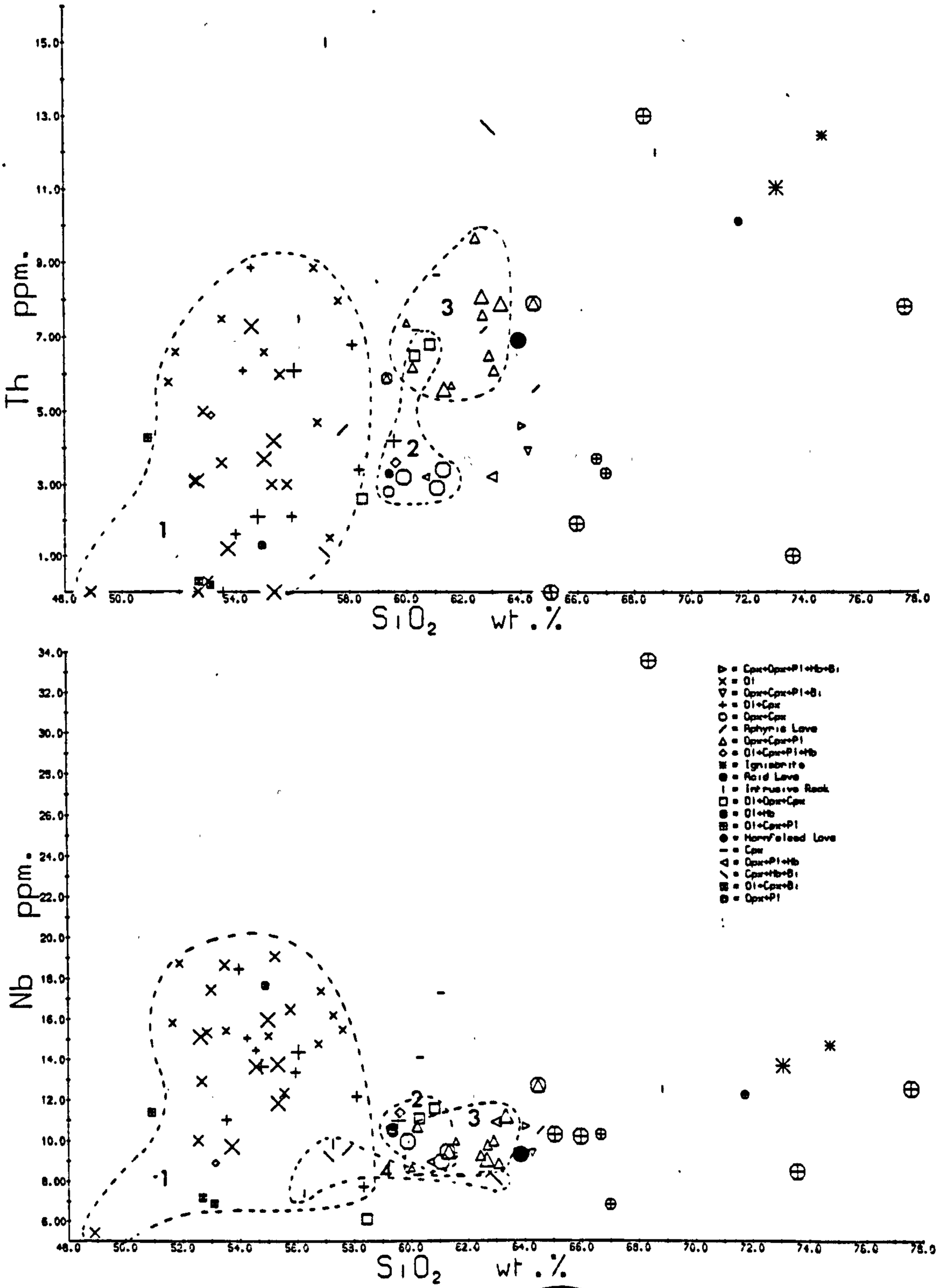

Fig. 4.1 c & d

Field boundaries as Fig. 4.1 a & b

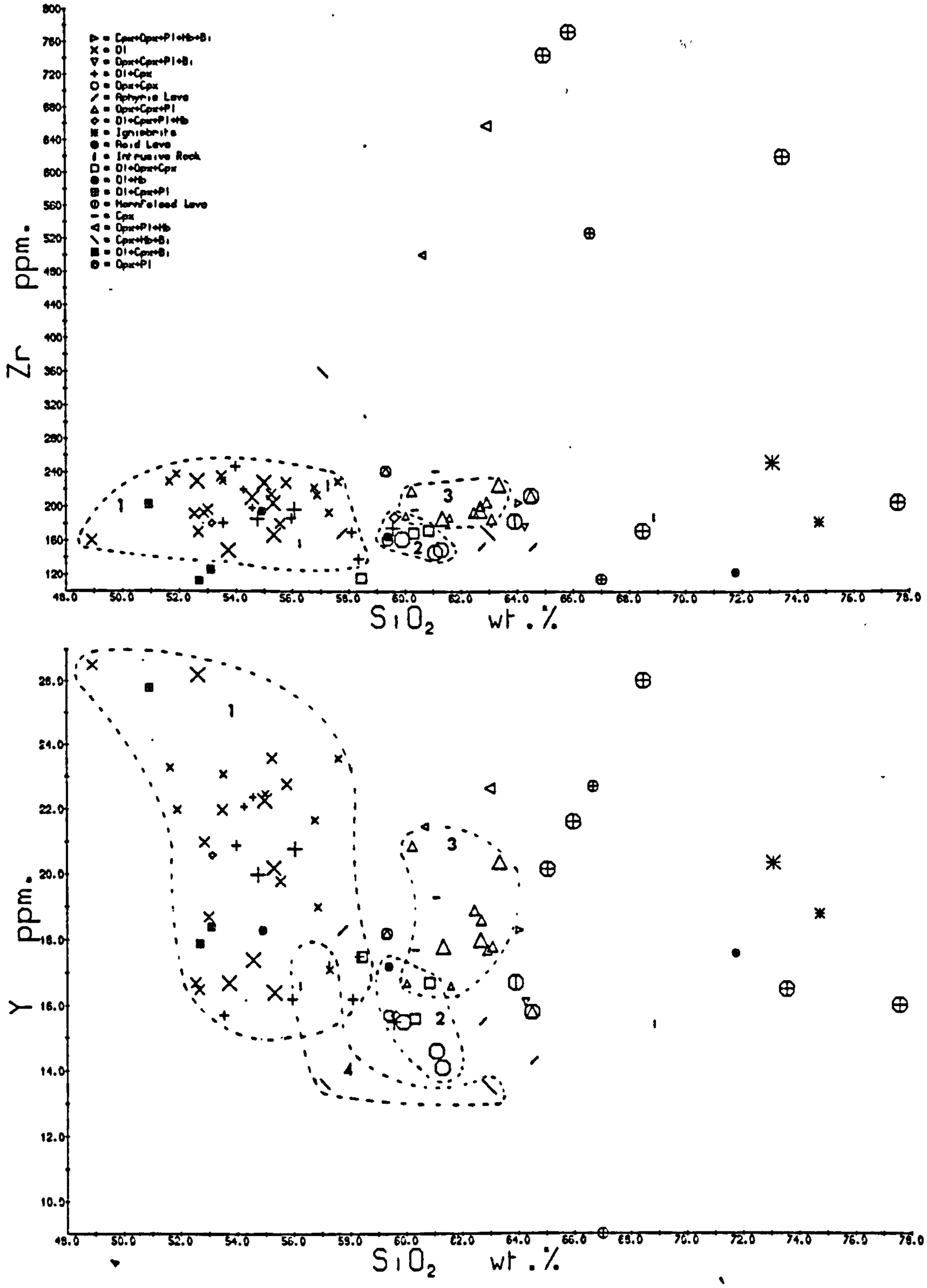

LORNE PLATEAU

Fig. 4.1 e & f

Fields as Fig. 4.1 a & b

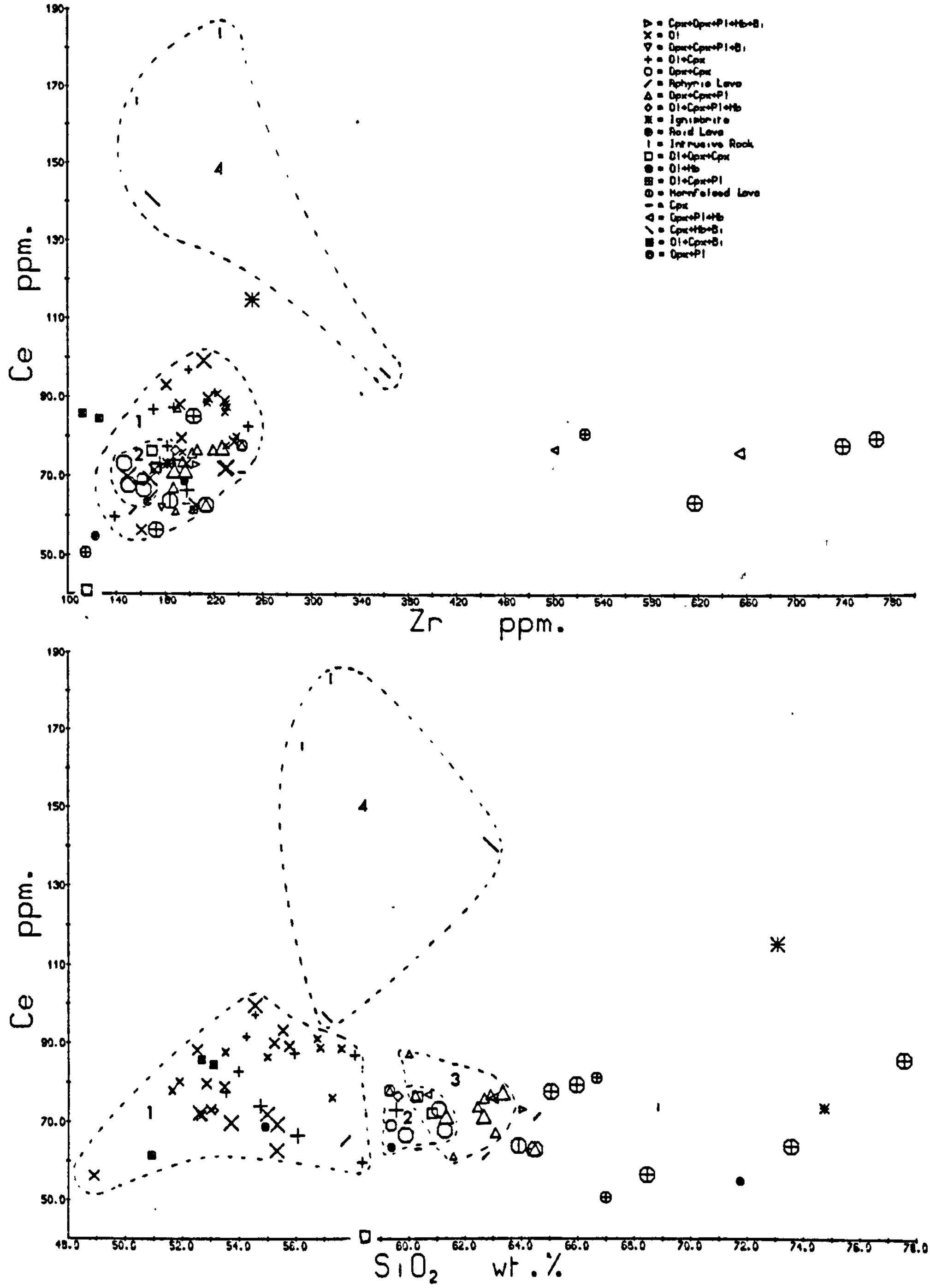

LORNE PLATEAU

Fig. 4.2 a & b : Bulk rock variation diagrams
Fields as Fig. 4.1, conventions as section 3.3

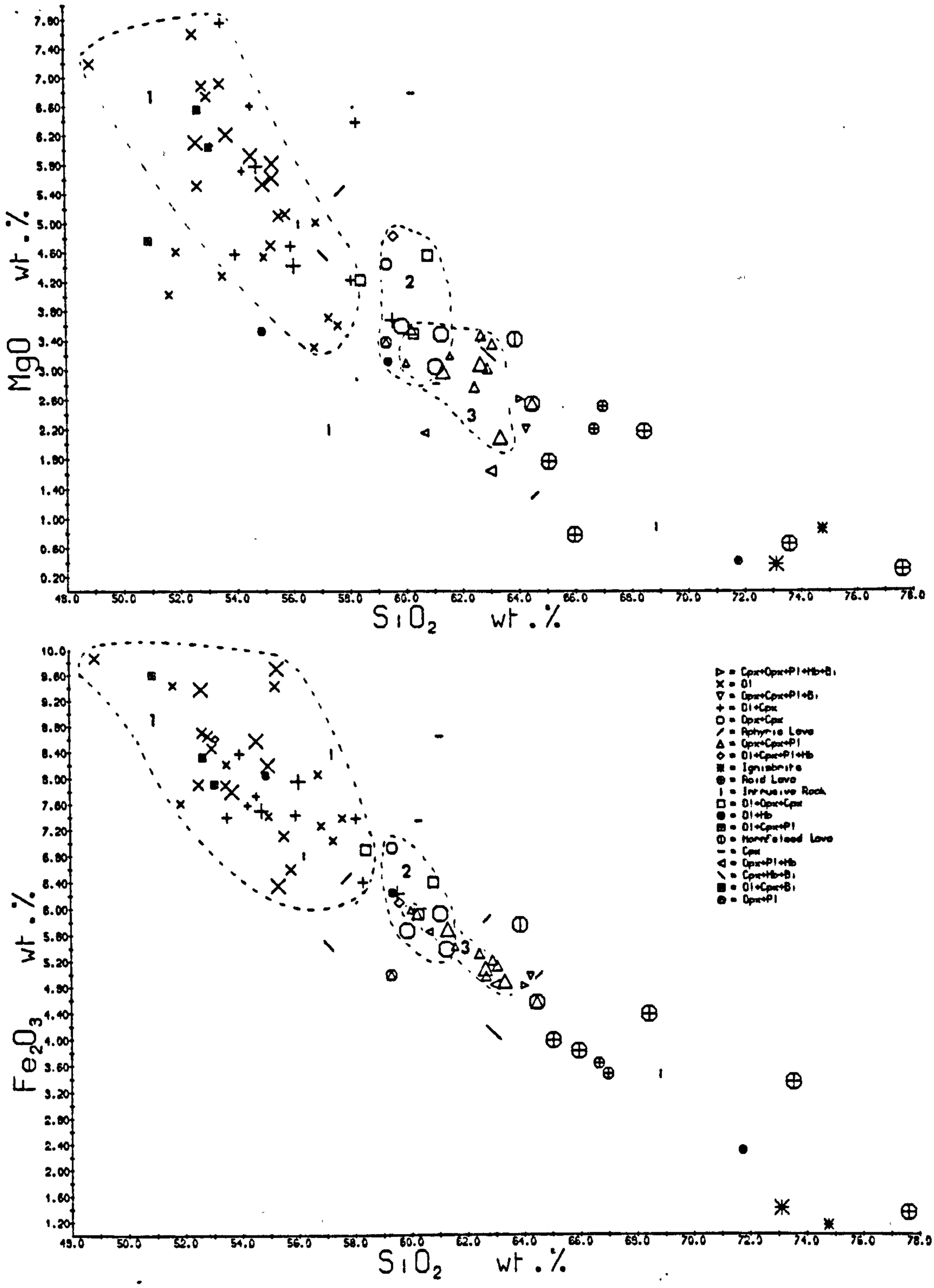

Fig. 4.2 c & d

Fields as Fig. 4.1

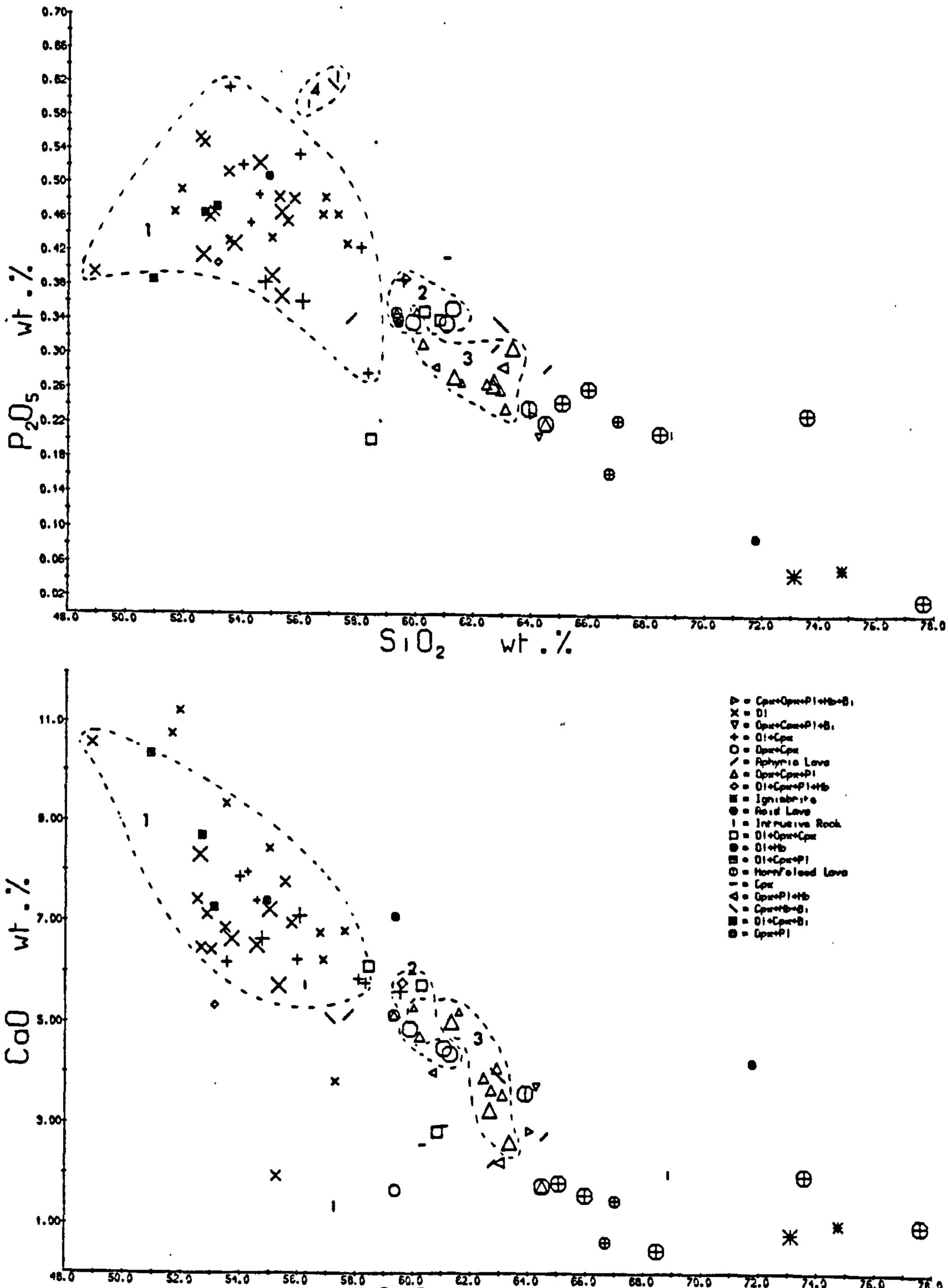

LORNE PLATEAU

Fig. 4.2 e & f

Fields as Fig. 4.1

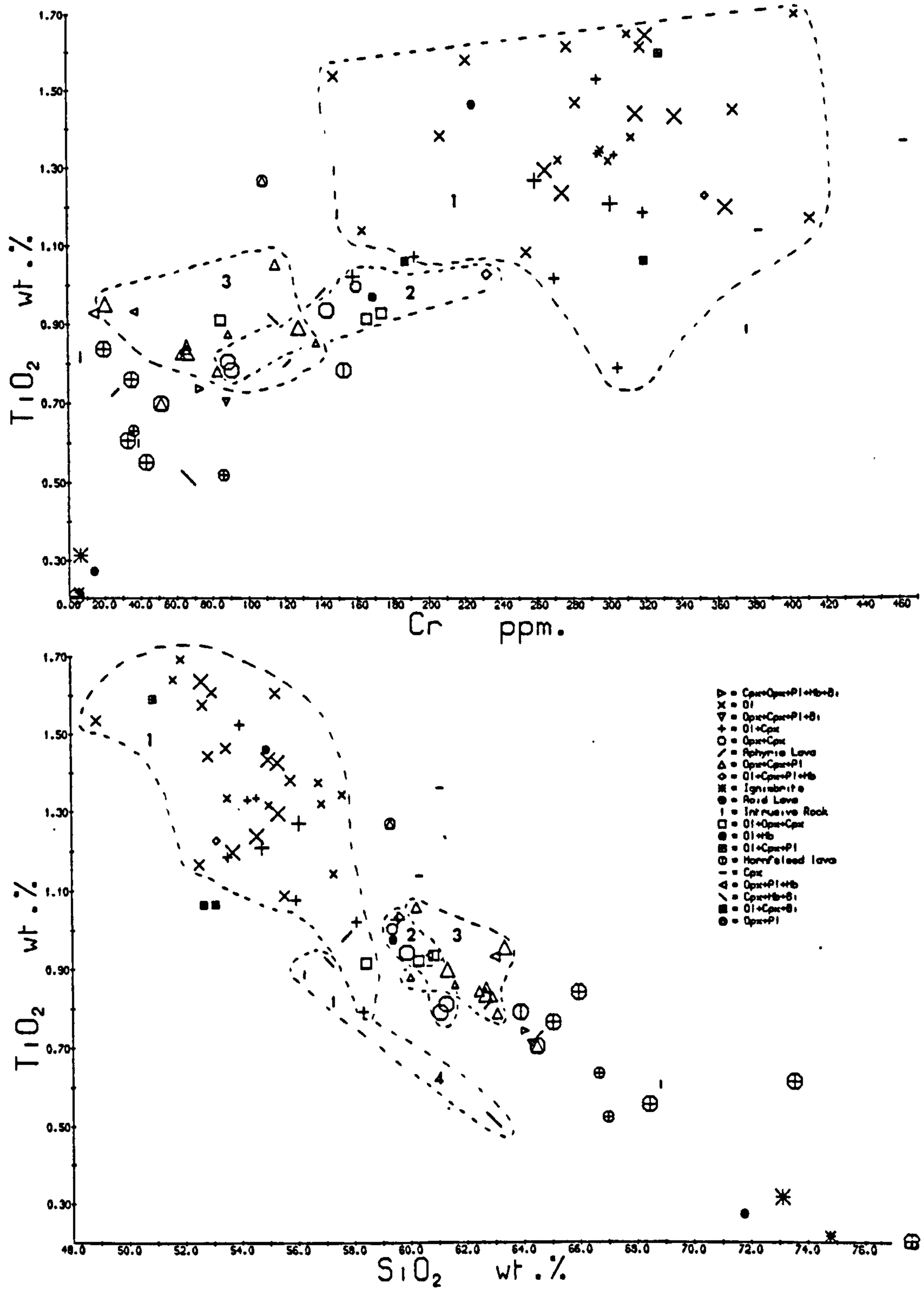

LORNE PLATEAU

Fig. 4.2 g & h

Fields as Fig. 4.1

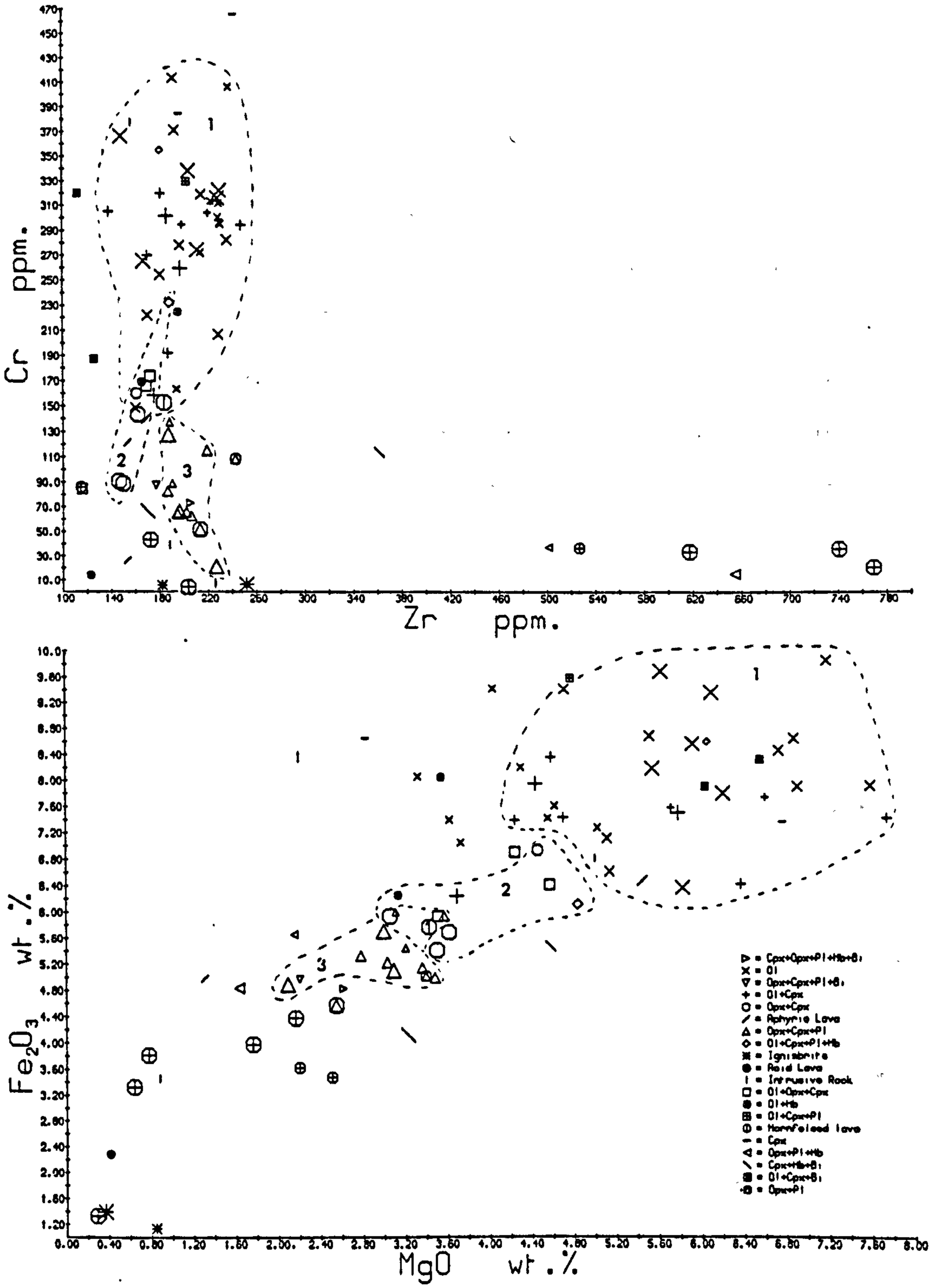

elements thought by Groome and Hall (1974) to show smooth variation with silica, and that the associations are not transitional with increasing silica content. The petrochemistry of the rocks in each major phenocryst association will therefore be discussed.

(b) Ol-phyric samples (@1)

Samples with olivine as the sole silicate phenocryst contain olivine pseudomorphs and occasional opaque oxide microphenocrysts in a plagioclase-augite-oxide groundmass. The rocks contain up to 15% modal phenocryst olivine, generally decreasing with increasing silica, although the most basic rock, L23, is phenocryst-poor (<1%). Silica varies from 48.9 to 57.6%, and no elements show smooth variation with silica, although general negative correlation exists for Fe, Mg, Mn, Cr and V, and general positive correlation for Rb, Nb, K and La/Y. Variation diagrams for other elements against silica show no clear trends, and are greatly scattered, despite the appearance in most cases of smooth variation when all rocks are considered (Fig. 4.2).

It is clear from Fig. 4.2 that the rocks do not lie on an olivine control line, and are therefore not genetically related by fractional crystallisation of the phenocrysts. It is apparent that samples with olivine and clinopyroxene as the only phenocrysts are not chemically distinguished from ol-phyric samples, and therefore this group will be treated prior to further discussion of the

chemistry.

(c) Ol-cpx-phyric samples (@7)

These rocks are petrographically very similar to ol-phyric samples, but additionally contain up to 3% of almost colourless augite phenocrysts. Rare samples also have opaque oxide phenocrysts, probably titanomagnetite (L155). The clinopyroxene is chemically a diopsidic augite (e.g. pyroxene analyses 1 and 12, Table C2) with low Al, Ti, Na and generally high Cr. Bulk-rock silica content varies between 53.5 and 59.5%, so that the average (Table 4.1) is more siliceous than that for the ol-phyric samples, and average concentrations of other elements differ according to the 'smooth trends' with increasing silica of Fig. 4.2. Substantial chemical overlap exists between the two groups, and the rocks show the same scattered variation in Figs. 4.1, 4.2. Variation diagrams using other elements as indices of differentiation, e.g. MgO, Cr and Zr, show a similar degree of scatter: it may therefore be concluded that no single-stage, single-source petrogenetic mechanism can create the observed variation.

The chemical variation discussed so far could be produced by a two-stage fractional crystallisation process; for example, the general variation trends of Table 4.1 may have been generated by high pressure fractional crystallisation, with scatter superimposed through lower pressure fractionation. A number of lines of evidence

suggest that this is not the case, of which the strongest is the use of the concentrations of elements with low crystal-liquid distribution coefficients ('incompatible elements'), which, even in multi-stage fractional crystallisation, should maintain constant ratios with evolution. The identity of such elements of course depends on the composition of the crystallising assemblage, but Pearce and Norry (1979) suggest that, assuming that liquids of basaltic composition are not in equilibrium with minor phases, Zr/Nb should be insensitive to fractional crystallisation or variation in degree of partial melting.

Although there is general positive correlation between Zr and Nb for the ol- and ol-cpx-phyric samples, there is still substantial scatter (Fig. 4.3b). Fig. 4.3a demonstrates the result of this scatter on the Zr/Nb ratio: for ol- and ol-cpx-phyric samples this varies between 11 and 30, although all except three have Zr/Nb between 11 and 16. This variation is substantially greater than that for any region illustrated by Pearce and Norry (1979), although the range for Hawaiian basalts is comparable to the restricted range for the Lorne samples. The presence of biotite and resorbed amphibole in some of the basic Lorne lavas suggests that equilibration with minor phases is a distinct possibility; however, Zr and Nb content of these phases is low, and therefore a high degree of crystallisation or large variation in degree of partial melting with these phases residual would be required to generate the observed Zr/Nb variation. These mechanisms would lead to major variation

LORNE PLATEAU

Fig. 4.3 a & b : Bulk rock variation diagrams

Fields as Fig. 4.1, conventions as section 3.3

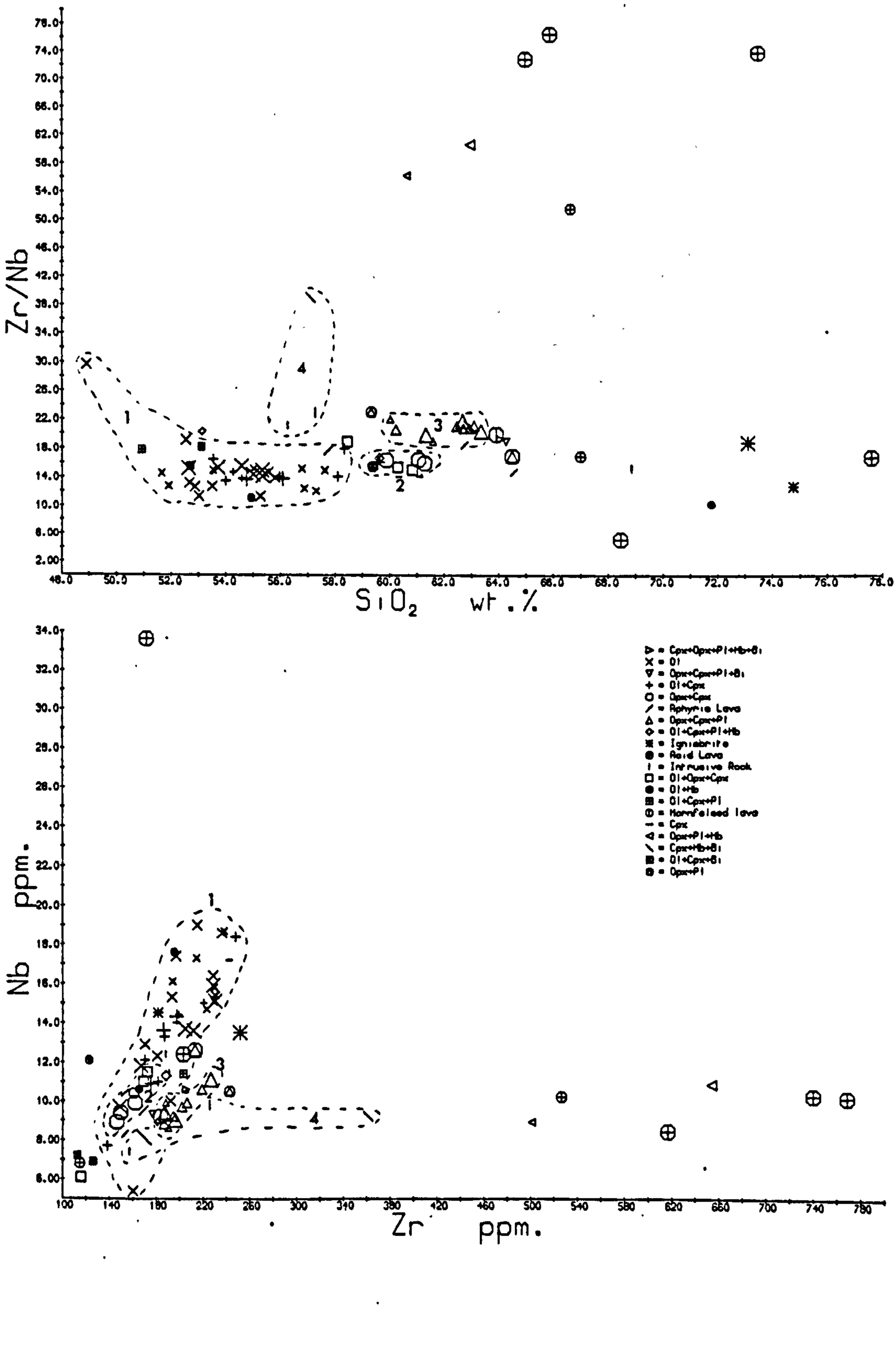

LORNE PLATEAU

Fig. 4.3 c & d

Fields as Fig. 4.1

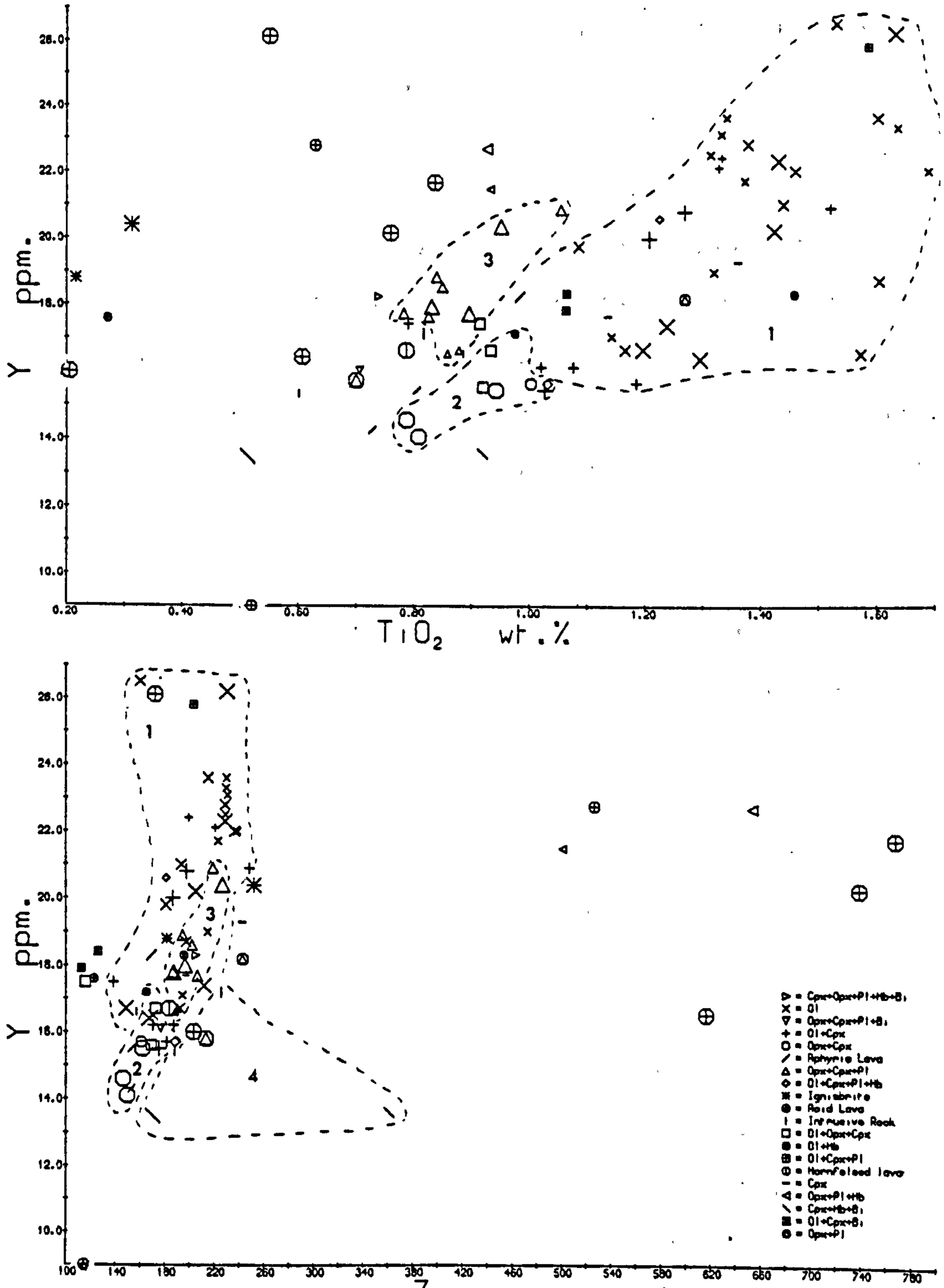

in the rest of the chemistry, particularly in Si, which would correlate with Zr/Nb variation. This is not observed (Fig. 4.3). Ilmenite has substantially higher Zr and Nb concentrations (e.g. analysis 2, Table C4) and equilibration with ilmenite-bearing assemblages could therefore lead to change in Zr/Nb (Chapter 3).

In addition to the general positive Zr-Nb correlation, there is also general positive correlation between Zr and Y, Ti and Y (Fig. 4.3), Ti and Nb and to some extent between Ti and Zr. Conversely, correlations between Zr and Ce (Fig. 4.1e) and between Ti and P are poor; Ce and P being elements which remain incompatible unless apatite is a fractionating phase.

Such Ti-Zr-Y-Nb relations, with relatively constant inter-element ratios, are commonly found in volcanic suites (Pearce and Norry, 1979), and may usually be interpreted as the products of partial melting or fractional crystallisation events. The direction of evolution on the Zr versus Nb diagram should be the direction of Cr and Ni decrease providing that plagioclase is not the sole fractionating phase, for one or both of Cr and Ni partition strongly into all mafic minerals (e.g. Gill, 1978). In these samples, there are good Sr-K, Sr-P, Sr-Ba, Sr-Rb and Sr-La/Y positive correlations (Fig. 4.4), implying that plagioclase can not be an important fractionating phase (Chapter 3). The range in Zr and Nb concentrations implies about 50% crystallisation of the parent magma if both are

LORNE PLATEAU

Fig. 4.4 a & b : Bulk rock variation diagrams
Fields as Fig. 4.1, conventions as section 3.3

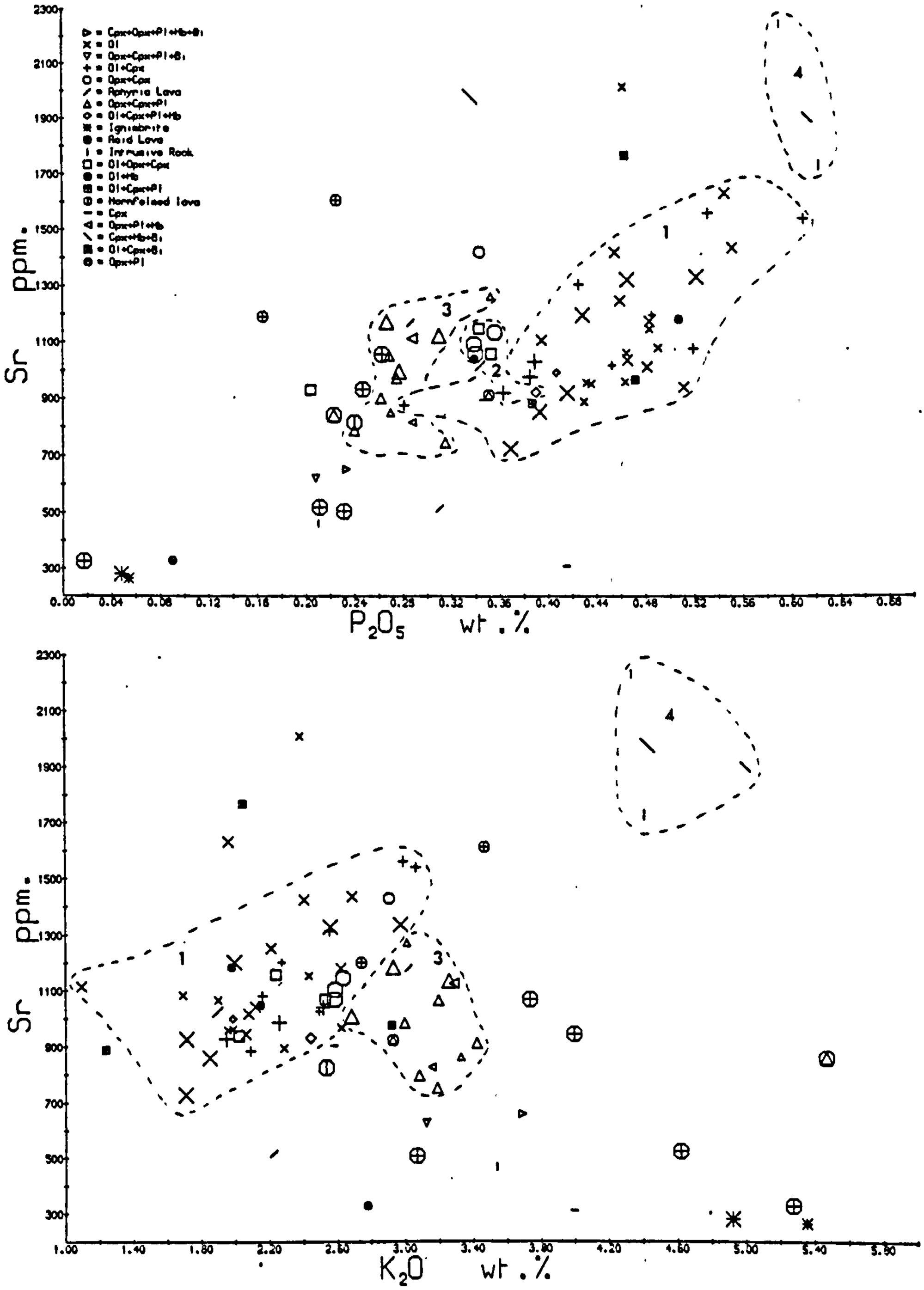

LORNE PLATEAU

Fig. 4.4 c & d

Fields as Fig. 4.1

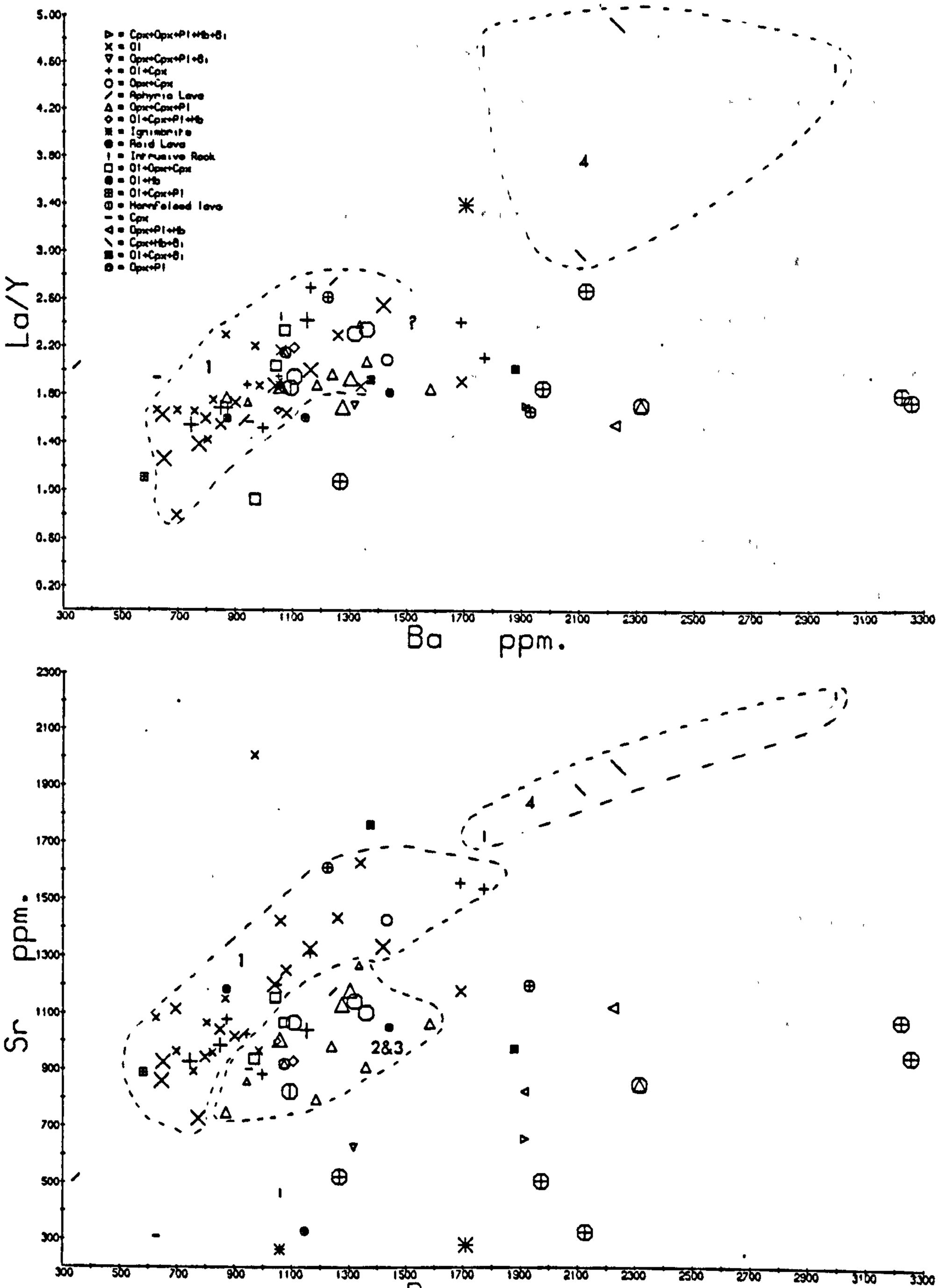

regarded as incompatible; such a large degree of crystallisation is likely to produce substantial reduction in Cr and Ni concentrations. For example, if the bulk distribution coefficient for Cr was as low as 2, the Rayleigh equation predicts halving of the Cr content of the liquid on 50% crystallisation. The same argument applies if Zr and Nb are regarded as compatible, for it is most improbable that they could be more compatible than Cr. No systematic depletion in Cr content occurs either with increase or decrease of Zr (Fig. 4.2). If fractional crystallisation of small amounts of ilmenite (or magnetite, Pearce and Norry, 1979) produces the variation in Zr/Nb by preferentially removing Nb, then Cr and Ni will also decrease with increasing Zr/Nb, so that, at constant Nb, there should be systematic decrease in Cr with increasing Zr. No such pattern is displayed (Fig. 4.5). Zircon separation, the final possibility suggested by Pearce and Norry (1979) for change in Zr/Nb by fractional crystallisation, may be ruled out because of the improbability of early zircon crystallisation from a basalt-basaltic andesite liquid with only about 200 ppm Zr. It may be concluded that even multistage fractional crystallisation can not produce the observed chemical variation.

(d) Opx-cpx-phyric and related samples (@8)

Rocks of this phenocryst association have a few phenocrysts of augite and pseudomorphed orthopyroxene in a

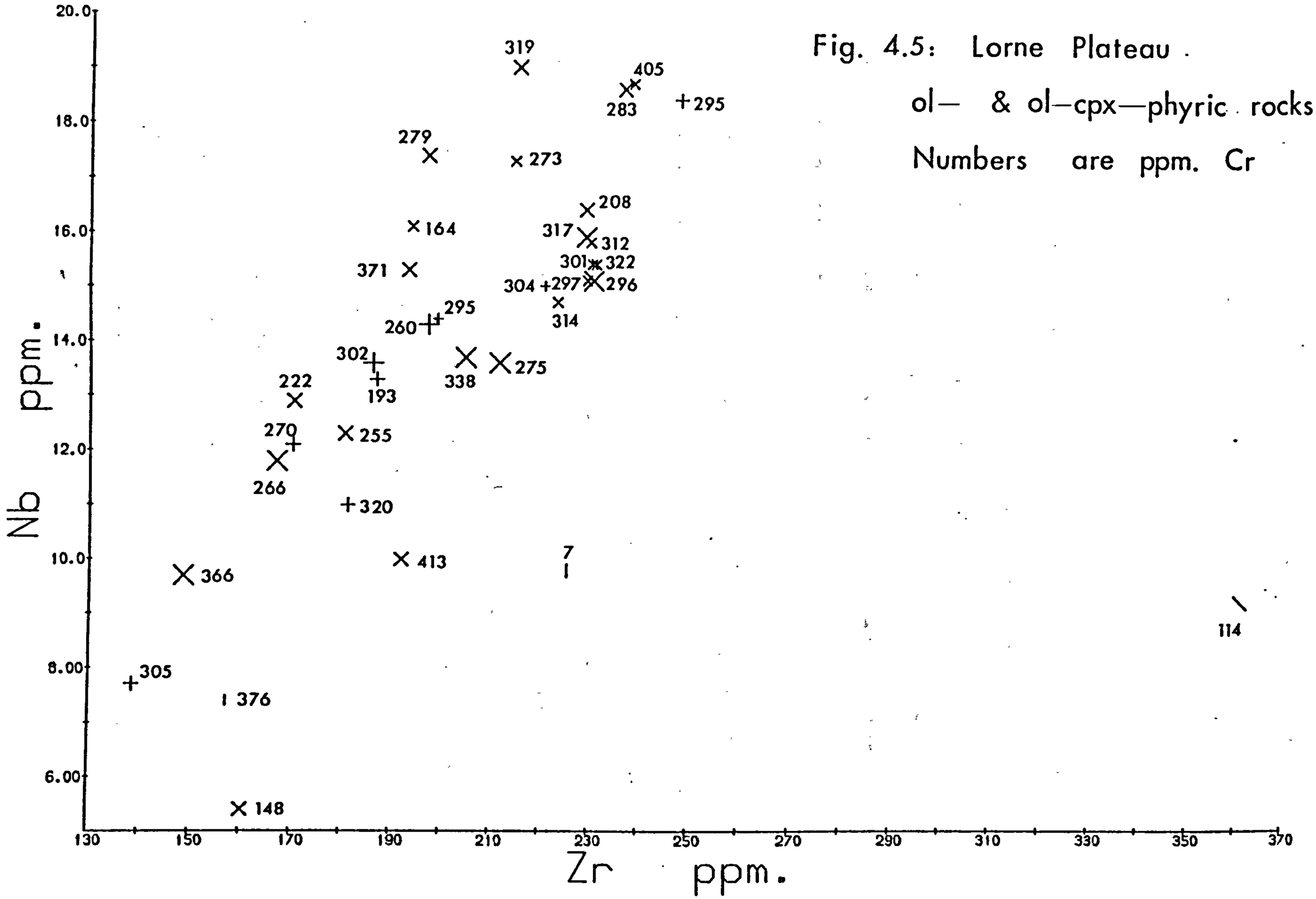

Fig. 4.5: Lorne Plateau .

ol— & ol—cpx—phyric rocks

Numbers are ppm. Cr

generally trachytoid feldspathic groundmass. Only four samples have been collected, but five other samples (L50-52, L21 and L61) show nearly identical chemistry, with the exception of substantially higher Th for samples L51 and L52 (Fig. 4.1). These two have phenocryst olivine in addition, but are not chemically transitional to the ol-cpx-phyric samples. L50 has olivine and augite phenocrysts with rare resorption pseudomorphs after amphibole and rare plagioclase, while the original nature of the phenocrysts in L61 is a little difficult to determine. L21 is the most siliceous ol-cpx-phyric sample, but has more affinities with the opx-cpx-phyric group.

Augite phenocrysts from L50 and L51 are very similar to those from the ol-cpx-phyric samples, and in particular do not have higher Fe/Mg than the pyroxenes from the more basic groups, contrary to the suggestion of Groome (1972). Single rounded crystals of quartz with a reaction rim of very low Ti, low Al augite (analysis 9, Table C2) or amphibole are very common in rocks of this group, and were interpreted as 'xenolithic' by Kynaston and Hill (1908, p.64). Groome believed them to be relatively high pressure phenocrysts, because of the lack of reaction rims around rare schist xenoliths. The absence of reaction rims around large aggregates of quartz grains (?quartzite xenoliths) and their presence around single crystal quartz in GC10 suggests that Groome's interpretation was correct, although quartzite xenoliths in the Ballachulish quartz-diorite display wide augite-hornblende coronae (Muir, 1953).

The silica range in this group is small, from 59 to 62%, but even in this range fairly smooth depletions are observed for Ti, Ca (unaltered samples), Mg, Fe, Cr, Ni, Sc and V (e.g. Fig. 4.2), contrasting strongly with the behaviour of these elements in the more mafic samples. Concentrations of these elements are lower than in more mafic samples (Table 4.1), as expected from the 'smooth' variation trends with silica for the Lorne lavas as a whole, but there appears to be a composition gap between this group and the more mafic samples, particularly evident for Nb, Ce (Fig. 4.1), Ti and P (Fig. 4.2). Zr/Nb is between 14 and 16, which is identical within analytical error and closely comparable with the average Zr/Nb of the mafic rocks (Fig. 4.3). Variation diagrams against Cr (e.g. Fig. 4.2) demonstrate that Ti, Zr, Y and Nb decrease smoothly with increasing differentiation (i.e. with decreasing Cr, Ni and increasing SiO_2). This may suggest fractional crystallisation of an assemblage including amphibole or biotite+zircon (Pearce and Norry, 1979) or possibly ilmenite. LREE may decrease slightly with differentiation, but as with Y, Nb and also Rb the amount of variation involved is close to the analytical precision limit. K_2O increases smoothly by 7% relative if the three more altered samples are ignored, Ba appears to increase by 22% relative (from about 1100 ppm in L21, 10, 50 and 51 to about 1350 ppm in L14 and L45), but Rb increases by a maximum of only 7%. This combination might suggest fractional crystallisation of a biotite-bearing assemblage (Chapter 3) rather than an amphibole-bearing one, but it should be noted that the

distribution coefficients are poorly known, and the variations in Rb, Nb and Y are close to the limits of analytical precision. Further, resorption pseudomorphs after amphibole occur in L50, suggesting that amphibole may be more plausible.

A model of fractional crystallisation of a biotite- or amphibole-bearing assemblage from a more mafic composition could therefore produce some features of the chemical variation of this group of rocks, but certain difficulties remain. Prominent amongst these are the lack of measurable Zr in amphiboles from higher Zr lavas in Glencoe, indicating D(Zr, hb) <0.6; the Th concentrations of L51 and L52; and the scatter in P_2O_5 concentrations between 0.33 and 0.38% unrelated to Cr content, which is considerably greater than the scatter introduced by analytical imprecision (Table B7). It is believed that variation within this group can not be adequately explained by fractional crystallisation.

(e) Opx-cpx-pl-phyric samples (@13)

Rocks with this common phenocryst association are in general phenocryst-rich, with up to 40% plagioclase, and correspond to the hypersthene-andesites of Kynaston and Hill (1908). The feldspar is usually calcic andesine, and the clinopyroxene is an augite low in Ti, Al and Na, with Fe/Mg significantly greater than that in samples lacking phenocryst plagioclase. The pyroxene is commonly reverse

zoned. Apatite, magnetite and ilmenite are common additional phenocrysts.

Silica varies from 60 to 63.5%, and in this small range there are fairly smooth depletion trends for Fe, Ca, Cr, Ni, Sc and, with the exception of the most siliceous sample, for P, Ti and possibly Al (e.g. Fig. 4.2). The rocks fall on the smooth overall variation trends of Table 4.1, but show marked differences from the opx-cpx-phyric and related samples which are not simply related to the slightly higher average silica of the opx-cpx-pl-phyric rocks. In particular, K, Th, Rb, Sc, V, Zr and Y are substantially higher in the opx-cpx-pl-phyric rocks, while P is lower. LREE and Nb show no differences, so that Zr/Nb is higher and La/Y, and also K/Rb, are lower in the opx-cpx-pl-phyric rocks (e.g. Figs. 4.1-4.3). These differences, in particular that of Zr/Nb, strongly suggest that the two main rock groups in the 59-64% SiO_2 range are neither derived from each other nor from the same parent magma by fractional crystallisation processes. Cumulus enrichment has probably played little part in creating the chemical differences, for Al contents of the two groups are very similar, and do not increase much with increasing amount of phenocryst plagioclase (e.g. from L30, <10%, to L128, >35% phenocryst plagioclase).

Zr/Nb varies between 19 and 22, close to the range expected through analytical imprecision, and both Zr and Nb increase fairly smoothly with decreasing Cr content (Fig.

4.2), suggesting that fractional crystallisation of a Zr-, Nb-poor assemblage could explain the variation in this group. However, only one of the ol- and ol-cpx-phyric samples has Zr/Nb in this range, and therefore derivation of the group by fractional crystallisation of one of the more mafic magmas is improbable.

Y, K, and less clearly, Ce and Rb, also increase with increasing Zr and SiO_2 and decreasing Cr (Figs. 4.1-4.3), and K, Rb, Zr and Nb all show about 20% enrichment over the full Cr depletion. Ce and Y seem to be less incompatible, with only about 15% enrichment. Fractional crystallisation of the phenocryst phases could probably give rise to the main variation trends, for apatite could account for the depletion in P_2O_5 and the less than perfectly incompatible behaviour of Y and LREE (Chapter 3). This possibility is difficult to test by least squares extract calculations because of the small amount of variation involved, and the difficulty of identifying the primary major element chemistry of small numbers of samples when modified by alteration. The far from perfect linear relationships of LREE, P and Ti with silica and Cr may suggest that, again, a more complex petrogenetic mechanism should be invoked.

(f) <u>Cpx-hb-bi-phyric samples</u> (@15)

Only two samples of this association have been analysed, but they have very distinctive chemistry. Both have small augite phenocrysts (analysis 5, Table C2; very

similar to augites in the more mafic samples but slightly richer in K), much apatite, resorption pseudomorphs probably after hornblende but possibly after biotite, and anhedral phlogopitic mica (analysis 1, Table C2). Ilmenite microphenocrysts and augite-rimmed quartz crystals are also present in L113. Samples L54 and L55 from two minor intrusions, one of which is augite-apatite-biotite-phyric, have very similar chemistry to L113. These four rocks show K_2O/Na_2O close to or greater than 1, extremely high Sr and Ba (>2000 ppm), and very high K, P and La/Y. L125 is more siliceous than the others, and accordingly has lower P etc., but the three more basic samples plot at the high Sr, Ba, K, P, Rb, La/Y end of the positive correlations between these parameters in the ol- and ol-cpx-phyric samples (Fig. 4.4). Zr/Nb is somewhat higher than the average for mafic samples, and rocks of this group also have much lower Ti, Fe, Sc, V and lower Cr, Y and Nb than the bulk of the more mafic Lorne rocks (Figs. 4.1-4.2).

(g) Other phenocryst associations

A number of other phenocryst associations of very distinctive chemistry exist. Two samples with ?clinopyroxene as the sole phenocryst phase are siliceous (60-61% SiO_2) but have extremely high Cr (470 ppm) and very high Ni, Sc, Ti and Fe relative to other Lorne andesites (Figs. 4.1-4.2). Two basic samples with phenocrysts of olivine, augite and conspicuous pale brown phlogopite, frequently associated with calcite, have low concentrations

of Th, Nb and Zr, but relatively high LREE.

A wide variety of more acid lavas exists, of which the most conspicuous is a group very rich in Zr (up to 780 ppm), poor in Th and Nb but relatively rich in Y. The only other very Zr-rich lavas are two opx-pl-hb-phyric andesites; these have similarly low Th and Nb, and are low in Cr and Ni relative to other Lorne andesites. This group of high-Zr rocks has very high Zr/Nb (50-80), which, using the criteria of Pearce and Norry (1979) would suggest fractional crystallisation of magnetite. This is not confirmed by V concentrations, which are identical to those of more normal andesites. The small number of acid lavas collected does not allow detailed discussion of their possible origins, but they are undoubtedly polygenetic.

4.2 : GLENCOE

The O.R.S. rocks of Glencoe outcrop within a small elliptical area bounded by the Glencoe Boundary Fault, and were interpreted by Bailey and Maufe (1960) as a cylindrical block preserved by caldera collapse. The rocks rest on Dalradian and Moinian metasediments, and are cut by the NE-SW dyke swarm, which has created the elliptical shape of the complex by NW-SE extension. The rocks in places form a roof to the Cruachan Granite, about which there is considerable contact-metamorphism.

The O.R.S. sequence is dominated by volcanic rocks;

the stratigraphic succession (Table 4.2) and petrography have been described by Bailey and Maufe (1960) and Taubeneck (1967). There is some similarity with the Lorne sequence in that rocks with little or no phenocryst plagioclase are overlain by notably plagioclase-phyric rocks, with intervening ignimbrites and hornblende-phyric andesites. Groome (1972), however, believed that the Glencoe rocks were different, and older, on chemical and isotopic grounds. The isotopic argument was disputed by Brown (1975) who stated that the Glencoe data did not form an isochron within error. The chemical grounds noted by Groome were higher Al, Rb and lower Mg, Cr and Ni at Glencoe, and, in acid rocks, lower Fe/Mg. The new data disclose that the Lorne and Glencoe rocks are generally chemically indistinguishable, although there is a tendency to lower La/Y in the mafic rocks at Glencoe.

Table 4.2 : Stratigraphic sequence of O.R.S. rocks of Glencoe (interpretations from Taubeneck, 1967, and Roberts, 1966).

Group	Thickness ft/m	Lithologies	Interpretation
7	300/100	Hb-andesite, rhyolite, ignimbrite	Island volcano in crater lake
6	50/15	Shales, sandstones	Caldera lake deposits
5	250/80	Ignimbrite	2nd phase of caldera subsidence
4	900/300	Hb-andesite	
3	250/80	Sandstones, breccias	Caldera deposits, talus
2	450-2000 /150-600	Rhyolite, andesite, ignimbrite	1st phase of caldera subsidence
1	1500/500	Basalts, andesites	Lorne Plateau lavas

The Glencoe lavas show similar overall variation trends to those of Lorne, and there are very few deviations

from straight-line variation with silica for a number of elements (Fig. 4.6). As with the Lorne lavas, the apparently simple pattern does not hold for the LIL and high field strength elements, nor is a simple pattern produced by considering variation against Cr (Fig. 4.7). The rocks are on the whole more siliceous than those of Lorne, and the andesites of groups 1 and 2 (Table 4.2) resemble the Lorne opx-cpx-phyric group. They are phenocryst-poor, have little or no phenocryst plagioclase, and may show augite-rimmed quartz crystals and resorption pseudomorphs after amphibole. Clinopyroxenes tend to be slightly more iron-rich than those from Lorne opx-cpx-phyric samples. The andesites of groups 1 and 2 however show much greater variation in SiO_2 and Zr/Nb than the opx-cpx-phyric rocks of Lorne (Fig. 4.7).

The hornblende-andesites of group 4 are not directly comparable to any Lorne rocks, and have phenocrysts of andesine-labradorite, slightly resorbed pargasite-hastingsite, pseudomorphed orthopyroxene, magnetite, apatite and sometimes biotite or augite, closely similar to Lorne augites (analysis 16, Table C2). They have higher Zr, LREE, Y and Zr/Nb than the group 1 and 2 rocks (Fig. 4.7), and show no evidence of cumulus enrichment (e.g. higher Al_2O_3). It is noteworthy that the two petrographically similar rocks from Lorne also have much higher Zr than average Lorne rocks, but do not show higher than average LREE. The group 5 ignimbrites are again high Zr, Ce, Y rocks, but the one andesite analysed from group 7, and a later porphyritic microdiorite dyke, may represent a return to the lower Zr of

Fig. 4.6 a & b : Bulk rock variation diagrams
Field marked for Ben Nevis lavas
Conventions as section 3.3

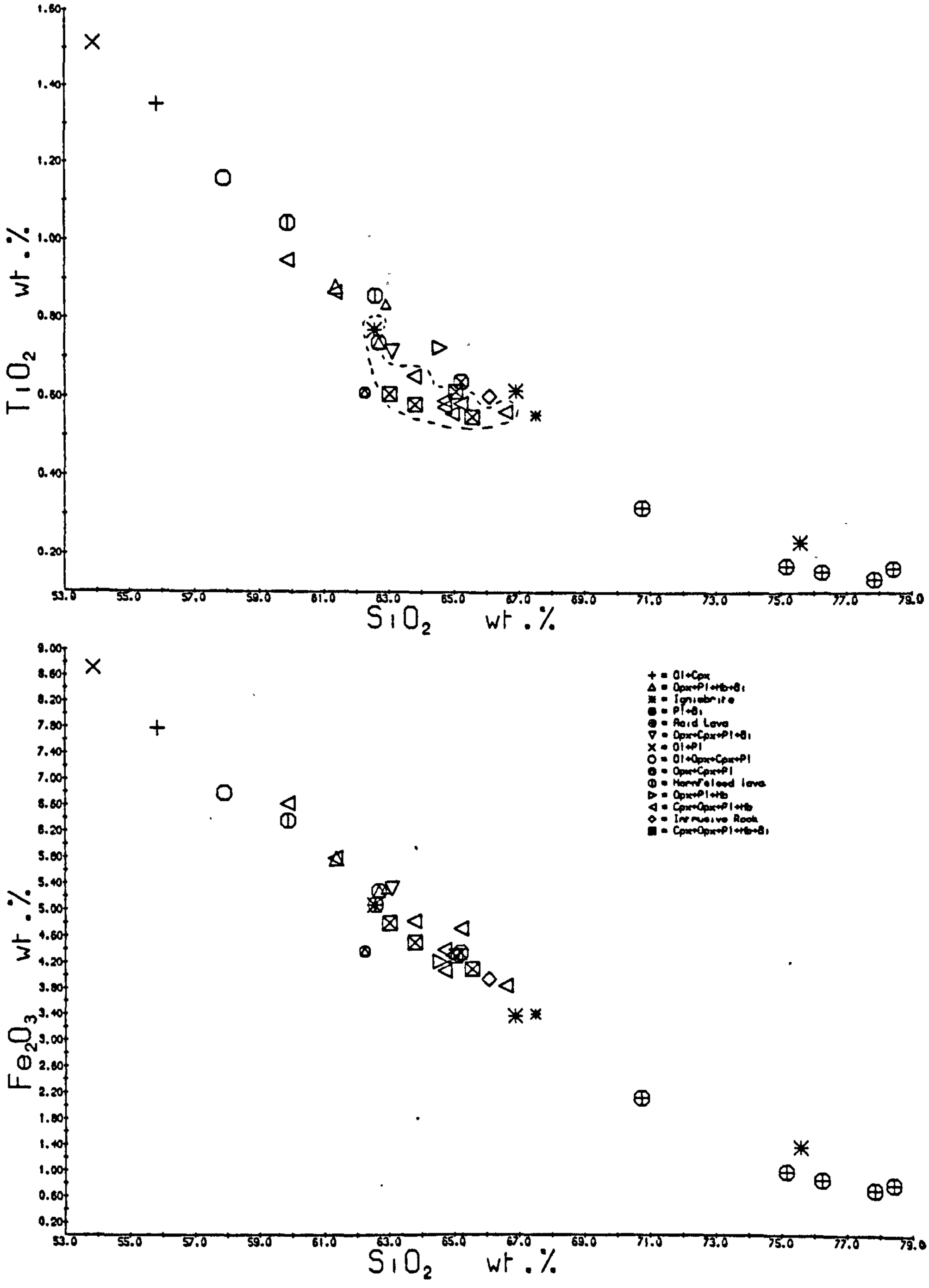

GLENCOE AND BEN NEVIS

Fig. 4.6 c & d

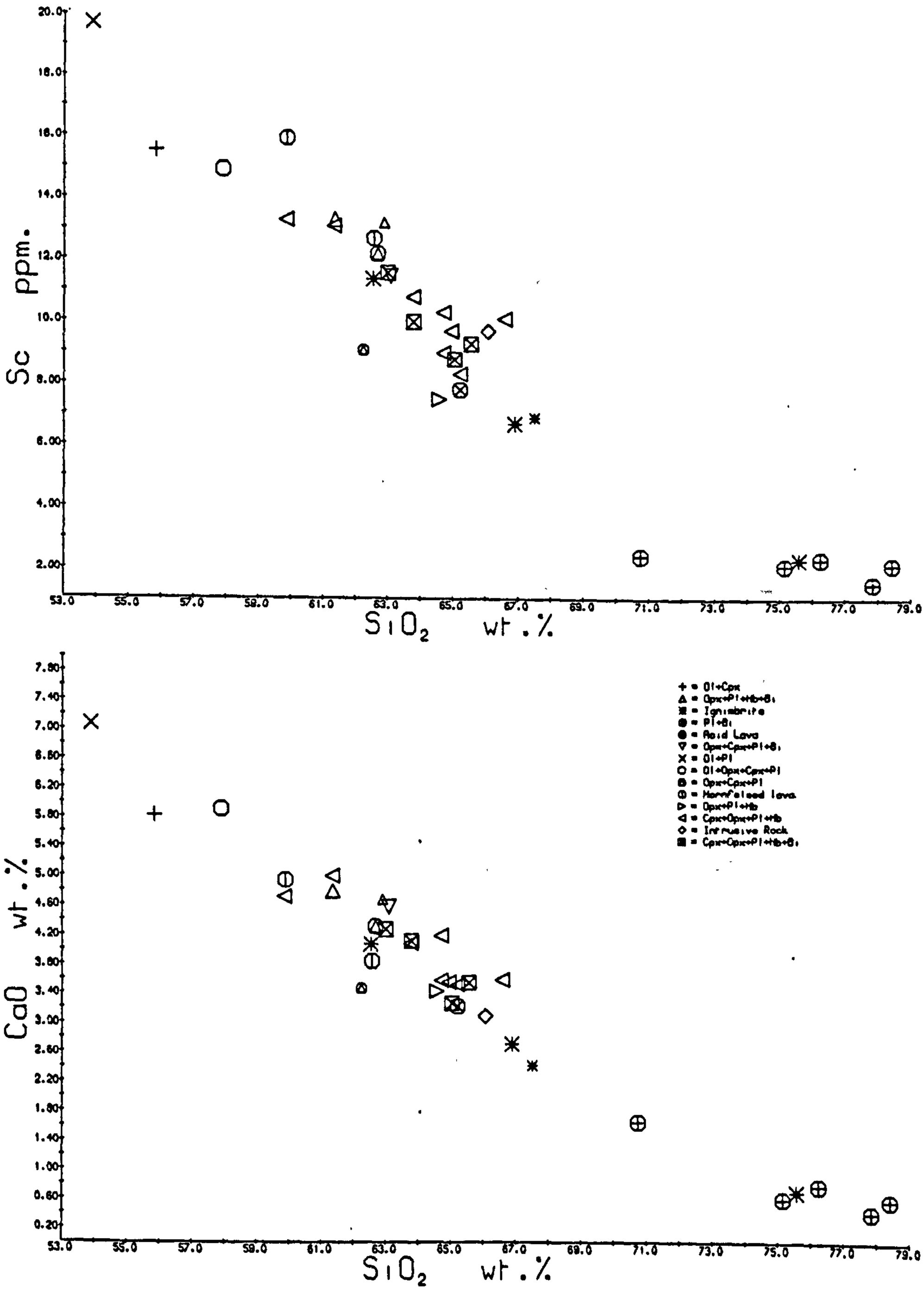

Fig. 4.7 a & b : Bulk rock variation diagrams. Fields are:

1 = Ben Nevis lavas

2 = Samples from groups 4 & 5, Glencoe

Conventions as section 3.3

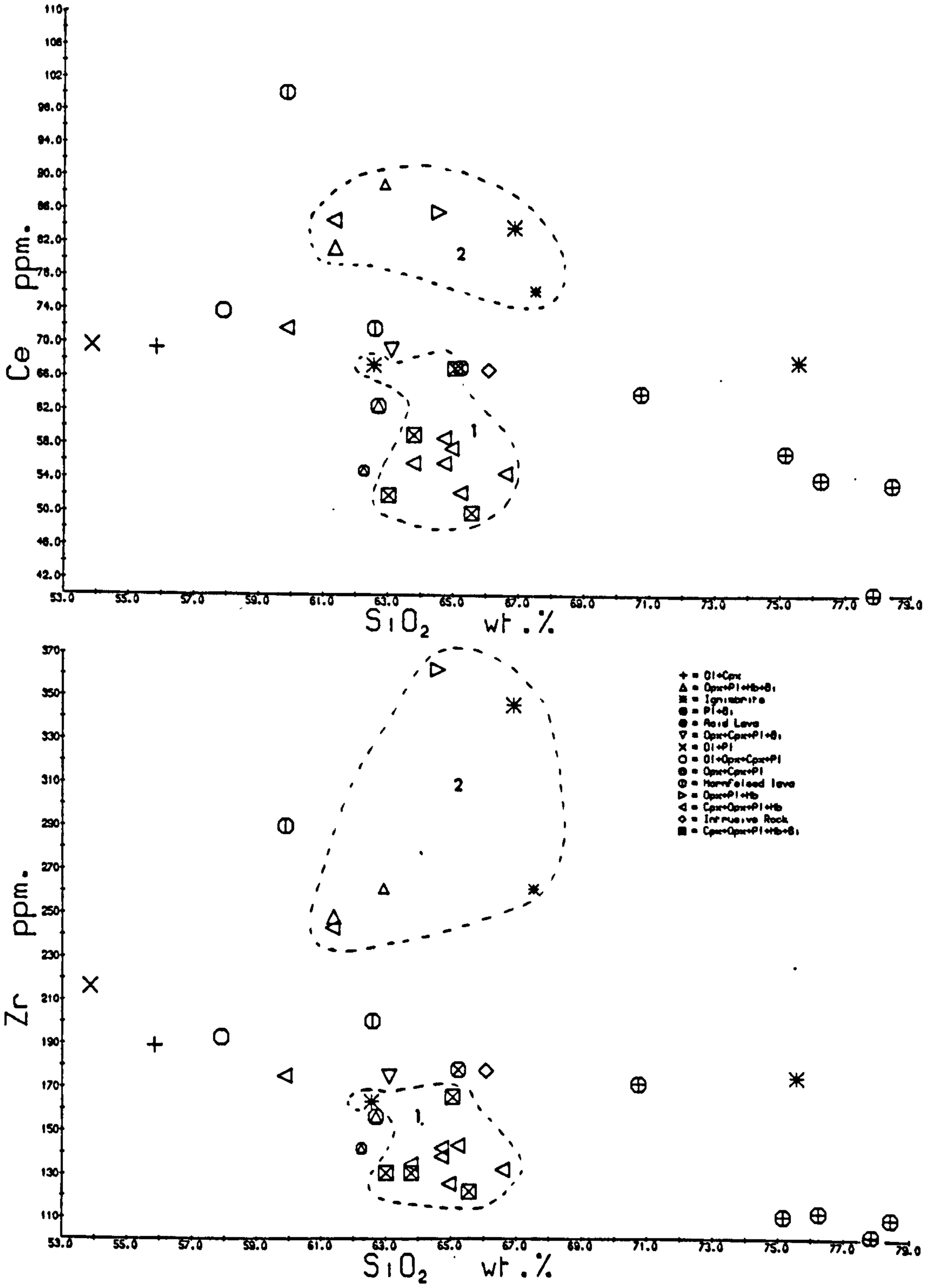

GLENCOE AND BEN NEVIS

Fig. 4.7 c & d

Field is for samples from Ben Nevis

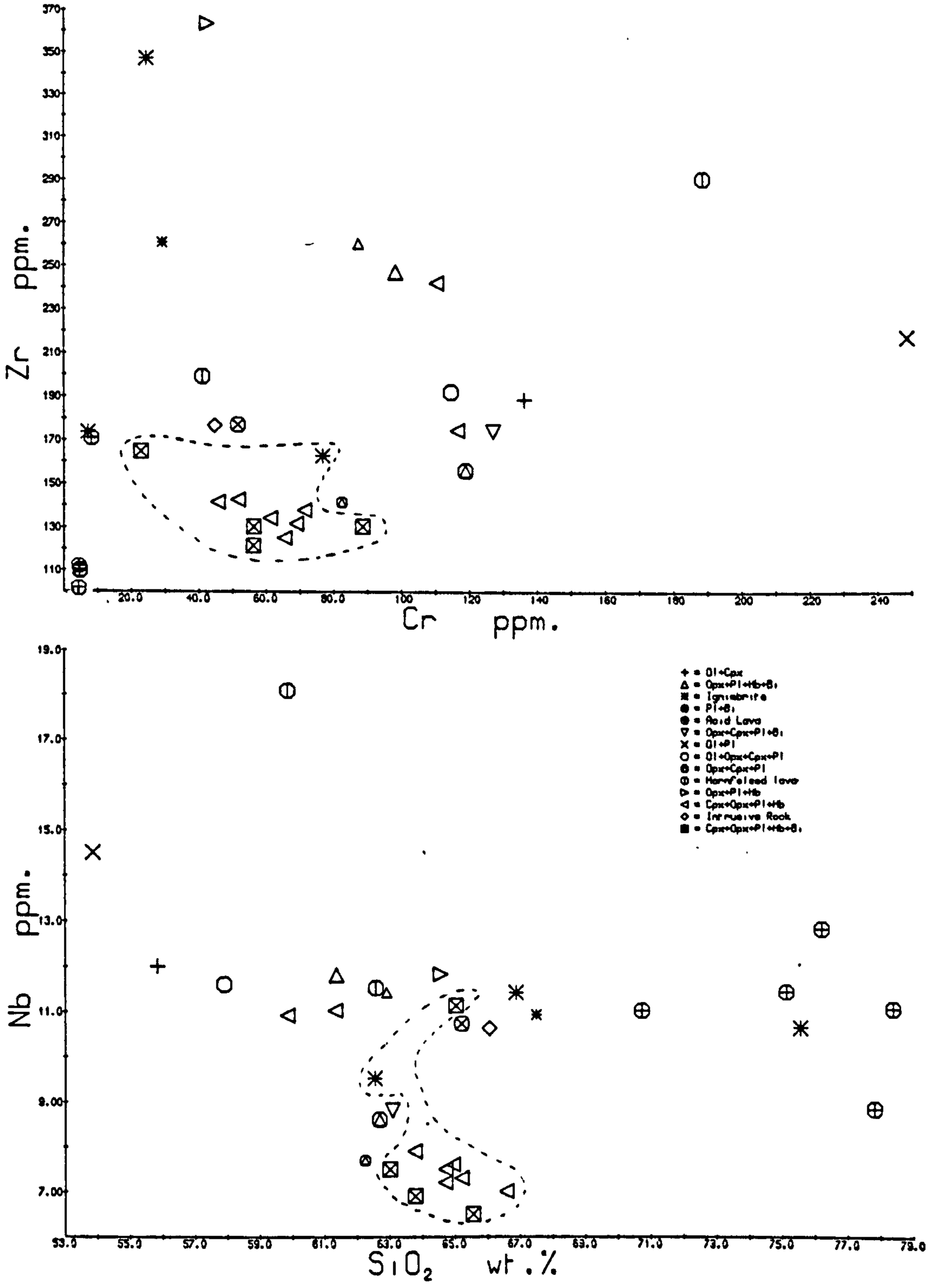

GLENCOE AND BEN NEVIS

Fig. 4.7 e & f

Fields as Fig. 4.7 a & b

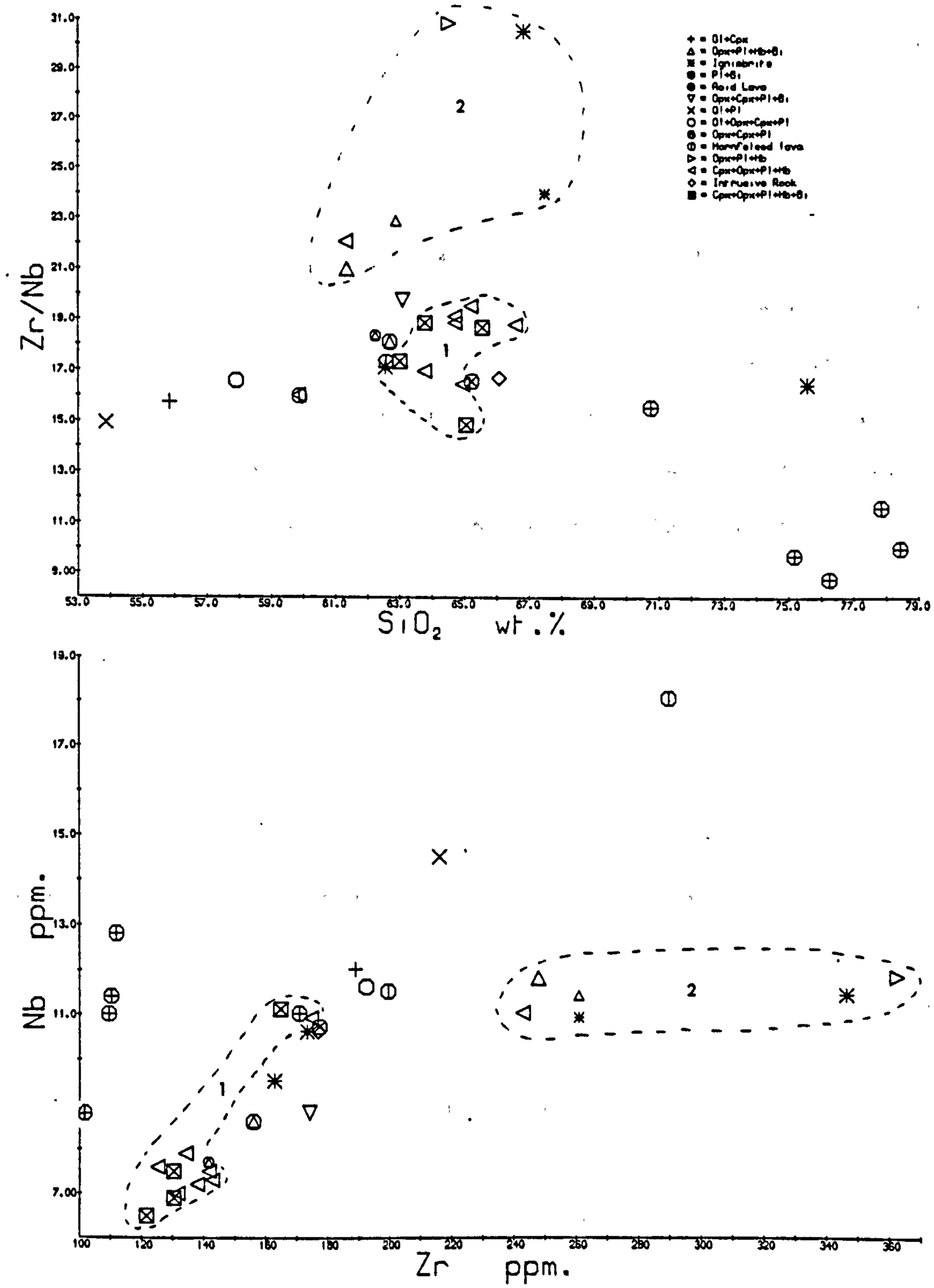

groups 1 and 2.

There appears to be a measure of stratigraphic control on chemistry, although it should be noted that a hornfelsed group 1 lava (GC19) shows group 4 levels of Zr, Y and LREE, and therefore the apparent stratigraphic control may be the result of the small number of samples collected. General similarity between the Glencoe and Lorne lavas is very strong, and it is believed that volcanism in the two areas was closely related in time and petrogenesis. Again, multistage fractional crystallisation can not account for all of the chemical variation, and even the groups 1 and 2 andesites, despite having a narrower range in Zr/Nb than the full sample population, show much variation in detail.

4.3 : BEN NEVIS

In common with the rocks of Glencoe, the O.R.S. of Ben Nevis was thought by Bailey and Maufe (1960) to be preserved as a cylindrical block downfaulted during caldera collapse. The rocks rest on Dalradian metasediments, and are metamorphosed by the Ben Nevis Inner Granite. The sequence is about 2000 ft (600 m) thick (Bailey and Maufe, 1960) and consists mainly of hornblende-andesite lavas and agglomerates with thin basal conglomerates and shales.

All samples collected have phenocrysts of slightly resorbed pargasite-hastingsite, andesine-labradorite, titanomagnetite, apatite, actinolite after clinopyroxene and

rare chlorite after orthopyroxene. A few show a small amount of phenocryst biotite in addition. Quartz phenocrysts are absent. Plagioclase is slightly poorer in Or than Glencoe plagioclase, but amphiboles are similar in both areas, with much variation in Ti, Al and K.

The petrochemistry of the Ben Nevis plutonic complex has been described by Haslam (1968), who suggested that the lavas formed part of the same magmatic suite. The samples collected have a small silica range (62.5 to 67%), and fall on the Glencoe variation trends for Al, Mg, Fe, Ca, Na, Mn, Ni, Cr, Zn, Sr, Sc, V and Ba (e.g. Fig. 4.6), although variation within the Ben Nevis range is seldom systematic. Ti and P are slightly lower in the Ben Nevis samples than in Glencoe acid andesites, and all other 'incompatible' elements are substantially lower (Table 4.1, Fig. 4.7). K/Rb is higher at Ben Nevis, but some Glencoe rocks have closely comparable Zr/Nb.

The higher K/Rb and lower Rb of the Ben Nevis samples suggest that they are less evolved than the Glencoe andesites, unless biotite was a fractionating phase. In either case identical Cr, Ni and Sr content of the Glencoe and Ben Nevis acid andesites precludes derivation of one from the other by fractional crystallisation (Chapter 3). Derivation of the Ben Nevis samples from the more basic Glencoe rocks would require fractional crystallisation of a biotite-, amphibole- or ilmenite-bearing assemblage to produce the lower Zr and Nb. However, intermediate points

on Fig. 4.7f include BN1 and BN2, and it is reasonable to infer that these would represent intermediate positions in any suggested fractional crystallisation scheme. However, their major element and compatible trace element chemistry is nearly identical with the rest of the Ben Nevis lavas (Fig. 4.6), suggesting that such a scheme is most unlikely. Further, Ben Nevis amphibole and biotite have Zr below the microprobe detection limit of about 150 ppm, and no zircon has been observed in thin section. The Zr analyses do not confirm the 4000 ppm reported from a Ben Nevis hornblende by Haslam (1968).

Variation of LIL and high field strength element concentrations within the Ben Nevis samples is not related to their Cr content (Fig. 4.7), but the biotite-bearing samples, excepting BN1, are the poorest in Zr and Nb. Again, therefore, the apparently simple genetic relationships suggested by smooth compatible element variation are not confirmed by the behaviour of the 'incompatible' trace elements.

4.4 : SW HIGHLANDS - CONCLUSIONS

Despite much variation in detail, the Old Red Sandstone volcanic rocks of the SW Grampian Highlands are very similar in broad outline.

(a) Petrography and mineral chemistry

Rocks more basic than 60% silica are characterized by the paucity of phenocryst plagioclase, and all rocks without phenocryst plagioclase have a low total phenocryst content. Quartz, believed to be a high pressure phenocryst phase (section 4.1d), is often present in rocks without phenocryst plagioclase, within the silica range 57.1 to 64.6%. At the basic end of this silica range, quartz is perhaps only a near-liquidus phase above 10 kb (Green and Ringwood, 1968), suggesting a sub-crustal source for the magmas. Phenocryst clinopyroxene is a diopsidic augite, with a little variation in Fe/Mg uncorrelated with host rock silica (Fig. 4.8). Ti and Al contents vary greatly within a single phenocryst, and do not correlate with host rock Ti and Al. All averaged clinopyroxene analyses fall within the tholeiitic (subalkaline) field of Le Bas (1962) for TiO_2 and tetrahedral Al. Na content is low and variable. Rocks rich in phenocryst plagioclase do not show good correlation between silica content and %Ab in the feldspar (Fig. 4.8), although the only plagioclase-phyric basalt (L73) has a calcic labradorite, unlike the normal labradorite-andesine. Or content of plagioclase may be a function of host rock K_2O, but the few alkali feldspars analysed occur in medium-grained aggregates with plagioclase (L68) which may be xenolithic or autolithic. Orthopyroxene phenocrysts are in general restricted to more siliceous rocks.

Fig. 4.8 a & b : Phenocryst chemistry of SW Highland O.R.S. lavas

a = atomic Ca, Mg, Fe for pyroxenes, amphiboles and biotites

b = the composition of plagioclase as a function of host rock silica

Average core compositions only plotted.

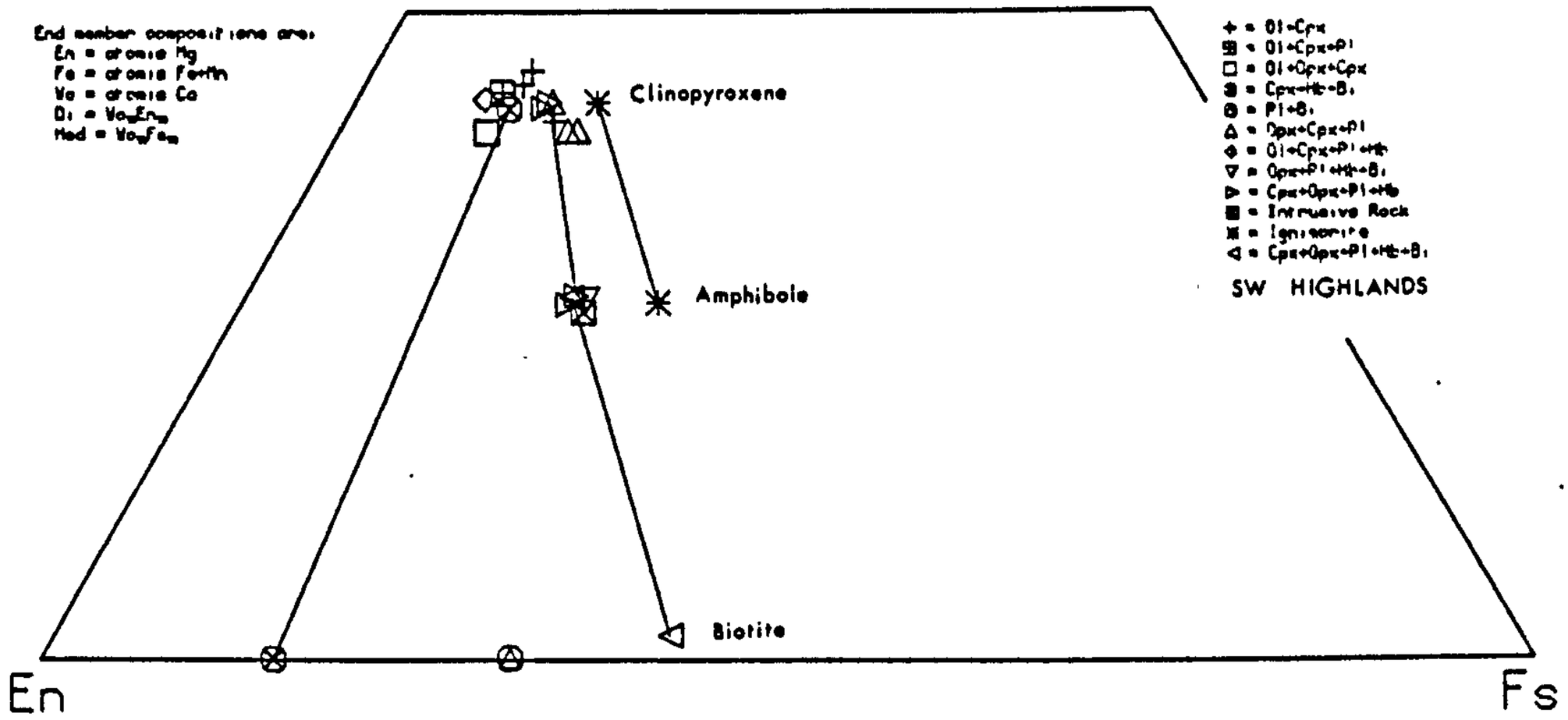

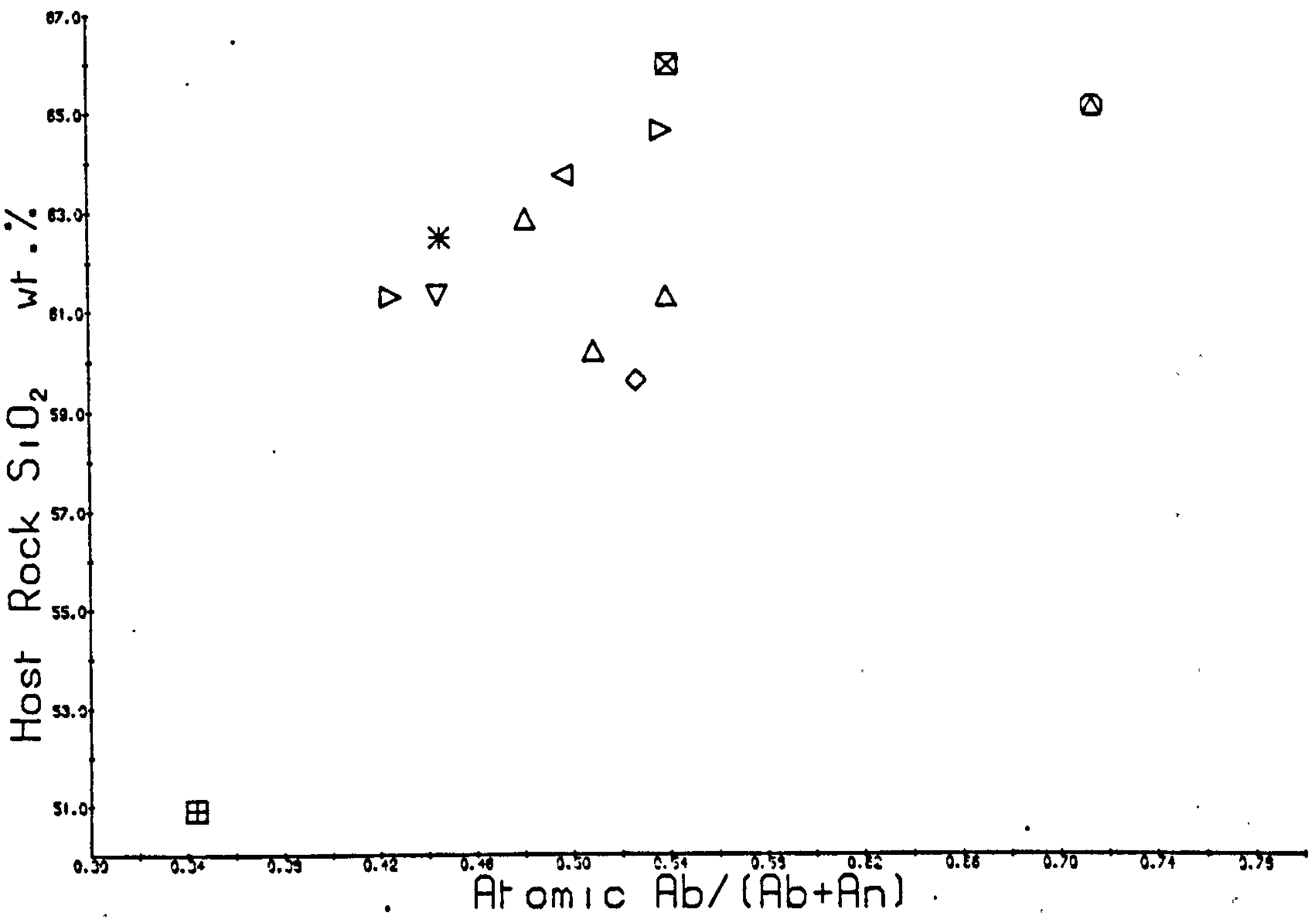

(b) Normative characteristics

Six of the samples collected have small amounts of normative nepheline, if a wt% $Fe_2O_3/(FeO+Fe_2O_3)$ ratio of 0.2 is chosen, but of these, five have LOI>3.3%, and the introduction of calcite or alkalis during alteration may explain the undersaturation. The sixth, L141, is fresh, and the 0.65% normative nepheline may be original. 21 rocks are olivine-hypersthene normative; while a number of these are altered it is probable that most were originally olivine-normative. There is some evidence that olivine-normative rocks may have higher Sr and LREE. However, most of the rocks are quartz-normative, and they clearly do not resemble alkali basalt differentiation series. Almost all samples with more than 66% silica are peraluminous, a frequent feature of calc-alkaline rocks.

(c) Chemical characteristics

Groome and Hall (1974) noted that the lavas of northern Lorne show a typical calc-alkaline trend of little relative iron enrichment on an FMA diagram, and the data presented here for all the SW Highland volcanics follow a similar trend, and plot in the calc-alkaline field of Miyashiro (1974) on an SiO_2 - Fe/Mg diagram. High alumina concentrations are often thought to be typical of calc-alkaline basic rocks, but the SW Highland rocks plot in the low-Al, tholeiitic, field of Irvine and Baragar (1971). Alkali contents are high, and place the rocks in the

alkaline field of Kuno (1968), but they are transitional between high-K calc-alkaline and shoshonitic (Fig. 9.1) on the classification of Peccerillo and Taylor (1976). Use of Ti, Zr, Y, Nb and Sr as suggested by Pearce and Cann (1973) to determine the tectonic setting of basaltic rocks suggests that the rocks are non-alkaline to transitional (Y/Nb>1), but the very high Sr, high Zr and low Y cause them to plot outside the fields given by Pearce and Cann (1973) on Ti-Zr-Y and Ti-Zr-Sr diagrams. In both cases, however, the SW Highland rocks plot close to the fields for calc-alkaline basalts. The unusual Zr-Nb relationship, in which more siliceous rocks frequently show lower Zr and Nb, was only recognized by Pearce and Norry (1979) in some Andean-type volcanic arc rocks.

The bulk of the evidence favours classification of the SW Highland volcanics as high-K calc-alkaline, and they are best compared with Andean-type volcanic arc rocks, in which comparably high levels of Ba, Sr and LREE have been reported (e.g. western U.S.A., Ewart, in press). The very high Ni and Cr are most unusual features for high-K calc-alkaline suites (e.g. Jakes and White, 1972), although concentrations little lower are again reported from the western U.S.A. (Ewart, in press). The high Ni and Cr imply that little fractional crystallisation of mafic minerals, particularly olivine, can have occurred during ascent. Fractional crystallisation of olivine or other mafic minerals would lead to higher Al_2O_3 and lower Ni and Cr comparable with most calc-alkaline volcanic suites.

(d) Source of magmas

(i) More basic rocks of Lorne

The high Ni and Cr content of the lavas must imply a mantle contribution, and the very high La/Y could imply equilibration with garnet. The elements Ba, Sr, P and LREE are probably incompatible with any mantle mineral assemblage below the plagioclase-spinel lherzolite transition zone, which is likely to have been shallower than the Moho below the O.R.S. mountains. The positive correlation between these elements, with K and Rb (Fig. 4.4) is not the result of fractional crystallisation of the magmas, for there is no correlation between depletion in Cr, Ni and increase in LILE (e.g. Fig. 4.9). The lack of correlation suggests that variable degrees of partial melting of a single source is also an unlikely mechanism, for Ni and Cr would increase and the LILE decrease with increasing degree of partial melting. The relatively high degrees of partial melting implied by the highest Cr and Ni contents would also require extremely high LILE contents in the mantle prior to melting. For example, a rough calculation may be made on the amount of Ce which must be removed from the column of mantle directly underlying the Lorne Plateau to form a 2000 ft (600 m) sequence of lavas with an average 80 ppm Ce. Assuming that melt will not have coalesced from a much wider area than the present lava outcrop, a 30 km high column of mantle with an initial 1.5 ppm Ce must have had its entire Ce content removed. Since no partial melting mechanism is this efficient, a much deeper column of mantle must have been

LORNE PLATEAU

Fig. 4.9 a & b : Bulk rock variation diagrams
Lorne ol- and ol-cpx-phyric samples,
cpx-hb-bi-phyric samples and related intrusions
Conventions as section 3.3

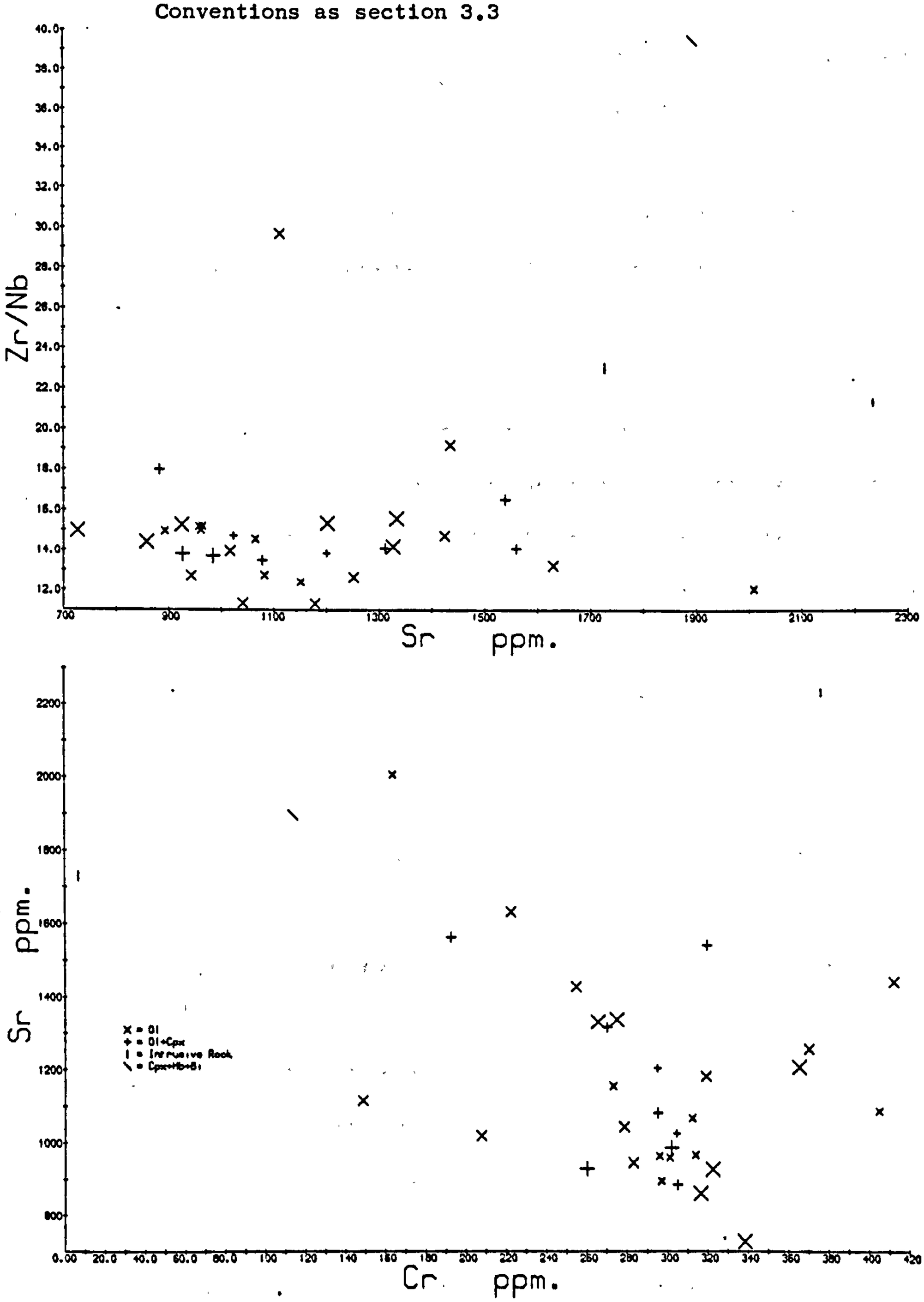

involved: it seems implausible that conditions could be favourable to melting over such a large thickness of mantle, and that melt could be created over the substantial depth range required without much modification to the compatible element chemistry. Furthermore, variation in Zr/Nb suggests that a single source model is not viable, and lack of correlation between Zr/Nb and LILE (e.g. Fig. 4.9) suggests that a simple binary contamination model between a mantle derived melt and a substance with different Sr and Zr/Nb is also untenable.

The chemistry therefore implies three separate controlling processes: a mantle source region controlling Cr and Ni, a process to provide LILE (e.g. a LILE- rich contaminant) and a process to provide two-fold variation in Zr and Nb, with some variation in Zr/Nb ratio. Derivation of the high levels of Sr by crustal contamination is thought to be unlikely because of the low initial $^{87}Sr/^{86}Sr$ of 0.7044 determined for Lorne (Brown, 1975). The conclusion that the Sr is of mantle origin, however, prevents the use of the initial ratio as a control on the degree of crustal contamination. A large crustal contribution with moderate Sr and high $^{87}Sr/^{86}Sr$ would be swamped by the high levels of mantle Sr. Brown (1975) reports somewhat higher initial $^{87}Sr/^{86}Sr$ at Glencoe (0.7049), and suggests that this may be the result of crustal contamination.

Since Sr correlates with K, Rb, Ba, La/Y and P, it is probable that the high level of all these parameters is of

mantle origin. The lack of correlation with Zr/Nb or with Zr could, however, be produced by contamination by crustal Zr and Nb.

(ii) More siliceous lavas

With minor exceptions, the more siliceous lavas of Glencoe, Ben Nevis and the opx-cpx- and opx-cpx-pl-phyric rocks of Lorne lie on smooth variation trends with silica for the major elements and the compatible trace elements, which extend from the most basic to the most acid volcanic products. The variation of LIL and high field strength elements precludes the conclusion that all are related by a single fractional crystallisation model, and suggests that they are better considered as a number of small groups. Variation within these groups might in some cases be ascribed to fractional crystallisation of biotite- or amphibole-bearing assemblages but this is not borne out by detailed examination of whole rock and mineral chemical data. Furthermore, significant crystal settling in such siliceous and hence viscous magmas is improbable, particularly in the case of such phases as biotite. Volcanic rocks possibly parental to the siliceous suites have not been identified, despite the abundance of basic rocks at Lorne. There is no control over the degree of crustal contamination that these rocks may have suffered, although the Ni, Cr and Sr contents appear to be mantle derived. Since no parental magmas can be identified, it would appear that andesites with silica well in excess of

60% may be direct melts of a sub-crustal source.

The chemistry of the SW Highland volcanic rocks is thus extremely complex in detail, although they may be considered as high-K calc-alkaline to shoshonitic. The range in magma compositions implies that the existence of separate magma generations for the intrusive rocks, as suggested by Groome and Hall (1974) is more than likely, and the rocks should not be viewed as the differentiation products of a single 'Devonian parent magma' (Bailey, 1958). The bulk of the volcanic rocks appear to have been produced in the mantle by processes including partial melting, mixing and contamination, but do not appear to have been significantly modified by fractional crystallisation.

CHAPTER 5 : NORTH MIDLAND VALLEY

Lower Old Red Sandstone rocks outcrop in a number of inliers near the southern margin of the Midland Valley of Scotland, and continuously from Stonehaven to Arran along the northern margin. In the north the rocks are dominantly conglomerates and sandstones but considerable thicknesses of volcanic rocks are interbedded with the sediments. The O.R.S. sequences overlap the Highland Boundary Fault Zone onto the Dalradian metasediments of the Highlands and onto the Cambro-Ordovician Highland Border Series. The Lower O.R.S. outcrop is disposed about a broad NE-SW trending paired anticline-syncline, and is bounded to the south by the Upper Old Red Sandstone unconformity or by the Ochil Fault. The crest of the Ochil-Sidlaw Anticline is faulted into a graben in the Carse of Gowrie, which is occupied by Upper O.R.S. sediments.

Armstrong and Paterson (1970) described six major lithostratigraphic groupings in the Lower Old Red Sandstone of the northern Midland Valley, of which all but the youngest contain volcanic rocks. The stratigraphy is summarized in Table 5.1.

The rocks of the Ochil Volcanic Formation have been somewhat arbitrarily divided for collecting purposes into three areas: the Sidlaw Hills and Moncreiffe Hill, the western Ochil Hills, and the hills of northern Fife.

Table 5.1 : Lower Old Red Sandstone stratigraphy of the northern Midland Valley, with location of volcanic horizons (after Armstrong and Paterson, 1970). Figures are thicknesses in ft/m.

Group	Stonehaven -St. Cyrus	S of Montrose	Dundee	Perth	Highland Border
Strathmore 6500/2000	no volcanic rocks				
Garvock 5000/1525	Garvock lavas 800/250				
Arbuthnott 7000/2100	Morphie or Bruxie Hill Member 800/250 St. Cyrus Member 2000/650 Dunnichen Member 500/150	Ethie Haven Member 1000/320 East Hills Member 500/150 Ferryden Member 1300/400	Broughty Ferry lavas 1200/400 ?Tealing lavas 300/100	Ochil Volcanic Formation 8000/2400	Volcanic rocks of Glenisla and Blairgowrie. Conglomerate with volcanic clasts
Crawton 2200/670	Crawton Volcanic Formation 100/30 Conglomerates and sandstones with acid volcanic clasts and 2 thin lavas				Lintrathen Porphyry 500/150
Dunnottar 5450/1660 Stonehaven 5100/1550	Tremuda Bay Volcanic Formation 200/60 Conglomerates and sandstones with volcanic clasts and 2 thin lavas				

The Sidlaw Hills are separated from the rest of the outcrop by a wide tract of alluvium, but the Ochil and North Fife Hills have continuous outcrop. The division here was placed at Glen Farg, for Geikie (1900, pp.25,32) suggested that the paucity of pyroclastic rocks in Glen Farg may be due to its distal position relative to centres of activity in the Ochil and North Fife Hills. In these three areas it is not yet possible to use stratigraphic subdivisions of the volcanic sequence of more than very local significance, but in the remainder of the Midland Valley, the Montrose region, a detailed stratigraphic-geographic subdivision may be employed (Fig. 5.1).

Fig. 5.1 : The Montrose Region

Boundaries from Armstrong and Paterson 1970

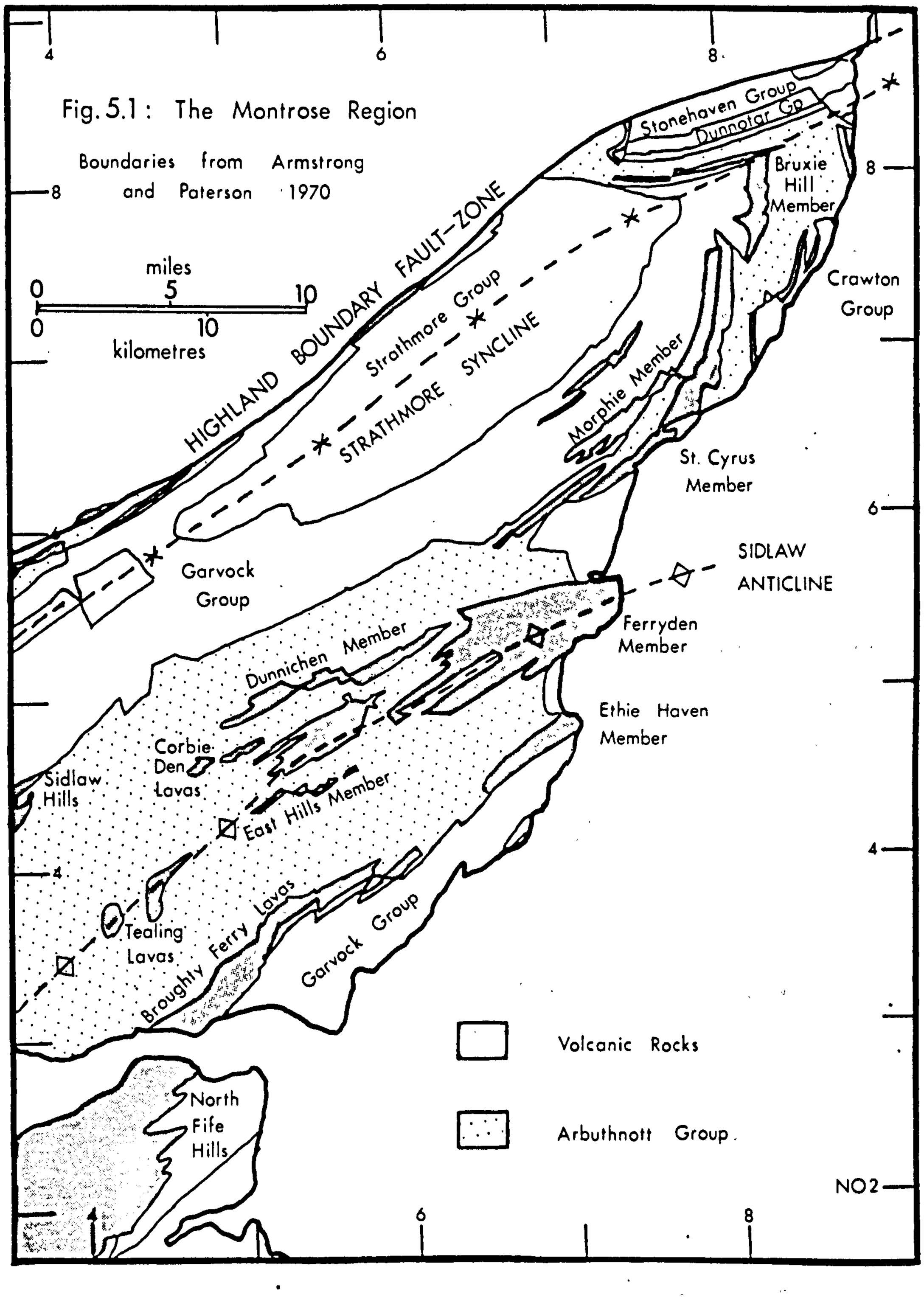

5.1 : MONTROSE REGION

The stratigraphy and petrography of some of the Old Red Sandstone volcanic rocks of the Montrose region have been described by Campbell (1913) for Kincardineshire, by Jowett (1913) for the coast between Montrose and Red Head (Ferryden and Ethie Haven Members) and by Robson (1948) for the inland area south of Montrose. Robson (1948) noted that the Montrose volcanic sequence lacked acid members, in contrast to the Old Red Sandstone volcanic sequence of the Ochil Hills.

(a) Rocks older than the Arbuthnott Group

Very coarse conglomerates dominate the pre-Arbuthnott Group strata, and most of the volcanic rocks occur as clasts in these, although there are a few lava flows. The latter are predominantly basic in composition, and contrast with the more siliceous nature of the volcanic clasts noted by Armstrong and Paterson (1970), which range from hypersthene-, hornblende- and biotite-andesites to rhyolites. The bulk of the clasts in the conglomerates are, however, Highland-derived (Campbell, 1913), and Waterston (1965) believed that the contrast was the result of interdigitation of acid Highland material with more basic flows originating in the Ochil-Sidlaw region.

Samples SC1-9 were collected from clasts in these conglomerates. They are mineralogically very varied,

although all have phenocrysts of a hydrous mineral. One sample has augite-rimmed quartz ?phenocrysts (SC4), and the rocks are similar to some of the Western Highland acid andesites. Silica varies from 60 to 77%, and the rocks are mostly corundum-normative, although this may in part be an effect of alteration. Trace element concentrations are very variable, and the rocks are most unlikely to be simply genetically related. This is indicated by the occurrence of acid rocks (>70% SiO_2) with both low and high concentrations of elements such as Zr, Nb, Y, and LREE, and by very variable Zr/Nb at constant Cr (c.f. SC6 and SC7). Despite this variability, it is notable that these samples have considerably less Sr, and, in general, less Ba, than otherwise comparable acid andesites from Lorne and Glencoe. Further collection of volcanic clasts may provide useful petrogenetic information, but at present they are important in that they demonstrate that very high Sr concentrations in Highland volcanic rocks are restricted to the west.

In situ volcanic rocks older than the Arbuthnott group in Kincardineshire comprise a few thin andesite flows, of which one in the Dunnottar Group is a bi-opx-cpx-pl-phyric andesite (SC10), chemically similar to some of the clasts; and the Tremuda Bay and Crawton Volcanic Formations. Four samples (SC11-14) have been collected from these latter formations. Each is petrographically distinctive, especially the type Crawton Basalt (SC13), with large tabular plagioclase phenocrysts in addition to the olivine ± augite of the other three. The samples are basic (51-53%

SiO_2), olivine-hypersthene normative and moderately high-alumina (16%). The one evolved sample (SC13) shows substantial iron enrichment relative to Mg, and plots in the tholeiitic field of Miyashiro (1974). Although the rocks have Y/Nb>1, suggesting sub-alkaline affinities (Pearce and Cann, 1973), they have concentrations of Nb, Ti, P and LREE comparable with those of many alkali basalts. All four samples have Zr/Nb almost identical at about 13, but SC11, despite relatively low Cr and Ni, has lower Zr and Zr/Y and is thought to be less closely related than the other three.

The three more closely related samples show variation trends which may probably be accounted for by fractional crystallisation of the phenocryst phases olivine, plagioclase and clinopyroxene, although some minor opaque oxide may be involved. Zr, Th, Nb, LREE and P all show about 80% increase from SC14 to SC13, suggesting that SC13 represents about 40% crystallisation. Ni, Mg, Cr and Mn decrease and K, Rb, V, Ba, and Y all increase, while most other elements show a stepped change consistent with removal of olivine from SC14, followed by clinopyroxene and plagioclase. The small number of samples does not permit verification of this hypothesis by least squares extract calculations. The minor difference in Al contents between the three samples suggests that the chemistry of SC13 has not been significantly affected by plagioclase accumulation.

The one remaining <u>in situ</u> volcanic rock in pre-Arbuthnott Group strata is the Lintrathen Porphyry,

which was shown to be an ignimbrite by Paterson and Harris (1969). The sample collected is rich in crystal clasts of quartz, plagioclase, biotite, hornblende, apatite, muscovite and phlogopite, and is unusual for the presence of three micas, although it is probable that at least one of these is an accidental xenocryst. It is strongly LREE enriched (La/Y = 2.5, approximately the same as the Crawton lavas) and has high Th, Nb, K, Rb but low Zr (Zr/Nb=6).

(b) Dunnichen/East_Hills_Members

Lavas belonging to these members of the Montrose Volcanic Formation are typically nearly aphyric, and show a few pseudomorphs after olivine and rarer labradorite (analysis 16, MT4) in a feldspathic groundmass, with opaque oxides and subophitic or intersertal augite. The one exception, MT5, has apatite phenocrysts with a few haematitic pseudomorphs possibly after olivine, and is chemically very similar to a number of apatite-phyric rocks from the Ferryden Member. This group of rocks, the "trachyandesites", will be treated together in section 5.1(e).

The rocks collected are silica-poor (52.6-55.3%), alumina-rich (>17.8%), poor in Ni and Cr (<27, <10 ppm respectively) and are quartz- or very slightly olivine-normative except where modified by alteration. They have fairly high Fe/Mg, but all fall within the calc-alkaline field of Miyashiro (1974). In common with the

SW Highland and pre-Arbuthnott Group volcanics, they show concentrations of LIL elements comparable to those in alkali basalts, although Sr and Ba are substantially lower than at Lorne. There are no significant chemical differences between the Dunnichen samples and MT1 and 3, and Zr/Nb is identical within precision, between 18 and 20. MT4 has substantially higher concentrations of LIL elements than the rest of the group, and Rb and P show greater enrichment than Y, Zr, Nb, K and LREE. The enrichment in Rb could be produced by about 30% crystallisation of a liquid with composition MT1, assuming that Rb was incompatible in the crystallising phases. Ni, Sc, Ti and particularly V show substantially lower concentrations in MT4, suggesting that fractional crystallisation of an assemblage including either amphibole or an opaque oxide could explain the observed variation. Again, the small number of samples and the altered nature of two of them does not permit the quantification of such a hypothesis by least squares extract calculations.

(c) Ethie Haven Member

Samples collected from Ethie Haven are rich in olivine and augite phenocrysts. All except MT42 have infrequent bytownite-labradorite microphenocrysts. Olivines are magnesian (Fo82-86, anal. 1, MT45) and Ni-rich; calculation using the data of Roeder and Emslie (1970) suggests that this is not far from the equilibrium olivine, and it is probable that the chemistry of MT45 has not been

seriously modified by olivine accumulation. Clinopyroxene phenocrysts are low-Na diopsidic augites (e.g. anals. 18 and 21; MT45, 42), but include some plotting within the alkaline field of Le Bas (1962). However, these latter include both core and rim compositions, and both TiO_2 and tetrahedral Al vary substantially between phenocrysts in the same rock, although the average augite analyses from the two rocks are nearly identical. It is believed that this is the result of localized melt heterogeneities arising during rapid crystallisation. The samples are quartz- or slightly olivine-normative, have SiO_2 from 53.8 to 55% and high MgO (6.5-9%), Ni (>150 ppm) and Cr (300-540 ppm), with moderate alumina (about 16%). These are much higher MgO, Ni and Cr concentrations than in the Dunnichen/East Hills samples, and the Ethie Haven rocks also have higher concentrations of Ca and Sc, and slightly lower Fe, Ti, Sr and many other LIL and high field strength elements. This suggests that the two groups could be related by fractional crystallisation processes, with olivine and clinopyroxene as the major crystallising phases. This possibility will be further discussed in section 4.1(i).

Zr/Nb varies within the limits of precision, and does not rule out an origin of the chemical variation within the Ethie Haven samples by fractional crystallisation, or by olivine accumulation, for the most magnesian sample, MT42, has the greatest quantity of modal olivine. The latter possibility is difficult to test. If MT42 is assumed to represent a liquid composition, then the increase in Zr

shown by the other samples implies roughly 9% crystallisation of this. A somewhat higher degree of crystallisation is implied by LREE data (about 16%) and somewhat lower by data for Y (7%). K and Rb concentrations appear to have been changed by alteration, but Ba suggests about 20% crystallisation. No element shows systematic variation in the three more evolved samples, and variation in many of the major elements is unrelated to the more magnesian nature of MT42. While it may not be conclusively demonstrated, it is thought unlikely that fractional crystallisation was the only process operating to produce chemical variation in these rocks.

(d) St. Cyrus Member

The volcanic rocks of the St. Cyrus Member were thought by Armstrong and Paterson (1970) to be at the same stratigraphic level as the Ethie Haven Member. Two of the samples collected have olivine and occasional feldspar phenocrysts, and are more magnesian and less siliceous than the third, which is phenocryst rich and has additional phenocryst ortho- and clinopyroxene. The overall chemistry of the rocks is similar to that of the Ethie Haven samples, but St. Cyrus samples have much lower Zr/Nb (Fig. 5.2), and since MgO, Cr and Ni concentrations are little different, the St. Cyrus lavas are most unlikely to be related to those of Ethie Haven by fractional crystallisation processes. Variation within the St. Cyrus Member is not simple, for although MT23 has the highest Zr, Y, Ti, Nb, P, and Al and

lowest Ni and Cr, it has lower LREE than the other samples, and is high in MgO.

(e) Ferryden Member

The members of the Montrose Volcanic Formation previously discussed display a high degree of chemical individuality, well expressed by a constant distinctive Zr/Nb for each member (Fig. 5.2). The Ferryden Member displays a greater range of lithologies and chemistries, and has a range of Zr/Nb from 14 to 22. Alumina also shows a wide range, and it is possible to divide the rocks of this member using Al content (Table 5.2).

Table 5.2 : Petrochemical characteristics of alumina-based subdivisions of the Ferryden Member.

Al_2O_3	Samples	Silica range	Cr	Phenocrysts	Zr/Nb
18.4-.8	24,25,35	53.7-54.5	7-8	rare ol, pl	17.5-18.2
17.9	9,27,29	60.3-62.2	6-12	rare ap,ol,pl ("trachyandesites")	22
17.8	26	52.2	113	ol,pl	20
16.9-17.3	38-40	54.6-55.8	114-127	ol,pl	14.5-15.5
16.5	41	59.9	232	opx,pl	16.2
15.8-16.1	36,37	57.6-.7	298-321	ol,opx,pl	14-14.8

Rocks of the high-alumina group have many similarities with those of the Dunnichen/East Hills Members, but have significantly lower Zr/Nb, lower Fe, Ti, P, Sc, V, Zr, Y and LREE and higher Ni, Al and Sr. These two groups are unlikely to be derived from each other by fractional crystallisation processes because of their identical concentrations of K, Rb and Ba. Derivation by separate

fractional crystallisation events from a similar parent is, however, possible (section 5.11).

Most of these Al-based divisions have distinctive Zr/Nb ratios, and therefore derivation from each other by processes of fractional crystallisation is unlikely. For MT36-40, Zr/Nb varies within the range of analytical error, and does not therefore preclude derivation of MT36 and 37 from the other three or vice versa by fractional crystallisation. If this were the case, the positive correlation between Cr, Ni and silica could only be generated by crystallisation of a very siliceous assemblage (>58% silica; MT36,37 parental) or of an assemblage with perhaps >80% plagioclase (MT36,37 derivative). No plausible combination of phases can produce such a siliceous crystallising assemblage, and furthermore, both K and Zr also correlate positively with silica, Cr and Ni. If Cr is incompatible in the crystallising assemblage (ie. >80% plagioclase), then over 60% crystallisation is implied by the increase in Cr content. No other element, normally incompatible, shows such an increase. It is thought most unlikely that any of the Al-based subdivisions of the Ferryden Member could be derived from another by fractional crystallisation processes.

The high-alumina, apatite-phyric, relatively siliceous samples described as "trachyandesite" are worthy of special note. The name "trachyandesite" was given because of the resemblance of these rocks to ones so named

by Francis et al. (1970) in the Ochil Hills. It is, however, recognized that they are no more alkaline than many other rocks in the Northern Midland Valley, and certainly do not display normative or pyroxene characteristics of alkaline rocks. Three samples of the Ferryden Member and one of the East Hills Member have been classified as "trachyandesite". They are nearly aphyric, and therefore their high alumina content may not be ascribed to plagioclase accumulation. Zr, Nb and Th are very high, with concentrations in excess of 600, 27 and 21 ppm respectively. It is notable that such high concentrations of Th are comparable to those found in peralkaline rhyolites (Macdonald and Bailey, 1973) although in these Zr and particularly Nb are substantially higher. Sc and V are much lower than in the more mafic rocks of the region, and Ni is further reduced from the low levels of the high-alumina basic andesites (Dunnichen Member etc.). Sr is also considerably lower, suggesting substantial fractional crystallisation of plagioclase. Enrichment factors for the LIL and high field strength elements relative to the high alumina rocks are given in Table 5.3, and are consistent with the derivation of the "trachyandesites" by fractional crystallisation of a plagioclase-rich assemblage with accessory apatite.

Table 5.3 : Enrichment factors for LIL and high field strength elements in the "trachyandesites" relative to high-alumina basic andesites, Montrose.

K	Rb	Ba	Th	Zr	Nb	La	Ce	Nd	Y	P	Sr
2.2	3.2	1.5	3.3	2.6	2.2	1.9	1.9	1.6	1.2	1.0	0.6

The lack of rocks intermediate on these possible fractional crystallisation trends prevents deduction of the particular mafic suite of the Montrose Volcanic Formation from which these "trachyandesites" may be derived and this precludes the use of least squares extract calculations to quantify a model. It is not impossible that the 70% crystallisation of one of the mafic liquids calculated from the Rb enrichment could result in increase of the Zr/Nb ratio by a small amount (Pearce and Norry, 1979). A number of elements show systematic variation within the "trachyandesites" with increasing silica and decreasing MgO. The Ferryden samples show increases in La, Rb, Zr and K, constant Ce and decreasing P with increasing silica, but comparable changes in other 'incompatible' elements are not significant relative to the analytical precision. The decrease in P implies that apatite is a fractionating phase. The sample from East Hills is relatively rich in V and particularly Fe (Fig. 5.2), and may be derived from a parent with a somewhat different composition, but by the operation of similar fractional crystallisation processes.

(f) Morphie/Bruxie Hill Member

The seven samples collected from this member are all

phenocryst-rich and five have phenocryst orthopyroxene, in addition to small quantities of olivine. Orthopyroxene may mantle olivine or vice versa. Pyroxenes are magnesian and Cr-rich, orthopyroxene being bronzite and clinopyroxene the diopsidic augite low in Na, Ti and Al that is typical of the province (e.g. anals. 19 and 20, MT10). Phenocryst plagioclase is variable, but generally labradorite. All seven samples are quartz-normative, fairly siliceous (55-57.7%), and have moderately low alumina (15.9-16.5%). Ni and Cr are high (110-208 and 193-343 ppm respectively). No systematic relationships exist between element concentrations and silica or MgO content, and the most magnesian, least siliceous sample has the highest concentrations of Ni, Cr, P, Ti, K, Ba, Sr, Zr, Nb and LREE. Zr/Nb varies from 14.5 to 17.5, and does not correlate with Zr or Cr. It is highly unlikely that such a suite of rocks could be related by fractional crystallisation nor is there any evidence suggesting a genetic relationship with any other member of the Montrose Volcanic Formation.

The samples collected from Glenbervie, on the NW limb of the Strathmore Syncline, are opx-cpx-pl-phyric andesites similar in many ways to the Bruxie Hill lavas, but detailed examination of Table B17 discloses some differences e.g. lower P. The low K of the Glenbervie samples is attributed to hydrothermal alteration of the groundmass glass (Chapter 2). These lavas were thought to be part of the Bruxie Hill Member by Campbell (1913), but Armstrong and Paterson (1970) believe that they are the approximate equivalents of the

MONTROSE REGION

Fig. 5.2 a & b : Bulk rock variation diagrams

Lettered fields refer to the major rock groups of Table 5.4, field T to the "trachyandesites" (Table 5.2).

Conventions as section 3.3

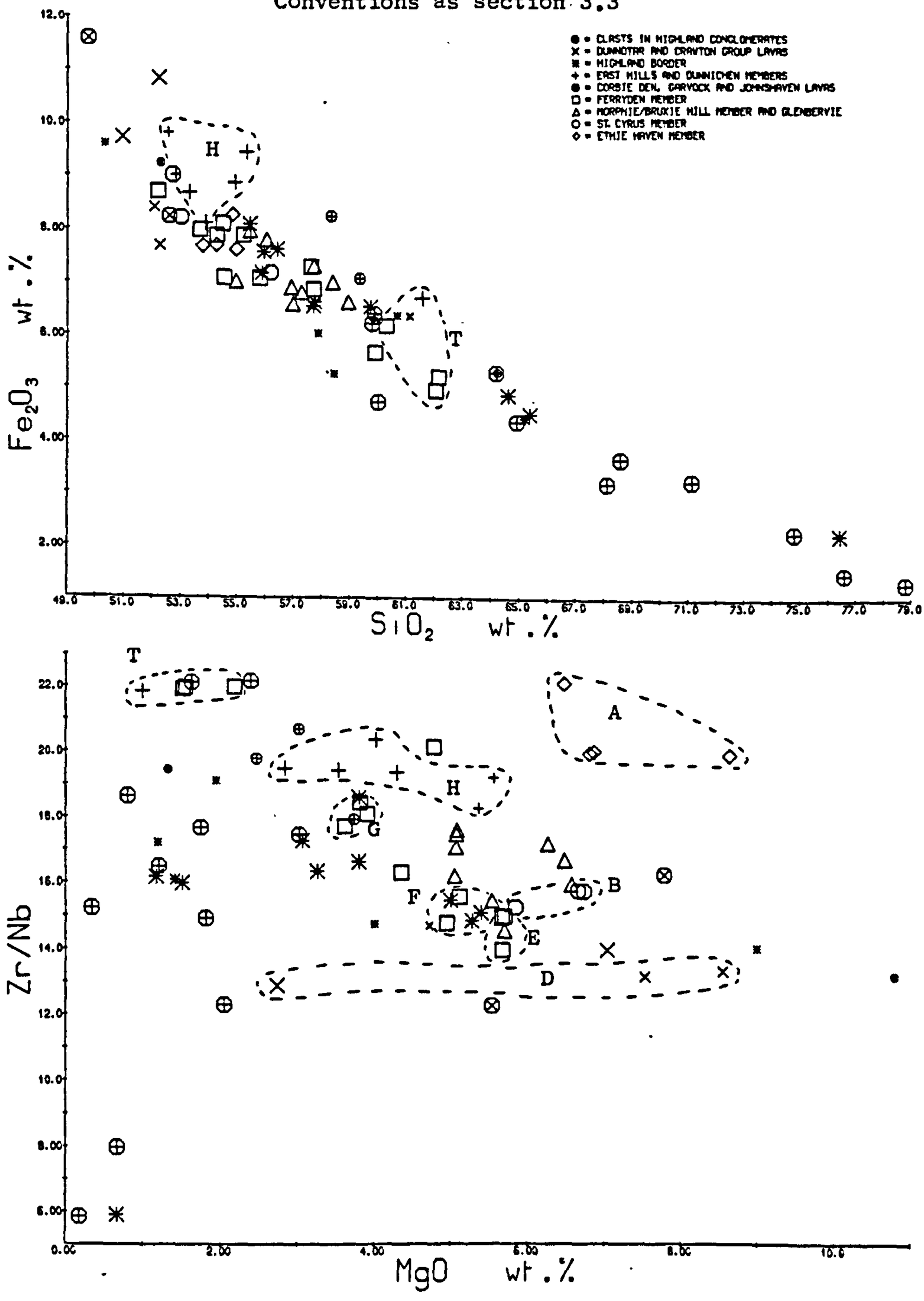

MONTROSE REGION

Fig. 5.2 c & d

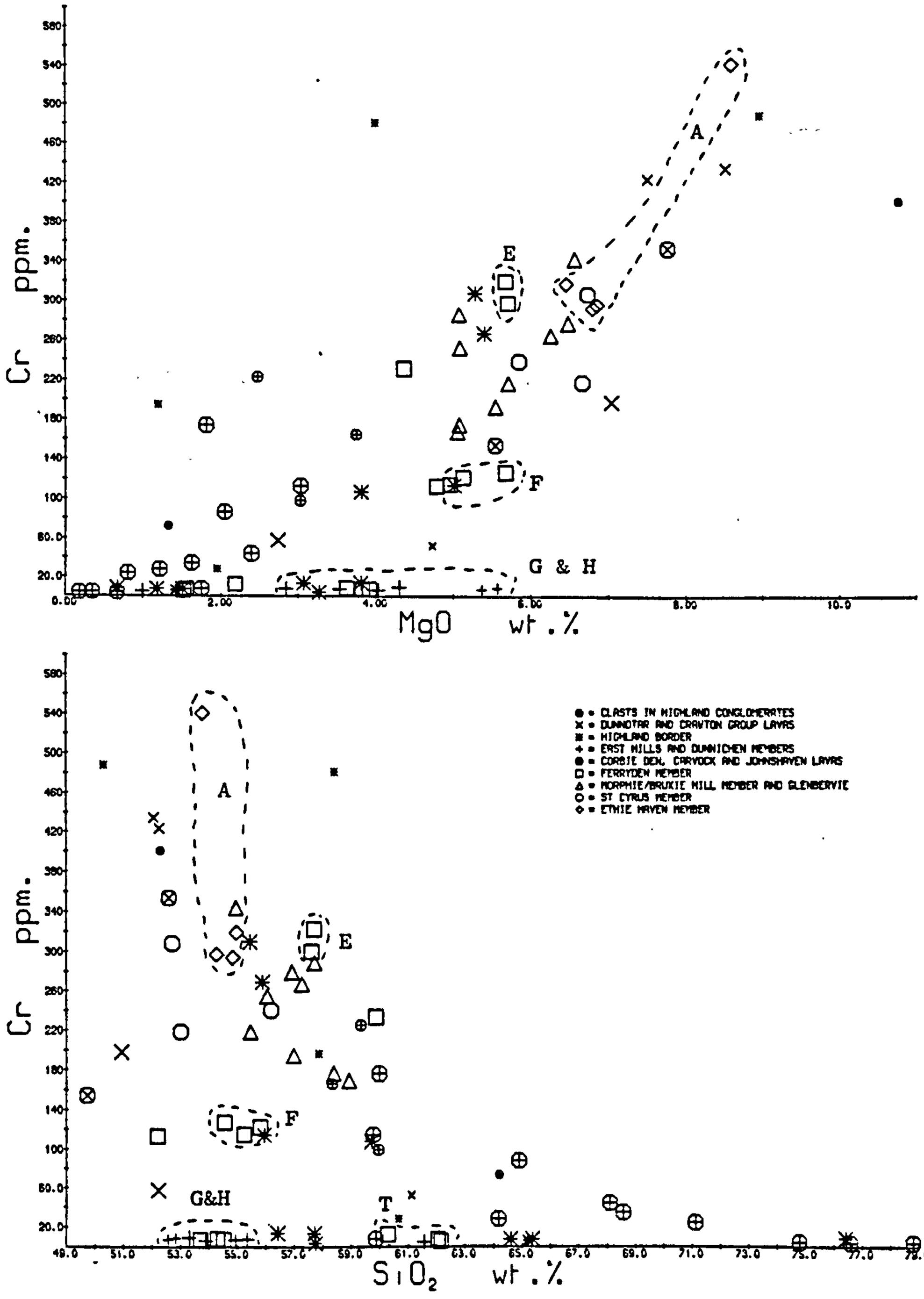

MONTROSE REGION

Fig. 5.2 e & f

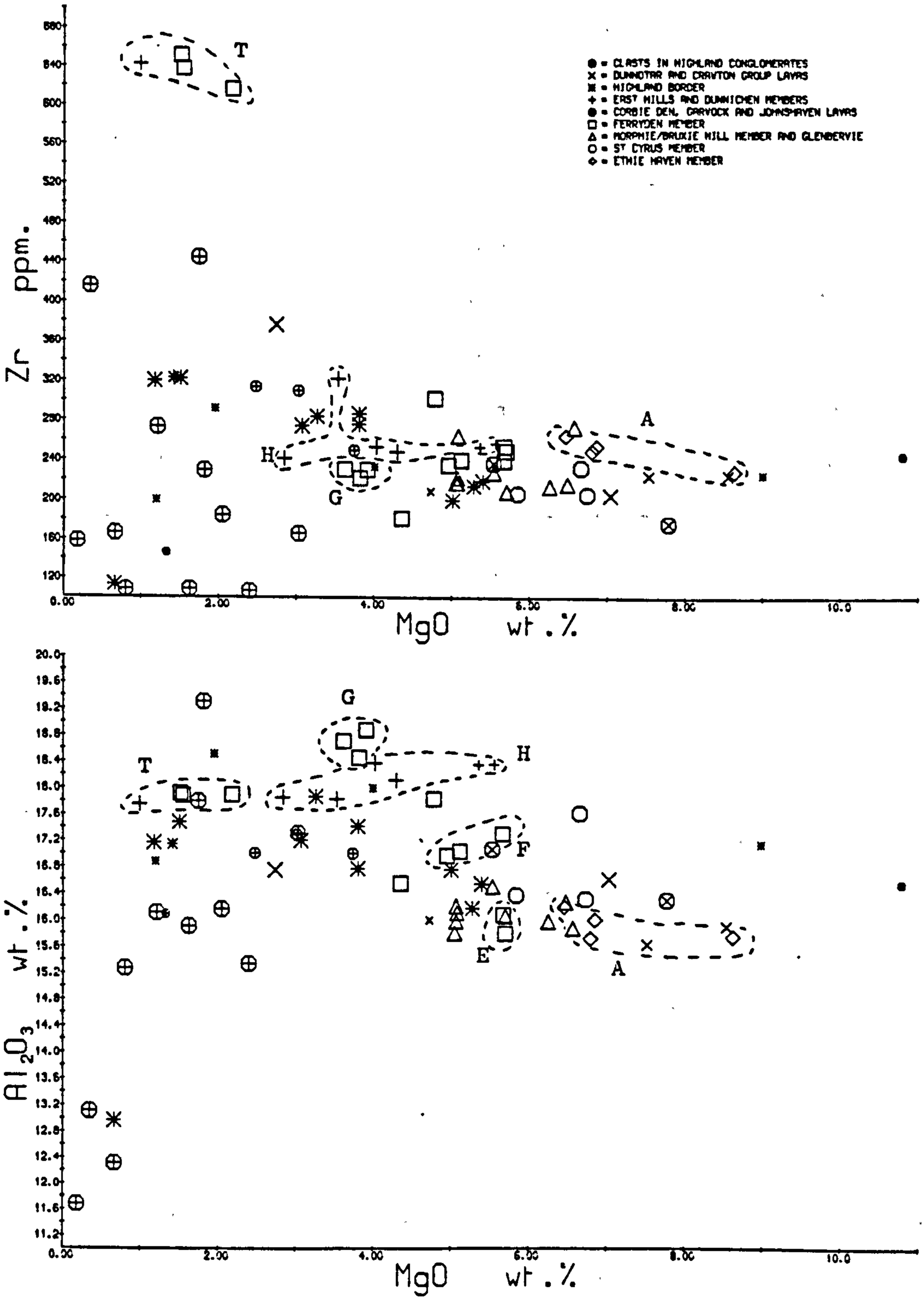

St. Cyrus Member.

(g) Highland Border Lavas

Volcanic rocks assigned to the Arbuthnott Group by Armstrong and Paterson (1970) outcrop at a number of places on the steeply dipping NW limb of the Strathmore Syncline, in close proximity to the Highland Boundary Fault. The main area of outcrop is between Kirriemuir and Dunkeld, with smaller areas near Crieff, Callander and Aberfoyle. All samples collected are quartz-normative, except for one highly altered sample from near Callander. They are very variable, and range from olivine-phyric basic rocks to hornblende-biotite dacites. The rocks from the Kirriemuir-Blairgowrie area frequently contain augite-rimmed quartz ?phenocrysts, and MT53 shows aggregates of pyroxenes and opaque minerals, possibly resorption pseudomorphs after amphibole. None of the rocks with less than 59% silica show much phenocryst plagioclase. Only one of the more basic samples has high alumina (MT33), and this is nearly aphyric, and has very low Ni and Cr. Wide variation in Zr/Nb exists, and it is unlikely that any of the rocks can be related by fractional crystallisation processes, although the number of samples available is too small to verify this.

Conglomerates containing volcanic and Highland metamorphic clasts are common in the Arbuthnott Group of the NW limb of the Strathmore Syncline. Four volcanic clasts have been collected from these conglomerates, all

plagioclase-phyric andesites. They are less variable than those from the Kincardineshire conglomerates, and have relatively low Al and Sr (400-600 ppm), and high concentrations of Th, K and Rb.

(h) Garvock Lavas

The one sample collected from the thin, ill-exposed volcanic rocks of the Garvock Group is an olivine-normative ol-phyric basalt. It has a high Fe/Mg ratio, believed to be primary, and falls in the tholeiitic field of Miyashiro (1974) on an SiO_2-Fe/Mg diagram. Despite this, concentrations of other elements are not abnormal, although Ti and P are relatively high.

(i) Montrose Region : Discussion and Conclusions

The volcanic rocks of the Montrose region have many general chemical similarities to those of the SW Highlands, particularly in being a quartz- or slightly olivine-normative suite of rocks with concentrations of LIL elements, Ti, Zr and Nb comparable to those of many alkaline suites. The stratigraphy, in conjunction with phenocryst mineralogy, Zr/Nb, Al, Ni and Cr allows the identification of a large number of petrochemically distinct rock groups. Each group shows relatively little compositional variation; in some cases such variation as exists may be explained by fractional crystallisation hypotheses (e.g. Dunnichen/East Hills Member, "trachyandesites") and in others can not

(e.g. St. Cyrus, Bruxie Hill). The groups therefore form tight clusters of points on variation diagrams, although the overall impression of these is of highly scattered calc-alkaline trends (Fig. 5.2).

Use of MgO instead of silica as an index of variation gives greater separation of the samples with less than 60% SiO_2, and is therefore preferred. Most importantly, it indicates that the high alumina samples are more evolved than samples with lower Al, a distinction not brought out by the use of silica as an index of variation, for silica concentrations of these are relatively low.

It is clear that the groups of samples, or even the least evolved sample from each group, do not lie on the same liquid line of descent from a common parent. The following interrelationships are possible between the various groups:

1/ Each group represents a position along a unique liquid line of descent from a common parent. Different groups therefore represent different combinations of phases crystallising from the same parent, at, for example, different P, T.

2/ Each group represents a stage on a liquid line of descent controlled by crystallisation of the same phases, but derived from a different parental liquid.

3/ A combination of 1 and 2, in which each group represents a stage on a unique liquid line of descent from a unique parent magma.

4/ Each group represents different degrees of partial

melting of the same source, possibly including disequilibrium melting.

5/ A more complex mechanism, possibly involving the melting of several sources, followed by crystallisation, contamination or magma mixing during ascent.

The chemical parameters believed to be most relevant to these possibilities are listed in Table 5.4.

Consideration of the first possibility requires the identification of possible parental liquids. The high Cr of group A rocks, in particular MT42, suggests that they are mantle-derived, and that little fractional crystallisation of mafic minerals can have occurred since separation of the melt from its mantle source. This is also true for groups B-E, Table 5.4. Fractional crystallisation of plagioclase is not precluded, however.

It was noted in Chapter 4 that Zr/Nb may only be changed during fractional crystallisation (of phases excluding ilmenite, magnetite and zircon) if the degree of crystallisation is high, for the differences in distribution coefficients between Zr and Nb are small for olivine, pyroxenes, amphiboles, biotite, garnet or plagioclase (Pearce and Norry, 1979). Further, fractional crystallisation of ilmenite- or magnetite-bearing assemblages can only lead to change in Zr/Nb with substantial depletion in V and Cr, elements which have high crystal-liquid distribution coefficients for these phases. Fractional crystallisation of zircon is most unlikely in

TABLE 5.4 : Chemical characteristics of the major lava groups of the Montrose region. Evolved samples omitted. Oxides in wt.%, trace elements in ppm.

Group	SiO_2	Al_2O_3	K_2O	Sr	P_2O_5	Ce	La/Y	TiO_2	Zr	Zr/Nb	Cr
A - Ethie Haven	54-55	15.7-16.2	?	560-630	0.36	62-76	1.2-1.3	1.29-1.34	228-264	20.0-22.5	300-560
B - St. Cyrus	53-56	16.3-17.6	1.9	580-690	0.33-.39	59-66	0.9-1.5	1.28-1.71	205-232	15.5	210-310
C - Morphie/Bruxie Hill	55-58	15.9-16.5	2.0	457-546	0.29	59-71	1.1-1.5	1.12-1.40	208-264	14.5-17.5	200-290
D - Crawton	52	15.6-15.9	1.7-1.9	770-830	0.50	93-112	1.8-2.1	1.50-1.66	224	13	430
E - Ferryden (MT36,37)	57.5	15.8-16.1	2.3	564	0.35	70-73	1.4-1.5	1.3	249-254	14.0-14.8	310
F - Ferryden (MT38-40)	54-56	17.0-17.3	?1.9	666-737	0.37	70-75	1.2-1.5	1.48-1.54	235-240	14.5-15.5	120
G - Ferryden high-alumina	53-55	18.5-18.9	2.0	690-740	0.37	67-70	1.0-1.1	1.53-1.56	222-230	17.5-18.2	<10
H - East Hills/ Dunnichen	53-55	17.8-18.4	2.0	634-673	0.44	71-80	1.0-1.1	1.70-1.76	241-256	18.0-20.2	<10

these basic andesites. It is therefore clear that groups A, B, D of Table 5.4 may not be derived from a common parent. The higher Si and K of groups C and E suggests that these could be derived by the fractional crystallisation of plagioclase-rich assemblages from magmas of groups A, B or D. Zr/Nb, and the difficulty of creating lower La/Y except by major apatite crystallisation, precludes derivation of groups C and E from either of groups A and D. The data given in Table 5.4 do not prevent group B liquids from being parental to those of groups C and E, but since both groups B and C are believed to be polygenetic (sections 5.1 d and f), and show wide spreads in La/Y and, for group C, Zr/Nb, it is clear that discussion of a liquid line of descent is meaningless.

It has been previously demonstrated that group F may not be derived from group E by fractional crystallisation processes (section 5.1e). Since there is only moderate depletion in Cr and no Zr enrichment relative to the more Cr-rich groups A-E, Zr/Nb ratio precludes derivation of group F from groups A and D. Therefore, group F may only be derived by fractional crystallisation from groups B and C, and by the argument of the previous paragraph, discussion of a liquid line of descent is meaningless.

It was noted in section 5.1(e) that groups G and H are not part of the same liquid line of descent. The low Cr, Ni and high alumina of these samples suggest that these groups could have been derived by fractional crystallisation

of olivine and clinopyroxene from a magma represented by one of the more mafic compositions of the area, comparable, for example, with the model of Gandy (1973a) for the derivation of high-alumina basalt from olivine-tholeiite by the fractional crystallisation of olivine and clinopyroxene. This can not have involved a high degree of crystallisation, for K, Zr and Ce contents are little, if at all higher than in the more mafic rocks of the region. Substantial magnetite or ilmenite separation is precluded by comparable, or higher, V contents in these high-alumina rocks. Therefore Zr/Nb is unlikely to have changed substantially from that of the parent liquid: groups G and H may therefore not be derived by fractional crystallisation of magmas from groups B, D, E and F, and Zr/Nb for groups A and C is also distinctly different. Further, derivation from group A would imply at least 23% crystallisation (Ti data); Zr, which is only an important minor constituent of Ti-rich phases such as ilmenite, would suggest <11% crystallisation of MT42. Group G shows a smaller increase in Ti, but no increase in Zr at all from MT42. It is very difficult to decrease Zr/Ti by fractional crystallisation of any phase except zircon (Pearce and Norry, 1979). Further evidence against fractional crystallisation comes from the relatively large enrichment in P, but very small enrichments in LREE.

It seems highly probable that no group of lavas in the Montrose region can be related to another by a fractional crystallisation process.

The second hypothesis for interrelationships between the groups, derivation of each group by the same fractional crystallisation process from different parental liquids, is extremely difficult to test by geochemical argument, for it is impossible to recognize the phase assemblage crystallised. Instead, less satisfactory arguments based on volume relationships must be resorted to. The individual group chemistries previously discussed require at least 6 different mafic magma bodies all differentiating more or less simultaneously, with only two of these mafic magmas (MT42 and SC14) being sampled in the present collection. This is most unlikely, and is made more unlikely by the difficulty of generating eight unrelated primitive magmas at roughly the same place.

The third hypothesis can combine the better features of the first two, but suffers from most of the difficulties of the second, and it becomes harder still to test. Different degrees of partial melting of the same mantle source, and the possibility of disequilibrium melting, are also difficult to test, for much depends on the phase composition of the source region. However, Zr/Nb is unlikely to vary much in the different partial melts, unless there is a residual Zr-rich phase, for example ilmenite.

The chemical variation of the rocks of the Montrose region clearly requires a very complex genetic mechanism. There are a number of parallels here with the complexities of the SW Highland volcanics: it is thought, however, that

further discussion should be postponed until after the description of the Ochil Volcanic Formation. It is possible that this formation contains mafic magmas not represented in the smaller outcrops at Montrose.

5.2 : THE SIDLAW HILLS

To the SW of the Montrose region, volcanic rocks appear at the junction between the Arbuthnott and Garvock Groups near Glamis and thicken to the south and west to form the volcanic sequence of the Sidlaw Hills, lying on the northern limb of the Sidlaw Anticline (Fig. 5.1). The stratigraphy and petrography of the rocks of various parts of the Hills have been described by Harry (1956,1958), Davidson (1932) and Gandy (1973a). These authors described a volcanic sequence dominantly composed of basalt and basic andesite, with very subordinate andesites and a "trachyandesite" at Craighead (Harry, 1956). No *in situ* acid rocks occur, but the conglomerates overlying the volcanic rocks near Perth are rich in acid clasts. A few horizons of sandstone are intercalated in the volcanic sequence.

In the course of the current research, a selection of the samples collected by Gandy (1973a) has been reanalysed, together with a number of new samples from the Moncreiffe Hill - Perth area.

(a) Ol-phyric, ol-pl-phyric, ol-cpx-pl-phyric and aphyric samples (@1,@11,@12,@20)

None of the samples are truly aphyric, and those classified as aphyric lavas have occasional microphenocrysts of olivine and plagioclase. These are the dominant phenocryst phases in the Sidlaw lavas; clinopyroxene is seldom abundant, and only occurs in the most phenocryst-rich rocks. These phenocrysts are set in a plagioclase-rich groundmass, with intersertal opaque oxide and either subophitic or intersertal clinopyroxene. Many rocks contain groundmass chlorite, which may be replacing both glass and, in some rocks, olivine. Gandy (1973b) has shown that olivine and plagioclase are the liquidus phases of the lavas at atmospheric pressure, and suggested that the chemical variation of the entire Sidlaw suite was controlled by fractional crystallisation of these, with minor ilmenite and possibly clinopyroxene, at low pressure. High scatter on the variation diagrams (Gandy, 1973a) was attributed to phenocryst accumulation and to a range of immediately parental high alumina basalt magmas.

Olivine has not been found fresh, but phenocryst clinopyroxenes are the low Na, Ti, Al diopsidic augites characteristic of the province. They show substantial variation within each rock in Ca, Mg, Ti and Al, not readily correlated with zoning. Plagioclase is labradorite, and neither plagioclase nor clinopyroxene composition is closely related to host rock chemistry.

The rocks are mainly quartz-normative, although a few contain minor normative olivine (up to 4%). Silica varies from 51.5 to 58.5%, although most rocks have less than 56% silica. Few elements show unscattered variation with silica (Fig. 5.3); in particular, the lack of a systematic relationship with Ni strongly suggests that olivine-dominated fractional crystallisation can not give rise to the variation in silica content. Further, separation of 40% olivine, 60% clinopyroxene from olivine-tholeiite to produce a range of high-alumina basalts as suggested by Gandy (1973a) followed by further olivine separation would be most unlikely to produce basic andesites with >100 ppm Ni.

Use of MgO as an index of evolution as at Montrose provides better separation of the basic andesites on variation diagrams (Fig. 5.4). Although there is considerable scatter, it will be noted that there are broad increases in Al and Ti with decreasing Cr and MgO, contrasting with the predictions of the petrogenetic model of Gandy (1973a) involving fractional crystallisation of olivine, plagioclase and minor ilmenite. There is little correlation between Al content and amount of phenocryst plagioclase (ol-cpx-pl-phyric rocks are generally richest in phenocryst plagioclase), suggesting that plagioclase accumulation has not played an important part in generating the scatter.

'Incompatible' elements in general increase with

SIDLAW HILLS

Fig. 5.3 a & b : Bulk rock variation diagrams

Conventions as section 3.3

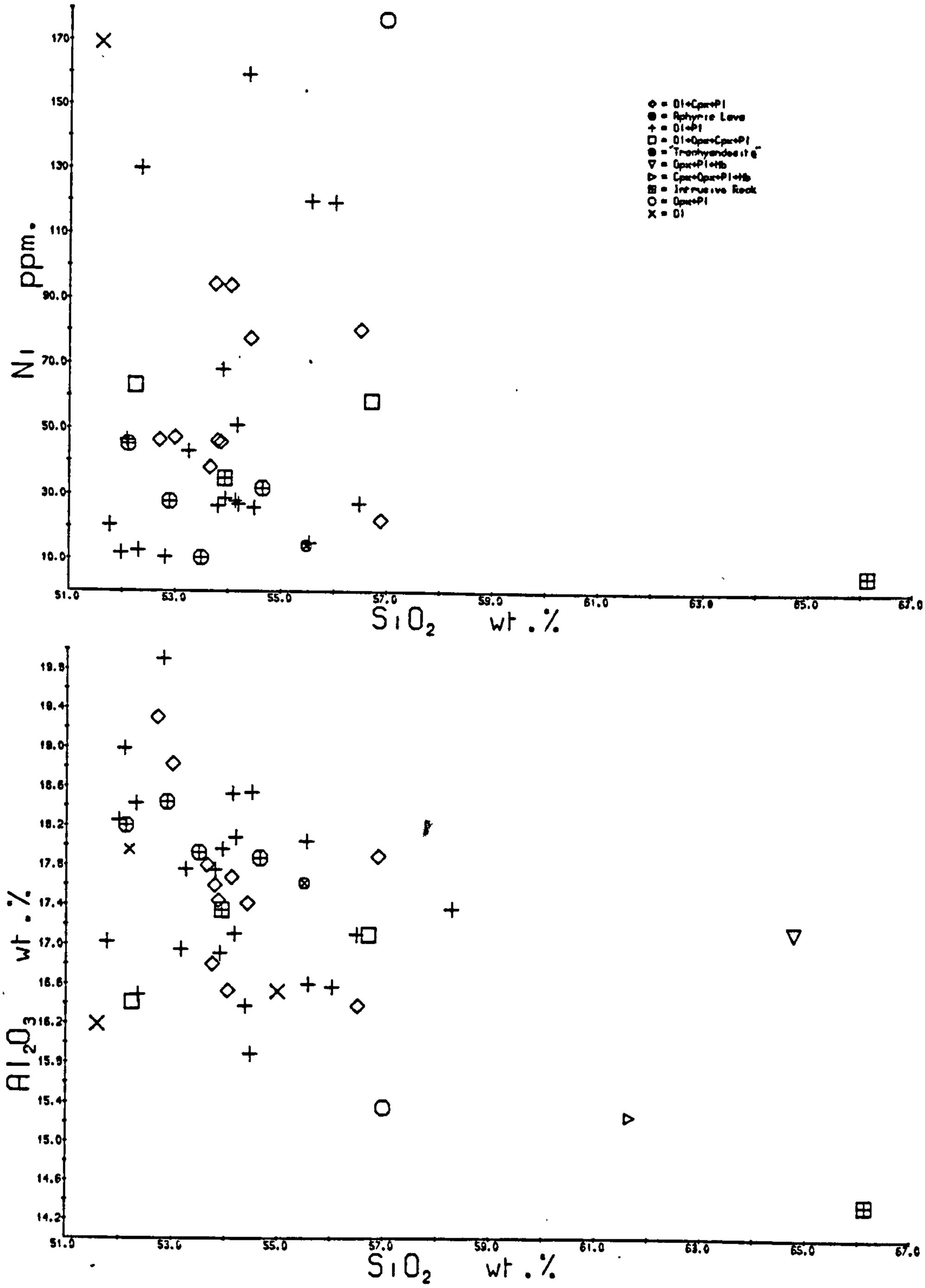

SIDLAW HILLS

Fig. 5.4 a & b : Bulk rock variation diagrams:

Conventions as section 3.3

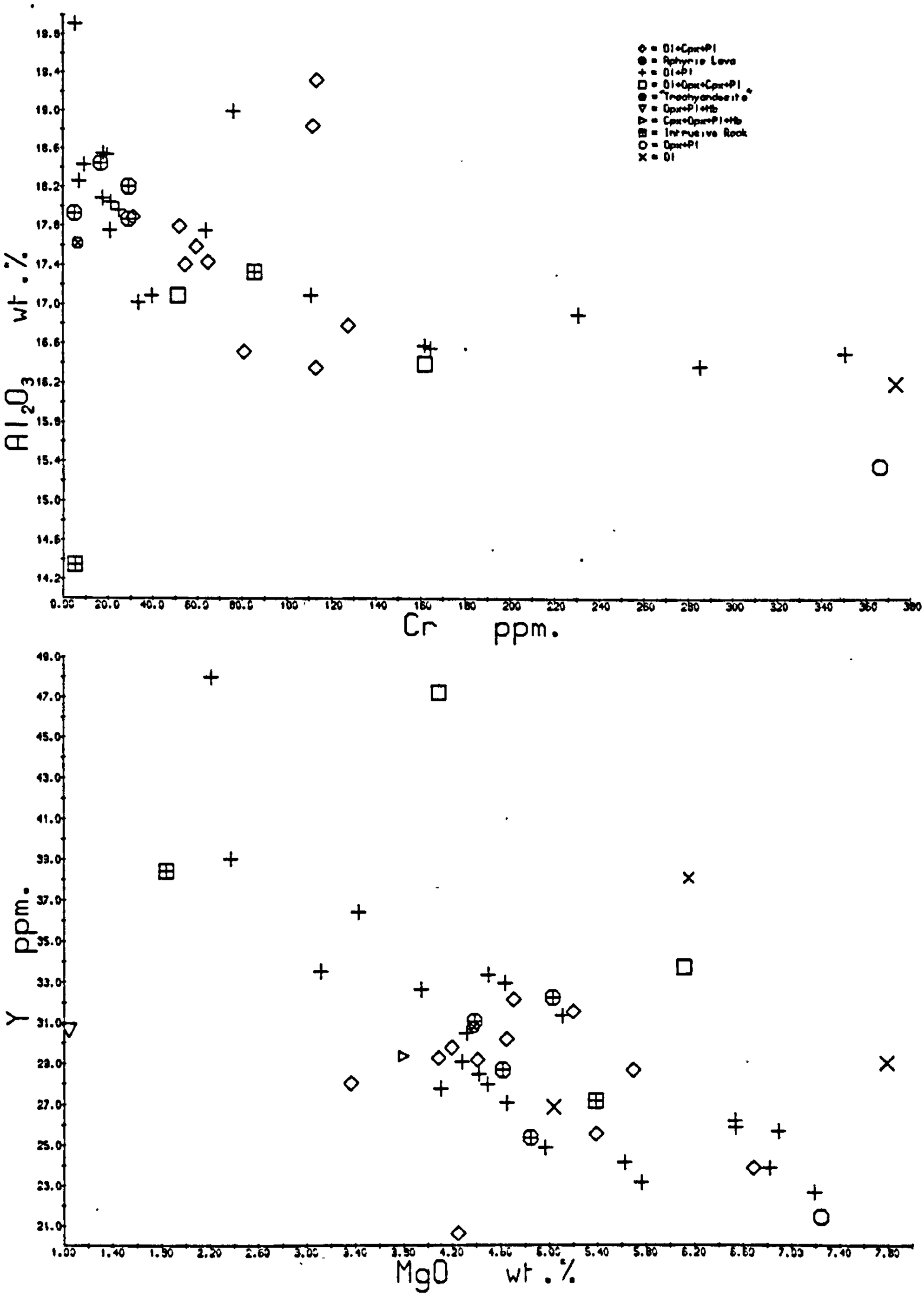

SIDLAW HILLS

Fig. 5.4 c & d

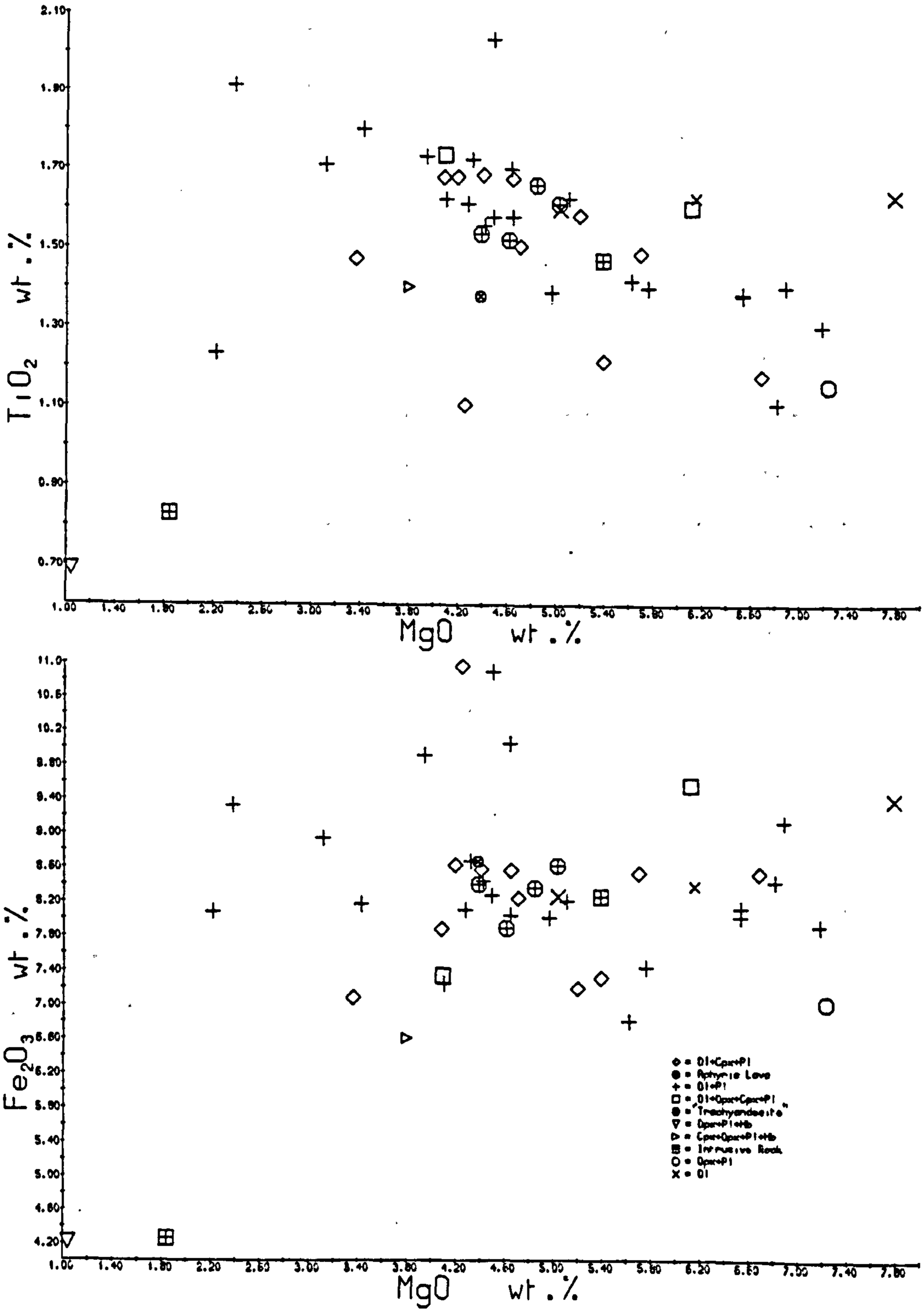

decreasing MgO, (Figs. 5.4,5.5), but there is much scatter, reflected in wide variation in Zr/Nb ratio from 14.5 to 29. Correlation of 'incompatible' element concentrations with Cr is poor, although in general the most Zr, Nb enriched samples have low Cr. Zr/Nb does not correlate with Cr, and again it may be concluded that the Sidlaw lavas may not be derived by multistage fractional crystallisation or partial melting processes from a common source.

Because of the lack of an external criterion by which to divide the rocks, it is very difficult to investigate whether individual groups of rocks can be derived from others by fractional crystallisation processes. Comparison with the variation diagrams for samples from the Montrose region shows that the Sidlaw lavas cover the full range of chemistries displayed by individual members of the Montrose Volcanic Formation. No basic andesite with <4.6% MgO has <17% alumina: at Montrose, only the Highland Border rocks have alumina in this region. A few samples have substantially higher alumina than the Dunnichen/East Hills rocks, but also have higher Ni (40 ppm) and Cr (100 ppm). It is clear that derivation of all high-alumina rocks by simple fractional crystallisation of olivine and clinopyroxene from a common parent is not a viable hypothesis.

(b) Orthopyroxene-bearing samples (@5, @10)

Phenocryst orthopyroxene is present in three samples

SIDLAW HILLS

Fig. 5.5 a & b : Bulk rock variation diagrams

Conventions as section 3.3

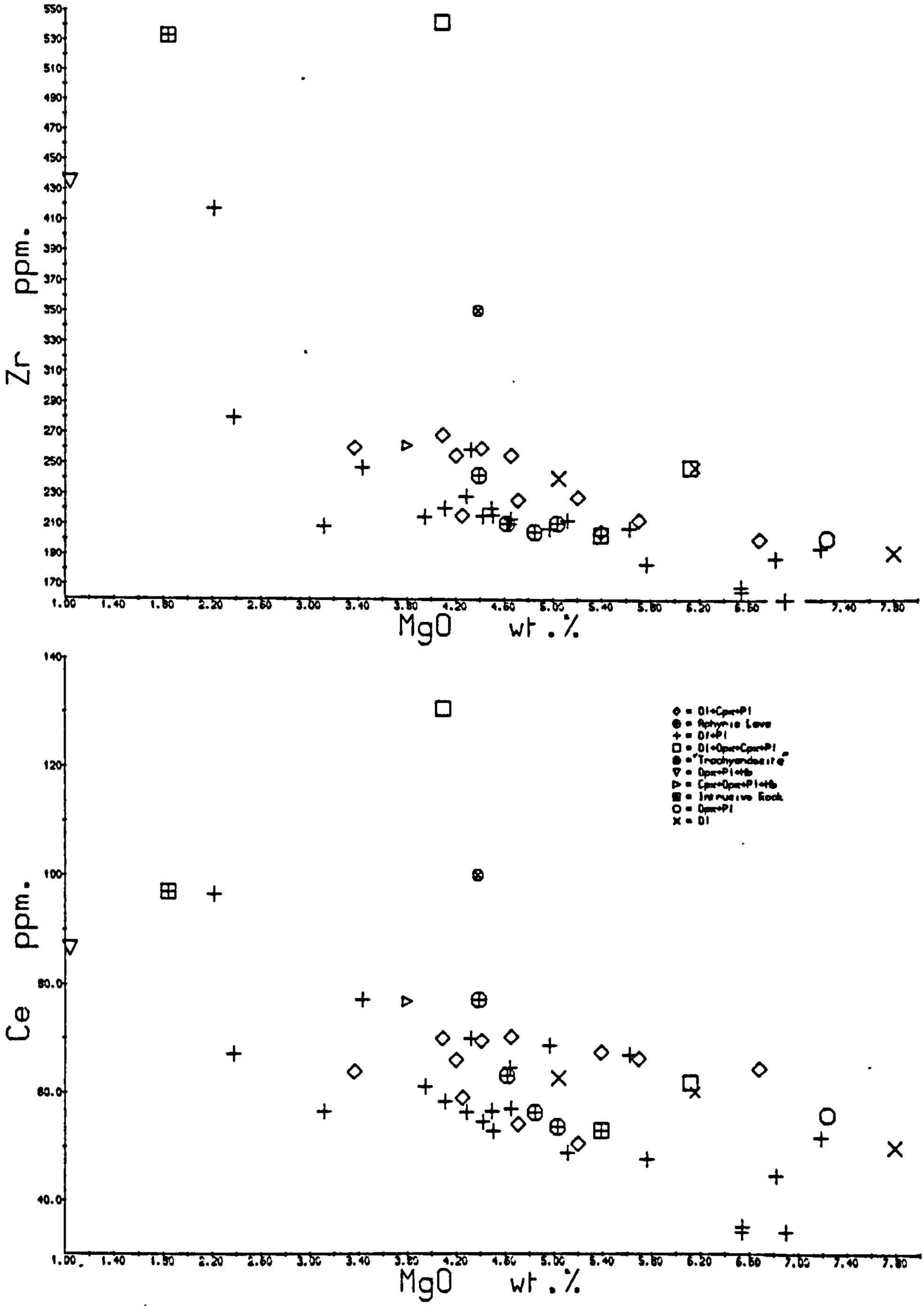

SIDLAW HILLS

Fig. 5.5 c & d

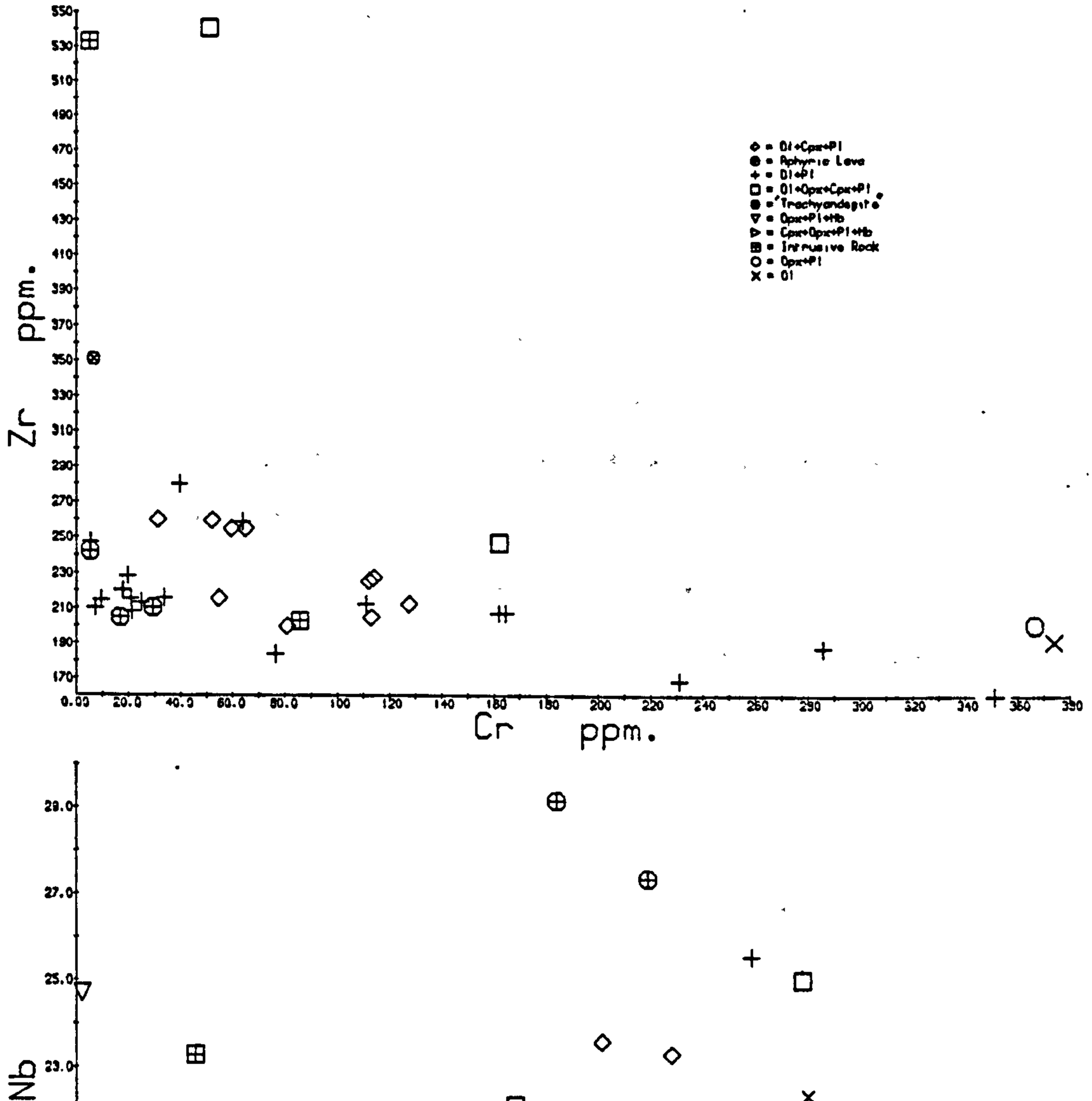

from the Sidlaw Hills. In one of these, it is a magnesian bronzite rich in Ni and Cr (anal. 22, S44), and is associated with sodic labradorite (anal. 19, S44). This sample was described by Gandy (1973a) as an orthopyroxene-phyric andesite, for it contains 57% silica, but it is one of the most Ni-, Cr-, Mg-rich rocks in the Sidlaw Hills. It is also rich in K and Rb, and for its MgO content, relatively rich in other generally 'incompatible' elements. It has therefore a number of similarities to the Ferryden samples MT36,37, but differs from these in detail, e.g. Zr/Nb ratio. Sr content is greater than that of other comparably mafic Sidlaw lavas, and therefore fractional crystallisation of a plagioclase-dominated assemblage can not produce the incompatible element enrichment. Fractional crystallisation of mafic minerals would reduce Ni and Cr: it may be concluded that no other Sidlaw composition could produce S44 by fractional crystallisation.

The two other orthopyroxene-bearing samples contain olivine and clinopyroxene in addition. Orthopyroxene is Cr-poor hypersthene (anal. 25, S52), plagioclase is labradorite-andesine and clinopyroxene the typical diopsidic augite low in Ti, Na and Al (Table C2, anals. 24 and 26, S13 and S52). Plagioclase is considerably richer in Or, and clinopyroxene in Fs, than those from the ol-cpx-pl- and ol-pl-phyric samples. Orthopyroxene is frequently mantled by clinopyroxene or by small olivines. The two samples are strongly enriched in Y (Fig. 5.4) relative to rocks with comparable MgO, and are also enriched in Zr (Fig. 5.5). S13

is also strongly enriched in other generally incompatible elements, with Ba the only exception. Sr is depleted relative to the bulk of the rocks; it is probable that fractional crystallisation of plagioclase-rich assemblages can explain the incompatible element enrichment, but, again, identification of a parental magma is very difficult. The difference in Zr/Nb between S13 and S52 suggests that these are not cogenetic, but S13 has comparable Zr/Nb to the Montrose "trachyandesites". Zr, Nb, Ce and several other elements show linear relations with MgO between S13 and the Montrose "trachyandesites", possibly suggesting that S13 is immediately parental in a fractional crystallisation process. Major elements, in particular Al and Ti, suggest that this can not be a simple process, however.

(c) <u>"Trachyandesite"</u>

The Sidlaw "trachyandesite", or "high-K andesite" of Gandy (1973a) is very different, both mineralogically and chemically, from the Montrose "trachyandesites". It is quite strongly sericitized, and use of K as a major classificatory parameter is therefore unsatisfactory. The sample is, however, highly enriched in Zr, LREE, Ba, P and Rb relative to rocks with comparable MgO (Figs. 5.4, 5.5), and depleted in Sc and Ca. Y is not enriched, and the sample is probably not related to S13 and S52@10. The sample may be a product of a further process of fractional crystallisation operating in the Sidlaw Hills.

(d) Sidlaw Hills : Conclusions

The chemical variation of the lavas of the Sidlaw Hills may not be generated by fractional crystallisation of olivine, plagioclase and minor ilmenite from a range of high-alumina basalts, themselves generated by olivine and clinopyroxene separation from a primary olivine-tholeiite, as proposed by Gandy (1973a). The chemistry of the Sidlaw Hills lavas is very variable, and encompasses the full range of variation of the samples collected from the Montrose region. Despite this variety, the Sidlaw lavas display the high levels of 'incompatible' elements characteristic of the rest of the province, and demonstrate calc-alkaline trends with little relative iron enrichment. Since it is not possible to separate the Sidlaw samples on a satisfactory stratigraphical or geographical basis, it becomes impractical to demonstrate that fractional crystallisation processes may not generate some of the compositions observed from other sampled compositions. By analogy with the Montrose region, it is believed that no extensive liquid line of descent could be recognized within the Sidlaw samples.

While the Sidlaw lavas include rare compositions appropriate for the genesis of the high-Al, low-Ni, -Cr lavas of East Hills/Dunnichen by olivine-clinopyroxene separation, there are several other high alumina samples in the Sidlaw Hills subtly different from those of Dunnichen. A number of these have relatively high Ni and Cr contents.

It is not possible to determine whether all high-alumina rocks are the products of such fractional crystallisation processes, and it remains possible that they have been generated by the partial melting of a source poor in Ni and Cr.

5.3 : THE WESTERN OCHIL HILLS

The Old Red Sandstone volcanic rocks of the Ochil Hills west of Glen Farg outcrop on both limbs of the Ochil-Sidlaw Anticline. The base of the volcanic sequence is not seen, but it is overlain by and intercalated with sediments belonging to the Garvock Group on the northern limb of the anticline. Overlying sediments on the southern limb are not seen, for the volcanic sequence is truncated by the Ochil Fault in the west, and by the Upper Old Red Sandstone unconformity in the east. Total thickness of volcanic rocks is believed to be in excess of 8000ft (2400m; Francis *et al.*, 1970). The volcanic rocks are cut by a number of intermediate and acid dykes, and by a variety of sills, bosses and laccoliths thought to be closely related to the volcanism. There are larger diorite bodies close to the Ochil Fault near Tillicoultry.

Geikie (1900) and Francis *et al.* (1970) have described the field occurrence and petrography of the volcanic rocks. A wide variety of rock types has been recorded, both lavas and pyroclastic rocks, and Francis *et al.* (1970, p.25) noted that the different lava-types were

distributed in an almost random manner both laterally and vertically. Hornblende-andesites were, however, believed to be restricted to the lower parts of the volcanic pile, and the coarsest agglomerates to areas close to the Ochil Fault. This latter feature was thought to imply proximity to a line of vents along or close to the Fault (Francis et al., 1970, p.27).

The rocks collected show strong similarities, both chemical and petrographic, to the rocks of the Sidlaw and Montrose areas. They differ mainly in the greater development of siliceous rocks, including opx-cpx-pl- and hb-opx-cpx-pl-phyric andesites, "trachyandesites" and the acid lavas of Craig Rossie. There is a corresponding paucity of Ni- and Cr-rich rocks, although many rocks are again considerably richer in these than the average andesite of Jakeš and White (1972). A wide range of phenocryst associations is present, but very few rocks lack phenocryst plagioclase, and over half the samples collected have phenocryst orthopyroxene, in contrast to the statement by Taylor (1972) that orthopyroxene was 'very uncommon' in the volcanic rocks south of Dunning.

Taylor (1972) described a trimodal distribution of silica content from the volcanic rocks of the Ochil Hills south of Dunning. This is not evident when rocks from a wider area are considered, and it is believed that this trimodality results from the unrepresentative collection inevitable in this small, poorly exposed area.

(a) Olivine-bearing samples

Only one sample with olivine as the sole phenocryst has been collected; all other olivine-bearing samples have phenocryst plagioclase, and many contain both orthopyroxene and clinopyroxene. Only one of these has fresh orthopyroxene. This is a bronzite, and the host rock, OC15, although siliceous (56.8%), is the most Cr-rich rock collected in the area. There are therefore some parallels with S44@5 (section 5.2b). Clinopyroxenes are the typical diopsidic augites low in Na, Ti and Al, and again there is much variation within the phenocrysts of a single rock, including, on rare occasions, pyroxenes plotting within the alkaline field of Le Bas (1962). This is again thought to be due to localized melt heterogeneity arising during rapid crystallisation (section 5.1c). Plagioclase is usually labradorite or andesine. Little correlation exists of phenocryst association and chemistry with host rock chemistry.

These rocks show a very wide range in chemistry not related to MgO or silica content (Fig. 5.6), even greater than that shown by the Montrose or Sidlaw volcanic rocks, although again, all rocks are quartz- or slightly olivine-normative. As discussed in previous sections, the high variability of Zr/Nb (15-36) suggests that derivation of the suite by fractional crystallisation of a common parent is most improbable, but as no non-chemical means of subdivision exists, it is difficult to rule out an origin by

Fig. 5.6 a & b : Bulk rock variation diagrams

Conventions as section 3.3

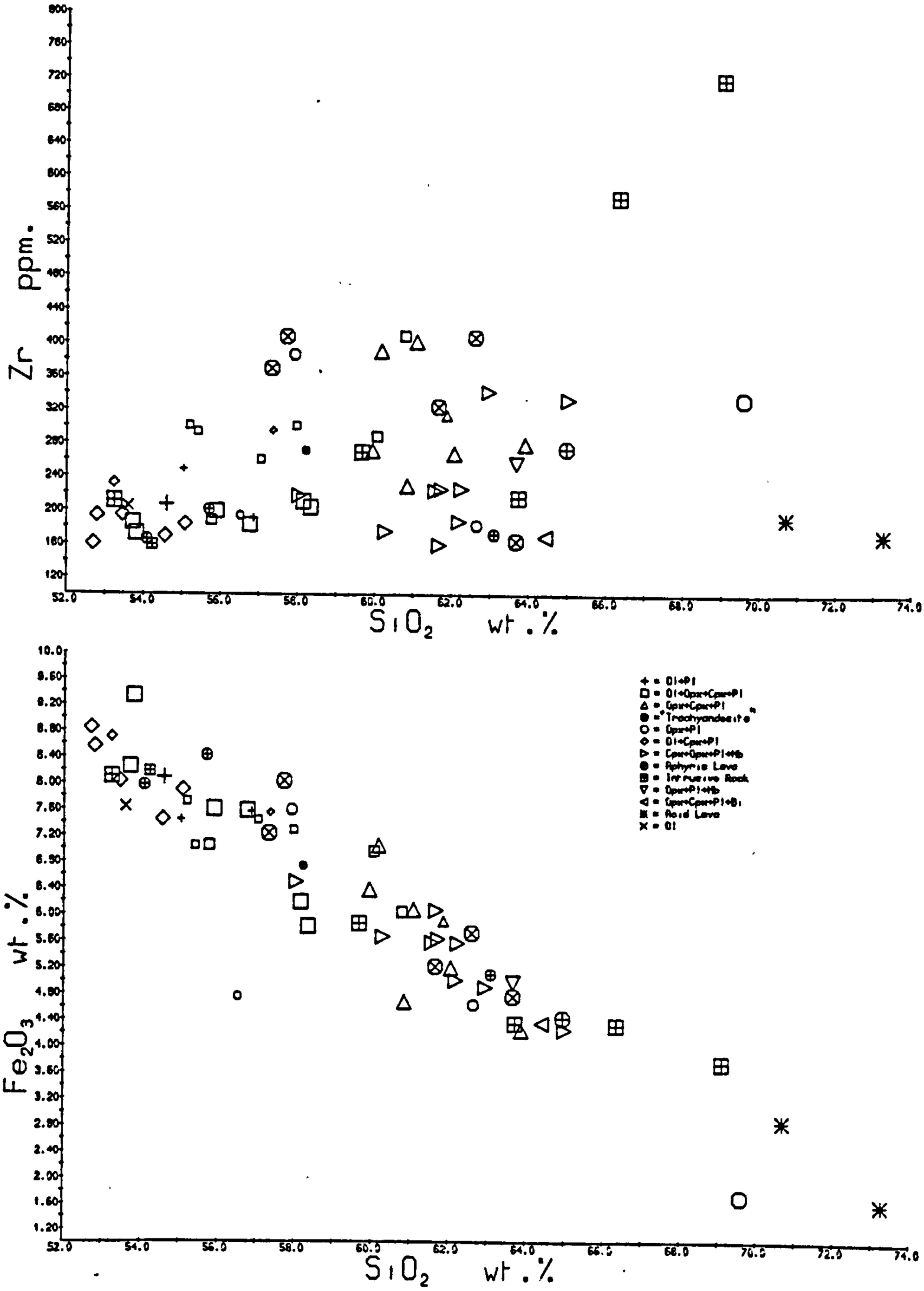

WESTERN OCHIL HILLS

Fig. 5.6 c & d

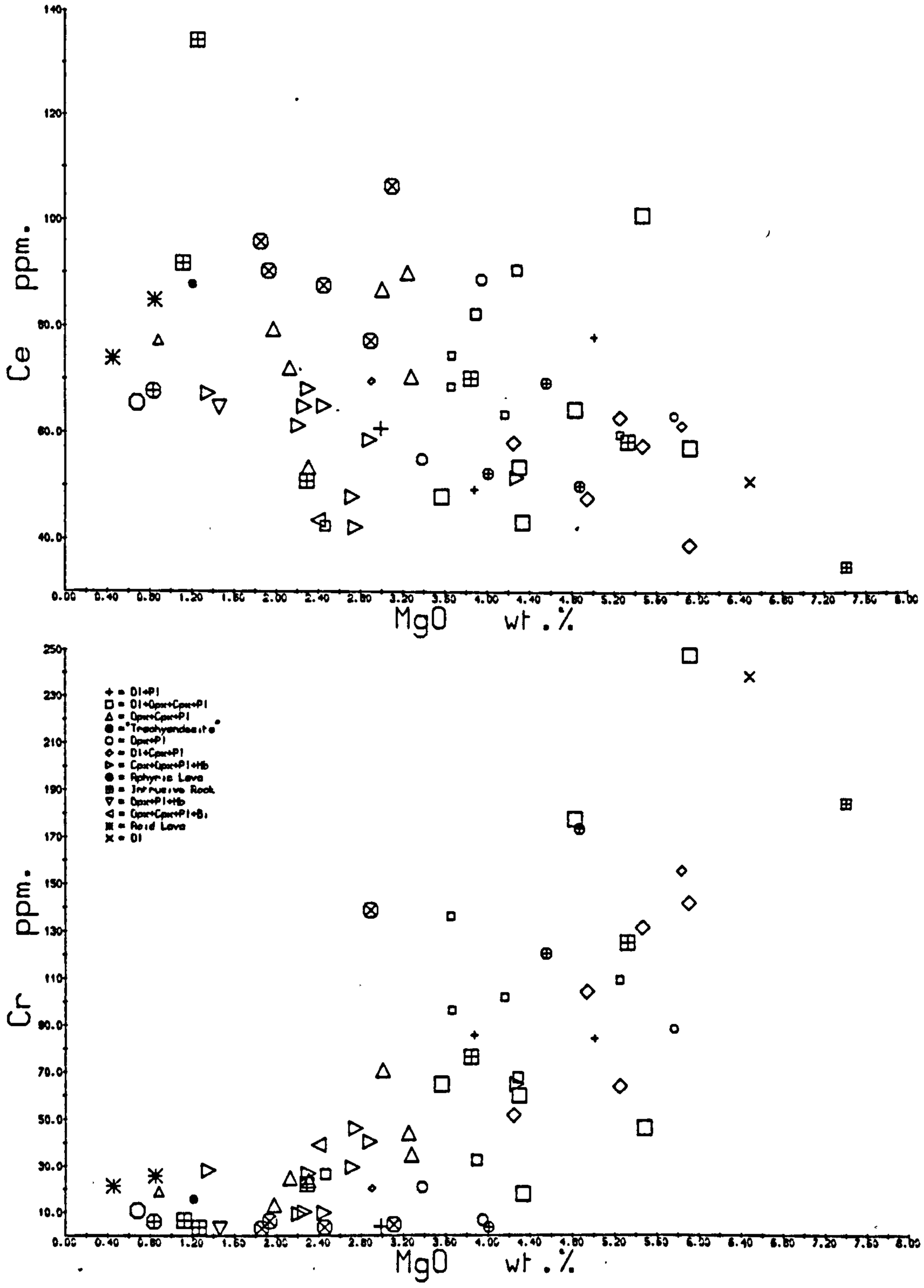

WESTERN OCHIL HILLS

Fig. 5.6 e & f

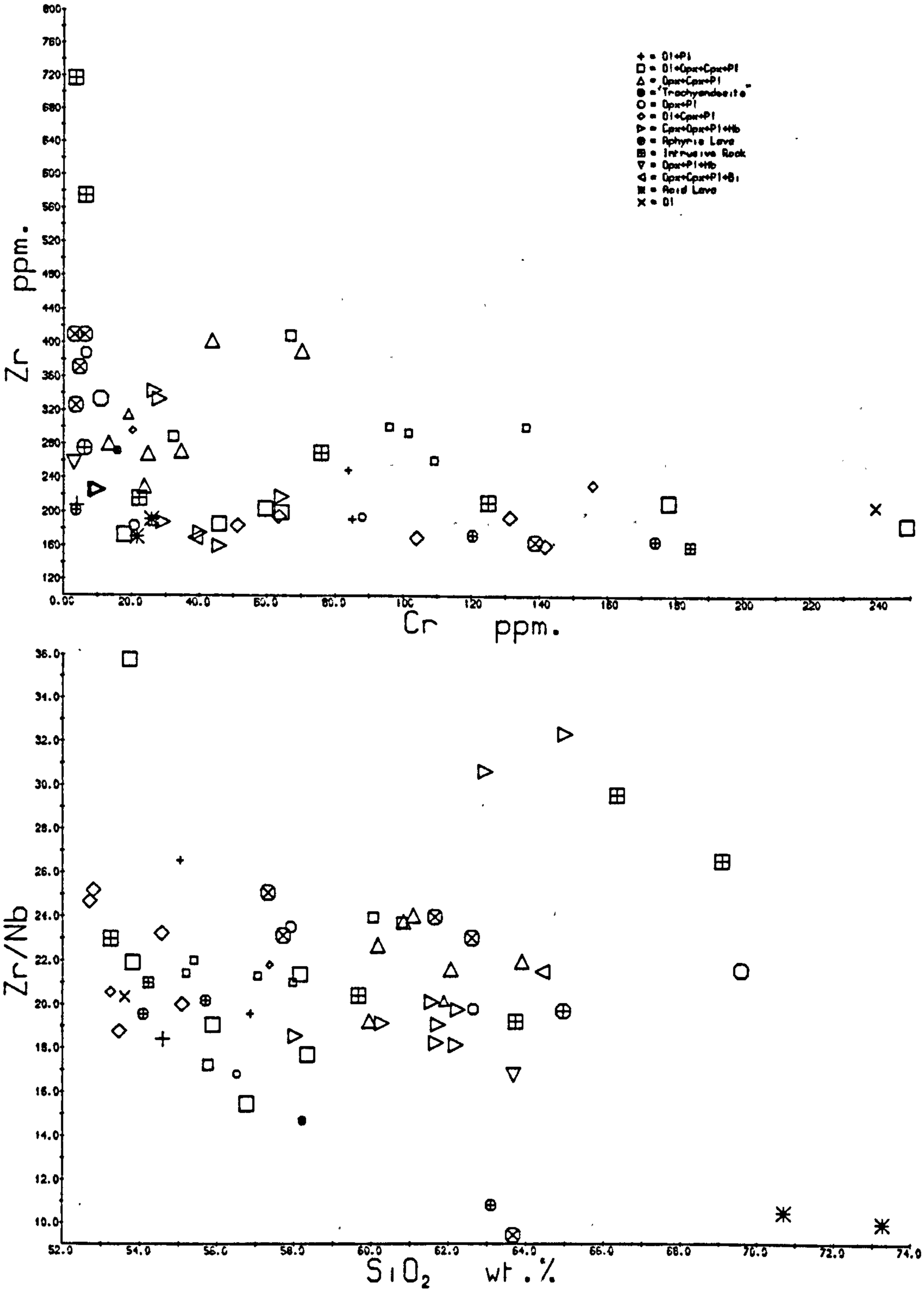

fractional crystallisation for small groups of samples. Small groups of samples which behave coherently may be recognized e.g. OC7, 8, 10. It should be noted that the ol-opx-cpx-pl-phyric samples are not as strongly enriched in generally incompatible elements as Sidlaw ol-opx-cpx-pl-phyric samples.

(b) Opx-cpx-pl-phyric samples (@13)

All samples with this phenocryst association have between 59.9 and 64% silica, 1.9 and 3.3% MgO (excluding one altered sample) and between 10 and 30 ppm Ni. Despite this apparently restricted composition, Zr varies from 220 to 400 ppm, Y between 19 and 40 and Ce between 55 and 90 ppm. The two samples with the highest incompatible element concentrations (OC7,8) also have high Ni, Cr, Sc and V relative to other opx-cpx-pl-phyric samples, but lower Sr and Al. This could suggest fractional crystallisation of an assemblage dominated by plagioclase, but it is unlikely that this could lead to increases in Ni and Cr. Furthermore, CaO concentrations are little different and Zr/Nb variation is outside the limit of analytical error. It may be concluded that the opx-cpx-pl-phyric rocks are unlikely to be all related to each other by fractional crystallisation processes. The phenocrysts are chemically comparable with those of the olivine-bearing samples, and the association may have apatite and magnetite in addition.

(c) Hornblende-andesites (@16)

As noted by Taylor (1972), phenocryst amphibole is absent from the basalts and basic andesites and it is never common in more siliceous rocks. The hornblende-andesites also contain phenocrysts of orthopyroxene, clinopyroxene, plagioclase and titanomagnetite. Some samples also have phenocryst apatite, and one contains rare pseudomorphs after olivine central to large aggregates of pseudomorphed orthopyroxene. The amphibole is a pargasitic hornblende, clinopyroxene is the typical low Ti, Al, Na diopsidic augite and orthopyroxene is bronzite-hypersthene. Plagioclase is labradorite or andesine, although two crystals partly enclosed in amphibole in OC67 zone from An84 inside the amphibole out to An50. Plagioclase is poorer in Or than that from samples with olivine-bearing associations.

With the exceptions of OC65 and OC67, the rocks have Zr/Nb within the range of analytical error. These two rocks are strongly enriched in Zr and Rb, slightly enriched in P, La, K, Si and depleted in Na, Y, Fe, Mg and Ti relative to other hornblende-andesites. The closely similar values of Cr, Ni, V, Sc and Sr strongly suggest that the two groups may not be derived by fractional crystallisation of a common parent. The most mafic sample, OC23, has substantially higher levels of Ni and Cr, but also has more Zr and Nb than many of the remaining five. These five show a good linear increase in Zr and Nb with decreasing Cr (Fig. 5.6). It seems possible that these five are related by fractional

crystallisation of a common parent, but as previously, the small variation does not permit the use of extract calculations to deduce the possible crystallising assemblage. Any parental magma must have been significantly poorer in Zr and Ce than any other composition analysed in the region.

(d) "Trachyandesites" (@18)

Rocks described as trachyandesites by Francis et al. (1970) and classed as dacites by Taylor (1972) form yet another petrographically and chemically heterogeneous group. They are generally sparsely porphyritic with a groundmass dominated by a subtrachytic arrangement of plagioclase laths. Phenocrysts include calcic andesine, diopsidic augite with slightly higher Na, Ti and Al than average (anals. for OC27, Table C2), but well within the tholeiitic (subalkaline) field of Le Bas (1962), titanomagnetite, orthopyroxene, hornblende and apatite in various combinations. The rocks are not notably more alkaline than many other rocks described as andesites by Francis et al. (1970), and the term "trachyandesite" is therefore a misnomer; it is still useful to refer to them as a group, and the term has therefore been retained in quotes.

The "trachyandesites" vary from 57 to 64% silica, and most of them are poor in Ni and Cr, with Ni>Cr, like the "trachyandesites" of the Montrose region. The one relatively Ni-rich sample is also the most siliceous, and,

together with one more altered sample (OC24) has very much lower Zr/Nb (10-15) than the remaining four samples (Zr/Nb=23-26). These four samples are themselves chemically very variable, and one (OC63) is much poorer in V, Ti, Y and also Zr and Nb than the remainder. This could possibly suggest fractional crystallisation of an ilmenite-rich assemblage, but this can not satisfactorily explain the silica variation. In addition, OC63 has much lower K and Rb than the other three. It seems likely that at least three magmas differing in 'incompatible' element ratios are required to generate the Ochil "trachyandesites". They show some broad similarities to the Montrose and Sidlaw "trachyandesites", particularly in their strong enrichment in P relative to most Midland Valley samples, but 'incompatible' element concentrations differ in details which may not be attributed to fractional crystallisation.

(e) Western Ochil Hills : Conclusions

It is clear from the preceeding discussion that Taylor's (1972) model for the petrogenesis of rocks with <63% silica by the wet partial melting of quartz-eclogite at 27-30kb can not explain the variations in Ni and Cr or in 'incompatible' element ratios, unless the eclogite was extremely heterogeneous. He believed that more siliceous rocks were derived by the fractional crystallisation of plagioclase, clinopyroxene and amphibole from wet andesitic magma. While a wide variety of andesitic magmas was apparently available, the very low Zr/Nb of the Craig Rossie

'rhyodacites' precludes their derivation from most of the andesites of the Western Ochil Hills by fractional crystallisation of zircon-free assemblages (Chapter 3). Early crystallisation and settling of zircon from liquids with only about 250 ppm Zr is thought to be unlikely.

The rocks of the Western Ochil Hills are very similar to those of the Sidlaw Hills and the Montrose Volcanic Formation, for they again show great chemical variety within broad calc-alkaline trends. Since no satisfactory non-chemical method of rock classification exists, it is again impractical to deduce whether individual rock groups can be related by fractional crystallisation processes to the more mafic lavas of the area or to a small number of parental magmas. Where a rock group may be delineated using petrographic and chemical criteria, for example, five of the hornblende-andesites, no other composition in the Ochil Hills can be immediately parental. Comparison with the Montrose region suggests the conclusion that no extensive liquid line of descent controlled by fractional crystallisation exists in the Ochil Hills.

5.4 : NORTH FIFE HILLS

Old Red Sandstone rocks of the Ochil Volcanic Formation outcrop in a range of hills along the south side of the Firth of Tay from Glenfarg to Newport-on-Tay, and cross the Tay at Dundee as the Broughty Ferry Lavas. These rocks are all on the southern limb of the Ochil-Sidlaw

Anticline. The volcanic sequence is thinner than in the western Ochil Hills, and in general thins to the east. The volcanic rocks are underlain by and intercalated with sandstones containing a Lower Old Red Sandstone fauna (Geikie, 1902, p.30) and are unconformably overlain by Upper Old Red Sandstone sediments. Only a few small intrusions are present south of the Tay, but there is a large suite of basic intrusions, probably mainly sills and plugs, near Dundee. The thick sill at Newburgh noted by Geikie (1900, p.30) is now believed (M.A.E. Brown, pers. comm., 1979) to be at least one lava flow. A K-Ar date of 394±5 Ma was reported by Evans et al. (1971) for some lavas near Tayport.

Geikie (1900,1902) and Harris (1928) have described the stratigraphy and petrography of the rocks south of the Tay and of the Broughty Ferry lavas respectively. There is again wide variety in lithology, and Geikie (1902, p.48) noted that there was no rational pattern in distribution of different petrographic types with position in the volcanic sequence. Most of the lavas contain phenocryst plagioclase (labradorite-andesine), almost always coexisting with one or more of the following: forsteritic olivine (up to Fo86), bronzitic orthopyroxene, titanomagnetite and low Na, Ti, Al diopsidic augite. Hornblende-andesites comparable to those of the western Ochil Hills are lacking, and pseudomorphed amphibole phenocrysts have only been observed in an acid lava clast from an agglomerate at Broughty Ferry, and from some nearly aphyric lavas akin to the "trachyandesites" at Auchtermuchty. These latter lavas contain an abundance of

coarse-grained xenoliths, which will be described later. Phenocryst biotite is restricted to the "dacites" of Geikie (1902).

The samples analysed show a range in silica from 50 to 80%, but there is a marked composition gap between the dominant lavas with <62% silica and the "dacites" of Geikie (1902) with >70% (Fig. 5.7). The only sample analysed in this gap was from a clast in an agglomerate (OC89). Only one nepheline-normative sample exists, and this may be due to secondary introduction of calcite. Most of the rocks are quartz-normative, although some of the most magnesian are slightly olivine-normative. They are all rich in LILE, high field strength elements and often in Ni and Cr relative to the average andesite of Jakeš and White (1972), and are thus closely comparable to the rocks of the province described previously.

As elsewhere in the northern Midland Valley, few elements show good linear correlation with increasing silica, although a number show general increases (K, Rb, Th, LREE) or general decreases (Fe, Mg, Ca, Ti, Sc and V). Other elements, particularly Al, P, Ni, Cr and Zr, are very highly scattered. Variation diagrams with MgO show little improvement in scatter, although Al and Na show broad increases, and Cr and Ni decreases, with decreasing MgO (Fig. 5.7).

Zr/Nb is very variable at all silica concentrations

NORTH FIFE HILLS

Fig. 5.7 a & b : Bulk rock variation diagrams

Conventions as section 3.3

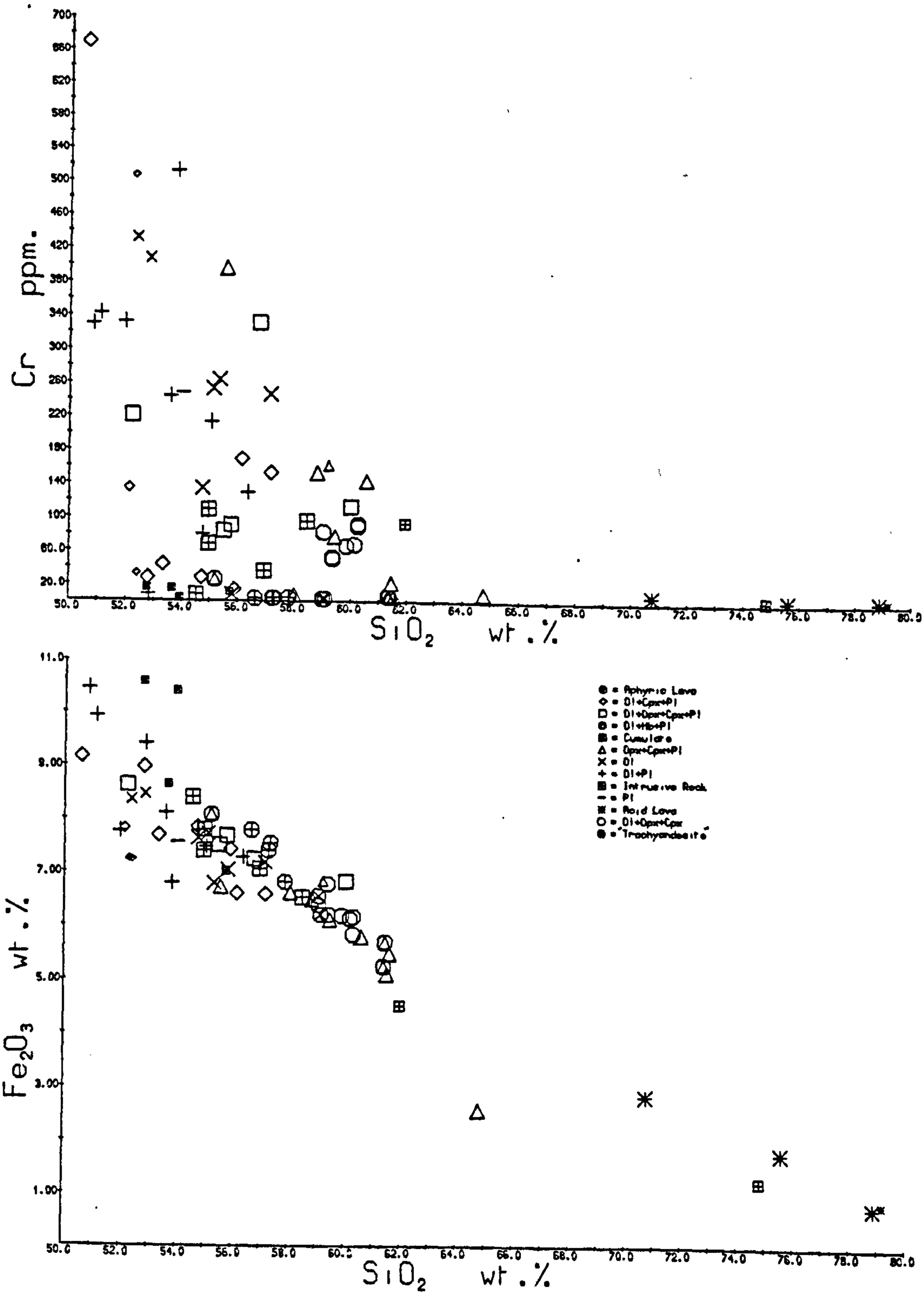

NORTH FIFE HILLS

Fig. 5.7 c & d

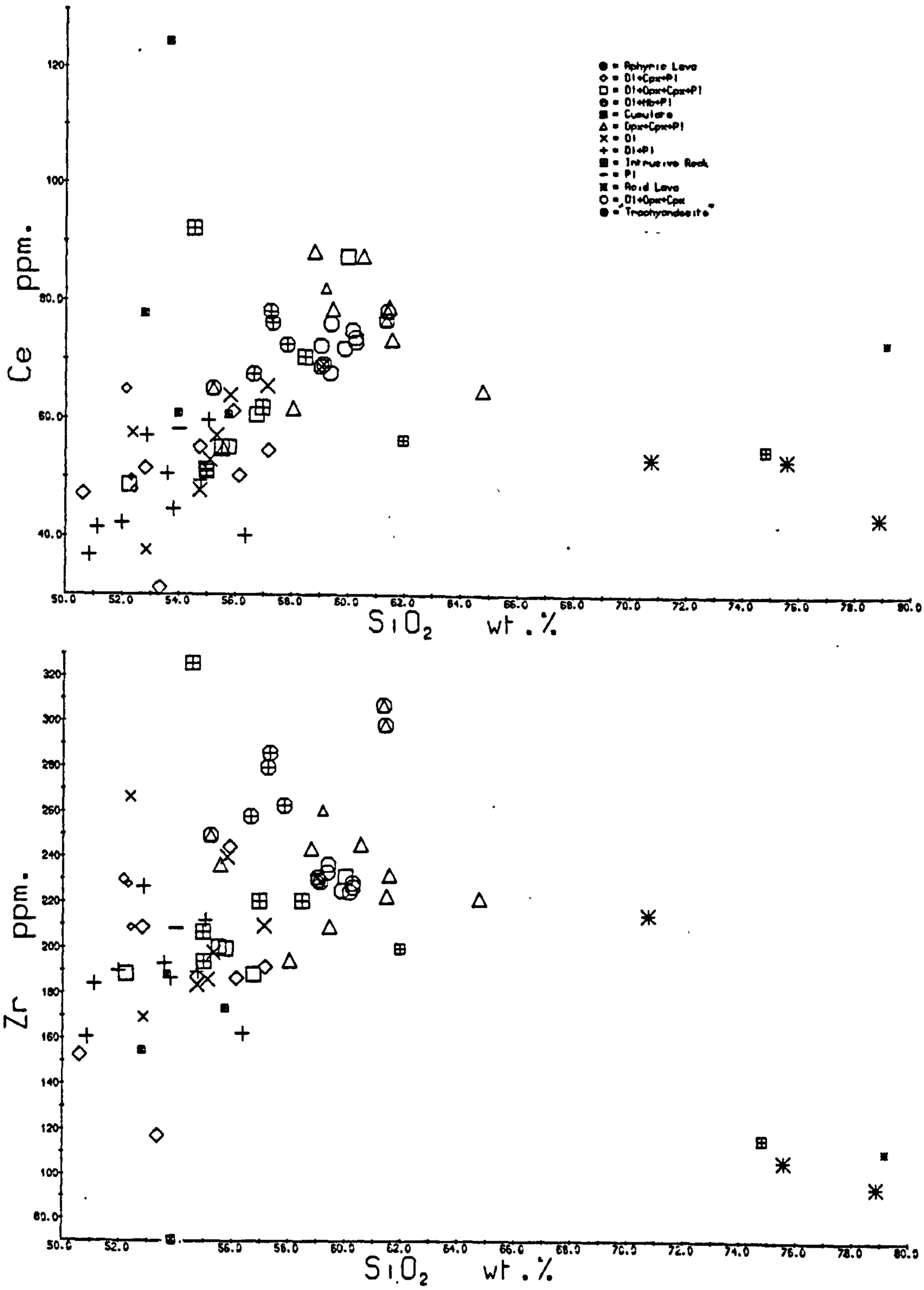

NORTH FIFE HILLS

Fig 5.7 e & f

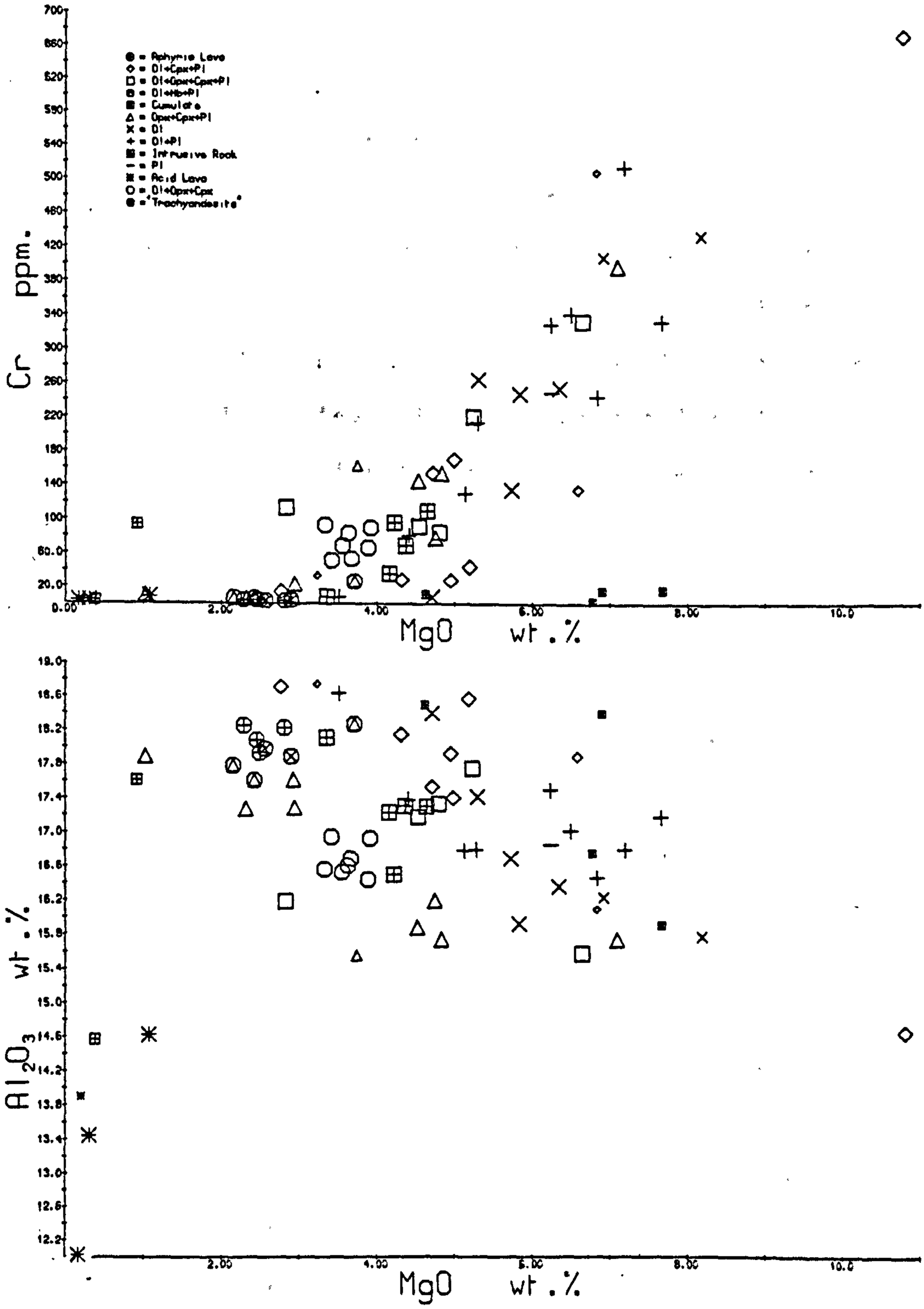

(Fig. 5.8), with a range between 14 and 30 for mafic samples, and correlations between Zr and Nb, Cr and Zr and Cr and Nb are poor: it may therefore be concluded that most of the volcanic rocks of the North Fife Hills may not be related to each other by fractional crystallisation processes. As with the Sidlaw and west Ochil Hills, however, it is not possible to subdivide the rocks by stratigraphical or geographical criteria, and therefore the recognition of small groups of samples of roughly constant Zr/Nb, for which hypotheses of fractional crystallisation may be tested, is impractical. By analogy with the Montrose region, it is again believed that no large suite of rocks conforming to a liquid line of descent is likely to be found.

Use of phenocryst assemblage as a method of classification indicates that a few of the more siliceous assemblages have constant Zr/Nb, and that therefore the rocks with these assemblages might be related by fractional crystallisation.

(a) Acid Lavas (@19)

The three acid lavas collected from the "dacites" of Geikie (1902), together with the Lucklaw Hill ?intrusion, also described by Geikie (1902) as a "dacite", have closely similar Zr/Nb, much lower than that of any other rock collected from the area. This is due to their low Zr content. Reduction of Zr/Nb with evolution by fractional

NORTH FIFE HILLS

Fig. 5.8 a & b : Bulk rock variation diagrams

Conventions as section 3.3

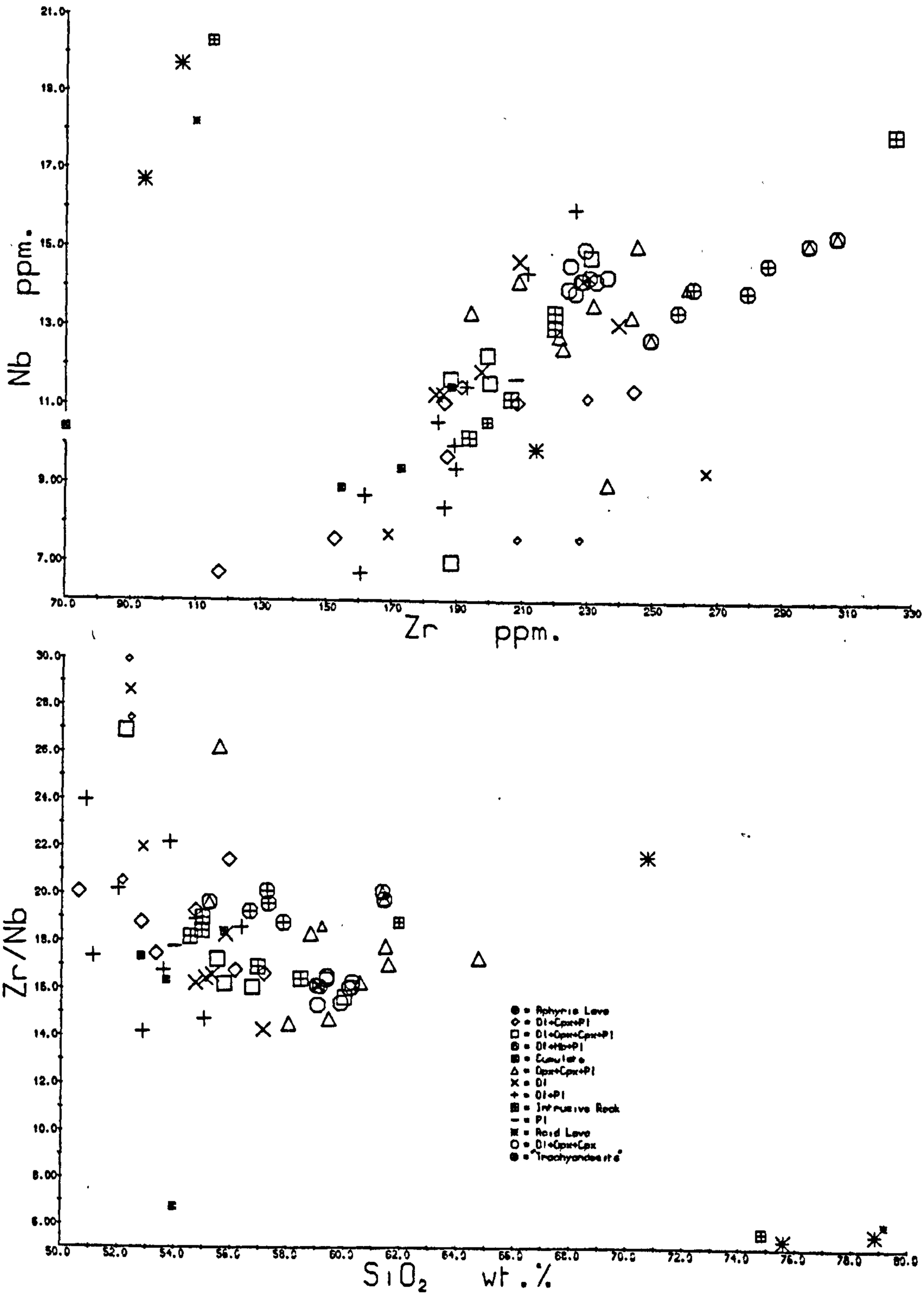

NORTH FIFE HILLS

Fig. 5.8 c & d

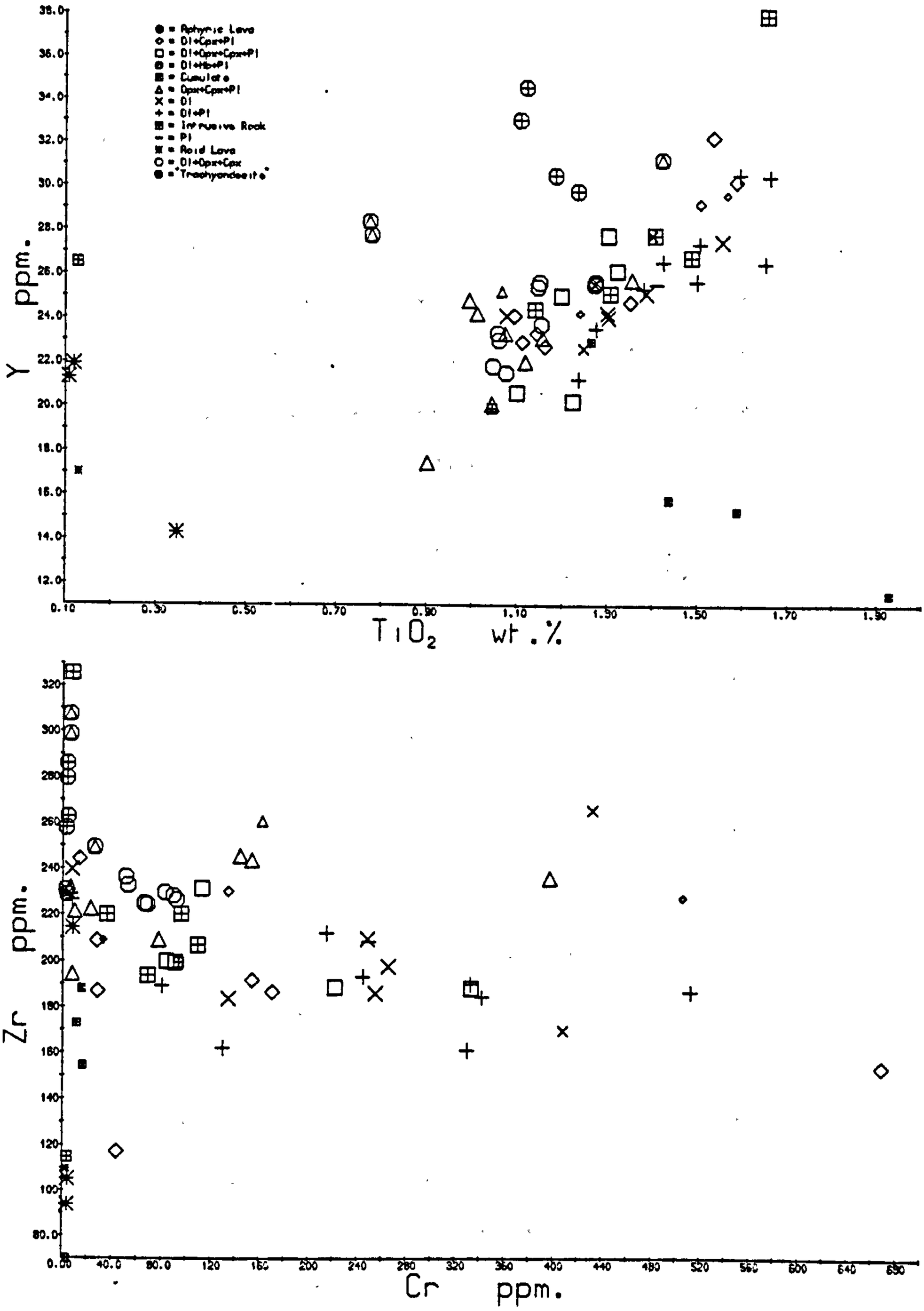

crystallisation would require the separation of zircon (Pearce and Norry, 1979). This is believed to be a most improbable mechanism, for Zr contents of the rocks are low, and Th would probably also be substantially reduced by zircon separation. Further, no intermediate rocks exist in such a fractional crystallisation scheme, and therefore it is believed that the "dacites" may not be generated by fractional crystallisation of any of the more mafic lavas of the area. Within the group, excepting the more altered sample, Zn, Fe, Zr, Nb, Y and LREE all decrease slightly with increasing silica content. This variation may not be significant, however, for a small number of rocks probably affected by secondary silicification.

(b) Aphyric and Ol-hb-pl-phyric samples (@20, @38)

Both of these groups outcrop in geographically restricted areas. The lavas classified as aphyric are all from the horizon described as a sill by Geikie (1900), and have very rare phenocrysts of plagioclase and magnetite in a groundmass of subtrachytoid plagioclase with intersertal ortho- and clinopyroxene. The ol-hb-pl-phyric lavas are restricted to the top of the sequence near Auchtermuchty, and are again nearly aphyric, but are most unusual for the province in containing an abundance of coarse-grained xenoliths. Elsewhere the only inclusions in the lavas are medium-grained aggregates with mineralogy similar to that of their host rocks, which may be interpreted as autoliths; or rarely, inclusions of country rock (e.g. phyllites at Lorne

and shales in the Cheviot Hills). At Auchtermuchty inclusions are abundant and show great variety. The commonest contain large crystals of pseudomorphed amphibole, plagioclase (An50 zoned to An40), a low-Cr, low-Al titanomagnetite, pleochroic apatite and rare oxidised biotite, set in a sparse matrix of devitrified glass (anals. for OC88A, Table C2). Examples of this are OC88A and D, while OC88E is a finer-grained variety with the same mineral assemblage. The host lava is very altered, but contains phenocrysts of the same minerals with additional pseudomorphed olivine. The overlying flow is xenolith-free and in addition has phenocryst diopsidic augite, whose cores are Ti- and Al-rich relative to most of the other analysed clinopyroxenes, plotting in the alkaline field of Le Bas (1962). However, it should be noted that the host rock is no more 'alkaline' than many other samples from the North Fife Hills. The similarity of the inclusion mineral assemblage and the host rock phenocrysts suggests that the xenoliths are cognate.

Other xenoliths contain pseudomorphs after olivine, orthopyroxene and (?) clinopyroxene in addition to the phases noted previously, with the possible exception of biotite. Examples of these are OC88B and OC87A (not analysed); plagioclase in OC88B zones from An84 to An57, with the more sodic plagioclase rimming partly carbonated euhedral cores. These xenoliths are sometimes layered, and may be interpreted as fragments of a layered cumulate. Accidental xenoliths include a rounded fragment of

quartzite, most probably derived from underlying O.R.S. conglomerates, and a fragment containing large elongate alkali feldspar crystals in a coarse quartz-rich mosaic. No metamorphic fragments comparable to those described by Graham and Upton (1978) from a number of localities in Carboniferous volcanic rocks have been found either at Auchtermuchty or anywhere else in the Old Red Sandstone.

Relative to other rocks of the area with comparable MgO, both groups of lavas are low in K, Th, Rb, Ba, Ce, Ni, Cr, Sc and high in Al, Fe, Ca, P, Ti, Zr and Y: there are therefore some similarities with the "trachyandesites" elsewhere in the northern Midland Valley. While the two groups of lavas have many similarities, they do not belong on the same liquid line of descent: this is particularly clear on a Ti-Y diagram (Fig. 5.8c), where Y increases with evolution of the 'aphyric' lavas, but decreases with evolution of the ol-hb-pl-phyric samples. Three of the coarse-grained amphibole-rich cognate xenoliths from Auchtermuchty have been analysed in an attempt to identify a possible bulk fractionating composition. While the compositions of the three analysed show marked differences, especially for the more mobile elements, they are all much lower in Zr, Nb and Y than the host lava, and Zr/Nb is slightly lower, in accord with the suggestion of Chapter 3 that Zr/Nb should never decrease with fractional crystallisation unless zircon is involved. The xenoliths are also very poor in Ni and Cr, which, since they contain phases with high crystal-liquid distribution coefficients

for these elements, implies that they crystallised from Ni- and Cr-poor magmas, such as their host rocks, but not OC86. It is clear from Fig. 5.8c (Ti-Y) that fractional crystallisation of the assemblage represented by these xenoliths could not generate the chemical variation of the ol-hb-pl-phyric rocks.

In contrast, the Y/Ti variation for the 'aphyric' lavas intersects the field of the xenoliths, and their variation in Ti-Y-Nb-Zr could be explained by fractional crystallisation of the xenoliths. This is not true for P, however, and it is unlikely that the assemblage of the xenoliths could crystallise from the 'aphyric' lavas. The four samples of 'aphyric' lava may be separated chemically into two pairs: in OC97 and OC99 V is much lower (60 ppm) and P_2O_5 substantially higher (0.6%) than in OC80 and 95 (115 ppm and 0.44% respectively). Other differences are:

Higher in 99 and 97: Na, Mn, Nb, Zn, Zr, Y, Nd, Zr/Nb, K/Rb, and possibly Ce, La and Sr.

Lower in 99 and 97: Ni, Sc, Ti, Ca, Al, Cu, Ba, K, Rb and possibly Th.

OC97 and 99 appear to be the most evolved: if the evolution is to be explained by fractional crystallisation then biotite must be a major crystallising phase. This is thought improbable for reasons previously stated, and in particular because it is unlikely that biotite would crystallise from a magma poor in K relative to many others in the area. The Auchtermuchty xenoliths are therefore probably only related to their host rocks, and have no

general significance, for there are no rocks which could be generated by separation of these xenoliths from a parental magma. No layered olivine-bearing xenoliths of sufficient size for analysis have been found, and it is possible that these would have more petrogenetic significance.

(c) Ol-opx-cpx-phyric samples (@9)

Rocks with this phenocryst association, together with the two North Fife "trachyandesites", outcrop on both sides of the Tay, and their close chemical similarity suggests that direct correlation could be made across the Tay. These two groups are relatively low alumina, high Cr, Ni rocks, contrasting with the "trachyandesites" of the rest of the Midland Valley. While chemically closely similar, they still display an unsystematic internal scatter for many elements (e.g. Fig. 5.8c), and it is thought most unlikely that they could be derived by fractional crystallisation of the same parent.

(d) Dundee Intrusions

The rocks of the intrusions around Dundee have between 54 and 59% silica, and show a range in Zr/Nb between the two groups described above. Even at constant Zr/Nb there is substantial chemical variation e.g. between OC137 and OC150. It is again thought that they are not very closely related.

(e) North Fife Hills : Conclusions

The Old Red Sandstone volcanic rocks of the North Fife Hills are similar to those throughout the northern Midland Valley. Again they display very varied petrography and chemistry, particularly well expressed by variation in Zr/Nb. General correlations exist between many elements and silica or MgO, but scatter on variation diagrams is probably the result of superposition of a number of chemically coherent rock groups. Identification of these groups is not practical and, by analogy with the Montrose region, it is believed that very few compositions could be related by fractional crystallisation processes. The unusual occurrence of xenoliths of cumulate appearance at Auchtermuchty probably has no general petrogenetic significance.

In previous sections the possibility of generating high alumina basalt by separation of olivine and clinopyroxene from olivine-tholeiite has been discussed. In the North Fife Hills there exist a number of high alumina basalts with high MgO, Ni and Cr. Most prominent amongst these are OC102, with 17.5% Al_2O_3, 183 ppm Ni and 330 ppm Cr, and OC85, which, if they represent liquid compositions, require the existence of primitive high-alumina magma. It is difficult, however, to rule out the possibility of plagioclase accumulation in either of these samples.

5.5 : NORTH MIDLAND VALLEY : CONCLUSIONS

The Old Red Sandstone volcanic rocks of the northern Midland Valley show great variety in detailed chemistry, but there are many broad petrochemical features in common between the several outcrop areas.

(a) Mineral Chemistry and Petrography

Most clinopyroxenes analysed from rocks of the northern Midland Valley are diopsidic augites low in Na, Ti and Al, very similar to those analysed from the SW Highlands. Variation between phenocrysts in a single rock is often large; while a few analysed points have Ti and Al concentrations within the alkaline field of Le Bas (1962), the vast majority are subalkaline (Fig. 5.9b). Pyroxene Ti and Na show broad correlation with their host rock chemistry (e.g. Fig. 5.9a), but it is believed that the Ti, Na, Al content of a particular pyroxene was mainly controlled by localized melt heterogeneities produced during rapid crystallisation. Fs content does not increase systematically with host rock silica (Fig. 5.9d), although there is a broad correlation with host rock FeO/(FeO+MgO). The small variation in Fs content of clinopyroxene, and the generally bronzitic composition of orthopyroxene (Fig. 5.9c), even in siliceous rocks, suggest that the host rocks are of calc-alkaline rather than tholeiitic affinities. The few fresh olivines are Mg-rich, with the exception of that from a small gabbroic intrusion near Glenfarg.

Fig. 5.9 a & b : Phenocryst chemistry of North Midland Valley O.R.S. volcanic and intrusive rocks.

a = clinopyroxene TiO_2 as a function of host rock TiO_2

b = clinopyroxene TiO_2 and atomic tetrahedral Al

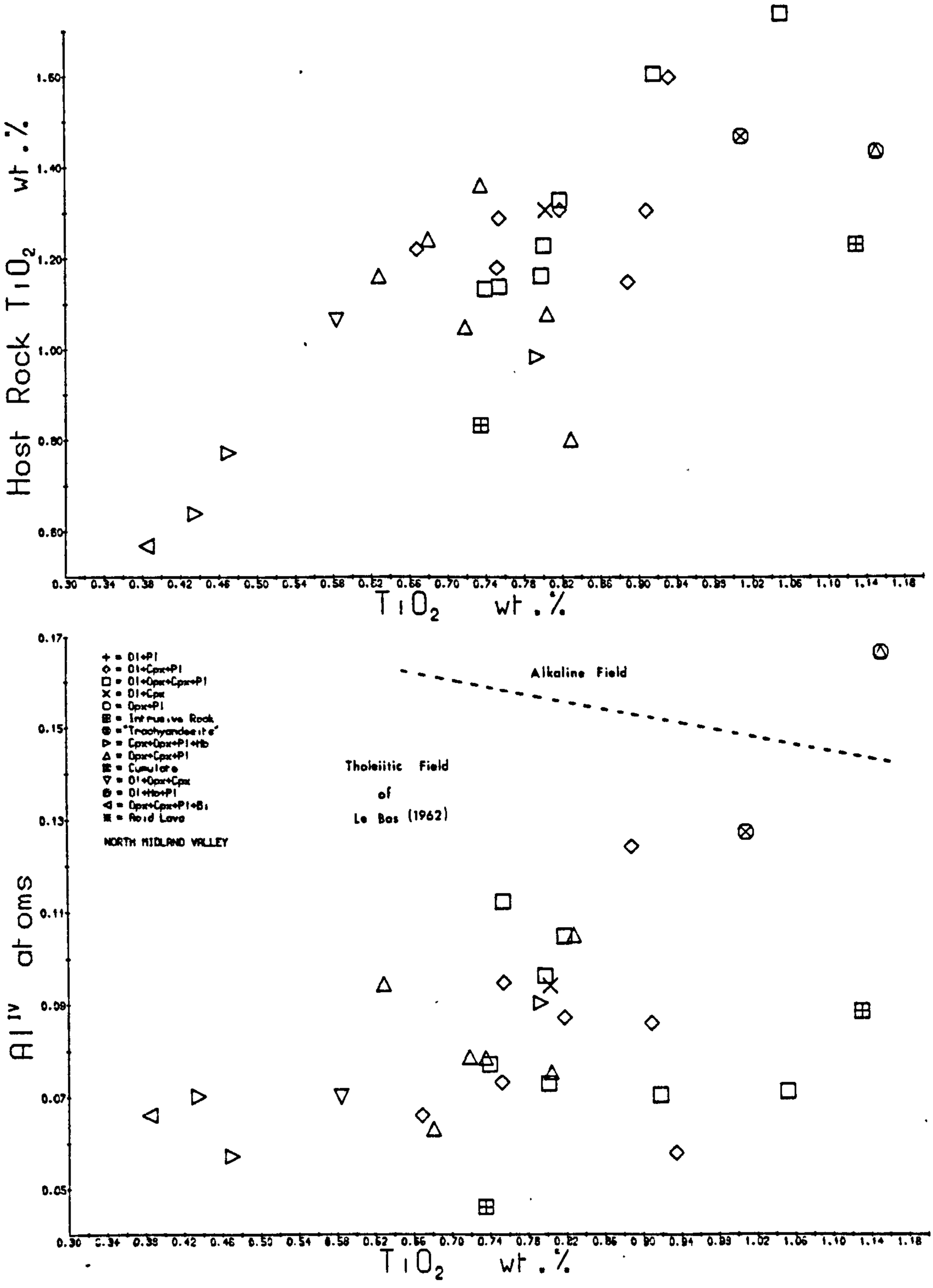

Fig. 5.9 c & d

c = atomic Ca, Mg, Fe for pyroxenes, olivines and amphiboles

d = the composition of clinopyroxene as a function of host rock silica

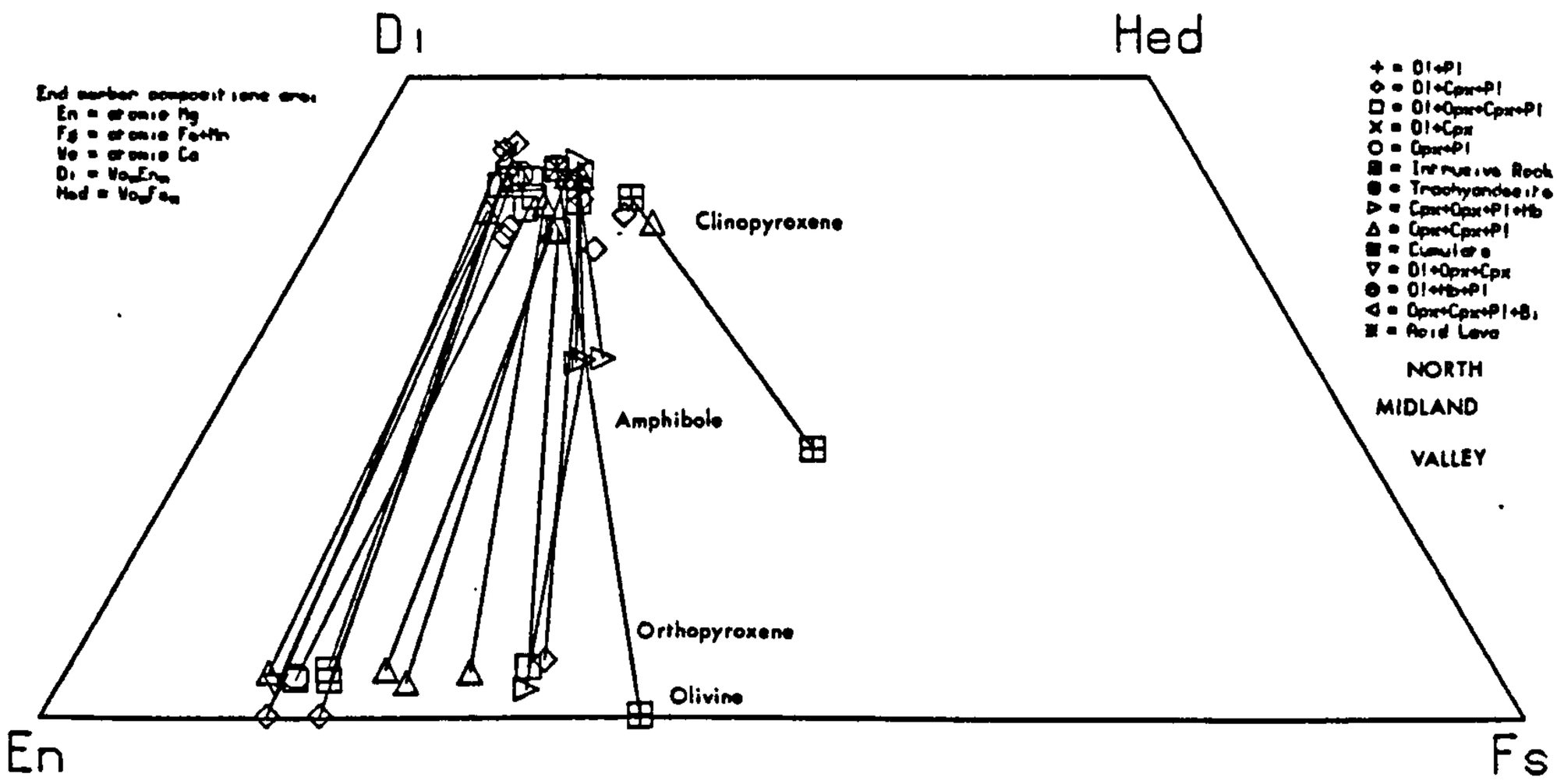

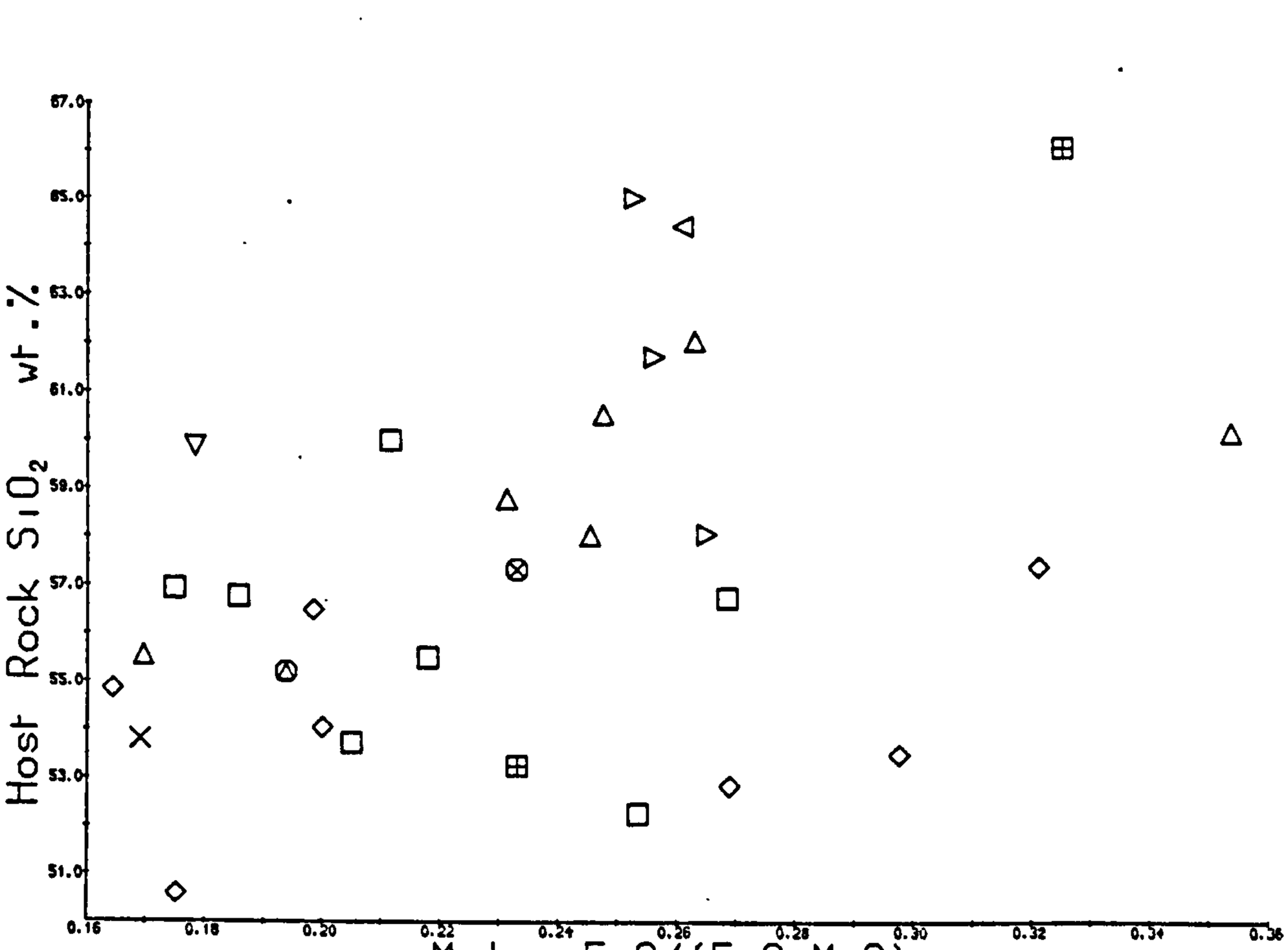

Fig. 5.9 e & f

e = plagioclase end-members

f = the composition of plagioclase as a function of host rock silica

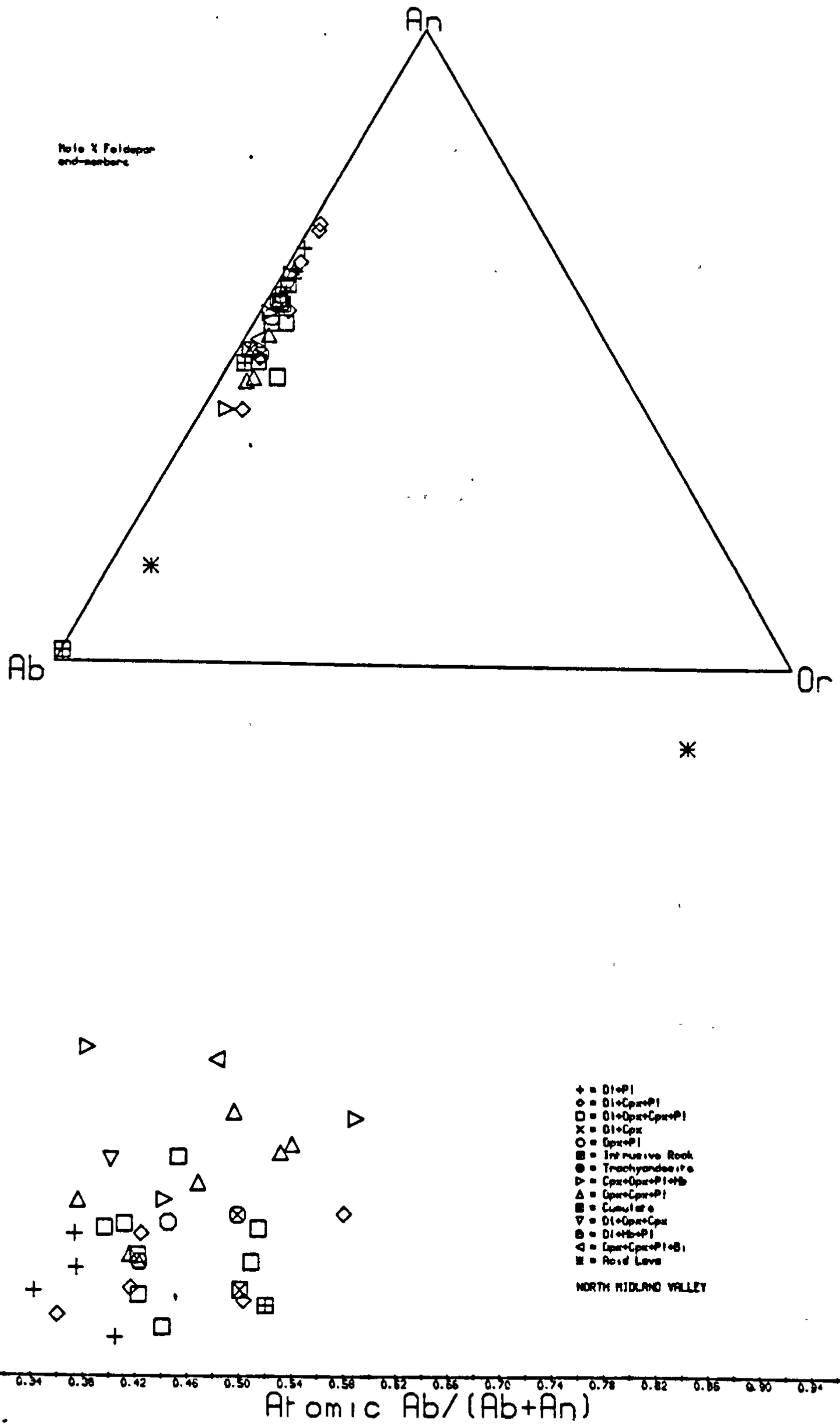

Most of the rocks analysed contain phenocryst plagioclase, contrasting with the rocks of the SW Highlands. This is generally labradorite-andesine, and its composition shows little correlation with host rock silica content (Fig. 5.9f). Or content of plagioclase may be related to host rock potash or to coexistance with K-rich phases, so that the plagioclase from hornblende- and biotite-bearing andesites generally has lower Or (Fig. 5.9e). Spinels are Cr-, Al-poor titanomagnetites, although those from OC152 contain up to 10% Cr_2O_3.

(b) <u>General Chemical Characteristics</u>

Very few of the rocks analysed have normative nepheline, and, when they do, it is probably always due to the secondary introduction of calcite. The rocks are dominantly quartz-normative, although a few are mildly olivine-normative. Rocks with >62% silica are often peraluminous. Most rocks have low Fe/Mg, and only a very small number plot outside the calc-alkaline field of Miyashiro (1974). The inference that the lavas are calc-alkaline is further supported by the high-alumina nature of many. The lavas all have high concentrations of LIL and high field strength elements, and vary between calc-alkaline and shoshonitic on the classification of Peccerilo and Taylor (1976). Many rock analyses compare closely with average data from several continental margin calc-alkaline suites reported by Ewart (in press).

While a wide range in silica concentrations is represented in the region, most rocks have less than 60%. This is particularly true for the North Fife and Sidlaw Hills and for the Montrose area, but acid andesites are not uncommon in the western Ochil Hills. This latter area and the Sidlaw Hills are poor in very Ni-, Cr-rich rocks relative to the other two, although such rocks do exist in all areas. These rocks can not have undergone much separation of mafic mineral phases since derivation from a mantle source region.

(c) Constraints on Petrogenetic Models

It is clear from the variation diagrams that the different rock-types can not be related by a single petrogenetic process. In particular, the great variation in relative and absolute amounts of LIL and high field strength elements shows little correlation with concentrations of elements compatible in mafic mineral phases, and can therefore not be due to multistage fractional crystallisation processes. The origin of some small groups of rocks by fractional crystallisation of a range of parental Ni-, Cr-rich magmas is however possible. For example, the siliceous, Cr-rich bronzite-andesites may have been generated by separation of plagioclase, while the Ni-, Cr-poor high-alumina samples may have been generated by separation of mafic mineral phases. For both of these however, magmas with sufficiently low concentrations of LIL elements to be parental are absent or very rare. Arguments

based on volume relations therefore suggest that many low-Ni, -Cr lavas may therefore be only slightly modified primitive melts, for large quantities of more mafic magmas not parental to these were able to reach the surface. It remains possible that all low-Ni, -Cr samples were derived by fractional crystallisation of mafic magmas essentially unrepresented at the surface.

The following hypotheses are possible:

1/ Most of the lavas seen at the surface are primary melts only slightly modified by fractional crystallisation during ascent, whose LIL and high field strength element geochemistry implies variation in source composition (Zr/Nb ratio), and probably also variation in degree of partial melting, nature of residuum etc. This requires an extremely heterogeneous mantle, and generation of the large volume of rocks very rich in LIL elements would require a very incompatible element-enriched mantle or the coalescence of melts from unreasonably large regions of mantle (section 4.4).

2/ The Ni-, Cr-, Mg-rich lavas seen at the surface are only slightly modified primary melts as before, but others are products of the fractional crystallisation at crustal levels of magmas not represented among the more mafic lavas of the area. This would imply the existance in the same area of large volumes of varied mafic magmas which fractionally crystallised and never reached the surface, and of further large volumes of varied mafic magma which reached the surface but did not undergo high level fractional

crystallisation. Those magmas which did not reach the surface must have been much poorer in LIL and high field strength elements than observed mafic lavas and therefore, since exposed mafic lavas may have high LILE content, the variation in LILE of primary melts must have been very large, and the mantle source much more heterogeneous in LILE than required by the first hypothesis. Neither of these hypotheses is therefore satisfactory.

3/ Variation in LILE and high field strength elements may have been superimposed on a small range of major element compositions by processes such as contamination or magma mixing. The major element compositions may have been generated by fractional crystallisation of a single parent magma, or may themselves represent only slightly modified primary magmas. In the latter case, equilibration with mantle can not have occurred for the more siliceous lavas, and in the former several different fractional crystallisation paths are required to generate the variety of major element-Ni-Cr compositions observed. These difficulties may be easily overcome by allowing some modification of major element chemistry by the contamination, although the most attractive feature of the hypothesis is the use of a contaminant enriched in LIL and high field strength elements to provide the high concentrations of these in the northern Midland Valley lavas.

There are strong parallels with the chemistry of the SW Highland lavas, for which three controlling processes

were inferred (section 4.4) on the basis of correlations between LIL and high field strength elements. Similar positive correlation exists in the north Midland Valley lavas (Fig. 5.10), both among Ni- and Cr- rich lavas of the whole region, and for most rocks in the individual outcrop areas. Few of these correlations are very good, and a simple binary contamination model is most unlikely. Positive correlations of note include SiO_2:La/Y, Zr:Nb, K:Rb, K:Ba, Sr:Ba, Sr:La/Y, Ti:Y and also Ce+La+Nd:Zr. The ΣLREE:Zr correlation is in contrast to the lack of correlation between Ce and Zr at Lorne. There may also be negative correlation between Sr and Y.

Positive correlations between these elements can not in general be explained by fractional crystallisation of mafic mineral phases, for enrichment in LILE is unrelated to depletion in Cr. Some scatter on diagrams involving Sr may be attributed to fractional crystallisation of plagioclase, but scatter on Zr-Nb and ΣLREE-Zr diagrams implies that the contamination process was not binary, for Zr/Nb and Ce/Zr show much variation at constant Zr. No correlation between Zr/Nb and other parameters has yet been found.

No evidence for the origin of the contaminants is yet available from isotopic work. The resemblance of the correlations between LIL elements in the north Midland Valley rocks to those in the ol- and ol-cpx-phyric rocks of Lorne strongly suggests that the same process gave rise to variation in LILE concentrations in both regions. Since the

low initial $^{87}Sr/^{86}Sr$ from Lorne implies a mantle origin for the Sr, it would be reasonable to infer that the concentrations of LILE in the northern Midland Valley rocks also have a mantle origin. It follows from this inference, and the discarding of hypothesis 2, p. 163, that a number of quite silica-rich magmas were present in the mantle prior to contamination with LILE.

The Old Red Sandstone volcanic rocks of the Northern Midland Valley are a calc-alkaline to shoshonitic suite with high concentrations of LIL and high field strength elements, and in many rocks, high Ni and Cr. The latter rocks can have undergone little fractional crystallisation of mafic minerals since separation from a mantle source, and there is evidence to suggest that many low Ni, Cr lavas may also not have suffered much fractional crystallisation. Enrichment and variation in incompatible element concentrations and ratios may best be explained by a complex contamination process, possibly involving contamination in both mantle and crust.

NORTH MIDLAND VALLEY

Fig. 5.10 a & b : Some relationships between LIL and high field strength elements in North Midland Valley O.R.S. igneous rocks. All samples plotted have >80 ppm. Ni and >140 ppm. Cr. Conventions as section 3.3

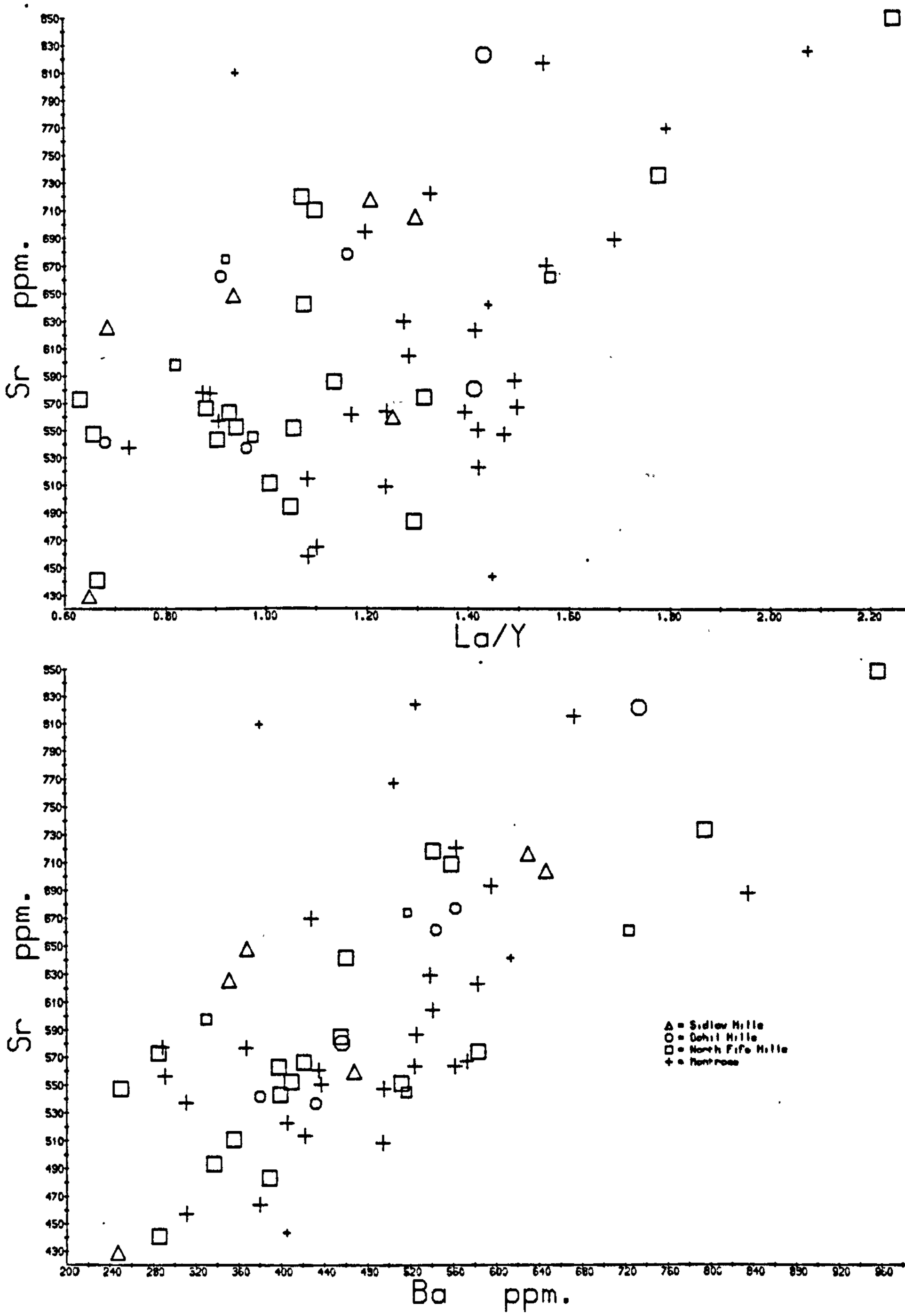

NORTH MIDLAND VALLEY

Fig. 5.10 c & d

All samples plotted have >80 ppm. Ni and >140 ppm. Cr.

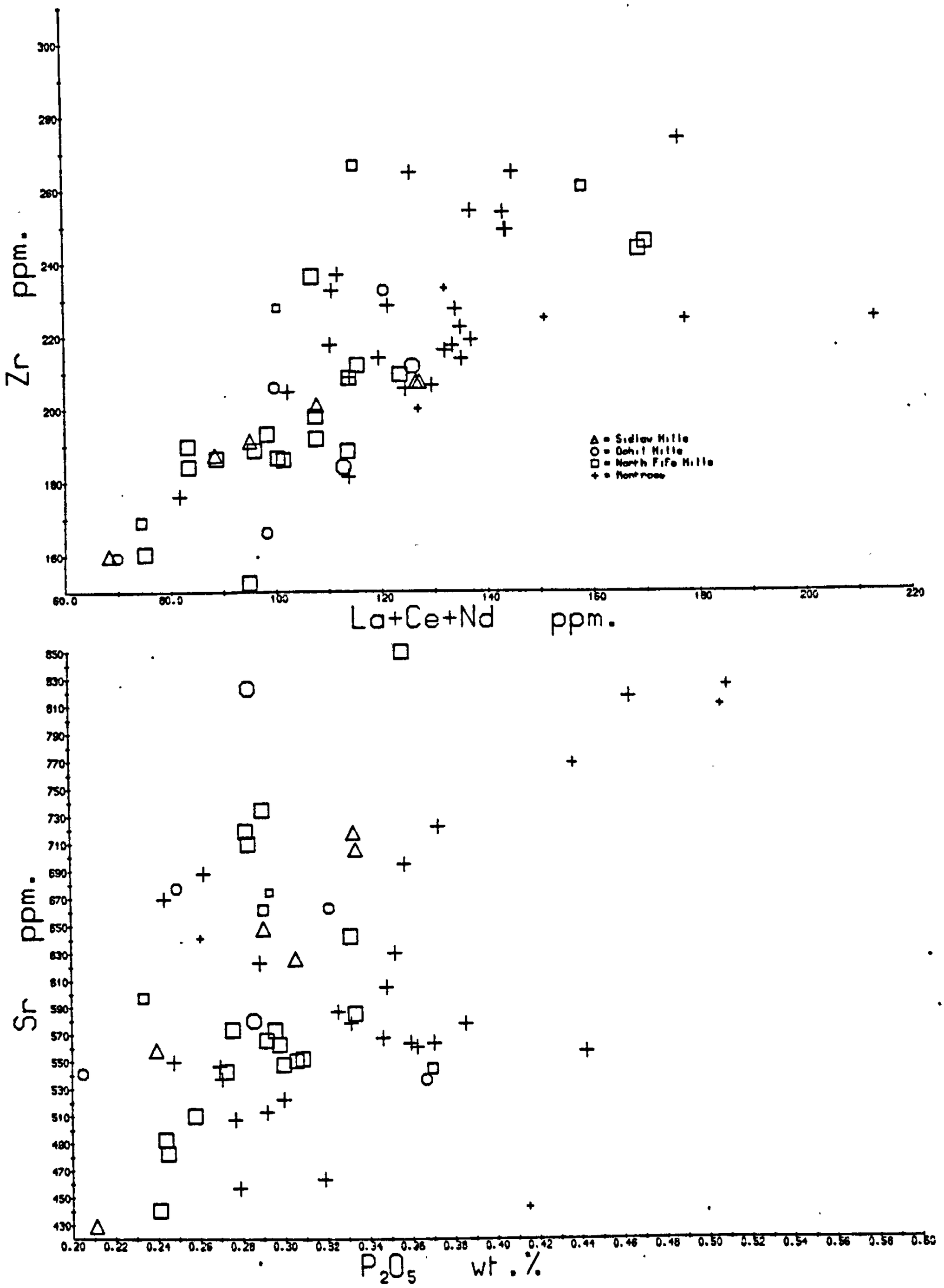

SIDLAW HILLS

Fig. 5.10 e & f

Full sample population from Sidlaw Hills is plotted.

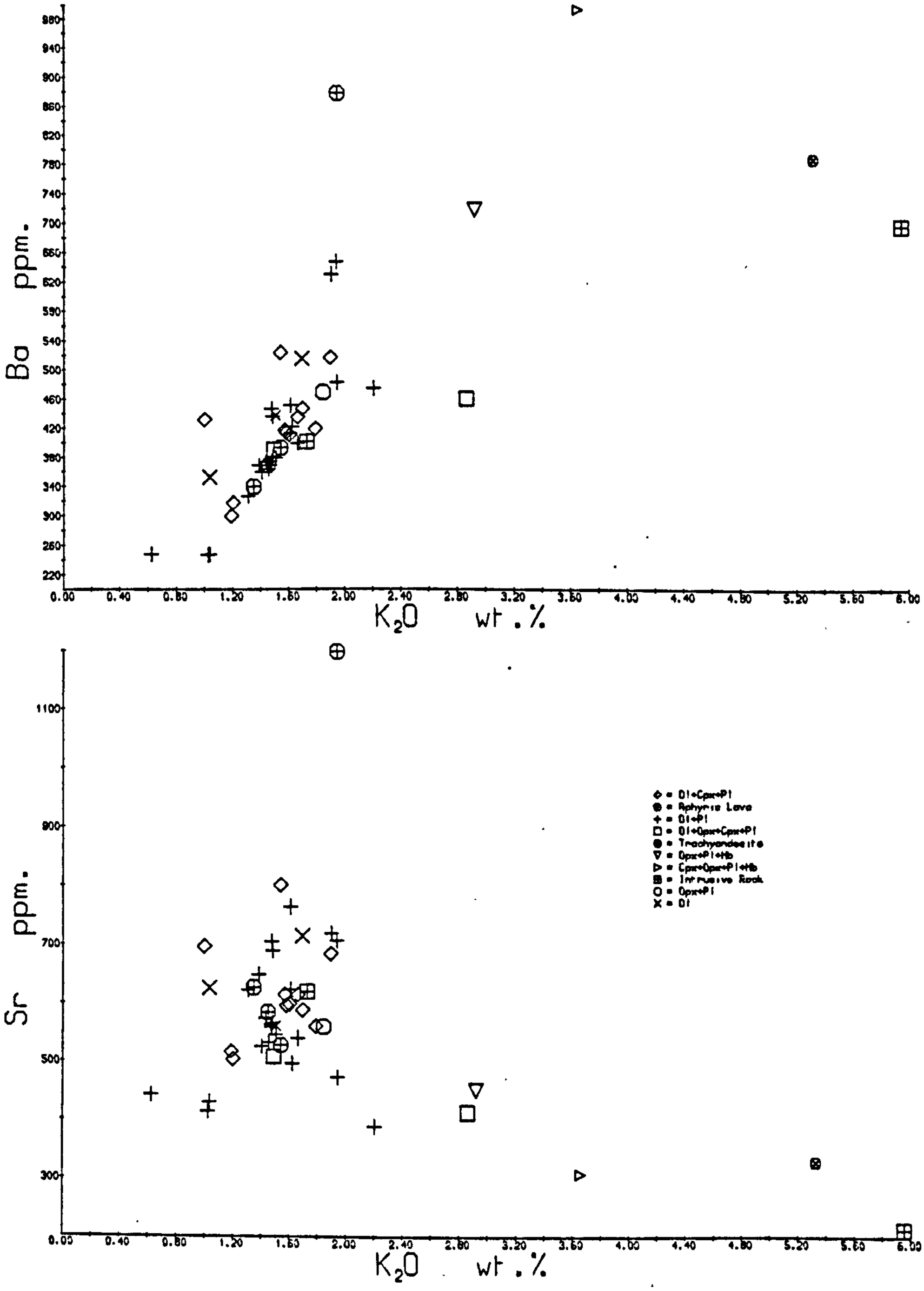

SIDLAW HILLS

Fig. 5.10 g & h

Full sample population from Sidlaw Hills is plotted.

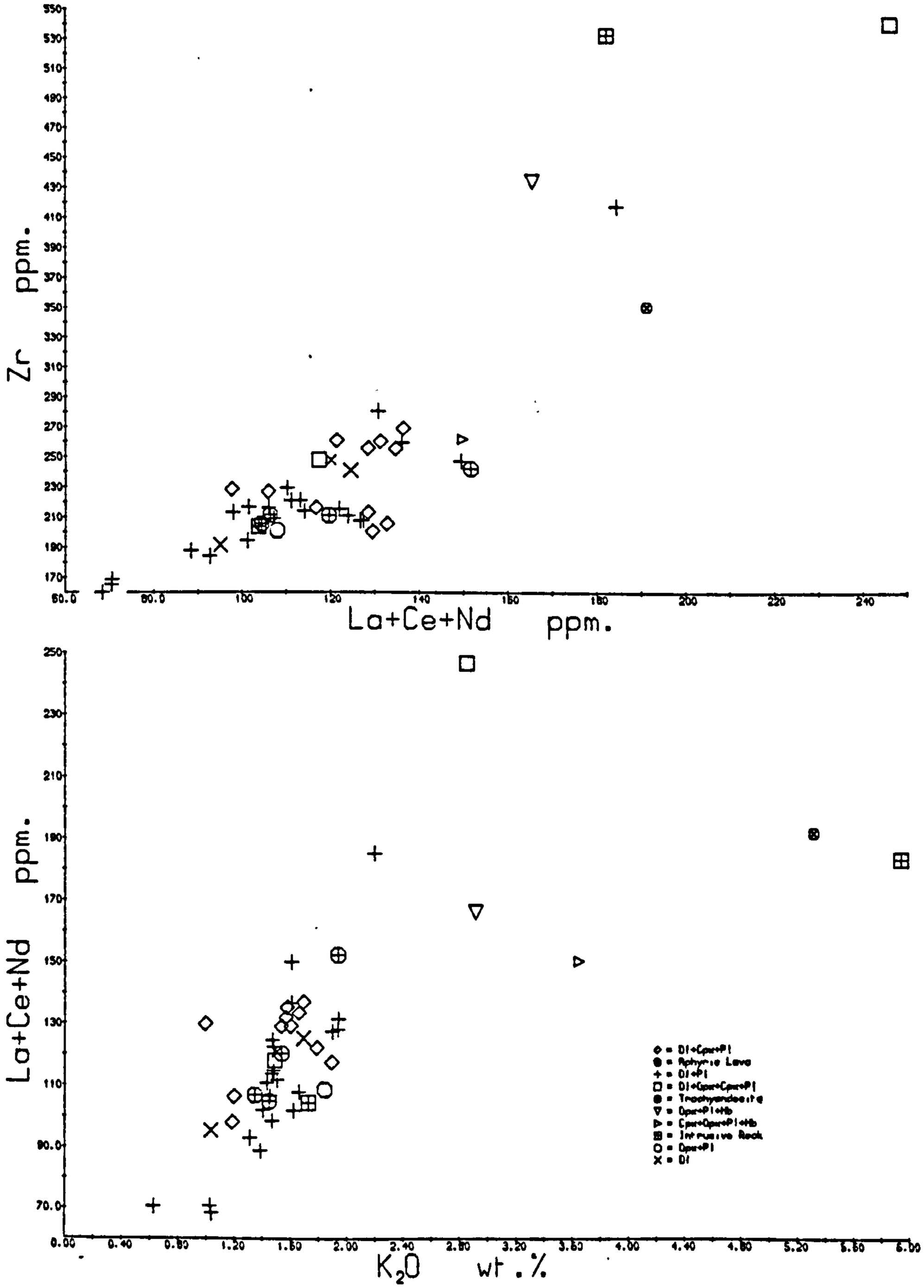

CHAPTER 6 : SOUTH MIDLAND VALLEY

The Lower Old Red Sandstone rocks of the southern Midland Valley outcrop discontinuously in a range of hills just north of the Southern Uplands Fault. In the NE Lower O.R.S. conglomerates rest unconformably on a sequence of sandstones and mudstones, some of continental facies, which may possibly all be of pre-Wenlock age (Mitchell and Mykura, 1962). Further SW, Lower O.R.S. rocks appear to rest conformably on the Silurian rocks of the Lesmahagow and Hagshaw Hills inliers (M. Gallagher, pers. comm., 1979), where again continental facies sediments occur higher in the Silurian sequence, and the youngest graptolite fauna recovered is upper Llandovery. Further SW in Ayrshire, the Lower O.R.S. rests unconformably on Ordovician strata. Throughout the region, Upper Old Red Sandstone and Carboniferous sediments rest unconformably on the Lower O.R.S.

The region is structurally more complex than the regions previously discussed, and the Lower O.R.S. is much folded and faulted, in particular close to the Southern Uplands Fault. The volcanic rocks of the Pentland Hills and of the Carrick Hills in Ayrshire are only gently inclined, and Mykura (1960) and Eyles *et al.* (1949) have described stratigraphical sequences in these areas, with total thicknesses of volcanic rocks in excess of 6000 ft (2000 m) and 1500 ft (500 m) respectively. Thicknesses of volcanic rocks in the smaller discontinuous outcrops close to the

Southern Uplands Fault or in the small region west of Distinkhorn are not known, but in some areas these must be well in excess of 1000 ft (300 m ; e.g. near Biggar). The rocks of these areas have been described by Geikie (1897) and by Richey et al. (1930). The volcanic rocks of the region can easily be divided into a number of outcrop areas, and each area could be treated separately, but unfortunately, with the exception of the Ayrshire Coast, exposure is very poor throughout the region and the rocks in many exposures are too severely altered to be suitable for detailed petrochemical study. The region has therefore been divided into the two areas of Ayrshire and the Pentland Hills; the former includes the Carrick Hills and the areas near Distinkhorn and Straiton, and is separated by some very poorly exposed ground near Dalmellington from the most southwestern of several discontinuous outcrops assigned to the Pentland Hills.

6.1 : THE PENTLAND HILLS

The stratigraphy and petrography of the volcanic rocks of the Pentland Hills (sensu stricto) have been described by Mykura (1960) and Peach et al. (1910). These authors have separated the sequence into a number of groups characterized by being dominantly basic, "trachytic", or acidic. The sequence dips gently SE and is overlain by westward-dipping Upper O.R.S. and Carboniferous sediments in the west. The top of the volcanic sequence is cut off by the Pentland Fault in the east, although rocks to the north

of the main hill-range are thought to be at a higher horizon (Mitchell and Mykura, 1962). None of the subdivisions of the Pentland sequence can be traced further SW than Carlops. The volcanic rocks and underlying Silurian are cut by a number of intrusions, of which the Lyne Water Diorite and the Tinto and Black Hill Felsites are the largest. Mykura (1960) suggested that the Black Hill Felsite could have been an extrusive dome.

The volcanic sequence is mainly composed of lava flows, although acid pyroclastic horizons are not uncommon, particularly near West Linton. A wide range of lava lithologies has been observed among the samples collected, and, since exposure is poor and degree of alteration high, it is likely that these form only a small part of the range actually present. Most of the samples collected are closely comparable with lithologies present in the northern Midland Valley, although basic samples lacking phenocryst plagioclase are more common in the Pentland Hills, as are acid rocks, while rocks with phenocryst clinopyroxene are relatively rare. Phenocryst compositions are closely comparable to those in the north Midland Valley.

Samples from the Pentland Hills show a comparable chemical range to that described from the northern Midland Valley, with large scatter on most variation diagrams (Fig. 6.1). The occurrence of rocks with silica as low as 47% is in contrast to the 50% minimum of the north Midland Valley, while rocks with silica >60% are not uncommon. A number of

PENTLAND HILLS

Fig. 6.1 a & b : Bulk rock variation diagrams

Conventions as section 3.3

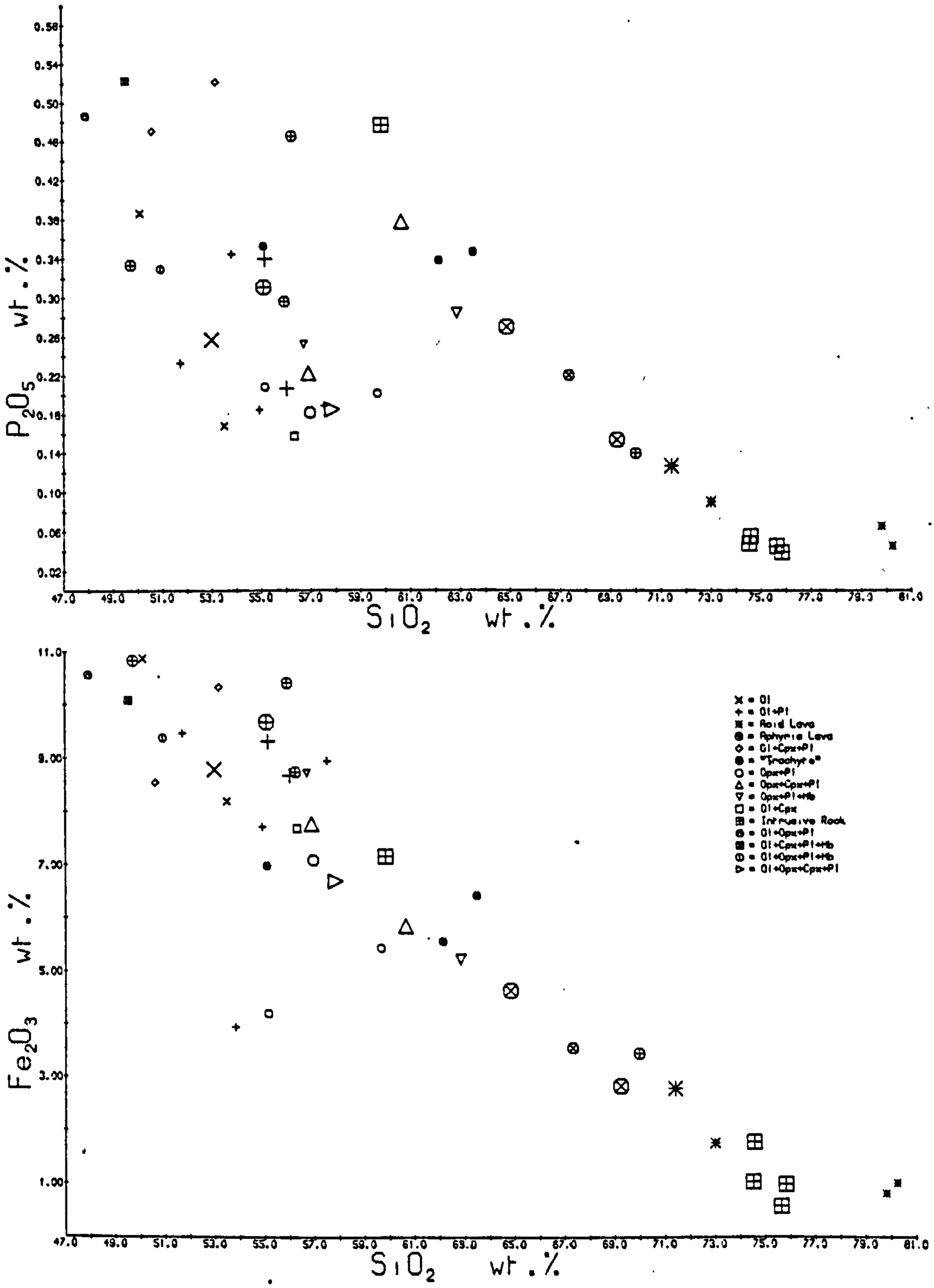

PENTLAND HILLS

Fig. 6.1 c & d

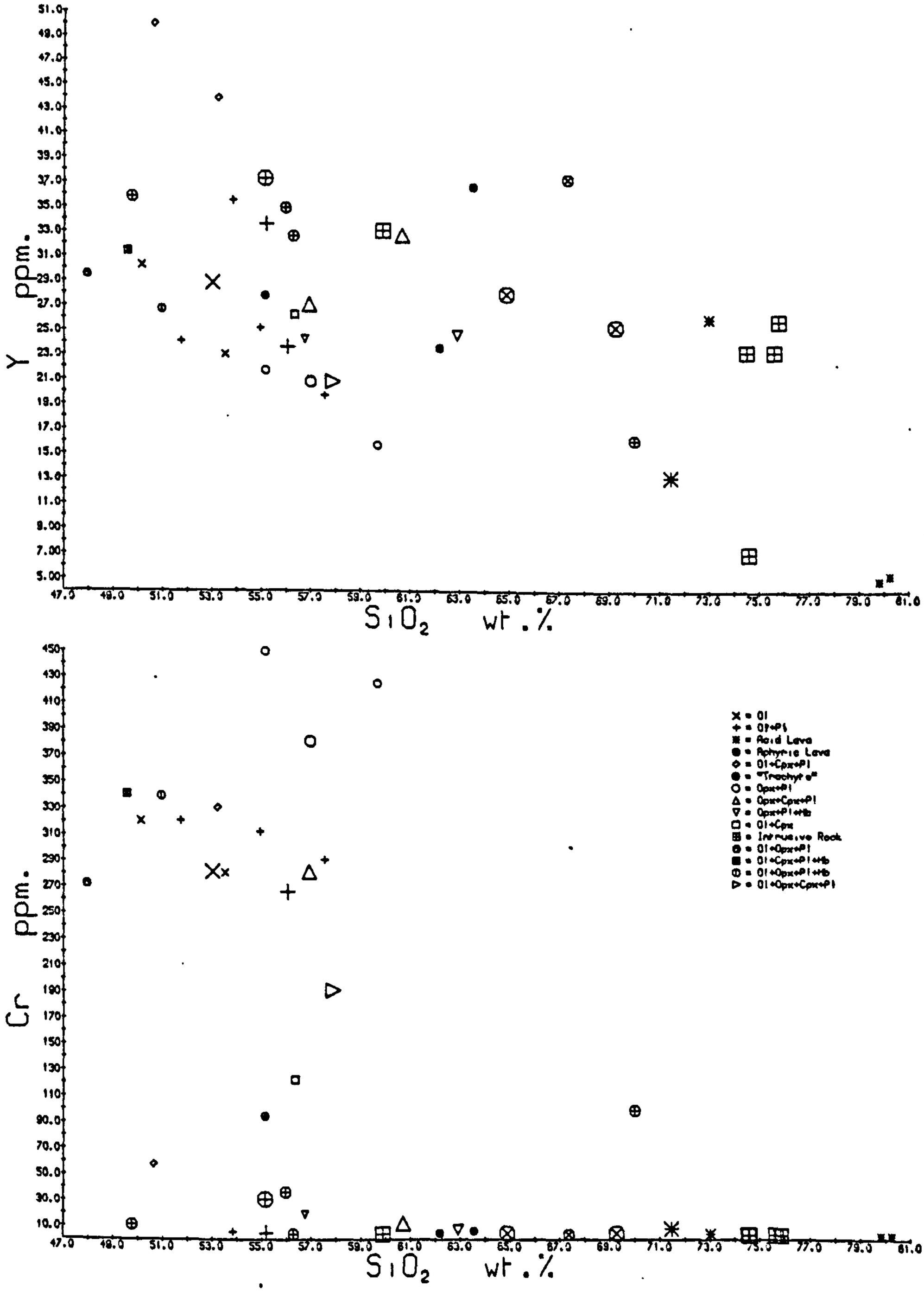

PENTLAND HILLS

Fig 6.1 e & f

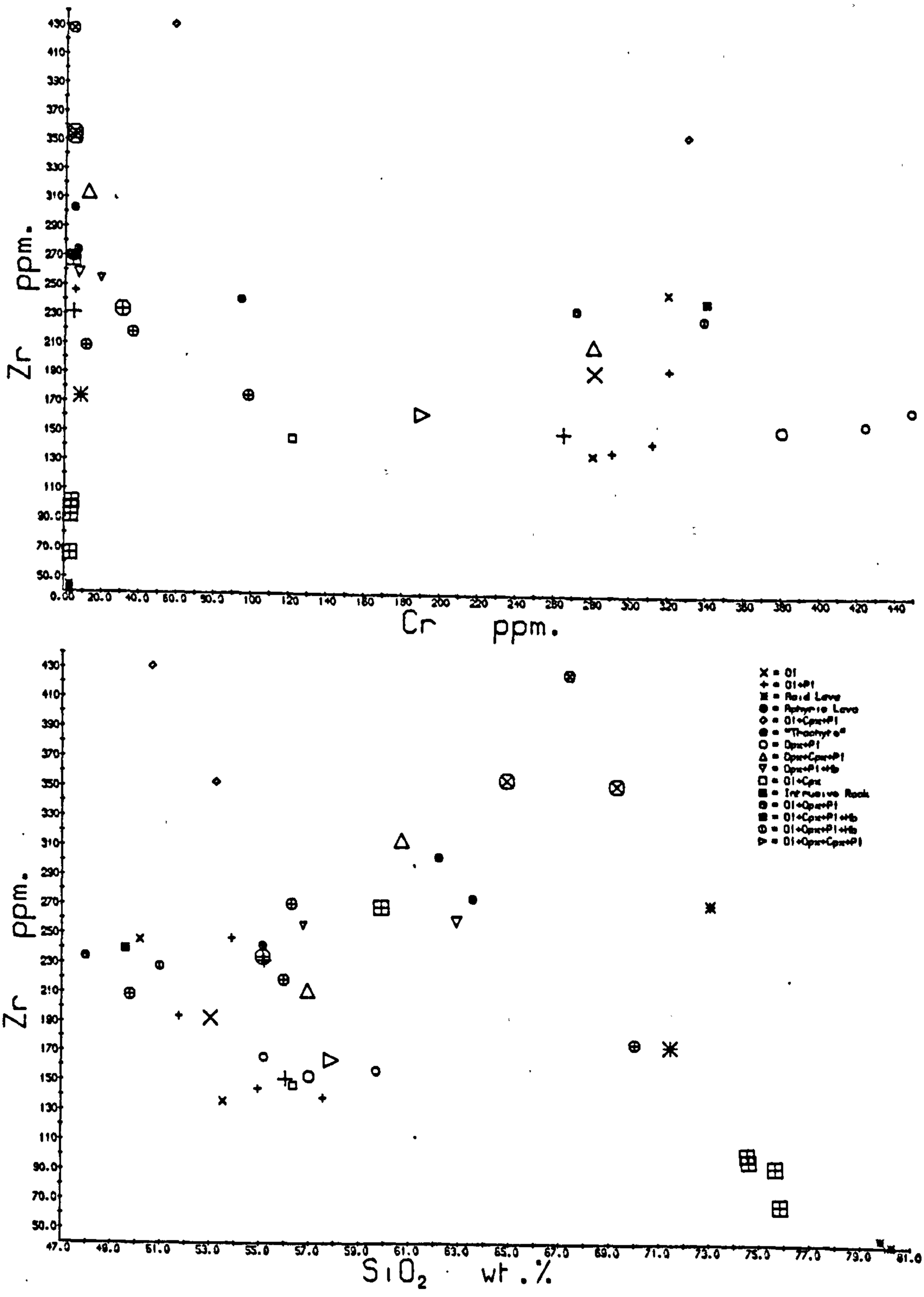

rocks are strongly nepheline-normative, but these all show high LOI and CaO, and the nepheline can be attributed to introduction of calcite on alteration. Only one relatively fresh rock (PE5) has normative olivine. Basic rocks include both moderate- and high- alumina types, and Ni and Cr may be high in both. LIL and high field strength elements show much variation unrelated to SiO_2, MgO or Cr concentrations, but concentrations of LIL elements in many rocks are closer to typical calc-alkaline values (Jakeš and White, 1972) than in rocks from further north. Zr/Nb varies between 12 and 32 in basic rocks, and shows no systematic variation with Cr content. There does not appear to be any relationship between chemistry and position in the stratigraphic succession of Mykura (1960), and the data available suggests that the Allermuir Group, at least, does not have any distinctive chemical features, but itself shows great variety. The arguments discussed in sections 5.1(i) and 5.5 again apply, and suggest that no extensive liquid line of descent generated by fractional crystallisation or partial melting exists among the rocks of the Pentland Hills and areas to the SW.

The occurrence of three andesites (PE14-16, 55-60% SiO_2) comparable to the bronzite-andesites of the north Midland Valley is notable. These are the most Cr-rich rocks in the area (370-450 ppm) and are also very Ni-rich (150-250 ppm), and presumably have similar petrogeneses to the north Midland Valley bronzite-andesites. It is unlikely that these rocks could be related by fractional crystallisation,

for Zr/Nb shows significant variation (12-17).

With the exception of one of the bronzite-andesites, all samples with more than 59% silica show good negative correlation with silica for P, Fe, Al and Ti, which could be taken to suggest a close genetic relationship (e.g. by fractional crystallisation). This group includes all rocks mapped as trachytes by Mykura (1960), which, as with the "trachyandesites" of the northern Midland Valley, are no more alkaline than many rocks mapped as andesites. With one exception all these rocks have low Ni and Cr. Despite the appearance of being closely related, Zr, Nb and Y do not vary systematically, and Zr/Nb again shows very low values in the most siliceous rocks (2-6). The variation in Y is particularly notable in samples from the Tinto Felsite, from which garnet has been recorded (Herriot, 1956). The one garnet-bearing sample (PE28) has much lower Y than the other three (Fig. 6.1), and also has lower Sc, elements which partition strongly into garnet (Chapter 3). This suggests that garnet separation may have occurred during ascent of the magma, a view which is supported by the observed zonation of garnet crystals (Table C3) from relatively grossular-rich to spessartine-rich compositions. Comparison with the data of Green (1977) suggests that generation of these silicic melts occurred below 20 km depth (<7% spessartine in core compositions).

As with the rocks of the northern Midland Valley there are broad correlations between concentrations of

PENTLAND HILLS

Fig. 6.2 a & b : Bulk rock variation diagrams

Conventions as section 3.3

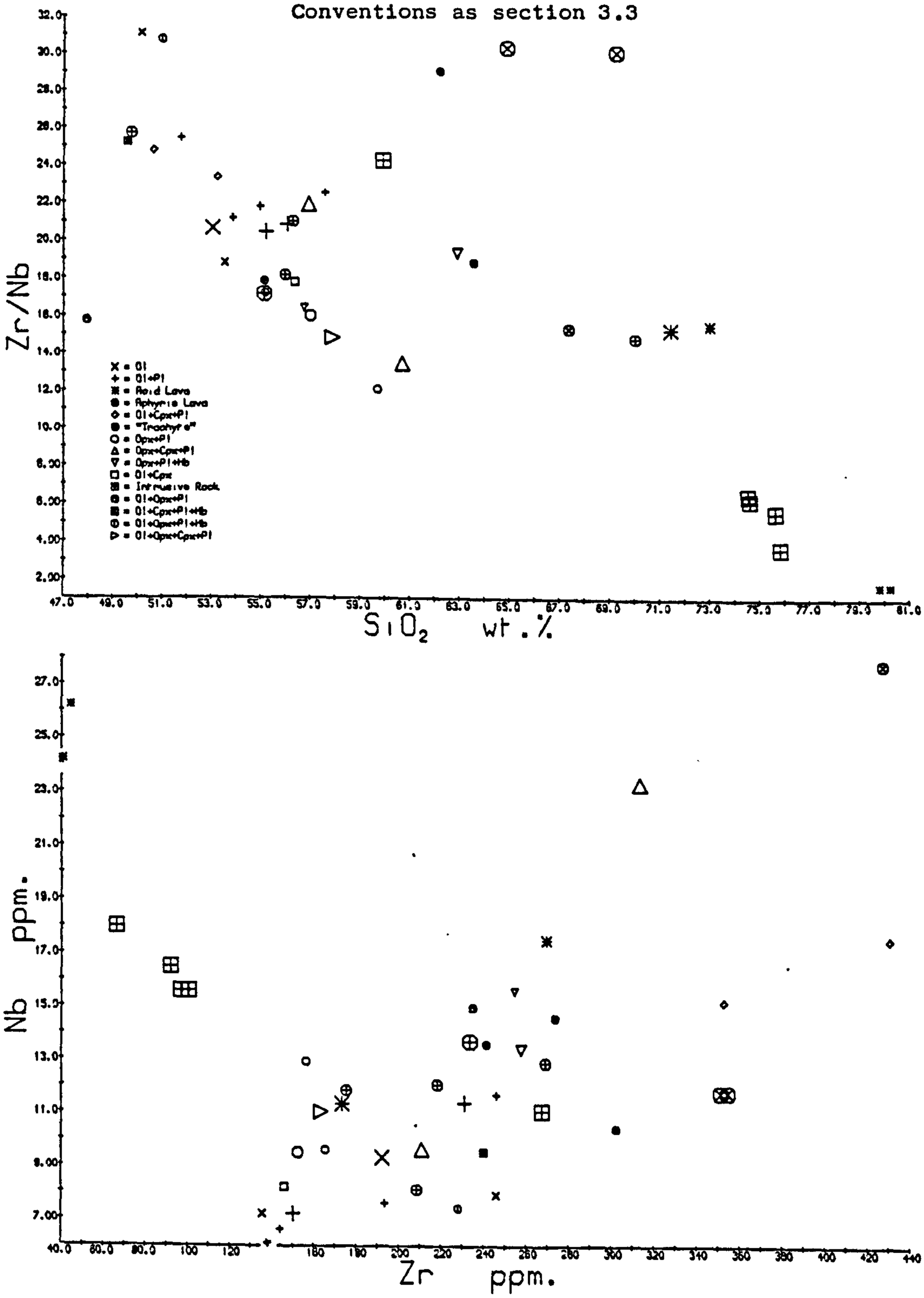

PENTLAND HILLS

Fig. 6.2 c & d

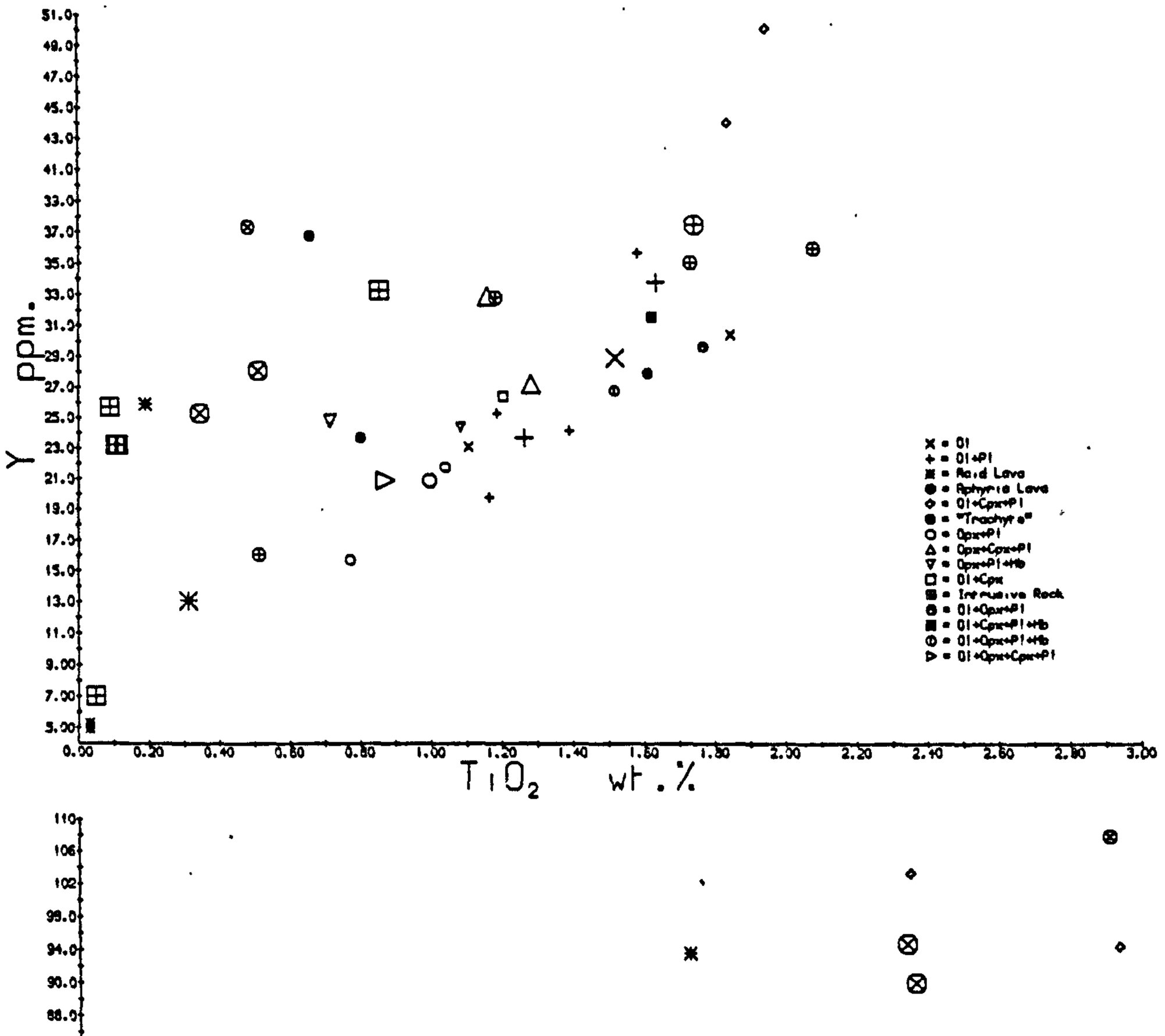

PENTLAND HILLS

Fig. 6.2 e & f Vertical lines for samples with > 58% SiO_2

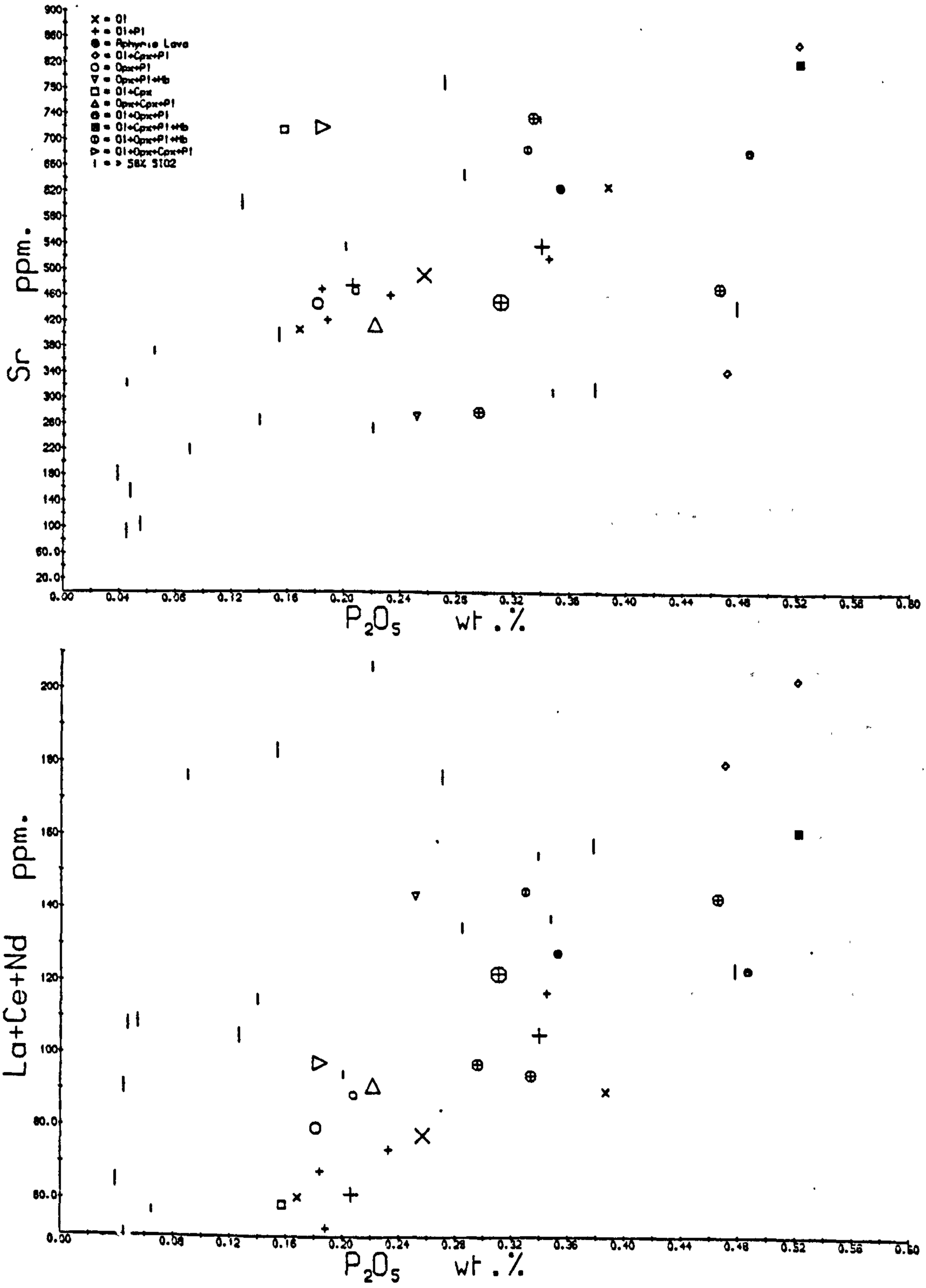

various pairs of LIL and high field strength elements in less siliceous rocks (<58% SiO_2; Fig. 6.2). Zr-Ce and Ti-Y correlations are particularly good, but with the exception of P-ΣLREE, the poor correlations between LIL elements may be the result of the mobility of Sr, Rb, K and Ba during alteration. Despite this, the broad correlations between LIL elements include concentrations lower than many from the northern Midland Valley. Decrease in Zr/Nb appears to correlate broadly with decreasing Ti and increasing SiO_2, in contrast to the rocks from further north.

6.2 : AYRSHIRE

The volcanic rocks of the Ayrshire Lower Old Red Sandstone outcrop in three main areas: the gently northward-dipping mass of the Carrick Hills and neighbouring coast, a small synclinal area near Distinkhorn and an intensely faulted area at Straiton, close to the Southern Uplands Fault. In all areas, a considerable thickness of sandstones and conglomerates outcrop below the lavas, which in the first two areas rest unconformably on the Llandovery and Ordovician rocks of the Straiton region. In all three areas the top of the volcanic sequence is cut off by the unconformity at the base of the Upper O.R.S. A number of intrusions are present in each area, of which the most important are the large Distinkhorn granodioritic complex and the Fore Burn Complex near Straiton. The Distinkhorn Complex has some similarities with the granodiorites of the Southern Uplands (Pidgeon and Aftalion, 1978).

Pyroclastic rocks are again uncommon in the volcanic sequences of all three areas, and the range of lava lithologies described by Tyrell (1913) is smaller than in the Pentland Hills. Acid rocks are only present as intrusions or as clasts in some of the interbedded conglomerates, although some of the lavas mapped as andesites (Eyles et al., 1949) may be dacitic (e.g. AY12). The bulk of the rocks collected contain phenocryst plagioclase and orthopyroxene, in association with olivine and sometimes clinopyroxene in more basic rocks, or with clinopyroxene alone in more siliceous rocks, but there is no precise relationship between phenocryst mineralogy and host rock silica. Hornblende phenocrysts are restricted to the more siliceous rocks, and biotite is absent.

Orthopyroxenes are usually bronzitic, and clinopyroxenes the typical diopsidic augites low in Ti, Al and Na, even in rocks with 65% SiO_2 (AY12), but pyroxenes analysed from two samples (AY35, 38) from the Straiton area are unusually iron-rich, although the host rocks do not have particularly high Fe/Mg. These relatively iron-rich pyroxenes zone to more normal Mg- and Cr-rich compositions, suggesting that the cores did not crystallise from their host magma. These clinopyroxenes typically show much chloritic material after exsolution lamellae parallel to (001): this is interpreted as the alteration product of exsolved pigeonite. Phenocryst plagioclase is generally labradorite-andesine, but calcic bytownite occurs in one of the Straiton samples (AY38) and zones to andesine.

All except six altered rocks are quartz-normative, and except for an acid sill, all rocks collected have between 50 and 66% SiO_2. No element shows good linear variation with silica (Fig. 6.3); however, K (Fig. 9.1) and Rb show a relatively unscattered enrichment with SiO_2 increase while Fe, Mg, Ca, V and Sc show a concomitant highly scattered decrease. The whole rock chemistry does not appear to be related to phenocryst association, geographic location or stratigraphical position. Use of MgO or Cr as indices of variation does not improve the scatter; Cr and Ni in particular show no systematic variation with either MgO or SiO_2, and LIL and high field strength elements tend to show rough <u>positive</u> correlation with Cr.

Zr/Nb shows substantial variation (16-31) which is not correlated with Cr content, and, in contrast to the Pentland Hills, it does not appear to have negative correlation with SiO_2 or TiO_2. However, there is again a prominent positive correlation between Ti and Y (Fig. 6.4), and between La/Y and silica. It is notable that samples from Distinkhorn tend to show higher, and those from Straiton lower than average La/Y and Sr, and hence, for more basic rocks, there is a poor Sr-La/Y correlation. Values for both of these are distinctly lower than their values in the north Midland Valley, as are concentrations of LREE and P. However, there is no Sr-P or K-Zr correlation, and Zr-Ce correlation is poor.

It is clear that there is again no extensive liquid

AYRSHIRE

Fig. 6.3 a & b : Bulk rock variation diagrams

Conventions as section 3.3

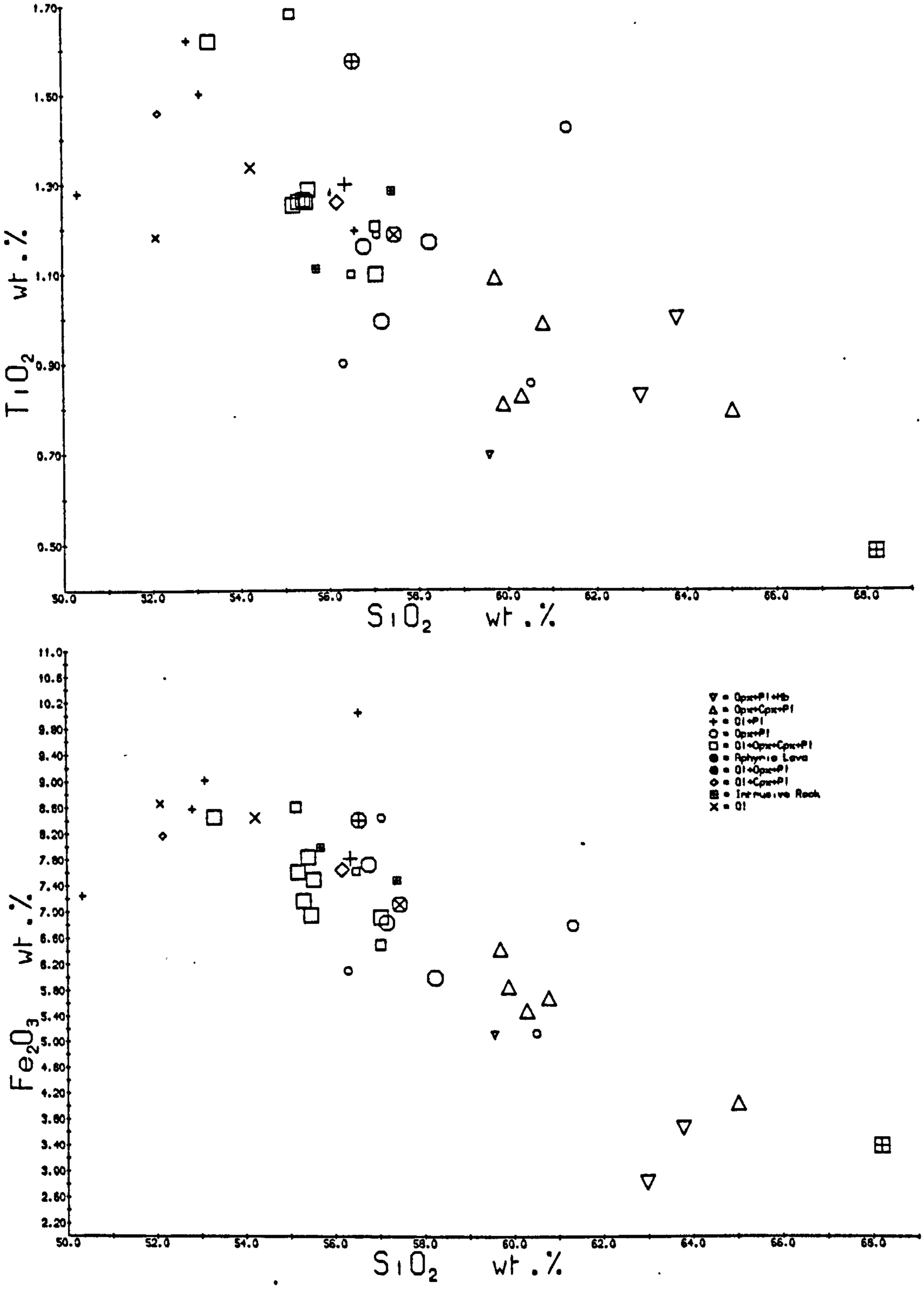

AYRSHIRE

Fig. 6.3 c & d

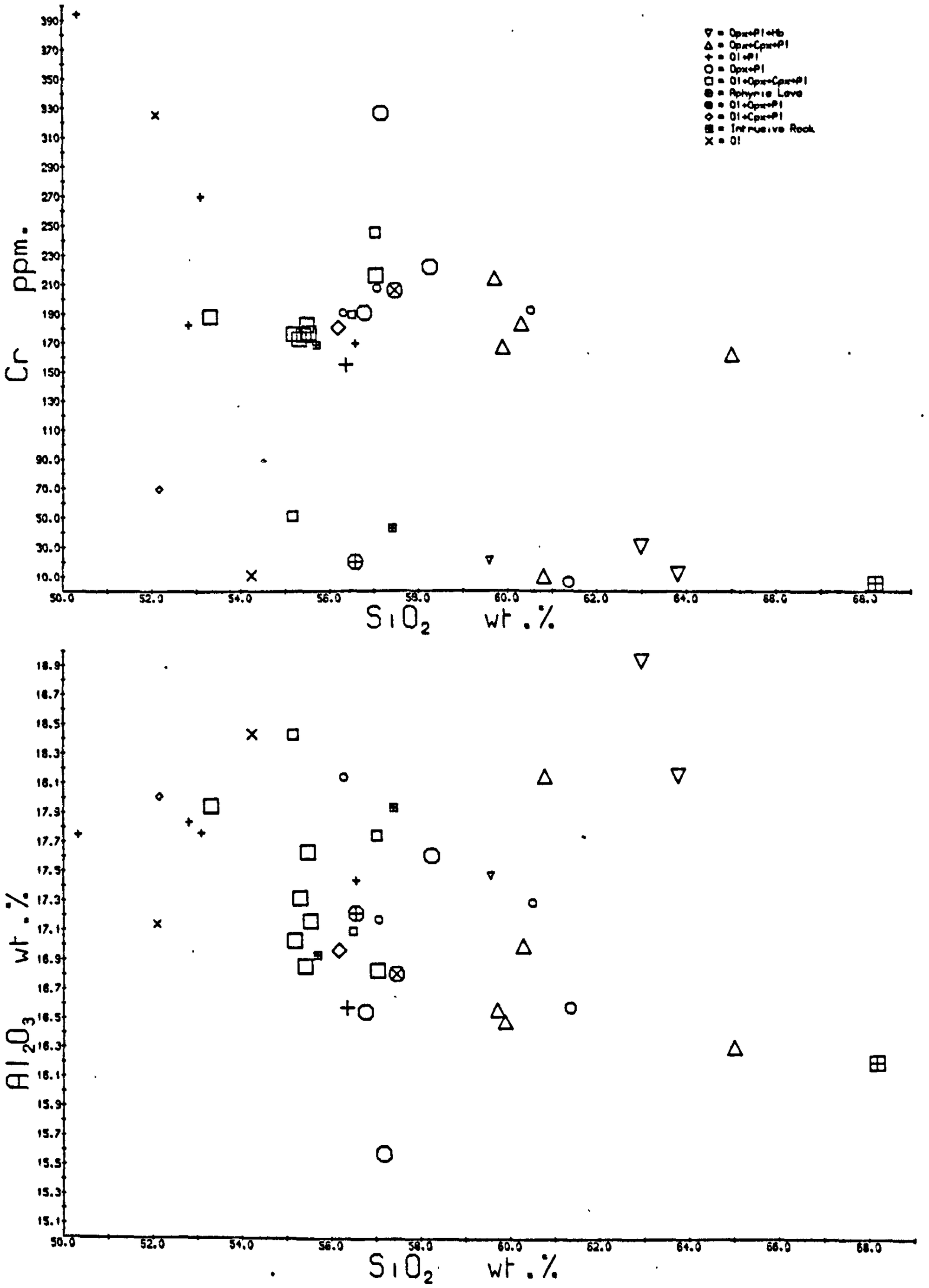

AYRSHIRE

Fig. 6.3 e & f

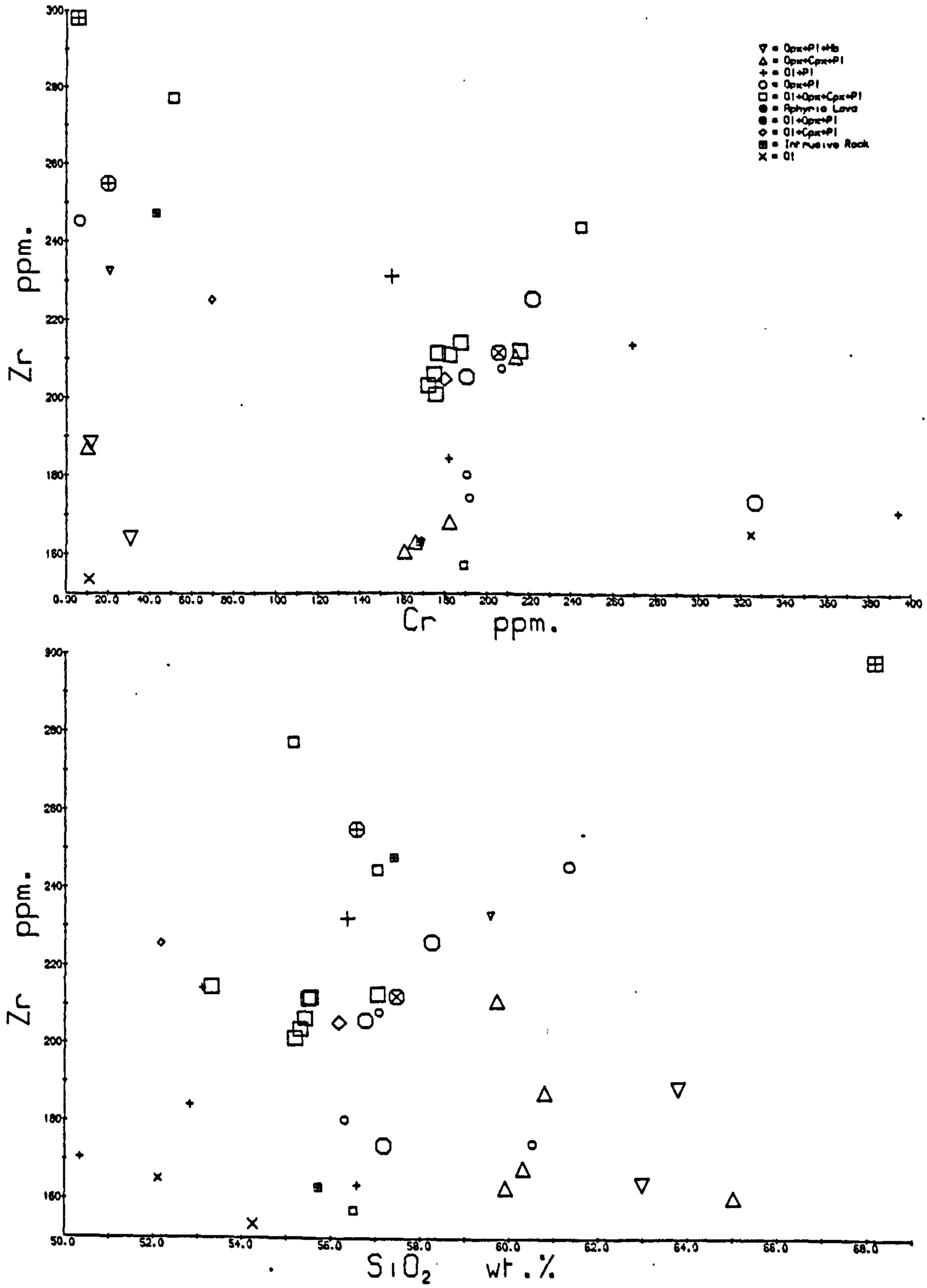

AYRSHIRE

Fig. 6.4 a & b : Bulk rock variation diagrams

Conventions as section 3.3

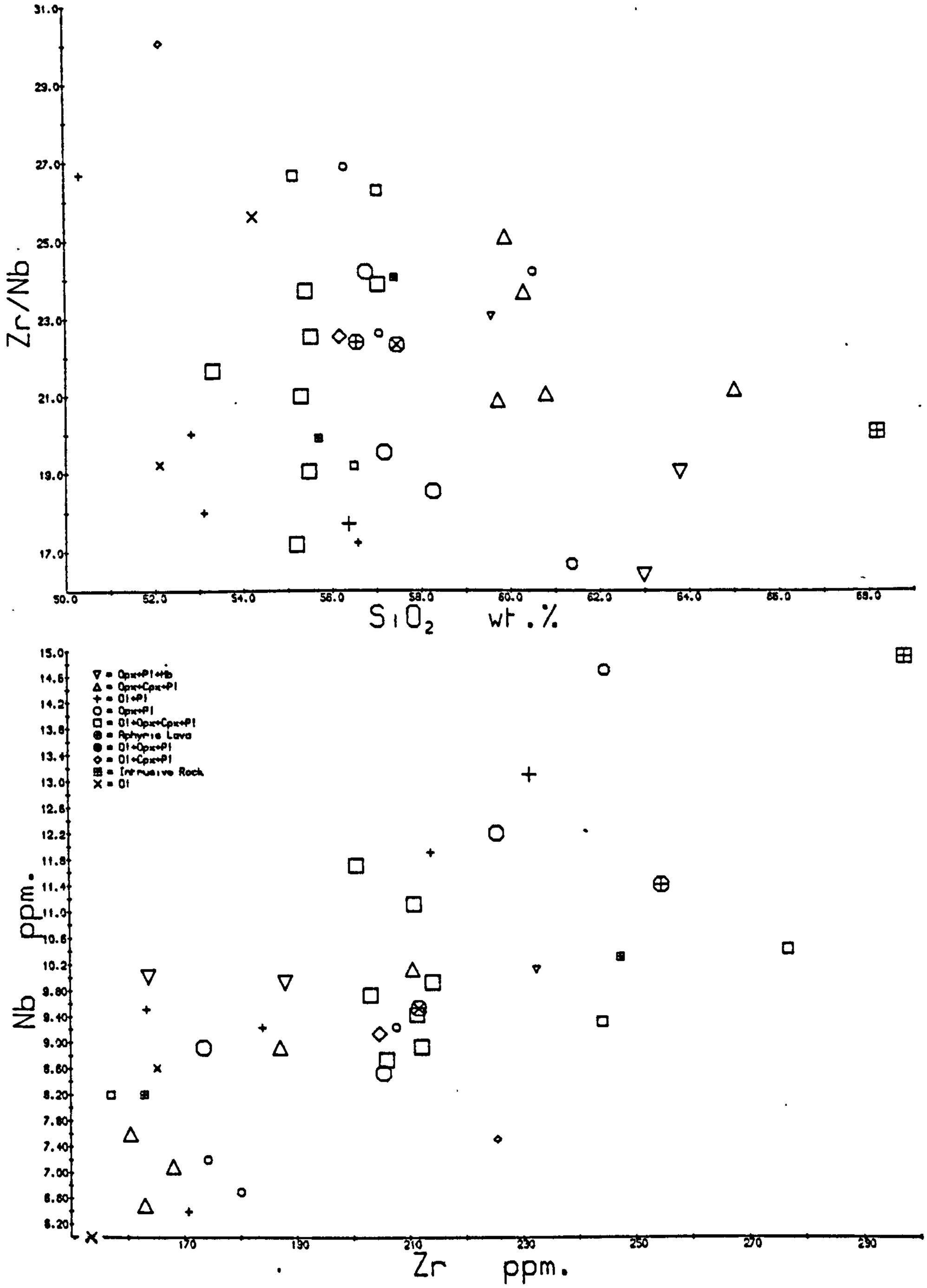

AYRSHIRE

Fig. 6.4 c & d

Fields for samples from Straiton and Distinkhorn

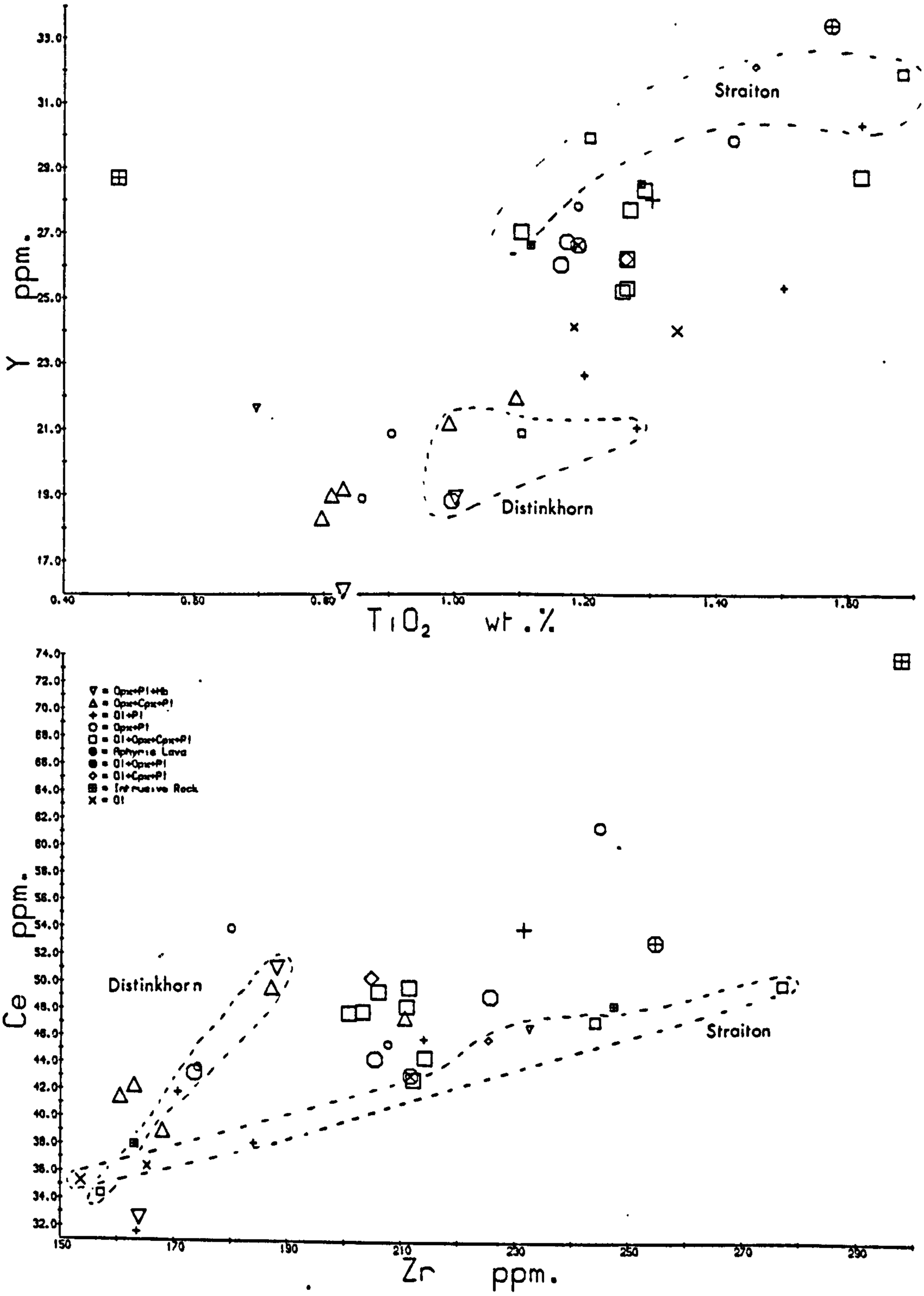

AYRSHIRE

Fig. 6.4 e & f

Fields for some Straiton and Distinkhorn samples

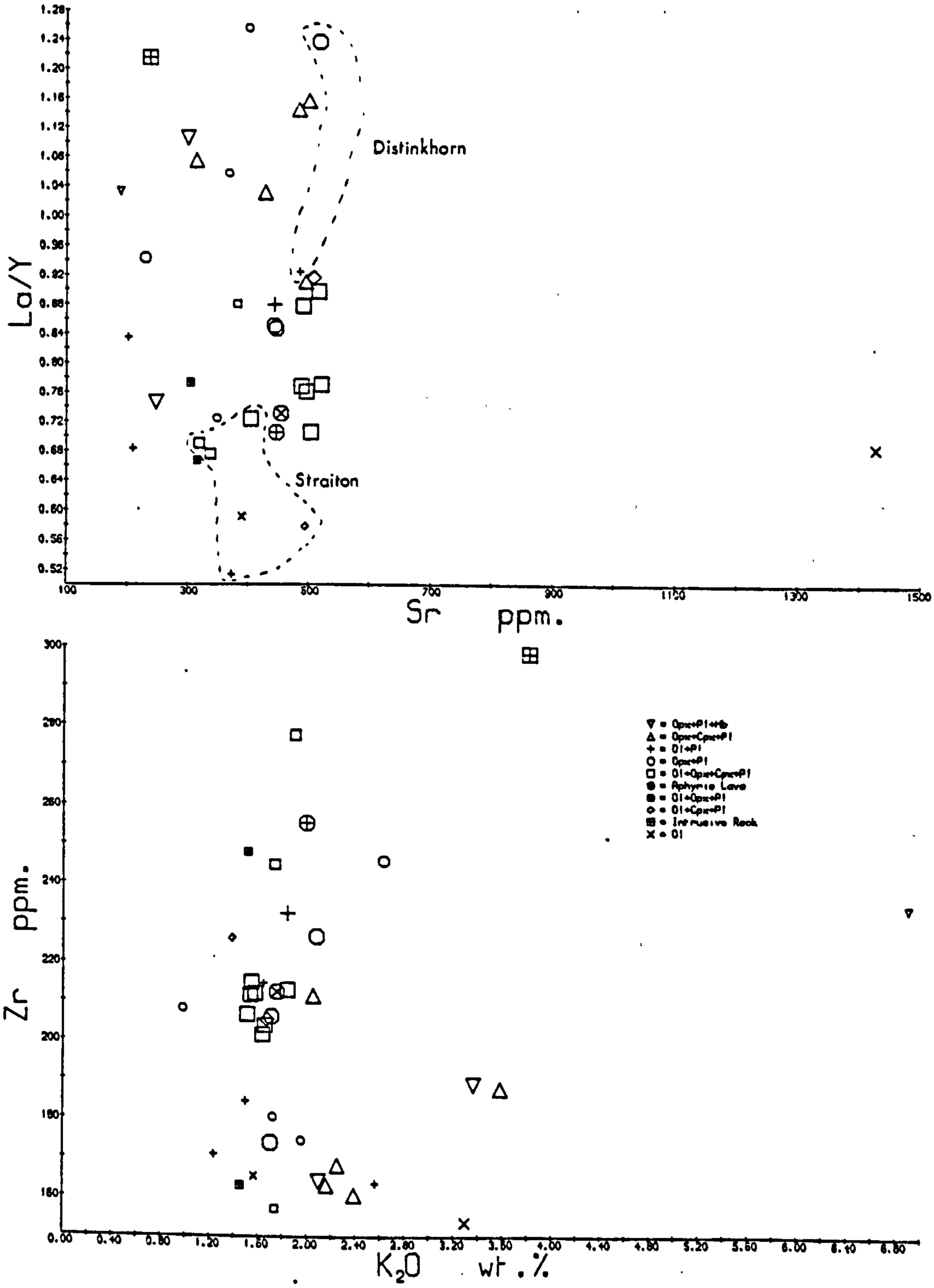

line of descent controlled by fractional crystallisation or partial melting in the Lower Old Red Sandstone volcanic rocks of Ayrshire.

6.3 : SOUTH MIDLAND VALLEY : CONCLUSIONS

The Lower Old Red Sandstone volcanic rocks of the south Midland Valley have considerable similarity to those of the north, particularly in the complexity of their chemical and mineralogical variation.

(a) Phenocryst chemistry (Fig. 6.5)

Clinopyroxenes are typically low Na, Ti, Al diopsidic augites, plotting within the non-alkaline field of Le Bas (1962). Orthopyroxenes are generally bronzites, even in samples with up to 65% SiO_2, suggesting that the rocks have calc-alkaline affinities. More iron-rich pyroxenes are present in the basic andesites of Straiton, and may indicate the existence of higher Fe/Mg, perhaps tholeiitic, liquids here. However, the reverse zoning of these Straiton pyroxenes suggests a complex crystallisation history. Composition of phenocryst plagioclase varies from bytownite to oligoclase and is generally unrelated to host-rock silica content.

(b) Chemical affinities

Most of the samples collected are quartz-normative,

Fig. 6.5 a & b : Phenocryst chemistry of South Midland Valley O.R.S. lavas.

a = atomic Ca, Mg, Fe for pyroxenes and biotites

b = the composition of plagioclase as a function of host rock silica

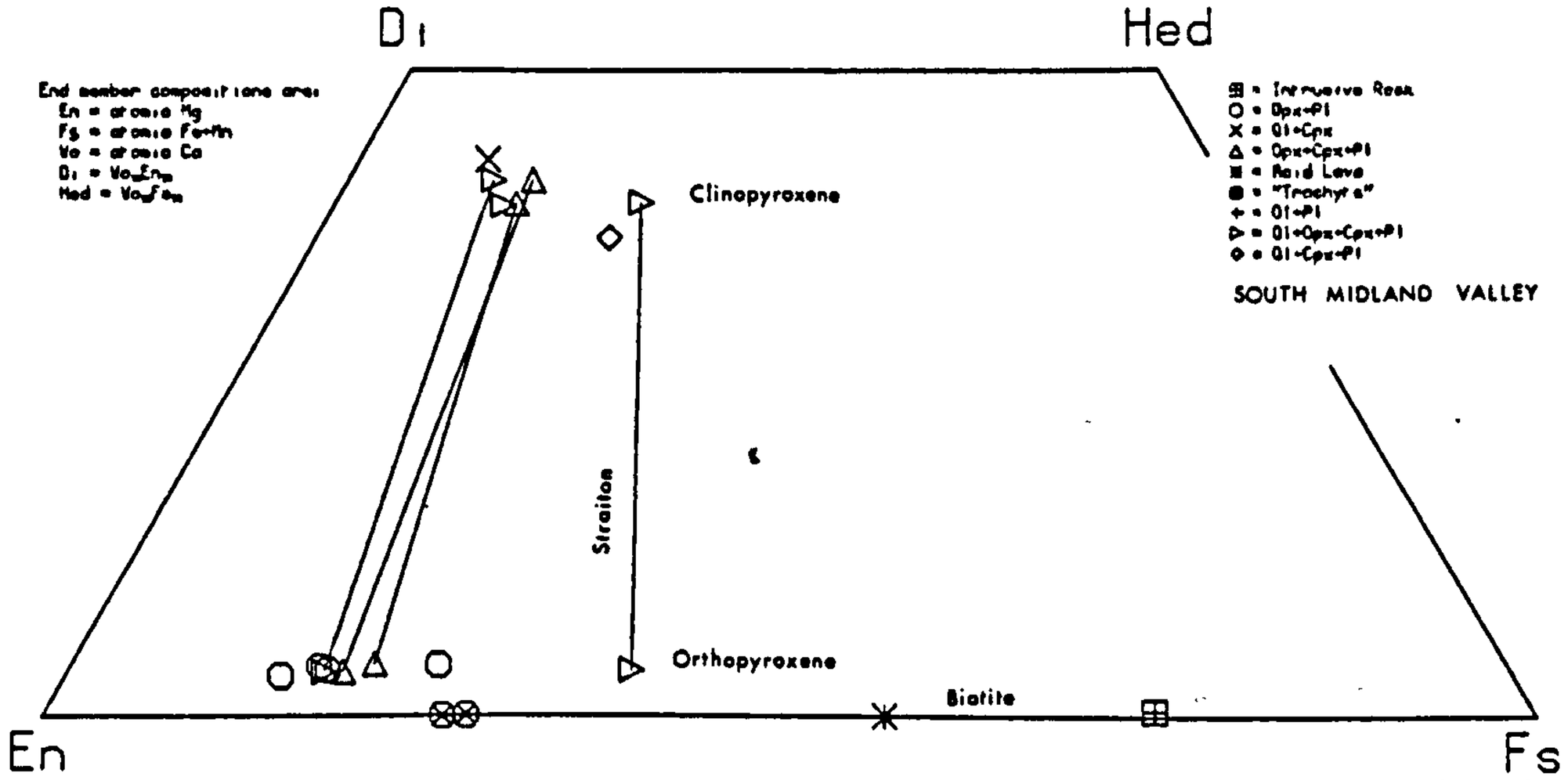

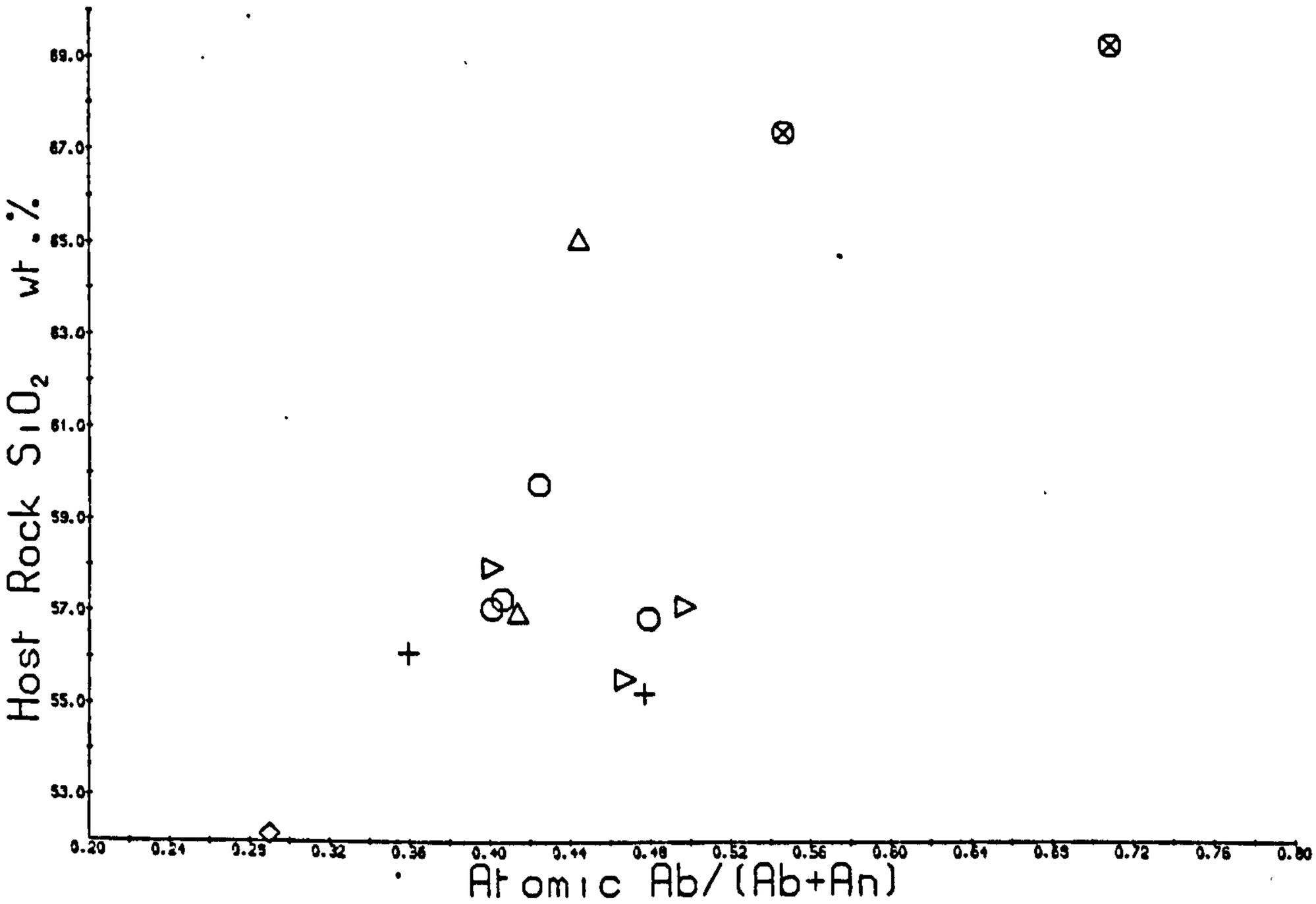

and most normative olivine and nepheline in other samples can be ascribed to secondary introduction of calcite. Except for two highly altered samples from the Pentland Hills, all samples have Fe/Mg within the calc-alkaline field of Miyashiro (1974), although basaltic and andesitic rocks include both moderate and high-alumina varieties. LIL and high field strength elements again have high concentrations, and many samples show concentrations of total alkalis within the alkaline field of Kuno (1968). As with the rest of the province, however, the dominantly quartz-normative nature, the pyroxene chemistry and the low Fe/Mg strongly suggest that the rocks are best described as calc-alkaline.

Many of the samples plot outside the named fields on the Ti-Zr-Y and Ti-Zr-Sr diagrams of Pearce and Cann (1973). In common with rocks from further north, most samples plot to the Zr-rich side of the field for calc-alkaline basalts on the former diagram: this is probably due to the overall high concentrations of LIL and high field strength elements in rocks of the province.

(c) Constraints on petrogenetic hypotheses

Very few element pairs show good correlation in samples from the south Midland Valley: the best correlation is provided by TiO_2-Y, or by Ce-Zr in the Pentland Hills. Many rocks are Ni- and Cr-rich, even samples with up to 65% SiO_2 (AY12), implying that they can not have suffered much fractional crystallisation of mafic minerals. Such

siliceous samples have Sr contents comparable to those of more basic rocks: the silica enrichment is therefore not caused by fractional crystallisation of calcic plagioclase.

Using such conclusions, the wide variability in Zr/Nb ratio, and the arguments of section 5.5, it is concluded that no extensive liquid line of descent controlled by fractional crystallisation or partial melting exists within the Lower O.R.S. volcanic rocks of the south Midland Valley. The wide variation in LIL and high field strength element concentrations in the Pentland Hills, and to a lesser extent in Ayrshire, can probably only be explained by a contamination model.

CHAPTER 7 : THE CHEVIOT HILLS

Lower Old Red Sandstone rocks south of the Southern Uplands Fault in Scotland outcrop in two areas: a small area of volcanic rocks and sediments at St. Abb's Head and Eyemouth, Berwickshire, and a much larger area of dominantly volcanic rocks forming the Cheviot Hills. The volcanic rocks of the two areas are petrochemically very different, and therefore the rocks of St. Abb's Head will be treated in the next chapter.

The Lower O.R.S. of the Cheviot Hills rests unconformably on Wenlockian greywackes and shales, and is overlain unconformably by the Upper O.R.S. of Roxburghshire and the Carboniferous sediments of Northumberland. The Lower O.R.S. occupies a very large tract of country, but because of poor exposure little is known of its detailed stratigraphy, thickness or structure. Carruthers *et al.* (1932) have described the field occurrence and petrography of the rocks. With the exception of an acid agglomerate at the base, the Lower O.R.S. consists almost entirely of lavas, although thin impersistent horizons of tuff and sandstone occur in several places. Carruthers *et al.* (1932) describe the occurrence of biotite-phyric rhyolites ("mica-felsites") above the basal agglomerate; "pitchstone-andesites" and rare horizons of "oligoclase-trachyte" at higher levels; but otherwise conclude that the volcanic series is a very monotonous accumulation of pyroxene-andesites. The lava pile is

intruded by a large number of dykes and sills and in places forms the roof to the Cheviot Granite.

Mitchell (1972) has reported the results of some K-Ar age determinations on rocks from the Cheviot Hills. The lavas were thought to have been erupted about 380-390 Ma ago.

(a) Pyroxene-andesites and "Pitchstone-andesites"

90% of rocks collected from these divisions of Carruthers et al. (1932) have the phenocryst association plagioclase-orthopyroxene-clinopyroxene-apatite-opaque oxide, and since collection has probably been biased towards less common varieties, it is likely that lavas with this phenocryst association provide more than 90% of the total volcanic sequence. Three samples from these divisions also contain rare resorption pseudomorphs after phenocryst biotite, and one sample does not appear to contain phenocryst pyroxene. This petrographic monotony is in striking contrast to rocks from elsewhere in the O.R.S. volcanic province.

In an attempt to provide a method of petrographic classification on variation diagrams comparable to that used in other areas, rocks with the phenocryst assemblage opx-cpx-pl have been subdivided according to their groundmass texture: this may be vitrophyric, hyalopilitic or a coarse or fine granular aggregate of feldspars and quartz.

Some groundmass textures are transitional, however. All rocks described as "pitchstone-andesites" by Carruthers et al. (1932) are vitrophyric with fresh glass in their groundmass and fresh mafic phenocrysts. These authors suggested (p. 14) that the "pitchstone-andesites" represented a minor magmatic type which was less susceptible to alteration through having an impermeable glassy groundmass. However, severely altered vitrophyric samples are common throughout the Cheviot Hills, and non-vitrophyric types containing fresh orthopyroxene are not uncommon (Appendix A). The distinction of a separate "pitchstone-andesite" rock type is therefore not valid.

Phenocryst orthopyroxene is bronzite-hypersthene (Table C2) and clinopyroxene is a low Ti, Al, Na augite. Fe/Mg of pyroxenes is slightly higher in the two vitrophyric samples analysed, but these are also the most silica-rich rocks. Phenocryst plagioclase is oscillatory-zoned labradorite-andesine. In sample C51, where there is additional phenocryst biotite, the phenocryst plagioclase is poorer in Or than that from other lavas (Fig. 7.3). Apatite analyses are presented in Table C2: REE contents are comparable to those predicted using the distribution coefficients of Nagasawa (1970). The opaque oxide is almost always ilmenite, in contrast to the dominance of titanomagnetite elsewhere in the province, and this may be very zirconian (Table C4).

The pyroxene-andesites are all quartz-normative, and

vary between 61 and 66% SiO_2. Fe/Mg is low, and the rocks all fall in the calc-alkaline field of Miyashiro (1974), although they only have moderate alumina (16%). They are very rich in LIL and high field strength elements, particularly in K, Rb, LREE and Th. K_2O/Na_2O is close to 1, but Ba and Sr are not particularly high. They are thus comparable with some high-K andesites (e.g. Jakes and White, 1972), although Ni and Cr concentrations are much higher than the values quoted by these authors. Fe, Ti, P and less clearly, V and Sc show good negative correlation with silica (Fig. 7.1), as do Ca, Mg and Sr if allowance is made for alteration (Chapter 2). K and Rb increase with increasing silica in fresher samples, but anomalously low values are given by the "pitchstone-andesites", believed to be due to interaction with meteoric water (Chapter 2). Such interaction is also suggested by an oxygen isotope study of the Cheviot Granite (A.N. Halliday, pers. comm., 1979). Otherwise, little relationship exists between chemistry and groundmass textural types, although vitrophyric samples often have lower Y.

Over the full range of samples collected there appears to be depletion in Zr, Cr, Ni and LREE and increase in Th with increasing silica (Fig. 7.2). Within the pyroxene-andesites, however, there is very good positive correlation between Ni and Cr, and Zr and LREE increase slightly with reduction in Cr (Fig. 7.2). Zr/Nb varies between 17 and 21; while this is a narrower range than in the regions discussed in previous chapters it is

CHEVIOT HILLS

Fig. 7.1 a & b : Bulk rock variation diagrams

Conventions as section 3.3

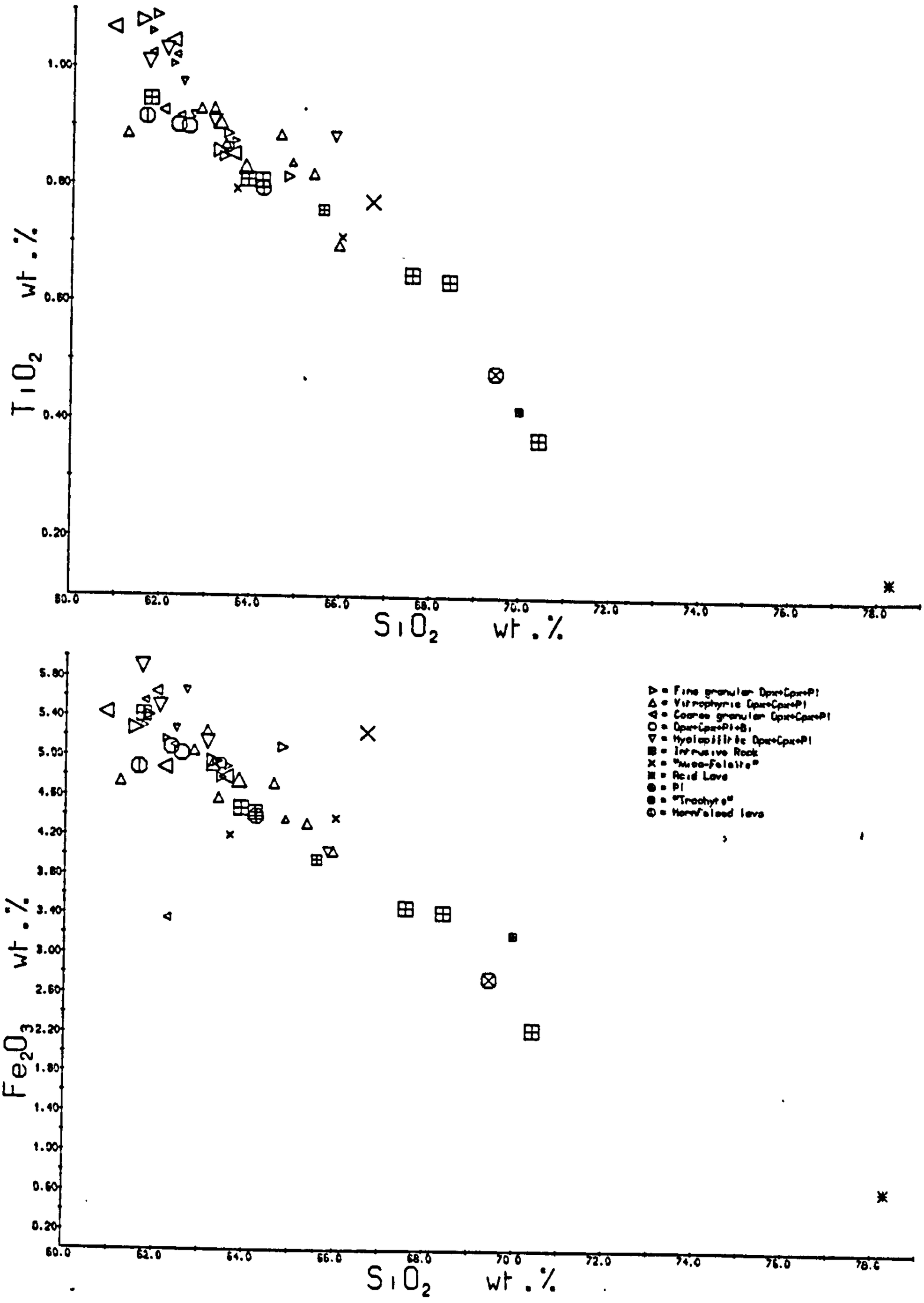

CHEVIOT HILLS

Fig. 7.1 c & d

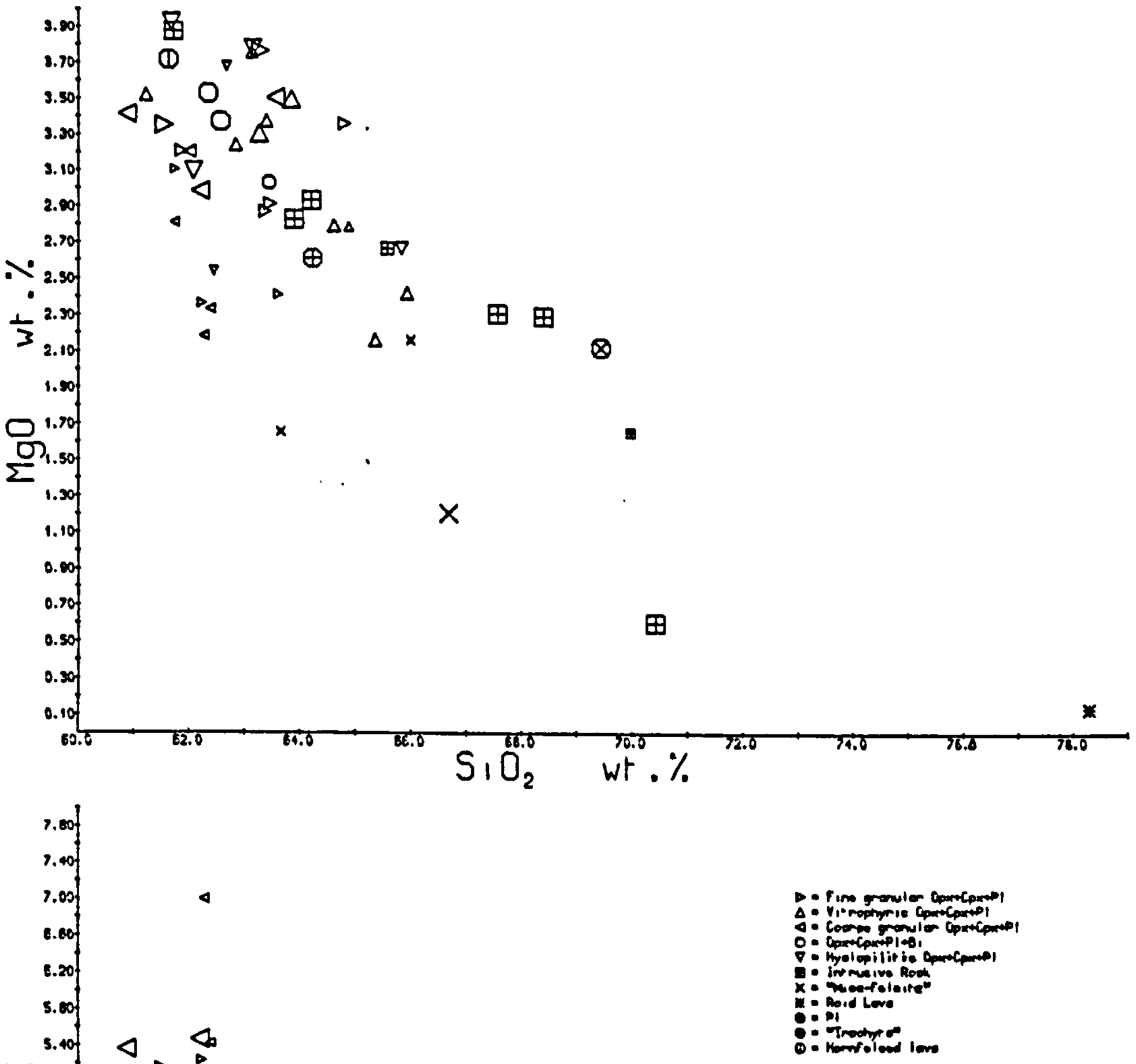

CHEVIOT HILLS

Fig. 7.1 e & f

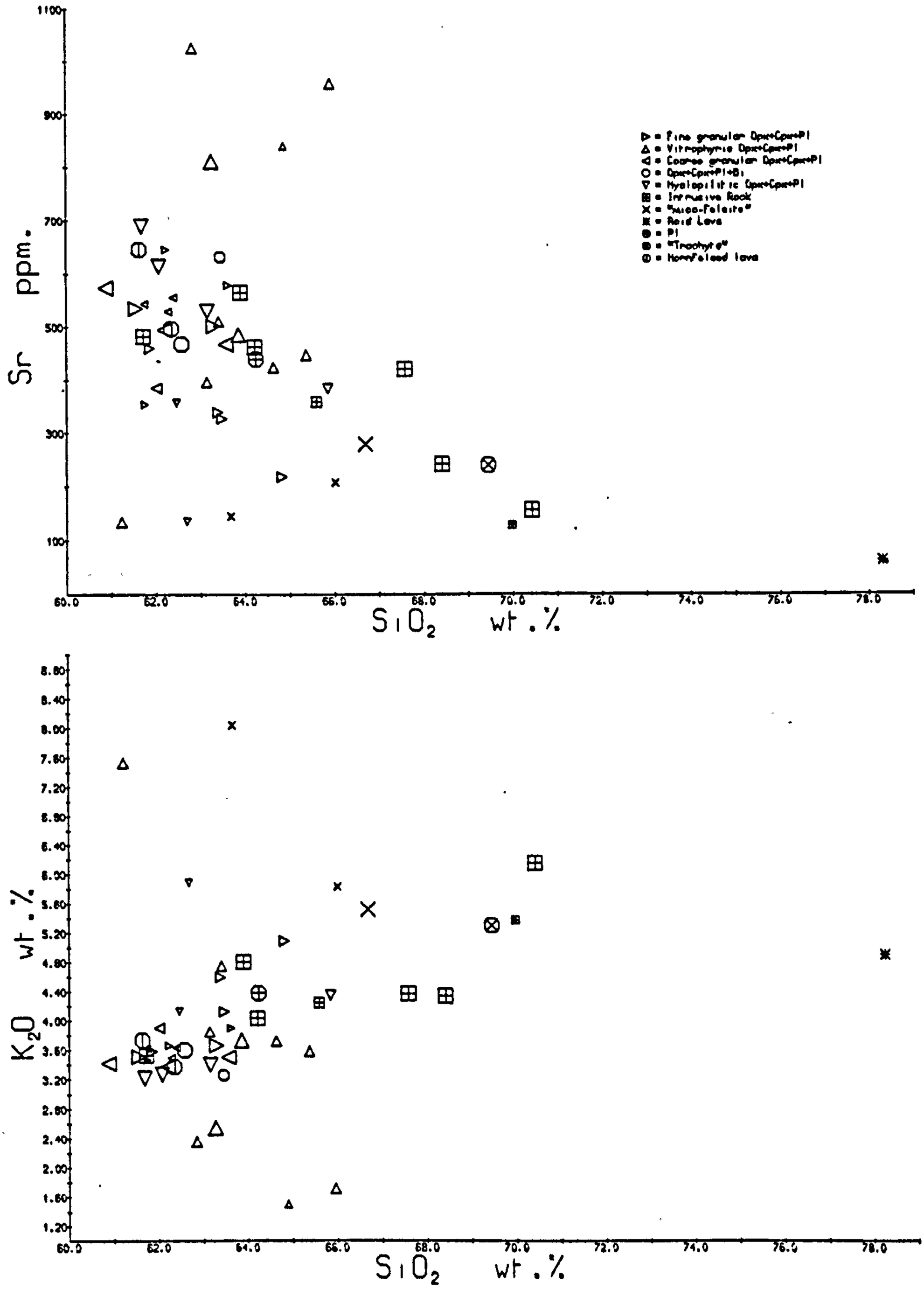

CHEVIOT HILLS

Fig. 7.2 a & b : Bulk rock variation diagrams

Conventions as section 3.3

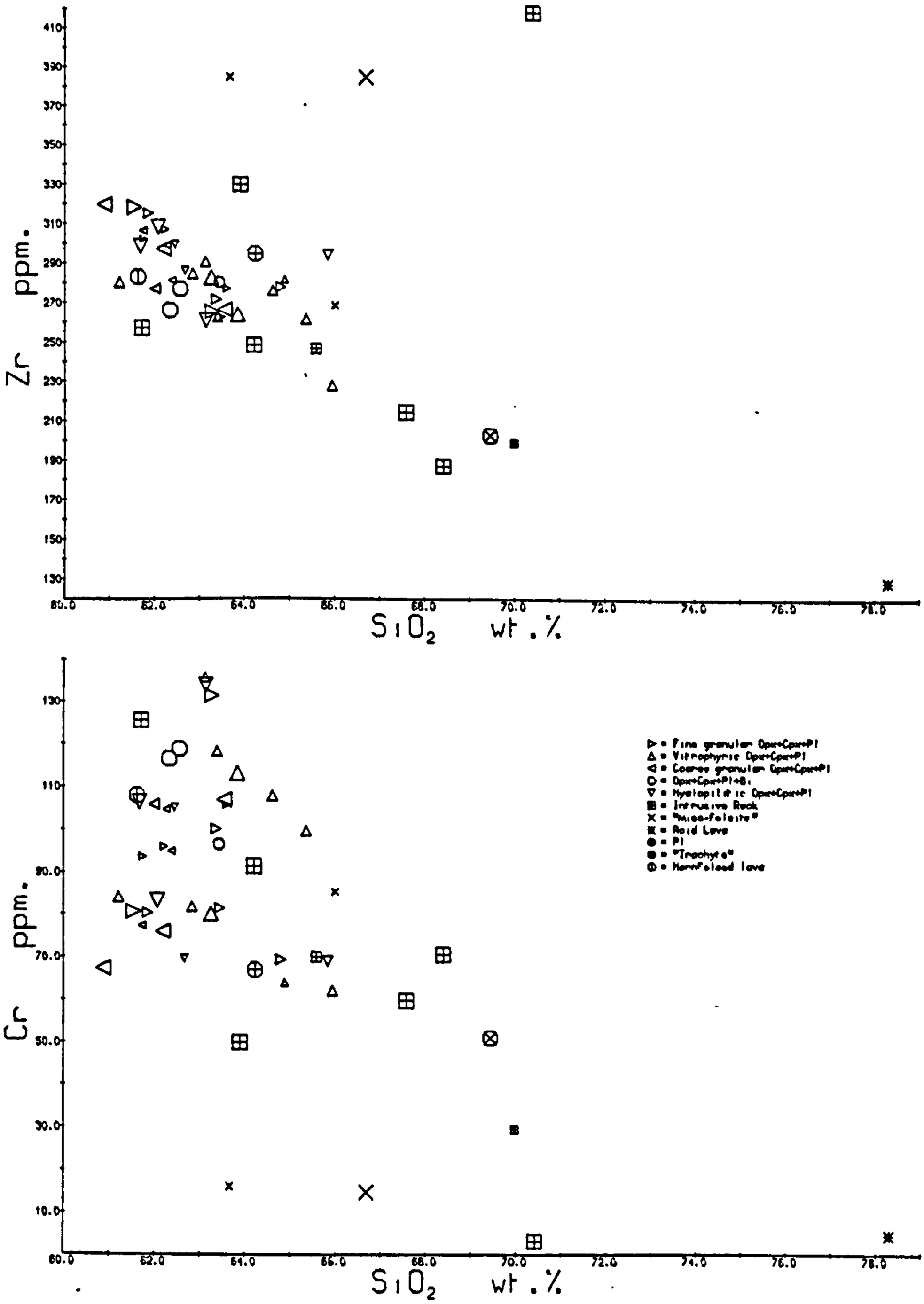

CHEVIOT HILLS

Fig. 7.2 c & d

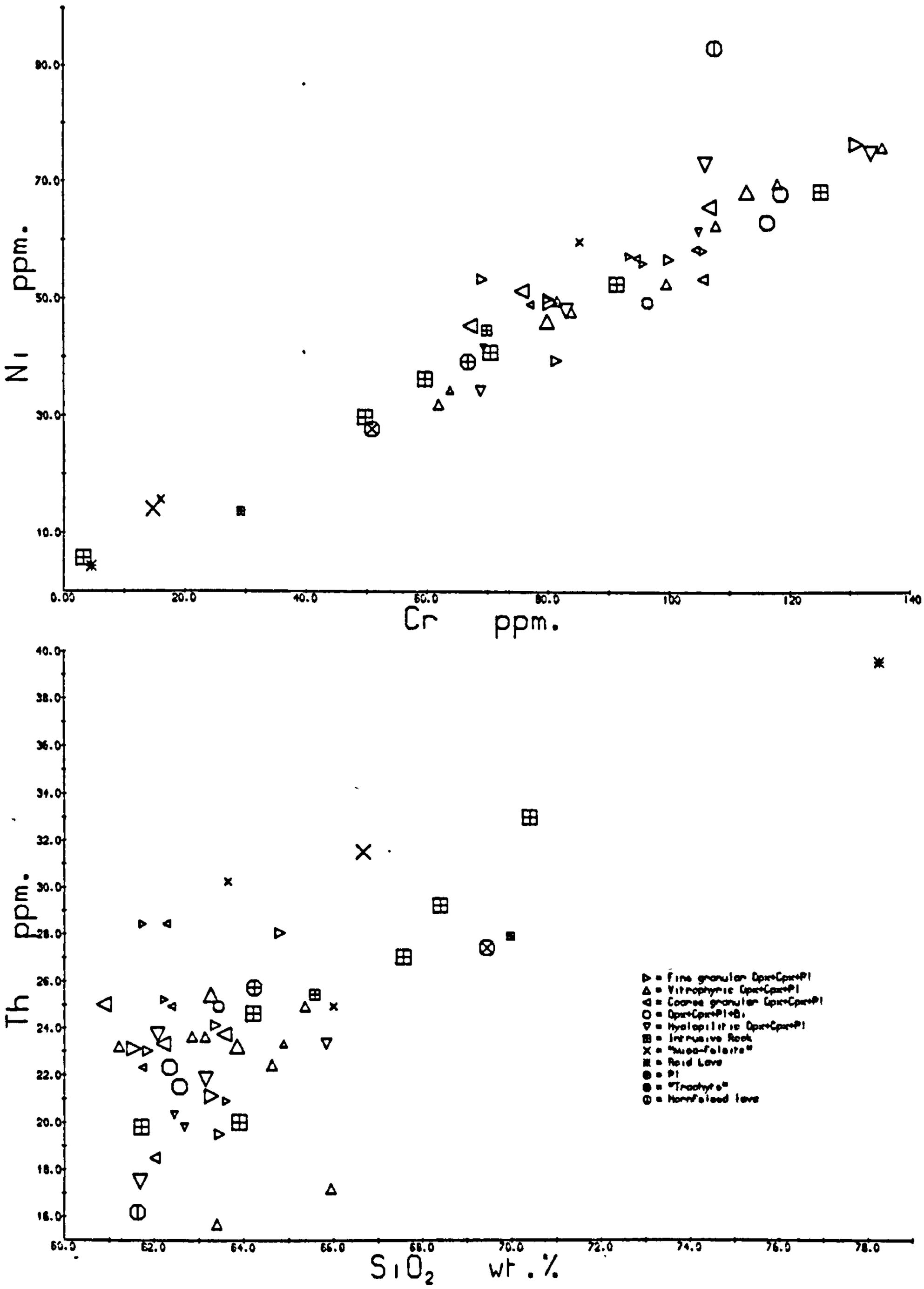

CHEVIOT HILLS

Fig. 7.2 e & f

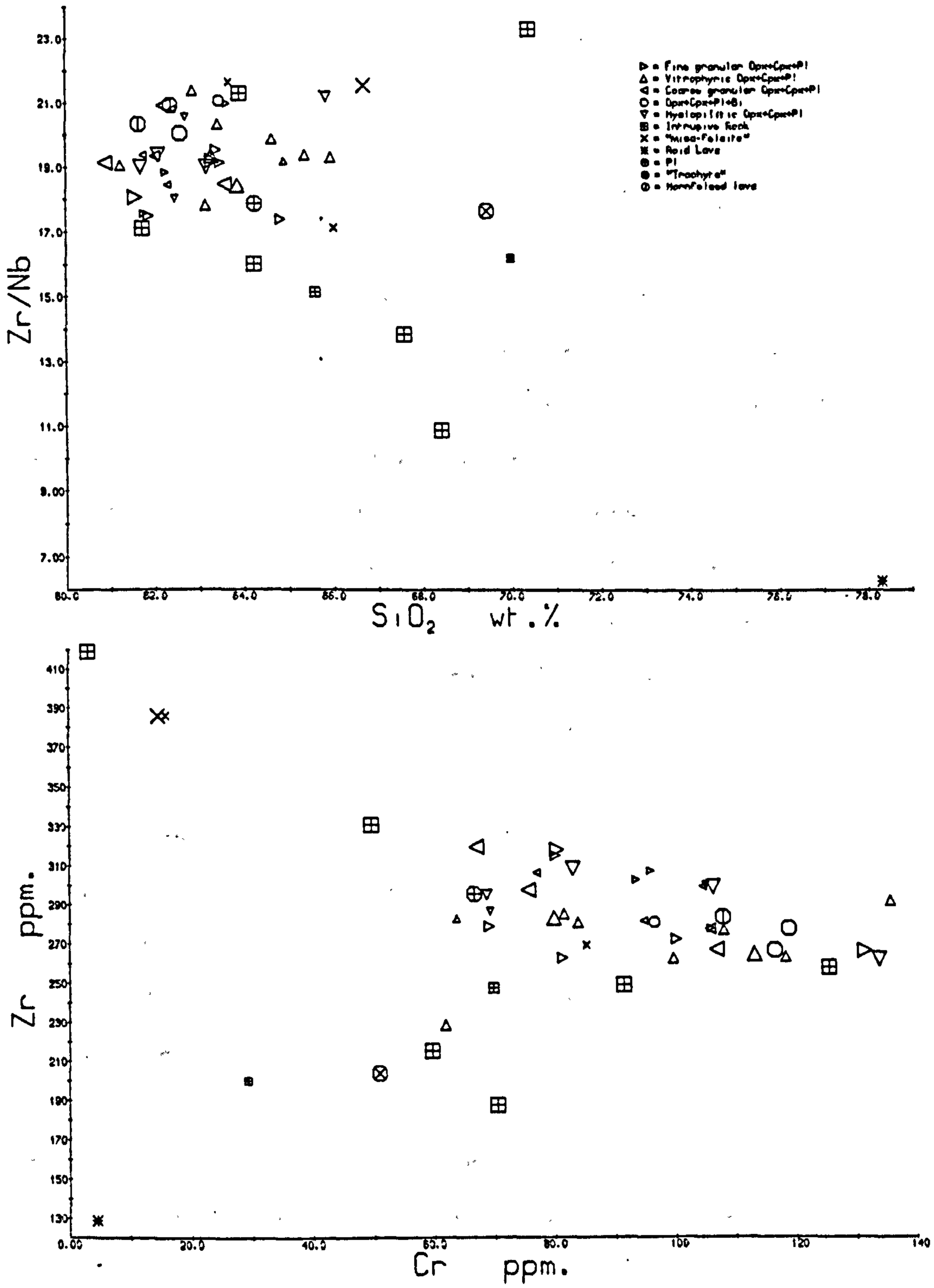

nevertheless significant within analytical precision. Zr/Nb does not correlate with Cr, SiO_2 or TiO_2, despite the presence of phenocryst ilmenite, suggesting that the pyroxene-andesites may not be derived by fractional crystallisation of a single parent magma.

The major element variation has been modelled using the least-squares computer program MODES, written by D.J. Humphries and based on that of Wright and Docherty (1970). Initial and final compositions with 62 and 70% silica have been estimated from the variation diagrams: it is recognized that this range is wider than the variation of the pyroxene-andesites, but all elements used in the calculation show approximately linear variation with silica in this range for all rocks (Fig. 7.1). To make allowance for discrimination by the program in favour of high concentration elements, the elements used (all major elements except Mn) have been inversely weighted approximately according to their concentrations. Average phenocryst compositions have been taken from C7. The program yields a good fit (sum of squares of residuals=1.08) for fractional crystallisation of the phenocrysts in proportion 63.3% pl - 17% opx - 14.9% cpx - 3.28% ilm - 1.49% ap, which are very close to the relative proportions of the phenocrysts. The residuals for all elements are well within scatter on the variation diagrams. 43% crystallisation is required to produce silica enrichment from 62 to 70%.

Rb and Th data agree well with a model of 43% crystallisation, for both nearly double over this silica enrichment. However, Zr, Nb, Y and LREE decrease over this range, suggesting that D(bulk) for these elements is greater than 1. Using maximum reasonable values of D(Zr) for cpx=1, for opx=0.1, for pl=0.1, for ilm=10 and for ap=0.1, then D(Zr,bulk)=0.56. Similarly, D(Ce,bulk)=0.77, assuming values from Gill (1978) and D(Ce,ap)=40, although increasing this to 50 increases D(Ce,bulk) to 0.91. These values are very dependant on the proportions of apatite and ilmenite in the fractionating assemblage, but P and Ti were weighted to obtain minimal residuals, and therefore the error in proportions of these phases should be trivial.

The conflict between predicted and real behaviour of these elements may perhaps be related to the the increases shown by these elements with decreasing Cr. Here, LREE appear more compatible than Zr, consistent with their relative bulk distribution coefficients calculated above, although Zr is still more compatible than predicted. This relationship, and the scattered Ni-SiO_2 and Cr-SiO_2 distributions, could be explained by a two-stage fractional crystallisation process, in which magmas parental to the first stage are not represented in the Cheviot Hills. The first stage may have led to a range of magmas with comparable major element composition, but including some slightly more evolved ones with lower Cr, Ni and higher Zr, LREE. The behaviour of Sr is reasonably consistent with the suggested amount of plagioclase extraction, although actual

depletion in Sr is larger than that predicted. The lack of Ba enrichment with silica is not satisfactorily explained by this model, nor is variation in Y and La/Y (Fig. 7.4), for Y should be less compatible in this assemblage than La (Chapter 3).

(b) "Oligoclase-trachyte"

Only one sample with this lithology has been collected, and it is severely altered. It is nearly aphyric, quartz-normative, siliceous and not significantly richer in alkalis than some of the more siliceous andesites (Fig. 7.1). It lies on the general variation trends with silica described in section (a), but its low Zr, Nb, Y and LREE can not be explained by further fractional crystallisation of the phenocryst minerals from the andesites. Biotite+zircon extraction (Pearce and Norry, 1979) can not explain the lack of K and Th depletion relative to the andesites.

(c) "Mica-felsites"

The "mica-felsites" collected in the course of this research are all feldpar-phyric, and no samples have been found of the type with biotite as the sole phenocryst phase, described by Carruthers et al. (1932). In addition to biotite, the samples contain phenocrysts of plagioclase, alkali feldspar, apatite, ilmenite and ?clinopyroxene, pseudomorphed by carbonate. They are all badly altered, and

the alkali feldspars are now near the pure K end-member.

The three samples collected have between 63 and 67% silica, and can not therefore be described as rhyolites (c.f. Carruthers et al., 1932; Mitchell, 1972). Two samples, together with two intrusive rocks (C23 and C58), are enriched in Rb, K, Zr, Th, LREE and to a lesser extent Nb and Y relative to the pyroxene-andesites, and they are depleted in Cr, Ni, Mg, P and possibly Sr. This could suggest fractional crystallisation of a pyroxene-andesite magma, but it is difficult to explain the lack of silica enrichment and the incompatibility of LREE (La and Zr enrichments are comparable) when apatite must be an important part of the crystallising assemblage. The third "mica-felsite" sample (C55) is not chemically distinguishable from the pyroxene-andesites.

(d) Intrusive rocks

All intrusive rocks sampled have a similar mineralogy to the lavas, although phenocryst quartz appears in more siliceous varieties, and phenocryst biotite is more common. All clinopyroxenes analysed from intrusive rocks are notably more calcic than lava clinopyroxenes, and orthopyroxene is less calcic (Fig. 7.3). Ti and Al show a much more restricted compositional range than in lava pyroxenes. This suggests that the crystallisation of the intrusive rocks occurred at lower temperatures and that it was closer to equilibrium. Plagioclase is generally poorer in Or than

Fig. 7.3 a & b : Phenocryst chemistry of Cheviot igneous rocks.

a = atomic Ca, Mg and Fe for pyroxenes and biotites

b = plagioclase end-members

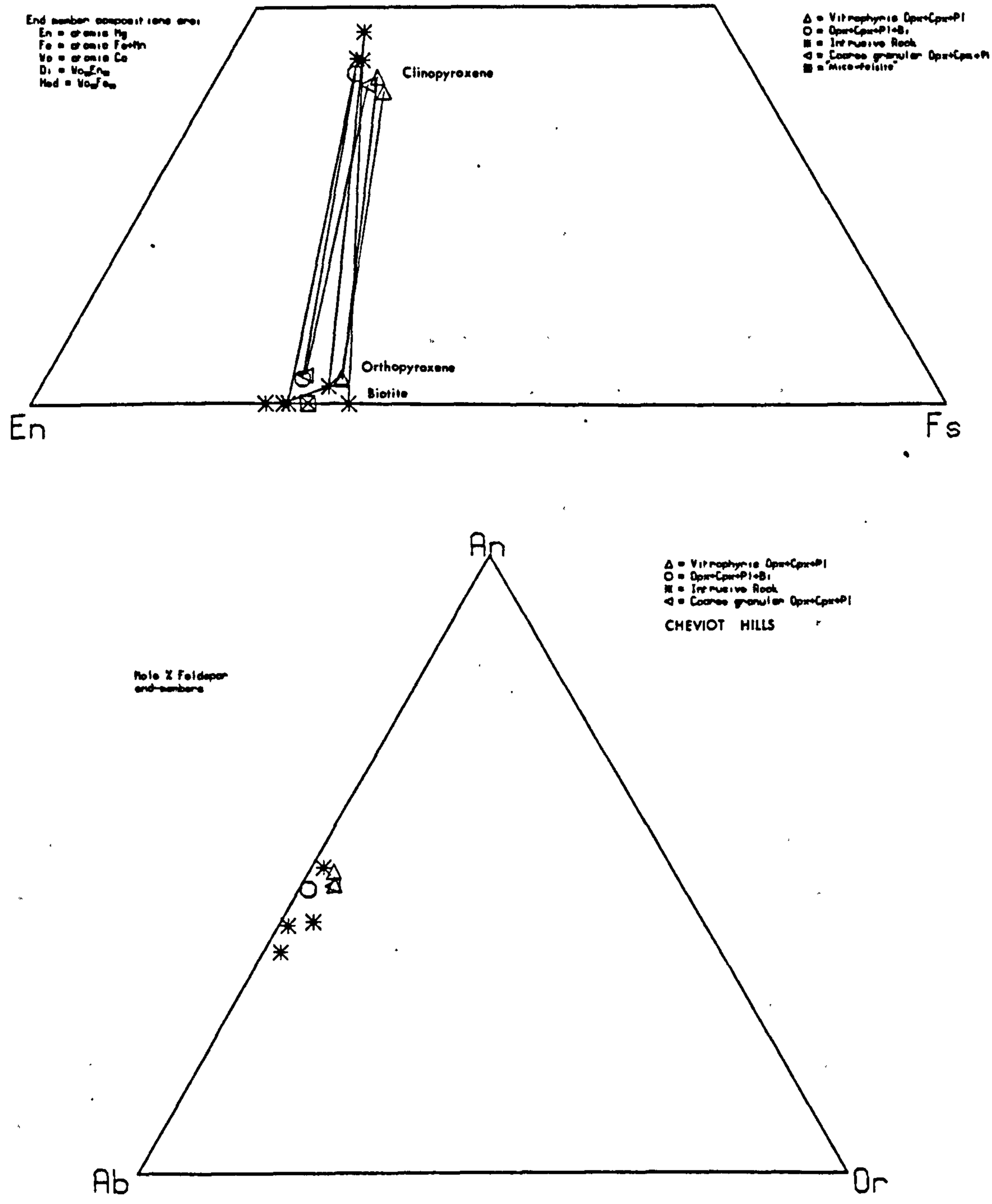

equivalent lava plagioclase.

With the exception of the two samples which appear to be related to the "mica-felsites" (section e), all the intrusive rocks fall on the general trends described in section (a) for all elements except Y and Nb, which remain constant and increase respectively, with increasing silica. The behaviour of Y gives rise to roughly constant La/Y, contrasting with the broad increase in La/Y with silica shown by the lavas (Fig. 7.4). Zr concentrations are slightly lower than those in the lavas.

C62 is an example of the marginal 2-pyroxene variety of the Cheviot Granite, interpreted by Carruthers *et al.* (1932) as the result of contamination of granitic magma by andesite. The lower temperature nature of the pyroxenes suggests that these are unlikely to be xenocrystal from the lavas, as suggested by Carruthers *et al.* (1932, p.93). Jhingran (1942) compared the analyses of a "pitchstone-andesite" and a sample of marginal 'granite', and concluded that contamination was more likely to have been the result of incorporation of sediment. The major difference between the two analyses quoted by Jhingran (1942) lies in the K_2O content, and the low K of the "pitchstone-andesite" quoted is probably the result of alteration, as suggested in Chapter 2. The marginal variety of the Cheviot Granite is chemically almost identical to the bulk of the pyroxene-andesites.

CHEVIOT HILLS

Fig. 7.4 a & b : Bulk rock variation diagrams

Conventions as section 3.3

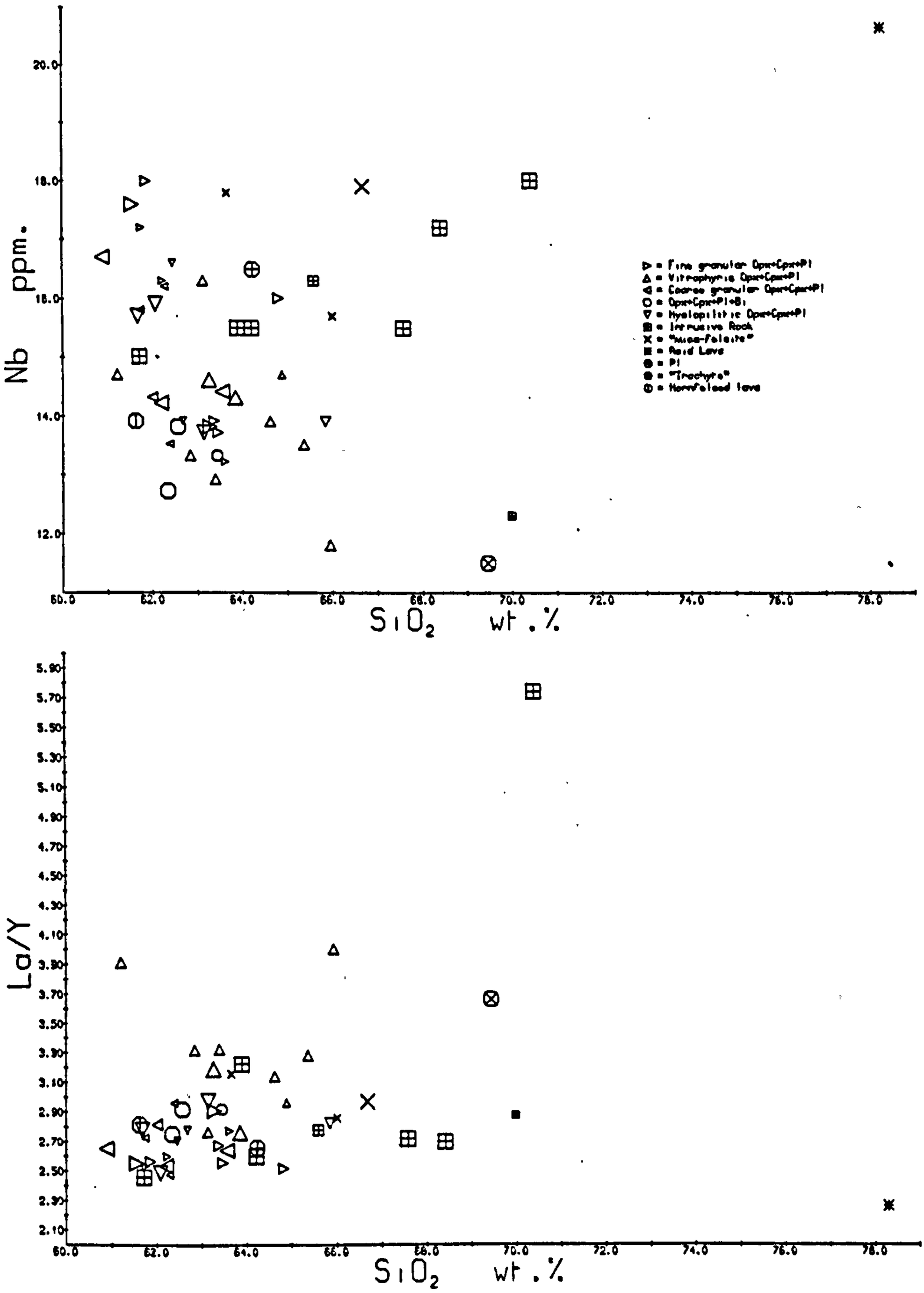

C41, a severely altered clast from the basal agglomerate, is the only true rhyolite collected from the Cheviot Hills. For most elements it falls on the same variation trends as the intrusive rocks e.g. for Nb and La/Y, Fig. 7.4, but is far more siliceous than any intrusive rock collected. In common with most rhyolites of the province it has low Zr and very low Zr/Nb.

(e) Conclusions

With very few more siliceous exceptions, the volcanic rocks of the Cheviot Hills are a group of high-K calc-alkaline 2 pyroxene-plagioclase-phyric andesites, closely similar in their petrography and chemistry. This monotony is most unusual for rocks of the Old Red Sandstone Volcanic Province. Their limited major element variation may be ascribed to fractional crystallisation of the phenocryst phases: this can also generate the major element variation of all other Cheviot samples, apart from P_2O_5 in the "mica-felsites".

Trace element variation can not be accounted for by this model. Most samples are high in Ni and Cr relative to averages quoted by Jakeš and White (1972) and by Ewart (in press), and they are also very rich in LREE, Th and Rb. LREE, Th, Y, Zr and Nb do not vary systematically with silica. With the exception of the most siliceous andesite, the "trachyte", and a number of intrusive rocks, the elements Zr, Nb, Th and LREE increase with reducing Cr,

suggesting that variation in these elements could be produced by minor differences in immediately parental magmas with about 60% silica. This could suggest a two-stage fractional crystallisation process, but it is difficult to account for the high levels of Ni and Cr, unless plagioclase was a major fractionating phase in the first stage. Fractional crystallisation of the phenocrysts, the second stage, does not satisfactorily account for the Ba and Y variation.

Halliday and Stephens (in press) have noted that acid members of the Southern Uplands plutons characteristically have higher $^{87}Sr/^{86}Sr$ (0.706) than more basic ones (0.704), and suggest that the acid members could be derived by the melting of Lower Palaeozoic sediments. Such melts may have had lower concentrations of LIL and high field strength elements than the Cheviot andesites. The observed depletions in these elements with increasing silica could represent a mixing line between a lower crustal- or mantle-derived melt, very rich in incompatible elements, with a more siliceous melt derived from the lower Palaeozoic sediments. The isotopic data on the volcanic rocks, and the chemical data on the sediments needed to test this hypothesis are not yet available. It will be noted, however, that the melt derived from the sediments is required to be very Th rich, and the hypothesis can not explain the variation in Y among the pyroxene-andesites.

CHAPTER 8 : MINOR OCCURRENCES OF O.R.S. VOLCANICS

8.1 : ST. ABB'S HEAD / EYEMOUTH

Old Red Sandstone volcanic rocks in Berwickshire are well exposed in the sea cliffs of St. Abb's Head where they are faulted against Llandovery greywackes inland (Greig, 1975). To the south and west there are a few small inland outcrops where O.R.S. sediments and volcanic rocks rest unconformably on Silurian. The fairly thick (2000 ft, 600 m; Greig, 1971, p.50) southward dipping sequence at St. Abb's Head consists mainly of sparsely porphyritic lavas, often much veined by carbonate. Olivine and orthopyroxene are the only phenocrysts observed in samples from St. Abb's Head, and no biotite has been found (c.f. Greig, 1975, p.122). Where olivine occurs alone it is generally euhedral, but where orthopyroxene is present it generally mantles subhedral olivine. Phenocrysts are never common, and occur in a trachytoid or subophitic groundmass of plagioclase, clinopyroxene (rarely fresh) and opaque oxides. Both plagioclase and amphibole phenocrysts occur in the rocks near Eyemouth, but the collection is biased towards plagioclase-phyric samples, for these were specifically chosen from the collection of the Institute of Geological Sciences. No phenocryst minerals were found in sufficiently fresh condition to permit microprobe analysis.

The samples analysed range from 53 to 72% SiO_2 and are all quartz-normative. All samples from St. Abb's Head

are basic andesites with a maximum of 58% SiO_2 but samples from Eyemouth have a wider silica range. Fe/Mg is low, and all samples plot within the calc-alkaline field of Miyashiro (1974). Alumina is moderate (16%). A few elements show fairly good linear variation with silica (e.g. Fe, Cr; Fig. 8.1) despite the severe alteration, but immobile LIL and high field strength elements all show two variation trends with silica, particularly evident for P and LREE (Fig. 8.1). Each trend includes samples from both St. Abb's Head and Eyemouth.

One of these trends, the 'rapid enrichment trend', shows good positive correlation between concentrations of 'incompatible' elements and silica over the small range of silica present (53.8 to 57.5%). Nb more than doubles over this silica range (Fig. 8.1), and P, Zr and Ce show about 70% enrichment. Ti and Y show smaller increases, about 25 and 43% respectively, but Ni, Cr and V all reduce by a factor of about 30% (Fig. 8.1). If the trend were generated by fractional crystallisation, then bulk distribution coefficients for these three elements must all be close to 1.7. Comparable D(Sr,bulk) is suggested by the Sr concentrations of the two samples of PAS 3 (SA1 and SA20). These relationships suggest a possible origin of the trend by fractional crystallisation of an assemblage with silica close to that of the parental magma. The very small reduction in Cr and Ni over the 50% crystallisation derived from the Nb data implies that plagioclase was dominant in the fractionating mineral assemblage; the Sr data and the

Fig. 8.1 a & b : Bulk rock variation diagrams

Conventions as section 3.3

ST. ABB'S HEAD & EYEMOUTH

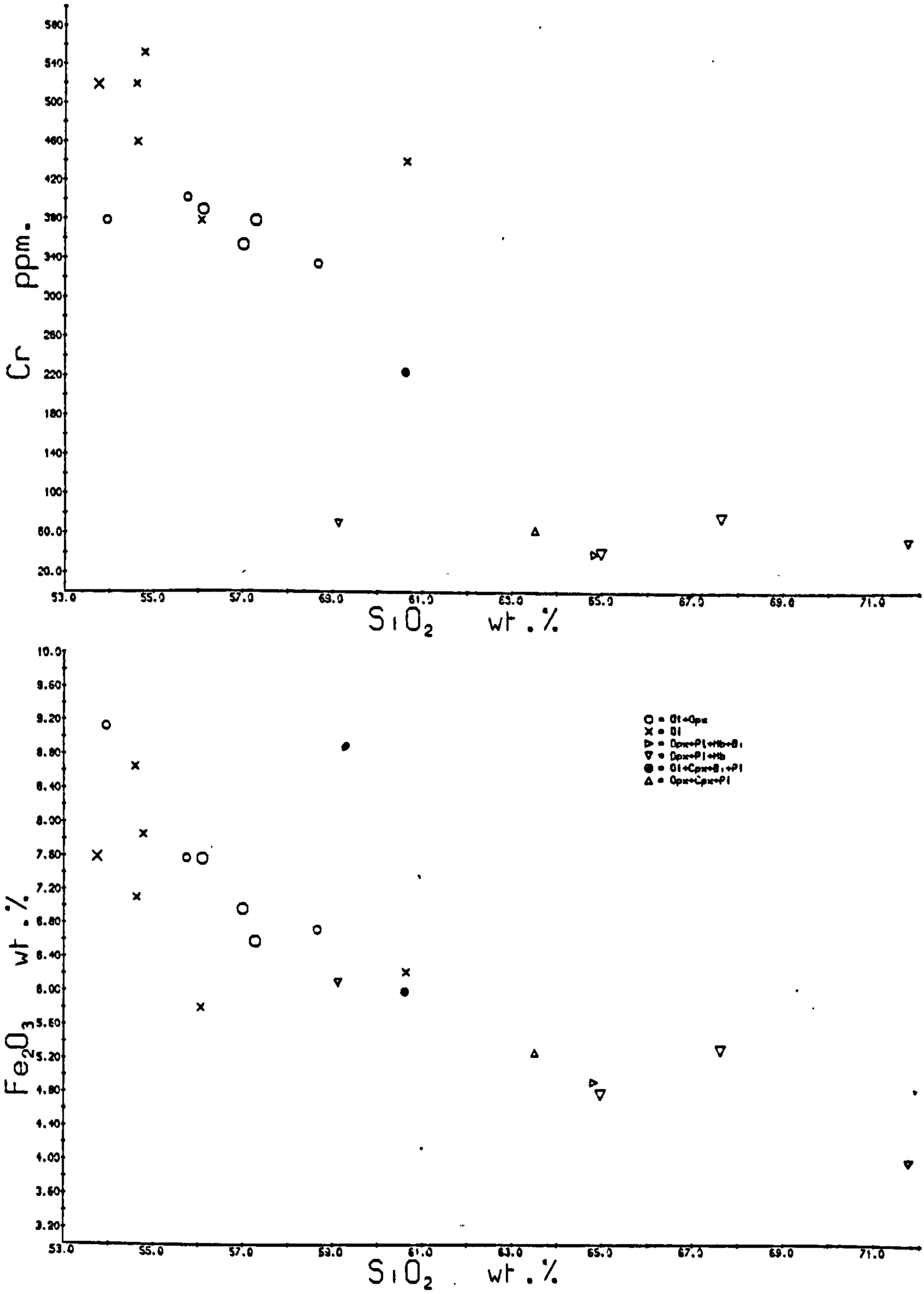

Fig. 8.1 c & d

ST. ABB'S HEAD & EYEMOUTH

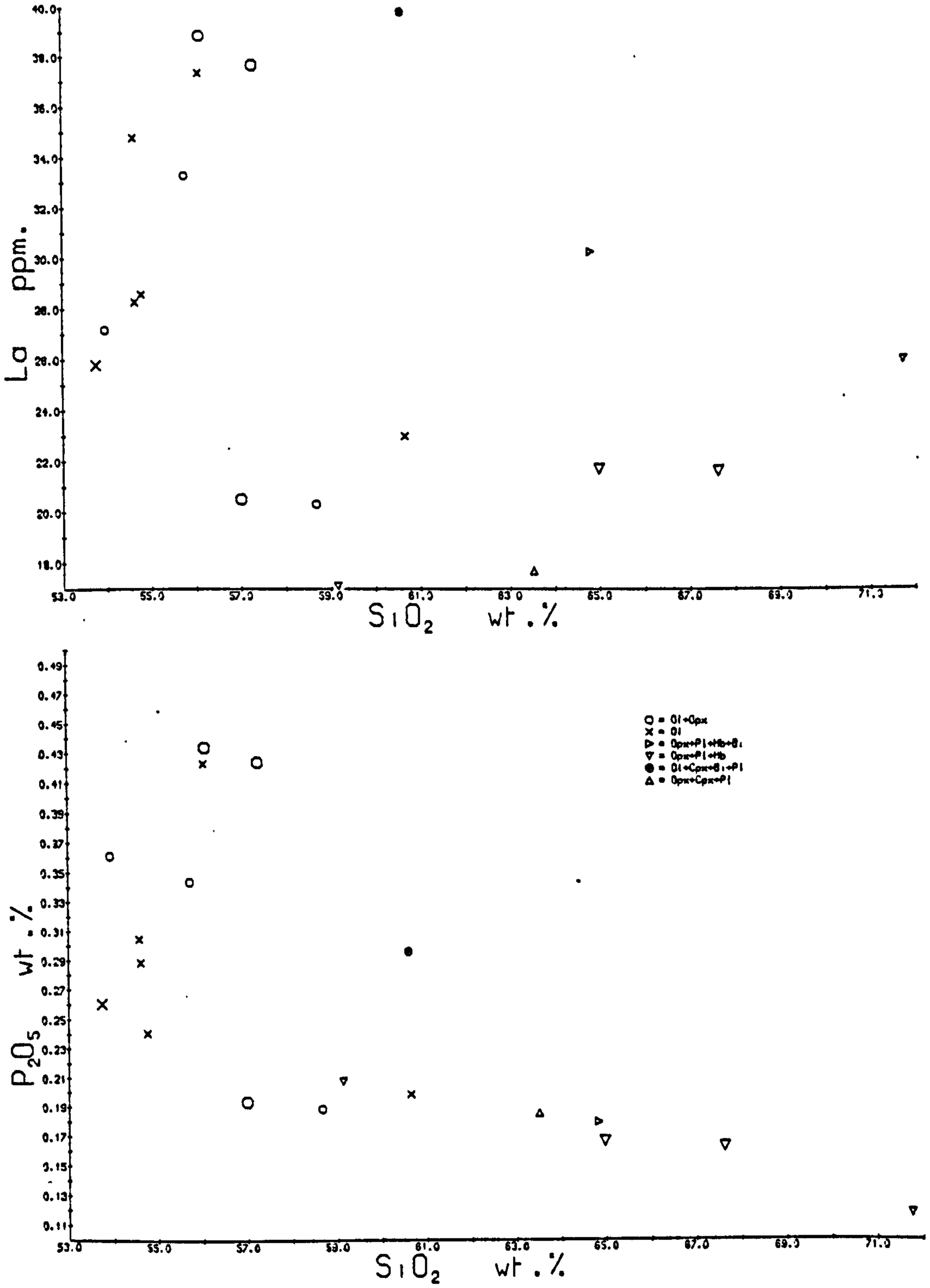

Fig. 8.1 e & f

ST. ABB'S HEAD & EYEMOUTH

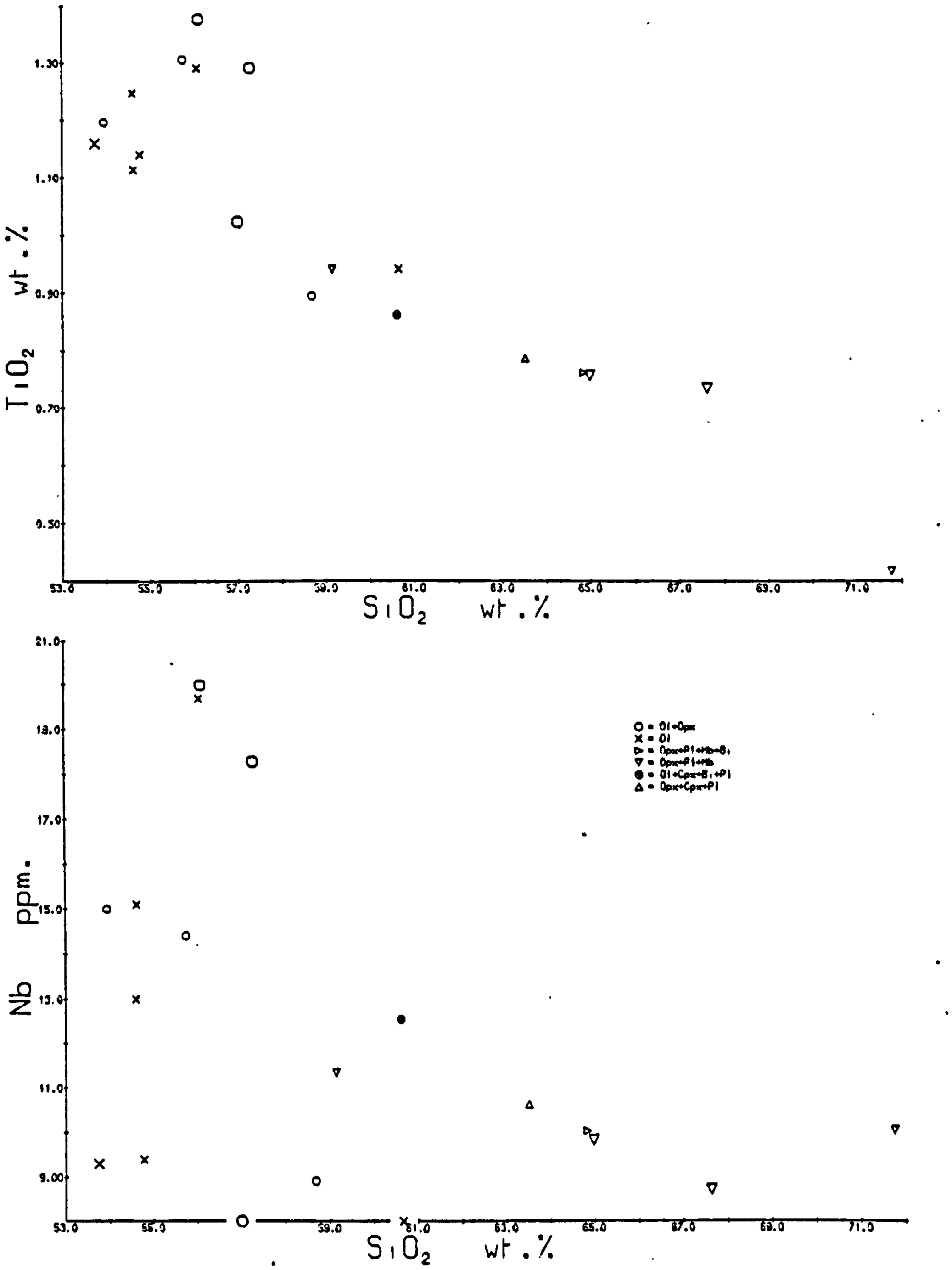

Fig. 8.1 g & h

ST. ABB'S HEAD & EYEMOUTH

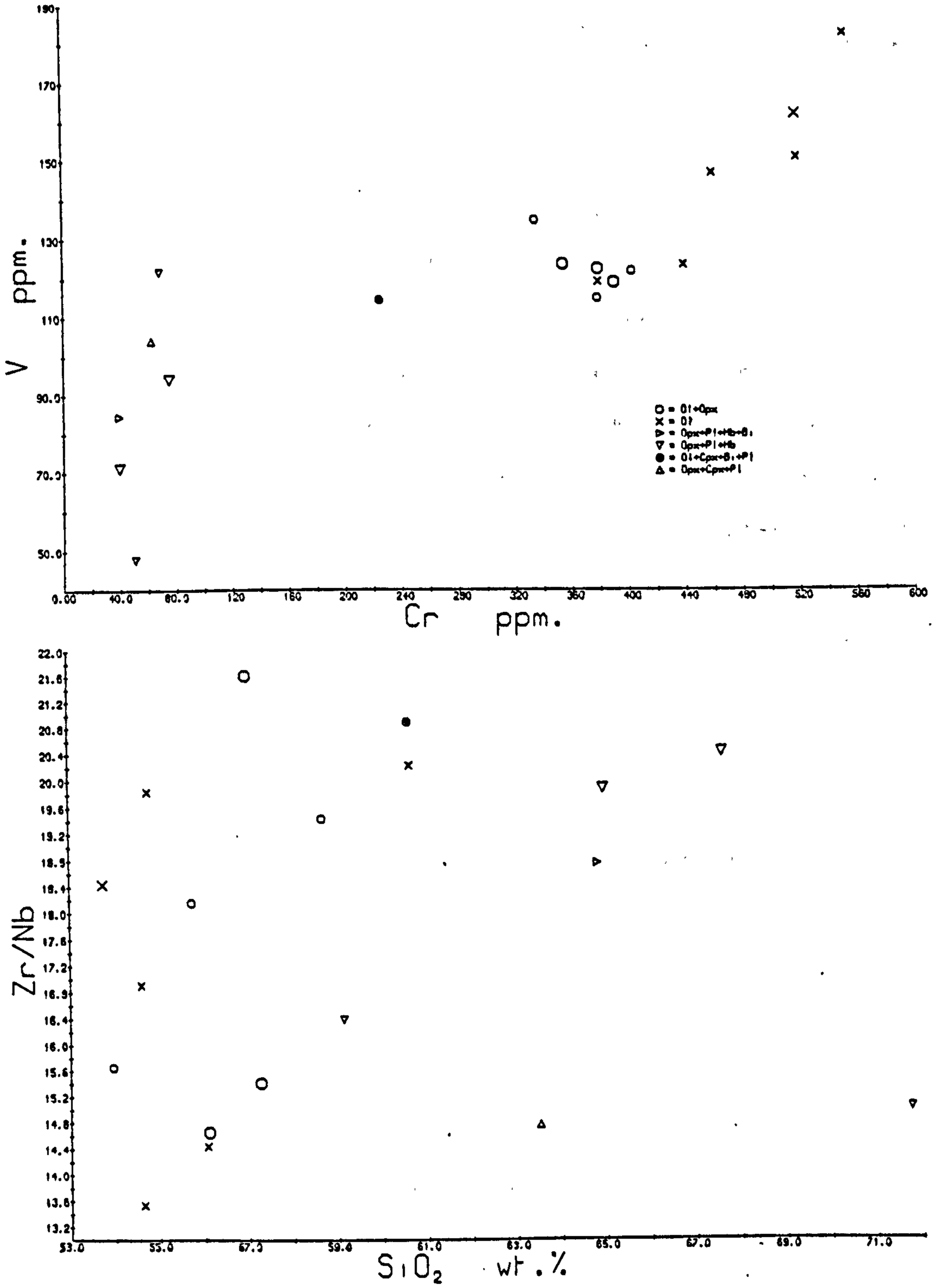

small variations in Al suggest that plagioclase must constitute some 60% of this assemblage. It is clear that this variation may not be generated by fractional crystallisation of the phenocryst minerals, olivine and orthopyroxene, and it is difficult to choose a combination of 40% ferromagnesian minerals-60% plagioclase to yield D(Ni,bulk) = D(Cr,bulk) = D(V,bulk) = 1.7. In particular, only amphibole, magnetite and biotite have distribution coefficients in excess of 1.5 for V (Gill, 1978), but separation of these minerals would lead to greater silica enrichment than that observed. Further evidence that fractional crystallisation is unlikely to produce the variation is provided by the variability in Zr/Nb ratio (13.5-20, Fig. 8.1), which has no correlation with SiO_2, Cr or Zr. This observation also rules out variation in the degree of partial melting of a single source, unless zircon was a residual phase.

SA17, a more siliceous sample which appears to be related to the 'rapid enrichment trend', has lower concentrations of P, Ti, Zr and Nb than the most siliceous sample of this trend. Th and LREE concentrations are, however, the highest in the area. The chemistry of this rock is not far removed from that of the least siliceous Cheviot andesites, and it is possible that they are genetically related. Since the relation of this sample to the 'rapid enrichment trend' is unclear, and also because the origin of the trend itself is debatable, further discussion of the possible relationship between the

St. Abb's and Cheviot lavas can only be speculative.

In addition to the 'rapid enrichment trend', a group of rocks showing low concentrations of 'incompatible' elements and little increase with increasing silica may be termed the 'flat' trend. Such rocks show a good negative correlation with silica for P, Fe and Ti (Fig. 8.1) but somewhat erratic scatter for most other elements. All plagioclase-phyric samples have low Ni and Cr. Considerable variation in Zr/Nb strongly suggests that rocks of the 'flat' trend may not be related to each other by fractional crystallisation or partial melting processes. One interesting feature is the occurrence of a sample (SA12) with much higher Y (44 ppm.) than any other from the area. This sample is also greatly enriched in La, Nd and Sm relative to other rocks of the 'flat' trend, but not in Ce. Possible interpretations may be based on the existence of two oxidation states for Ce, which could make it more susceptible to alteration than La, Nd, Sm and Y, or more probably this could be a magmatic negative Ce anomaly inherited from the source region.

The volcanic rocks of St. Abb's Head and Eyemouth do not closely resemble those from other areas of the province. Particularly unusual is the relatively simple phenocryst mineralogy which appears to correlate with chemistry (ol-opx-phyric samples have lower Ni, Cr and V than ol-phyric samples), and the existence for many elements of two very distinct variation trends with silica. All ol- and

ol-opx-phyric samples have high Ni and Cr (maxima 286 and 551 ppm. respectively), implying that these are mantle-derived, but the small number of samples and the high degree of alteration prevent any detailed petrochemical discussion. The rocks may be described as calc-alkaline.

8.2 : IRELAND

Old Red Sandstone strata including volcanic rocks outcrop both north and south of the Iapetus suture in Ireland, as defined by Phillips et al. (1976). Little is known about the volcanic rocks in the south, but they appear to be a few thin acid lavas and tuffs associated with very thick Upper O.R.S. in Co. Kerry (House et al., 1977, p.63), and they have not been sampled in the present study. In the north of Ireland, O.R.S. volcanic rocks are known from three areas: near Cushendall, Co. Antrim; the Fintona block, Co. Tyrone, and the Curlew Mountains inlier, near Boyle, Co. Roscommon. A welded tuff in the Upper Silurian strata of Clare Island, Co. Mayo, has yielded a K-Ar age of 412±8 Ma (Cocks et al., 1971, p.119), and may be part of the O.R.S. volcanic province. At Letter Hill, Castlebar, Co. Mayo, deformed Lower O.R.S. or Silurian andesites have been reported (House et al., 1977, p.58).

(a) Cushendall

On the Antrim coast, unfossiliferous O.R.S. rocks rest unconformably on Dalradian metasediments and are

overlain unconformably by Triassic sediments. The O.R.S. contains abundant andesite boulders, and a body of quartz-andesite or dacite (the Cushendall Porphyry) near the top has been variously interpreted as lava flows (House et al., 1977, p.58) or as an intrusion (Wilson, 1972). volcanic clasts from the conglomerates (NI2, 3) are rich in phenocryst plagioclase, associated with amphibole, orthopyroxene and biotite. They are quartz-normative, siliceous (67.6-69.6% SiO_2), moderately aluminous (16%) and have high Ni and Cr (>20, >50 ppm respectively) for such siliceous rocks. They have high Ba (>1300 ppm.), Sr and La/Y, and may best be compared with some of the Ben Nevis andesites.

The sample from the Cushendall Porphyry (NI1) appears to have phenocrysts of olivine, orthopyroxene, alkali feldspar, biotite and quartz, and has a correspondingly unusual chemistry, with >10% K_2O and 63% SiO_2. It is not certain whether the K_2O is primary or the result of alteration. Ba and Rb are also high, while P, Zr, LREE, Ni and Cr are all at least double their concentrations in the andesite clasts. Zr/Nb is also substantially higher. It is clear that these three rocks are not related by fractional crystallisation processes, but apart for the high K in NI1 they are not unusual for the O.R.S. province.

(b) Fintona

O.R.S. rocks in Counties Fermanagh and Tyrone are

faulted against Dalradian metasediments and rest unconformably on the Llandovery of the Pomeroy inlier (Wilson, 1972). The sediments are probably very thick and include several horizons of volcanic rocks, of which the most important, the Barrack Hill Member, may be 1600 ft (500 m) thick (Wilson, 1972). Apart from this member, the volcanic rocks are severely altered and badly exposed, but it appears that they are all quartz-normative, fairly siliceous (66-68%) and only sparsely porphyritic. Phenocrysts include plagioclase, both ortho- and clinopyroxene, and rare resorption pseudomorphs probably after amphibole. They are not chemically distinguishable from rocks elsewhere in the province. The sample from the Barr Church Member (NI10), although less siliceous, has lower Ni, Cr and higher 'incompatible' element concentrations than samples from Barrack Hill. The latter have substantially lower P, K, Ba and Sr than the Cushendall rocks. NI5 and 6 are fairly rich in Ni and Cr (>40, >85 ppm respectively).

(c) Curlew Mountains

The probable O.R.S. rocks of the Curlew Mountains form a small inlier lying unconformably below Carboniferous strata, and probably resting unconformably on Lower Palaeozoic rocks in the west. Charlesworth (1960) described the O.R.S. sequence and noted the occurrence of volcanic rocks at two horizons. The lower horizon was thought to be a 2000 ft (600 m) thick sequence of hornblende-andesites,

although some doubt was expressed over whether these were in fact extrusive. The upper horizon was believed to be from 50 to 100 ft (15-30 m) thick, consisting of plagioclase-pyroxene-phyric andesites and 'nodular lavas' (?autobreccias).

Exposure is minimal and there is some doubt whether the three samples collected were <u>in situ</u>; it is also uncertain to which volcanic horizon they belong. The samples are petrographically very different (Table A1) but are not abnormal for the province. Hornblende occurs only as very rare resorption pseudomorphs, and one sample contains fresh phenocryst orthopyroxene. All three are quartz-normative, and silica varies from 59 to 67%, the most siliceous sample having phenocryst quartz. Fe, Ti, P, V and Sr show good linear depletion with increasing silica, but the most siliceous sample is the most Cr-rich (116 ppm). Concentrations of LREE, Zr and Nb are relatively constant. K, P and particularly Ba and Sr are substantially lower than in Cushendall samples, and are closely comparable to their concentrations at Fintona.

(d) <u>Conclusions</u>

The O.R.S. volcanic rocks of the north of Ireland are not dissimilar to those of Scotland, and probably form part of the same volcanic province. While the rocks are generally siliceous, those from Fintona and the Curlew Mountains have significantly lower Ba, Sr and also P and K

than samples from Cushendall (Fig. 8.2).

8.3 : ARRAN

Lower Old Red Sandstone conglomerates in Kintyre (Friend and Macdonald, 1968) and on Arran are rich in volcanic clasts, and on Arran Tyrell (1928) described the occurrence of a basalt lava flow at several localities. This is olivine-phyric, and is cut by numerous closely spaced carbonate veins. The sample collected in this study is olivine-normative, has 53% SiO_2, and is rich in Ni and Cr (240, 340 ppm respectively). Zr and particularly LILE show very high concentrations, only slightly lower than in the Lorne cpx-hb-bi-phyric samples (section 4.1f).

A number of samples have been collected from clasts in the O.R.S. conglomerates of Arran. Tyrell (1928) described hornblende-feldspar-phyric andesites from these clasts; samples collected in the present study are varied and include 2 pyroxene-plagioclase-phyric types as well as amphibole- and biotite-phyric varieties. These are all siliceous (59-70% SiO_2) and all except one are quartz-normative. AR10 is slightly nepheline-normative, and has 10.8% K_2O: it is not certain whether this is primary or the result of alteration. The remaining samples are chemically comparable to the clasts of Cushendall (section 8.2a), in particular in their high concentrations of Ba and Sr (Fig. 8.2), although Y is never as low as at Cushendall, and the rocks are more varied. Many samples have fairly

Fig. 8.2 a & b : Bulk rock variation diagrams

Conventions as section 3.3

ARRAN AND IRELAND

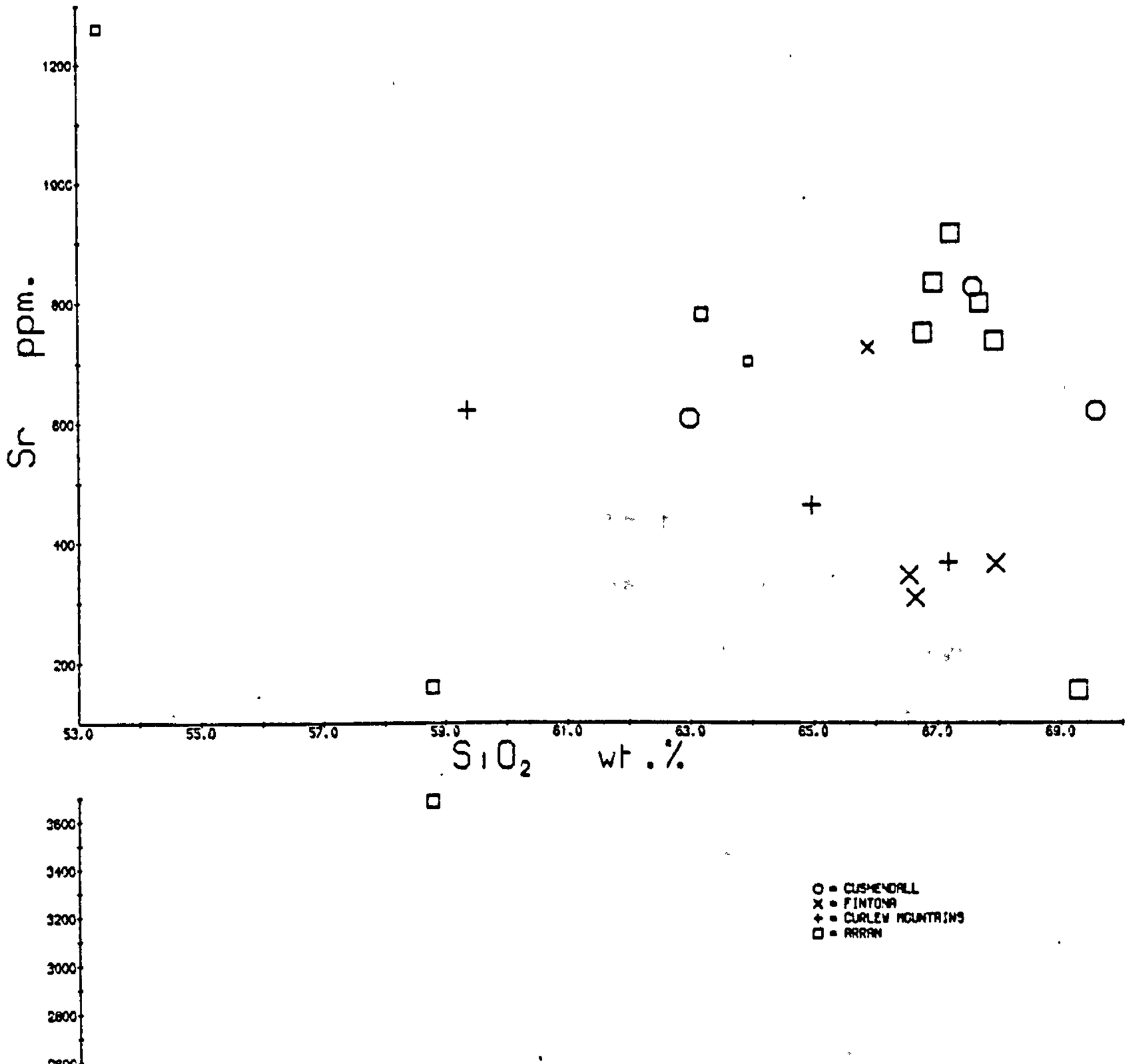

high Ni and Cr (maxima 51 and 121 ppm respectively) despite their high silica. Hornblende-granophyre forms a further clast type (AR11): this has low Sr, Ni and Cr, and high Zr and Y. This clast was probably not derived from an O.R.S. source region.

8.4 : HUNTLY

A number of sedimentary outliers variously assigned to the Lower and Middle O.R.S. rest unconformably on the Dalradian and Moinian metasediments of the northeast Grampian Highlands. A hornblende-andesite lava and an olivine-basalt ?sill were described by Read (1923) from the Bogie outlier, a northward continuation of the Rhynie outlier. Read also noted the occurrence of a similar lava near Buckie, Banffshire (interpreted as a sill in the underlying Dalradian by Peacock *et al.*, 1968, p.42) and an andesite sill near Cullen.

Exposure in the Bogie outlier is poor, and the only *in situ* sample collected (NG2) is a vesicular andesite rich in phenocryst augite and plagioclase, with rare olivine. In addition NG1, an ol-pl-phyric sample with an ophitic augite-plagioclase groundmass, was recovered from a loose block; this is closely similar to the olivine-basalt described by Read (1923). These two samples are quartz-normative and have 59 and 54% SiO_2 respectively, and for their silica contents do not have particularly high Ni and Cr. P, Zr, Nb, Th, Y and LREE are high, but are

comparable to their concentrations in the pre-Arbuthnott Group lavas of the Montrose region (Section 5.1a) and most major elements are close to their levels at Montrose.

NG3 was collected from near Buckie and is a plagioclase-hornblende-phyric andesite. It is siliceous (65% SiO_2) and very rich in Rb and Th. Many elements show linear variation with silica between this and the two samples from Huntly, and Zr/Nb is almost identical for the three samples. LREE concentrations are closely comparable but Y, Zr and Nb are depleted relative to the Huntly samples.

8.5 : SHETLAND

O.R.S. strata outcrop over much of eastern Scotland north of the Great Glen Fault and its possible continuation into Shetland, the Walls Boundary Fault (Flinn, 1961). The sedimentary history of this large area was dominated by the Orcadian Lake. With the exception of Orkney and Shetland, the absence of contemporaneous volcanic rocks contrasts strongly with their abundance further south, and clasts of volcanic origin in the sediments have only been described from the Black Isle (Horne and Hinxman, 1914, p.63). Even these are very uncommon, and none was found in the present study.

The stratigraphy of the Shetland Old Red Sandstone has been reviewed by Mykura (1976) who considered that five

From Mykura (1976)

Fig. 8.2c

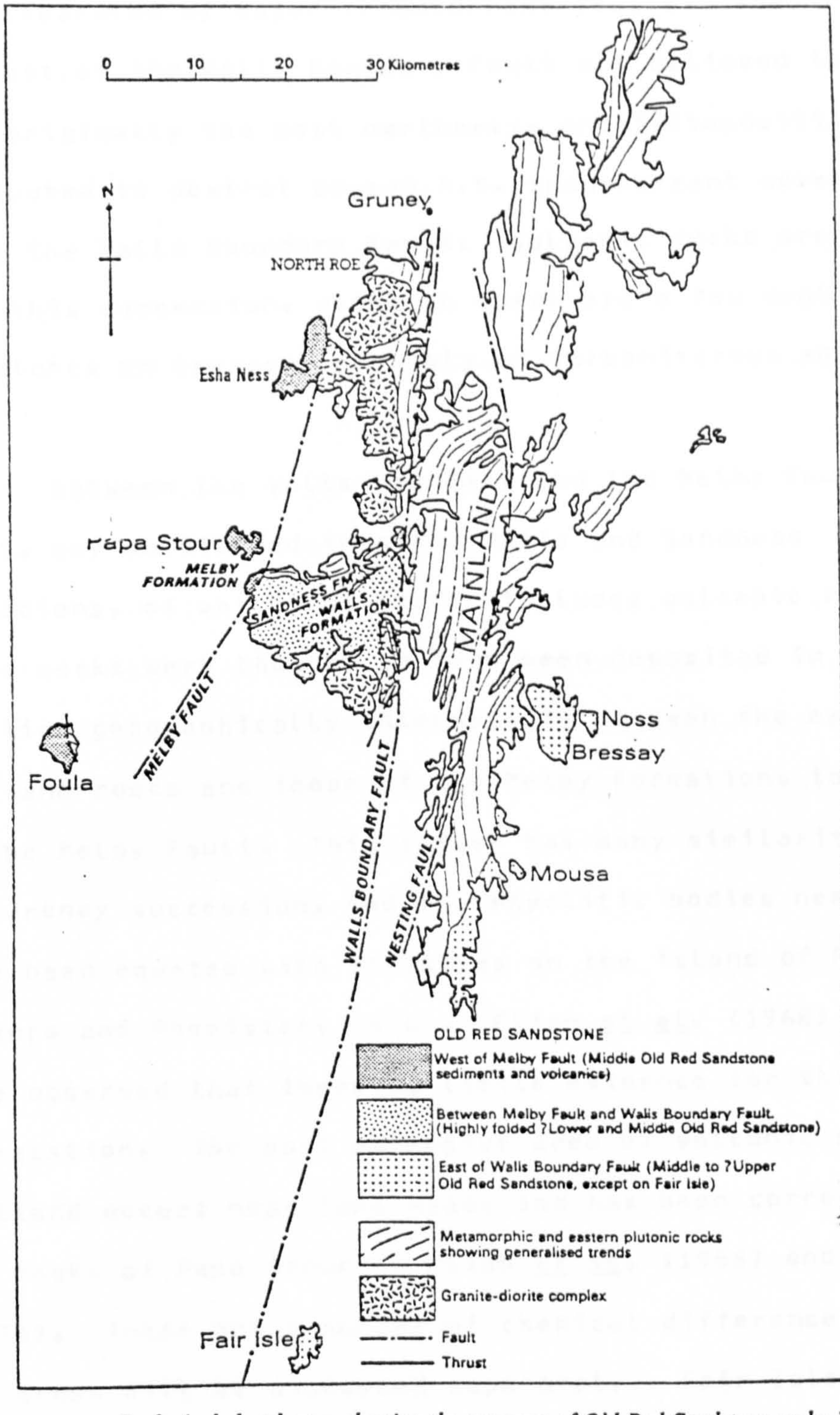

Geological sketch-map showing the outcrops of Old Red Sandstone rocks in Shetland and their structural relationships

distinct sedimentary sequences could be recognized, in the main separated by major transcurrent faults. The area to the east of the Walls Boundary Fault was believed to have been originally the most northerly, and juxtaposition was attributed to dextral post-O.R.S. transcurrent movement along the Walls Boundary Fault. Volcanic rocks are absent from this succession, although there are a few vent structures on Bressay, probably of Carboniferous age.

Between the Walls Boundary and the Melby Faults the O.R.S. may be divided into the Walls and Sandness Formations, of which the latter includes volcanic rocks. These rocks were thought to have been deposited in a position geographically intermediate between the east Shetland rocks and those of the Melby Formation, to the west of the Melby Fault. This latter has many similarities to the Orkney succession, and two rhyolitic bodies near the top have been equated with rhyolites on the island of Papa Stour (Mykura and Phemister, 1976). Flinn et al. (1968) however, have observed that there is little evidence for this correlation. The most extensive area of volcanic rocks in Shetland occurs near Esha Ness, and has been correlated with the rocks of Papa Stour by Flinn et al. (1968) and by Mykura (1976). There are a number of chemical differences, and the two areas will be discussed separately. Fair Isle and Foula also have distinct O.R.S. sedimentary sequences, although the general equivalence of the Fair Isle and Walls sequences has been suggested by Mykura and Phemister (1976, p.264). These last two areas lack volcanic rocks.

(a) Esha Ness

The O.R.S. sequence of Esha Ness is dominantly volcanic, and has been described by Finlay (1930) and summarized by Mykura (1976). The oldest beds are sandstones, which are faulted (?Melby Fault) against the Northmaven plutonic complex, but the rest of the sequence is volcanic, and rock types described include olivine-basalts, andesites, pyroxene-andesites, rhyolites and tuffs, with a mugearite and an ignimbrite. The field boundaries between these rock types (1-inch geological map, Northern Shetland) appear to be based on the presence or absence of macroscopic olivine or plagioclase. In particular, none of the four rocks collected from the area mapped as mugearite may be called a mugearite; all they have in common is their paucity of phenocrysts.

The volcanic rocks collected fall into five groups, defined by petrography and silica content. The 'basalts' (SH4, 37-39) have 51-54% SiO_2 and are sparsely porphyritic with olivine, plagioclase and in one case clinopyroxene. The 'andesites' (SH7-10) have 59 to 61% SiO_2 and SH7-9 have the phenocryst assemblage opx-cpx-pl-ap-mt, although SH10 appears to lack clinopyroxene and apatite. Clinopyroxene is a relatively iron-rich augite (anal. 89, SH9) and is rich in chlorite lamellae parallel to (001), interpreted as pseudomorphed exsolved pigeonite. In one case (SH8), these lamellae are arranged symmetrically about a twin plane, and the same herring-bone arrangement persists into an anhedral

chlorite core. This suggests the presence of early formed pigeonite, and the exsolution relationships greatly resemble those described from Straiton, Ayrshire (section 6.2).

The 'dacites' (SH1-3, 12, 13, 40, 41) have 63 to 70% silica and are rich in phenocryst feldspar, some of which is probably sanidine, although the rocks are severely altered. Mafic phenocrysts include oxide-rich pseudomorphs possibly after iron-rich pyroxene and others which may have been fayalitic olivine or hornblende. The ignimbrites have 67% SiO_2 and are rich in plagioclase and alkali feldspar crystal clasts. One severely altered rhyolitic rock has been collected, with 78% SiO_2. It should be noted that the outcrop area is very small, and therefore the composition gaps between these rock types may have no genetic significance.

Except for three basalts, all rocks are quartz-normative. SH38 has 2% normative nepheline, but this may be attributed to alteration. Pyroxenes analysed from SH9 have low Na, Ti and Al (anal. 89), plotting within the tholeiitic field of Le Bas (1962). A number of rocks, particularly 'dacites' (Fig. 8.3b), show Fe/Mg within the tholeiitic field of Miyashiro (1974), and all rocks have low to moderate alumina (<16.5%). These criteria, and the relatively iron-rich pyroxenes, suggest that the rocks are best classified as transitional between calc-alkaline and tholeiitic, despite the high levels of K_2O (Fig. 8.3).

Fig. 8.3 a & b : Bulk rock variation diagrams

Conventions as section 3.3

ORKNEY AND SHETLAND (field for Esha Ness ignimbrites)

a : boundaries from Peccerilo and Taylor (1976)
b : boundary from Miyashiro (1974)

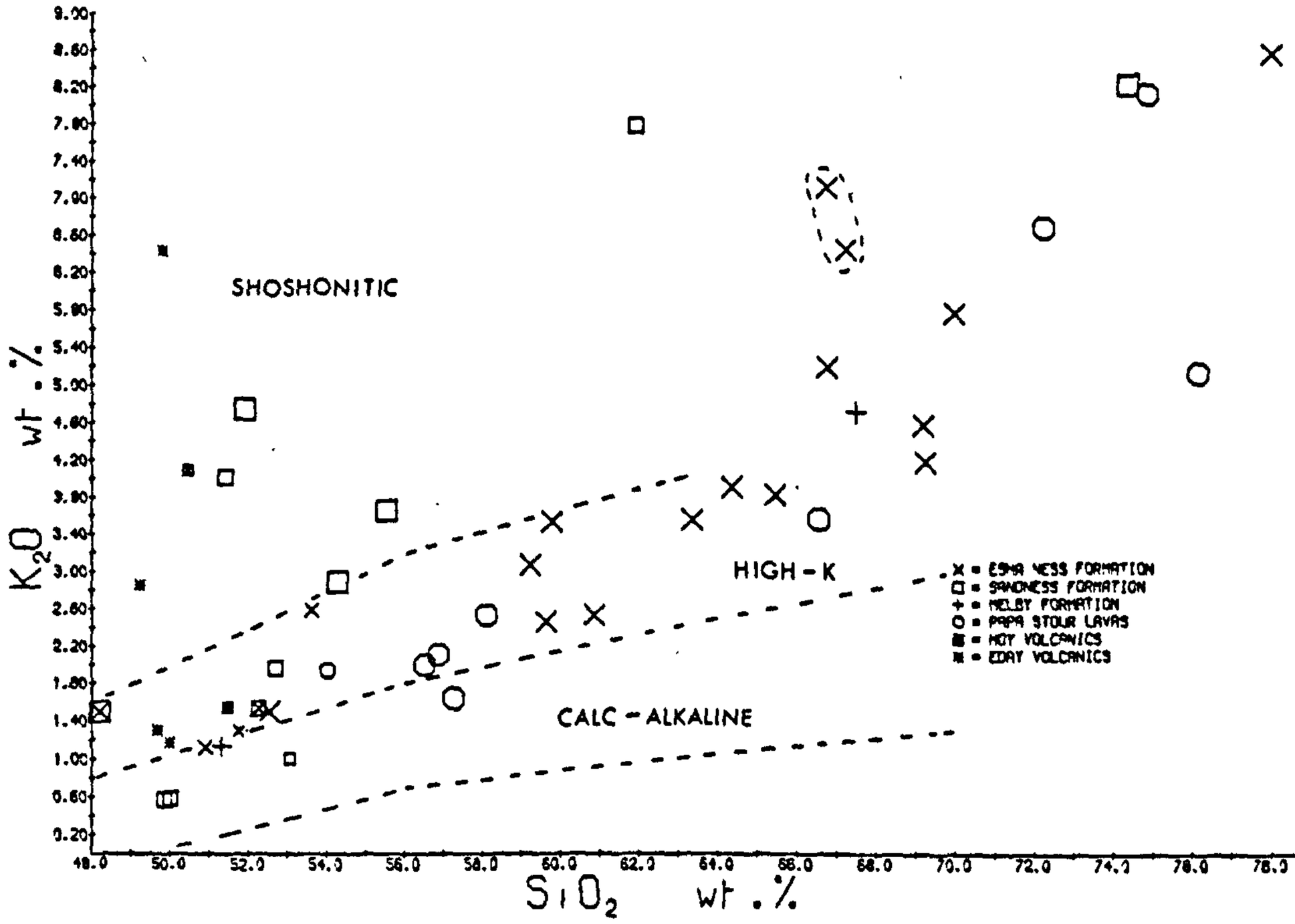

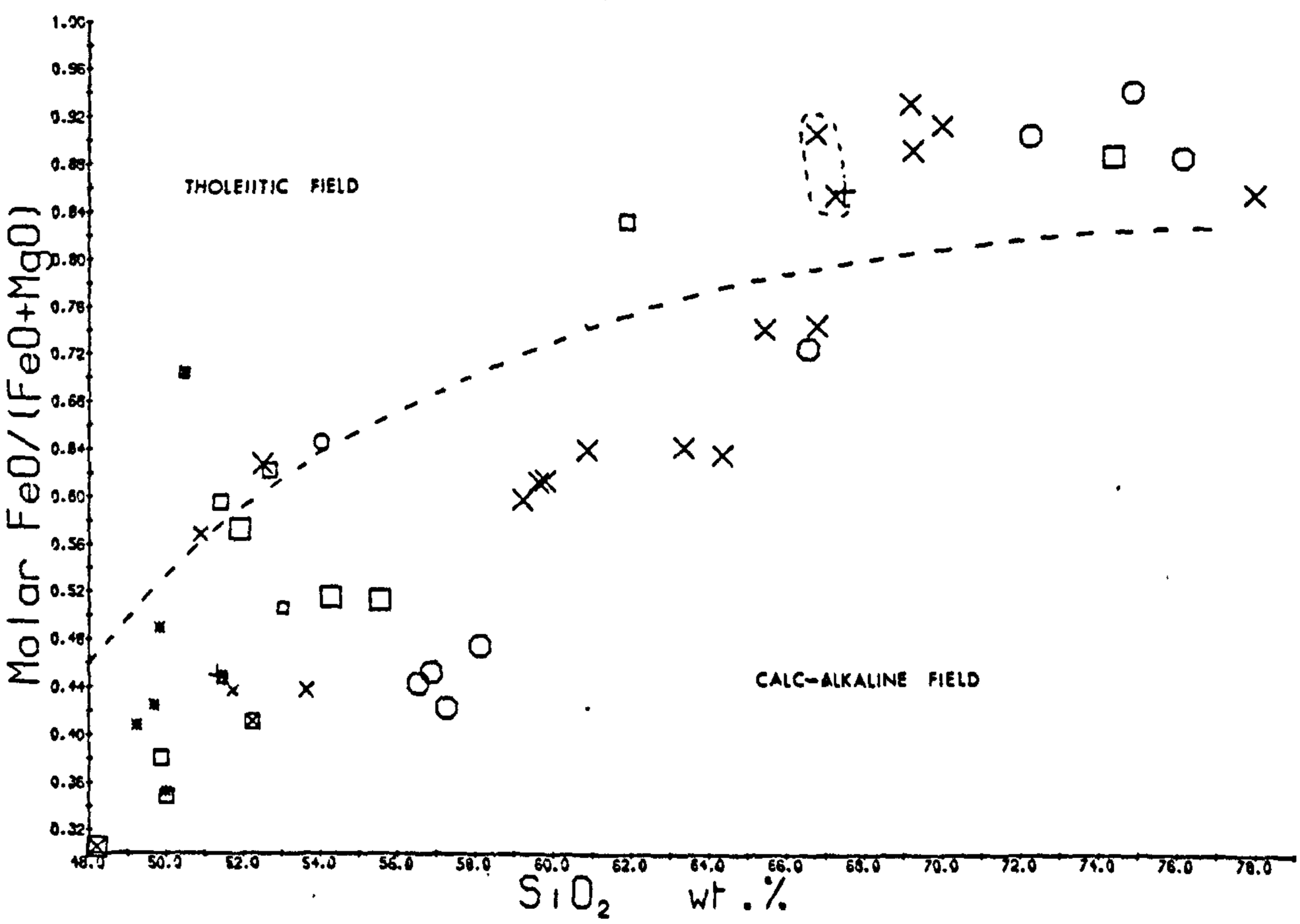

Fig. 8.3 c & d

Field for Esha Ness ignimbrites.

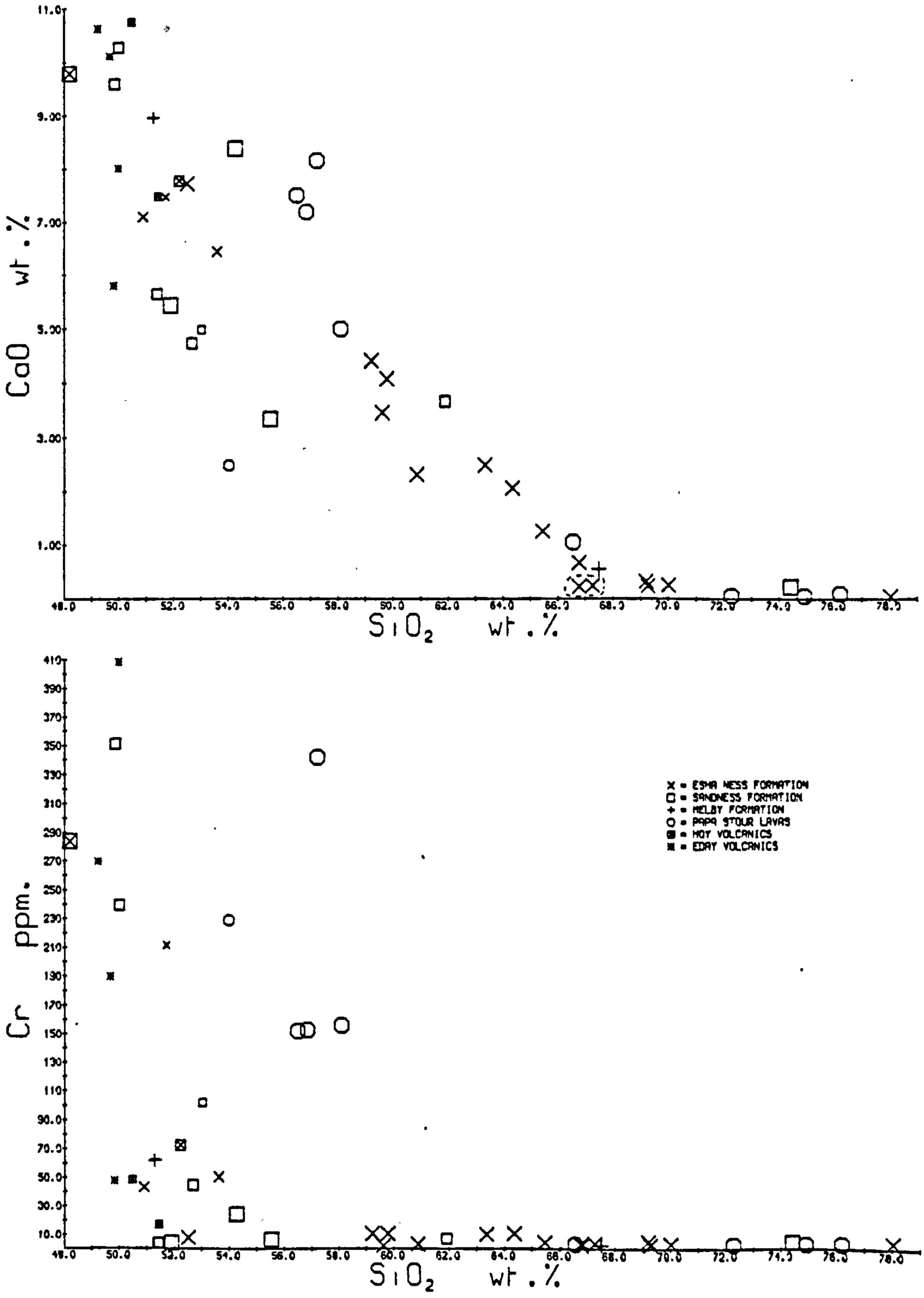

Fig. 8.3 e & f

ORKNEY AND SHETLAND

Field for Esha Ness ignimbrites

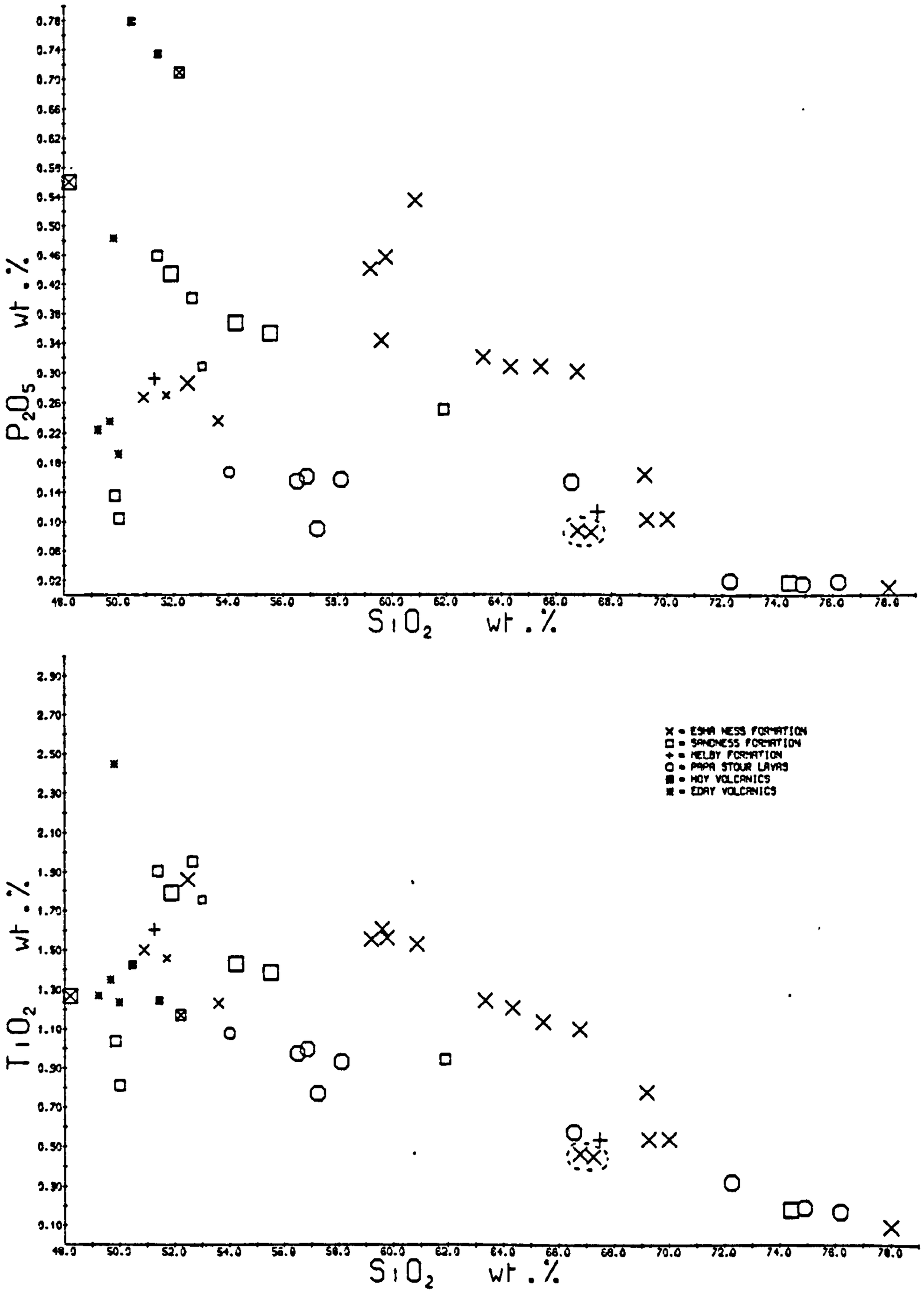

Fig. 8.3 g & h

Field for Esha Ness ignimbrites

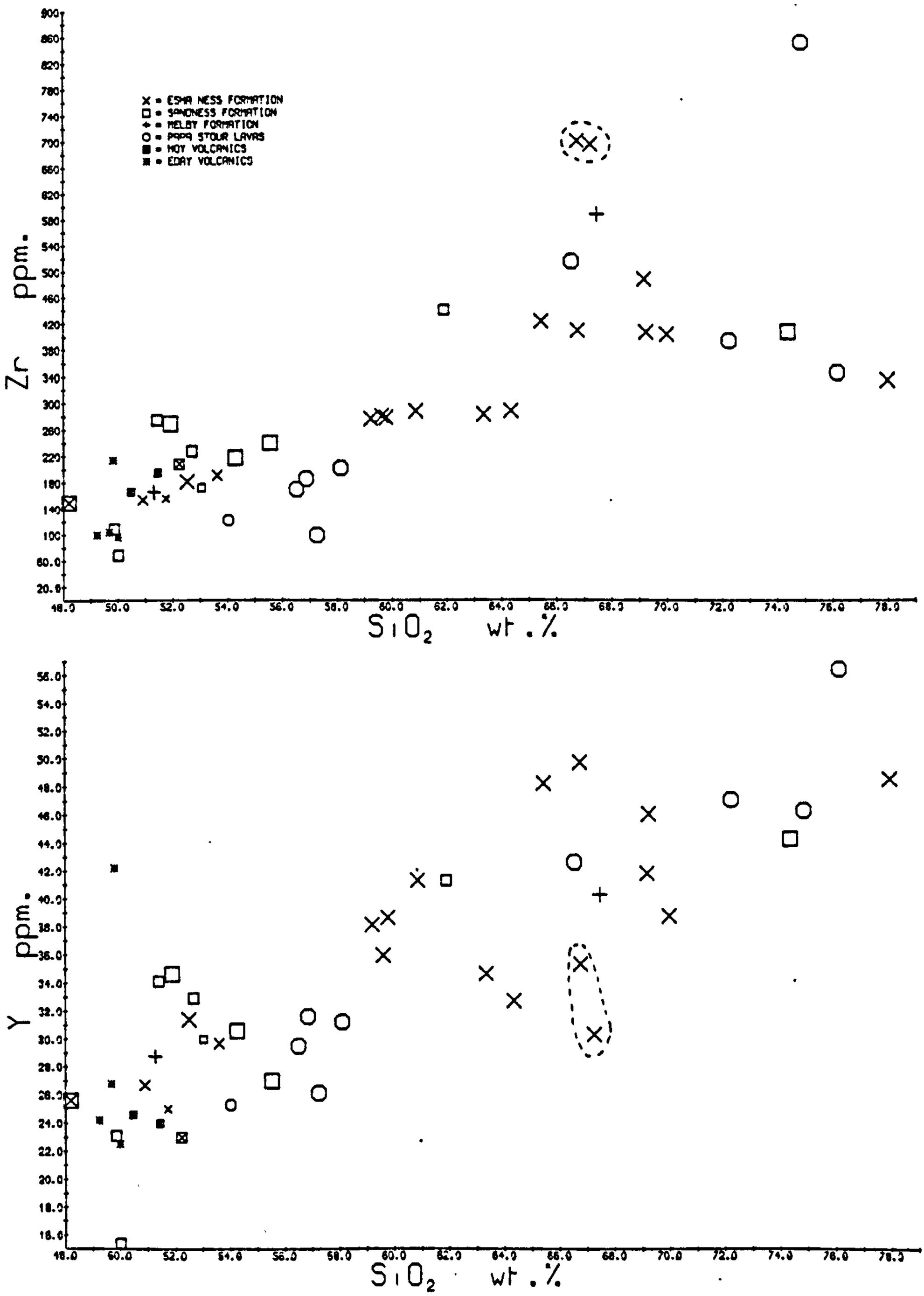

Fig. 8.3 i & j

ORKNEY AND SHETLAND

Field for Esha Ness ignimbrites

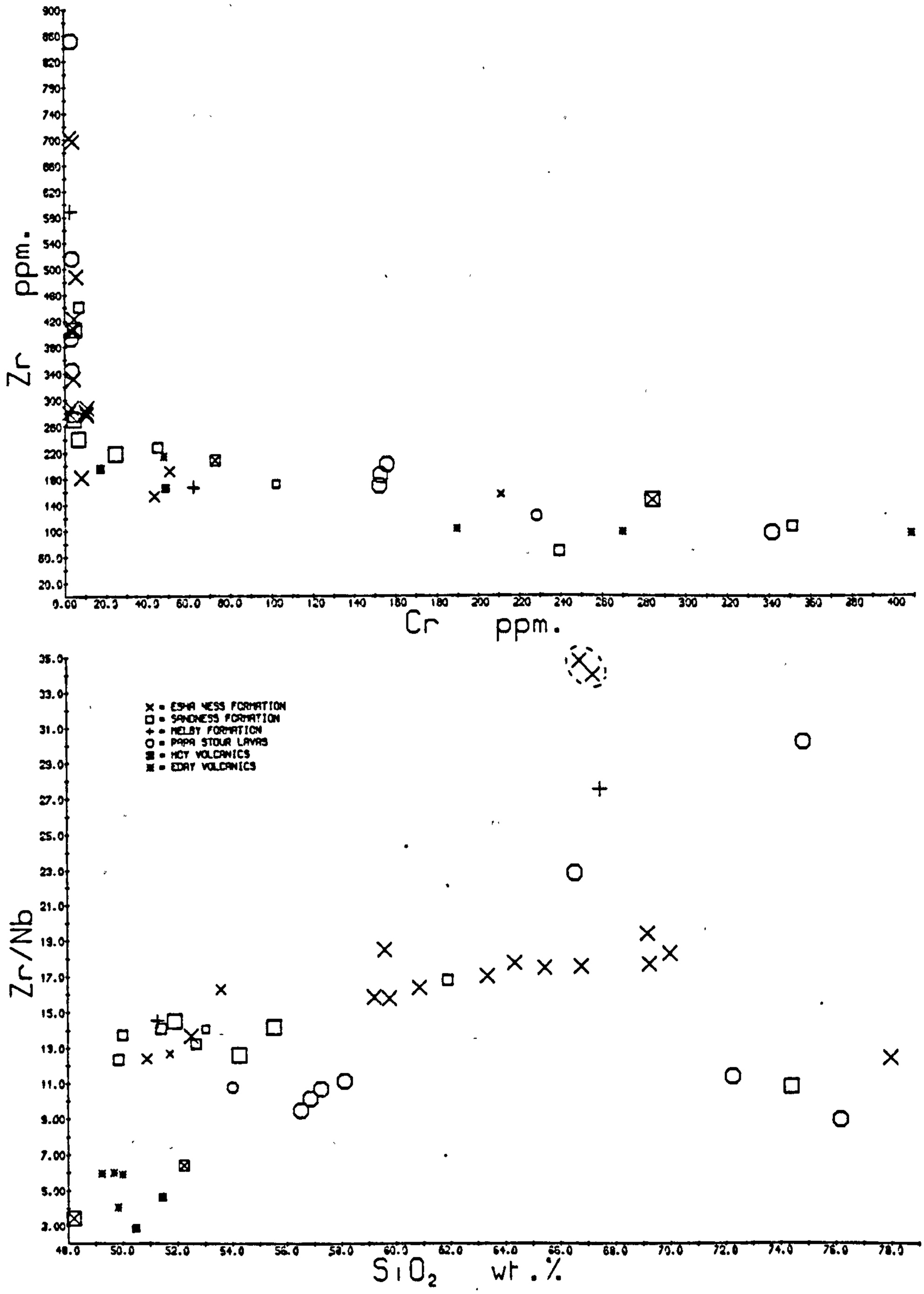

With the exceptions of the ignimbrites and the rhyolite, all samples show excellent negative correlation with silica for Al and Ca (Fig. 8.3c). Close negative correlation with silica also exists for Fe, Ti and Mg, and to a lesser extent for V and Sc, in the andesite-dacite range. Ni and Cr are always lower than 18 and 11 ppm respectively in rocks with more than 54% SiO_2, contrasting strongly with the situation elsewhere in the O.R.S. volcanic province, although the lack of compositions between 54 and 59% SiO should be noted. One of the 'basalts' (SH4) also has very low Ni and Cr, and has the highest concentrations of Fe, Ti, V and also Ca and Sc. P concentrations are at a maximum in the andesites (Fig. 8.3e). Zr, Nb, Y and LREE all show fairly good positive correlation with silica, and La/Y and Zr/Nb show slight increases with increasing silica (Fig. 8.3j). These relationships suggest that the suite could be genetically related by fractional crystallisation. The variation in Zr/Nb from 12 to 19 correlates well with increasing SiO_2 and Zr: the three-fold increase in Zr suggests a high degree of crystallisation, and the increase in Zr/Nb may be well explained by an implication of Pearce and Norry (1979) that D(Zr/Nb)<1 for most plausible fractionating minerals (Chapter 3).

The variation described above for the basalts may probably be accounted for by fractional crystallisation of the phenocryst minerals olivine and plagioclase, associated with minor chrome-spinel. However, the enrichment in Ti and V in SH4 is not associated with enrichment in Zr or Nb, and

the highly altered state of the basalts leads to difficulty in the development of a quantitative model.

The change from basalt to andesite is marked by 1.5X enrichment in Zr and Nb, 1.8X enrichment in LREE, and substantial depletion in Ca, Mg, Sc, V, Fe, Al and Ti (in order, with greatest depletion in Ca). This suggests the incoming of at least one extra liquidus phase; for example plagioclase, clinopyroxene, orthopyroxene or titanomagnetite. Major element variation from SH4 to SH9 (an andesite) and from SH9 to SH12, a dacite, has been modelled using the computer program MODES, using the weighting facility as in Chapter 7. Mineral analyses were taken from SH9, together with an estimated titanomagnetite and the orthopyroxene from AY35 (cpx analyses of SH9 and AY35 compare closely). A very good fit (sum of squares of residuals $\Sigma r^2=0.03$) is given for fractional crystallisation of 7.3% mt, 3.3% opx, 0.3% ap, 15% cpx and 32.8% pl from SH4 to form SH9. This model is supported by the nearly constant Sr, and the c. 1.5X enrichments in Zr and LREE, which will be partially retained by titanomagnetite and apatite. These elements, together with Sc, V and Ni, have been modelled using the Rayleigh equation for perfect fractional crystallisation and the distribution coefficients of Gill (1978) and Pearce and Norry (1979). Reasonable agreement is provided by Zr, LREE, Sr and Sc, but in the latter case only if D(Sc,cpx) is taken as 4. V content of SH9 is too high for the required amount of magnetite separation (assuming D(V,mt)=24) and Ni and Cr are higher in SH9 than SH4, even

though D(Ni,bulk)=2.5. It is clear that SH9 may not be derived by fractional crystallisation of a liquid of composition SH4, but it is believed that it could be derived from a liquid immediately parental to SH4 with higher concentrations of Ni and Cr.

Chemical variation among the four andesites is substantial for P, V, LREE and Fe (Fig. 8.3), and this variation is correlated with smaller changes in Mg, Sc and Y. SH10, the apatite-free andesite, has highest P, LREE and lowest Fe, Mg, V, Sc: it is suggested that this variation could result from minor variation in the relative proportions of phases crystallised from a basaltic parent.

The variation between SH9 and the dacites (e.g. SH12) is not well modelled by fractional crystallisation of the phenocrysts of SH9 ($\Sigma r^2=5$) although a better fit is provided for generation of a less siliceous dacite, SH40 ($\Sigma r^2=1.2$). Both of these models have large residuals for Ti, suggesting that a Ti-rich phase should be incorporated into the model. Recognition of the mafic phenocrysts in the dacites is difficult, and it is possible that one of them may have been a Ti-rich amphibole.

The ignimbrites show much higher Zr/Nb than other rocks, mainly due to their very high Zr content, while the rhyolite has slightly lower Zr/Nb. It is possible that the rhyolite represents the final stage in the fractional crystallisation sequence, but this is difficult to model

because of the severe alteration.

Despite the small area of rocks exposed at Esha Ness, there is good evidence that the suite may be derived by multistage low pressure fractional crystallisation. The first stage involved separation of an olivine-dominated assemblage from a magma close in composition to an olivine-tholeiite, and was followed by crystallisation of orthopyroxene (or pigeonite), clinopyroxene, plagioclase, titanomagnetite and apatite, and later by a Ti-rich phase. Major iron enrichment in andesites and dacites is prevented by crystallisation of titanomagnetite, but the rocks are transitional between calc-alkaline and tholeiitic. The area is thus distinguished from the rest of the province, where fractional crystallisation processes have been inferred to be of minor importance. The principal petrochemical differences are as follows:

1/ Gently increasing Zr/Nb with increasing SiO_2 and Zr.

2/ Positive correlation between SiO_2 and Zr, Nb, Y and LREE, despite the later crystallisation of apatite and Ti-rich phases.

3/ Good correlation between phenocryst mineralogy and host rock SiO_2.

4/ Very low Ni and Cr in rocks with >54% SiO_2, and the absence of rocks with low Ni and low 'incompatible' elements, and of rocks with high Ni and high 'incompatible' elements.

It is possible that variation in Zr/Nb in the basalts

is significant, and that the petrogenesis is not quite as simple as presented above. Because of the high degree of crystallisation implied above within the basalt range, and from basalt to andesite, andesite to dacite, incompatible element concentrations increase rapidly with SiO_2: the most mafic rocks have low K_2O(<1.4%), low LREE (<30 ppm La) and low Ba (?500 ppm) relative to many rocks in the rest of the province.

(b) Melby - Papa Stour

The two rhyolites of Melby are severely altered, and the one analysed (SH20) compares well with the Esha Ness ignimbrites, although similarity between two such acid rocks is not necessarily significant. A sparsely ol-pl-phyric lava is exposed on the Holm of Melby, an island in the Sound of Papa; this is basaltic (SH36), and compares very closely with the moderate-Ni, -Cr basalts of Esha Ness (SH38, 39), except for the more mobile elements Ba, Rb, K and Na. It is suspected that the high and variable Zn concentrations are also due to alteration.

The rocks of the island of Papa Stour have been described by Mykura and Phemister (1976). They were assigned to the Middle O.R.S. on the basis of correlation with the Melby rhyolites, which overlie sediments with a rich fish fauna. The sequence consists of at least four 'basalt' flows, overlain by tuffs, sandstones and two thick rhyolite lavas. The samples collected from the basic flows

have olivine and plagioclase phenocrysts, with olivine common in SH32, but SH27, 29 and 30 are all sparsely porphyritic. SH31 is an altered coarse-grained variant. SH30 contains rare phenocrysts of relatively iron-rich augite, low in Ti, Al and Na (anal. 90), and augite-rimmed orthopyroxene in addition. With the exception of the altered sample, they are all quartz-normative. They are not basalts (54-58% SiO_2), but have much higher Ni and Cr than most Esha Ness samples (Fig. 8.3d), suggesting that the rocks of these two areas can not be related by fractional crystallisation. In addition, Zr/Nb is much lower at Papa Stour, and is constant for all mafic samples. Fe/Mg is low, and the rocks are best described as calc-alkaline. SH32 has the highest concentrations of Mg, Ni, Cr, Ca, [illegible] Sc and V, and the three other fresh samples are enriched in P, LREE, Rb, Ba, Zr and Nb by an amount which could be attributed to about 40% crystallisation of a liquid of composition SH32. Ti, Y and Sr are slightly enriched in the evolved samples (Fig. 8.3). It is suggested that these four samples are likely to be related by fractional crystallisation, not of the phenocryst phases, but possibly of an assemblage rich in clinopyroxene at higher pressure. The small number of samples available does not permit quantitative modelling by extract calculations. The most mafic sample has very low concentrations of many incompatible elements compared with rocks elsewhere in the province e.g. 0.09% P_2O_5, 220 ppm Sr and 34 ppm Ce.

The rhyolites contain phenocrysts of sanidine and

sometimes plagioclase, with some pseudomorphs possibly after hornblende. Two have Zr/Nb similar to that of the mafic rocks, but the other two have high Zr/Nb comparable to the Esha Ness ignimbrites (Fig. 8.3). All four have moderate to low Ba, perhaps attributable to fractional crystallisation of sanidine, but the four are very variable for most elements, and the small number of samples does not permit the suggestion of petrogenetic hypotheses.

The new chemical data suggests a review of the correlation proposed by Finlay (1930), Flinn *et al.* (1968) and Mykura (1976) between the Esha Ness, Papa Stour and Melby volcanic rocks. It is considered unwise to use probably impersistent rhyolites as a basis for correlation, and more emphasis should be placed on basic lavas and ignimbrites. The mafic lavas of Papa Stour are very different from those of Esha Ness, particularly in Zr/Nb, P_2O_5, Ni and Cr, but that of the Holm of Melby is very similar to the Esha Ness basalts. Ignimbrites have not been recorded from Papa Stour, but are known from Melby (Mykura and Phemister, 1976, p.151). It is therefore suggested that Esha Ness - Holm of Melby - ?Melby formed a single volcanic region, from which Papa Stour was distinct. These differences may be explained by postulating a transcurrent fault in the Sound of Papa, or by invoking an age difference between the two areas.

(c) Sandness Formation

The Sandness and Walls Formations lie between the Melby and the Walls Boundary Faults, and are separated from each other by the Sulma Water Fault. The Walls Formation is wholly sedimentary, but the Sandness Formation contains a number of thin lava flows and pyroclastic horizons described as the Clousta Volcanic Rocks. The occurrence and petrography of these have been described by Mykura and Phemister (1976). The rocks have suffered polyphase deformation, and sometimes low-amphibolite facies metamorphism. The effects of the deformation may often be seen in thin section; for example, the dislocation of phenocryst plagioclase in SH23.

Mykura and Phemister (1976) have described pyroxene-andesites, basalts and ignimbrites from the Clousta Volcanic Rocks. Most rocks collected in the course of this research are sparsely porphyritic with olivine and plagioclase, although SH23 has abundant calcic labradorite (anal. 78) and diopsidic augite phenocrysts. A few of the latter are rich in Ti and tetrahedral Al, but the average (anal. 88) plots within the tholeiitic field of Le Bas (1962). A severely altered ignimbrite sample and an apparently acid clast rich in sanidine from the Clousta Tuff have also been collected.

The mafic rocks include two slightly nepheline-normative samples (0.5% ne), but this can be

attributed to alteration. Three further samples are olivine-hypersthene normative. Silica varies from 50 to 55%, and SH23, the 'pyroxene-andesite' with abundant phenocryst plagioclase from Burga Water (Mykura and Phemister, 1976, p.92), has 50% SiO_2 and is Ni- and Cr-rich. Several rocks have Fe/Mg within the tholeiitic field of Miyashiro (1974), and they may be described as transitional between calc-alkaline and tholeiitic. Zr/Nb is identical within analytical error (12-14.5) and the rocks can not be distinguished from those of Esha Ness on the basis of Zr/Nb (Fig. 8.3). SH23 has the lowest concentrations of most incompatible elements (e.g. 69 ppm Zr), but does not have the highest Ni or Cr. The high alumina of SH23 suggests that the low incompatible element concentrations may be due to plagioclase accumulation, for in general samples with higher incompatible elements have lower Ni and Cr.

The chemical variation may be due to fractional crystallisation of olivine, clinopyroxene and plagioclase, with additional spinel for the two more siliceous rocks (SH15, 16). This is suggested by enrichment in V, Ti and Fe and depletion in Mg, Ni, Cr, Ca and Sc between SH23, 25 and SH18, 19, 22 and 24. Over this same range, Sr, Y and V increase by a factor of about 1.8; Ti by about 2.4; Zr, Nb and P by about 3.5; Ba and LREE by about 6 and K, Rb and Th by about 7. It should be noted that the lack of silica enrichment over the large degree of crystallisation necessary will occur if $D(SiO_2, bulk)=1$, which may be the case during separation of the assemblage ol-cpx-pl, although

it is surprising that the phase assemblage seems not to have changed over such a large degree of crystallisation. Separation of titanomagnetite can generate the higher silica and lower Fe, Ti and V of SH15 and 16.

While the more evolved rocks show significantly higher incompatible element concentrations and lower Sc and V than the Esha Ness basalts, there is broad similarity between the two areas (Fig. 8.3), and the most mafic Esha Ness rocks generally fall on the variation trends for Sandness rocks. This suggests the possibility that the parental magmas of each were in many ways similar, although Esha Ness rocks all have lower Al.

The apparently acid clast from the Clousta Tuff has only 62% SiO_2, but 7.8% K_2O. Zr/Nb is close to that of basic Sandness rocks and it is conceivable that this could be derived by further fractional crystallisation of the basic Sandness magmas. The ignimbrite has lower Zr/Nb, comparable with the Papa Stour rocks (Fig. 8.3), but it is greatly altered and little can be concluded concerning its petrogenesis.

(d) Shetland : Conclusions

The three volcanic sequences of Shetland form three petrochemically distinct groups. The basic and intermediate rocks of each sequence can be related by fractional crystallisation processes. This is in strong contrast to

rocks from elsewhere in the province, where Ni- and Cr-rich rocks frequently have high concentrations of incompatible elements. The compositions of Shetland lavas often imply a large degree of crystallisation of parental magmas deficient in incompatible elements. These parental magmas, while not primary magmas, are represented in Shetland by a few rocks with 100-200 ppm Ni, and have lower concentrations of incompatible elements than observed from elsewhere in the province.

8.6 : ORKNEY

Most of the rocks exposed in Orkney have been assigned to the Old Red Sandstone (Wilson *et al.*, 1935) on the basis of abundant fish faunas. Volcanic rocks are present at two horizons in the O.R.S. sequence: near the base of the Eday Flags (Middle O.R.S.) and at the base of the Hoy Sandstone (?Upper O.R.S.). The rocks associated with the Eday Flags on Shapinsay and at Deerness comprise lavas and associated intrusions (Kellock, 1969). The lavas are sparsely ol-pl-phyric with a groundmass of plagioclase, augite, analcite and other zeolites, and the intrusive rocks are coarse-grained with the same mineralogy. Kellock (1969) compared the rocks with the Carboniferous teschenites and alkali basalts of the Midland Valley, although the analcite may be secondary. Two of the samples have normative nepheline, but this can be attributed to the introduction of carbonate on alteration. All four rocks have 49-50% SiO_2, but a significant range in Ni and Cr concentrations exists.

The three samples with higher Ni (OR5, 7, 8) show increases in Zr, Nb, Y, P, Ti and LREE with decreasing Cr, while Zr/Nb is constant at about 6. (Fig. 8.3j). Y/Nb>1 for these three samples, suggesting that they are not alkaline (Pearce and Cann, 1973), and most immobile incompatible elements have low concentrations similar to those at Esha Ness, although Nb is slightly higher. OR6, however, has 52 ppm Nb and Y/Nb<1. Such high Nb is not known from elsewhere in the O.R.S. province. Ti in OR6 is closely comparable to its concentrations in Carboniferous alkali basalts (Macdonald 1975) but in the other three Ti is much lower. It is believed that OR5, 7 and 8 are olivine-tholeiites similar to the Shetland rocks, and that the intrusive rock OR6 is probably younger, and Carboniferous.

The volcanic rocks of Hoy are thought to be of Upper Devonian age (House *et al.*, 1977) because of the occurrence of *Holoptychius*, an Upper O.R.S. fish, in the Caithness equivalents of the immediately overlying Hoy Sandstone (Mykura, 1976, p.89). A K-Ar stepwise degassing age of 368±8 Ma has been reported by Halliday *et al.* (1977). Tuffaceous sediments are overlain by the Hoy lava(s) which were described as ol-pl-phyric by Mykura (1976). Olivine is fresh in two samples and has composition Fo83 (anal. 4, OR3). Plagioclase is generally bytownite (anal. 77, OR3), and there are also frequent phenocrysts of augite. This is often rich in Ti and tetrahedral Al (anal. 87, OR3) and most analysed points plot in the alkaline field of Le Bas (1962). An isotropic groundmass mineral is probably analcite.

All four samples have normative nepheline (3-5% ne), and since two samples have fresh olivine the nepheline is believed to be primary. Silica varies from 48 to 52% and OR3 is rich in Ni and Cr. Nb is very high (32-58 ppm) and Zr/Nb very low (3-6). There is no correlation between Zr and Nb, or between these and depletion in Cr or Ni: the rocks can not therefore be related by fractional crystallisation. Y/Nb is less than 1 and La/Y, P_2O_5 and Sr are much higher than any other rock from Shetland and Orkney (Fig. 8.3). They may therefore be described as alkali basalt and hawaiite, but their low Ti distinguishes them from the younger Carboniferous alkali basalts. Whitford (1975) noted that alkali basalts erupted in subduction-related magmatic arcs characteristically have low Ti.

CHAPTER 9 : SPATIAL VARIATION, DISCUSSION AND CONCLUSIONS

9.1 : CHARACTERISTICS OF THE O.R.S. VOLCANIC SUITE

The volcanic rocks associated with the Old Red Sandstone in Britain have a number of features in common. The most important are:

(a) Most rocks are quartz-normative. Basic rocks are sometimes olivine-hypersthene normative, but apart from the Hoy lavas, significant normative nepheline is never present in rocks free from secondary carbonate.

(b) Y/Nb is greater than 1, except in the Hoy lavas. This suggests a non-alkaline suite (Pearce and Cann, 1973).

(c) Ti and Al contents of phenocryst clinopyroxene are low, generally falling within the non-alkaline field of Le Bas (1962), with the exception of those from the Hoy lavas.

These three features imply that the suite is non-alkaline, but concentrations of LIL elements and Zr are often comparable to those of alkaline suites. In particular, the classification of Peccerillo and Taylor (1976) describes many rocks as shoshonitic (Fig. 9.1); but using the above criteria these rocks are not alkaline.

(d) Few rocks show much iron enrichment relative to Mg, and with the notable exception of some samples from Shetland (Fig. 8.3) almost all samples fall within the

Fig. 9.1 : K_2O : SiO_2 variation diagrams for the main O.R.S. volcanic regions, with boundaries from Peccerilo and Taylor (1976) between shoshonitic, high-K, calc-alkaline and tholeiitic suites (as Fig. 8.3). Conventions as section 3.3.

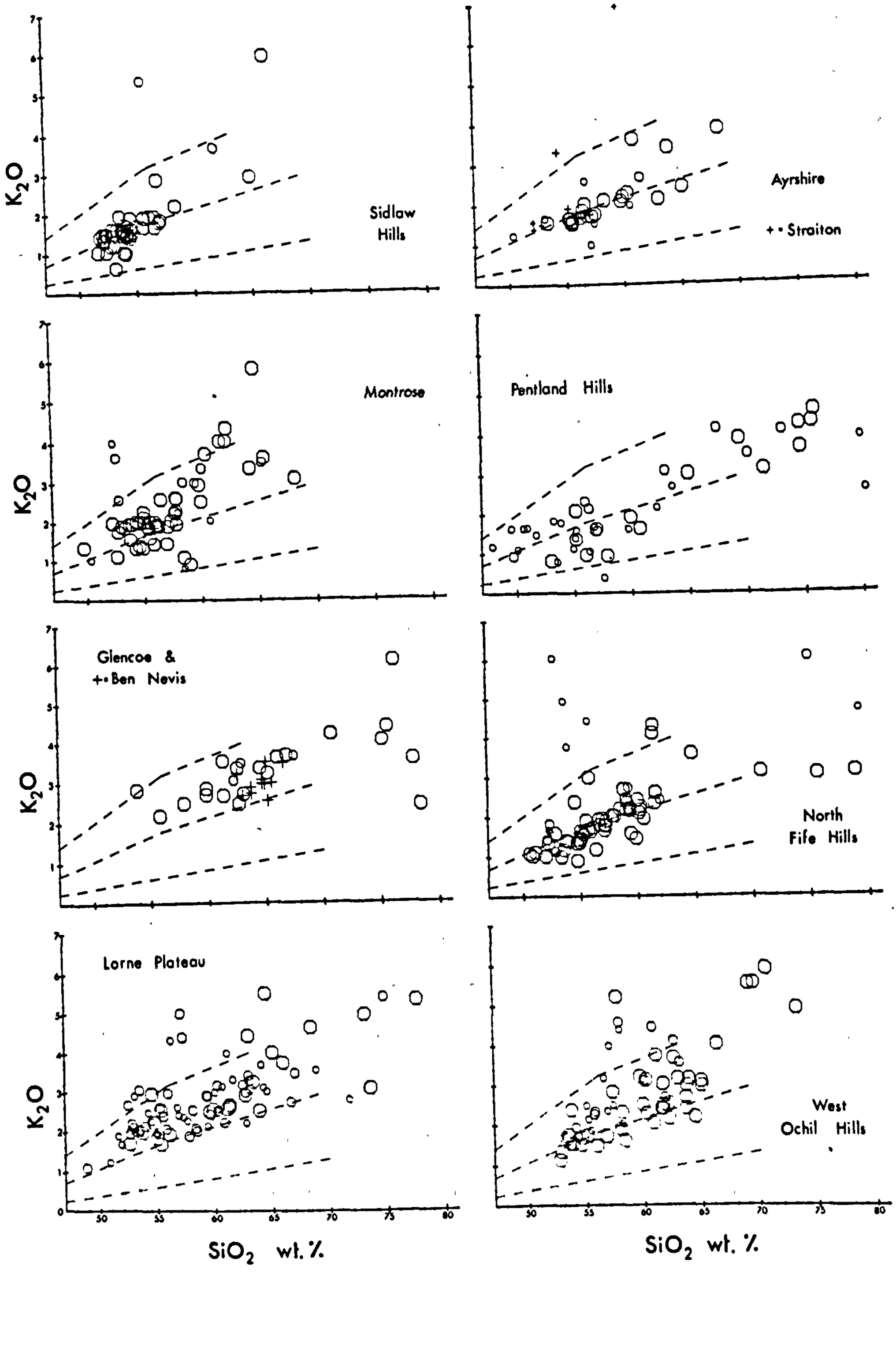

calc-alkaline field of Miyashiro (1974).

(e) Phenocryst pyroxene seldom has atomic Mg/(Mg+Fe) lower than 70, even in siliceous rocks. Exceptions occur at Shetland and at Straiton, Ayrshire, where exsolution relationships indicate the former presence of pigeonite.

(f) In the three regions of the province where volcanic rocks outcrop over a wide area (SW Highlands, North Midland Valley, South Midland Valley) all silica concentrations from 50 to 80% are well represented. The smaller outcrop areas into which these may be divided often show a preponderance of a more restricted silica range, but this may be due to the locations of these areas relative to eruptive foci. In these three regions, rocks with <53 and >65% SiO_2 are relatively less common. Of the other outcrop areas, only the Cheviot Hills provide a volcanic suite in which basic rocks (<60% SiO_2) may never have been present.

(g) Alumina concentrations are never lower than 14.6% in basic and intermediate lavas, and samples with around 16% Al_2O_3 are common. Many therefore plot within the tholeiitic field on the Al_2O_3 - normative plagioclase composition diagram of Irvine and Baragar (1971).

(h) Rocks with high concentrations of Ni (>60 ppm) and Cr (>100 ppm) are abundant throughout the province. Many such samples are silica-rich, and several have >65% SiO_2. Rocks with around 57% SiO_2, 180 ppm Ni and 350 ppm Cr are common in the Midland Valley. Most Ni-, Cr-rich samples have low alumina (<16.5%).

Features (d) to (f) strongly suggest that the rocks are best described as calc-alkaline, with the rocks of Shetland transitional to tholeiitic. The high Ni and Cr of the low-alumina rocks could suggest that far less separation of mafic phases has occurred during ascent than in most modern calc-alkaline suites: this can resolve the ambiguity of point (g), for separation of mafic phases will result in higher alumina. This suggests that the term "high alumina basalt" (Kuno, 1960) is of little genetic relevance in describing the mafic members of calc-alkaline suites.

(i) A wide range in lava chemistries at constant silica is present in the rocks of each outcrop area. This can only be attributed to fractional crystallisation in the various geographic subareas of Shetland: elsewhere variation in ratios of incompatible trace elements such as Zr/Nb implies a complex contamination history for the magmas.

(j) Many outcrop areas show broadly constant or in some cases decreasing concentrations of Zr and Nb with increasing silica. Pearce and Norry (1979) noted this unusual behaviour of 'incompatible' trace elements only in continental margin calc-alkaline suites. High concentrations of LIL elements comparable to those in the O.R.S. province are only to be found among modern calc-alkaline suites in those developed on continental margins e.g. the western U.S.A. (Ewart, in press).

9.2 : SPATIAL VARIATION IN MODERN CALC-ALKALINE SUITES

Modern calc-alkaline suites are almost exclusively associated with zones of lithospheric plate convergence. To some extent a semantic equivalence has grown up, and volcanic rocks associated with plate convergence are often loosely termed calc-alkaline, while calc-alkaline rocks have been used as evidence for the existence and interaction of minor plates in areas not clearly related to major plate convergence. The close spatial and temporal relation of the O.R.S. volcanic province to the closure of Iapetus (section 1.1) confirms that this province was developed at a zone of plate convergence.

More specifically, most modern calc-alkaline suites overlie Benioff zones of intermediate-deep focus earthquakes, and thus characteristically form arcuate volcanic zones, in some way genetically related to lithospheric subduction. This association has led to the use of calc-alkaline volcanic suites as evidence for palaeo-subduction, and the O.R.S. suite has been used by Phillips *et al.* (1976) as evidence for termination of northward subduction under Scotland during the Devonian. The occurrence of modern calc-alkaline volcanic rocks in the western U.S.A. and Turkey (e.g. Lambert *et al.*, 1974), where no Benioff zones have been recognized, suggests that care should be taken in the direct equation of calc-alkaline magmatism with active subduction.

Petrographic and chemical variation across and along subduction-related magmatic arcs has received much attention in the literature. Kuno (1966) observed variation across the Japanese arc from tholeiitic ('pigeonitic') volcanoes nearest the trench in the east, through calc-alkaline ('hypersthenic') volcanoes to alkaline volcanoes in the west. Dickinson and Hatherton (1967) observed that a close relationship existed between the K content of andesites at constant silica and the depth of the Benioff zone beneath the volcano, and hence with depth (h) to the subducting lithosphere. K content at constant silica was determined from a regression line drawn on a K_2O-SiO_2 variation diagram. Ninkovich and Hays (1972), Nielson and Stoiber (1973) and Dickinson (1975) showed that the K-h relation was closely dependant on the type of magmatic arc, with those located on continental margins showing the highest K for constant h. Similar variation for many other LIL and high field strength elements has been summarized by Jakeš and White (1972) and by Arculus and Johnson (1978), but the data is often vague, and Arculus and Johnson (1978) describe a number of examples where K-h variation does not appear to occur. Variation along a magmatic arc was described from the Lesser Antilles; variation along the arc has also been described in Indonesia (Whitford, 1975) where a southeastward decrease in $^{87}Sr/^{86}Sr$ was used to infer decreasing crustal contribution in this direction.

In addition to the spatial variations, Jakeš and White (1972) have also drawn attention to broad chemical

changes occurring during the evolution of a magmatic arc. Tholeiitic volcanism was believed to dominate the early stages of arc evolution, with alkaline (?shoshonitic) volcanoes occurring late in the arc development. The evidence for this is frequently ambiguous (Arculus and Johnson, 1978).

The origin of these spatial and temporal variations has been discussed by many authors, but detailed discussion is often hampered by the lack of comprehensive chemical data. Cawthorn (1977) noted that the variation in K content at constant silica described by Dickinson (1975) was critically dependant on the origin of the positive correlation between K_2O and SiO_2. If this were due to fractional crystallisation then K_{55}, $K_{57.5}$ and K_{60} as defined by Dickinson (1975) would be functions of the silica content of the bulk extract. For example, high partial pressures of oxygen could lead to fractional crystallisation of magnetite (Osborn, 1962), resulting in lower K at constant silica than magmas separating a more silica-rich assemblage. Fractional crystallisation of amphibole-bearing assemblages (Cawthorn and O'Hara, 1976) would also lead to relatively low K at constant silica. A similar criticism applies if the silica variation is generated by variation in the degree of partial melting of a common source: variation in residual phases could lead to variation in K content at constant silica. However, variation in both partial melt residua and fractionating assemblage could be related to depth of magma generation.

It is clear that the true nature of spatial and temporal variation in calc-alkaline suites can only be elucidated if the origin of the silica variation is known, or if we can infer the compositions of primitive magmas from which the lava compositions seen at the surface may be derived by crystal separation. In both cases, it is essential to consider a comprehensive body of accurate chemical data, rather than restricting discussion to K_2O and SiO_2.

9.3 : SPATIAL CHEMICAL VARIATION IN O.R.S. MAFIC ROCKS

The O.R.S. volcanic province is most unusual for calc-alkaline suites in its great abundance of rocks with high Ni and Cr. Some 20% of the rocks collected have >100 ppm Ni and >150 ppm Cr; these include rocks from the SW Grampian Highlands, the North and South Midland Valley, Arran, St. Abb's Head, Orkney and Shetland. 600 and 1200 ppm respectively are close to the maximum Ni and Cr concentrations observed in natural liquid compositions; fractional crystallisation of mafic minerals from such compositions results in rapid depletion in Ni and Cr, for distribution coefficients are high for these elements in mafic phases (Gill, 1978).

For example, if such compositions were parental to the rocks of the O.R.S. volcanic province, then an assemblage with D(Ni,bulk)=7 could generate the 100 ppm Ni of many of these rocks with only 25% crystallisation.

Higher D(Ni,bulk) is likely if olivine formed a major part of the crystallising assemblage, while large contributions from clinopyroxene or spinel would result in major depletion in Cr. It is clear that crystal separation of mafic phases can not produce more than 25% relative variation in LIL elements in rocks with >100 ppm Ni. Furthermore, Ni and Cr concentrations can be used as indices of differentiation, and more than some 20% relative variation of LIL elements at constant Ni and Cr can not be generated by separation during ascent of different proportions of mafic phases.

Fig. 9.2 demonstrates that approximately 6-fold variation in Ba and Sr exists among rocks with >100 ppm Ni in the O.R.S. volcanic province. The strong positive correlation between Ba and Sr may not be generated by separation of plagioclase during magma ascent: it is therefore concluded that any primary magmas parental to these rocks must have shown comparable variation in Ba and Sr content. The very minor significance of separation of mafic phases during ascent is emphasized by the total absence of correlation between increase in Ba and Sr and decrease in Ni and Cr. The correlation between Ba and Sr demonstrated for Lorne in Chapter 4 forms part of the overall correlation throughout the whole province, and there is clear correlation between geographic position and content of Ba and Sr in rocks with >100 ppm Ni. Low concentrations are dominant in the South Midland Valley and high concentrations are dominant in the SW Grampian Highlands.

Fig. 9.2 a & b : Bulk rock variation diagrams for samples with >100 ppm Ni and >150 ppm Cr.

Conventions as section 3.3

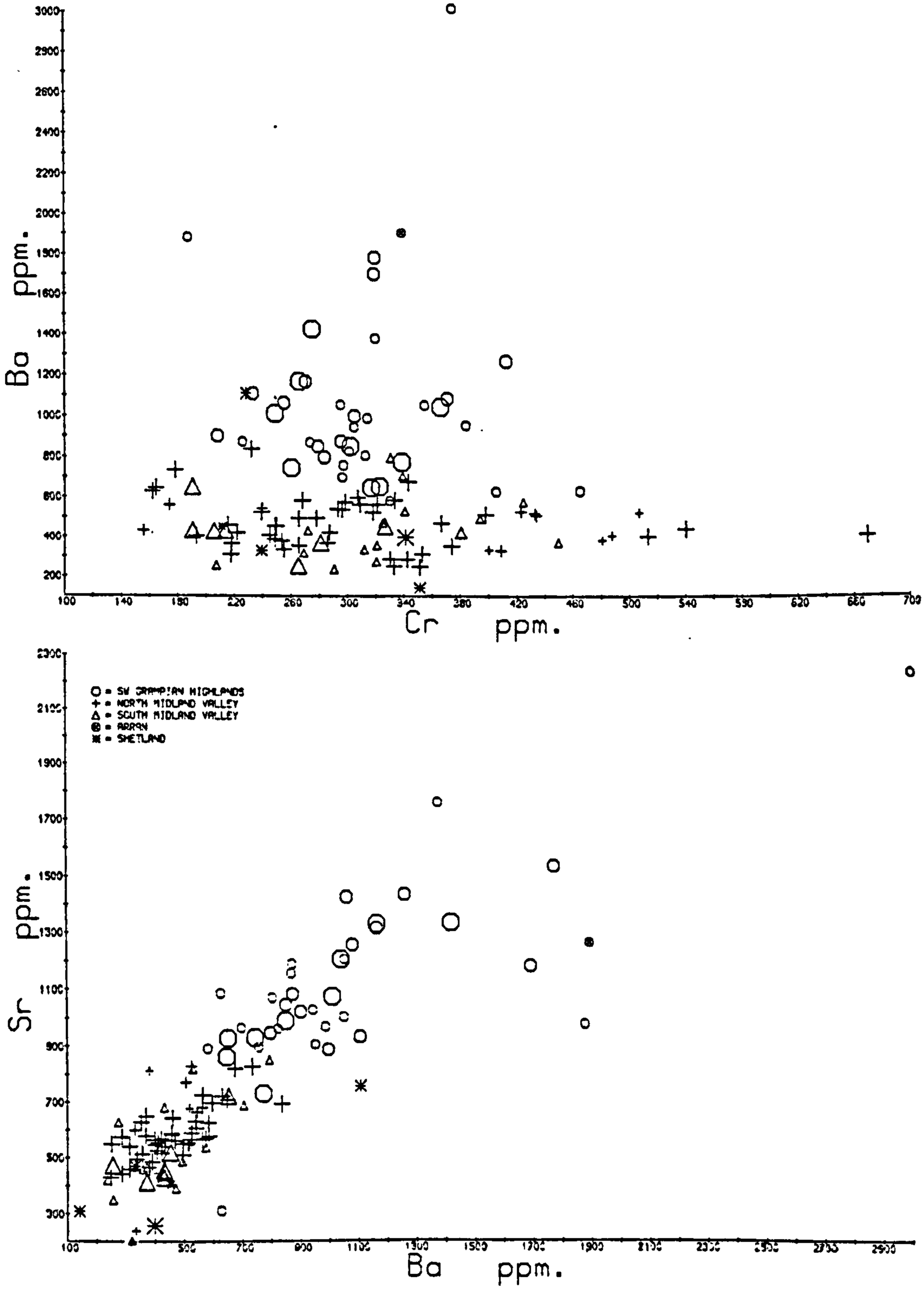

Fig. 9.2 c & d : samples with >100 ppm Ni and >150 ppm Cr

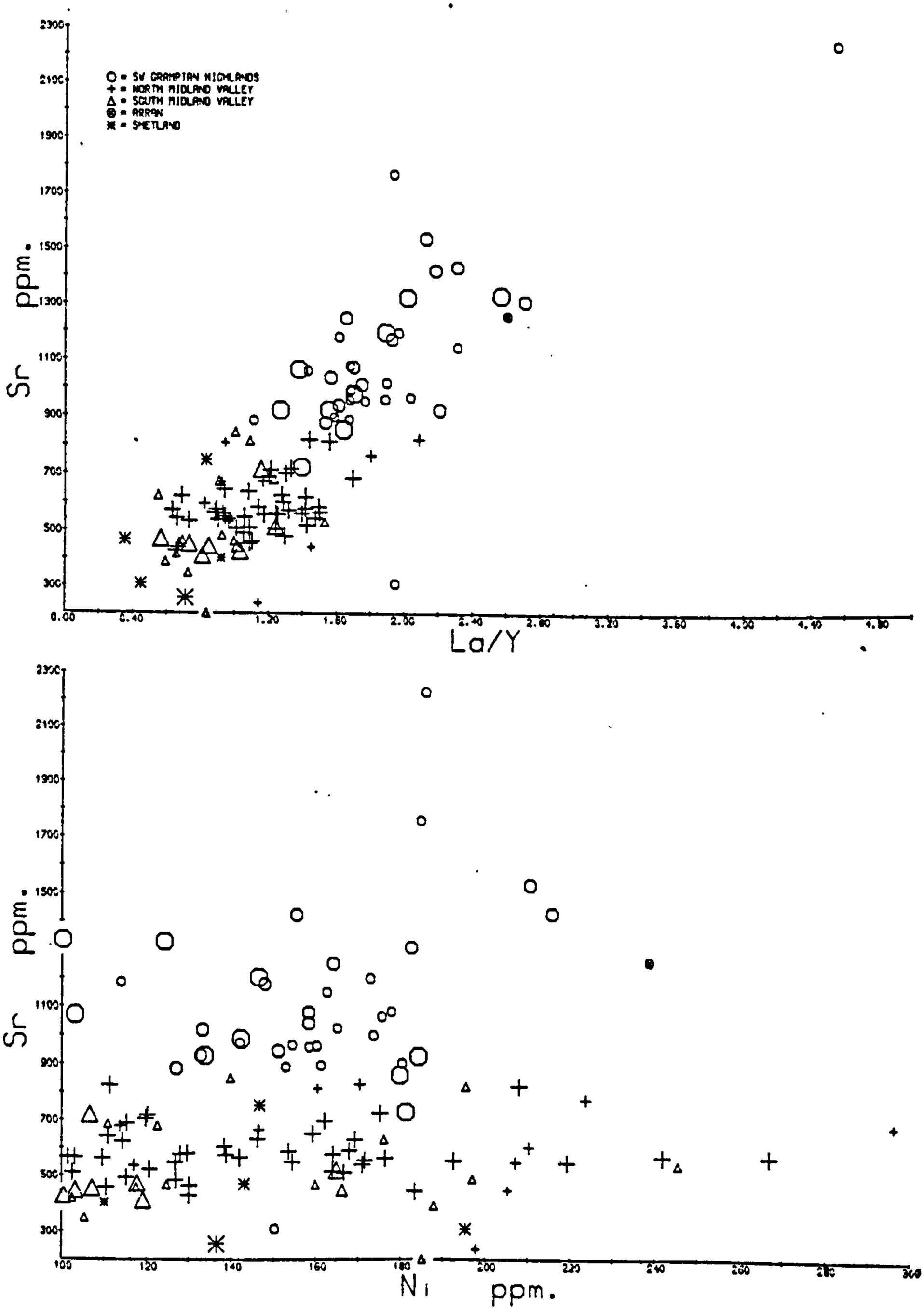

Fig. 9.2 e & f : samples with >100 ppm Ni and >150 ppm Cr

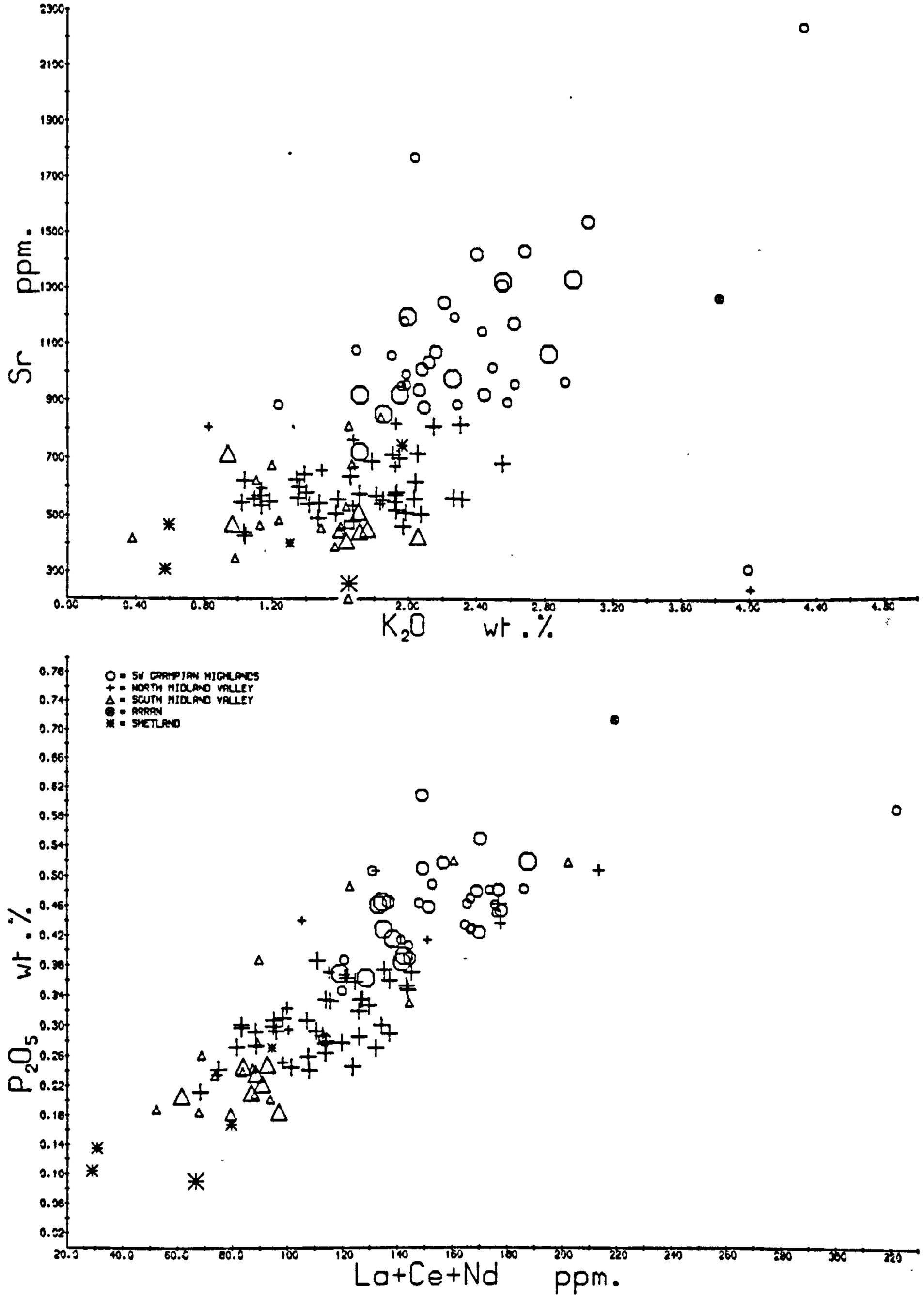

Fig. 9.2 g & h : samples with >100 ppm Ni and >150 ppm Cr

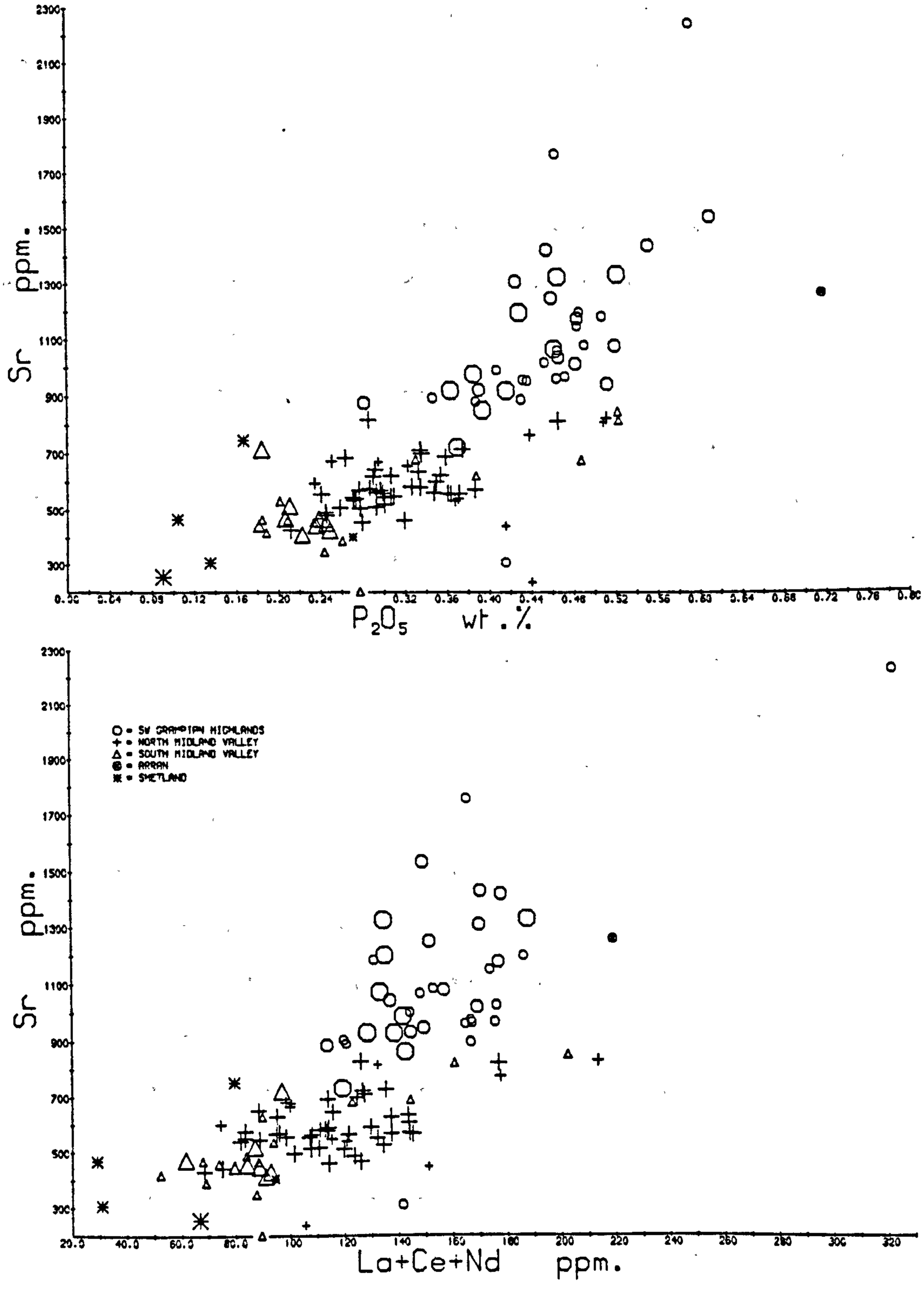

Similar correlations exist for Sr-La/Y and P_2O_5- LREE, although the relationships between Sr-K, Sr- LREE and Sr-P_2O_5 are curved, with greatest variation in Sr between the SW Highlands and the North Midland Valley, while P and LREE variation is large between the South and North Midland Valley.

Confirmation that comparison is being made between otherwise similar rocks (e.g. for SiO_2, Ni and Cr) is given by the great similarity between the average compositions of rocks with >100 ppm Ni from these three areas (analyses 1-3, Table 9.1). The striking equivalence of most elements is strong evidence for the existence of a fundamental process causing increase in Sr, Ba, P, LREE, K, (La/Y) and possibly Nb and Rb, and decrease in Y and possibly also Sc on a traverse from the South Midland Valley to the SW Grampian Highlands. Difference in the averages for other elements is perhaps significant for Ca and Mg: the high average LOI of South Midland Valley rocks suggests that this is probably a function of alteration. 25% and 75% quartiles are given for some of these parameters in Table 9.2: the variation is comparable to that displayed by the means, demonstrating that the means are not seriously dependant on atypical high or low values for elements in one or two samples.

This spatial variation in LIL elements is encountered in a traverse roughly perpendicular to the suture of Phillips et al. (1976). The variation is comparable to that described from many calc-alkaline suites (section 9.2).

TABLE 9.1 : Average analyses of samples with > 100 ppm. Ni

1 = SW Highlands, 2 = North Midland Valley, 3 = South Midland Valley,
4 = St. Abb's Head/Eyemouth, 5 = Shetland

	1	2	3	4	5
SiO_2	54.95	54.58	54.66	56.11	52.57
Al_2O_3	16.46	16.37	16.86	16.35	17.08
Fe_2O_3	7.95	7.77	8.10	7.31	9.40
MgO	5.37	6.52	5.09	6.27	6.22
CaO	6.91	7.33	8.36	6.44	7.61
Na_2O	3.82	3.60	3.72	3.36	3.88
K_2O	2.34	1.69	1.43	2.04	1.22
TiO_2	1.32	1.36	1.28	1.17	1.03
MnO	0.10	0.11	0.10	0.08	0.27
P_2O_5	0.45	0.32	0.27	0.31	0.15
Total	99.67	99.65	99.87	99.44	99.43
LOI	3.32	1.79	4.47	4.81	2.66
Ni	158	157	143	220	146
Cr	308	316	302	426	274
V	168	162	175	135	178
Sc	22	24	26	24	32
Cu	30	28	34	31	24
Zn	80	76	133	122	399
Sr	1103	589	515	510	437
Rb	40	37	34	48	49
Th	4	6	7	4	2
Zr	200	211	197	220	111
Nb	14	12	9	13	9
Ba	1045	465	436	534	486
La	37	28	22	30	16
Ce	81	61	49	61	30
Nd	38	29	25	29	14
Sm	7	6	6	5	2
Y	20	25	25	25	23
No.	38	53	22	12	5

TABLE 9.2 : Interquartile ranges for selected chemical parameters.

All samples with >100 ppm. Ni.

	South Midland Valley		North Midland Valley		SW Highlands	
	25 percentile	75 percentile	25 percentile	75 percentile	25 percentile	75 percentile
Sr	428	626	540	644	928	1201
K_2O	1.13	1.66	1.37	1.93	1.99	2.58
Ba	336	493	374	554	797	1105
La/Y	0.69	1.03	0.93	1.36	1.61	2.02
SiO_2	51.7	57.2	52.5	56.5	53.1	56.1
Cr	265	339	242	360	274	330
No. of samples	22		53		38	

9.4 : SPATIAL CHEMICAL VARIATION IN LESS MAFIC ROCKS

Direct comparison between the spatial chemical variation described in section 9.3 and that described by workers on other calc-alkaline suites is only possible if the entire range of volcanic products is considered, although the demonstration in section 9.3 of a wide range in primary magma compositions is believed to be more fundamental than variations in element concentrations at constant silia (section 9.2). This is particularly true where the origin of the silica variation is not understood, as is the case for most of the O.R.S. regions, with the prominent exception of Shetland.

The criticism by Cawthorn (1977) of the K-h relationship, that variation in K at constant SiO_2 can easily be generated by differences in the Si and K content of a fractionating assemblage (section 9.2), will apply to any element that shows correlation with silica. When an element shows no correlation with silica, variation in the SiO_2 content of the extract can not change the concentration of the element at a particular evolved silica composition. Sr shows little or no correlation with silica in O.R.S. lavas with less than about 65% silica (e.g. Fig. 9.3), and therefore spatial variation in Sr can not be generated by geographic changes in the silica content of an extract in a fractional crystallisation model. Regression lines for Sr against SiO_2 have been computed for each area using the program VARPLOT (Appendix D7; perpendicular-to-line

Fig. 9.3 : Sr : SiO_2 variation diagrams for the main volcanic regions. Conventions as section 3.3.

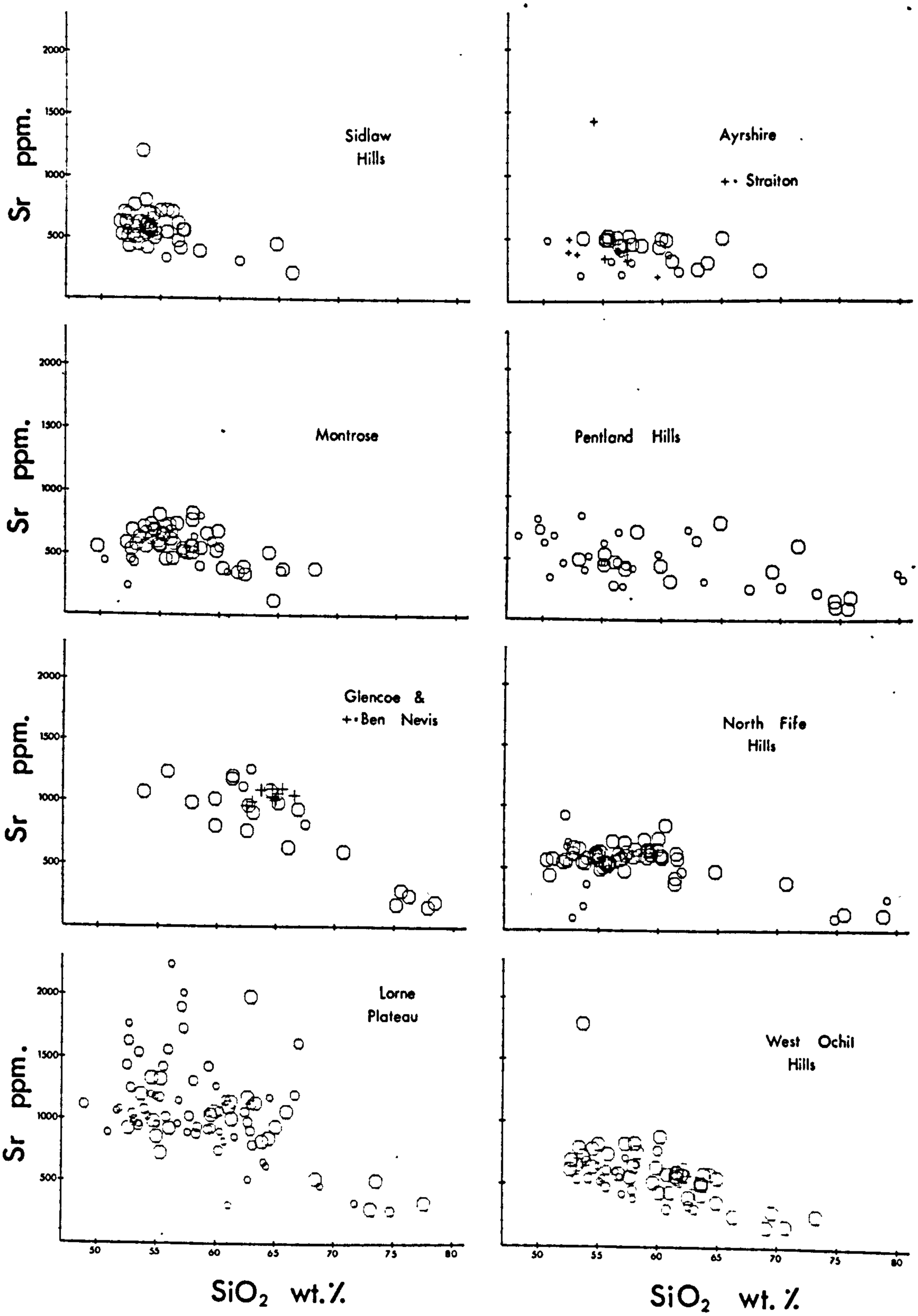

Fig. 9.4 a & b : Regression lines for each area for samples with <65% SiO_2, <3% LOI. Symbols refer to the major regions:
○ = SW Grampian Highlands, + = North Midland Valley,
△ = South Midland Valley, * = Shetland (Esha Ness)

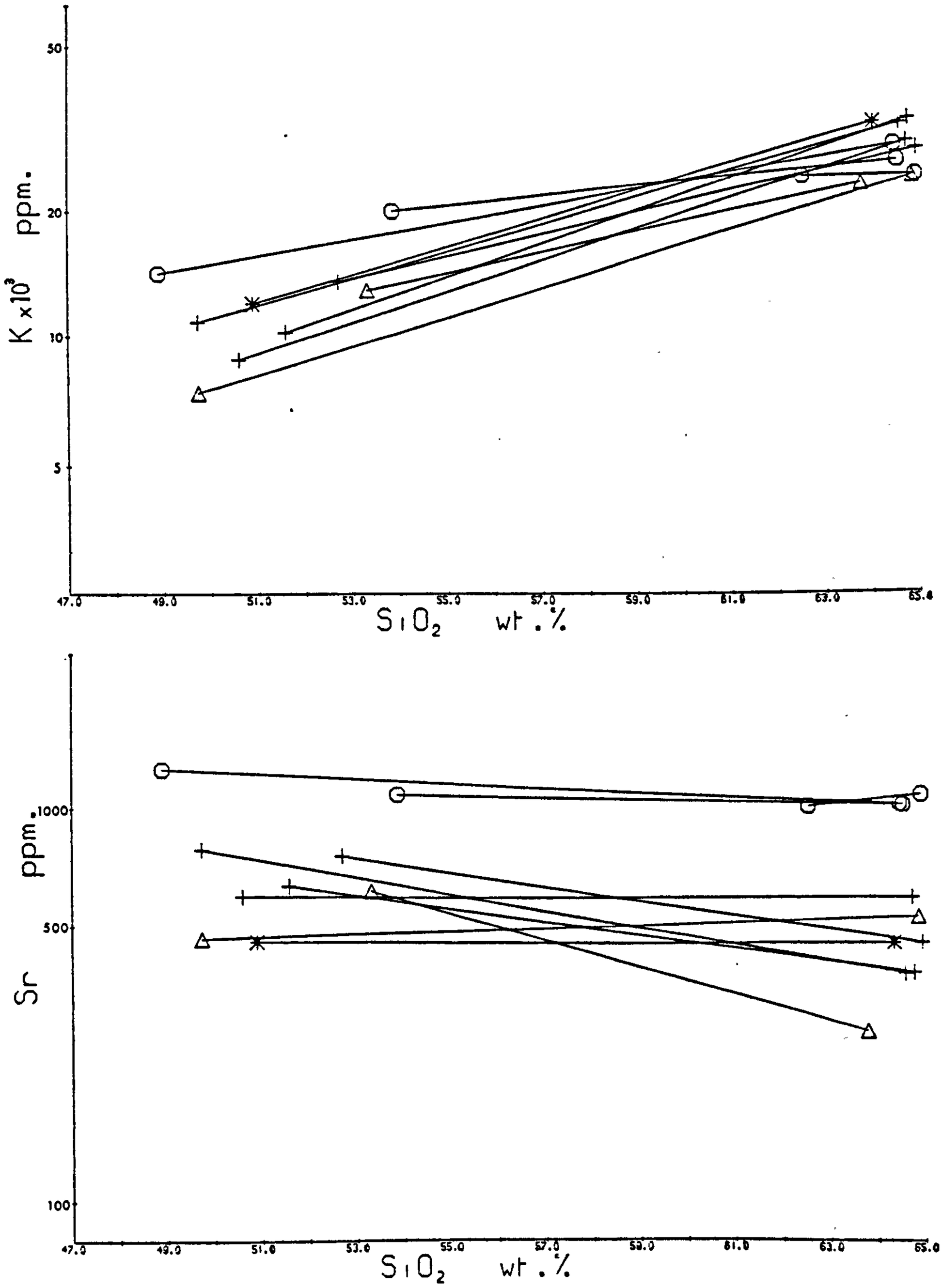

Fig. 9.4 c & d : Regression lines for each area for samples with <65% SiO_2. Symbols as Fig. 9.4 a & b

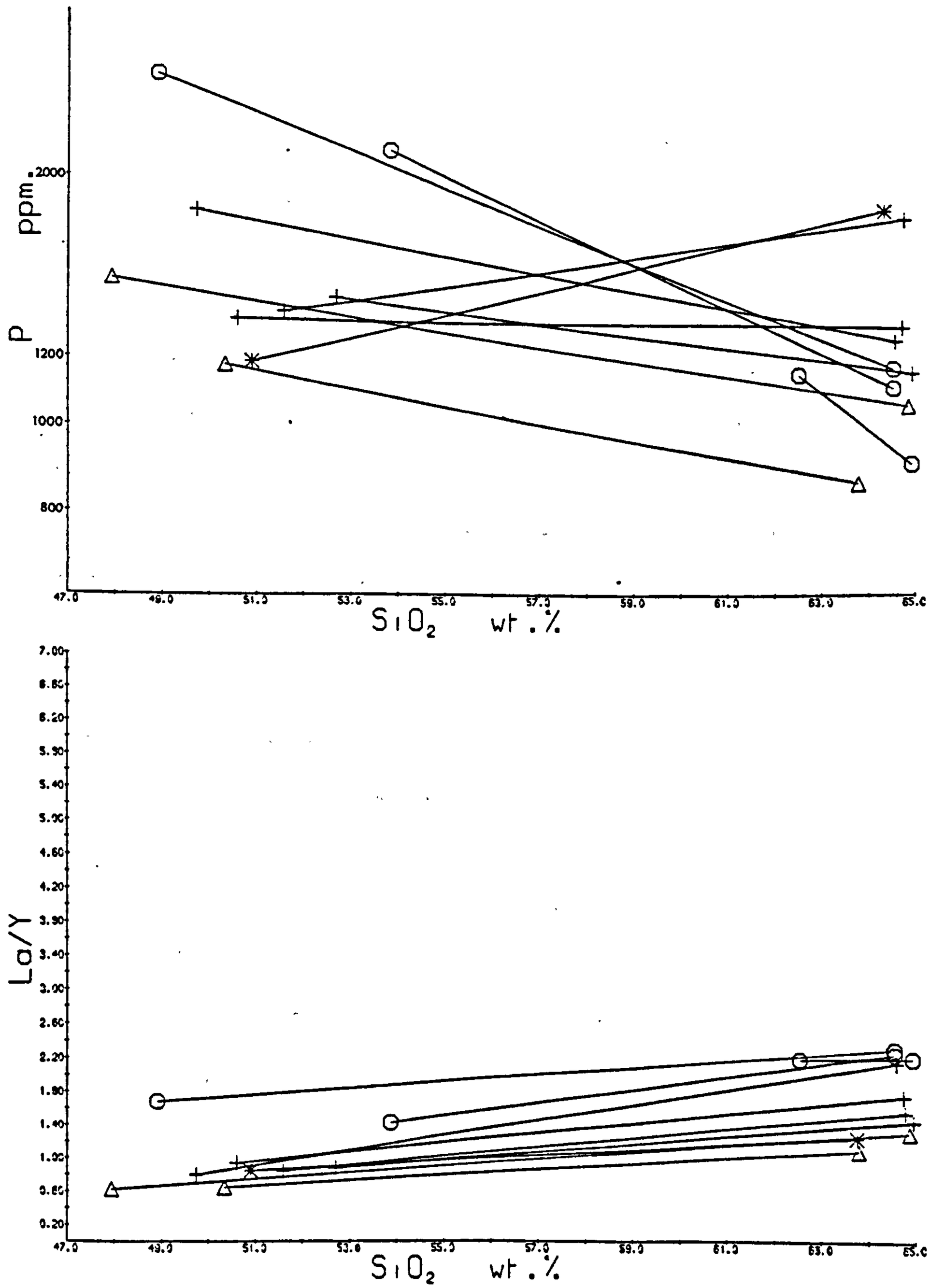

procedure), and are given in Fig. 9.4. Sr concentrations in the SW Highlands, the North Midland Valley and the South Midland Valley are readily distinguished using this method, and the variation is similar to that described in section 9.3.

Despite the aforegoing criticisms of the K-h relationship, regression lines have also been computed for many geochemical parameters which do show correlation with silica: for example, for K, La/Y and P_2O_5, Fig. 9.4. The same spatial variation is shown, namely that at constant silica, samples from the SW Highlands have highest Sr, Ba, K, La/Y, P and LREE, while samples from the South Midland Valley have the lowest values of these parameters. These data are directly comparable to the spatial variations described from modern calc-alkaline magmatic arcs, related, by Dickinson (1975) and many other authors, to the depth to the descending lithospheric plate.

There is therefore abundant evidence that the Old Red Sandstone volcanic province was generated in response to subduction beneath the northwestern continental margin of the Iapetus Ocean.

9.5 : SUBDUCTION DIRECTION

Chemical variation in the O.R.S. volcanic province as a whole is not well described by distance perpendicular to the suture of Phillips *et al.* (1976). Fig 9.5 demonstrates

Fig. 9.5 : Ranges of Sr and La/Y plotted against distance from suture of Phillips et al. (1976). The cpx-hb-bi-phyric rocks of Lorne and some altered rocks are omitted from the ranges. Outcrop areas are shown as rectangles if they have significant width normal to the suture, and as a dot (e.g. area 6) if only a small number of samples is represented. The Irish and Arran areas are shown dotted for clarity.
Numbers refer to: 1 = Esha Ness, 2 = Papa Stour, 3 = Sandness Formation, 4 = Shapinsay/Deerness, 5 = Hoy, 6 = Huntly, 7 = Ben Nevis, 8 = Glencoe, 9 = Lorne Plateau, 10 = Montrose, 11 = Highland Border, 12 = Sidlaw Hills, 13 = North Fife Hills, 14 = West Ochil Hills, 15 = Pentland Hills, 16 = Distinkhorn, 17 = Ayrshire Coast, 18 = Straiton, 19 = St. Abb's Head & Eyemouth, 20 = Cheviot Hills, 21 = Arran, 22 = Cushendall, 23 = Fintona, 24 = Curlew Mountains.

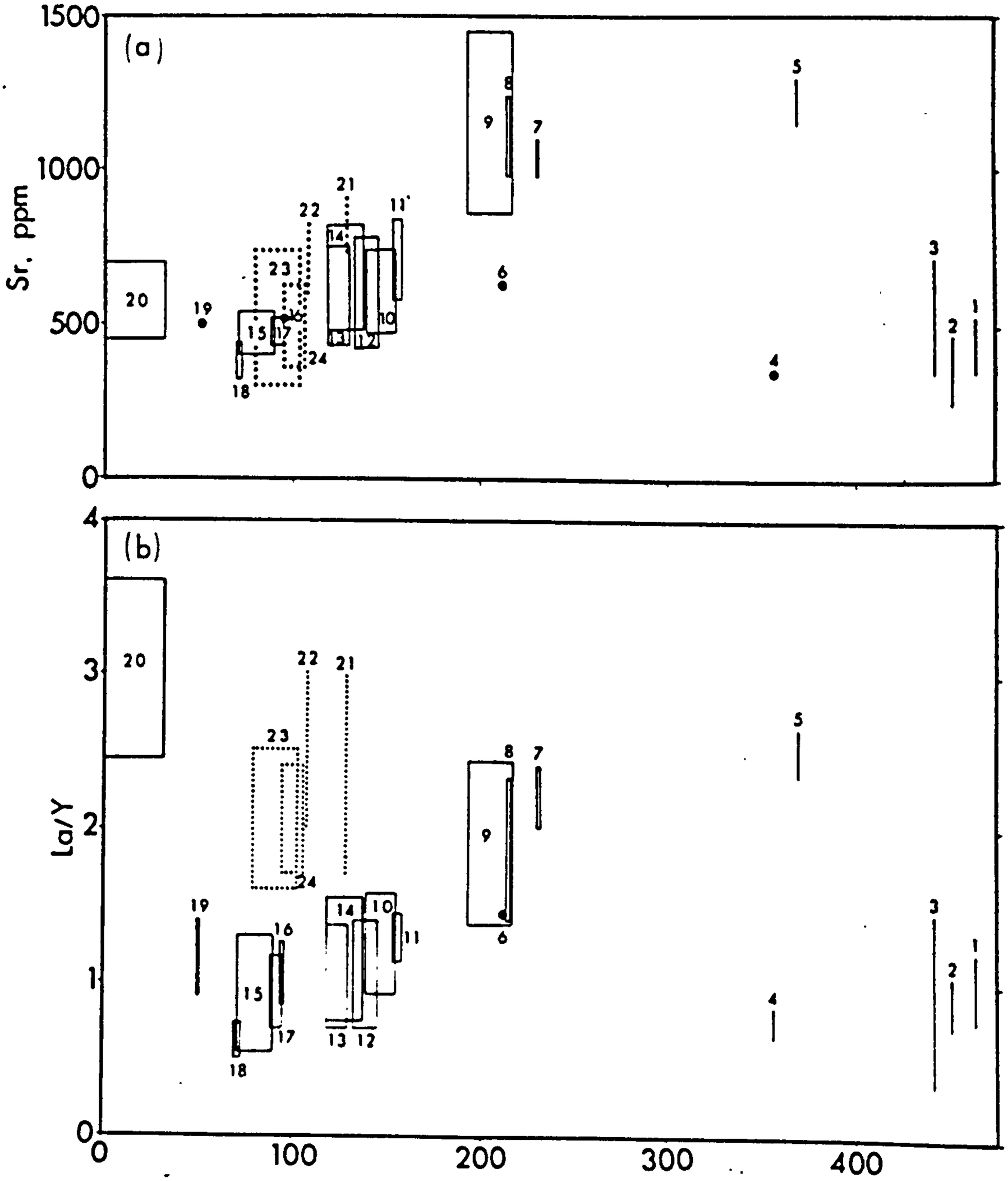

that the range in Sr and La/Y values exhibited by basic and intermediate rocks of each outcrop area only correlates well with distance from the 'suture' for areas in the North and South Midland Valley and in the SW Grampian Highlands. With respect to these regions, all areas with apparently anomalous low levels of Sr and La/Y lie geographically to the northeast of a line joining the South Midland Valley and Lorne (Fig. 1.1), while, with the exception of the Cheviot Hills and St. Abb's Head, all areas with apparently anomalous high levels of La/Y and Sr (Ireland and Arran) lie to the southwest of this main volcanic region.

There is considerable difficulty involved in discussion of the significance of these relationships, for Fig. 9.5 does not include any measure of SiO_2, Ni or Cr, and comparison between the siliceous rocks of Ireland and rocks from the rest of the province is hazardous. The following points should be noted:

(a) A lava with >100 ppm Ni and >150 ppm Cr is present on Arran (AR2). This has very high concentrations of LIL elements, comparable with those at Lorne (Fig. 9.2). More siliceous rocks from both Arran and Cushendall have higher concentrations of LIL elements than those from further southwest in Ireland (Fig. 8.2), and higher than those of siliceous rocks in the Midland Valley.

(b) The most mafic sample from Huntly (NG1) has 90 ppm Ni and 157 ppm Cr. It is therefore unlikely that concentrations of LIL elements in this sample have been greatly changed by fractional crystallisation of mafic

phases. Both Sr and La/Y are lower than in SW Highland rocks and comparable to their levels in the North Midland Valley. More siliceous samples from Huntly also have relatively low Sr and La/Y, as do the Highland-derived volcanic clasts in the O.R.S. conglomerates of Kincardineshire (section 5.1a).

(c) Chemical variation in the volcanic rocks of Shetland is controlled by fractional crystallisation, and values of K at constant silica for Shetland are a little higher than those in the North Midland Valley. However, the few Ni- and Cr-rich rocks present all have much lower concentrations of LIL elements (Fig. 9.2). These are the only Shetland rocks directly comparable with the Ni-, Cr-rich lavas of the rest of the province. The average analysis of these rocks is given in Table 9.1: while concentrations of Sr, P, LREE and K are much lower than those for areas on the Scottish mainland, the analyses are not wholly comparable because of differences in SiO_2. Shetland lavas are transitional between calc-alkaline and tholeiitic (Fig. 8.3).

(d) The older lavas of Orkney (Eday Flags) are closely comparable with mafic lavas in Shetland (section 8.6), and have equally low LIL element concentrations. The younger lavas of Orkney (Hoy) are alkaline and are perhaps unrelated to the rest of the province.

(e) The lavas of the Cheviot Hills have La/Y values comparable to those of Lorne, but Sr and Ba are much lower, even in equally siliceous rocks. La/Nd is substantially higher than at Lorne (Fig. 9.6): it is

Fig. 9.6 a & b : Bulk rock variation diagrams for samples with between 60 and 65% SiO_2. N.B.1 : similarity to Fig. 9.2 c; N.B.2 : Anomalous behaviour of Cheviot samples.

Conventions as section 3.3

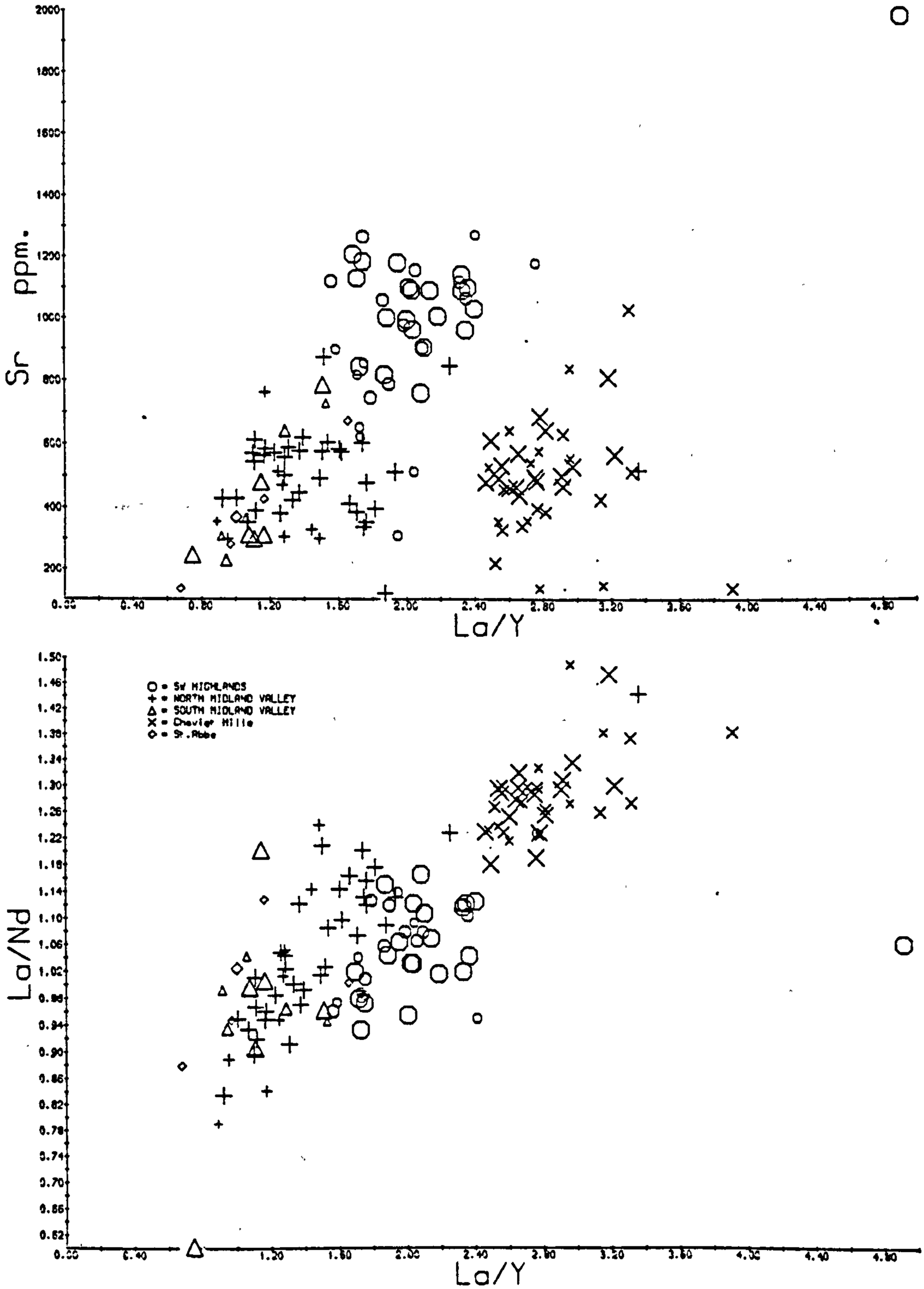

important that while enrichment of LREE relative to HREE (Y) shows considerable spatial variation, enrichment within the LREE (La/Nd) does not, with the exception of the Cheviot lavas.

(f) Due to alteration, the behaviour of Sr and Ba in the St. Abb's Head lavas is not known. The average analysis of St. Abb's Head Ni- and Cr-rich lavas is given in Table 9.1. While not directly comparable with elsewhere (SiO_2, Ni, Cr, V), concentrations of LIL elements appear to be similar to those in the North Midland Valley (column 2).

If the correlations between LILE concentrations and La/Y displayed in Fig. 9.2 are believed to be the result of subduction-related processes (section 9.7), it is reasonable to suggest that the Cheviot lavas, and possibly those of St. Abb's Head, were not related to the same subduction zone as the remainder of the province. Supporting evidence for this exception comes from the unusual petrography and chemistry of rocks in these areas, and perhaps in their unusual positioning on an accretionary sedimentary wedge.

If this exception is accepted, the simplest tectonic model that can explain the spatial variation in LIL element concentrations in the province requires a major change in strike of the surface expression of the subduction zone off the east coast of Scotland. It is proposed that the plate convergence responsible for the Old Red Sandstone volcanic province took place in a nearly east-west direction, and that the southeast margin of the American-Scottish plate was

an arcuate zone of active plate consumption, concave northwards.

Such a subduction geometry would allow the tholeiitic/calc-alkaline transitional rocks of Shetland to lie relatively close to the surface trace of the subduction zone, while the LILE-rich rocks of the SW Highlands and Arran would lie furthest from the surface trace. The position suggested in Fig. 9.7 is critically dependant on several assumptions:

(i) That, with the exception of the Cheviot Hills and St. Abb's Head, all the volcanic rocks are related to the same subduction zone. Multi-subduction zone models could easily account for the observed variation, but they are not necessary.

(ii) That the volcanic rocks are not widely disparate in their ages. This may not be a valid assumption for the relationship of Shetland and Orkney to the mainland, but the Huntly and Arran rocks are generally considered to be part of the Lower O.R.S.

(iii) That the levels of La/Y and LILE were directly related to the depth to the Benioff zone (section 9.7).

(iv) That the angle of dip of the Benioff zone was relatively constant throughout the province. Variation in the angle of dip does not however allow much change in the position of the surface trace.

A number of additional lines of evidence support the suggestion of a change in strike of the subduction zone from

Fig. 9.7 : Suggested Position of Surface Trace of the Late Silurian Subduction Zone

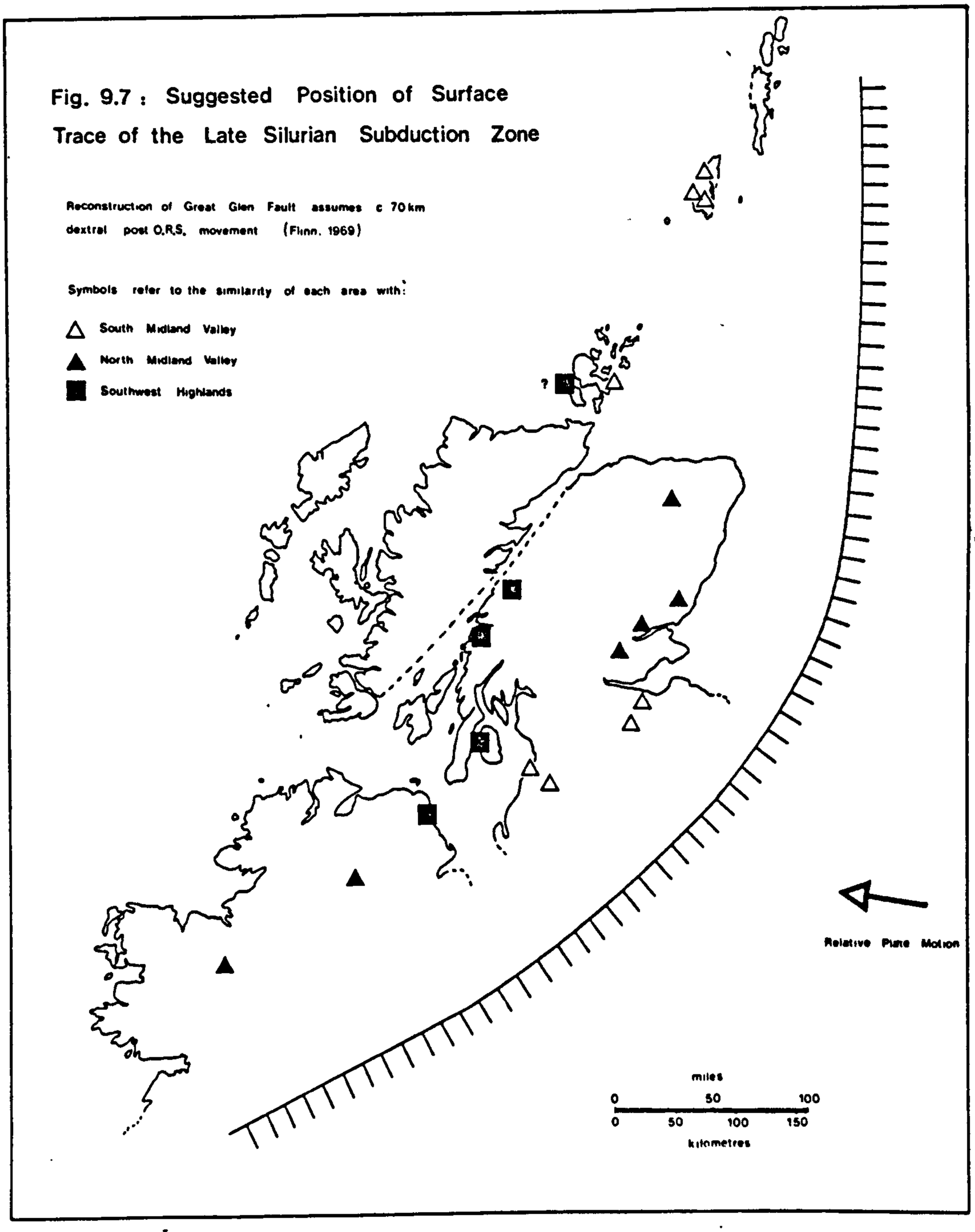

ENE in southern Scotland and Ireland to NNE in the North Sea:

(a) The change in strike of the Great Glen Fault and of Dalradian metasediments from ENE in the SW Grampian Highlands to N in Shetland. While both of these probably pre-date the development of the O.R.S. province, they may be indicative of a regional change in strike existing until final closure of Iapetus. The presence of a possibly ophiolitic complex on Unst and Fetlar, Shetland, provides additional evidence for the proximity of Shetland to a subduction zone, although these again probably pre-date the O.R.S. volcanic rocks.

(b) Chemical and isotopic variation among the younger granites of the Scottish Highlands is not well characterized by distance from the ENE-striking suture of Phillips et al. (1976). Instead, the chemical and isotopic composition of the granites appears to vary from east to west (Stephens, pers. comm., 1979). The north-south orientation of a belt of syenitic plutons in the northern Highlands from Ben Loyal to Glendessary may also be significant, although these are now known to be Ordovician (van Breemen et al., 1979).

(c) Phillips et al. (1976) extrapolate their suture ENE from Scotland to join the southeastern front of the Scandinavian Caledonides (their Fig. 9). This would imply that the entire Scandinavian nappe pile, and the east Greenland Caledonides, were developed on the continent to the northwest of Iapetus, a most unlikely possibility in view of the generally southeastward

translation of the Scandinavian nappes (Strand and Kulling, 1972, p.50). While the suture position is more a function of the shape of the opposing continental masses than of subduction zone position, the occurrence of Lewisianoid basement in Shetland (Pringle, 1970) and of abundant allochthonous continental basement in the Scandinavian nappes strongly suggests that both the suture, and the trace of the subduction zone by which closure occurred, must be located between Shetland and Scandinavia. This implies a major change in strike for the suture in the North Sea, and perhaps a corresponding change in subduction zone strike.

It is evident that the change in strike of the subduction zone suggested by the chemical data fits the tectonics of the area more satisfactorily than the consistently ENE striking suture and E-W striking northern subduction zone of Phillips et al. (1976). It should be noted that the subduction direction suggested is almost perpendicular to that used by Phillips et al. (1976) in their model of oblique collision, and therefore casts doubt on many of the conclusions reached by these authors.

9.6 : THE SILURO-DEVONIAN OROGENY IN BRITAIN

The British Isles are unique among the Atlantic Caledonides in their lack of major tectonism and metamorphic activity associated with final closure of Iapetus. If nappe tectonics be considered diagnostic of collision orogeny,

then collision orogeny did not take place in Britain at the time of closure. Despite this, abundant evidence for orogeny is preserved in the great thicknesses of Old Red Sandstone conglomerates in the Midland Valley of Scotland. It is believed that this apparent paradox can be resolved by considering the implications of sections 1.3 and 9.5.

(a) Timing of subduction

The convincing evidence for northwestward subduction preserved in the Southern Uplands accretionary sedimentary wedge (McKerrow et al., 1977) indicates that subduction was active from at least the Caradoc to the Wenlock. Pre-O.R.S. volcanic rocks suggested by Mitchell and McKerrow (1975) to be due to this subduction are the Wrae volcanics (now known to be peralkaline, Thirlwall, in prep.) and the 'andesite' clasts in Southern Uplands greywackes (described by Kelling, 1962, p.126, as petrographically comparable to some of the rocks of Bail Hill, Sanquhar, now known to be an alkaline volcanic complex, M. McMurtry, pers. comm., 1979). The only volcanic rocks north of the suture of Phillips et al. (1976) which can confidently be related to subduction are therefore those of the Old Red Sandstone, but these are commonly thought to be of Devonian age, post-dating the last accretionary slice in the Southern Uplands.

Calc-alkaline volcanism possibly post-dating subduction has been suggested in the Cascade Range, U.S.A.: the occurrence of bronzite-andesites at Mount Shasta,

California, has been reported by Anderson (1977), who interpreted them as the result of the "melting of a refractory source rock", initiated by continued volatile loss from a stationary segment of subducted lithosphere. The bronzite-andesites of the O.R.S. province are not comparable with these, however, for they are rich in LIL elements. A time delay between an increment of subduction and its associated magmatic event is not unlikely, but no calc-alkaline volcanic province is known that wholly post-dates its associated subduction.

Recalling the unsatisfactory state of the evidence for a Devonian age for the Scottish Lower O.R.S. (section 1.3), it is suggested that the bulk of the Scottish Lower O.R.S., and possibly some of that described as Middle O.R.S. (Shetland), may in fact be of Silurian age, and directly associated with the subduction responsible for the Southern Uplands accretionary prism of McKerrow et al. (1977).

If the Scottish Lower Old Red Sandstone is of Silurian age, then the large thickness of conglomerates in the Midland Valley can not be used as evidence for end-Silurian orogeny, and the paradox noted earlier is partially resolved. It is therefore necessary to re-examine briefly the entire status of the Siluro-Devonian Orogeny in Britain.

(i) Scottish Highlands: all nappe tectonics and metamorphism is Ordovician or earlier (van Breemen and Boyd, 1972). Very minor open folds may be younger, but

it is probable that the Highlands acted as a nearly rigid block by the end of the Ordovician. The O.R.S. conglomerates probably indicate the uplift and erosion of the mountains of the Grampian Orogeny, of Ordovician age (Lambert and McKerrow, 1976).

(ii) Midland Valley: pre-O.R.S. rocks are only present in the south, where their relationship to the O.R.S. varies from ?conformity to unconformity. In both cases, there is a transition from marine to continental facies near the base of the Wenlock, and it is not improbable that such a transition could be accompanied by the development of local unconformity. Most of the folding in the South Midland Valley inliers may postdate the local Lower O.R.S.

(iii) Southern Uplands (and Girvan area): folding and cleavage development in the sediments of the accretionary prism could be mainly related to the accretionary process and sediment dewatering. The subaerial volcanic rocks of St. Abb's Head and the Cheviot Hills lie unconformably on the rocks of the prism, but they need not be younger than the youngest segment of the prism on which they rest. However, these volcanic rocks are not thought to be related to the rest of the province; and they may well be younger.

(iv) Lake District: Soper and Moseley (1978) have inferred major end-Silurian orogeny on the basis of a common penetrative cleavage direction in major rock groups of Arenig to Ludlow age, and suggested that this was dated by the contemporaneity of the final stages of

cleavage formation with the injection of the Shap Granite (394 Ma). However, the common direction does not necessarily imply that the cleavage was formed at the same time throughout the Lake District. In addition, there is no evidence that the Silurian rocks in the south of the Lake District were originally present throughout the area, for chemical (Fitton and Hughes, 1970) and age (Downie and Soper, 1972) differences between the Eycott and Borrowdale Volcanic Groups imply that these may no longer be used to infer the existence of a pre-Carboniferous Lake District anticline. Apart from the Silurian rocks in the south, and the immediately adjacent Ordovician, there is therefore little evidence for end-Silurian orogeny in the Lake District.

(v) Wales: there is reasonable evidence that cleaved Silurian rocks were originally present throughout much of North and Central Wales, and end-Silurian orogeny is accepted here.

It is concluded that major Siluro-Devonian deformation in Britain was probably restricted to the southern Lake District and Wales, and can not accurately be described as a major orogeny. The great contrast in structural complexity between this deformation and the end-Silurian nappe structures of Scandinavia therefore requires explanation.

(b) Direction of Subduction

The arcuate surface trace of the O.R.S. subduction zone has great implications for the geometry of plate movements in the British-Scandinavian sector of the Caledonides. Strongly curved magmatic arcs are known in modern Indonesia, and such arcs imply one of two geometrical possibilities:

(i) Deformation of the descending plate, allowing perpendicular plate convergence throughout the length of the subduction zone;.

(ii) A major transcurrent component to subduction in regions where the orientation of the surface trace of the subduction zone is subparallel to the relative direction of motion of the opposing plates.

It is probably not feasible to distinguish between these possibilities when all traces of oceanic crust have been destroyed, but it is believed that the second can be used to explain the tectonic contrast between Britain and Scandinavia at the end of the Silurian.

Major collision orogeny could be expected where the direction of relative plate motion was perpendicular to the surface trace of the subduction zone. Collision orogeny could therefore occur on the Shetland-Scandinavia sector of the subduction zone if relative plate motion was east-west. Plate convergence along the sector between Ireland and southern Scotland would then be less than 45° oblique to the

subduction zone, and would perhaps result in much less intense deformation. The occurrence of granulite facies gneissose blocks in Carboniferous vents close to the suture in central Ireland (Strogen, 1974), and the existence of a normal crustal thickness along the LISPB seismic section (Bamford et al., 1978) suggest that the opposing continents did come into contact in this sector, although some ambiguity exists in the geological interpretation of the seismic data. Further speculation on the actual geometry of collision is considered unjustified because of the lack of information concerning the shape of the northwest margin of the European plate.

It is believed that the rarity of calc-alkaline volcanic rocks of Silurian age on the European plate can be used as evidence against final closure being accomplished by the collision of two opposing subduction zones (c.f. Phillips et al., 1976), although the significance of the c. 400 Ma granitoids of northern England and southern Scotland, and of the Cheviot and St. Abb's Head lavas, remains to be investigated. These lavas and plutons are thought to be of early Devonian age, a little younger than the O.R.S. volcanic province to the north of the Southern Uplands Fault. More detailed modelling will need to be based on an accurate geochronological study of the O.R.S. lavas, together with a trace element chemical study of the plutonic rocks.

9.7 : ORIGIN OF SPATIAL CHEMICAL VARIATION

The complex chemical variation described from most of the O.R.S. volcanic province was ascribed to multi-source contamination models in sections 4.4, 5.5 and 6.3. As discussed in section 9.3, the wide variation in LIL element concentrations of rocks with >100 ppm Ni and >150 ppm Cr can not be generated by fractional crystallisation, and requires the existence of primary magmas with a wide range of LILE concentrations in a single area, and an increase in overall LILE concentrations correlated with increasing depth to the inferred Benioff zone. Since correlation between LILE concentrations is colinear for variation both within a single area and throughout the whole province, it is believed that any mechanism proposed to explain LILE variation with depth to the Benioff zone must also be able to provide LILE variation within a single area.

The existence of a descending lithospheric plate allows five possible contributory sources to the eventual magma composition: the upper and lower continental crust; the mantle; the subducted lithosphere and any sedimentary material subducted with the descending plate. The greater the number of sources invoked in a final model the harder this becomes to test, and therefore models will be discussed in order of increasing complexity.

(a) Single source models

The high Ni and Cr concentrations of many of the rocks imply derivation of parental magmas by the partial melting of a Ni- and Cr-rich source material. Both upper crustal material and subducted sediments are likely to contain less Ni and Cr than many of the lavas, and if the subducted oceanic crust was comparable to modern mid ocean ridge basalts, Ni and Cr would again be lower than their concentrations in many O.R.S. lavas (Sun et al., 1979, Fig. 2). The cumulates and mantle underlying the subducted oceanic basalts are likely to be highly refractory: it is not believed that significant volumes of melt could be derived from this source. Little is known of the chemical characteristics of the lower continental crust, but it is unlikely to have much Ni and Cr, assuming that it is not ultramafic.

The only single source that can provide adequate Ni and Cr is therefore the mantle. It was observed in section 4.4 that generation of thick sequences of LILE-rich volcanic rocks such as the Lorne Plateau lavas requires the total removal of many LILE from unreasonably large volumes of even fairly enriched mantle (2x chondrite). A single mantle source region is therefore required to be highly enriched in LIL elements. If this also involved enrichment in Rb/Sr and Nd/Sm then the values of $^{87}Sr/^{86}Sr$ and $^{143}Nd/^{144}Nd$ could be used to indicate the longevity of the enrichment. The relatively low $^{87}Sr/^{86}Sr$ at Lorne (Brown, 1975) suggests that either

enrichment had not been long in existence, requiring a recent influx of LIL elements, or that Rb/Sr was not enriched. Depth-correlated variations in LILE concentrations could then be generated by an increase in mantle LILE with depth.

Such a model for the K-h variation has been discounted by many authors e.g. Dickinson and Hatherton (1967) and Cawthorn (1977). It is believed to be unlikely because of the extreme nature of the necessary enrichment in LILE, and the development of the enrichment not long before volcanism would require an additional source of incompatible elements. Furthermore, the failure of Rb, Zr and possibly Th and Nb to show depth variation (Fig. 9.8, Table 9.1), and the negative correlation between Y and depth, suggests either that enrichment was restricted to a particular group of incompatible elements, or that these elements were located in refractory phases, and that the Y-bearing phase (?garnet) became more refractory with depth. Both of these possibilities are thought to be unlikely, and the difficulty of producing the observed variation in incompatible element ratios within a single area is believed to be strong evidence against any single source model.

(b) Dual source models

Using the same argument as previously, the high Ni and Cr of many rocks requires that some part of these melts must originate in the mantle. Since the main difficulty

Fig. 9.8 a & b : Bulk rock variation diagrams for samples with >100 ppm Ni and >150 ppm Cr.

Conventions as section 3.3

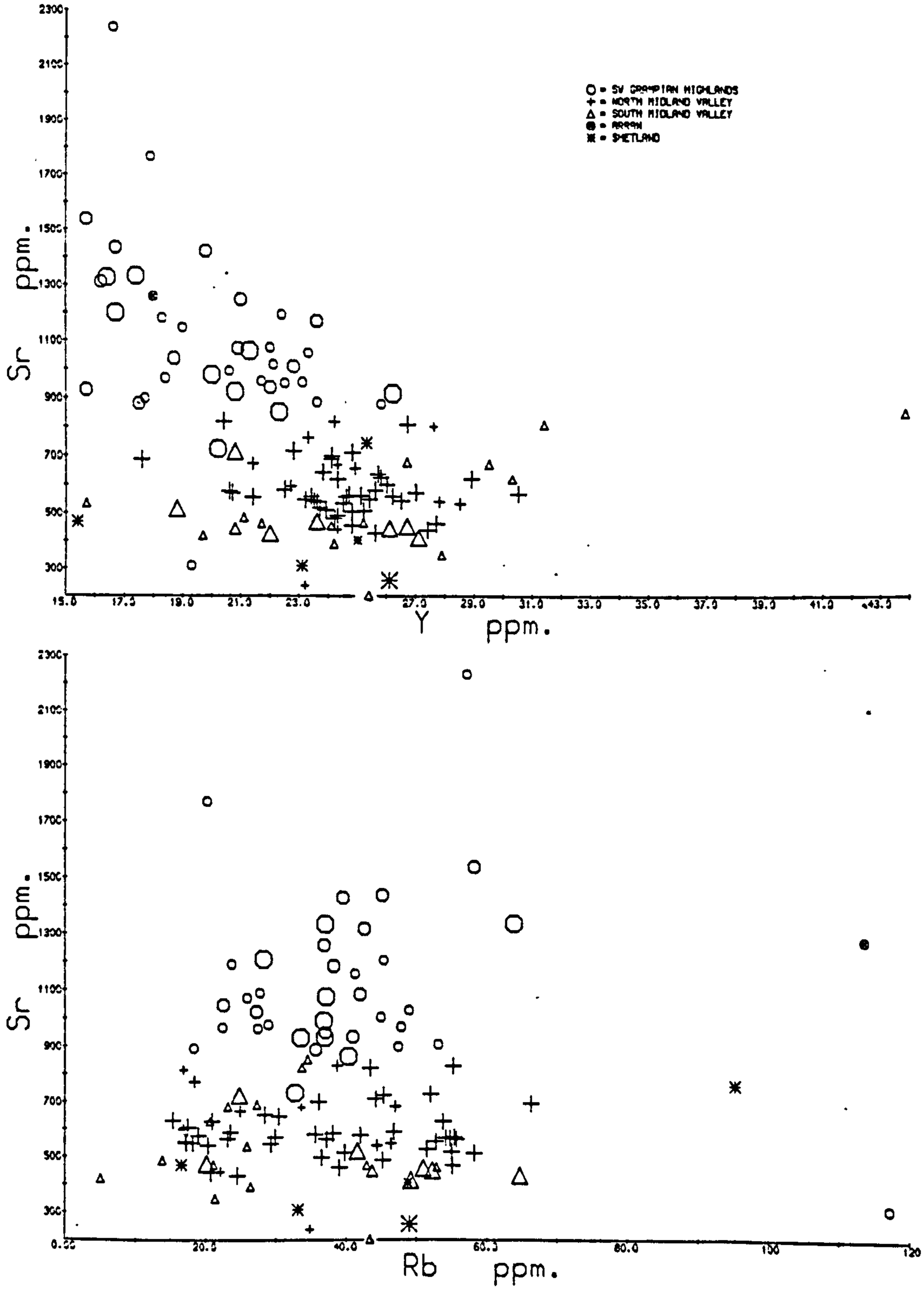

Fig. 9.8 c & d : samples with >100 ppm Ni, and >150 ppm Cr

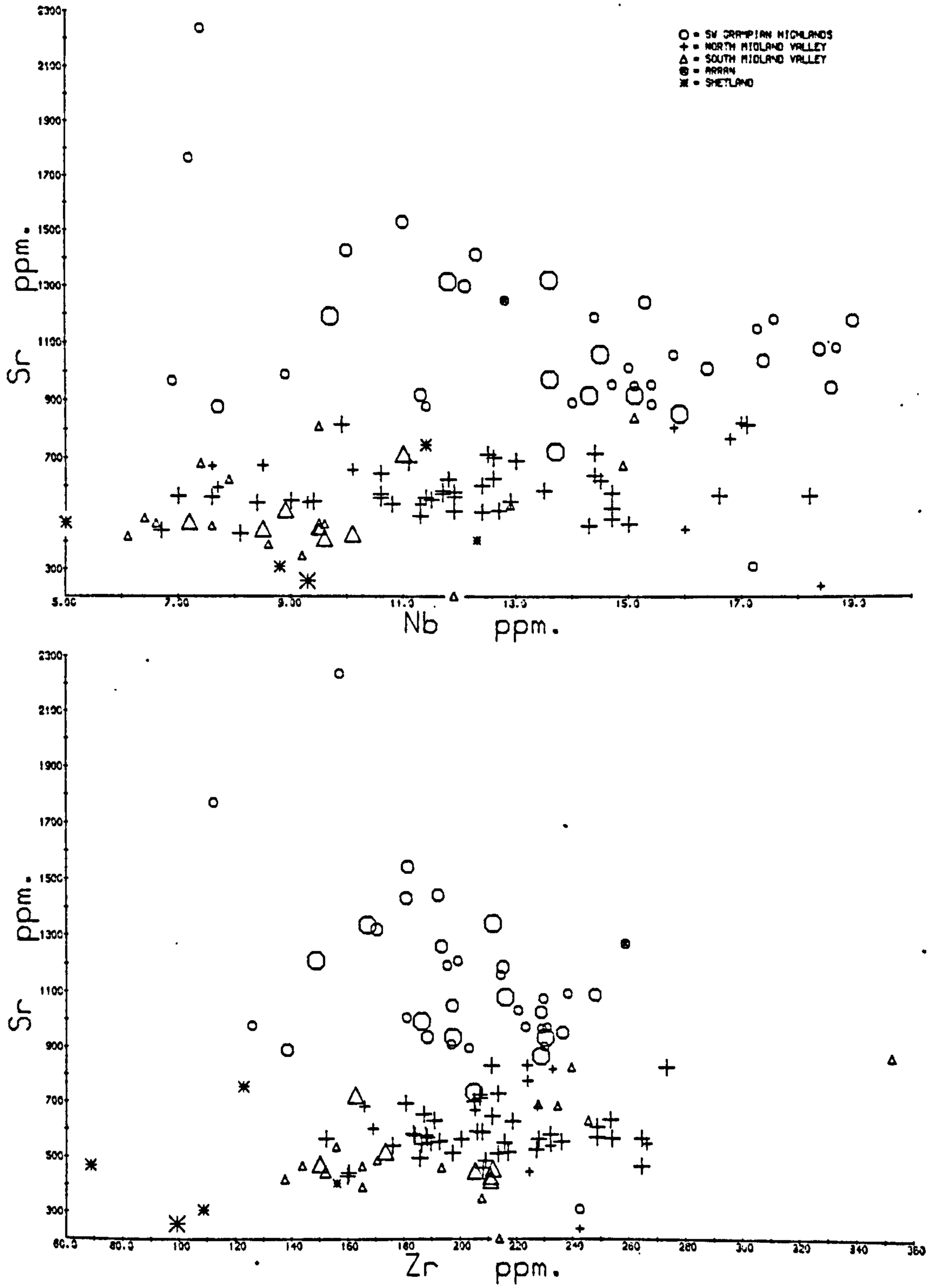

Fig. 9.8 e & f : Regression lines for each area for samples with 65% SiO_2. Symbols refer to the major regions:
○ = SW Grampian Highlands, + = North Midland Valley,
△ = South Midland Valley, ✳ = Shetland (Esha Ness)

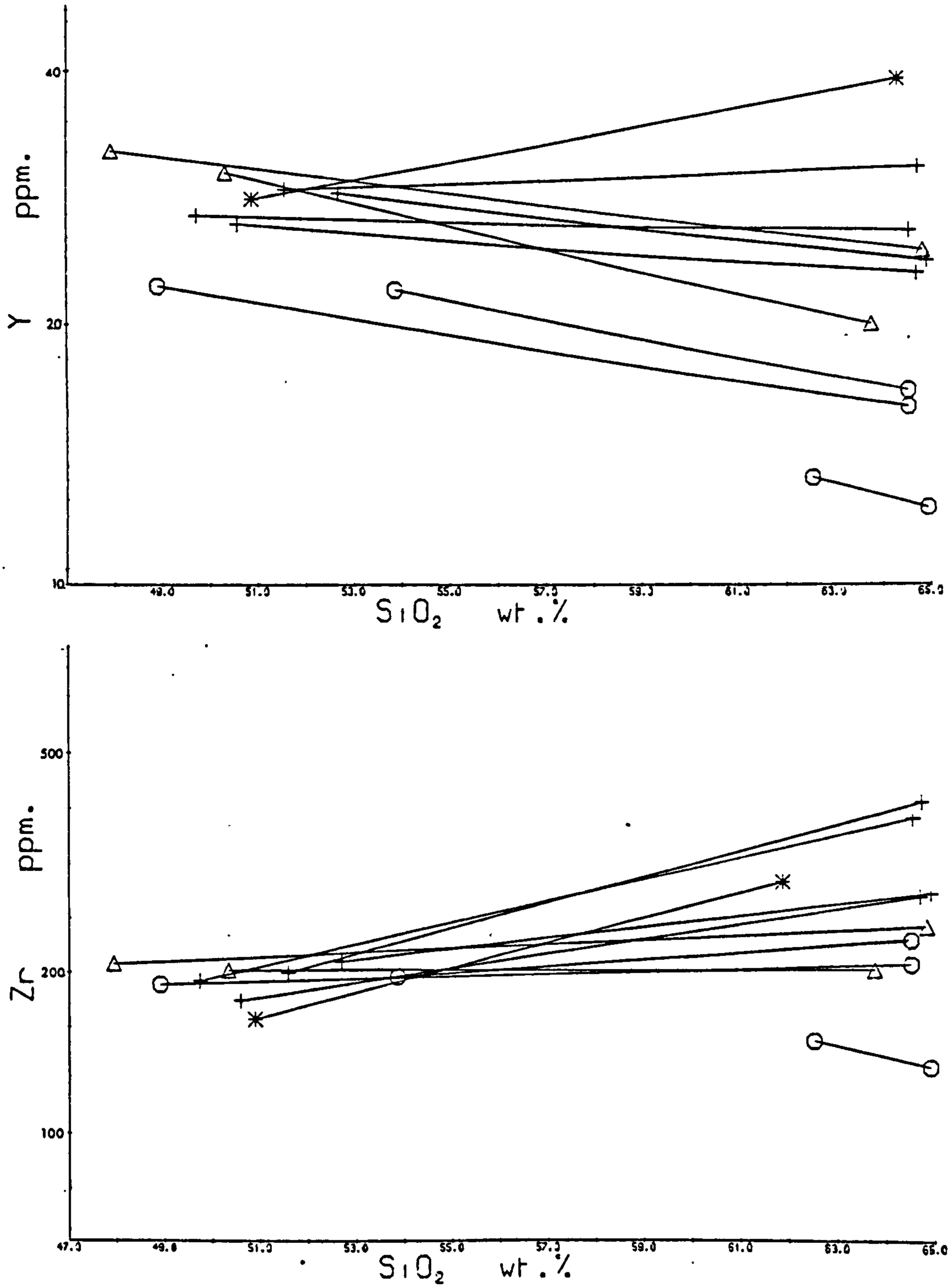

with single-source mantle derivation is the high concentrations of incompatible elements, the basic function of an additional source region is to provide a contaminant rich in incompatible elements, varying proportions of which can be added to a mantle melt to provide a wide range of incompatible element concentrations with only minor change in major element composition.

Generation of higher LIL element concentrations through the interaction of mantle-derived melt with thicker crust to the northwest can not satisfactorily account for the low levels of these elements in Huntly and Shetland. The low initial $^{87}Sr/^{86}Sr$ of the Lorne lavas was used in Chapter 4 to infer that the high Sr was not crustally derived, but interpretation of this isotopic result is hazardous because of the northwestward decrease in Rb/Sr. It is very difficult to envisage a model for this Rb/Sr depletion involving crustal contamination. Derivation of the high concentrations of incompatible elements by contamination with lower crustal material is unlikely to produce an increase with depth to the subduction zone. Furthermore, if the lower crust was of Lewisian character, it is improbable that a contaminant rich in incompatible elements could be derived from it.

It is difficult to suggest criteria which could indicate the extent to which subducted sediments contributed to the magmas. They are probably capable of providing a source for small quantities of melt very rich in

incompatible elements, but it is difficult to suggest a reason for the increase in LIL element concentrations with depth to the Benioff zone. This requires a greater relative volume of sediment-derived melt or melts richer in LILE with increasing depth. Neither of these possibilities is thought to be likely, and the failure of Zr, Rb and Nb to increase with depth requires an unusual combination of refractory phases.

Interaction of subducted oceanic crustal material and overlying mantle can occur by transfer of either melts or hydrous fluids. In either case, the existence of an increase in LIL element concentrations with depth to the Benioff zone implies that the contaminant becomes richer in LIL elements with depth or that the relative proportion of contaminant to mantle-derived melt increases. Cawthorn (1977) has reviewed the suggestions of several authors for the origin of K-h variation involving a melt contribution from the slab. These include the breakdown of hydrous phases in the slab, buffering of the K_2O content of the magmas by sanidine, and decrease in D(K,bulk slab) with pressure. Models involving particular phases are specific for K, and can not generate the variation observed in the O.R.S. province for many other LIL elements.

Little evidence is available for the behaviour of LILE distribution coefficients with pressure: it is thought to be most unlikely that those for Sr, Ba, LREE, P and K in an eclogitic assemblage would decrease by the large amount

required with no corresponding change in those for Rb, Zr and Nb. Change in relative proportions of slab and mantle melt is unlikely to result in contamination by a greater proportion of slab melt at greater depths, unless slab dehydration at shallower levels results in greater melting of the overlying mantle. Change in proportions of contaminant and mantle melt requires lower concentrations of Rb, Zr and Nb in deeper slab melts: this would probably require the retention of these elements in refractory slab phases, and is thought to be unlikely.

It is probable that a slab-derived hydrous fluid would be able to transport LIL in preference to high field strength elements from the slab into the overlying mantle, in a manner analogous to the behaviour of these two groups of elements during metamorphism. This might therefore provide a model for the separation of the two groups of incompatible elements, not readily accomplished by melting processes. The high degree of light rare earth enrichment at Lorne could be produced without the need to invoke residual garnet, or separation of garnet during ascent, for Y would not be readily transported by the hydrous fluid.

The hypothesis satisfactorily explains the failure of Zr, Ti and Y to correlate with the LIL elements, and slight correlation of LILE with Nb could be ascribed to minor transport of Nb as ionic complexes. However, Rb is likely to be one of the most readily transported LIL elements in a hydrous fluid. Furthermore, it is not clear how

contamination by slab-derived hydrous fluid can generate the depth increase, for the bulk of the dehydration of the subducting lithosphere is likely to take place at relatively shallow levels. The PT regime of the descending lithosphere is not sufficiently well-known to permit accurate prediction of the stability limit of amphibole, which is probably the most important hydrous phase, although phases such as hydrogarnet have been proposed at higher pressures. It is nevertheless believed that the quantity of hydrous fluid released by the descending lithosphere will decrease with increasing depth, and that therefore increase of LILE with depth by this model requires major increase in D(LILE,hydrous fluid/slab) with pressure. This has been demonstrated by Mysen (1979) for LREE in a garnet-peridotite, but is thought unlikely to be the case for all the elements involved.

(c) Zone-refining

Best (1975) suggested that the K-h relation could be produced if magmas (or hydrous fluids) generated in the vicinity of the subducted lithosphere were able to zone-refine (or scavenge) incompatible elements from the overlying mantle wedge, resulting in higher K with an increased path length to the surface. The enrichment process is only limited by the distribution coefficient for a particular element between the fluid and the mantle phase assemblage, and variation within a single outcrop area can be attributed to differences in the rate of fluid ascent, or

to heterogeneity in the mantle resulting from the passage of earlier fluids. This mechanism would be most effective for incompatible elements present at grain boundaries, in fluid inclusions or in defect structures, but the ascending fluid would probably not incorporate incompatible elements held in minor phases, unless it was sufficiently superheated to allow melting of these phases.

Various minor mantle phases have been invoked to explain trace element characteristics of 'primary' magmas; for example, phlogopite (Beswick 1976) and apatite (Beswick and Carmichael, 1978). If such phases are present then the incompatible element concentrations of a particular zone-refining primary magma will be a function of the concentrations acquired at the site of melting, the ascent rate, the path length to the surface and the distribution of minor phases along this path. The failure of Zr, Rb, possibly Th and to a lesser extent Nb to show depth-correlated variation might suggest the presence in the mantle of minor phases rich in these elements. These phases are not required to be refractory, as is the case in previously discussed models, and the wide variation in these elements uncorrelated with Sr or LREE in a single outcrop area, e.g. Lorne, could be due chance melting and incorporation of these phases into some of the ascending fluids.

This interaction between ascending fluids and incompatible elements occurring both within discrete phases

and dispersed through the mantle can probably account for most of the observed spatial and local variation in relative and absolute abundances of incompatible elements in the Ni- and Cr-rich rocks. The absence of constant ratios between the incompatible elements that increase most with depth can be ascribed to the partial buffering of most elements by minor phases. For example, K_2O shows little increase relative to Sr between the North and South Midland Valley, while P_2O_5 and LREE appear to increase more rapidly than Sr over this part of the depth range (Fig. 9.2). The close correlation between P_2O_5 and ΣLREE and the curved Sr-P, Sr-ΣLREE relations could suggest minor buffering of P and LREE concentrations by apatite in the north, but otherwise it is difficult to suggest the identity of the minor phases. For example, the failure of Rb to show a depth increase coupled with the intermediate behaviour of K could suggest the presence of phlogopite, but it is doubtful whether D(K/Rb,phlog) is sufficiently low to provide readily apparent variation in K but none in Rb. Ilmenite is perhaps the most plausible phase to prevent a Zr-h relation, but the existence of a slight Nb-h relation is difficult to reconcile with D(Zr/Nb)<1 for most phases. The decrease in Y with depth (Fig. 9.8) can not be satisfactorily explained by this process, unless interaction with a greater height of garnet-bearing mantle can result in loss of Y from the ascending fluids. This could also produce the slight decrease in Sc with depth (Table 9.1).

While the scavenging/zone refining process provides

the most satisfactory dual source explanation for the depth variation and for variation within a single area, some doubts must be expressed concerning the dynamics of the process. The zone-refining presumably occurs by diffusion of incompatible elements into the ascending fluid: if ascent was diapiric then diffusion rates are probably too slow to provide sufficient enrichment. The alternative is to invoke percolation of the ascending fluid through the mantle: this may involve equilibration with the mantle throughout ascent for the major elements. Insufficient high pressure experimental work is available to suggest the sort of compositions that might result, but the hypothesis requires some of these to be very siliceous: seven of the rocks with >100 ppm Ni and >150 ppm Cr have over 59% SiO_2, and bronzite-andesites with 56-59% SiO_2 are very common. Many rocks much more siliceous than these also have high Ni and Cr, frequently in excess of 60 and 100 ppm respectively. The zone-refining hypothesis could imply that these too had passed through the mantle, for such rocks display a similar variation in incompatible element concentrations (e.g. Fig. 9.6a), and can not be derived by fractional crystallisation of any of the more mafic magmas (sections 4.4d, 5.5c, 6.3c). High pressure experimental determination of the phase relations of some of these compositions would be of great value.

A further problem arises concerning the genesis of many rocks poor in Ni and Cr. While the few of these that are rich in incompatible elements may probably be generated

by fractional crystallisation (e.g. the "trachyandesites" of Montrose, section 5.1e), many have equivalent or lower concentrations of incompatible elements than the Ni- and Cr-rich rocks of the same area (e.g. the East Hills/ Dunnichen Member, section 5.1b). It was concluded in section 5.5c that these were most likely to represent partial melts of a Ni-, Cr-poor source, although their derivation by fractional crystallisation from primitive incompatible element-poor magmas, never seen at the surface, could not precluded. If the latter was the case, then the entire spatial variation of mafic rocks in the O.R.S. province would have to be a result of chance: this can not be accepted. It is possible, however, that relatively little separation of mafic phases is required to reduce Ni and Cr to these levels, and that the parental magmas need not have been much poorer in incompatible elements.

Alternatively, the Ni-, Cr-rich magmas could be parental to the low-Ni, -Cr rocks if differentiation took place prior to contamination. If this differentiation occured at relatively shallow depths (<60 km), then the contamination process must have involved the mixing of magmas produced at these levels with the fluids which had ascended through and zone-refined the mantle wedge. Serious volumetric problems are encountered here, for the great advantage of the zone-refining process would be lost, whereby the incompatible element-depth variation is believed to be due to zone-refining through different path lengths to the surface. An extra variable would be introduced into the

chemical equation: the relative proportion of zone-refining fluid to sub-crustal melt. The relatively constant levels of K and Sr in many parts of the Midland Valley (e.g. Figs. 9.1, 9.3 for the Sidlaw Hills, the North Fife Hills and Ayrshire) are most unlikely to be due to high level mixing, for it would be expected that at least some of the high level magmas parental to rocks such as those of Dunnichen and East Hills would reach the surface. The relatively uniform levels of these elements are far better explained by allowing a wide range in Ni, Cr and SiO_2 concentrations in the primary magmas formed in the vicinity of the subducted slab. A third source component is therefore believed to be necessary to generate the volcanic rocks of the O.R.S. province: the subducted slab.

The melting processes in the vicinity of the subducted slab are not understood, for their chemical features are difficult to isolate from the effects of later contamination. It is possible that the positive K-SiO_2 correlation has its origin in this region, with the K later augmented by zone-refining. The striking La/Y-SiO_2 and Ti-Y correlations in the rocks of many areas may also originate at this early stage in petrogenesis.

(d) Petrogenetic summary

It is believed that a model along the following lines could have generated the chemical variation of the rocks of the O.R.S. volcanic province:

(i) Generation of melts in the subducted slab and in the immediately overlying mantle with a wide range in SiO_2, Ni and Cr concentrations. Subducted sediment may also play a part in initial magma generation.

(ii) Percolation of melts through the overlying mantle wedge, resulting in the zone-refining of incompatible elements from grain boundaries, and sometimes the melting of minor phases rich in LIL and high field strength elements. The increase in incompatible element concentrations from the South Midland Valley to Lorne is directly related to the increased path length available for zone-refining to melts arising from successively deeper levels.

(iii) Minor separation of mafic phases in the later stages of ascent can reduce Ni and Cr concentrations and could possibly destroy evidence for major element equilibration with mantle.

(iv) Minor fractional crystallisation at crustal levels may generate a few rocks greatly enriched in Zr, Nb etc. e.g. the "trachyandesites" of Montrose. Major fractional crystallisation at this level appears to have taken place in Shetland.

(v) Melting of the lower continental crust with hybridisation may generate some of the most siliceous magmas, with lower incompatible element concentrations than in many more basic magmas.

The great complexity of the chemical variation inevitably means that the evidence for some of these

conclusions is a little unsatisfactory, and further work, particularly isotopic and experimental, is required before detailed petrogenetic models can be suggested for the various rock groups. It is believed that further work on rocks of the province, possibly leading to refutation of some of the above conclusions, would be of great value, for some of the implications of the model discussed above are of considerable importance for the genesis of all calc-alkaline rock suites. The zone-refining process will result in a mantle heterogeneously depleted in grain boundary incompatible elements, but not necessarily infertile: any melts forming at a later date should show the effects of this (e.g. the Scottish Carboniferous volcanic rocks). Further, there is no reason to suggest that the zone-refining process should be restricted to calc-alkaline rocks, and any magma generated below the uppermost mantle is probably capable of zone-refining during its passage to the surface.

ACKNOWLEDGEMENTS

I am most grateful to Dr. J.G. Fitton and Dr. B.G.J. Upton for suggesting this research project, for their constant interest and encouragement throughout, and for their helpful comments on the various stages of this thesis.

I am very grateful to Professor Sir Frederick Stewart and Professor G.Y. Craig for placing the facilities of the Grant Institute of Geology at my disposal. The receipt of a Natural Environment Research Council Research Studentship is gratefully acknowledged.

I also wish to thank everyone with whom I have discussed the various ideas presented herein, especially my fellow research students Messrs. A.M. Graham and P.M. Jackson.

I would also like to express my appreciation to the following persons for the large amount of technical advice and assistance that I have received throughout the course of this research.

Mr. K. Cameron and his assistants for making most of the thin sections and probe slides, and for help in making the others.

Dr. J.G. Fitton, Dr. E. Boyle and Mr. G.R. Angell for assistance and advice on XRF techniques.

Dr. P.G. Hill, Mr. C. Begg and Mrs. S. O'Hara for their great help in electron microprobe techniques, and in particular for their immediate assistance at any mishap and for their maintenance of an extremely efficient microprobe laboratory.

Dr. G. Yarwood for my introduction to the Edinburgh computer system; the authors of the various computer programs that I have used, particularly Dr. D.J. Humphries; and the staff of the Edinburgh Regional Computing Centre, without whose assistance little of this work could have been completed within three years.

Mrs. D. Baty and Mrs. K. Swanson for photographing and printing some of the diagrams, and for their assistance with draughting.

Mrs. T. Grieve for assistance in the library.

Mr. P. Aspen for the efficient curation of my samples.

Several people kindly donated specimens for analysis; I should particularly like to thank Messrs. M.A.E. Brown, D.C. Greig and R.W. Elliot of the Institute of Geological Sciences, Edinburgh, and Mr. E. Kellock.

REFERENCES

ABBEY, S., 1977. Studies in "standard samples" for use in the general analysis of silicate rocks and minerals. Part 5: 1977 edition of "usable" values. Geol. Surv. Canada Paper, 77-34.

ANDERMAN, G. and KEMP, J.W., 1958. Scattered X-rays as internal standards in X-ray emission spectroscopy. Anal. Chem., 30, 1306-1309.

ANDERSON, A.T., 1977. Bronzite-andesite: indicator of dead subduction? (abstract). IASPEI/IAVCEI Assembly, Durham, p.48.

ARCULUS, R.J., 1973. The alkali basalt, andesite association of Grenada, Lesser Antilles. Unpubl. Ph.D. Thesis, Univ. of Durham.

ARCULUS, R.J. and JOHNSON, R.W., 1978. Criticism of generalized models for the magmatic evolution of arc-trench systems. Earth Planet. Sci. Letters, 39, 118-126.

ARMSTRONG, M. and PATERSON, I.B., 1970. The Lower Old Red Sandstone of the Strathmore Region. Institute of Geological Sciences Report No. 70/12.

BAILEY, E.B., 1958. Some chemical aspects of South-West Highland Devonian igneous rocks. Bull. geol. Surv. Gt. Br., 15, 1-20.

BAILEY, E.B. and MAUFE, H.B., 1960. The Geology of Ben Nevis and Glen Coe and the surrounding country. Mem. geol. Surv. Gt. Br. (Scotland).

BAMFORD, D., NUNN, K., PRODEHL, C. and JACOB, B., 1978. LISPB-IV. Crustal structure of Northern Britain. Geophys. J. R. Astr. Soc., 54, 43-60.

BEST, M.G., 1975. Migration of hydrous fluids in the upper mantle and potassium variation in calc-alkalic rocks. Geology, 3, 429-432.

BESWICK, A.E., 1976. K and Rb relations in basalts and other mantle-derived materials: Is phlogopite the key? Geochim. Cosmochim. Acta, 40, 1167-1183.

BESWICK, A.E. and CARMICHAEL, I.S.E., 1978. Constraints on mantle source compositions imposed by phosphorus and the rare-earth elements. Contrib. Mineral. Petrol., 67, 317-330.

BLUCK, B.J., 1978. Sedimentation in a late-orogenic basin : the Old Red Sandstone of the Midland Valley of Scotland. In: D.R. Bowes and B.E. Leake (eds.) 'Crustal evolution in northwestern Britain and adjacent regions'. Geol. J. Spec. Issue, 10, 249-278.

BRIDEN, J.C., MORRIS, W.A. and PIPER, J.D.A., 1973. Palaeomagnetic studies in the British Caledonides - VI: Regional and global implications. Geophys. J. R. Astron. Soc., 34, 107-134.

BROWN, G.C., 1979. Some geochemical and geophysical constraints on the origin and evolution of Caledonian granites. In: A.L. Harris, C.H. Holland and B.E. Leake (eds.) 'the Caledonides of the British Isles'. J. geol. Soc. Lond. Spec. Issue.

BROWN, J.F., 1975. Rb-Sr studies and related geochemistry on the Caledonian calc-alkaline igneous rocks of N.W. Argyllshire. Unpubl. D.Phil. Thesis, Univ. of Oxford.

CAMPBELL, R., 1913. The geology of south-eastern Kincardineshire. Trans. R. Soc. Edinb., 48, 923-960.
CARRUTHERS, R.G., BURNETT, G.A. and ANDERSON, W., 1932. The Geology of the Cheviot Hills. Mem. geol. Surv. Gt. Br. (England and Wales).
CAWTHORN, R.G., 1977. Petrological aspects of the correlation between potash content of orogenic magmas and earthquake depth. Mineral. Mag., 41, 173-182.
CAWTHORN, R.G. and O'HARA, M.J., 1976. Amphibole fractionation in calcalkaline magma genesis. Am. J. Sci., 276, 309-329.
CHARLESWORTH, H.A.K., 1960. The Old Red Sandstone of the Curlew Mountains Inlier. Proc. R. Irish Acad., 61B, 51-58.
CHURCH, W.R. and GAYER, R.A., 1973. The Ballentrae Ophiolite. Geol. Mag., 110, 497-510.
COCKS, L.R.M., HOLLAND, C.H., RICKARDS, R.B. and STRACHAN, I., 1971. A correlation of Silurian rocks in the British Isles. Geol. Soc. Lond. Special Report No. 1, 136pp.
DAVIDSON, C.F., 1932. The geology of Moncreiffe Hill, Perthshire. Geol. Mag., 69, 452-464.
DEWEY, J.F., 1969. Evolution of the Appalachian/Caledonian orogen. Nature, 222, 124-129.
DICKINSON, W.R., 1975. Potash-depth (K-h) relations in continental margin and intra-oceanic magmatic arcs. Geology, 3, 53-56.
DICKINSON, W.R. and HATHERTON, T., 1967. Andesite volcanism and seismicity around the Pacific. Science, 157, 801-803.
DOWNIE, C. and SOPER, N.J., 1972. Age of the Eycott Volcanic Group and its conformable relationship to the Skiddaw Slates in the English Lake District. Geol. Mag., 109, 259-268.
DUNCUMB, P. and JONES, E.M., 1969. Electron probe microanalysis: an easy to use computer program for correcting quantitative data. Tube Investments Research Laboratories, Saffron Walden, Cambridge.
DUNHAM, K.C., 1974. Granite beneath the Pennines in north Yorkshire. Proc. Yorks. geol. Soc., 40, 191-194.
ERCC, 1974. Edinburgh IMP language manual. R. McLeod (ed.).
ERCC, 1976. EMAS User's Guide. R. McLeod (ed.), Edinburgh Regional Computing Centre, 137pp.
ERCC, 1977. ERCC Graphics Manual. Edinburgh Regional Computing Centre.
EVANS, A.LL., MITCHELL, J.G., EMBLETON, B.J.J. and CREER, K.M., 1971. Radiometric age of the Devonian polar shift relative to Europe. Nature Phys. Sci., 229, 50-51.
EWART, A., in press. The mineralogy and petrology of Tertiary to Recent orogenic volcanic rocks: with special reference to the andesitic-basaltic compositional range. In: R.S. Thorpe (ed.) 'Orogenic andesites and related rocks'. J. Wiley, London.
EYLES, V.A., SIMPSON, J.B. and MACGREGOR, A.G., 1949. The Geology of Central Ayrshire. Mem. geol. Surv. Gt. Br. (Scotland).
FINLAY, T.M., 1930. The Old Red Sandstone of Shetland. Part II: North-western area. Trans. R. Soc. Edinb., 56,

671-694.
FITTON, J.G. and GILL, R.C.O., 1970. The oxidation of ferrous iron in rocks during mechanical grinding. Geochim. Cosmochim. Acta, 34, 518-524.
FITTON, J.G. and HUGHES, D.J., 1970. Volcanism and plate tectonics in the British Ordovician. Earth Planet. Sci. Letters, 8, 223-228.
FITTON, J.G., THIRLWALL, M.F. and HUGHES, D.J., in press. Volcanism in the Caledonian orogenic belt of Britain. In: R.S. Thorpe (ed.) 'Orogenic andesites and related rocks - part IX: Andesitic volcanism throughout the Earth's history'. J. Wiley, London.
FLINN, D., 1961. Continuation of the Great Glen Fault beyond the Moray Firth. Nature, 191, 589-591.
FLINN, D., 1969. A geological interpretation of the aeromagnetic maps of the continental shelf around Orkney and Shetland. Geol. J., 6, 279-292.
FLINN, D., MILLER, J.A., EVANS, A.L. and PRINGLE, I.R., 1968. On the age of the sediments and contemporaneous volcanic rocks of Western Shetland. Scott. J. Geol., 4, 10-19.
FRANCIS, E.H., FORSYTH, I.H., READ, W.A. and ARMSTRONG, M., 1970. The Geology of the Stirling District. Mem. geol. Surv. Gt. Br. (Scotland).
FRIEND, P.F. and MACDONALD, R., 1968. Volcanic sediments, stratigraphy and tectonic background of the Old Red Sandstone of Kintyre, W. Scotland. Scott. J. Geol., 4, 265-282.
GALE, N.H., BECKINSALE, R.D. and WADGE, A.J., 1979. A Rb-Sr whole rock isochron for the Stockdale Rhyolite of the English Lake District and a revised mid-Palaeozoic time scale. Jl geol. Soc. Lond., 136, 235-242.
GANDY, M.K., 1973a. The Petrology and Geochemistry of the Lower Old Red Sandstone Lavas of the Sidlaw Hills, Perthshire. Unpubl. Ph.D. Thesis, Univ. of Edinburgh.
GANDY, M.K., 1973b. Melting relations of some calc-alkaline lavas from the eastern Sidlaw Hills, Perthshire, Scotland. Earth Planet. Sci. Letters, 19, 230-234.
GEIKIE, A., 1897. The ancient volcanoes of Great Britain. 2 vols. MacMillan, London.
GEIKIE, A., 1900. The Geology of Central and Western Fife and Kinross. Mem. geol. Surv. Gt. Br. (Scotland).
GEIKIE, A., 1902. The Geology of Eastern Fife. Mem. geol. Surv. Gt. Br. (Scotland).
GILL, J.B., 1978. Role of trace element partition coefficients in models of andesite genesis. Geochim. Cosmochim. Acta, 42, 709-724.
GOLDSCHMIDT, V.M., 1954. 'Geochemistry'. Clarendon Press, Oxford.
GRAHAM, A.M., in preparation. Genesis of the igneous rock suite of Grenada, Lesser Antilles. Unpubl. Thesis, Univ. of Edinburgh.
GRAHAM, A.M. and UPTON, B.G.J., 1978. Gneisses in diatremes, Scottish Midland Valley: petrology and tectonic implications. Jl geol. Soc. Lond., 135, 219-228.
GREEN, T.H., 1977. Garnet in silicic liquids and its possible use as a P-T indicator. Contrib. Mineral. Petrol., 65, 59-67.

GREEN, T.H. and RINGWOOD, A.E., 1968. Genesis of the calc-alkaline igneous rock suite. Contrib. Mineral. Petrol., 18, 105-162.

GREIG, D.C., 1971. British Regional Geology : The South of Scotland. H.M.S.O., Edinburgh. 125pp.

GREIG, D.C., 1975. St. Abb's Head. In: G.Y. Craig and P.McL.D. Duff 'The Geology of the Lothians and southeast Scotland'. Edin. Geol. Soc. excursion guide, Scottish Academic Press, Edinburgh.

GROOME, D.R., 1972. The geochemistry of the Old Red Sandstone volcanic rocks of northern Lorne, Argyllshire. Unpubl. Ph.D. Thesis, Univ. of London.

GROOME, D.R. and HALL, A., 1974. The geochemistry of the Devonian lavas of the northern Lorne Plateau, Scotland. Mineral. Mag., 39, 621-640.

HALLIDAY, A.N., McALPINE, A. and MITCHELL, J.G., 1977. The age of the Hoy lavas, Orkney. Scott. J. Geol., 13, 43-52.

HALLIDAY, A.N. and STEPHENS, W.E., in press. Compositional variation in the Galloway plutons. In: M.P. Atherton and J. Tarney (eds.) 'The origin of granite batholiths - geochemical evidence'. Shira Press.

HARLAND, W.B., SMITH, A.G. and WILCOCK, B., 1964. The Phanerozoic Time-scale. Q. Jl geol. Soc. Lond., 120 (supplement).

HARRIS, J.W., 1928. Notes on the extrusive igneous rocks of the Dundee district. Trans. Edinb. Geol. Soc., 12, 105-110.

HARRY, W.T., 1956. The Old Red Sandstone lavas of the western Sidlaw Hills, Perthshire. Geol. Mag., 93, 43-56.

HARRY, W.T., 1958. The Old Red Sandstone lavas of the eastern Sidlaws. Trans. Edinb. geol. Soc., 17, 105-112.

HART, S.R. and DAVIS, K.E., 1978. Nickel partitioning between olivine and silicate melt. Earth Planet. Sci. Letters, 40, 203-219.

HARVEY, P.K., TAYLOR, D.M., HENDRY, R.D. and BANCROFT, F. An accurate fusion method for the analysis of rocks and chemically related materials by X-ray fluorescence spectrometry. X-ray Spectrometry, 2, 33-44.

HASLAM, W.H., 1968. The cystallisation of intermediate and acid magmas at Ben Nevis, Scotland. J. Petrology, 9, 84-104.

HELLMAN, P.L., SMITH, R.E. and HENDERSON, P., 1977. Rare earth element investigation of the Cliefden outcrop, N.S.W., Australia. Contrib. Mineral. Petrol., 65, 155-164.

HERRIOT, A., 1956. Notes on the occurrence of garnet in the felsite of Tinto, Lanarkshire. Trans. Geol. Soc. Glasgow, 22, 94-99.

HOLLAND, J.G. and BRINDLE, D.W., 1966. A self-consistent mass absorption correction for silicate analysis by X-ray fluorescence. Spectrochim. Acta, 22, 2083-2092.

HORNE, J. and HINXMAN, L.W., 1914. The Geology of the country round Beauly and Inverness. Mem. geol. Surv. Gt. Br. (Scotland).

HOUSE, M.R., RICHARDSON, J.B., CHALONER, W.G., ALLEN, J.R.L., HOLLAND, C.H. and WESTOLL, T.S., 1977. A

correlation of the Devonian rocks in the British Isles. Geol. Soc. Lond. Special Report No. 7. 110pp.

IRVINE, T.N. and BARAGAR, W.R.A., 1971. A guide to the chemical classification of the common volcanic rocks. Canad. Jl Earth Sci., 8, 523-548.

JAKEŠ, P. and WHITE, A.J.R., 1972. Major and trace element abundances in volcanic rocks of orogenic areas. Geol. Soc. Am. Bull. 83, 29-40.

JHINGRAN, A.G., 1942. The Cheviot Granite. Q. Jl geol. Soc. Lond., 98, 241-254.

JOWETT, A., 1913. The volcanic rocks of the Forfarshire coast and associated sediments. Q. Jl geol. Soc. Lond., 69, 459-482.

KELLING, G., 1962. The petrology and sedimentation of Upper Ordovician rocks in the Rhinns of Galloway, south-west Scotland. Trans. R. Soc. Edinb., 65, 107-137.

KELLOCK, E., 1969. Alkaline basic igneous rocks in the Orkneys. Scott. J. Geol., 5, 140-153.

KYNASTON, H. and HILL, J.B., 1908. The Geology of the country near Oban and Dalmally. Mem. geol. Surv. Gt. Br. (Scotland).

KUNO, H., 1960. High-alumina basalt. J. Petrology, 1, 121-145.

KUNO, H., 1966. Lateral variation of basalt magma type across continental margins and island arcs. Bull. Volc., 29, 195-222.

KUNO, H., 1968. Differentiation of basalt magmas. In: H.H. Hess 'Basalts: the Poldervaart Treatise on rocks of basaltic composition'. J. Wiley, New York. pp623-688.

LAMBERT, R.St.J., HOLLAND, J.G. and OWEN, P.F., 1974. Chemical petrology of a suite of calc-alkaline lavas from Mount Ararat, Turkey. J. Geol., 82, 419-438.

LAMBERT, R.St.J. and McKERROW, W.S., 1976. The Grampian Orogeny. Scott. J. Geol., 12, 271-292.

LE BAS, M.J., 1962. The role of aluminium in igneous clinopyroxenes with relation to their parentage. Am. J. Sci., 260, 267-288.

LEE, G.W. and BAILEY, E.B., 1925. The pre-Tertiary Geology of Mull, Loch Aline and Oban. Mem. geol. Surv. Gt. Br. (Scotland).

MACDONALD, R., 1975. Petrochemistry of the early Carboniferous (Dinantian) lavas of Scotland. Scott. J. Geol., 11, 269-314.

MACDONALD, R. and BAILEY, D.K., 1973. The chemistry of the peralkaline oversaturated obsidians. U.S. Geol. Surv. Profess. Paper, 440-N-1, N1-N37.

McKERROW, W.S., LEGGETT, J.K. and EALES, M.H., 1977. Imbricate thrust model of the Southern Uplands of Scotland. Nature, 267, 237-239.

MELVIN, J., 1977. Sedimentological studies in Upper Palaeozoic sandstones near Bude, Cornwall and Walls, Shetland. Unpubl. Ph.D. Thesis, Univ. of Edinburgh.

MITCHELL, A.H.G. and McKERROW, W.S., 1975. Analogous evolution of the Burma orogen and the Scottish Caledonides. Geol. Soc. Am. Bull., 86, 305-315.

MITCHELL, G.H. and MYKURA, W., 1962. The Geology of the neighbourhood of Edinburgh. Mem. geol. Surv. Gt. Br. (Scotland).

MITCHELL, J.G., 1972. Potassium-argon ages from the Cheviot Hills, northern England. Geol. Mag., 109, 421-426.

MIYASHIRO, A., 1974. Volcanic rock series in island arcs and active continental margins. Am. J. Sci., 274, 321-355.

MORTON, D.J., 1979. Palaeogeographical evolution of the Lower Old Red Sandstone basin in the western Midland Valley. Scott. J. Geol., 15, 97-116.

MUIR, I.D., 1953. Quartzite xenoliths in the Ballachulish Granodiorite. Geol. Mag., 90, 409-428.

MYKURA, W., 1960. The Lower Old Red Sandstone igneous rocks of the Pentland Hills. Bull. geol. Surv. Gt. Br., 16, 131-155.

MYKURA, W., 1976. British Regional Geology : Orkney and Shetland. H.M.S.O., Edinburgh. 149pp.

MYKURA, W. and PHEMISTER, J., 1976. The Geology of Western Shetland. Mem. geol. Surv. Gt. Br. (Scotland).

MYSEN, B.O., 1979. Experimental determination of crystal-vapour partition coefficients for rare earth elements at 30 kbar pressure. Ann. Rep. Dir. Geophys. Lab. (Carnegie Inst. of Washington). Yearbook Carnegie Inst. of Washington, 1977-8, 689-695.

NAGASAWA, H., 1970. Rare earth concentrations in zircons and apatites and their host dacites and granites. Earth Planet. Sci. Letters, 9, 359-364.

NESBITT, R.W., MASTINS, H., STOLZ, G.W. and BRUCE, D.R., 1976. Matrix corrections in trace element analysis by X-ray fluorescence: an extension of the Compton scattering technique to long wavelengths. Chem. Geol., 18, 203-213.

NIELSON, D.R. and STOIBER, R.E., 1973. Relationship of potassium content in andesitic lavas and depth to the seismic zone. J. Geophys. Res., 78, 6887-6892.

NINKOVICH, D. and HAYS, J.D., 1972. Mediterranean island arcs and the origin of high potash volcanoes. Earth Planet. Sci. Letters, 16, 331-345.

NORRISH, K. and HUTTON, J.T., 1969. An accurate X-ray spectrographic method for the analysis of a wide range of geological samples. Geochim. Cosmochim. Acta, 33, 431-453.

OSBORN, E.F., 1962. Reaction series for sub-alkaline igneous rocks based on different oxygen pressure conditions. Amer. Mineral., 47, 211-226.

PANKHURST, R.J. and O'NIONS, R.K., 1973. Determination of Rb/Sr and Sr/ Sr ratios of some standard rocks and evaluation of X-ray fluorescence spectrometry in Rb-Sr geochemistry. Chem. Geol., 12, 127-136.

PATERSON, I.B. and HARRIS, A.L., 1969. Lower Old Red Sandstone ignimbrites from Dunkeld, Perthshire. Institute of Geological Sciences Report No. 69/7.

PEACH, B.N., CLOUGH, C.T., HINXMAN, L.W., GRANT WILSON, J.S., CRAMPTON, M.B., MAUFE, H.B. and BAILEY, E.B., 1910. The Geology of the neighbourhood of Edinburgh. Mem. geol. Surv. Gt. Br. (Scotland).

PEACOCK, J.D., BERRIDGE, N.G., HARRIS, A.L. and MAY, F., 1968. The Geology of the Elgin district. Mem. geol. Surv. Gt. Br. (Scotland).

PEACOCK, M.A., 1931. Classification of igneous rock series. J. Geol., 39, 54-67.

PEARCE, J.A. and CANN, J.R., 1973. Tectonic setting of basic volcanic rocks determined using trace element analyses. Earth Planet. Sci. Letters, 19, 290-300.

PEARCE, J.A. and NORRY, M.J., 1979. Petrogenetic implications of Ti, Zr, Y and Nb variations in volcanic rocks. Contrib. Mineral. Petrol., 69, 33-47.

PECCERILO, A. and TAYLOR, S.R., 1976. Geochemistry of Eocene calc-alkaline volcanic rocks from the Kastamonu area, northern Turkey. Contrib. Mineral. Petrol., 58, 63-81.

PHILLIPS, W.E.A., STILLMAN, C.J. and MURPHY, T., 1976. A Caledonian plate tectonic model. Jl geol. Soc. Lond., 132, 579-609.

PIDGEON, R.T. and AFTALION, M., 1978. Cogenetic and inherited zircon U-Pb systems in granites: Palaeozoic granites of Scotland and England. In: D.R. Bowes and B.E. Leake (eds.) 'Crustal evolution in northwestern Britain and adjacent regions'. Geol. J. Spec. Issue No. 10, 183-220.

PRINGLE, I.R., 1970. The structural geology of the North Roe area of Shetland. Geol. J., 7, 147-170.

READ, H.H., 1923. The Geology of the country round Banff, Huntly and Turriff. Mem. geol. Surv. Gt. Br. (Scotland).

READ, H.H., 1961. Aspects of Caledonian magmatism in Britain. Liv. and Manch. Geol. J., 2, 653-683.

REYNOLDS, R.C., 1963. Matrix corrections in trace element analysis by X-ray fluorescence: estimation of the mass absorption coefficient by Compton scattering. Amer. Mineral., 48, 1133-1143.

RICHEY, J.E., ANDERSON, E.M. and MACGREGOR, A.G., 1930. The Geology of North Ayrshire. Mem. geol. Surv. Gt. Br. (Scotland).

ROBERTS, J.L., 1966. Ignimbrite eruptions in the volcanic history of the Glencoe cauldron subsidence. Geol. J., 5, 173-184.

ROBSON, D.A., 1948. The Old Red Sandstone volcanic suite of eastern Forfarshire. Trans. Edinb. geol. Soc., 14, 128-140.

ROEDER, P.L. and EMSLIE, R.F., 1970. Olivine-liquid equilibrium. Contrib. Mineral. Petrol., 29, 275-289.

ROSE, H.J., ADLER, I and FLANAGAN, F.J., 1963. Use of La203 as a heavy absorber in X-ray fluorescence analysis of silicate rocks. U.S. Geol. Surv. Profess. Paper 450-B, 80-82.

RUNDLE, C.C., 1979. Ordovician intrusions in the English Lake District. Jl geol. Soc. Lond., 136, 29-38.

SCHNETZLER, C.C. and PHILPOTTS, J.A., 1970. Partition coefficients of rare-earth elements between igneous material and rock-forming mineral phenocrysts - II. Geochim. Cosmochim. Acta, 34, 331-340.

SMITH, R.E. and SMITH, S.E., 1976. Comments on the use of Ti, Zr, Y, Sr, K, P and Nb in classification of basaltic magmas. Earth Planet. Sci. Letters, 32, 114-120.

SOPER, N.J. and MOSELEY, F., 1978. Structure. In: F. Moseley (ed.) 'The Geology of the Lake District'. Yorks. Geol. Soc., Leeds, 45-67.

STATHAM, P.J., 1975. Quantitative X-ray energy spectrometry:

the application of a Si(Li) detector to electron microprobe analysis. Unpubl. Ph.D. Thesis, Univ. of Cambridge.

STILLMAN, C.J. and WILLIAMS, C.T., 1979. Geochemistry and tectonic setting of some Upper Ordovician volcanic rocks in east and southeast Ireland. Earth Planet. Sci. Letters, 42, 288-310.

STRAND, T. and KULLING, O., 1972. Scandinavian Caledonides. John Wiley, London. 302pp.

STROGEN, P., 1974. The sub-Palaeozoic basement in Central Ireland. Nature, 250, 562.

SUN, S.-S., NESBITT, R.W. and SHARASKIN, A.Y., 1979. Geochemical characteristics of mid-ocean ridge basalts. Earth Planet. Sci. Letters, 44, 119-138.

TARLO, L.B. and GURR, P.R., 1964. The Lower Old Red Sandstone of the Lorne Cuvette. Advan. Sci., 20(87), 446 (summary).

TAYLOR, D.M., 1972. The geochemistry and petrology of the andesites and associated igneous rocks of an area of the Ochil Hills, near Dunning, Perthshire. Unpubl. Ph.D. Thesis, Univ. of Nottingham.

TAYLOR, S.R., KAYE, M., WHITE, A.J.R., DUNCAN, A.R. and EWART, A., 1969. Genetic significance of Co, Cr, Ni, Sc and V content of andesites. Geochim. Cosmochim. Acta, 33, 275-286.

THEISEN, R. and VOLLACH, D., 1967. Tables of X-ray Mass Absorption Coefficients. Verlag Stahleisen M.B.H., Dusseldorf.

THIRLWALL, M.F., in preparation. Peralkaline rhyolites from the Ordovician Tweeddale lavas, Peebleshire. Submitted to Scott. J. Geol.

TYRELL, G.W., 1914. A petrographical sketch of the Carrick Hills, Ayrshire. Trans. Geol. Soc. Glasgow, 15, 64-83.

TYRELL, G.W., 1928. The Geology of Arran. Mem. geol. Surv. Gt. Br. (Scotland).

VAN BREEMEN, O., AFTALION, M. and JOHNSON, M.R.W., 1979. Age of the Loch Borrolan complex, Assynt, and late movements along the Moine Thrust Zone. Jl geol. Soc. Lond., 136, 489-495.

VAN BREEMEN, O. and BOYD, R., 1972. A radiometric age for pegmatite cutting the Belhelvie mafic intrusion, Aberdeenshire. Scott. J. Geol., 8, 115-120.

WADGE, A.J., GALE, N.H., BECKINSALE, R.D. and RUNDLE, C.C., 1978. A Rb-Sr isochron for the Shap granite. Proc. Yorks. geol. Soc., 42, 297-305.

WATERSTON, C.D., 1965. Old Red Sandstone. In: G.Y. Craig (ed.) 'The Geology of Scotland'. Oliver and Boyd, Edinburgh, 269-308.

WESTOLL, T.S., 1945. A new cephalaspid fish from the Downtonian of Scotland, with notes on the structure and classification of ostracoderms. Trans. R. Soc. Edinb., 61, 341-357.

WESTOLL, T.S., 1951. The vertebrate-bearing strata of Scotland. Rep. XVIII Int. geol. Congr. Gt. Br., Pt. 11, 5-21.

WHITFORD, D.J., 1975. Strontium isotopic studies of the volcanic rocks of the Sunda arc, Indonesia, and their petrogenetic implications. Geochim. Cosmochim. Acta,

39, 1287-1302.
WILLIAMS, A., 1972. Distribution of brachiopod assemblages in relation to Ordovician palaeogeography. In: N.F. Hughes (ed.) 'Organisms and continents through time'. Spec. Pap. Palaeont., 12, 241-269.
WILSON, H.E., 1972. Regional geology of Northern Ireland. H.M.S.O., Belfast.
WILSON, G.V., EDWARDS, W., KNOX, J. and STEPHENS, J.V., 1935. The Geology of the Orkneys. Mem. geol. Surv. Gt. Br. (Scotland).
WRIGHT, T.L. and DOCHERTY, P.C., 1970. A linear programming and least squares computer method for solving petrologic mixing problems. Geol. Soc. Am. Bull., 81, 1995-2008.

APPENDIX A : PRE-ANALYTICAL PROCEDURES

A1 : SAMPLE COLLECTION

Samples were collected with the object of displaying the full range of chemical and petrographic variation found in the rocks of each area of volcanic outcrop, with each part of that range being represented by the samples least affected by alteration. While collection has been primarily from lava flows, in some areas samples have been collected from minor intrusions into the volcanic pile, and from clasts of volcanic origin in Old Red Sandstone conglomerates. Coastal, quarry and riverside exposures were best suited to the collection of less altered samples, for collection could here be restricted to the compact central portions of flows, instead of the characteristically autobrecciated and vesicular tops and bases. In most areas, however, exposure is limited, and unusual rock types have been collected despite their state of alteration. The shortage of exposure, and variation in appearance of altered rocks, have probably led to underrepresentation of some rock types, but it is thought that this is not a serious problem.

Where possible, samples of at least 4" (10cm) diameter were collected, and as much weathered material as possible was removed in the field. Sampling was based on a geographic division of the province into 15 outcrop areas, and samples are identified by prefixing numbers with letters indicative of the outcrop area. The rocks of any one outcrop area are not necessarily genetically related.

A2 : SELECTION OF SAMPLES FOR ANALYSIS

All samples collected have been examined petrographically, initially to determine their degree of alteration and the likely effect of this on a possible analysis. Where several well-defined petrographic types were identified, the less altered samples of each type were selected for analysis. As far as possible, the analysed samples represent the full range of primary petrographic variation present in the samples collected from each area. A total of 597 samples have been analysed, and are listed in Table A1. In order to maintain constant analytical quality, only new analyses have been used, and the majority of the samples have been collected by the author.

Table A1 : List of samples analysed, localities and brief petrographies.
Abbreviations: ol=olivine; opx=orthopyroxene; cpx=clinopyroxene; hb=hornblende; pl=plagioclase; ksp=alkali feldspar; qz=quartz; bi=biotite; ap=apatite; mt=spinel; ilm=ilmenite; cc=calcite.
% refers to approximate volume percent phenocrysts.
Alteration state numbers (PAS) are: 1=ol fresh; 2=opx fresh; 3=both cpx,pl fresh ; 4=either of cpx,pl fresh; 5=none fresh (Chapter 2).
Where an alternative specimen number is quoted, the sample

is from another worker's collection: SA12-21, SH36-41, OC152-153 and OR1-4 are from the Scottish collection of the Institute of Geological Sciences (S-numbers); OR5-8 were collected by Kellock (1969); S18-52 were collected by Gandy (1973a; M-numbers); and AR10 and AR11 were collected by Dr. J.E. Dixon.

Sample	Grid Reference	Phenocrysts	%	PAS	Comments
LORNE					
L1@24	NM980349	cpx-pl-bi-hb-?opx-mt-ap-qz	25	5	
L3@1	NM924371	ol	5	4	
L4@1	NM924373	ol-mt	15	4	
L5@14	NM922375	opx-cpx-pl-bi	25	5	
L8@1	NM871319	ol	10	3	
L9@7	NM888338	ol-cpx	10	3	
L10@8	NM886339	opx-cpx	5	3	
L11@8	NM886339	opx-cpx	5	4	
L12@1	NM902342	ol	7	4	
L13@1	NM904342	ol	8	4	qz-cc amygdales
L14@8	NM909343	opx-cpx-qz	3	3	
L18@1	NM903338	ol-?cpx	6	4	
L19@1	NM883312	ol	13	4	
L21@7	NM885309	ol-opx-cpx-qz-?pl-?ap	5	3	
L22@20	NM864275	qz-?pl-?hb	4	4	pl xenocrystal
L23@1	NM859278	ol-?pl	1	3	
L24@7	NM915343	ol-cpx	7	3	
L25@1	NM924343	ol	7	4	
L26@7	NM933345	ol-cpx	9	3	
L28@13	NM968341	pl-opx-cpx-ap-mt	25	4	
L30@13	NM961327	pl-opx-cpx-ap-mt	20	4	
L34@45	NM986337	ol-pl-hb-cpx	20	5	
L35@21	NM985342	pl-?hb		5	ignimbrite
L38@20	NM985305	?opx	0	5	cc veins
L41@20	NN044285	opx-?hb	0	4	
L42@19	NN040285	pl	5	5	?autobreccia
L43@22	NM980288	pl-mt-?ksp	20	5	?dyke-rock
L44@1	NM908334	ol	7	3	
L45@8	NM904318	opx-cpx	5	3	
L50@45	NM911299	ol-cpx-pl-hb-qz	7	3	
L51@9	NM914296	ol-opx-cpx-?hb	6	3	
L52@9	NM916285	ol-opx-cpx-?hb	8	5	
L54@22	NM831280	cpx-bi-ap-?pl	15	5	Ferry Plug
L55@22	NM823258	?bi-?cpx	0	5	Gallanach neck
L56@1	NM791278	ol	10	3	
L58@1	NM793279	ol	7	4	
L61@47	NM889284	?ol-?opx-?hb-qz	5	5	
L63@47	NM887265	ol-opx-bi-pl-?hb-?cpx	5	5	
L64@7	NM892265	ol-cpx	6	3	
L65@7	NM816237	ol-cpx	14	3	
L67@1	NM821235	ol	7	3	
L68@1	NM889248	ol-?qz	8	3	pl-rich ?autoliths
L71@1	NM908242	ol-?opx	5	5	
L73@12	NM922240	ol-cpx-pl	15	3	
L75@19	NM922242	pl-hb-bi-mt-?ol	6	5	
L77@19	NM932226	pl-hb	15	5	

L79@13	NM947234	opx-cpx-pl-mt-ap	25	4	
L82@25	NN113289	pl, schistose screen in Etive complex			
L86@13	NN013290	opx-cpx-pl-mt-ap	32	5	
L87@3	NN012290	cpx-qz	24	5	
L91@3	NN013283	cpx-qz	20	5	
L92@19	NN014282	pl-bi-ap-?hb	6	5	
L95@13	NN018278	opx-cpx-pl-mt-ap	22	5	
L97@7	NN027265	ol-cpx	9	3	
L98@6	NM937282	pl-opx-hb-mt-ap	22	5	
L99@19	NM946278	pl	1	5	
L100@6	NM944278	pl-opx-hb-mt-ap	30	5	
L101@9	NM944283	ol-opx-cpx	7	3	
L102@13	NM947286	pl-opx-cpx-mt-ap	32	4	
L113@15	NM824217	?hb-cpx-bi-qz	18	3	
L120@19	NM804201	pl-qz-opx	15	5	
L121@13	NM813213	pl-opx-cpx-mt-ap	34	4	
L122@26	NM843198	ol-cpx	6	3	cc-bi aggregates
L125@15	NM834225	?hb-cpx-bi	12	3	
L126@7	NM857201	ol-cpx	6	3	
L128@13	NM897205	pl-opx-cpx-mt	50	3	
L129@1	NM912204	ol	4	4	
L130@19	NM915205	pl-hb-bi-opx	6	5	
L131@5	NM924307	pl-opx-mt-ap	30	5	
L132@5	NM912199	pl-opx-mt-ap	36	4	
L133@1	NM846193	ol	5	5	cc veins
L137@26	NM875170	ol-cpx	10	4	cc-bi aggregates
L140@1	NM854163	ol	5	3	
L141@1	NM847156	ol	10	3	
L146@7	NM958154	ol-cpx	14	3	
L148@1	NM992241	ol	15	3	
L150@21	NM984235	pl-bi-?ksp-mt-ap	35	5	
L151@1	NM978238	ol	6	4	
L152@1	NM975235	ol	10	3	
L153@1	NM965232	ol	9	3	
L155@7	NM946238	ol-cpx-mt	11	3	
L156@19	NM956252	pl-opx-hb	8	5	
L157@13	NM956257	pl-opx-cpx-mt	50	5	
L158@13	NN013238	pl-cpx-?opx	30	5	
<u>GLENCOE</u>					
GC1@7	NN138555	ol-cpx	5	4	Group 1
GC3@44	NN144547	pl-opx-hb-bi-mt-ap	24	3	Gp 4
GC4@44	NN148538	pl-opx-hb-bi-mt-ap	27	3	Gp 4
GC5@21	NN153536	qz-pl-mt		5	Gp 5
GC6@17	NN155536	pl-bi-mt	45	5	Gp 7
GC8@19	NN158548	pl		5	Gp 2
GC10@14	NN162571	pl-opx-cpx-bi-qz	3	3	Gp 1
GC11@11	NN173568	ol-pl	10	5	Gp 1
GC12@10	NN174566	ol-cpx-opx-pl	3	3	Gp 1
GC13@19	NN181564	pl-?bi-ap	5	5	Gp 2, autobrecciated
GC16@19	NN196564	pl-?ksp-bi-?hb-mt	10	5	Gp 2
GC17@21	NN202563	pl-qz		5	Gp 2, ?lava
GC18@13	NN208562	pl-mt-?cpx-?opx	10	5	Gp 2
GC19@25	NN178511	?Gp 1 andesite hornfelsed by Cruachan Granite			
GC20@25	NN172516	pl-?opx-?hb	15	5	?Gp 4
GC23@6	NN172519	pl-hb-mt-?opx	18	5	Gp 4
GC24@21	NN172522	pl-qz-bi-ap		4	Gp 5
GC25@19	NN228527?	pl		5	Gp 2, hornfelsed

GC26@16	NN157583	opx-cpx-pl-mt-hb-qz	4	3	Gp 2
GC28@13	NN139552	opx-cpx-pl	5	4	Gp 1
GC29@16	NN147552	pl-opx-hb-cpx-mt-ap	28	3	Gp 4
GC30@22	NN160560	pl-hb-bi-mt-ap	33	4	NNE dyke
GC31@19	NN143548	pl-bi	5	5	Gp 2, ?autobrecciated
BEN NEVIS					
BN1@24	NN157729	pl-opx-mt-hb-bi-ap	18	4	?autobrecciated
BN2@21	NN160728	pl-hb-opx-cpx-mt-ap	18	3	?tuff
BN3@24	NN165722	pl-hb-opx-cpx-bi-mt-ap	37	3	
BN4@16	NN165722	pl-hb-cpx-opx-mt-ap	22	4	
BN5@24	NN164721	pl-hb-cpx-opx-bi-mt-ap	27	3	
BN6@16	NN162719	pl-hb-cpx-opx-mt-ap	10	4	
BN7@16	NN162718	pl-hb-cpx-opx-mt-ap	34	3	
BN8@16	NN165712	hb-pl-mt-cpx-?opx-ap	16	4	
BN9@16	NN167713	pl-hb-cpx-?opx-mt-ap	10	5	
BN10@16	NN157715	pl-cpx-opx-hb-mt-ap	19	3	
BN11@24	NN154716	pl-cpx-hb-mt-bi-?opx-ap	15	3	
MONTROSE REGION, pre-Arbuthnott group					
SC1-9 all from clasts in conglomerates					
SC1@6	NO879855	pl-?hb-?opx-ap	15	5	Stonehaven Gp
SC2@6	NO879855	pl-opx-?hb-mt	40	5	Stonehaven Gp
SC3@19	NO879855	pl-qz-hb-bi-mt-ap	45	4	Stonehaven Gp
SC4@16	NO880853	pl-hb-opx-cpx-mt-qz	40	3	Dunnotar Gp
SC5@19	NO879853	pl-hb-opx-mt	25	4	Stonehaven Gp
SC6@19	NO880849	pl-ksp-qz-bi-?hb-mt	20	4	Dunnotar Gp
SC7@25	NO880849	pl-?ksp-?hb-ap	8	5	Dunnotar Gp
SC8@16	NO880849	pl-opx-cpx-hb-ap	8	5	Dunnotar Gp
SC9@24	NO881847	pl-opx-cpx-hb-bi-mt-ap-?qz	30	4	Dunnotar Gp
SC10@14	NO881848	pl-opx-cpx-bi-mt-ap	35	4	Strathlethan Fm.
SC11@1	NO880828	ol	2	3	Tremuda Bay
SC12@7	NO878796	ol-cpx	1	3	Crawton
SC13@12	NO881797	ol-cpx-pl	20	3	Crawton
SC14@1	NO870768	ol	1	3	Todhead Point
SC15@19	NO870768	qz-pl-?ksp	15	5	clast, Crawton
SC16@21	NO275542	qz-pl etc.		4	ignimbrite
MONTROSE REGION, post-Crawton group					
MT1@11	NO505439	ol-pl	1	3	East Hills
MT2@11	NO458424	ol-pl	5	3	Corbie Den
MT3@1	NO519446	ol-?pl	1	3	East Hills
MT4@11	NO536447	ol-pl	1	3	East Hills
MT5@18	NO549451	ap-?ol	0	4	East Hills
MT6@1	NO506502	ol	1	5	Dunnichen
MT7@1	NO549517	ol	1	5	Dunnichen
MT8@1	NO557519	ol-?pl	1	3	Dunnichen
MT9@18	NO589496	ap-ol	1	4	Ferryden
MT10@10	NO822802	pl-opx-cpx-ol	10	2	Bruxie Hill
MT11@13	NO824805	pl-opx-cpx	10	2	Bruxie Hill
MT12@11	NO828787	ol-pl	15	3	Bruxie Hill
MT13@10	NO822791	pl-ol-opx-cpx	15	3	Bruxie Hill
MT14@12	NO816754	pl-ol-cpx	8	3	Bruxie Hill
MT15@13	NO758802	pl-opx-cpx-?ol	25	2	Glenbervie
MT16@13	NO758802	pl-opx-cpx-?ol	25	2	Glenbervie
MT17@1	NO736704	ol-?pl	6	3	Garvock Gp
MT18@10	NO772691	opx-ol-cpx-pl	8	3	Morphie
MT19@10	NO778673	opx-cpx-pl-ol	20	4	St. Cyrus
MT20@1	NO796669	ol	10	5	Johnshaven

MT21@10	NO734661	opx-cpx-ol-pl	5	3	Morphie
MT22@11	NO752646	ol-pl	6	3	St. Cyrus
MT23@1	NO757648	ol	4	4	St. Cyrus
MT24@11	NO677518	ol-pl	2	3	Ferryden
MT25@11	NO662535	ol-pl	2	3	Ferryden
MT26@11	NO668520	ol-pl	8	3	Ferryden
MT27@18	NO632494	ap-ol-pl	2	5	Ferryden
MT29@18	NO622526	ap-ol-pl	3	4	Ferryden
MT30@12	NO253537	ol-cpx-pl-qz	1	3	Glenisla
MT31@12	NO254537	ol-cpx-pl-qz	1	3	Glenisla
MT32@10	NO254536	ol-opx-cpx-pl-qz	4	3	Glenisla
MT33@20	NO232544	opx-pl-?qz-?ap	0	3	Glenisla
MT34@13	NO292537	opx-cpx-pl-ap-mt	25	3	Glenisla
MT35@20	NO648555	?ol-?pl	0	3	Ferryden
MT36@28	NO727568	ol-opx-pl	10	3	Ferryden
MT37@28	NO734567	ol-opx-pl	10	3	Ferryden
MT38@1	NO729558	ol	2	3	Ferryden
MT39@1	NO732556	ol	8	3	Ferryden
MT40@11	NO732554	ol-?pl	4	3	Ferryden
MT41@5	NO724542	opx-pl	15	3	Ferryden
MT42@7	NO701488	ol-cpx	18	3	Ethie Haven
MT43@12	NO705484	ol-cpx-?pl	10	3	Ethie Haven
MT44@12	NO706483	ol-cpx-pl	10	3	Ethie Haven
MT45@12	NO705481	ol-cpx-pl-mt	10	1	Ethie Haven
MT46@5	NO074405	opx-pl-ap-?hb	50	5	clast
MT47@13	NO074405	opx-cpx-pl-mt-ap	40	4	clast
MT48@10	NO074405	ol-opx-cpx-pl-mt-ap	20	4	clast
MT49@1	NO065406	ol	8	5	Dunkeld
MT50@20	NO092425	ol-opx-cpx-pl	0	2	Dunkeld
MT51@16	NO173482	opx-cpx-pl-?hb-?ol	25	5	clast
MT52@22	NO173482	pl-?ksp-bi-hb-qz-ap	40	4	clast
MT53@16	NO191515	pl-opx-cpx-?hb-qz	8	2	Blairgowrie
MT54@13	NN637109	pl-opx-?cpx-mt	25	5	Callander
MT55@1	NN638114	ol-cc	10	5	Callander
MT56@1	NS515998	ol-cc	10	5	Aberfoyle
MT58@19	NN875264	pl-hb-bi-mt-ap-?ol	15	5	Crieff
MT59@19	NN877266	pl-hb-bi-mt-ap-?opx	18	5	Crieff
MT60@19	NN875265	pl-hb-bi-mt-ap	15	5	Crieff
<u>SIDLAW HILLS</u>					
S1@12	NO125199	pl-ol-cpx	20	3	
S2@12	NO124200	pl-ol-cpx	30	3	
S4@20	NO123201	pl-?ol	1	3	
S5@11	NO122207	ol-pl	5	3	
S6@11	NO118205	pl-ol	3	3	
S8@11	NO161198	pl-ol	10	3	
S9@12	NO148193	pl-ol-cpx	10	3	
S10@20	NO109222	pl-ol	0	3	
S12@12	NO138227	pl-cpx-ol	35	3	
S13@10	NO139242	pl-ol-cpx-opx	18	3	
S15@12	NO184246	pl-ol-cpx-mt	20	3	
S16@11	NO169255	pl-ol	2	3	
S17@20	NO183279	pl	0	3	
S18@11	NO206260	ol-pl	7	3	M121
S19@11	NO241281	pl-ol	8	3	M13
S20@18	NO241281	pl-ol-mt	5	4	M142
S21@12	NO208281	pl-ol-cpx	15	3	M128
S22@20	NO206289	ol	0	3	M129
S23@11	NO210288	pl-ol	7	3	M135

Text cut off in original

S24@11	NO207285	pl-ol	3	3	M136
S25@12	NO207300	pl-ol-cpx	10	3	M86
S26@11	NO220298	ol-pl	3	3	M88
S27@11	NO212303	ol-pl	2	3	M82
S28@12	NO215301	pl-ol-cpx	28	3	M83
S29@12	NO208300	pl-ol-cpx	12	3	M85
S30@11	NO209316	pl-ol	8	3	M1
S31@11	NO221317	pl-ol	10	3	M10
S32@11	NO225315	pl-ol	11	3	M53
S33@11	NO232312	pl-ol	15	3	M55
S34@11	NO234311	pl-ol	2	3	M58
S35@11	NO238306	pl-ol-cpx	16	3	M59
S36@11	NO244321	pl-ol-cpx	17	3	M61
S37@6	NO261314	pl-?opx-?hb-mt-ap	3	5	M99
S38@16	NO313309	pl-opx-cpx-?hb	15	4	M107
S39@11	NO315310	ol-pl	5	3	M110
S40@22	NO282318	pl		4	M112
S41@22	NO282318	pl-cpx-mt		4	M114, segregatior
S42@12	NO242355	pl-ol-cpx	8	3	M104
S43@12	NO247354	pl-ol-cpx	20	3	M31
S44@5	NO265352	pl-opx	5	2	M96
S45@1	NO282359	ol	4	3	M102
S46@1	NO316384	ol	4	3	M116
S47@11	NO306401	pl-ol	8	3	M32
S48@11	NO305400	pl-ol	10	3	M41
S49@1	NO315411	ol	8	3	M24
S50@11	NO319408	pl-ol	5	3	M26
S51@11	NO323411	pl-ol	8	3	M28
S52@10	NO310417	pl-ol-cpx-opx	4	2	M18
<u>OCHIL HILLS, WEST OF GLENFARG</u>					
OC1@11	NS815972	pl-ol-?mt	15	5	cc vesicles
OC2@10	NS814981	pl-ol-opx-cpx	40	4	
OC3@10	NS814979	pl-ol-opx-cpx	35	4	
OC4@13	NS815986	pl-opx-cpx-mt	30	4	
OC5@10	NN857045	pl-ol-opx-cpx	40	5	
OC7@13	NN835019	pl-cpx-opx-mt-?ol-?hb	35	3	
OC8@13	NN843019	pl-opx-cpx-mt-ap-?ol	30	3	
OC9@10	NN851018	pl-opx-cpx-ol-?mt	40	4	
OC10@18	NN855016	pl-mt	10	4	
OC11@5	NN855015	pl-opx-mt-?cpx	8	5	
OC12@10	NN888072	pl-ol-cpx-?opx-mt-qz	20	4	
OC13@12	NN883061	pl-cpx-ol-mt	45	3	
OC15@10	NN994037	opx-cpx-pl-ol	14	2	opx mantled by ol
OC17@12	NN915047	pl-ol-cpx-mt	20	3	
OC18@12	NN915046	pl-ol-cpx	35	3	
OC19@13	NN913042	pl-cpx-?opx-mt-ap	18	4	
OC20@16	NN946057	pl-hb-cpx-opx-mt	35	3	
OC21@20	NN970054	ol-pl	0	3	?minor intrusion
OC22@10	NN986006	cpx-pl-opx-ol-mt-ap	60	3	sector-twinned cp
OC23@16	NN997024	pl-opx-cpx-hb-mt	35	3	ol in aggregate
OC24@18	NN913039	?ol-pl-?mt	3	5	much cc
OC25@16	NN937072	pl-opx-cpx-hb-mt	35	3	
OC26@16	NN937070	pl-opx-cpx-hb-mt	35	3	
OC27@18	NN935066	pl-?hb-mt-cpx-ap	4	3	
OC28@10	NS802979	pl-cpx-opx-ol-mt	28	3	
OC30@22	NS827971	pl-?hb-?opx	10	5	
OC31@10	NS826973	pl-opx-cpx-ol-mt	30	4	
OC32@5	NS828973	pl-?opx	8	5	clast

OC33@5	NS829971	pl-opx-mt	30	5	clast
OC35@18	NS848972	?ol-?hb	2	4	
OC36@13	NS848975	pl-cpx-opx-mt-ap	20	5	
OC38@20	NS847979	pl-ol	2	4	
OC39@20	NS879991	pl	0	5	
OC41@6	NN870002	pl-opx-ap-mt-?hb	12	4	
OC42@10	NN881014	pl-ol-cpx-opx	20	3	
OC43@13	NS897995	pl-opx-cpx-mt-ap	30	4	
OC44@11	NS900987	pl-ol	10	4	
OC47@22	NS912977	pl-hb-bi-cpx-mt-ap		4	diorite
OC48@22	NS913977	pl-?cpx		5	aplite vein
OC50@10	NS998998	pl-cpx-opx-ol-mt	60	3	
OC51@13	NO003030	pl-opx-cpx-mt	40	4	clast
OC52@10	NN974019	pl-ol-cpx-opx-mt	65	4	clast
OC53@16	NN965013	pl-hb-cpx-opx-mt-ap	30	3	
OC54@14	NO024022	pl-opx-cpx-bi-mt-ap	25	3	
OC55@22	NO054046	pl-hb-mt	15	5	dyke
OC56@16	NN944069	pl-cpx-opx-hb-mt-ap	35	3	
OC57@18	NN947076	pl-opx-cpx-ap-mt	5	4	
OC58@19	NN977127	pl-bi-qz	10	5	
OC59@19	NN975128	pl-bi-qz-ap	15	4	
OC61@16	NO021104	pl-cpx-opx-hb-mt	30	3	
OC63@18	NO092065	pl-mt-ap	3	5	
OC64@20	NO033140	pl	3	5	
OC65@16	NO042128	pl-hb-opx-cpx-ol-mt-ap	25	3	
OC67@16	NO042128	pl-hb-cpx-opx-mt-ap	25	2	
OC69@5	NO107095	pl-opx-mt	15	5	
OC71@22	NO113083	pl	10	4	diorite
OC72@22	NO124092	pl-ol-cpx-bi-mt-ap		1	gabbro
OC73@11	NO132097	pl-ol	10	4	
OC74@12	NO132097	pl-ol-cpx	40	3	
OC75@12	NO055166	pl-ol-cpx	5	3	
OC76@1	NO064161	ol	8	3	
OC77@10	NO088126	pl-cpx-ol-opx-mt	20	3	
OC78@12	NO149137	pl-cpx-ol	10	3	
OC79@12	NO091180	ol-pl-cpx	5	3	
<u>NORTH FIFE HILLS</u>					
OC80@20	NO163143	pl-mt	0	3	
OC81@12	NO155131	pl-cpx-ol	30	4	
OC82@12	NO165118	pl-ol-cpx	15	3	
OC83@10	NO177112	pl-ol-cpx-opx	20	2	
OC84@10	NO195113	pl-cpx-ol-opx	10	2	
OC85@10	NO189134	pl-ol-opx-cpx	25	3	
OC86@38	NO249120	pl-ol-cpx-hb	3	3	
OC87@38	NO249122	pl-hb-ol-ap-mt	4	5	gabbroic xenolith
OC88@38	NO239127	pl-hb-ol-ap-mt	4	5	
OC88A@34	NO239127	pl-hb-bi-ap-mt in glass			xenolith
OC88D@34	NO249122	pl-hb-ap-mt in glass			xenolith
OC88E@34	NO249122	as OC88D but finer-grained			
OC89@13	NO231133	pl-opx-cpx-mt-?hb	30	5	
OC90@1	NO228163	ol	8	3	
OC91@12	NO223166	pl-ol-cpx	30	3	
OC92@12	NO232168	ol-cpx-pl	4	3	
OC93@13	NO231179	pl-opx-cpx-mt	25	2	
OC94@13	NO233180	pl-opx-cpx-mt	30	3	
OC95@20	NO244176	pl-mt	0	3	
OC96@1	NO268171	ol	5	3	
OC97@20	NO282189	pl-mt	0	2	

OC98@13	NO337237	pl-opx-cpx-mt	30	2	
OC99@20	NO334219	mt	0	2	
OC100@11	NO331214	pl-ol	10	2	
OC101@1	NO356238	ol-pl	5	3	
OC102@11	NO358252	pl-ol	25	3	
OC103@13	NO363254	pl-opx-cpx	10	2	
OC104@11	NO365254	pl-ol	5	3	
OC105@1	NO357249	ol	2	3	
OC106@13	NO161333	pl-opx-cpx-mt	15	3	
OC107@22	NO375189	pl-opx		5	?intrusion
OC108@13	NO388173	pl-opx-cpx	2	2	
OC109@13	NO404192	pl-opx-cpx-mt	20	3	
OC110@12	NO422214	pl-cpx-ol	10	3	
OC111@22	NO419213	pl-bi-mt	4	5	Lucklaw Hill
OC112@12	NO430225	pl-ol-cpx-?opx-?hb	20	3	
OC113@11	NO446243	pl-ol	5	3	cc amygdale
OC115@11	NO393262	ol-pl	10	3	
OC116@4	NO389258	pl	20	3	
OC117@19	NO385258	?pl-bi	5	5	
OC118@11	NO407270	ol-pl	5	3	
OC119@11	NO402268	ol-pl	7	3	
OC120@12	NO400265	ol-pl-cpx	5	3	
OC121@12	NO418276	ol-pl-cpx	10	3	
OC122@9	NO426280	opx-cpx-ol-?pl	4	3	
OC123@9	NO426282	opx-cpx-ol-?pl	4	2	
OC124@9	NO426283	opx-cpx-ol-?pl	5	2	
OC126@19	NO397264	pl-bi-mt	4	3	tuffaceous
OC127@22	NO397264	pl-cpx-opx	25	5	?intrusion
OC128@19	NO397264	pl-bi-mt-ap	5	3	
OC129@1	NO424287	ol-mt	5	3	
OC130@18	NO447293	pl-?cpx	4	4	
OC131@10	NO451293	pl-opx-ol-cpx	25	3	
OC132@1	NO454293	ol-mt	8	3	
OC133@1	NO441276	ol-pl	10	2	
OC134@9	NO424265	opx-cpx-ol-?pl	6	3	
OC135@9	NO477333	cpx-pl-opx-ol	1	3	microphenocrysts
OC136@9	NO485338	opx-cpx-ol-?pl	5	3	
OC137@22	NO475355	pl-ol-cpx	25	3	?lava
OC138@9	NO504355	ol-opx-cpx-?pl	8	3	
OC139@22	NO489370	pl-ol-cpx	20	3	?lava
OC140@12	NO454311	pl-ol-cpx	10	3	
OC141@22	NO429329	rare ol,pl in doleritic pl-cpx-opx PAS=3			
OC143@22	NO392315	as OC141		3	
OC145@13	NO443310	pl-opx-cpx-mt	35	2	
OC146@19	NO444310	pl-bi-hb-mt	15	4	clast
OC147@18	NO446310	pl	2	4	
OC148@11	NO513375	ol-pl	5	3	
OC149@11	NO556386	pl-ol	15	3	
OC150@22	NO522417	pl-ol		3	doleritic
OC152@12	NO204165	ol-pl-mt-cpx	20	1	S60736
OC153@10	NO265174	pl-opx-cpx-ol	20	2	S54857
<u>PENTLAND HILLS</u>					
PE1@1	NT204677	ol	10	4	Warklaw Hill Gp
PE3@11	NT247692	pl-ol	1	4	much cc
PE3A@11	NT247692	pl-ol-mt	2	3	?Allermuir Gp
PE4@19	NT235667	pl-bi-mt	14	5	Capelaw Acid Gp
PE5@20	NT233668	pl	0	3	Capelaw Basic Gp
PE6@1	NT233663	ol	7	3	Allermuir Gp

PE8@11	NT223667	pl-ol	27	3	Capelaw Basic Gp
PE9@11	NT226658	pl-ol-cc	18	4	Allermuir Gp
PE10@20	NT226660	ol-pl	0	5	Allermuir Gp
PE11@12	NT207614	pl-ol-cpx	35	5	Carnethy Gp
PE12@29	NT186587	pl-?ksp-bi	4	5	Woodhouselee Gp
PE13@11	NT204675	pl-ol	21	4	Warklaw Hill Gp
PE14@5	NT161558	opx-pl	13	4	much cc
PE15@5	NT162558	pl-opx	16	2	
PE16@5	NT152550	opx-pl	17	2	
PE17@12	NT151550	pl-cpx-ol	16	4	qz vein
PE18@13	NT150549	pl-mt-cpx-ap-?opx	10	4	
PE19@29	NT119506	pl-?ksp-bi-qz	10	4	
PE20@29	NT083470	pl-?ksp-?hb-?bi	4	5	
PE21@6	NT041359	pl-hb-opx-mt	20	5	
PE22@20	NT034363	pl-?ol	1	4	
PE23@20	NT025363	pl-?ol	1	4	
PE24@7	NT003344	ol-cpx-?pl	5	4	
PE25@22	NS978346	bi-pl	0	5	Tinto Felsite
PE26@13	NT088440	pl-opx-cpx	21	2	
PE27@22	NS953344	pl-bi-qz	2	3	Tinto Felsite
PE28@22	NS954356	gt-pl-bi	4	5	Tinto Felsite
PE29@22	NS956339	pl	0	5	Pap Craig
PE31@22	NT184618	micropegmatite-bi-qz		4	Black Hill Felsit
PE32@28	NT187616	ol-?opx-pl	12	4	Allermuir Gp
PE33@20	NT190620	pl-?ol	2	4	Allermuir Gp
PE34@19	NT201636			5	Bells Hill Gp
PE36@19	NT201636			5	Bells Hill Gp
PE37@45	NT216642	ol-pl-cpx-?hb	5	3	Allermuir Gp
PE38@29	NT136454	bi-?pl	2	5	
PE39@29	NS989385	pl	2	5	
PE40@49	NS971373	ol-?hb-?opx-pl-bi	8	5	much cc
PE41@10	NS897332	pl-opx-cpx-ol	20	2	
PE42@6	NS895332	pl-hb-?opx-mt-ap	30	4	
PE44@11	NS865311	pl-ol	15	5	
PE46@20	NS854234	opx-?cpx-?ol	?	5	
PE48@1	NS710196	ol	5	4	
PE51@19	NS759249	pl-hb-bi-mt-ap	35	4	clast
AYRSHIRE (Carrick Hills unless otherwise stated)					
AY1@6	NS513343	pl-hb-opx-mt-ap	15	4	Distinkhorn
AY2@13	NS524348	pl-opx-?cpx-mt	15	5	Distinkhorn
AY3@11	NS567358	pl-ol	15	5	Distinkhorn
AY4@5	NS532352	pl-opx-?ol	15	2	Distinkhorn
AY5@10	NS502351	pl-ol-opx-?cpx	8	5	Distinkhorn
AY6@11	NS329172	pl-ol	20	4	
AY7@20	NS297179	pl-cpx-mt	1	3	
AY8@11	NS273181	pl-ol	10	3	
AY9@6	NS263174	pl-hb-?opx-?cpx	8	5	clast, much cc
AY10@28	NS268178	pl-opx-ol-mt	25	3	
AY11@5	NS269179	pl-opx-mt	25	4	
AY12@13	NS258170	pl-opx-cpx-mt	15	3	
AY13@5	NS258168	pl-opx-mt	20	2	
AY14@13	NS255166	opx-pl-cpx-?ol	15	3	
AY15@5	NS255164	pl-opx-?ol	10	5	
AY16@10	NS268178	pl-ol-cpx-opx	25	3	
AY17@12	NS248156	pl-ol-cpx	20	3	
AY18@5	NS252159	pl-opx	15	5	
AY19@13	NS254160	pl-cpx-opx-?ol	20	2	
AY19A@10	NS250160?	pl-ol-opx-cpx	35	3	

AY20@10	NS244139	pl-ol-cpx-opx	20	3	
AY21@22	NS238102	pl-?cpx	5	5	dyke
AY22@13	NS227100	pl-opx-cpx	15	3	
AY23@5	NS228101	pl-opx-?ol	20	4	
AY24@10	NS231103	pl-ol-opx-cpx	40	3	
AY25@10	NS205078	pl-ol-cpx-opx	30	3	
AY26@11	NS203077	ol-pl	5	5	
AY27@10	NS202076	pl-ol-cpx-opx	25	3	
AY28@5	NS278119	pl-opx	10	5	
AY30@1	NS456055	ol	5	5	Dalmellington
AY31@11	NS388034	ol-pl	5	5	Straiton
AY32@10	NS389033	pl-ol-cpx-opx	15	3	Straiton
AY33@22	NS355107	pl-opx-?bi-?cpx	70	5	?sill
AY34@22	NS349126	pl-?cpx-?hb-mt-ap	5	5	?sill
AY35@10	NS389019	pl-opx-cpx-ol	15	2	Straiton
AY37@10	NS393017	pl-opx-ol-cpx	40	5	Straiton
AY38@12	NS390016	pl-cpx-ol	45	3	Straiton
AY40@6	NX397994	pl-hb-opx-mt-ap	20	5	Straiton
AY41@1	NX398986	ol	2	4	Straiton
CHEVIOT HILLS					
C1@31	NT829277	pl-opx-?cpx-?ilm-ap	25	5	
C2@33	NT987269	pl-opx-?cpx-?ilm-ap	19	5	
C5@31	NT900353	pl-opx-cpx-?ilm-ap	34	5	
C7@30	NT884344	pl-opx-cpx-ilm-ap	43	2	
C8@30	NT868304	pl-opx-cpx-?ilm-ap	36	4	
C9@33	NT870303	pl-opx-cpx-?ilm-ap	44	2	
C10@31	NT880305	pl-opx-cpx-?ilm-ap	28	5	
C11@31	NT883307	pl-opx-cpx-?ilm-ap	40	3	
C12@30	NT884312	pl-opx-cpx-?ilm-ap	28	2	
C13@30	NT885313	pl-opx-cpx-?ilm-ap	30	3	
C15@33	NT860284	pl-opx-cpx-?ilm-ap	41	2	
C16@14	NT854266	pl-opx-cpx-?ilm-bi-ap	29	3	
C17@31	NT854263	pl-opx-cpx-?ilm-ap	29	4	
C18@32	NT853262	pl-opx-cpx-?ilm-ap	38	2	
C19@30	NT857261	pl-opx-cpx-?ilm-ap	38	3	
C21@31	NT853281	pl-opx-cpx-?ilm-ap	30	4	
C22@33	NU025126	pl-opx-cpx-?ilm-ap	25	5	
C23@22	NT958085	pl-bi-?ilm	15	5	Biddlestone Felsite
C27@30	NT890073	pl-opx-cpx-?ilm-ap	35	5	
C28@22	NT879078	qz-pl-bi	25	5	dyke
C29@32	NT876080	pl-opx-cpx-?ilm-ap	35	5	qz amygdales
C30@33	NT864112	pl-opx-cpx-?ilm-ap	40	4	
C31@31	NT846114	pl-opx-cpx-?ilm-ap	45	5	
C33@33	NT833110	pl-opx-cpx-ilm-ap	20	2	
C34@32	NT822106	pl-opx-cpx-?ilm-ap	20	5	
C35@52	NT819103	pl-ksp-cpx-bi-ilm-ap	16	5	
C36@31	NT824108	pl-opx-cpx-?ilm-ap	30	4	
C37@33	NT856113	pl-opx-cpx-?ilm-ap	33	5	
C38@32	NT996166	pl-opx-cpx-?ilm-ap	28	3	
C40@22	NT993164	pl-bi-ksp-qz-ap	35	5	dyke
C41@19	NT993160	?mafic mineral	1	5	clast
C43@32	NT914235	pl-opx-?cpx-?ilm-ap	28	4	
C44@31	NT877235	pl-opx-cpx-?ilm-ap	16	3	
C45@30	NT861235	pl-opx-cpx-?ilm-ap	30	2	
C46@33	NT869225	pl-opx-cpx-?ilm-ap	28	3	
C47@22	NT874234	pl-opx-?cpx-bi-?ilm-ap	50	5	dyke
C48@22	NT943267	pl-opx-cpx-bi-ilm-ap	29	3	?dyke

C49@4	NT942264	pl-?qz-?ilm-ap	30	5	
C50@14	NT898226	pl-opx-cpx-?ilm-ap-?bi	20	2	
C51@14	NT898223	pl-opx-cpx-ilm-ap-?bi	22	2	
C52@22	NT898223	pl-opx-bi-cpx-ilm-ap	30	3	?dyke
C54@33	NT826283	pl-opx-cpx-ilm-ap	27	2	
C55@52	NT853185	pl-ksp-cpx-bi-?ilm-?opx-?hb-ap	25	5	
C57@52	NT919101	pl-bi-?ilm-ap-?cpx	16	5	
C58@22	NT927116	pl-cpx-bi-?ilm-opx-ap	30	3	?dyke
C59@29	NT929113	pl-?bi	2	5	
C60@33	NT918112	pl-cpx-opx-?ilm-ap	25	5	
C61@32	NT908109	pl-cpx-?opx-?ilm-ap	20	5	
C62@22	NT959171	pl-opx-cpx-bi	32	2	Cheviot Granite
C64@25	NT962160	pl-cpx	?		hornfels
ST. ABB'S HEAD AND EYEMOUTH					
SA1@48	NU918683	ol-?opx	5	3	
SA2@48	NU917688	ol-opx	3	4	
SA5@48	NU912693	ol-?opx	5	4	
SA6@1	NU914693	ol-?opx	5	4	
SA7@48	NU918686	ol-opx	4	4	
SA8@1	NU918685	ol	4	4	cc amygdale
SA9@48	NU916686	ol-opx	5	4	
SA10@1	NU913687	ol	8	5	
SA11@1	NU912689	ol	8	4	
SA12@44	NU943561	pl-hb-opx-bi		5	S55969
SA13@6	NU951571	pl-hb-opx		5	S54186
SA14@1	NU950570	ol-?opx		4	S54163
SA15@6	NU941651	pl-hb-opx		5	S51899
SA16@6	NU941649	pl-?opx-?hb		5	S51902
SA17@51	NU921631	ol-pl-?cpx-?hb-bi-ap		4	S51875
SA18@13	NU942650	pl-opx-cpx		5	S50572
SA19@48	NU885649	ol-opx		4	S49457
SA20@1	NU954566	ol		3	S54167
SA21@6	NU898641	pl-hb-opx		5	S50541
IRELAND					
NI1@22	D2527	ol-opx-bi-?ksp-qz	10	5	Cushendall Porphyry
NI2@44	D2528	pl-opx-hb-?cpx-bi-ap	10	4	clast, Cushendall
NI3@44	D2528	pl-hb-opx-bi	18	4	clast, Cushendall
NI5@16	H6968	pl-opx-cpx-?hb	5	4	Fintona
NI6@16	H6968	pl-opx-cpx-?hb	8	3	Fintona
NI8@16	H6864	pl-opx-cpx-?hb	8	4	Fintona
NI10@5	H3956	pl-opx-mt-ap	5	5	Fintona
NI11@13	M5696	pl-opx-cpx-mt-?hb-qz	15	2	Curlew Mts
NI12@19	M5895	pl-qz-bi-opx	30	4	Curlew Mts
NI13@20	M5996	cpx-hb-?pl	1	3	Curlew Mts
ARRAN					
AR1@13	NR987372	pl-opx-cpx-mt-ap	25	4	clast
AR2@1	NR893367	ol	10	5	much cc
AR3@19	NR895365	pl-hb-bi-mt-ap	30	5	clast
AR5@19	NR895365	pl-hb-opx-bi-mt	35	5	clast
AR6@44	NR895365	pl-hb-opx-bi-mt	10	5	clast
AR7@19	NR895365	pl-hb-bi-ap	15	5	clast
AR8@13	NR895365	pl-opx-cpx-mt-ap	30	5	clast
AR9@13	NR895365	pl-opx-cpx-mt-ap	25	5	clast
AR10@13	NR381596	pl-opx-cpx-mt-ap		5	clast, AR77-27
AR11@22	NR381596	pl-hb-granophyre		3	clast, XAR7

HUNTLY					
NG1@11	NJ521324	ol-pl	2	3	
NG2@12	NJ518337	pl-cpx-ol	10	4	
NG3@22	NJ406645	pl-hb-opx	20	5	
SHETLAND					
SH1-SH13, SH37-SH41 from Esha Ness, SH14-SH19, SH22-SH25 from Sandness Formation, SH20, 21 from Melby Formation, SH27-SH36 from Papa Stour.					
SH1@52	HU228776	pl-?ksp-?ol/cpx-ap	15	5	
SH2@52	HU214769	pl-?ksp-?ol/cpx-?opx-ap	15	5	
SH3@52	HU212773	pl-?ksp-?opx-?ol-ap	20	5	
SH4@11	HU223805	pl-ol	2	3	
SH5@21	HU217807	ksp-pl-ap-?hb		5	
SH6@21	HU214806	ksp-pl-ap-?hb-cpx		4	
SH7@13	HU216805	pl-opx-cpx-mt-ap	10	3	
SH8@13	HU205783	pl-opx-cpx-mt-ap	35	4	
SH9@13	HU204782	pl-opx-cpx-mt-ap	35	3	
SH10@5	HU210795	pl-?opx	6	4	
SH11@19	HU239800	?pl	1	5	
SH12@52	HU242829	pl-?ksp-?ol/cpx/hb-ap-mt	15	5	
SH13@52	HU236810	pl-?ksp-?ol/cpx/opx-ap-mt	15	5	
SH14@19	HU325590	pl-ksp-?cpx-mt-ap	45	4	clast greenschist
SH15@11	HU327589	pl-?ol-?hb			
SH16@20	HU308579	chlor vesicles		3	
SH17@21	HU288565	?pl/ksp-qz		5	
SH18@20	HU290564	none	0	5	
SH19@20	HU274556	pl-ol	1	5	
SH20@19	HU185580	pl-mt-?bi-?hb	3	5	
SH22@20	HU226540	pl-?ol	1	4	
SH23@12	HU229539	pl-cpx-?ol	30	3	
SH24@11	HU230543	pl-?ol	3	4	
SH25@11	HU235543	pl-?ol	15	3	greenschist
SH27@11	HU185610	ol-pl	2	4	
SH28@19	HU186613	ksp-pl-?hb-mt	5	4	
SH29@4	HU167617	pl-?ol-?cpx	5	2	
SH30@10	HU167620	pl-opx-cpx-?ol	5	3	
SH31@11	HU167620	pl-ol	10	4	
SH32@11	HU149609	ol-pl	6	3	
SH33@19	HU162609	ksp-hb-mt	20	4	spherulitic
SH34@19	HU166592	ksp-hb-cpx	15	4	autobrecciated
SH35@19	HU180598	pl-ksp-opx-?hb-mt	20	4	
SH36@11	HU191586	ol-pl	4	3	S30602
SH37@11	HU243798?	ol-pl	5	4	S43372
SH38@1	HU241787	ol, much cc	5	4	S43409
SH39@12	HU207787?	ol-cpx-pl	2	3	S43630
SH40@52	HU251851	pl-?ksp-opx-cpx-mt-ap	15	4	S43347
SH41@52	HU242845	pl-?ksp-opx-cpx-mt-ap	15	4	S43344
ORKNEY					
OR1-OR4 from Hoy; OR5-OR8 from Deerness and Shapinsay					
OR1@12	HY176008	pl-ol-?cpx	?20	5	S60792
OR2@12	ND195989	pl-ol-cpx-?hb	?25	3	S60793
OR3@12	HY220036	ol-cpx-pl	?25	1	S60794
OR4@12	HY214040	ol-pl-cpx	?15	1	S60795
OR5@22	HY563032	ol	5	3	DL92
OR6@22	HY591038	pegmatitic		4	DL27

OR7@11	HY527149	ol-pl	10	4	DL76, zeolitised
OR8@11	HY527149	ol-pl	15	5	DL78, zeolitised

A3 : REDUCTION OF SAMPLES TO POWDER

Since most of the rocks are fine-grained and fairly homogeneous, only small sample weights, about 200g, are thought to be required to obtain a representative analysis. This hypothesis has been tested by the collection of more than one sample from a single flow on a number of occasions: analyses of these compare closely (e.g. OC93/94, OC87/88). Several samples crushed by Gandy (1973a) have been re-crushed, and both powders analysed. The results (Table A.2) compare well despite the phenocryst-rich nature of the rocks.

Samples selected for analysis were as far as possible trimmed of their weathered surfaces and reduced to about 1.5 in (4 cm) diameter using a Cutrock hydraulic splitter. Little powder was produced during splitting, and any surfaces contaminated by steel from the splitter were discarded. The rock fragments were then reduced to about 0.5 in (1 cm) diameter chips and powder using a Sturtevant open-door roll jaw-crusher, the powder being retained with the chips. Where possible, chips showing alteration features (e.g. amygdales) were discarded. Use of the jaw-crusher may result in minor contamination by steel, although none has been observed on inspection of the chips. The chips and powder were then ground for about 2 min using a tungsten carbide Tema swing mill. The resulting powder is no longer gritty to the touch when wet, and will pass 100 mesh. Grinding probably results in partial oxidation of iron (Fitton and Gill, 1970), and in contamination by W and Co, not affecting the present study. Samples S18, S21-27, S29, S31-42 and S44-46 were ground by Gandy (1973a) using a steel Tema mill; this contaminates the sample with Ni and Cr (e.g. Table A.2), and therefore samples of which sufficient was available were reground using a tungsten carbide mill, and for others Ni and Cr values are not quoted.

All equipment was thoroughly cleansed with acetone between samples, and the jaw-crusher was pre-contaminated at the beginning of each crushing session.

TABLE A2: Comparison between powders of S21 (M128) and S35 (M59) crushed by Gandy (1972) using a steel Tema mill, and by the author using a tungsten carbide Tema mill.

	steel Tema		WC Tema	
	S21	S35	S21	S35
SiO_2	53.74	55.56	53.29	56.01
Al_2O_3	16.80	16.60	16.87	16.40
Fe_2O_3	8.54	8.01	8.43	8.10
MgO	5.70$^+$	4.97$^+$	5.55	4.69
CaO	7.95	7.13$^+$	7.95	6.90
Na_2O	3.62	3.64	3.66	3.73
K_2O	1.54	1.90$^+$	1.52	1.97
TiO_2	1.49$^+$	1.39	1.45	1.40
MnO	0.12	0.10	0.13	0.09
P_2O_5	0.35$^+$	0.33	0.33	0.34
Sc	23	18	22	17
V	176	139	167	136
Cu	52$^+$	24	49	23
Ba	523$^+$	631	503	639
La	29	30$^+$	28	35

	steel Tema		WC Tema	
	S21	S35	S21	S35
Ni	516*	488*	95	120
Zn	64$^+$	83$^+$	73	73
Th	9$^+$	8	4	4
Rb	34	45	32	45
Sr	801$^+$	717$^+$	813	695
Y	29	25	28	26
Zr	213$^+$	207	206	207
Nb	11	13	10	13
Cr	219*	234*	127	162
Ce	66	68	66	66
Sm	5	4	7	8
Nd	34	29	35	31

* = contamination by steel from Tema

+ = outside 95% confidence limits, based on reproducability, Tables B1, B3.

APPENDIX B : X-RAY FLUORESCENCE ANALYTICAL TECHNIQUES

B1 : INTRODUCTION

Precise and rapid analytical procedures were made necessary by the large number of samples selected for analysis. The acquisition by the Grant Institute of a Philips PW1450/20 sequential automatic X-ray fluorescence spectrometer allowed the choice of XRF methods for all elements, in principle capable of rapid, precise and accurate measurements. The analytical techniques devised and the computer software written to handle the data are described in the following sections.

B2 : SAMPLE PREPARATION

The quality of an XRF analysis is dependant on a number of sample features, the relative importance of which is governed by the wavelength of X-rays used for analysis. Long wavelength radiation (K lines for elements of atomic number less than 20) is only weakly penetrative, and is strongly affected by minor mineralogical inhomogeneities close to the sample surface, and also by the surface finish. Accordingly, for the analysis of these elements, use of a pellet pressed directly from powder is not advisable and some form of homogenization procedure is required. Methods described in the literature involve fusion with a borate flux, and the grinding and pelleting of the glass so produced (e.g. Rose et al., 1963), or the direct casting of the melt to produce a glass disc (e.g. Norrish and Hutton, 1969; Harvey et al., 1973). The former method is unsuited to accurate analysis because of uncertainties in the amount of moisture adsorbed on the powdered glass. A direct casting fusion method based on that of Norrish and Hutton (1969) has therefore been used for preparation of samples for major element analysis. It should be noted that the 'major elements' are only definable for a particular rock: in the rocks analysed in this study, only Si, Al, Fe, Mg, Ca, Na, K, Ti, Mn and P had concentrations commonly above 1500 ppm, and hence these elements were treated as major elements. Following convention, these elements were determined as their oxides; the Fe2/Fe3 ratio was not determined because of the high degree of post-eruptive alteration, and a value of Fe203/(FeO+Fe203) wt.% of 0.2 was used in the normative calculations.

(i) Major Elements

The major elements provide nearly the total mass absorption of a sample, and therefore reference by calibration to samples of known different composition is unjustified. Possible methods of overcoming this difficulty include the use of standards very close in composition to the unknowns, or the use of an iterative correction procedure. The latter method relies to a great extent on the initial range of standards through which a first fit regression is calculated: if this is small, matrix

differences between the standards can lead to a meaningless regression line, and there are further difficulties in the selection of suitable mass absorption coefficients. The former method is time-consuming unless a method is chosen which involves dilution with an element with high absorption in the wavelength range of the major element K lines. This may conveniently be added as part of the flux in the fusion procedure of Norrish and Hutton (1969), and a mixture of lithium tetraborate, lithium oxide and lanthanum oxide is supplied commercially by Johnson Matthey Chemicals Ltd. as Spectroflux 105. Dilution by this in the constant flux:sample ratio of 5.3333:1 provides nearly constant composition samples, although they clearly differ in their pre-dilution chemistry. The extent to which the assumption of constant matrix is valid may be judged from the linearity of calibration graphs over large ranges in sample composition (Fig. B1).

Role of volatiles

On fusion, both sample and flux lose water and CO2, and much of the iron in the sample is oxidised. This creates difficulty in the production of a constant flux:sample ratio, and two fusions are required, with intervening flux addition, to allow for flux volatiles. Two methods of treating sample volatiles are currently in use at the Grant Institute, one of which involves ignition of the sample at 1100C before initial flux addition, thus requiring an extra preparation stage but leading to a total oxides sum close to 100%. In the second, extra flux is added to make up for volatile loss from the sample, giving total oxides of about 100%-H2O-CO2. All samples analysed in this study have been ignited prior to flux addition, and it is recommended that all samples with potentially high Loss on Ignition (LOI>4%) should be ignited, because of the uncertain contribution to total mass absorption involved in adding extra flux.

Procedure

Sample powders were dried overnight in small glass jars in an oven at 110°C to remove adsorbed water (H2O-), and about 1.05g was weighed into clean Pt-5%Au crucibles. Samples were ignited at 1100°C in a Gallenkamp furnace for at least 15 min, allowed to cool and then reweighed. Wt.% loss on ignition (LOI) was calculated. Ignition causes release of CO2, H2O, some Cl and possibly other volatiles, and gain of oxygen to allow almost complete oxidation of iron. This oxygen gain is relatively small, although in rare cases negative LOI may be reported. A consequence of this oxidation is that total iron may be calculated as Fe2O3.

Flux was then added to the ignited sample in the ratio 5.3333:1, a small amount of extra flux (c. 0.05g) being added to compensate for flux volatiles. The mixture was fused at 1100°C until the sample had completely dissolved (usually about 20 min unless the sample melted during ignition) and then allowed to cool. Platinum foil lids were

used to cover the crucibles in the furnace, to prevent contamination by furnace lining, and also whilst cooling, to prevent ejection of fracturing glass. Cooling was rapidly effected by placing the crucibles on a large block of stainless steel. The crucibles were reweighed and flux added to make up for flux volatile loss. This amount should be small (c. 0.01g) if sufficient was added after ignition, and hence its volatile content is trivial. The crucibles were transferred to Meker burners at about 1000°C, where the extra flux was dissolved. The crucibles were gently shaken to ensure melt homogeneity, and the melt poured onto graphite plattens inside stainless steel rings on a 240°C hotplate, followed immediately by quenching and moulding using an aluminium plunger, also at 240°C. The quenched glass discs were covered and allowed to anneal on the hotplate. Any remaining melt was shaken from the crucible and stored with the glass disc; the crucibles were plunged into water to cause cracking of any remaining glass adhering, and finally cleansed in warm 50% HCl for at least 20 min. Prior to reuse the crucibles were rinsed with distilled water and dried in an oven. In general, four crucibles were processed simultaneously, resulting in a production rate of about 2 discs per hour. The glass discs are essentially homogeneous and have a reproducable surface finish. Six discs of sample MT45 were produced to test reproducability (Table B1); for Ca, Na, K, Ti and P this is comparable to the precision (Table B7), although for other elements it is a little worse. Total oxides for the six discs varied considerably within the range 99.2 to 100.1%, and SiO2 correlates positively with total oxides, suggesting that the reproducability is inferior because of slight errors in operation of the fusion procedure. This also illustrates the value of sample ignition, in providing an analytical check of constant total oxides (section B9).

Table B1 : Reproducability of six discs of sample MT45.

	SiO2	Al2O3	Fe2O3	MgO	CaO	
Mean	54.529	15.589	8.248	6.743	8.023	
± 2-sigma	0.342	0.114	0.101	0.069	0.025	
	Na2O	K2O	TiO2	MnO	P2O5	LOI
Mean	3.317	1.356	1.281	0.115	0.347	1.542
± 2-sigma	0.104	0.011	0.007	0.016	0.004	0.100

(ii) Trace Elements

The high degree of dilution involved in disc preparation leads to difficulty in the analysis of small quantities of elements, and although trace elements with concentrations in excess of 100 ppm may easily be analysed, counting times must be long to provide adequate precision. Accordingly, pressed powder pellets have been used: problems of heterogeneity and surface finish were not encountered as Sc was the lightest element analysed, and mathematical

corrections may be made for matrix absorption (section B8).

A sample weight of 7g was used, calculated by Fitton (pers. comm., 1977) to allow 99% absorption of NbK radiation in a matrix of very low absorption (pure silica). More strongly absorbing matrices have been analysed using as little as 4g, and no significant differences have been observed using the different weights (Table B2).

Table B2 : Analyses of SA1 using 4g and 7g pellets.

	Ni	Zn	Th	Rb	Sr	Y	Zr	Nb	Cr	Ce
4g	187.5	112.3	7.8	55.1	524.1	29.3	280.2	17.2	375.9	79.9
7g	187.9	112.3	5.7	54.8	521.0	28.6	281.2	17.3	379.9	80.7

	Sm	Nd	TiO2W	Sc	V	Cu	Ba	La	TiO2CR
4g	5.4	34.2	1.239	22.0	126.7	16.3	534.2	36.9	1.242
7g	3.8	35.8	1.256	21.6	122.1	17.7	540.9	37.7	1.242

After shaking the bottle of powder, about 7g of sample was transferred to polished tungsten carbide pressing apparatus and a backing of powdered boric acid was added to the hand-pressed pellet. The apparatus was then compressed at about 10 ton/in^2 for about 1 minute using a Research and Industrial Instruments Company 30-ton hydraulic press. Analysis of powders compressed at 9 and 11 ton/in^2 and for longer times has shown no significant differences. The procedure can allow the production of about 20 pellets per hour. The apparatus was thoroughly cleansed with acetone between samples. Reproducability has been tested by making six pellets of MT45; the results (Table B3) are mainly comparable with the analytical precision (Table B7). The two exceptions are TiO2CR, where the inferior reproducability may be the result of minor Ti discrepancy (section B9), and Th, where there is a large difference in the two mean values for MT45. The spectrometer run for precision took place one month later than the reproducability run, and it is possible that the calibration had changed. This may also have bearing on the relatively high frequency of negative values quoted for Th (section B12).

Table B3 : Reproducability of six pellets of MT45.

	Sc	V	Cu	Ba	La	TiO2CR	Ni	Zn	Th
Mean	24.4	167.0	49.9	543.6	31.1	1.309	138.3	67.9	10.6
± 2-sigma	0.4	4.6	1.2	8.5	2.1	0.036	0.8	1.1	2.3

	Rb	Sr	Y	Zr	Nb	Cr	Ce	Sm	Nd	TiO2W
Mean	17.3	601.1	25.8	249.1	12.4	289.8	73.3	8.8	34.1	1.331
± 2-sigma	0.9	4.5	0.8	1.5	0.9	4.0	2.3	4.6	1.7	0.016

B3 : STORAGE OF PREPARED SAMPLES

Labelled glass discs were stored in labelled 2 in (60 mm) square sealed plastic bags with any spare glass from the fusion procedure. They are very durable if correctly prepared, but retention of spare glass allows remelting on Meker burners and the recasting of the glass disc in case of shattering. Prior to analysis the analytical surface was wiped with a clean tissue, but great care was taken to avoid touching this surface, which leads to contamination by Na from perspiration. Glass discs have been stored for longer than six months and re-run without significant change in their analysis.

Pressed powder pellets were stored in boxes; they are fairly durable unless the sample is water-poor or rich in groundmass glass, when splitting of sample from backing may occur. This may be overcome by repelleting, or by the use of six drops of a 2% aqueous solution of polyvinyl alcohol (PVA) as a binding agent. This was found to have no significant effect on an analysis. Prior to analysis boric acid debris etc. was blown from the analytical surface.

B4 : USE OF MONITOR

The PW1450/20 allows pre-selection of a wide range of measurement conditions and procedures by means of the PW1395 programmer, and permits counting for a number of elements (up to 13 have been used) on four samples without operator intervention. An XRF program therefore produces fixed format output of cyclical nature, each cycle pertaining to four samples.

In order to eliminate some effects of long-medium term machine drift (e.g. temperature or generator induced), the first sample position has always been occupied by a monitor sample, chosen for reasons of durability to be a glass disc made by solution of compounds of the elements of interest in a borate flux. The flux should not contain La in the case of a trace element monitor.

Drift corrections were made by ratio, of peak P_s^i minus background B_s^i counts for element i on sample s divided by counts on monitor peak P_m^i over the same time, and the resulting 'count ratio' was used as the primary XRF measurement instead of the more traditional count rate. Thus:

$$R_s^i = (P_s^i - B_s^i)/P_m^i$$

where R_s^i = count ratio for element i in sample s.

Prior to the acquisition of a Philips PW1466/20 60-position automatic sample changer in July 1978, a slightly different procedure was in use, which involved ratio to $P_m^i - B_m^i$. This is not thought to have any advantage, but it results in a slightly different calibration. Major elements for samples GC1-26, L, BN, PE1-37, OC1-27 and a few

S samples, were analysed using this procedure.

Elements were present in high concentrations in the monitors to allow the rapid location of peak angles and to prevent significant worsening of precision through the ratio procedure. XRF printout consists of count ratios to four decimal places, and therefore precision would be worsened if monitor concentrations were more than an order of magnitude greater than sample concentrations. This procedure relies on the assumption that the monitor is unaffected by exposure to X-rays between calibrations. This might be noticed in systematic variation of calibration constants over several calibrations; this has not been observed (Table B4), and repeat analyses of samples within the same calibration over a period of 4 months show no systematic change.

Table B4 : Secular change in major element calibration constants

	Aug. 1978		Jan. 1979		July 1979	
	m	c	m	c	m	c
Si	59.93	4.46	59.73	4.52	59.82	4.61
Al	18.61	0.15	18.48	0.20	18.44	0.19
Fe	20.67	-0.11	20.68	-0.11	20.63	-0.11
Mg	38.04	-0.15	37.66	0.00	36.64	-0.19
Ca	15.30	-0.03	15.28	-0.03	15.21	-0.02
Na	15.53	-0.32	15.97	-0.26	15.43	-0.34
K	8.59	-0.05	8.61	-0.04	8.58	-0.04
Ti	4.98	-0.05	4.98	-0.05	4.97	-0.06
Mn	1.15	0.03	1.69*	-0.07	1.09	0.01
P	2.79	0.00	2.75	0.00	2.89+	-0.00

m=calibration gradient, c=intercept. *=Mn analysed using LiF220. +=P analysed with different energy window.

The monitor also provides an indicator that the PW1450/20 is operating correctly, for times required for preset counts on the monitor are printed in the teletype output. Providing temperature-stable dispersing crystals are in use, monitor count rates should remain roughly constant, as should P_s^i/P_m^i and B_s^i/P_m^i for a given sample. This is usually true, but as yet unexplained exceptions have been observed on occasions of machine shutdown when using a tungsten anode X-ray tube. The value R_s^i, and hence the concentration, does appear to remain constant, however.

B5 : ANALYTICAL CONDITIONS

(i) Anode material of X-ray tube

Two high-voltage X-ray tubes are available at the Grant Institute, with chromium and tungsten anodes (Cr-tube and W-tube respectively). The latter tube is fitted with a relatively thick Be window, and is thus unsuitable for the excitation of long wavelength fluorescent radiation (NaK_α to PK_α), but provides a more intense continuum at short

wavelengths. There is thus a range of wavelengths for which the tubes provide comparable excitation: the cross-over point in efficiency is in the region of CrK_α. It is, however, better to analyze for the major elements together, so that the total oxides (section B9) may be used as an immediate analytical check. The Cr-tube is therefore used for Na, Mg, Al, Si, P, K, Ca, Ti, Mn and Fe, despite its lower efficiency for the last two. The CrK_β tube line interferes with MnK_α, but this may be largely removed by use of an aluminium filter across the tube window, or, less satisfactorily, by use of a high resolution crystal (LiF220). The latter method was used for samples SH, OR, MT, SC, AY, NI, PE37-51, OC88D, OC88E and OC152-3, and the MnO values for these samples are slightly less precise than usual.

Trace elements Sc, V, Cu, Ba and La are also analysed using the Cr-tube, which is more efficient for ScK_α, VK_α and probably for LaL_α, than the W-tube, while CuK_α is free from WL_α tube line interference, and BaL_{β_2} is in an optimum excitation position relative to the CrK_α tube line.

The elements Ni, Zn, Th, Rb, Sr, Y, Zr, Nb, Cr, Ce, Sm and Nd were analysed using the W-tube, for all of which it is more efficient.

(ii) Analytical lines and interferences

Analytical lines and machine conditions are listed in Table B6. Lines were in general chosen to provide high intensity with minimal interference. The main interferences are listed in Table B5 together with the corrections made. Interference corrections have been made by use of a series of synthetic standards described in section B7. For Sc, V and Nd, corrections have been made by counting on the interfering line, and the correction may be expressed, for example, as count ratio Sc per count ratio CaK_β. Back-interference by the analytical line does not affect the calculation of concentration, for the same proportional back-interference also affects the standards. For Y, Zr and Sm, corrections have been made by counting on another line of the interfering element i.e. RbK_α, SrK_α and CeL_{β_1}, and corrections may be expressed as before. The remaining corrections have been made using a previously determined interfering element concentration, and thus corrections are made after matrix correction, and may be expressed as μ-corrected count ratio per ppm interfering element. Correction coefficients are in most cases calculated by computer regression (section B10); while only the gradient of the correction graph is used, the intercept should be close to the calibration intercept. It should be noted that in the first two methods correction should in theory not be made across a sample major element absorption edge. This is unfortunately unavoidable for ScK_α, but a range of major element compositions has been used in derivation of the correction, and variation in correction with composition is trivial.

TABLE B5: Interferences on chosen analytical lines and backgrounds.

Line	Interference	Approx extent of Interference	Correction made
Mn K_α	Cr K_β	Unimportant for Cr <1500 ppm	None
P K_α	Ca K_β (2nd order)	Unimportant for CaO <20%	Narrow energy window
Mg K_α	Ca K_α (3rd order)	? 0.1% MgO for 20% CaO	None
Sc K_α	Ca K_β	1 ppm. Sc per % CaO	Regression
V K_α	Ti K_β	180 ppm. V per % TiO_2	Regression
La $L\alpha_1$	Ti K_α	5 ppm. La per % TiO_2	Regression
Ti K_β	Ba $L\beta_3$	0.00004 % TiO_2 per ppm. Ba	Yes
	V K_α	0.0004 % TiO_2 per ppm. V	Yes
Ni K_α	Y K_α (2nd order)	Unimportant for Y <400 ppm.	Narrow energy window
Y K_α	Rb K_α	0.22 ppm. Y per ppm. Rb	Regression
Zr K_α	Sr K_α	0.07 ppm. Zr per ppm. Sr	Regression
Nb K_α	La K_α (2nd order)	0.01 ppm. Nb per ppm. La	Regression
	Y K_β	Unimportant for Y <1000 ppm.	None
	U $L_{\beta 2,4}$	Unimportant for U<50 ppm.	None
Cr K_α	V K_β	0.05 ppm. Cr per ppm. V	Regression
Ce L_{β_1}	Nd $L\alpha_1$	Probably unimportant?	None
Nd $L\alpha_1$	Ce $L\beta_1$	0.01 ppm. Nd per ppm. Ce	Regression
Sm $L\alpha_1$	Ce $L\beta_2$	0.02 ppm. Sm per ppm. Ce	Regression
Cu background	Hf $L\alpha_1$	Unimportant for Zr <800 ppm	None
	Zr K_α (2nd order)		
Y, Zr, Nb backgrounds	U, Th	Unimportant for <500 ppm U, Th	None
Ce, Nd background	Cr K_α	Unimportant for Cr <800 ppm	None

TABLE B6: XRF analytical conditions

Line	Crystal	kV	mA	Collimator	Counter	Background offset 2θ°	Lower Level	Window
SiK_α	PE	50	45	C	F	+ 4.40	25%	60%
AlK_α	PE	60	45	C	F	- 5.75	25%	60%
FeK_α	LiF200	50	45	F	F	- 1.63	20%	60%
MgK_α	TlAP	60	45	C	F	+ 2.70	25%	50%
CaK_α	LiF200	50	30	F	F	- 3.00	25%	60%
NaK_α	TlAP	60	45	C	F	- 2.25	30%	50%
KK_α	LiF200	50	45	F	F	- 4.55	25%	60%
TiK_α	LiF200	50	45	F	F	+ 4.74	30%	50%
MnK_α	LiF200	60	45	F	F	- 1.00	15%	70%
PK_α	Ge	50	45	C	F	+ 3.14	35%	40%
ScK_α	LiF200	60	45	F	F	- 1.59	25%	60%
VK_α	LiF220	60	45	F	F	- 2.62	30%	50%
CuK_α	LiF200	60	45	C	F	+ 1.01	39%	26%
BaL_{β_2}	LiF220	60	45	F	F	+ 1.75	15%	60%
LaL_{α_1}	LiF200	60	45	C	F	- 1.08	30%	50%
NiK_α	LiF200	60	45	F	F	+ 1.33	25%	50%
ZnK_α	"	60	45	F	F	+ 0.80	25%	50%
ThL_{α_1}	"	90	30	F	FS	-	20%	60%
RbK_α	"	90	30	F	FS	+ 2.09	20%	60%
SrK_α	"	90	30	F	FS	-	20%	60%
YK_α	"	90	30	F	FS	+ 0.48	20%	60%
ZrK_α	"	90	30	F	FS	-	20%	60%
NbK_α	"	90	30	F	FS	- 0.40	20%	60%
CrK_α	"	60	45	F	F	+ 1.44 - 0.74	15%	60%
CeL_{β_1}	"	60	45	F	F	-	15%	60%
SmL_{α_1}	"	60	45	F	FS	- 0.48	20%	60%
NdL_{α_1}	"	60	45	F	F	- 1.34	15%	60%
TiK_β	"	60	45	F	F	- 1.54	30%	50%
CaK_β	"	60	45	F	F	-	25%	60%

Crystals

PE = Pentaerythritol,
Ge = Germanium,
TlAP = Thallium acid phthalate
LiF = Lithium Fluoride

Collimators

C = coarse, F = fine

Counters

F = gas flow proportional counter
FS = flow counter and scintillation counter.

(iii) Background positions .

Background positions have been chosen to be as close as possible to the peak without interference. In general, only one background position has been used for each element, giving rise to a small matrix dependant error. The error is trivial for the major elements, and contributions to the background count from interfering minor elements are very small relative to the major element peak height. Care should be taken to avoid interference by the La spectrum from the flux, however. For trace elements, background position is critical, and change in peak angle should always be accompanied by a corresponding change in background angle setting.

For trace element i in sample s:

$$X_s^i = m^i \mu_s^i R_s^i + c$$

where X_s^i is the concentration of i in s,
μ_s^i is the mass absorption coefficient of s at the wavelength of the i analytical line - $\lambda_{i,s} = \lambda_{i,s}$ if the peak and background positions are close,
m^i and c^i are the calibration gradient and intercept for element i respectively,
R_s^i is the 'true' count ratio, related to that measured by

$$R_s^i \text{ measured} = R_s^i \text{ true} + B*$$

where B* is the small discrepancy between true and measured backgrounds. Therefore:

$$X_s^i = m^i \mu_s^i R_s^i \text{ measured} - m^i \mu_s^i B* + c^i$$

The term $m^i \mu_s^i B*$ is thus a small matrix dependant error, proportional to the count ratio discrepancy between measured and true background, which should give rise to calibration lines with matrix dependant intercept. This has never been observed. Additionally, for wavelengths shorter than the FeK_α absorption edge, it is approximately true that

Background Intensity $B_s^i \propto 1/\mu_s^i$ (Anderman and Kemp, 1958)

and thus $B* \propto 1/\mu_s^i$

For such wavelengths, the $m^i \mu_s^i B*$ term becomes nearly matrix independant, and will form part of the calibration intercept constant. Where interference corrections have to be made, it is advisable to reduce the B* term as much as possible, and accordingly two backgrounds have been used for CrK_α. The steeply sloping continuum between ThL_α, and NbK_α presents difficulties in the use of two backgrounds, for there are a number of Th and U L lines which could cause interference. Only one intermediate background position has therefore been used, and the background has been assumed linear between this and the two end backgrounds. This assumption has been checked by counting for a number of intermediate background positions on the United States

Geological Survey (USGS) standard samples.

(iv) Vaccuum

All counting has been carried out under vaccuum. While air has relatively small absorption for short wavelength radiation, the flow counter window is subjected to less stress if vaccuum is permanent, and even for NbK$_\alpha$ substantially higher count rates are obtained.

(v) Angle and Pulse Height settings

The PW1450/20 allows pre-selection of goniometer angles and energy windows, and as these may remain unchecked for periods of one month or more, it is essential that they should be initially correctly set. The goniometer angle for a particular analytical line may change if the crystal d-spacing changes with temperature, or with a change in reflection geometry. The former only occurs with the penta-erythritol crystal (PE), and thus only affects Si and Al. While the monitor will correct for minor drifts, it is advisable to wait a few hours until the spectrometer has reached operating temperature before setting the angles for Si and Al. Change in reflection geometry usually produces substantial change in monitor count rates, and recalibration is advisable.

Automatic energy window selection is made possible by means of a variable potentiometer control of counter voltage, which is automatically set in relation to goniometer angle so that the first order reflection occurs at about the middle (50%) of the full energy window. This may drift if the initial counter high voltage changes, and, although the setting is seldom critical, the preset lower levels and windows in the XRF program on the PW1395 should be checked prior to recalibration. The monitors are convenient samples on which to check angles and energy distributions.

(vi) Counting times

In principle, counting times should be calculated from a required analytical precision, but use of a monitor complicates the calculation. Since the acquisition of the automatic sample changer, printout has consisted of count ratios to four decimal places, and it is difficult to allow for the rounding error in a precision-time calculation. A trial and error method has therefore been used, with precision being estimated by the repeated analysis of a single pellet or glass disc. Precision data for the analyses presented in this thesis are given in Table B7. Repeatability runs indicated that long exposure of single pellets or discs to X-rays did not cause deterioration.

For convenience in data processing, peak and background counts have been repeated four times each per sample for trace elements and 4 peaks, 2 backgrounds for major elements. This repetition allows the detection of

TABLE B7: Analytical Precision/Repeatability data.

	G2		AGV1		DTS1	
	Mean	± 2σ	Mean	± 2σ	Mean	± 2σ
SiO_2	69.32	0.210	59.62	0.240	40.57	0.146
Al_2O_3	15.48	0.058	17.12	0.062	0.40	0.006
Fe_2O_3	2.74	0.015	6.92	0.035	8,93	0.036
MgO	0.84	0.038	1.59	0.030	49.89	0.253
CaO	1.92	0.010	4.96	0.020	0.17	0.002
Na_2O	4.30	0.060	4.37	0.124	0.11	0.057
K_2O	4.49	0.014	2.96	0.013	(-0.02)	0.001
TiO_2	0.49	0.004	1.06	0.006	0.02	0.002
MnO	0.03	0.010	0.10	0.009	0.13	0.008
P_2O_5	0.13	0.005	0.48	0.007	0.01	0.003

16 CYCLES PER SAMPLE

	SR6		S32		JB1	
	Mean	± 2σ	Mean	± 2σ	Mean	± 2σ
Sc	15.7	0.4	21.7	0.6	26.2	0.5
V	162.7	3.1	133.1	4.5	194.0	2.8
Cu	29.9	0.5	22.2	1.0	53.9	0.8
Ba	893.7	7.0	408.2	4.1	554.1	5.7
La	44.9	2.0	30.6	2.8	40.2	2.0
TiO_2CR	0.73%	0.003	1.18%	0.003	1.27%	0.007%

19 CYCLES PER SAMPLE

	MT45	
	Mean	± 2σ
Ni	138.9	1.5
Zn	68.6	1.7
Th	4.6	2.2
Rb	16.7	1.2
Sr	603.6	2.0
Y	25.5	0.5
Zr	249.8	1.7
Nb	12.7	1.1
Cr	290.0	1.7
Ce	71.7	3.8
Sm	8.7	2.8
Nd	34.1	1.6
TiO_2W	1.34%	0.014

12 CYCLES

Oxides in wt.%; trace elements in p.p.m.

G2, AGV1, DTS1 and JB1 are international standards

S32, MT45 are samples from the present study

SR6 is a basaltic andesite from the volcano Stromboli, Italy

spurious counts (section B10). Unfortunately, the sample changer does not easily allow the use of different count times on peak and background, so that, for major elements, total peak time = 2 X total background time, and for trace elements, total peak time = total background time. There are minor exceptions in the cases of elements using the same background as another (Ce, Th, Rb, Sr, Y, Zr and Nb).

B6 : XRF OUTPUT

XRF output is printed simultaneously on teletype paper and onto punched paper tape. As the X-ray tube is the only analytical condition which must be manually selected, three programs are currently in use:

Program 90 : Major elements
91 : Cr-tube, trace elements Sc, V, Cu, Ba, La
91 : W tube, trace elements Ni, Zn, Th, Rb, Sr Y, Zr, Nb, Cr, Ce, Sm, Nd

Specimen output of these programs is presented in Tables B8-B10. It will be noted that TiO2 has been analysed in all three programs; it is used as an analytical check in the trace element programs (section B9).

B7 : STANDARDS

Glass discs for major element standards were prepared in the same way as the specimens (section B2). Standards used were USGS G2, GSP1, AGV1, BCR1, DTS1, PCC1; Centre de Recherches Petrographiques et Géochemiques (CRPG) GA, GH, BR; Geological Survey of Japan (GSJ) JG1, JB1 and National Bureau of Standards (NBS) NBS91 and NBS99A. Values were taken from Abbey (1977). These were all used without pre-ignition, but in addition ignited samples of the USGS and CRPG standards were used, with oxide % calculated from Abbey (1977) using the measured loss on ignition. This calculation may be easily performed using the computer program IGSTAN (source file: EGE007.IGSTAN). This effectively gives the USGS and CRPG standards double weighting. For computing purposes, ignited standards are named using the suffix -IG; sets of standards made with a new flux batch have a letter inserted between the sample name and the -IG, e.g. BCR1BIG. Hyphens should not be used in standard names during computer processing of the data. Fe for the ultramafic standards is not used in the calibration, and BR is given half weighting for silica (i.e. only the value for BRIG, BRBIG is used, not that of BR), because of possible matrix effects (section B8). No Mn value is quoted for NBS99A. The same standards were used for all the rocks analysed, although a new set was made up at the beginning of a new flux batch. A different selection of standards should be used if rocks are of more extreme composition.

Trace element standards require a slightly different procedure to the samples, for in using 7g of scarce international standard they must be almost permanent. Six drops of 2% PVA are therefore used as a pellet binder. PVA

TABLE B8 : Specimen output of XRF program 90 - major elements

Program number	Address – usually = Atomic number		Monitor count	Time (4·3s)	Sample 1 Ratio	Sample 1 Time	Sample 2 Ratio	Sample 2 Time	Sample 3 Ratio	Sample 3 Time	
90	2	2 01									
	3	2 02									
	4	2 03									
	14	1	400000	16349	8114	16349	8283	16349	7773	16349	Peaks
	14	1	400000	16413	8125	16413	8304	16413	7793	16413	Peaks
	14	1	400000	16417	8142	16417	8303	16417	7788	16417	Peaks
	14	1	400000	16425	8156	16425	8301	16425	7775	16425	Peaks
	64	2	24	16425	25	16425	25	16425			—
	14	1	400000	16431	8166	16431	8340	16431	7806	16431	Background
	64	2	24	16431	25	16431	26	16431			—
	13	1	200000	28083	9131	28083	10202	28083	6454	28083	Al Kα
	13	1	200000	28060	9169	28060	10181	28060	8466	28060	Al Kα
	13	1	200000	28063	9149	28063	10169	28063	8478	28063	Al Kα
	63	2	107	28063	111	28063	109	28063			—
	13	1	200000	28127	9144	28127	10208	28127	8466	28127	Al Kα
	63	2	110	28127	115	28127	109	28127			—
	26	1	200000	7643	5755	7643	5133	7643	6165	7643	Fe Kα
	26	1	200000	7614	5734	7614	5117	7614	6152	7614	Fe Kα
	26	1	200000	7633	5745	7633	5140	7633	6165	7633	Fe Kα
	76	2	41	7633	43	7633	42	7633			—
	26	1	200000	7654	5756	7654	5126	7654	6159	7654	Fe Kα
	76	2	44	7654	43	7654	41	7654			—
	12	1	200000	46567	2025	46567	1240	46567	1765	46567	Mg Kα
	12	1	200000	46558	2024	46558	1232	46558	1797	46559	Mg Kα
	12	1	200000	46644	2037	46644	1240	46644	1777	46644	Mg Kα
	62	2	500	46644	471	46644	503	46644			—
	12	1	200000	46454	2014	46454	1226	46454	1779	46454	Mg Kα
	62	2	489	46454	469	46454	501	46454			—
	20	1	400000	5466	3286	5466	1666	5466	4677	5466	Ca Kα
	20	1	400000	5469	3303	5469	1664	5469	4677	5469	Ca Kα
	20	1	400000	5465	3277	5465	1659	5465	4688	5465	Ca Kα
	70	2	8	5465	6	5465	10	5465			—
	20	1	400000	5463	3298	5463	1650	5463	4666	5463	Ca Kα
	70	2	6	5463	7	5463	9	5463			—
	11	1	20000	28687	4486	28687	6347	28687	5560	28687	Na Kα
	11	1	20000	28764	4454	28764	6256	28764	5411	28764	Na Kα
	11	1	20000	28446	4416	28446	6125	28446	5303	28446	Na Kα
	61	2	2041	28446	2014	28446	2073	28446			—
	11	1	20000	28363	4467	28363	6265	28363	5414	28363	Na Kα
	61	2	2093	28363	2093	28363	2054	28363			—
	19	1	400000	7385	1236	7385	2336	7385	1357	7385	K Kα
	19	1	400000	7388	1240	7388	2332	7388	1352	7388	K Kα
	19	1	400000	7391	1233	7391	2346	7391	1366	7391	K Kα
	69	2	9	7391	8	7391	8	7391			—
	19	1	400000	7387	1235	7387	2327	7387	1370	7387	K Kα
	69	2	8	7387	9	7387	9	7387			—
	22	1	200000	3577	3641	3577	2292	3577	3137	3577	Ti Kα
	22	1	200000	3572	3634	3572	2286	3572	3118	3572	Ti Kα
	22	1	200000	3587	3646	3587	2311	3587	3135	3587	Ti Kα
	72	2	31	3587	30	3587	31	3587			—
	22	1	200000	3590	3656	3590	2271	3590	3159	3590	Ti Kα
	72	2	28	3590	27	3590	27	3590			—
	25	1	10000	5626	5928	5626	8074	5626	6517	5626	Mn Kα
	25	1	10000	5578	5868	5578	8056	5578	6548	5578	Mn Kα
	25	1	10000	5619	5810	5619	7991	5619	6531	5619	Mn Kα
	75	2	4257	5619	4336	5619	4225	5619			—
	25	1	10000	5536	6027	5536	7973	5536	6451	5536	Mn Kα
	75	2	4160	5536	4114	5536	4191	5536			—
	15	1	40000	14248	1399	14248	901	14248	1268	14248	P Kα
	15	1	40000	14400	1455	14400	878	14400	1282	14400	P Kα
	15	1	40000	14330	1416	14330	899	14330	1241	14330	P Kα
	65	2	325	14330	320	14330	322	14330			—
	15	1	40000	14459	1435	14459	922	14459	1286	14459	P Kα
	65	2	317	14459	294	14459	317	14459			—
	2		3 01								
	3		3 02								
	4		3 03								
90											
	14	1	400000	16458	7979	16458	8453	16458	8118	16458	Si Kα

TABLE B9 : Specimen output of XRF program 91 - trace elements analysed on Cr-tube.

PROGRAM ADDRESSES — FOR PEAK, USUALLY + ATOMIC NUMBER										
91	2	1 01								
	3	1 02								
	4	1 03								
		COUNT	TIME	COUNT	TIME	COUNT	TIME			
18	2	131499	4000	110304	4000	157917	4000			
18	2	132220	4000	110407	4000	157914	4000			
18	2	131660	4000	110023	4000	158216	4000			
21	1	200000	46217	399	46217	361	46217	466	46217	Ca K_β
01	2	124	46217	119	46217	130	46217			
21	1	200000	46385	397	46385	356	46385	476	46385	
01	2	125	46385	116	46385	132	46385			
21	1	200000	46390	392	46390	358	46390	467	46390	Sc K_α
01	2	128	46390	118	46390	137	46390			
21	1	200000	46485	399	46485	363	46485	481	46485	
01	2	126	46485	118	46485	126	46485			
17	2	102136	10000	85889	10000	98987	10000			
17	2	102552	10000	85105	10000	99042	10000			Ti K_β
17	2	102283	10000	85606	10000	98927	10000			
00	2	595	4000	622	4000	593	4000			
00	2	626	4000	551	4000	632	4000			
00	2	596	4000	597	4000	603	4000			
23	1	200000	56682	1688	56682	1369	56682	1708	56682	
02	2	204	56682	194	56682	204	56682			
23	1	200000	56733	1711	56733	1367	56733	1726	56733	
02	2	202	56733	191	56733	204	56733			V K_α
23	1	200000	56901	1697	56901	1372	56901	1736	56901	
02	2	207	56901	203	56901	202	56901			
23	1	200000	56767	1692	56767	1362	56767	1727	56767	
02	2	205	56767	197	56767	209	56767			
29	1	200000	62508	3537	62508	3357	62508	3742	62508	
03	2	2276	62508	2317	62508	2267	62508			
29	1	200000	62463	3523	62463	3369	62463	3717	62463	
03	2	2271	62463	2303	62463	2264	62463			Cu K_α
29	1	200000	62326	3511	62326	3366	62326	3727	62326	
03	2	2264	62326	2300	62326	2238	62326			
29	1	200000	62787	3540	62787	3396	62787	3736	62787	
03	2	2255	62787	2305	62787	2246	62787			
56	1	200000	89715	1229	89715	1194	89715	948	89715	
04	2	439	89715	437	89715	445	89715			
56	1	200000	89678	1204	89678	1206	89678	946	89678	
04	2	444	89678	430	89678	442	89678			Ba $L\beta_2$
56	1	200000	89761	1207	89761	1206	89761	960	89761	
04	2	439	89761	441	89761	443	89761			
56	1	200000	89825	1200	89825	1196	89825	963	89825	
04	2	445	89825	436	89825	442	89825			
57	1	200000	56617	2088	56617	1910	56617	2003	56617	
05	2	1934	56617	1826	56617	1936	56617			
57	1	200000	56807	2074	56807	1915	56807	2005	56807	
05	2	1937	56807	1822	56807	1948	56807			La $L\alpha_1$
57	1	200000	56617	2071	56617	1927	56617	2015	56617	
05	2	1941	56617	1833	56617	1944	56617			
57	1	200000	56958	2090	56958	1918	56958	1995	56958	
05	2	1935	56958	1824	56958	1963	56958			
	2	1 04								
	3	1 05								
	4	1 06								
91										
18	2	130107	4000	141793	4000	130135	4000			

TABLE B1O : Specimen output of XRF program 91 - trace elements analysed on W-tube.

PROGRAM NUMBER — FOR PEAK, USUALLY ATOMIC NUMBER

	2	1 01									
	3	1 02									
	4	1 03									
91			count	time	count	time	count	time	count	time	
28	1	200000	11775	524	11775	2114	11775	703	11775		
01	2	219	11775	209	11775	209	11775				
28	1	200000	11790	528	11790	2119	11790	705	11790		
01	2	218	11790	212	11790	213	11790				
28	1	200000	11813	533	11813	2129	11813	687	11813		
01	2	219	11813	209	11813	215	11813				
28	1	200000	11803	536	11803	2113	11803	695	11803		
01	2	217	11803	211	11803	210	11803				
30	1	200000	9878	456	9878	1050	9878	447	9878		
02	2	287	9878	261	9878	281	9878				
30	1	200000	9866	467	9866	1047	9866	458	9866		
02	2	285	9866	262	9866	277	9866				
30	1	200000	9890	469	9890	1047	9890	458	9890		
02	2	294	9890	266	9890	280	9890				
30	1	200000	9875	455	9875	1058	9875	461	9875		
02	2	285	9875	266	9875	272	9875				
90	1	10000	556	Tau line should change in XRF kV, mA							
90	1	4000000	108603	288	108603	264	108603	286	108603		
90	1	4000000	108620	286	108620	263	108620	284	108620		
90	1	4000000	108451	290	108451	265	108451	286	108451		
90	1	4000000	108443	288	108443	263	108443	286	108443		
03	2	247	108443	239	108443	242	108443				
37	1	400000	25232	1078	25232	1107	25232	933	25232		
03	2	574	25232	537	25232	567	25232				
37	1	400000	25232	1071	25232	1094	25232	937	25232		
03	2	574	25232	534	25232	566	25232				
37	1	400000	25168	1066	25168	1098	25168	937	25168		
03	2	575	25168	530	25168	562	25168				
37	1	400000	25333	1095	25333	1108	25333	946	25333		
03	2	575	25333	537	25333	563	25333				
38	1	200000	7928	3263	7928	4175	7928	2881	7928		
38	1	200000	7929	3283	7929	4162	7929	2877	7929		
38	1	200000	7918	3265	7918	4177	7918	2863	7918		
38	1	200000	7911	3289	7911	4178	7911	2879	7911		
39	1	400000	42235	1766	42235	1663	42235	1688	42235		
04	2	1451	42235	1321	42235	1423	42235				
39	1	400000	41671	1756	41671	1660	41671	1672	41671		
04	2	1430	41671	1318	41671	1399	41671				
39	1	400000	41708	1751	41708	1646	41708	1673	41708		
04	2	1426	41708	1318	41708	1403	41708				
39	1	400000	41758	1762	41758	1667	41758	1674	41758		
04	2	1436	41758	1311	41758	1401	41758				
40	1	400000	19522	1835	19522	1971	19522	1827	19522		
40	1	400000	19471	1825	19471	1976	19471	1827	19471		
40	1	400000	19486	1842	19486	1978	19486	1838	19486		
40	1	400000	19487	1829	19487	1970	19487	1834	19487		
41	1	400000	49904	2295	49904	2097	49904	2271	49904		
05	2	2274	49904	2062	49904	2214	49904				
41	1	400000	49925	2314	49925	2095	49925	2266	49925		
05	2	2263	49925	2056	49925	2216	49925				
41	1	400000	49854	2299	49854	2101	49854	2274	49854		
05	2	2279	49854	2051	49854	2219	49854				
41	1	400000	50020	2312	50020	2091	50020	2263	50020		
05	2	2292	50020	2056	50020	2232	50020				
24	1	10000	828								
24	1	400000	18817	255	18817	842	18817	232	18817		
06	2	58	18817	67	18817	56	18817				
24	1	400000	18850	258	18850	856	18850	237	18850		
06	2	56	18850	66	18850	58	18850				
24	1	400000	18847	260	18847	851	18847	234	18847		
07	2	66	18847	81	18847	69	18847				
24	1	400000	18823	256	18823	849	18823	234	18823		
07	2	66	18823	82	18823	69	18823				
58	1	40000	43415	1930	43415	2429	43415	2120	43415		
58	1	40000	43016	1877	43016	2418	43016	2159	43016		
58	1	40000	43021	1863	43021	2441	43021	2146	43021		
58	1	40000	43314	1914	43314	2432	43314	2103	43314		
62	1	400000	159808	1069	159808	1151	159808	1090	159808		
09	2	934	159808	985	159808	930	159808				
62	1	400000	159181	1058	159181	1141	159181	1044	159181		
09	2	883	159181	994	159181	927	159181				
62	1	400000	159075	1074	159075	1140	159075	1067	159075		
09	2	910	159075	969	159075	902	159075				
62	1	400000	159247	1030	159247	1134	159247	1065	159247		
09	2	915	159247	952	159247	963	159247				
60	1	40000	49536	1982	49536	2578	49536	2172	49536		
08	2	1468	49536	1739	49536	1461	49536				
60	1	40000	49533	1966	49533	2651	49533	2197	49533		
08	2	1472	49533	1717	49533	1478	49533				
60	1	40000	49829	1991	49829	2633	49829	2237	49829		
08	2	1469	49829	1701	49829	1485	49829				
60	1	40000	49509	1946	49509	2574	49509	2181	49509		
08	2	1493	49509	1699	49509	1449	49509				
25	1	20000	2475	1601	2475	3389	2475	1357	2475		
26	2	95	2475	123	2475	136	2475				
25	1	20000	2492	1601	2492	3313	2492	1420	2492		
26	2	104	2492	117	2492	125	2492				
25	1	20000	2458	1587	2458	3265	2458	1418	2458		
26	2	110	2458	127	2458	104	2458				
25	1	20000	2469	1546	2469	3383	2469	1381	2469		
26	2	102	2469	142	2469	103	2469				
	2	1 04									
	3	1 05									
	4	1 06									
91											
28	1	200000	11783	713	11783	760	11783	571	11783		

Peak : Nickel K$_\alpha$ & 3 samples
Background : 3 samples only

N i K$_\alpha$

Zn K$_\alpha$

Th L$_{\alpha_1}$

Rb K$_\alpha$

Sr K$_\alpha$

Y K$_\alpha$

Zr K$_\alpha$

Nb K$_\alpha$

Cr K$_\alpha$

Ce L$_{\beta_1}$

Sm L$_{\alpha_1}$

Nd L$_{\alpha_1}$

Ti K$_\beta$

	Sc	V	Cu	Ba	La	Ni	Zn	Th	Rb	Sr	Y	Zr	Nb	Cr	Ce	Sm	Nd	TiO_2
SY3	*				*			*			*		*		*	*	*	
GSN					*			*								*	*	
PCC1				*	*	*		*			*	*	*	*	*	*	*	
UBN	x	x	x	x	x	*		*			*	*	*	*	*	*	*	
JB1													*					
JG1													*				*	
GSP1					*										*	*	*	
T1	*				*			*	*		*		*		*	*	*	
GH							*											
FKN	x	x	x	x	x		*	*	*		*	*	*		*	*	*	
DRN	x	x	x	x	x			*					*		*	*	*	
	GA, BR, G2, AGV1 and BCR1 used for all elements																	
INTSGA2			*			*			*				*	*	*		*	*
INTSGB2	*		*		*	*	*				*			*				*
INTSBA2			*			*							*	*	*		*	*
INTSBB2	*		*		*	*	*				*	*		*				*
INTSGA3			*			*								*				*
INTSGB3	*		*			*								*				*
INTSBA3			*			*								*				*
INTSBB3	*		*			*								*				*
INTSGA4			*			*								*				*
INTSGB4			*			*								*				*
INTSBA4			*			*								*				*
INTSBB4			*			*								*				*
INTSG			*			*							x	*		x		*
INTSB			*			*							x	*		x		*
INTSA			*			*	x	x	x	x	x	x	x	*	x	x	x	*

TABLE B 11: Standards used in trace element calibrations.

* = omitted by program

x = omitted by not including in run

makes little difference to count rates, with the possible exception of the lightest elements, where a systematic error of up to 0.5 ppm may have been introduced. Because of the doubtful values of some elements for many of the standards, a far wider range of standards has been used than for the major elements; Table B11 lists the standards used for each element. For very different rock types, it is recommended that a different set of standards should be used in the calibration. Standard concentrations were again taken from Abbey (1977), with some additional data from the originators of the standards.

In addition to the international standards, a set of synthetic standards has been made by Dr. J.G. Fitton and the author. These are identified by the prefix INTS- (for INTerference Standard) and fall into two groups, two of roughly granitic composition (INTSG-) and two basaltic (INTSB-). Johnson-Matthey specpure major element oxides were fused at 1400°C in platinum dishes to produce about 100g of trace element free glasses of basaltic and granitic composition. These were ground in a tungsten carbide Tema mill, and glass discs were made from the powder to confirm the major element composition of the base glasses (Table B12). Mixtures of these with specpure TiO2 were made to provide interference standards for Sc and V, and pellets were made of all these.

Table B12 : Major element composition of base glasses INTSG and INTSB, and of their derivatives.

	SiO2	Al2O3	Fe2O3	MgO	CaO	Na2O	K2O	TiO2
INTSG	73.30	14.04	2.13	0.00	2.06	3.91	3.90	0.00
INTSB	50.05	13.80	10.25	9.64	10.39	2.91	1.02	2.00
INTSA	61.67	13.92	6.19	4.82	6.22	3.41	2.46	1.00
INTSATI	60.92	13.74	6.10	4.74	6.12	3.37	2.43	2.29
INTSBTI	49.07	13.53	10.05	9.45	10.19	2.85	1.00	3.92

Portions of the base glasses were then spiked with accurately known quantities of stoichiometric trace element compounds, to give element concentrations of between 1000 and 2000 ppm. Compounds used are listed in Table B13.

Table B13 : Trace element compounds used for spiking synthetic glasses.

Element	Rb	Sr	Y	Zr	Nb	Sc	V	Cr
Compound	RbCl	SrCO3	Y2O3	ZrO2	Nb2O5	Sc2O3	NH4VO3	K2Cr2O7

Element	Ni	Cu	Zn	Ba	La	Ce
Compound	Ni(CH3CNO.CH3CNOH)2	CuO	ZnO	BaCO3	La2O3	CeO2

A pair of spiked glasses, suffixed -A and -B, was produced for both INTSG and INTSB, to allow different combinations of trace elements for interference corrections. The spiked glasses were then shaken in a polystyrene mixing vial using a Glen Creston mixer mill. To ensure homogeneity the spiked glasses were fused in the platinum dishes at

1400°C: the A series was fused first, and it would seem that this has lost Cu to the platinum, whence the B series has gained it. Cu values for these standards are therefore meaningless. It is possible that other elements have been similarly transferred, but only Ni and Cr show minor departures from the international standards calibration, and the synthetic standards are therefore not included in the calibrations for Ni and Cr. The resulting four glasses were ground in a tungsten carbide Tema mill and pellets made of the powders: these are INTSGA1, INTSBA1, INTSGB1 and INTSBB1. Three accurately weighed dilutions were made of the spiked glasses with base glasses, with mixing carried out by shaking in a mixer mill as before. Three more sets of four pellets were produced by this, suffixed 2, 3 and 4. All synthetic standards were pelletized using 2% PVA binding agent. The theoretical trace element composition of these sixteen pellets is given in Table B14.

Calibration consists of using the count ratios and the concentrations of the standards of Table B11 to determine m and c in the linear relation

$$X_s^i = m^i \mu_s^i R_s^i + c^i \qquad \text{(section B5)}$$

using regression procedures described in section B10.

B8 : MATRIX CORRECTIONS

The use of La2O3 in the flux for glass disc preparation and the five-fold dilution involved gives rise to a relatively constant matrix composition. It was therefore hoped that matrix correction would be unnecessary, and calibration lines were constructed from direct count ratio - concentration graphs. The ten graphs involved are presented in Fig. B1, and it is clear that a very high degree of linearity is obtained despite the wide variety of rock types used as standards, from dunite to granite. Linearity is particularly good for Mg, Ca, K, Ti and P, and it is improbable that matrix correction, with the attendant uncertainties in coefficients, could improve this. Matrix correction was applied to the silica calibration; while the resulting line was slightly different it was no more linear than the uncorrected calibration. Accordingly, for all elements determined on the glass discs, μ_s^i is given the value 1 in the equation at the end of section B7.

It is considered that a number of minor discrepancies do result from this lack of correction. In Fig. B1(a), it will be seen that BR and the ultramafic standards are divergent. Better total oxides are obtained if the calibration is placed closer to the ultramafic standards, and hence the SiO2 value of BR is not used in the calibration, equivalent to giving BR half weighting for silica. A 100% specpure silica disc then has a total of about 101%: a similar effect probably accounts for the high frequency of >100% totals for analysed rhyolites. A minor discrepancy in iron contents of the ultramafic standards is also possibly a matrix effect, and these values are not used

TABLE B14: Theoretical compositions of synthetic trace element standards. All values in ppm. Cu concentrations are incorrect due to exchange with Pt.

	Rb	Sr	Nb	Cr	Ni	Cu	Ba	La	Y	Sc	Zr	Zn	V	Ce
INTSBA1	1017	1017	1004	2528	2026	(1062)	1313	0	0	0	0	0	0	0
INTSGA1	2109	1125	1058	1058	1018	(1031)	2534	0	0	0	0	0	0	0
INTSBA2	414	414	409	1030	826	(433)	535	0	0	0	0	0	0	0
INTSGA2	877	468	440	440	423	(429)	1054	0	0	0	0	0	0	0
INTSBA3	83	83	82	206	165	(87)	107	0	0	0	0	0	0	0
INTSGA3	208	111	104	104	100	(102)	250	0	0	0	0	0	0	0
INTSBA4	19.4	19.4	19.1	48.2	38.6	(20.2)	25.0	0	0	0	0	0	0	0
INTSGA4	41.7	22.3	20.9	20.9	20.1	(20.4)	50.1	0	0	0	0	0	0	0
INTSBB1	0	0	0	0	0	(0)	0	1402	961	988	?4530	1053	1020	1047
INTSGB1	0	0	0	0	0	(0)	0	1017	998	998	1044	1011	1050	1037
INTSBB2	0	0	0	0	0	(0)	0	577	395	406	?1864	433	420	431
INTSGB2	0	0	0	0	0	(0)	0	430	422	422	441	427	444	438
INTSBB3	0	0	0	0	0	(0)	0	136	93.5	96	?441	102	99	102
INTSGB3	0	0	0	0	0	(0)	0	97	95	95	99	96	100	99
INTSBB4	0	0	0	0	0	(0)	0	28.5	19.5	20.1	?92.1	21.4	20.7	21.3
INTSGB4	0	0	0	0	0	(0)	0	18.6	18.2	18.2	19.1	18.5	19.2	18.9

Fig. B1 a & b : Major element calibration graphs

Symbols: ◆ = 'granites' (GA,GH,G2,JG1); ■ = 'ultramafics' (PCC1,DTS1,UBN)
▲ = 'intermediate rocks' (AGVi,GSP1,GSN,DRN,T1);
● = 'basalts' (BR,BCR1,JB1); △ = others (SY3,NBS91,NBS99A,FKN)

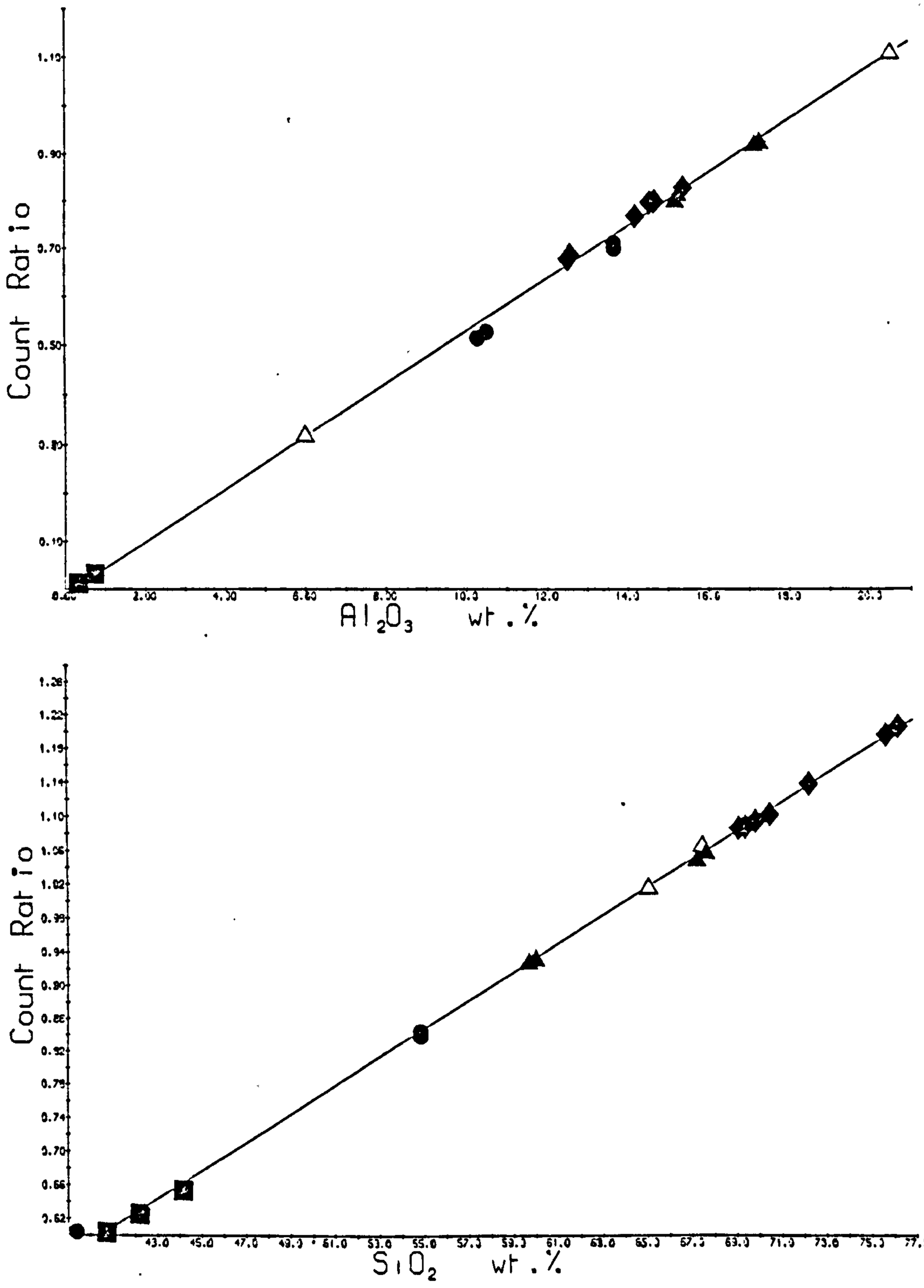

Fig. B1 c & d : Major element calibration graphs

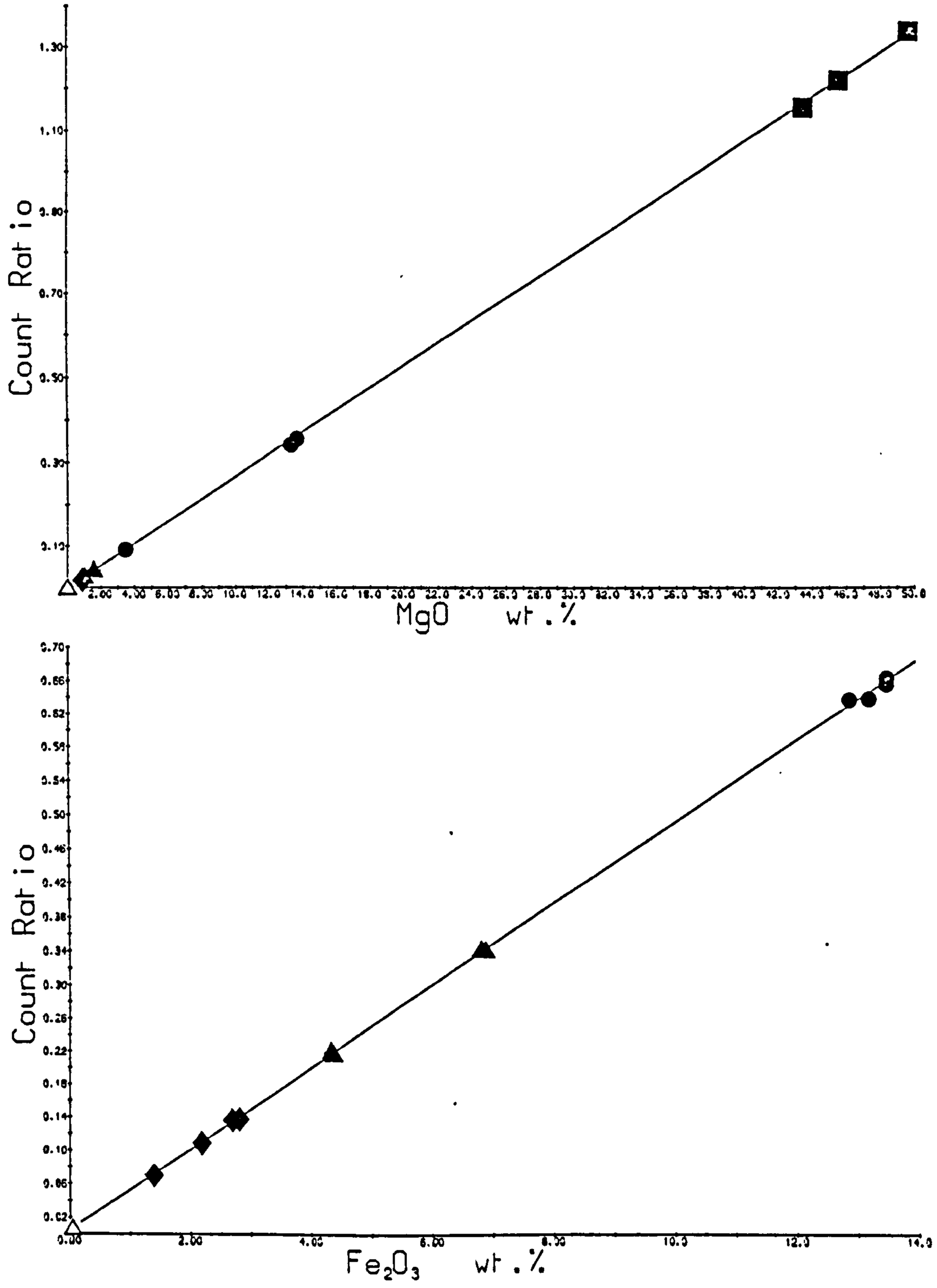

Fig. B1 e & f : Major element calibration graphs

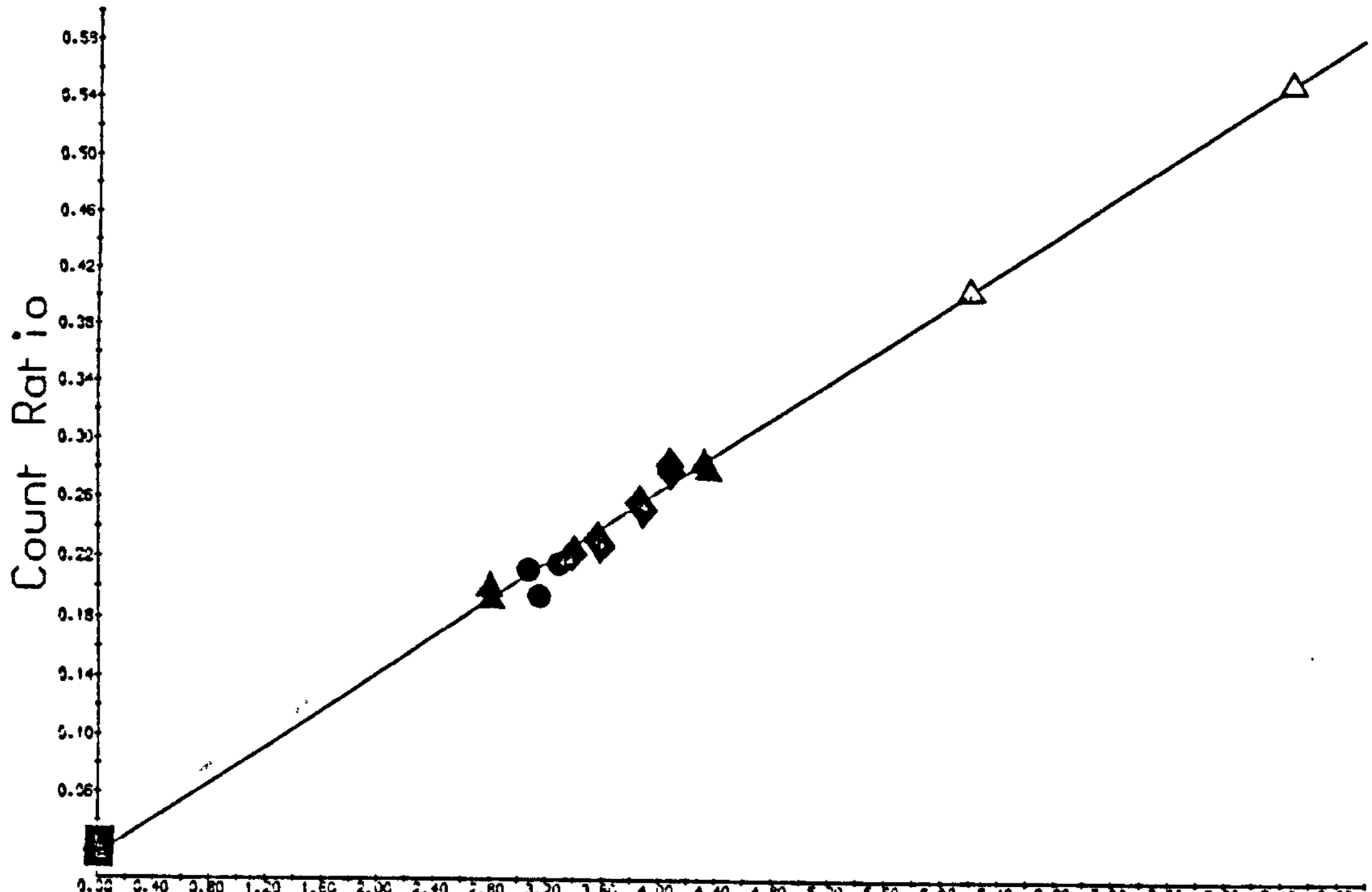

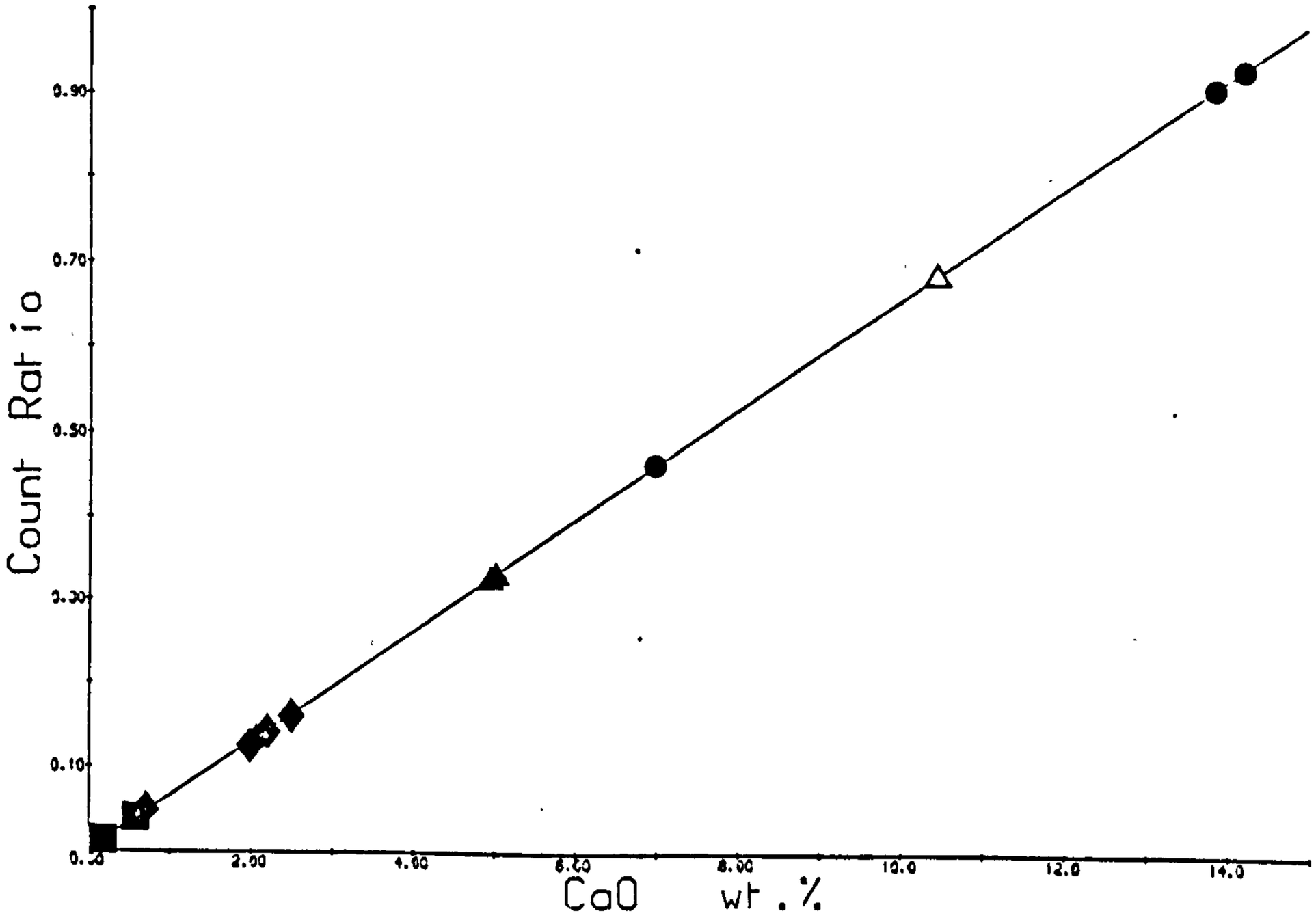

Fig. B1 g & h : Major element calibration graphs

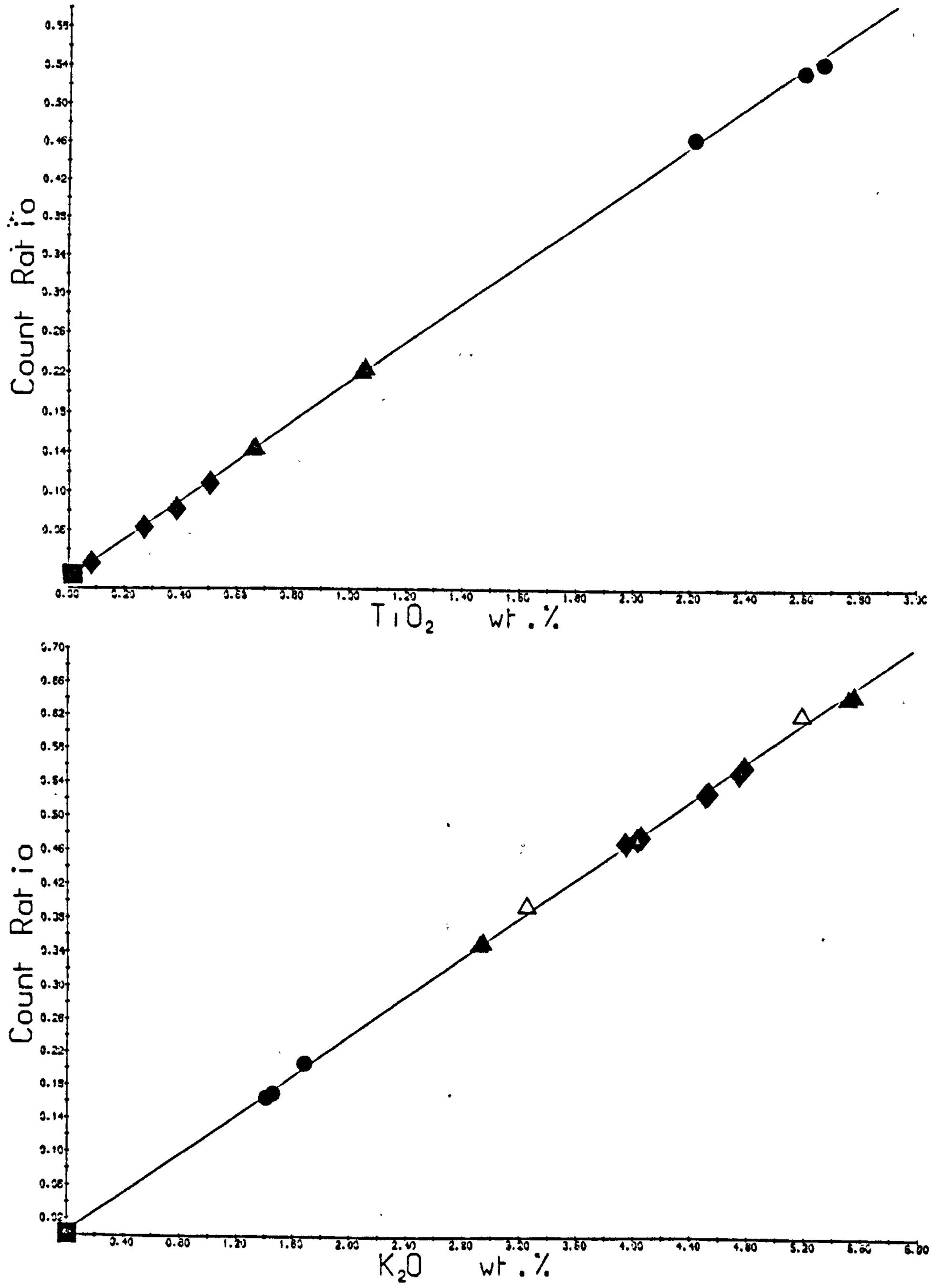

Fig. B1 i & j : Major element calibration graphs

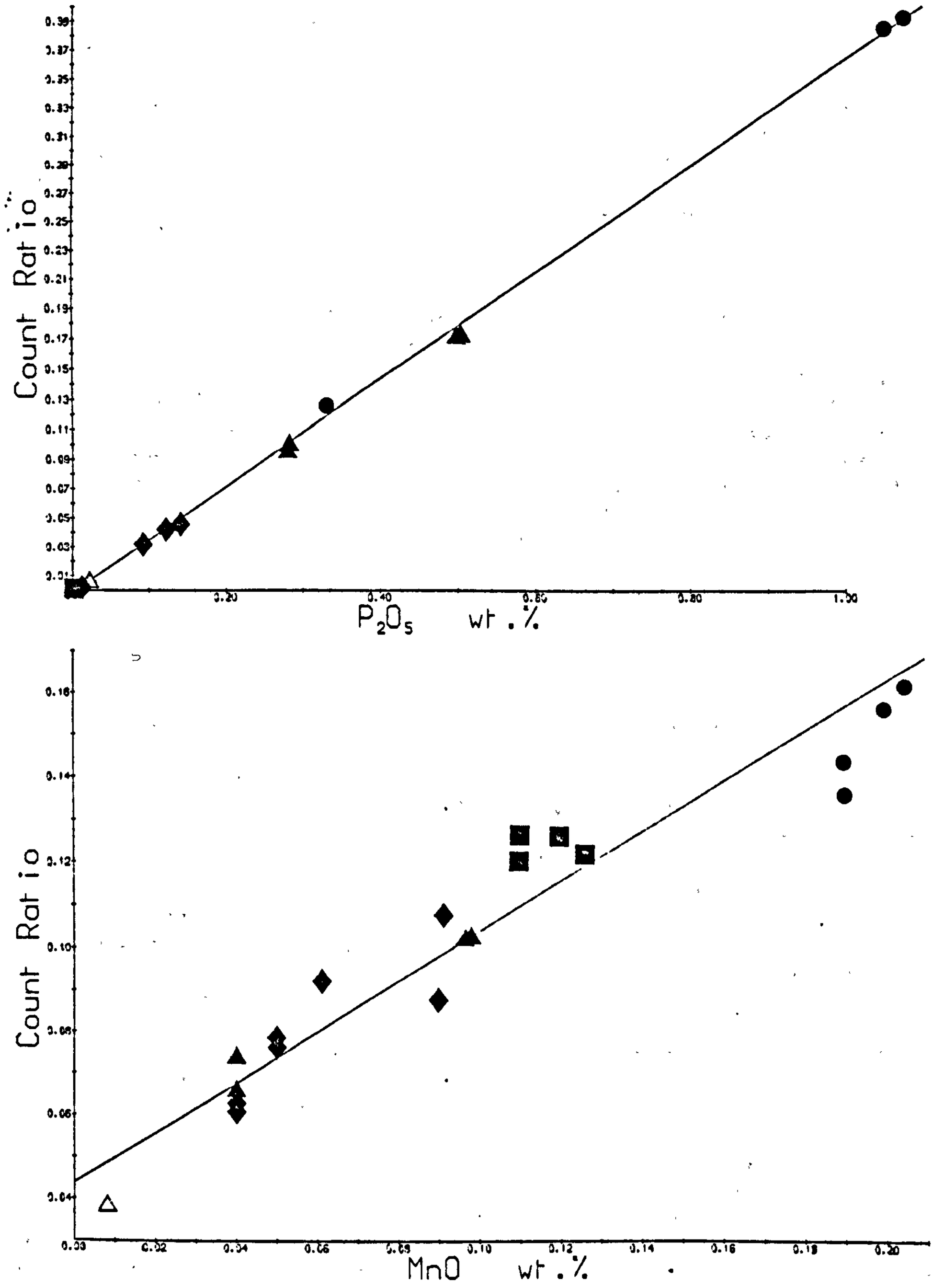

in calibration. Scatter in the MnO calibration is caused by the values in Abbey (1977) being quoted to only two decimal places. It is believed that the high degree of linearity of the calibrations is justification for not making matrix corrections, providing that the rocks analysed are not extreme in composition. More extreme compositions e.g. limestones may be brought into the calibration range by fusion with a known weight of a specpure oxide.

A number of methods have been used by previous workers for matrix correction of trace element data. A common method involves ratio to background, used, for example, by Gandy (1973a), and based on Anderman and Kemp (1958). The latter authors state that their method should not be used for wavelengths longer than the FeK_α absorption edge, but this has not prevented a number of workers from using the correction for V and Cr. The method states that

$$\mu_s^i \propto 1/B_s^i$$

at the wavelength of the i analytical line. Mass absorption coefficients for a number of USGS standards have been calculated using the data of Theisen and Vollach (1967). At all wavelengths shorter than CaK_α the coefficients of basaltic rocks are higher than those of granites. Superimposed chart recorder spectra for these standards between the wavelengths of CaK_α and NbK_α demonstrate that, with increasing wavelength, the basaltic background intensity increases towards the level of the granitic background, until, at wavelengths longer than CrK_α, the basaltic background is higher than the granitic, and, approximately,

$$\mu_s^i \propto B_s^i$$

This is the inverse of the Anderman-Kemp relation. The reason for this inversion is not understood, and requires further work. It is clearly unwise to use the Anderman-Kemp correction method until more is known about the $\mu_s^i - B_s^i$ relationship. In Fig. B2 calibration graphs are presented for Sc (K_α with longer wavelength than the FeK_α absorption edge) and Zr (K_α shorter than the FeK_α absorption edge) with matrix correction made by ratio to background. It is clear that they are both inferior to the calibrations produced using the same data, but with the matrix correction method described below (Fig. B3).

Other correction methods involve extra determinations of matrix absorption: an example is the method of Reynolds (1963), where the reciprocal of the intensity of the MoK_α Compton scatter peak, measured using a Mo-tube, is used as a mass absorption coefficient. This is closely related to the Anderman-Kemp method, for the scatter peak is merely a particularly intense segment of the background. It has the advantage of being accurately measurable, but suffers from the same disadvantages as the Anderman-Kemp method, although an extension of its applicability to wavelengths longer than the FeK_α absorption edge has been reported by Nesbitt et al.

Fig. B2 : Calibration graphs for Zr and Sc using the Anderman-Kemp matrix correction procedure. N.B. different calibration lines for acid and basic rocks. Symbols as Fig. B1..

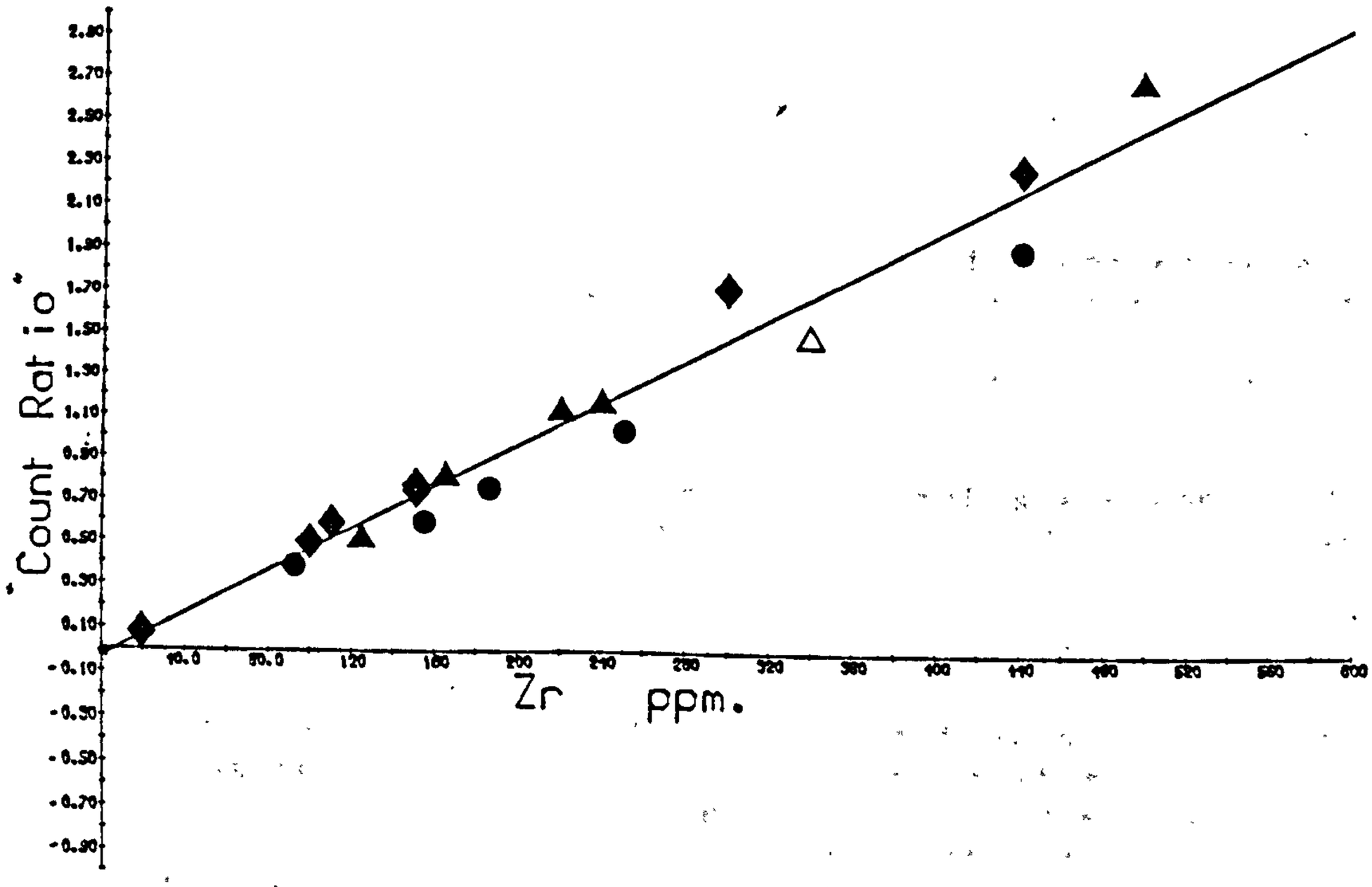

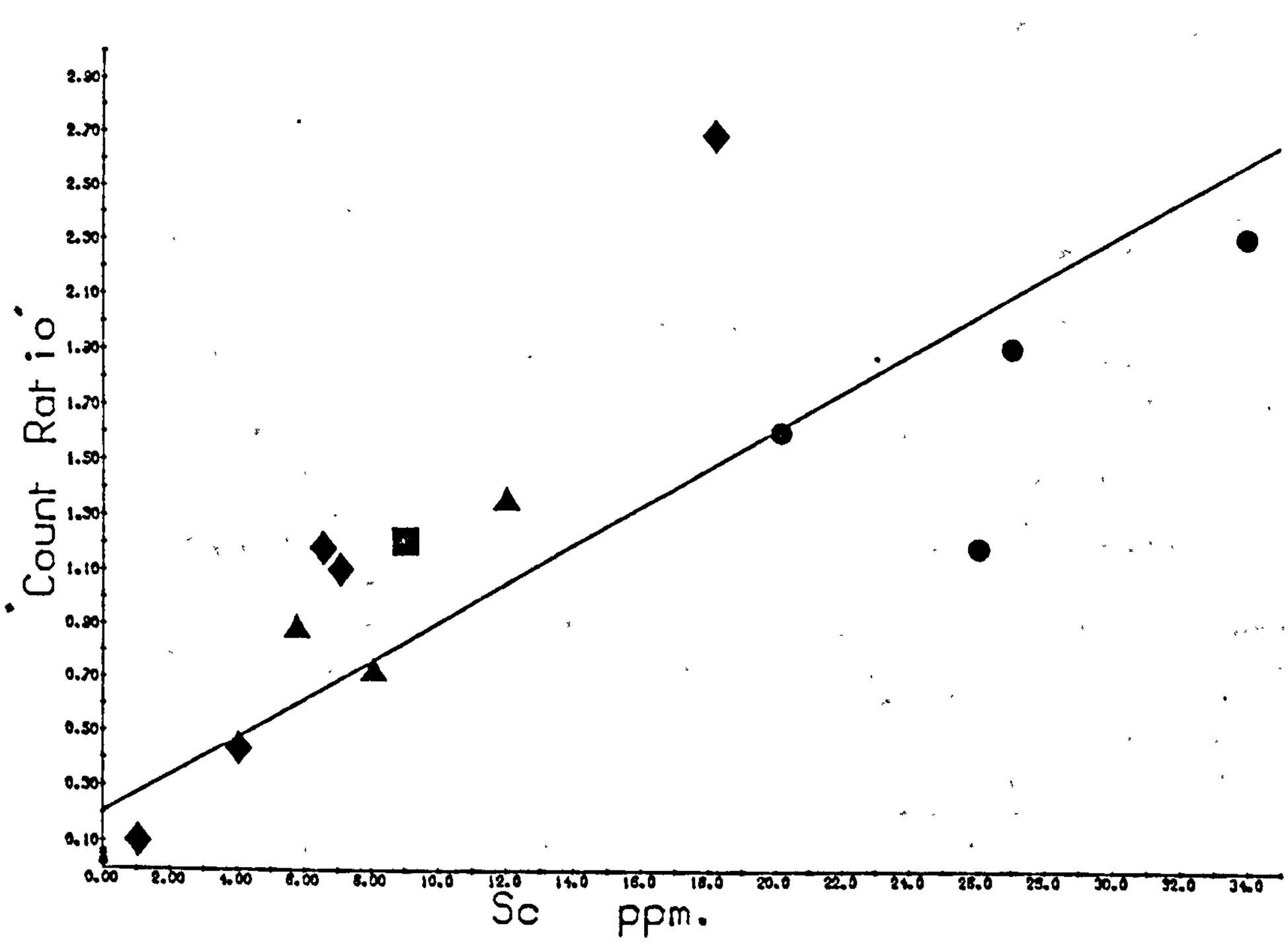

N.B. These calibrations have not been used in the calculation of Zr and Sc concentrations.

(1976). In addition, the method involves an extra determination for each sample, and is only strictly applicable to one wavelength. Some direct determination methods for μ_s^i have been reported, but these are very time-consuming, for they involve determination at every analytical wavelength.

By definition:

$$\mu_s^i = \sum_{z=1}^{z=92} \mu_z^i X_s^z$$

where μ_z^i is the mass absorption coefficient of pure element atomic number z at the wavelength of the i analytical line,
X_s^z is the weight fraction of element atomic number z in sample s.

Since around 99.5% of most samples are composed of the ten major elements analysed on glass discs with oxygen, this may be simplified to:

$$\mu_s^i = \sum_z \mu_z^i X_s^z \quad \text{for } z=8,\ 11\text{-}15,\ 19,\ 20,\ 22,\ 25,\ 26$$

and, if z is taken to refer to the oxide, so that μ_z^i is the mass absorption coefficient of the pure element oxide at the i analytical wavelength, the value for z=8 may be omitted. Coefficients of μ_z^i have been taken from Theisen and Vollach (1967), and may be easily converted to oxide coefficients. The calculation may be further simplified by use of the relation $\mu \propto 1/\lambda^3$, and thus, providing analytical lines for i_1 and i_2 are between major element absorption edges,

$$\mu_s^{i_1}/\mu_s^{i_2} = \text{constant, for all samples s}$$

Analytical lines for Sc, V, La and TiK_β lie between the CaK_α and TiK_α absorption edges, and oxide absorption coefficients calculated at TiK_α have been used for these lines by means of the above relation. Similarly, coefficients calculated at CrK_α have been used for analytical lines between the Ti and Mn K_α absorption edges (Cr, Ba, Ce, Nd, Sm), and at SrK_α for analytical lines with wavelengths shorter than the FeK_α absorption edge.

Examination of the tables of Theisen and Vollach (1967) discloses that the relation $(\mu_z^{i_1}/\mu_z^{i_2})$=constant, a subset of the previous relation, only holds true if elements z are in the same period, and, between elements in different periods, the discrepancy becomes greater the further separate i_1 and i_2 are. Lines relating to TiK_α and CrK_α are sufficiently close for this discrepancy to be very small, and no allowance has been made. For lines relating to SrK_α, 4th period oxide concentrations are multiplied by a factor of

$$\frac{(\mu_z^{i_1}/\mu_z^{i_2})\text{-4th period}}{(\mu_z^{i_1}/\mu_z^{i_2})\text{-3rd period}}$$

This factor ranges from 0.908 (Ni) to 1.024 (Nb). Oxygen is

Fig. B3 a & b : Trace element calibration graphs

Symbols as Fig. B1.

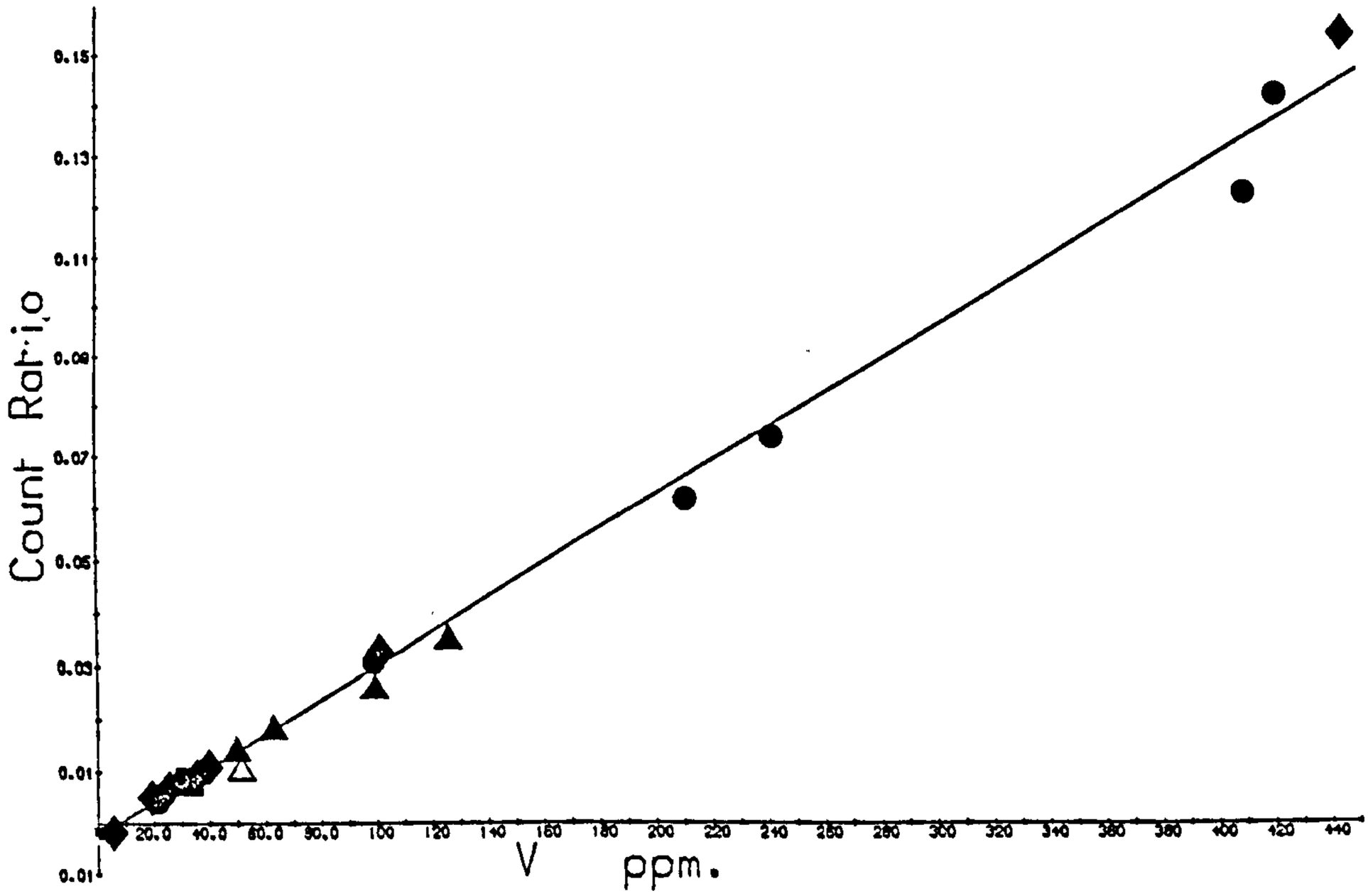

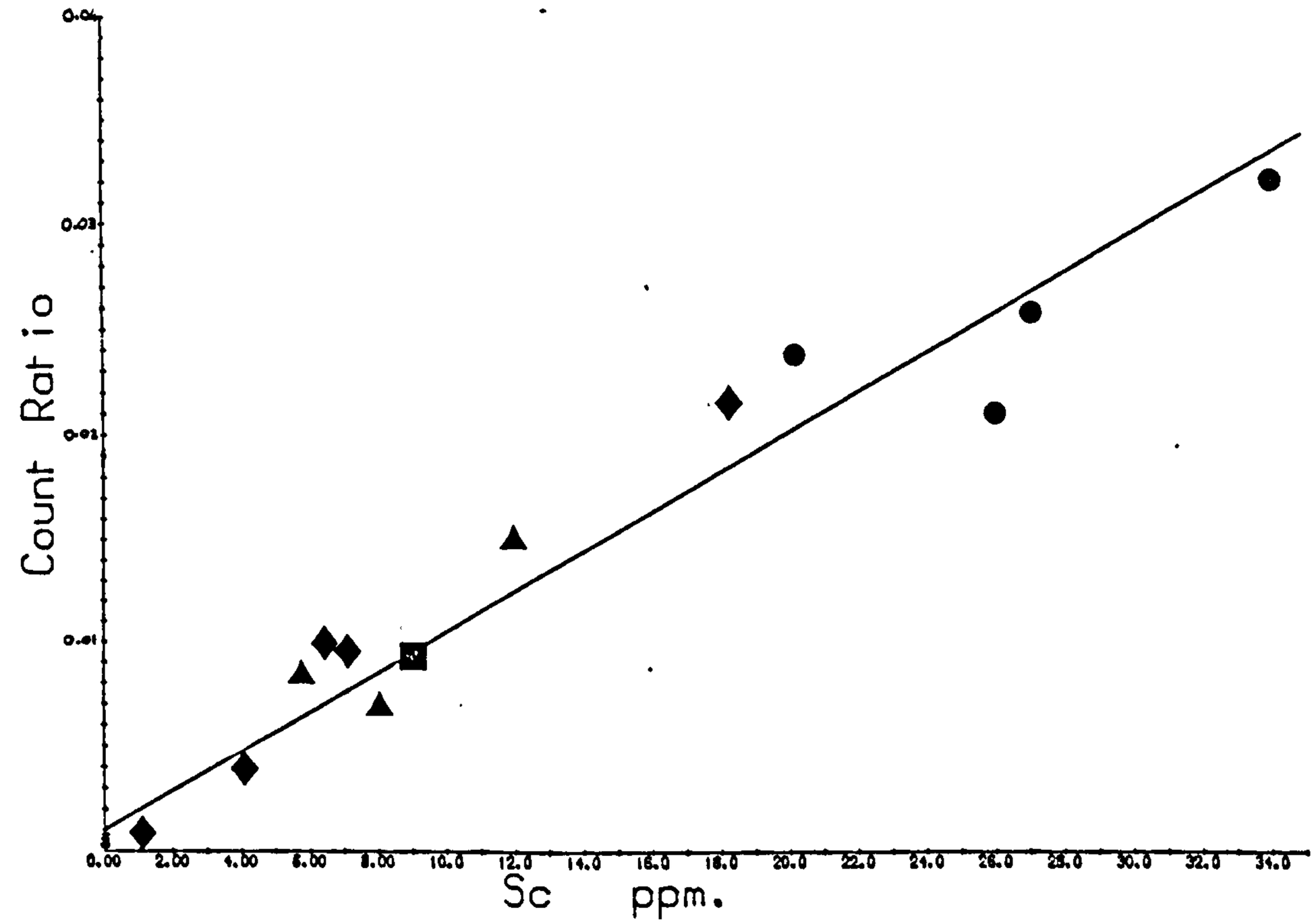

Fig. B3 c & d : Trace element calibration graphs

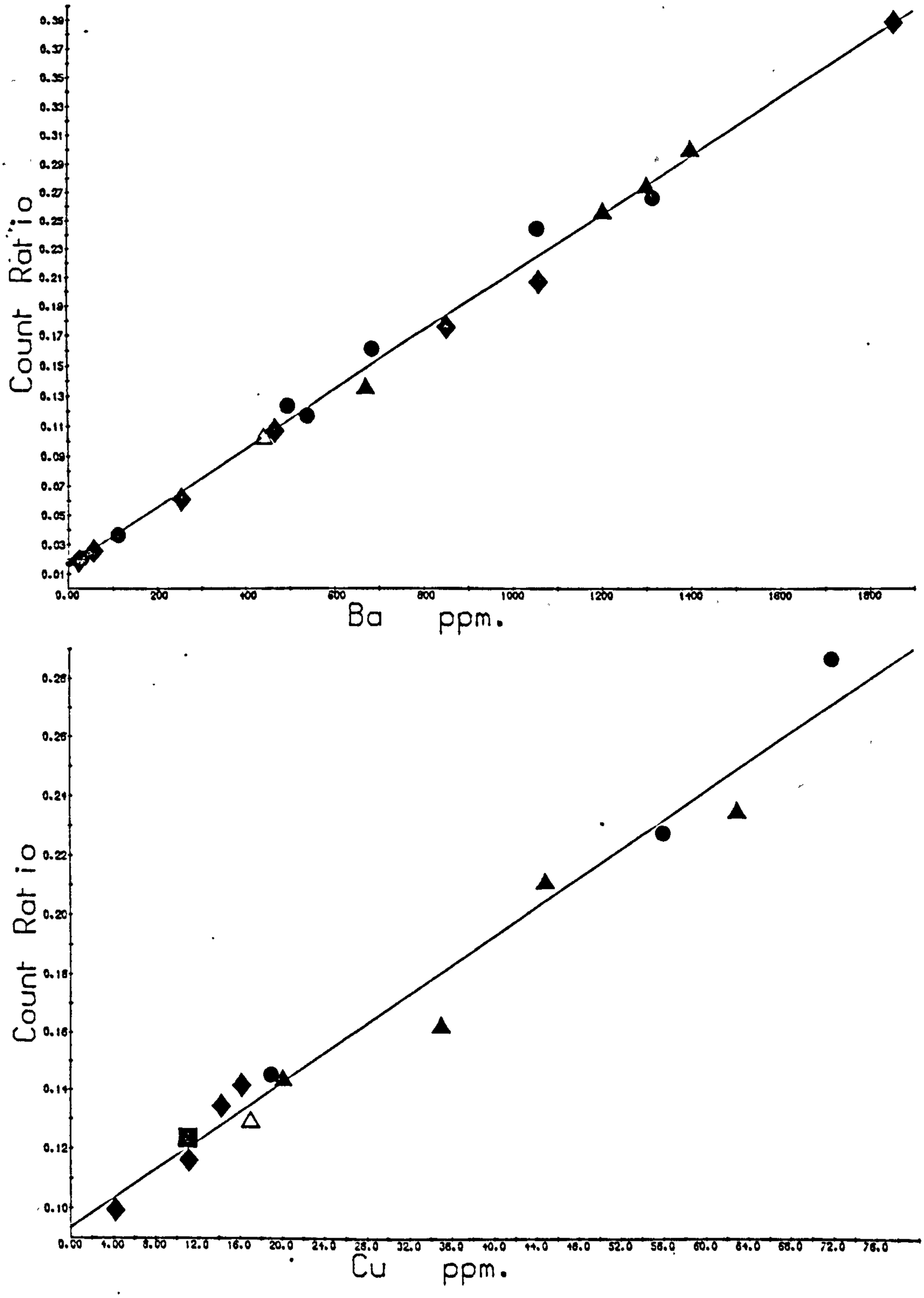

Fig. B3 e & f : Trace element calibration graphs

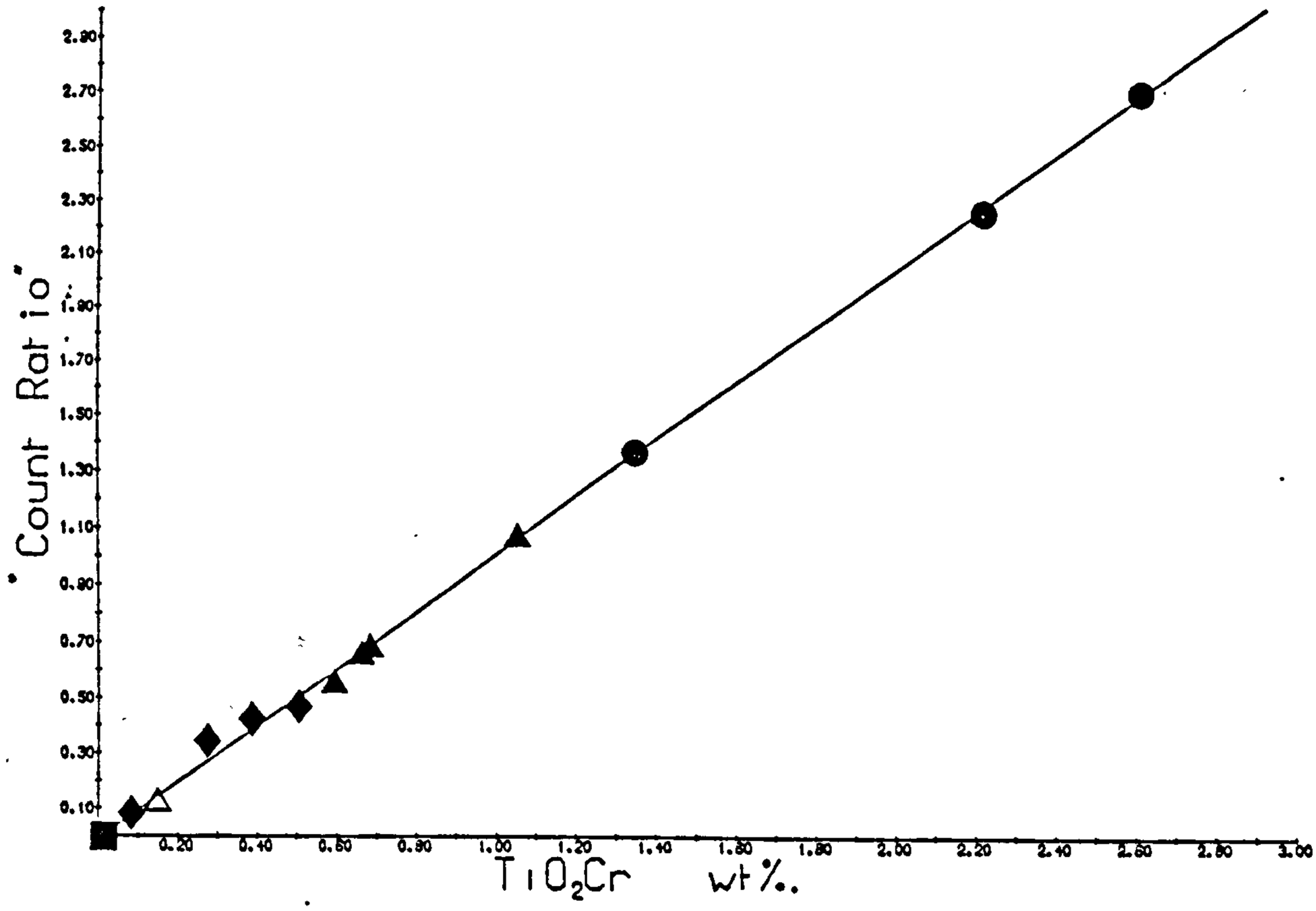

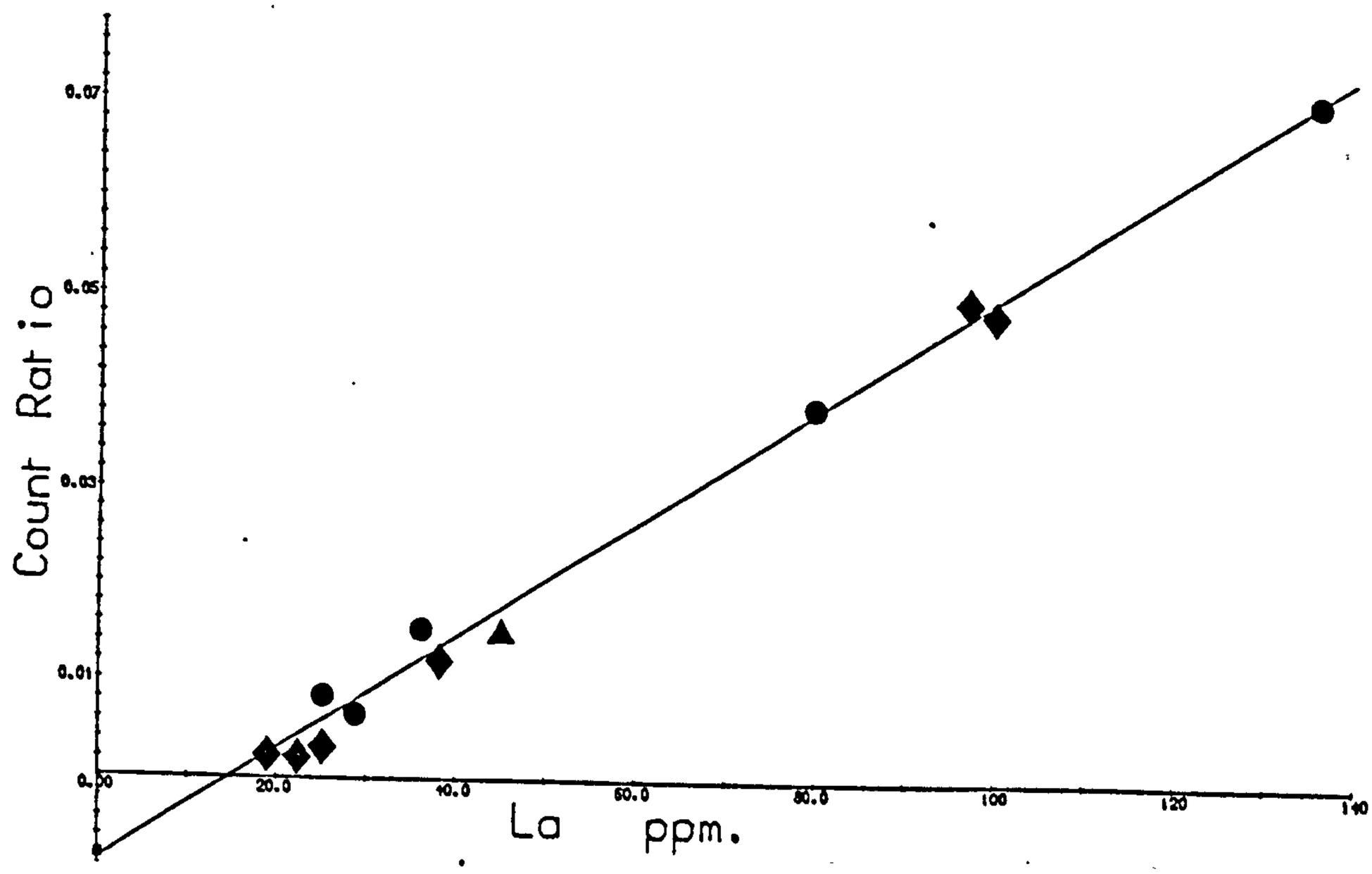

Fig. B3 g & h : Trace element calibration graphs

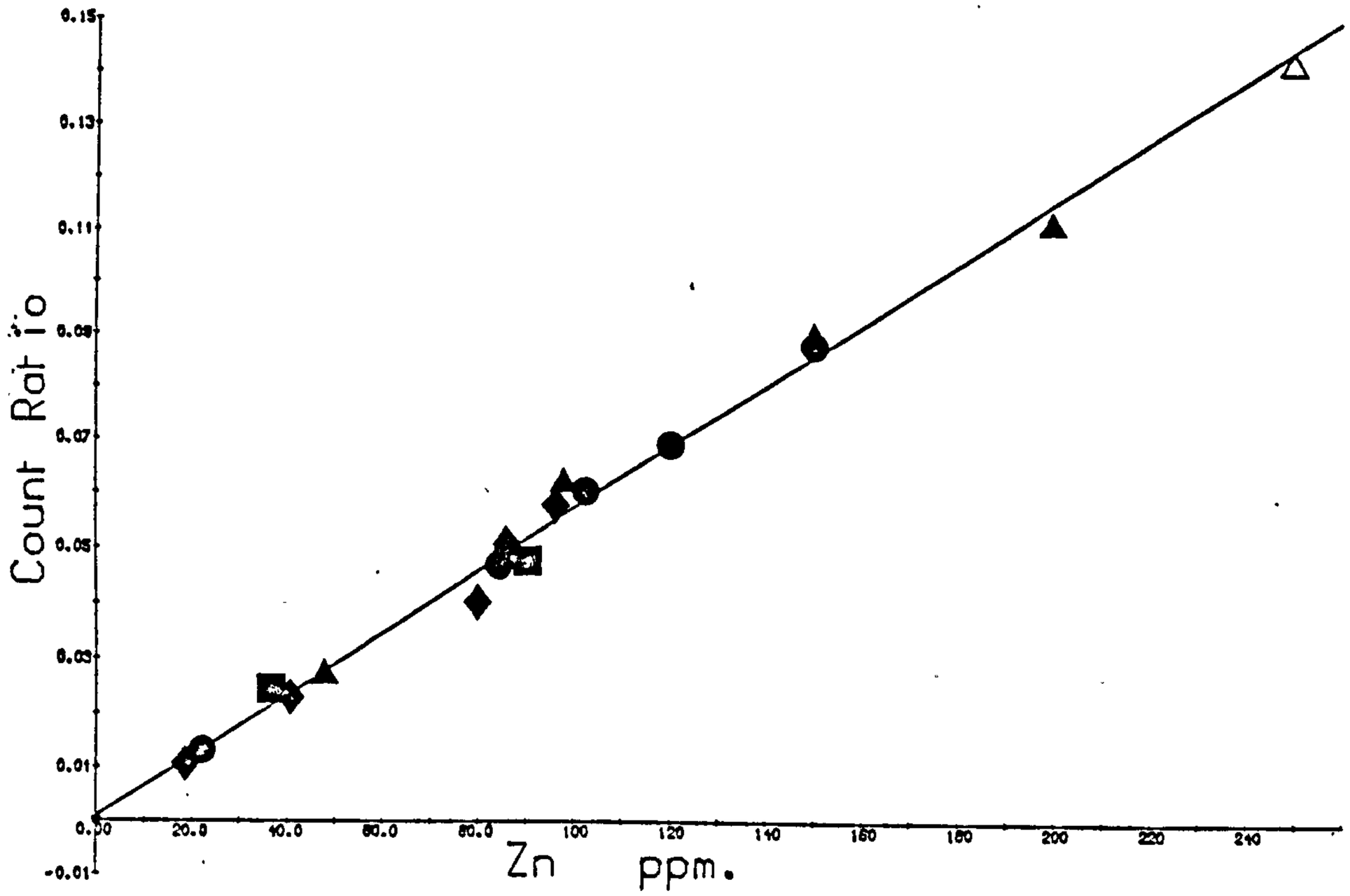

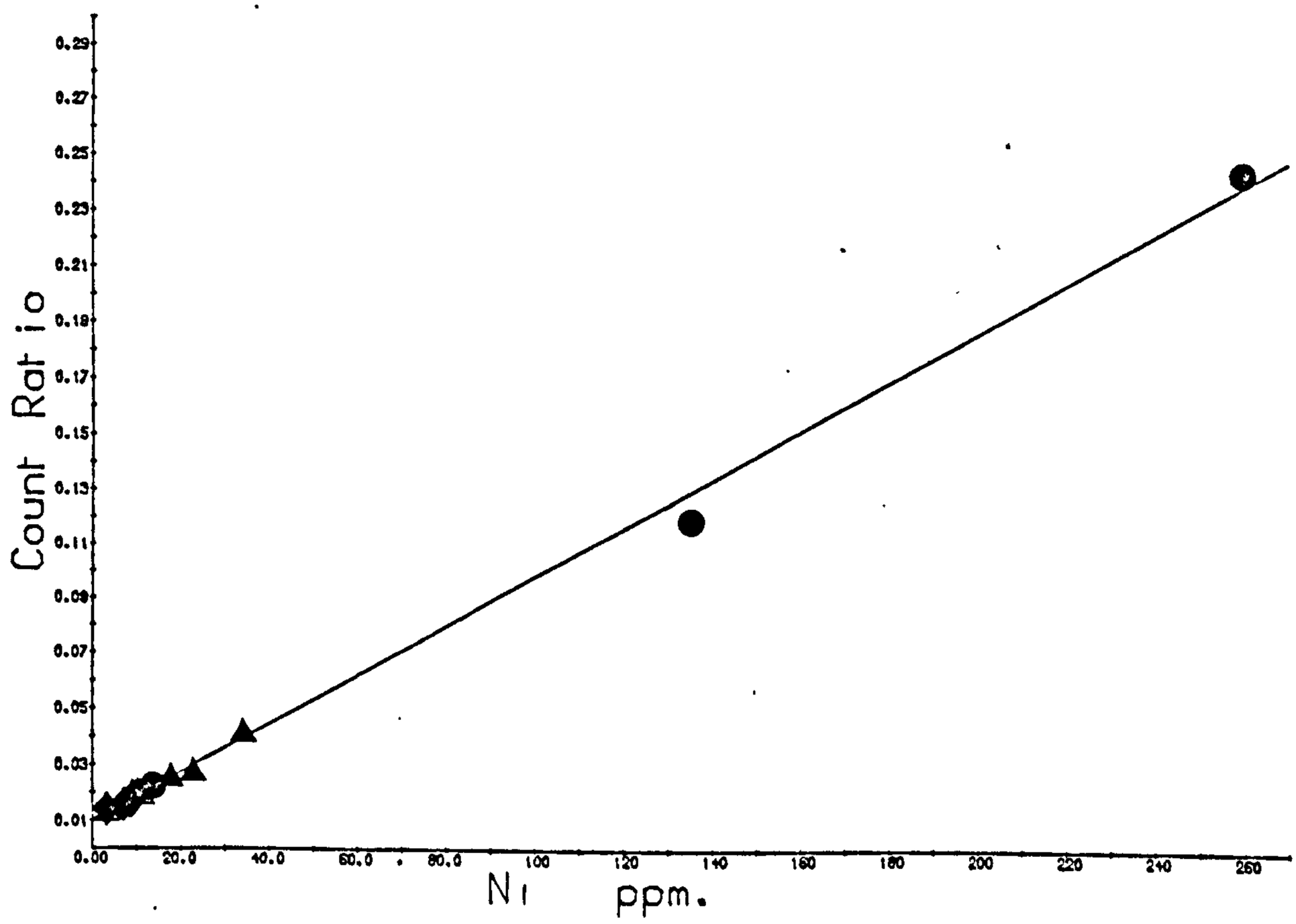

Fig. B3 i & j : Trace element calibration graphs

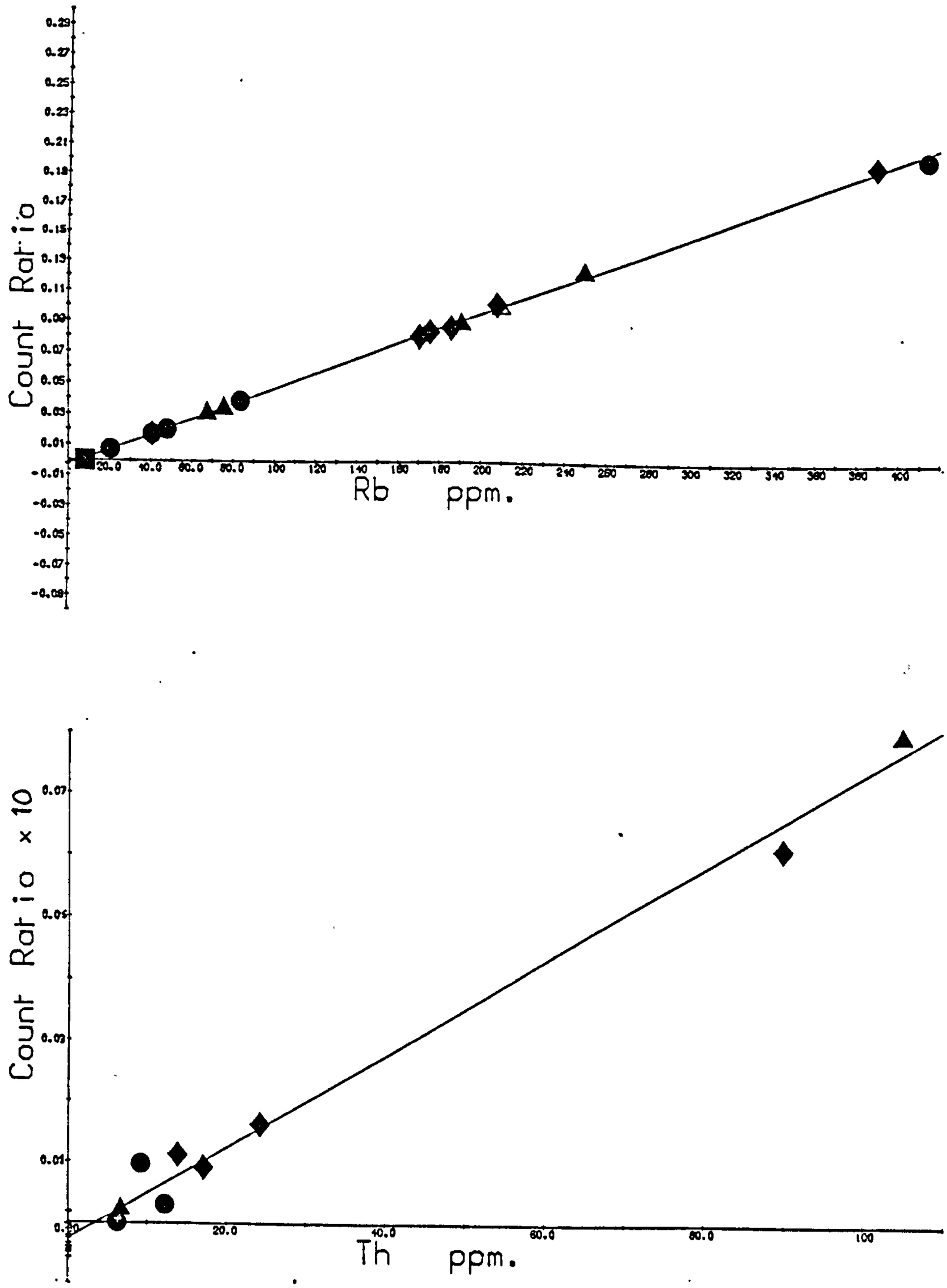

Fig. B3 k & l : Trace element calibration graphs

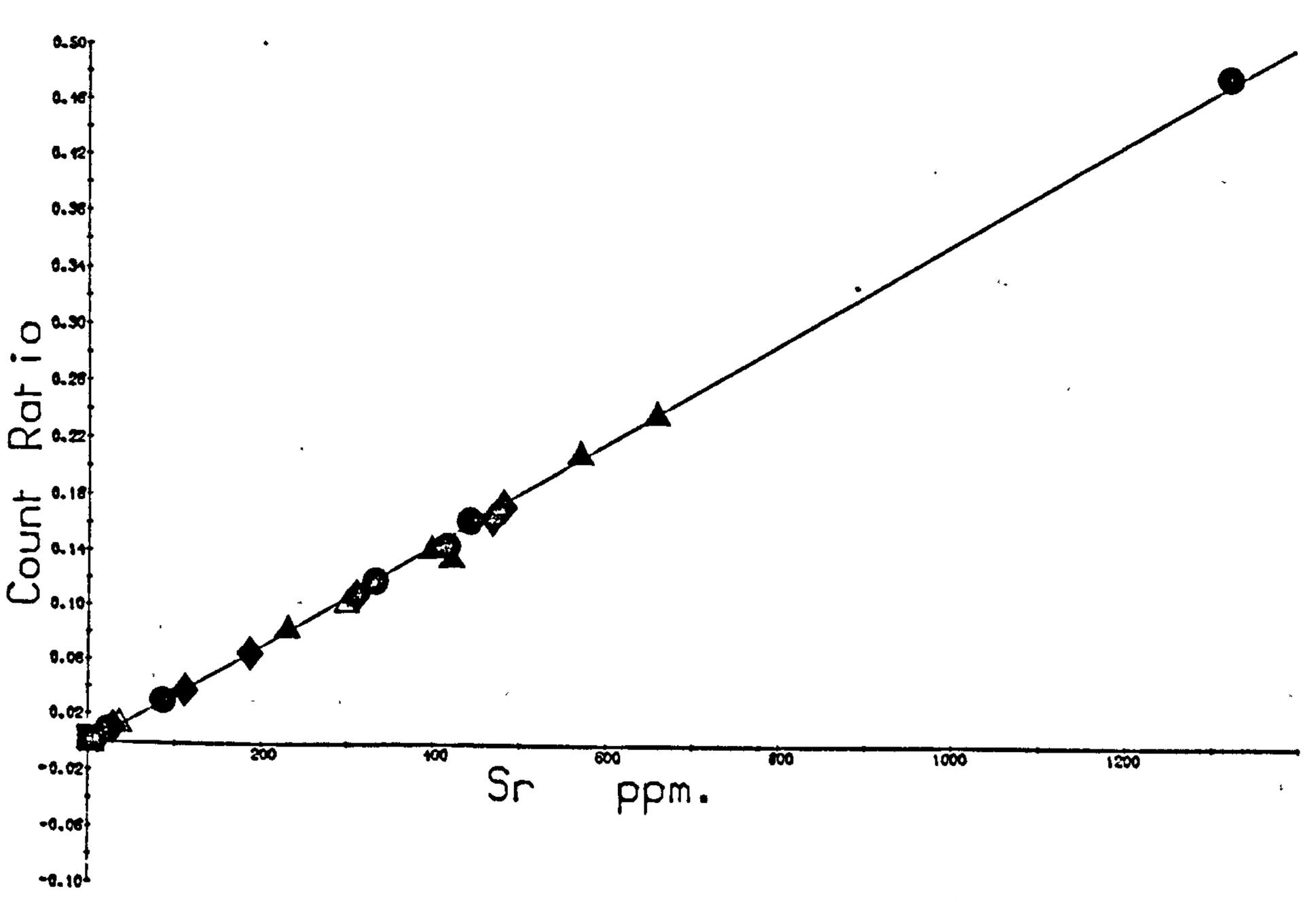

Fig. B3 m & n : Trace element calibration graphs

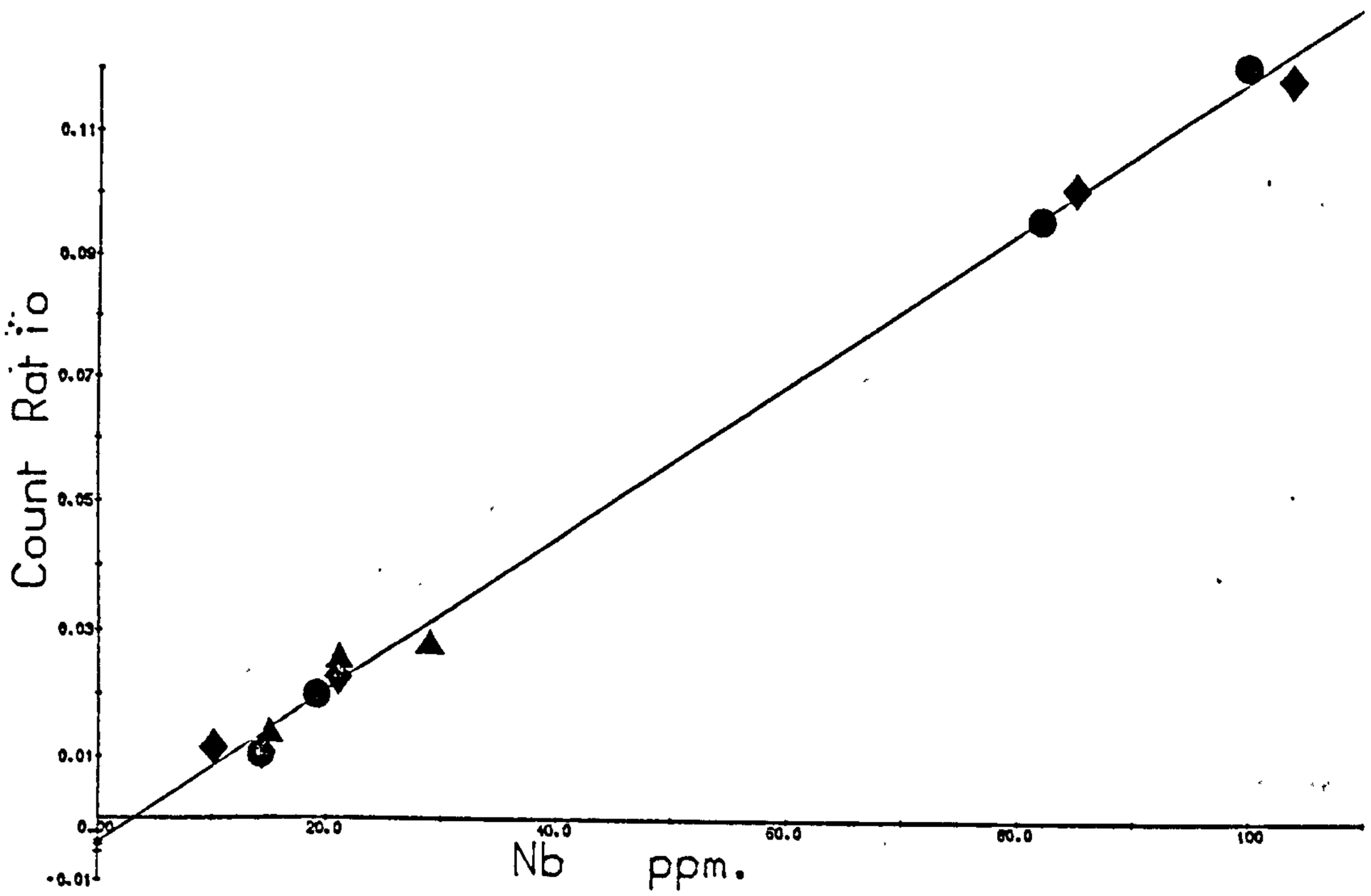

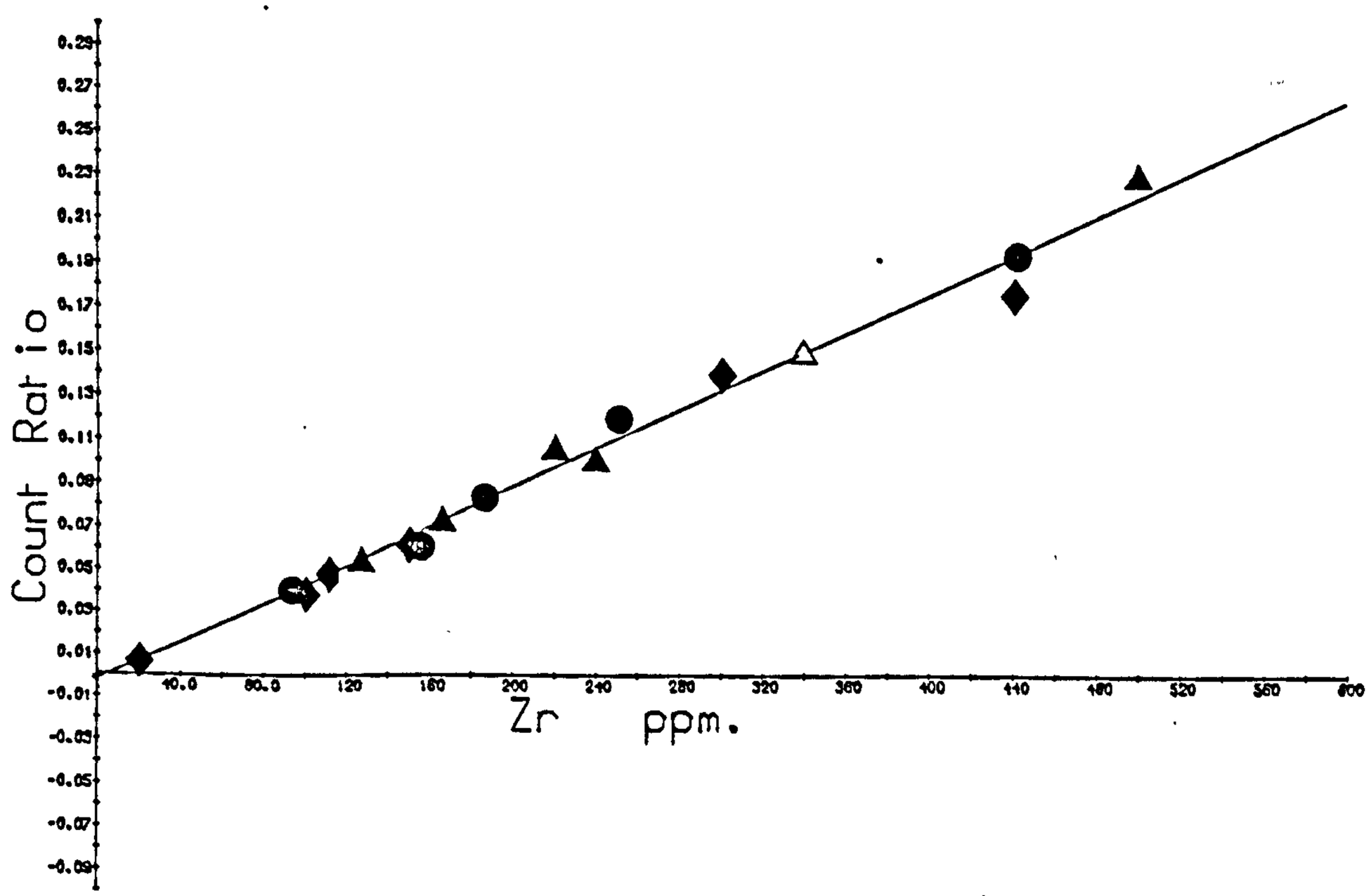

Fig. B3 o & p : Trace element calibration graphs

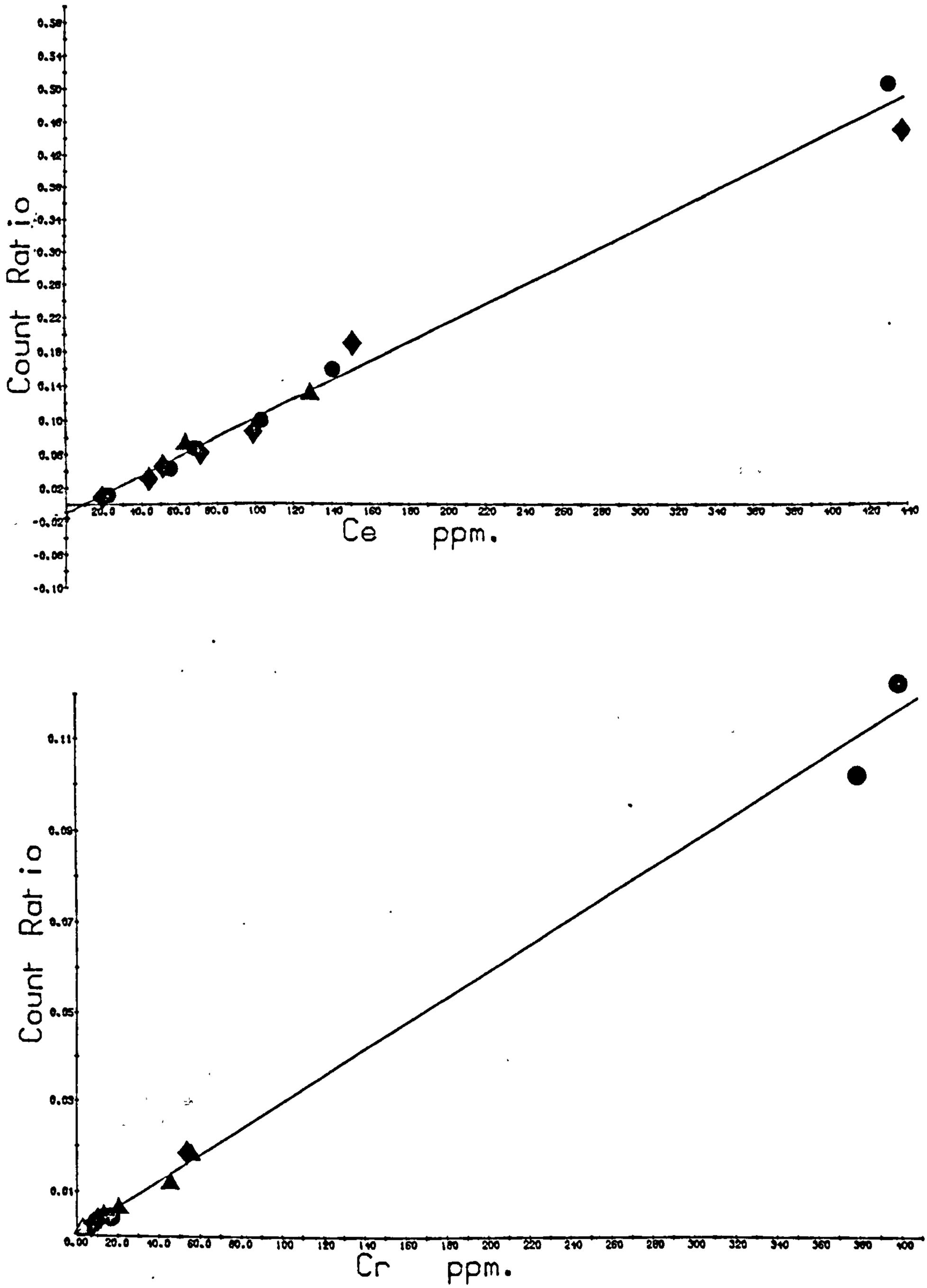

Fig. B3 q & r : Trace element calibration graphs

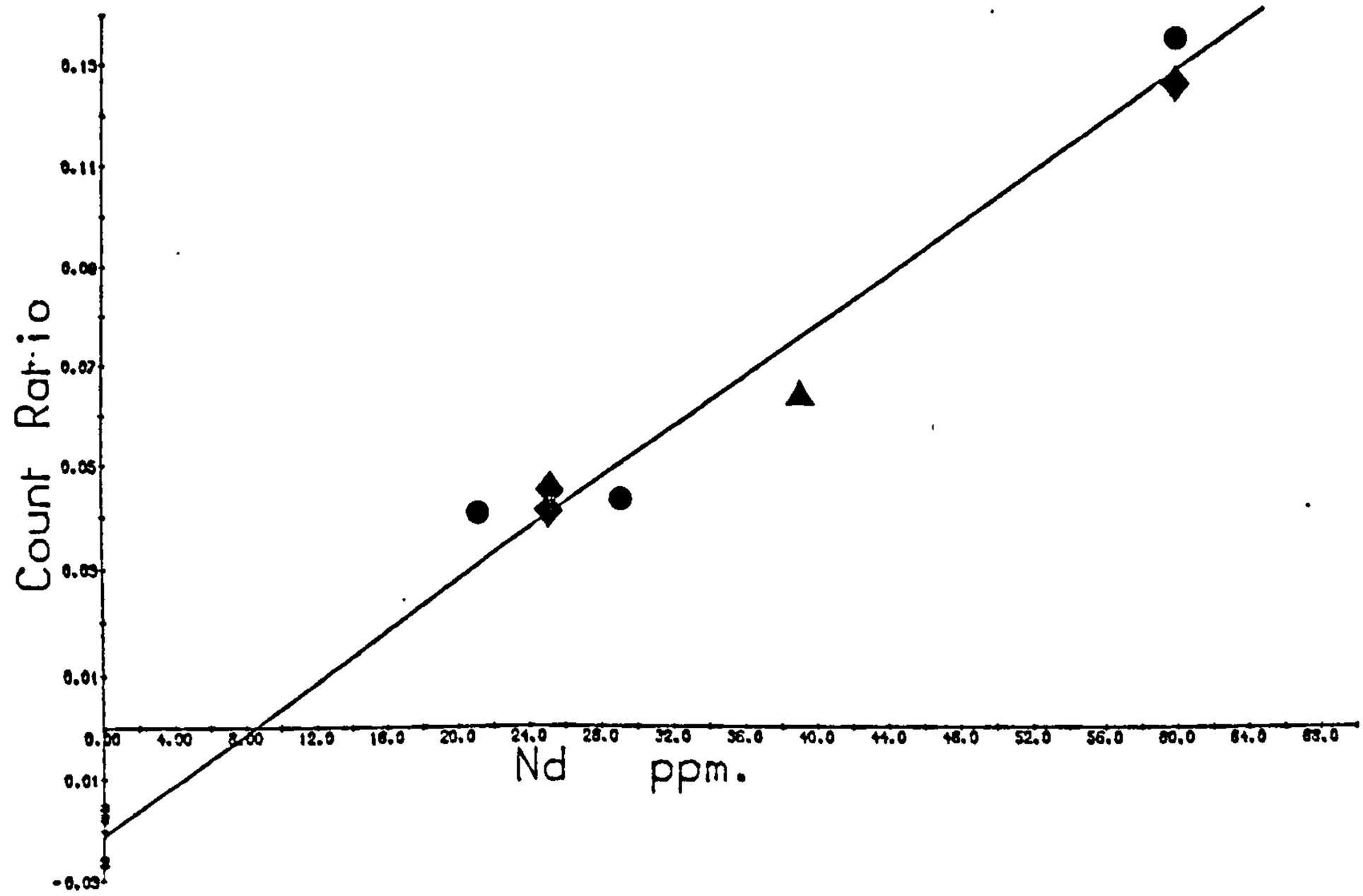

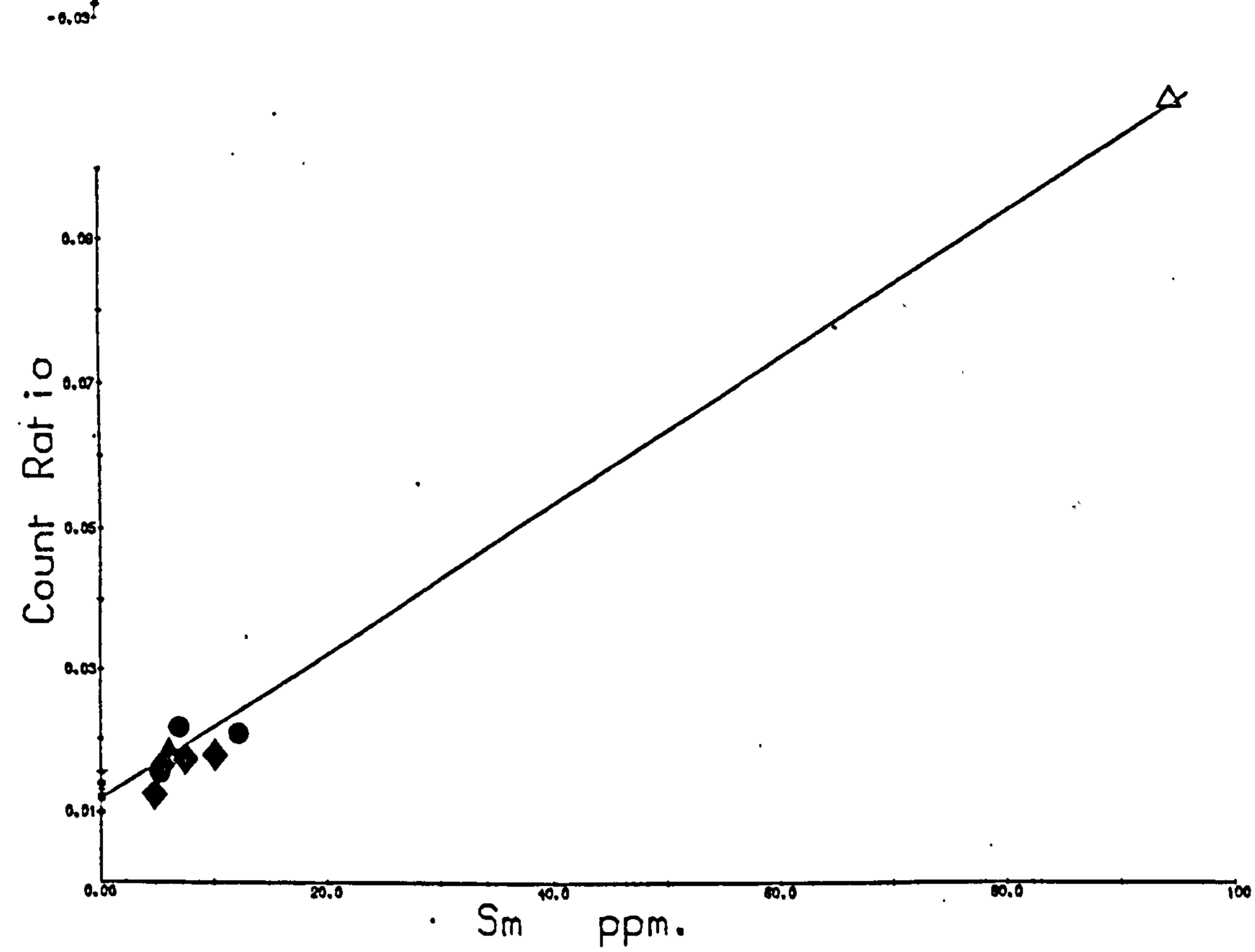

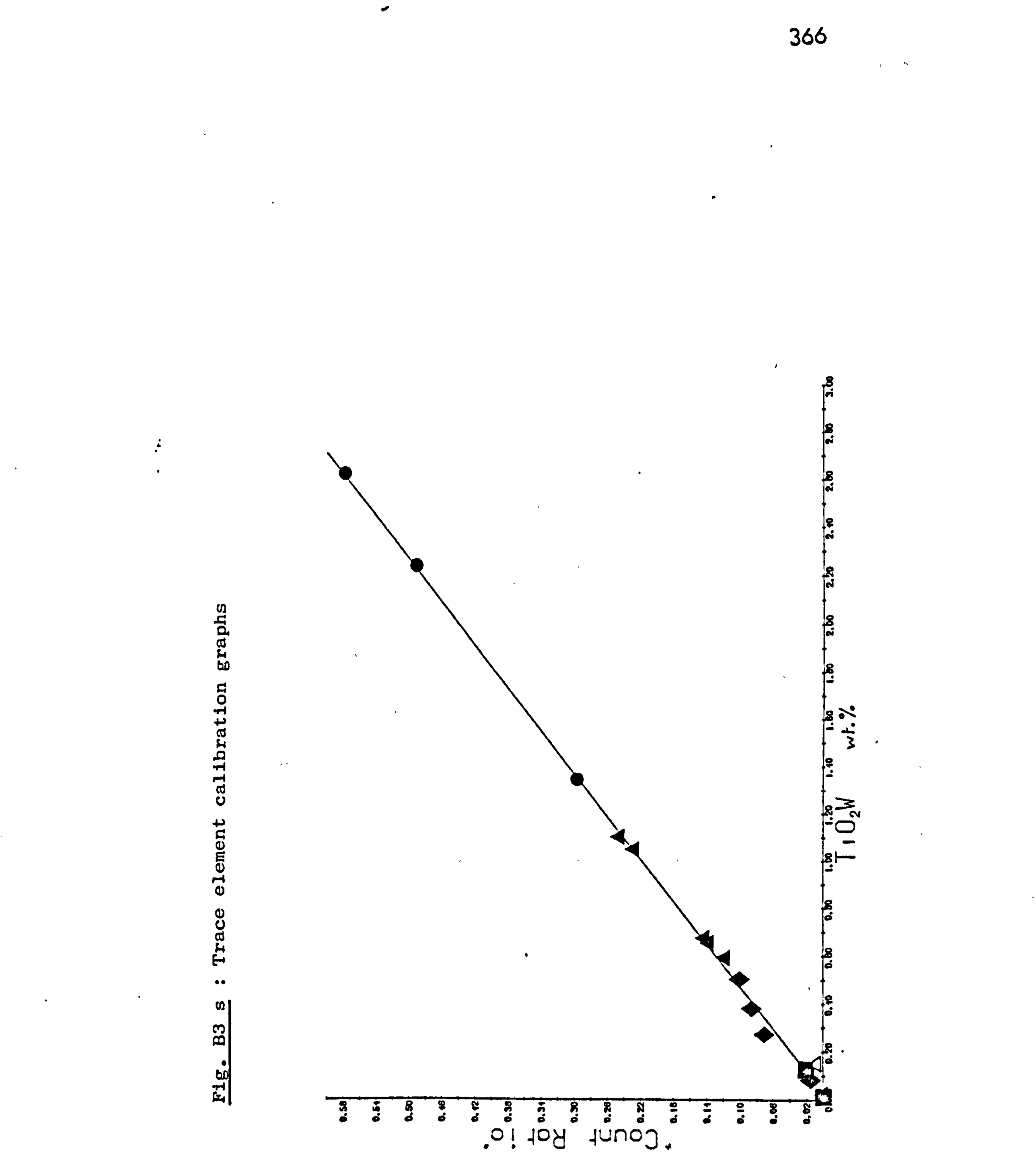

Fig. B3 s : Trace element calibration graphs

TABLE B15: Analytical Accuracy

Analyses of standard samples run as unknowns, not included in calibrations, compared with values from Abbey (1977). Major elements in wt.%, trace elements in ppm.

Major elements: sample GS-N

	SiO_2	Al_2O_3	Fe_2O_3*	MgO	CaO	Na_2O	K_2O	TiO_2	MnO	P_2O_5
XRF	66.09	14.81	3.82	2.30	2.45	3.60	4.687	0.662	0.060	0.269
Abbey (1977)	65.98	14.71	3.75	2.31	2.51	3.78	4.64	0.68	0.06	0.28

	XRF						Abbey (1977)					
	DR-N	FK-N	UB-N	W1	SY2	TB	DR-N	FK-N	UB-N	W1	SY2	TB
Sc	34	0	14	37	6	21	-	-	-	?35	?7	13.5
V	224	2	68	264	50	121	220	-	75	240	50	105
Cu	44	4	20	102	3	32	52	?3	30	110	4	50
Ba	398	198	40	175	460	777	380	?210	?45	160	460	720
La	20	2	3	12	67	51	-	-	-	?12	?85	?56

		Ni	Zn	Th	Rb	Sr	Y	Zr	Nb	Cr	Ce	Sm	Nd
XRF	W1	74	84	2	22	196	24	107	9	128	19	3	11
	SY2	11	260	427	226	270	124	288	37	9	157	13	72
	TB	44	98	19	189	164	33	188	20	107	103	7	43
Abbey (1977)	W1	78	86	2	21	190	25	105	?10	120	?23	?4	15
	SY2	10	250	?370	220	270	130	270	?25	10	?210	?16	?70
	TB	40	95	?19	180	155	?39	175	-	80	?115	?9	-

in the second period, but its contribution to the total mass absorption is so small that the error of up to 5% introduced in treating it as third period is trivial.

The accuracy of this method of matrix correction may be judged by the high degree of calibration linearity (Fig. B3), in particular for Rb, Sr, TiO2Cr and TiO2W, where standard concentrations are best known. Departures from linearity are mainly attributable to inaccurately known standard concentrations, although a few difficulties remain, in particular a low Zn value for GH, and low REE values for GSP1. It seems unlikely that these discrepancies are due to poor matrix correction, for they only apply to single samples: they may possibly be explained by sample inhomogeneity. It is possible that negative values for Ce and Nd in PCC1 are the result of a fault in matrix correction procedure, for this is common to all highly magnesian samples. Since these are usually also Cr-rich, it is difficult to separate this possible matrix effect from the effect of overlap of CrK_α onto the Ce, Nd background (section B5).

B9 : ANALYTICAL ACCURACY

Analytical accuracy is to a large extent measured by the linearity of the calibration graphs provided sufficient standards are used. In addition, a number of standards became available too late to be included in the calibration: these may be used as a measure of analytical accuracy (Table B15). Further confirmation of the accuracy of the trace element matrix correction procedure is provided by comparison (Table B16) with isotope dilution analyses of USGS standards for Rb and Sr, which is better than with the values of Abbey (1977).

Table B16 : Comparison of XRF and Isotope Dilution analyses (Pankhurst and O'Nions, 1973) for Rb and Sr.

Rb (ppm.)

	ID	XRF			Abbey (1977)
		Jan. '79	Feb. '79	April '79	
BCR1	47.3	48.4	46.7	47.9	47
AGV1	67.1	68.1	67.3	68.0	67
GSP1	254.7	255.3	256.1	254.9	250
G2	169.3	170.2	169.5	169.0	170

Sr (ppm.)

	ID	XRF			Abbey (1977)
		Jan. '79	Feb. '79	April '79	
BCR1	332.1	334.4	332.4	332.1	330
AGV1	662.0	661.1	659.4	657.6	660
GSP1	233.1	235.3	237.2	233.3	230
G2	476.3	476.4	476.9	474.7	480

In addition to the overall confirmation of accuracy, it is useful to have a check incorporated into each analysis made. For major elements, the total oxides forms such a check, for after ignition this should fall slightly less than 100%. The bulk of the analyses reported in Table B17 have totals between 99.2% and 100.2%, with the exception of a few rhyolites up to 100.8% (section B8). Discs giving totals outside this range were re-analysed.

The check chosen for trace element analyses was the analysis of TiO2 in the trace element programs, giving the values of TiO2Cr and TiO2W in Table B17, analysed respectively with the Cr-tube and W-tube trace elements. The analytical check consists of comparison between these and the TiO2 value determined on the glass disc. TiO2 was chosen because of its relatively low concentration, the high precision and accuracy of the glass disc analyses, and the ability to use mass absorption coefficients previously calculated for $TiK\alpha$. $TiK\beta$ was chosen as the analytical line because of its low intensity, the need to count on it as an interference correction for V, and because of interference on it from $VK\alpha$ and $BaL\beta_3$. This makes $TiK\beta$ comparable with the more difficult trace element lines. The high degree of linearity of both the TiO2Cr and the TiO2W calibrations (Fig. B3) is evidence for the accuracy of the $TiK\alpha$ mass absorption coefficients: the difference in linearity between these and most trace element calibrations is presumably mainly due to the greater accuracy of the Ti standard values.

Comparison between TiO2Cr, TiO2W and glass disc TiO2 is generally good, with the somewhat lower values of TiO2Cr probably due to its not being run with a monitor. Future Cr-tube trace element runs will include monitoring of TiK . A number of highly discrepant values are present, however, although the discrepancy is usually smaller for TiO2W. Particularly discrepant samples include OC93, OC94, S16, S17, S30 and S32. These pellets have been recycled, and remade, with no change, suggesting that the discrepancy is a sample effect, although samples that show it have little in common. The possibility that disc TiO2 was incorrect was eliminated by use of plasma source spectrometry on a number of samples, by Dr. J.N. Walsh of University of London Kings College. It is possible that other elements are incorrect for samples with high TiO2-TiO2W, most probably V, although it is difficult to suggest which until the reason for the Ti discrepancy is understood. The very close similarity for all elements except V and Zn between S29 (no Ti discrepancy) and S32 (high Ti discrepancy) suggests that the cause may lie in the behaviour of opaque oxides on pelleting. V and Zn data should perhaps be treated with caution for Ti discrepant samples.

B10 : DATA PROCESSING

Averaging of count ratios, calibration regressions, interference and matrix corrections were carried out using programs written by the author in the high level language

IMP (ERCC, 1974). The work was rapidly performed using the twin ICL 4-75 computers of the Edinburgh Regional Computing Centre (ERCC); forming part of the Edinburgh Multi-Access System (EMAS, ERCC, 1976). The system has a number of interactive terminals on which a user may operate his process i.e. manipulate data stored as files by transferring these from a user-restricted disc storage to a portion of active computer core. Geology user numbers begin with the letters EGEO, and programs described in the following sections are preserved as text files on EGEO07, but may be run by other EGEO users.

XRF punched paper tape output is transferred to ERCC where it is read in as a file on an EGEO process. Such a file contains no information of sample names, which are inserted in order of analysis at the beginning with separating spaces. The number '999' is inserted at the end of the file to provide an end-marker, and any XRF printing mistakes are corrected by means of the EMAS EDIT command prior to use of the programs.

The flow diagram of Fig. B4 illustrates the general course of XRF data processing from the EMAS command level, and is followed by the program listings.

(i) RATMAJ (Fig. B5)
Source file: XRFS ; Object file: XRFY
Input data: file of XRF output of program 90, with initial sample names and terminal 999 (Table B8).
Output: file of count ratios for the ten major elements for each sample (Fig. B6).
Spurious counts for peaks are detected if any of the three subsequent counts differs from the first by more than a constant (DIFF(J)) multiplied by the square root of the first count (INITP(A)).
Spurious counts for backgrounds are detected if the second count differs from the first by more than a constant amount (DIFF(J+10)).

(ii) MAJORS (Fig. B7)
Source file: XRFS ; Object file: XRFY
Input data: EITHER
File of direct XRF output from pre-sample loader program
OR: Count ratio file from RATMAJ
OR: Major element analyses (Fig. B10)
AND, in the first two cases, EITHER:
Concentrations of standards in file ANAL (Fig. B8)
OR: Calibration gradients and intercepts in file STDATA (Fig. B9)
Output: One or more of:
(a) Count ratio file (if direct XRF output used as input)
(b) Analysis file (Fig. B10). This should have LOI values inserted if samples were ignited.
(c) Norminput file (Fig. B11). This is the only output possible if analysis file is used as input.
(d) File STDATA (Fig. B9). This is updated with each new calibration.

Figure B4: Flow diagram of computer processing of XRF data.

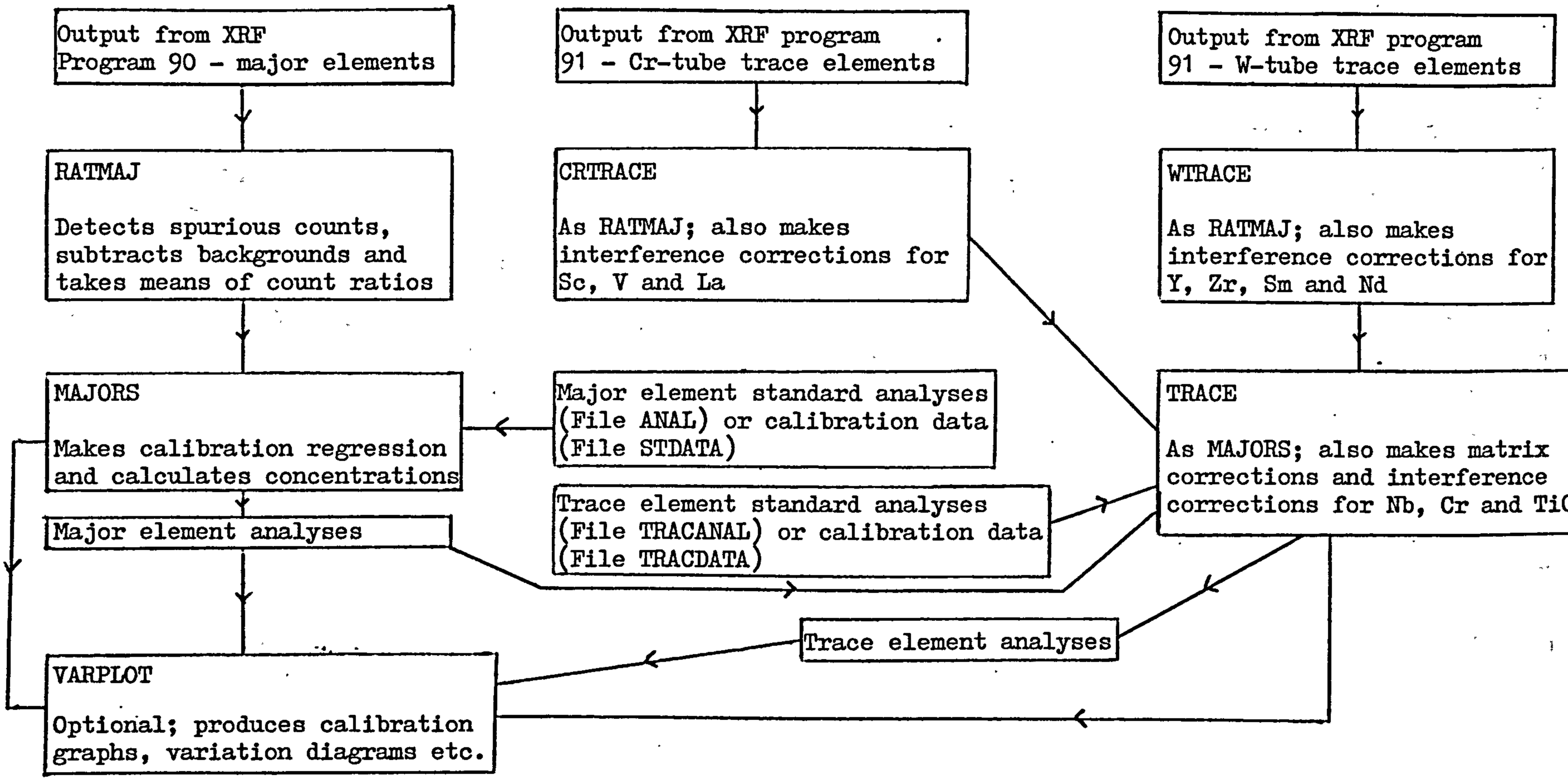

FIG. B5 : Compiled listing of program RATMAJ

```
1374    EXTERNALROUTINE RATMAJ
1375        DYNAMICROUTINESPEC PSTRG(STRINGNAME S)
1376        DYNAMICROUTINESPEC RTILLSP(STRINGNAME S)
1377        DYNAMICROUTINESPEC PROMPT(STRING(15) S)
1378        DYNAMICROUTINESPEC DEFINE(STRING(63) S)
1379        INTEGER NOSAMS,V,J,A,B,C,COUNT
1380        STRING(255) S,S1
1381        PROMPT('INPUT FILE: ');RSTRG(S)
1382        DEFINE('ST1,',S)
1383        PROMPT('CTRATIOFILE: ');RSTRG(S1)
1384        DEFINE('ST2,',S1)
1385        PROMPT('NO.OF SAMPLES: ');READ(NOSAMS)
1386        BEGIN
1387            REALARRAY CR(1:10,1:NOSAMS),RAT(1:3)
1388            CONSTREALARRAY DIFF(1:20)=1,1.3,1,1.7,.8,3.2,.8,.8,5.3,5.10,10,
1389                    20,3,100,3,5,250,40
1390             ! FACTORS USED IN DETECTION OF SPURIOUS COUNTS
1391            INTEGERARRAY Z(1:10),INITP,INITB(1:3)
1392            STRING(15) ARRAY NS(1:NOSAMS)
1393            SELECTINPUT(1)
1394             ! READS IN SAMPLE NAMES, SEPARATED BY SPACES.
1395            CYCLE V=1,1,NOSAMS
1396            RTILLSP(NS(V))
1397            REPEAT
1398            V=-3
1399        -1;CYCLE A=1,1,5
1400             RSTRG(S); IF S='999' THEN ->2
1401             ! END OF INPUT MARKER, OTHERWISE READS 5 LINES RUBBISH.
1402             REPEAT
1403             V=V+3
1404             CYCLE J=1,1,10
1405             ! 10 ELEMENTS
1406             CYCLE A=1,1,3
1407              RAT(A)=0
1408             REPEAT
1409             CYCLE C=1,1,3
1410            ! 3 PAIRS OF COUNTS FOR EACH ELEMENT.
1411             READ(Z(J))
1412             ! READS ATOMIC NUMBER OF EACH ELEMENT.
1413             CYCLE A=1,1,3
1414              READ(B)
1415             REPEAT
1416             CYCLE A=1,1,3
1417             ! 3 SAMPLES
1418             READ(COUNT); READ(B)
1419             IF C=1 THEN INITP(A)=COUNT ELSESTART
1420               IF !COUNT-INITP(A)!>DIFF(J)*SQRT(INITP(A)) START
1421            ! SPURIOUS PEAK CHECK
1422                NEWLINE
1423                PRINTSTRING('SPURIOUS COUNT FOR ELEMENT ');PRINT(Z(J),2,0)
1424                PRINTSTRING(', SAMPLE '.NS(V+A))
1425                FINISH
1426              FINISH
1427             RAT(A)=RAT(A)+COUNT
1428            ! PEAK ADDED
1429            REPEAT
1430            READ(B); READ(B)
1431            IF C=1 THEN READ(B) AND READ(B)
1432            ! PEAK
1433            CYCLE A=1,1,3
1434             READ(COUNT); READ(B)
1435             IF C=1 THEN RAT(A)=RAT(A)+COUNT ELSE RAT(A)=RAT(A)-COUNT*2
1436            ! ADD PEAK OR SUBTRACT TWICE BACKGROUND
1437            IF C=1 START
1438               IF !COUNT-INITP(A)!>DIFF(J)*SQRT(INITP(A)) START
1439                  NEWLINE
1440                  PRINTSTRING('SPURIOUS COUNT FOR ELEMENT ');PRINT(Z(J),2,0)
1441                  PRINTSTRING(', SAMPLE '.NS(V+A))
1442                  FINISH
1443               FINISH
1444               IF C=2 THEN INITB(A)=COUNT
1445               IF C=3 START
1446                  ! SPURIOUS BACKGROUND CHECK
1447                  IF !COUNT-INITB(A)!>DIFF(J+10) START
1448                     NEWLINE
1449                     PRINTSTRING('SPURIOUS COUNT FOR BACKGROUND ');PRINT(Z(J),2,0)
1450                     PRINTSTRING(', SAMPLE '.NS(V+A))
1451                     FINISH
1452                  FINISH
1453               REPEAT
1454               REPEAT
1455               CYCLE A=1,1,3
1456                RAT(A)=RAT(A)/40000
1457                CR(J,V+A)=RAT(A)
1458               REPEAT
1459               REPEAT
1460               ->1
1461            2;SELECTOUTPUT(2);SETMARGINS(2,1,130)
1462              SPACES(20)
```

FIG. B5 : continued. Program RATMAJ

```
1463            CYCLE J=1,1,10
1464            PRINT(Z(J),2,0)$SPACES(8)
1465            REPEAT
1466            NEWLINES(2)
1467            CYCLE V=1,1,NOSAMS
1468             PRINTSTRING(NS(V))$ SPACES(16-LENGTH(NS(V)))
1469            CYCLE J=1,1,10
1470             PRINT(CR(J,V),2,6)$ SPACE
1471            REPEAT
1472            NEWLINE
1473            REPEAT
1474            END

1475        END
```

FIG. B6 : Example of a major element count ratio file

	14	13	26	12	20	11	19	22	25	15
GA	1.094000	0.795325	0.138275	0.026375	0.161750	0.234650	0.474175	0.084809	0.087175	0.042225
GH	1.195800	0.681975	0.070450	0.003050	0.050025	0.258525	0.550700	0.026475	0.075900	0.003050
BR	0.587200	0.516350	0.636175	0.343975	0.910550	0.211725	0.167475	0.531375	0.155625	0.382825

FIG. B7 : Compiled listing of program MAJORS

```
70      ROUTINE INSTRG(STRINGNAME S)
71              SHORTROUTINE
72          INTEGER I
73          S=**
74          UNTIL I=NL CYCLE
75          READSYMBOL (I)
76          S=S.TOSTRING(I)
77          REPEAT
78          LENGTH(S)=LENGTH(S)-1
79          END

80      EXTERNALROUTINE RSTRG(STRINGNAME S)
81          INSTRG(S) UNTIL S#**
82          END

83      RECORDFORMAT MAJF(LONGREALARRAY STPC,STRAT(1:40),LONGREAL CALM,CALC)
84      EXTERNALRECORDARRAY CALIB(1:15) (MAJF)
85      EXTERNALSTRING(15) ARRAY ELNAME(1:15)
86      EXTERNALROUTINE MAJORS
87          DYNAMICINTEGERFNSPEC INTEGSTR(STRINGNAME S)
88          DYNAMICROUTINESPEC PRELOAD(STRING(63)S)
89          DYNAMICROUTINESPEC DEFINE(STRING(63)S)
90          DYNAMICROUTINESPEC PROMPT(STRING(15)S)
91          DYNAMICROUTINESPEC RSTRG(STRINGNAME S)
92          INTEGER B,C,J,K,V,T,G,EG,SNO,NOSAMS,BLOCK,EXIT
93          STRING(200) STANSUSED,OMIT,HT,PREL
94          STRING(200) S,S1,S2,S3,ROCK,HEAD,TAIL,ANSWER
95          LONGREALARRAY CT(0:3,1:6),PK,BG(0:3,1:10)
96          INTEGERARRAY STAN,Z(1:10),STANINIT,STANFINAL(1:15)
97          PROMPT("INPUT FILE: ");RSTRG(S3)
98          IF S3=".NULL" THEN ->60
99          ! .NULL IF INPUT IS FROM "RATMAJ" OUTPUT
100         DEFINE("ST1,".S3)
101         60:PROMPT("CTRATIO FILE: ");RSTRG(S1)
102         IF S1=".NULL" THEN ->25
103         DEFINE("ST2,".S1)
104         25:PROMPT("ANALYSIS FILE: ");RSTRG(S2)
105         IF S2=".NULL" THEN ->26
106         NEWLINE
107         PRINTSTRING("DO YOU REQUIRE LOSS ON IGNITION VALUES IN ANALYSIS")
108         PRINTSTRING(" FILE? (Y OR N)");NEWLINE
109         PROMPT("ANSWER: ");RSTRG(ANSWER)
110         DEFINE("ST3,".S2)
111         26:PROMPT("NORMINPUTFILE: ");RSTRG(S)
112         IF S=".NULL" THEN ->27
113         DEFINE("ST4,".S)
114         27:PROMPT("NO. SAMPLES: ");READ(NOSAMS)
115         IF S3=".NULL" AND S1=".NULL" THEN->35
116         NEWLINE
117         PRINTSTRING("STATE NO. OF GROUPS OF STANDARDS.")
118         ! NO. OF BATCHES OF STANDARDS IN INPUT SAMPLES
119         NEWLINE
120         PROMPT(": ");READ(BLOCK)
121         OMIT=**
122         IF BLOCK=0 THEN DEFINE("ST7,".'EGE007.STDATA") AND->35
123         ! BLOCK=0 IMPLIES NO NEW CALIBRATION
124         PROMPT("PRELOAD? ");RSTRG(PREL)
125         CYCLE Q=1,1,BLOCK
126         PRINTSTRING("STATE POSITION IN SEQUENCE OF SPECIMENS OF FIRST ")
127         PRINTSTRING("STANDARD OF GROUP ")
128         PRINT(Q,1,0);NEWLINE
129         PROMPT(": ");READ(STANINIT(Q))
130         PRINTSTRING("STATE POSITION IN SEQUENCE OF SPECIMENS OF FINAL ")
131         PRINTSTRING("STANDARD OF GROUP ")
132         PRINT(Q,1,0);NEWLINE
133         PROMPT(": ");READ(STANFINAL(Q))
134         REPEAT
135         OMIT="BR 1#;DTS1 26#;PCC1 26#;NBS99A 25#;DTS1IG 26#".C
  C                 "DTS1BIG 26#;PCC1IG 26#;PCC1BIG 26#"
136         !  ELEMENTS SHOWN FOR EACH STANDARD ARE NOT INCLUDED IN THE CALIBRATION
137         NEWLINE
138         PRINTSTRING("OMIT=".OMIT)
139         NEWLINE
140         PROMPT("CHANGE OMIT? ");RSTRG(HEAD)
141         DEFINE("ST7,".'STDATA")
142         IF HEAD="N" THEN->35
143         PROMPT("TYPE OMIT: ");RSTRG(OMIT)
144         35:DEFINE("ST6,".'EGE007.ANAL")
145         CYCLE J=1,1,10; STAN(J)=0 ; REPEAT
146         BEGIN
147             STRING(110) COUNTRATS
148             STRING(10) ARRAY NS(1:3,1:(NOSAMS//3+2))
149             LONGREALARRAY CR(0:3,1:10,1:(NOSAMS//3+2))
150             STRING(7) ARRAY ELEM(1:10)
151             ELEM(1)="SIO2"; ELEM(2)="AL2O3";  ELEM(3)="FE2O3"; ELEM(4)="MGO";
152             ELEM(5)="CAO"; ELEM(6)="NA2O"; ELEM(7)="K2O"; ELEM(8)="TIO2"
153             ELEM(9)="MNO"; ELEM(10)="P2O5"
154             IF S3=".NULL" THEN EG=NOSAMS//3+1 AND ->03
155             ! S3=".NULL" IMPLIES INPUT OF RATMAJ OUTPUT
```

FIG. B7 : continued. Program MAJORS

```
156             !
157             ! FOLLOWING LINES RELATE TO PRE-SAMPLE LOADER INPUT
158             SELECTINPUT(1)
159             IF S1=".NULL" THEN ->30
160             SELECTOUTPUT(2)%SET MARGINS(2,1,120)% SPACES(14)
161             30:EQ=0
162             01:EQ=EQ+1
163             CYCLE C=1,1,3
164             40:RSTRG(ROCK)
165             IF ROCK="999" THEN ->03
166             IF ROCK->HEAD.("<1>").TAIL THEN->40
167             IF ROCK->HEAD.("=").TAIL THEN TAIL->HEAD.(" ").ROCK
168             WHILE ROCK->(" ").ROCK CYCLE%REPEAT
169             NS(C,EQ)<-ROCK
170             REPEAT
171             IF NEXTITEM="<" THEN RSTRG(ROCK)
172             READ(Q)%RSTRG(HEAD)% CYCLE J=1,1,10
173             READ(Z(J))
174             CYCLE B=1,1,6
175             IF B=1 THEN ->02
176             READ(K)
177             02:READ(SNO)
178             CYCLE C=0,1,3
179             READ(CT(C,B))% READ(T)
180             CT(C,B)=CT(C,5)/(T/1000)
181             REPEAT%REPEAT
182             CYCLE C=0,1,3
183             PK(C,J)=(CT(C,1)+CT(C,2)+CT(C,3))/3
184             BG(C,J)=(CT(C,4)+CT(C,5)+CT(C,6))/3
185             PK(C,J)=PK(C,J)-BG(C,J)
186             REPEAT
187             CYCLE C=1,1,3
188             CR(C,J,EQ)=PK(C,J)/PK(0,J)
189             REPEAT
190             IF EQ=1 OR S1=".NULL" THEN ->09
191             PRINT(Z(J),2,0)% SPACES(7)
192             09:REPEAT
193             IF S1=".NULL" THEN ->01
194             CYCLE C=1,1,3
195             NEWLINE% IF EQ=1 AND C=1 THEN NEWLINE
196             PRINTSTRING(NS(C,EQ))% SPACES(10-LENGTH(NS(C,EQ)))
197             CYCLE J=1,1,10
198             PRINT(CR(C,J,EQ),2,6)% REPEAT% REPEAT
199             ->31
200             !
201             !
202             03:NOSAMS=(EQ-1)*3
203             STANSUSED=""
204             BEGIN
205                 STRING(7) TO
206                 INTEGER BG
207                 STRING(4) END
208                 STRING(2) A
209                 LONGREALARRAY P,R,ANALYSIS(1:10,1:NOSAMS)
210                 LONGREALARRAY MA,CX,ERR,EP,ER,ERP(1:10),LOI,TOT(1:NOSAMS)
211                 STRING(200) STNO
212                 STRING(10) ARRAY NO(1:NOSAMS)
213                 BG=-2
214                 END="-1"% A="."
215                 IF S3=".NULL" AND S1=".NULL" THEN->33
216                 IF S3=".NULL" THEN ->61
217                 CYCLE EQ=1,1,(NOSAMS//3)
218                 CYCLE C=1,1,3
219                 V=3*EQ+C-3
220                 CYCLE J=1,1,10
221                 R(J,V)=CR(C,J,EQ)% NO(V)=NS(C,EQ)
222                 REPEAT%  REPEAT
223                 REPEAT
224                 !
225                 ! START OF TREATMENT OF RATMAJ OUTPUT
226                 61:IF S3#".NULL" THEN ->62
227                 SELECTINPUT(2)
228                 CYCLE J=1,1,10% READ(Z(J))% REPEAT
229                 ! READS ATOMIC NUMBER
230                 CYCLE V=1,1,NOSAMS
231                 RTILLSP(NO(V))
232                 ! READS SAMPLE NAME
233                 CYCLE J=1,1,10
234                 READ(R(J,V))
235                 REPEAT%REPEAT
236                 ! READS TEN COUNT RATIOS
237                 62:CYCLE J=1,1,10
238                  ERR(J)=0% EP(J)=0% ER(J)=0% ERP(J)=0
239                 REPEAT
240                 IF BLOCK=0 THEN->11 ELSE ->12
241                 11:SELECTINPUT(7)
242                 ! NO RECALIBRATION, INPUT FROM STDATA
243                 CYCLE J=1,1,10
244                       RTILLSP(ELEM(J))% READ(MA(J))% READ(CX(J))
245                 ! READS ATOMIC NUMBER, CALIBRATION GRADIENT AND INTERCEPT
```

FIG. B7 : continued. Program MAJORS

```
246                 REPEAT: ->06
247                 !
248                 ! RECALIBRATION
249                 12:IF PREL='Y' THEN PRELOAD(**)
250                   CYCLE J=1,1,10
251                   ELNAME(J)=ELEM(J)
252                   REPEAT
253                   SELECTINPUT(6)
254                 ! INPUT FROM ANAL
255                 !
256                 ! GOES THROUGH EACH STANDARD IN INPUT COUNT RATIO FILE, AND TRIES TO
257                 ! FIND SAME NAME AMONG STANDARDS IN ANAL. STANDARD NAMES SHOULD BE
258                 ! EXACTLY AS WRITTEN ON DISC LABEL
259                 CYCLE Q=1,1,BLOCK
260                 CYCLE V=STANINIT(Q),1,STANFINAL(Q)
261                 05:RSTRG(STNO); IF STNO='STOP' THEN  ->13
262                 IF STNO#NO(V) THEN ->06 ELSE ->07
263                 06:RSTRG(STNO); ->05
264                 07:STANSUSED<-STANSUSED.' '.STNO
265                 ! A CORRESPONDING NAME HAS BEEN FOUND, AND IS ADDED TO A LIST OF STANDARDS
266                 ! USED IN THE CALIBRATION
267                 CYCLE J=1,1,10
268                 READ(P(J,V))
269                 ! READS 10 STANDARD PERCENT OXIDES, IN USUAL ORDER
270                 IF OMIT->HEAD.(STNO.' ').TAIL START
271                 B13:CYCLE EQ=1,1,LENGTH(TAIL)
272                      EXIT=740
273                    IF CHARNO(TAIL,EQ)=';' OR CHARNO(TAIL,EQ)=',' START
274                       HT=FROMSTRING(TAIL,1,EQ-1)
275                       IF Z(J)=INTEGSTR(HT) THEN EXIT=750 C
  C                                    AND EXIT
276                       IF CHARNO(TAIL,EQ)=';' THEN EXIT
277                       TAIL->HEAD.(',').TAIL
278                         EXIT=730;EXIT
279                       FINISH
280                    REPEAT
281                    IF EXIT=750 THEN->A13
282                      IF EXIT=730 THEN->B13
283                    FINISH
284                 ! LAST 15 LINES CAUSE EXCLUSION OF STANDARDS IN 'OMIT' FROM CALIBRATION
285                 !
286                 STAN(J)=STAN(J)+1
287                 ! STAN(J)= NO. OF STANDARDS USED IN JTH CALIBRATION
288                 CALIB(J)_STPC(STAN(J))=P(J,V)
289                 CALIB(J)_STRAT(STAN(J))=R(J,V)
290                 ! CORE STORE RECORDS SET TO STANDARD PERCENTS AND RATIOS
291                 EP(J)=EP(J)+P(J,V); ER(J)=ER(J)+R(J,V)
292                 ! EP= SUM OF PERCENTS, ER = SUM OF RATIOS
293                 ERR(J)=ERR(J)+(R(J,V))**2
294                 ERP(J)=ERP(J)+(R(J,V))*(P(J,V))
295                 ! ERR = SUM OF SQUARES OF RATIOS, ERP = SUM OF PERCENT-RATIO PRODUCTS
296                 A13:REPEAT
297                 13:SELECTINPUT(96);CLOSESTREAM(6);SELECTINPUT(6)
298                 REPEAT;REPEAT
299                 SELECTOUTPUT(7)
300                 CYCLE J=1,1,10
301                   CYCLE BQ=1,1,24
302                   IF CALIB(J)_STPC(BQ)=0 THEN CALIB(J)_STPC(BQ)=.00001
303                 ! SETS ANY REMAINING ZERO VALUES TO .00001 PREVENTS PLOTTING
304                 ! OF ZERO POINTS.
305                   REPEAT
306                 MA(J)=(STAN(J)*ERP(J)-(ER(J))*(EP(J)))/(STAN(J)*ERR(J)-(ER(J))**2)
307                 CX(J)=((EP(J))*ERR(J)-ER(J)*ERP(J))/(STAN(J)*ERR(J)-(ER(J))**2)
308                   CALIB(J)_CALM=MA(J)
309                   CALIB(J)_CALC=CX(J)
310                 ! OUTPUTTING OF NEW CALIBRATION DATA TO STDATA#4
311                 PRINTSTRING(ELEM(J));SPACES(12-LENGTH(ELEM(J)))
312                 PRINT(MA(J),4,5); SPACES(2)
313                 PRINT(CX(J),3,5); NEWLINE; REPEAT
314                 NEWLINES(2); PRINTSTRING(STANSUSED)
315                 ! PRINTS LIST OF STANDARDS USED IN CALIBRATION
316                 !
317                 08:IF S2='.NULL' THEN ->33
318                 IF ANSWER='N' THEN->NCL
319                 SELECTINPUT(98);SELECTOUTPUT(99)
320                 ! RETURNS OUTPUT/INPUT TO INTERACTIVE TERMINAL
321                 NEWLINE
322                 PRINTSTRING('LIST LOSS ON IGNITION VALUE IN RESPONSE TO PROMPT')
323                 PRINTSTRING(' OF SAMPLE NAME.')
324                 NEWLINE
325                 CYCLE V=1,1,NOSAMS
326                 PROMPT(NO(V).': ');READ(LOI(V))
327                 REPEAT
328                 !
329                 ! PRINTING OF ANALYSIS FILE
330                 NCL:SELECTOUTPUT(3); SET MARGINS(3,1,120)
331                 ELEM(3)='FE2O3T'
332                 SPACES(11)
333                 CYCLE J=1,1,10
334                 PRINTSTRING(ELEM(J));SPACES(9-LENGTH(ELEM(J)));IF J=3 THEN SPACE
```

FIG. B7 : continued. Program MAJORS

```
335                 REPEAT
336                 TO='TOTAL'
337                 SPACE
338                 PRINTSTRING(TO)
339                 IF ANSWER='N' THEN=>NL
340                 SPACES(6)
341                 PRINTSTRING('LOI')
342                 NL:NEWLINE
343                 CYCLE V=1,1,NOSAMS
344                 NEWLINES(2)
345                 TOT(V)=0
346                 PRINTSTRING(NO(V))| SPACES(9-LENGTH(NO(V)))
347                 CYCLE J=1,1,10
348                 ANALYSIS(J,V)=MA(J)+R(J,V)+CX(J)
349                 ! CALCULATES ANALYSIS AND SUMS TOTAL OXIDES
350                 TOT(V)=TOT(V)+ANALYSIS(J,V)
351                 REPEAT
352                 CYCLE J=1,1,10
353                 PRINT(ANALYSIS(J,V),3,3)|SPACE
354                 REPEAT
355                 SPACES(2)| PRINT(TOT(V),3,3)
356                 IF ANSWER='Y' THEN SPACES(4) AND PRINT(LOI(V),1,2)
357                 REPEAT
358                 NEWLINES(4)
359                 PRINTSTRING('STOP')
360                 ! 'STOP' FORMS ANALYSIS FILE TERMINATOR WHEN USED FOR MATRIX CORRECTIONS
361                 NEWLINES(8)
362                 CYCLE J=1,1,10
363                 RRINT(Z(J),2,0)|PRINT(MA(J),4,5)|PRINT(CX(J),5,5)
364                 NEWLINE
365                 REPEAT
366                 NEWLINES(2)|PRINTSTRING(STANSUSED)
367                 NEWLINES(2)|PRINTSTRING(OMIT)
368                 ! LAST SIX LINES PRINT COPY OF STDATA AT END OF ANALYSIS FILE
369                 !
370                 33:IF S='.NULL' THEN =>23
371                 SELECTOUTPUT(4)
372                 IF S3='.NULL' AND S1='.NULL' START
373                 ! TAKES ANALYSIS FILE INPUT AND PRODUCES NORMINPUT FILE
374                    SELECTINPUT(3)
375                    CYCLE J=1,1,10
376                    RTILLSP(ELEM(J))| REPEAT
377                    RSTRG(STNO)
378                    CYCLE V=1,1,NOSAMS
379                    RTILLSP(NO(V))
380                    CYCLE J=1,1,10
381                    READ(ANALYSIS(J,V))
382                    REPEAT
383                    RSTRG(STNO)
384                    REPEAT
385                    =>X23
386                    FINISH
387                 CYCLE V=1,1,NOSAMS| CYCLE J=1,1,10
388                 ANALYSIS(J,V)=MA(J)+R(J,V)+CX(J)
389                 REPEAT:REPEAT
390                 ! PRINTING OF NORMINPUT FILE
391                 X23:CYCLE V=1,1,NOSAMS
392                 ELEM(3)='FE203'
393                 PRINTSTRING(NO(V))|
394                 PRINTSTRING(A)|NEWLINE
395                 CYCLE J=1,1,10
396                 ! ROUTINE TAKES STANDARD ANALYSIS AND PUTS IT INTO ARRAY MAJ
397                 PRINTSTRING(ELEM(J))|PRINT(ANALYSIS(J,V),3,3)|SPACE
398                 IF J=5 THEN NEWLINE
399                 REPEAT
400                 NEWLINE
401                 IF V=NOSAMS THEN PRINTSTRING(END) ELSE PRINT(80,2,0)
402                 NEWLINE
403                 REPEAT
404                 23:END
405                    29:END
?   UNUSED LABEL     29
?   UNUSED NAME  COUNTRATS

406              END
```

```
AGV1IG
 60.074 17.322 6.881 1.559 5.030 4.336 2.947 1.056 0.098 0.503
BCR1IG
 54.844 13.679 13.519 3.490 6.979 3.290 1.680 2.220 0.190 0.330
DTS1IG
 40.676 0.290 8.599 49.825 0.150 0.007 0.001 0.013 0.110 0.002
```

FIG. B8 : Part of file ANAL - major element standard data

```
 14   59.72945    4.51928
 13   18.47972    0.19681
 26   20.68417   -0.10809
 12   37.66466    0.09285
 20   15.28127   -0.02784
 11   15.96797   -0.26075
 19    8.60696   -0.04338
 22    4.97556   -0.05071
 25    1.69021   -0.07403
 15    2.75345    0.00403
```

FIG. B9 : Example of file STDATA - gradients and interccpts of major element calibrations

	SIO2	AL2O3	FE2O3T	MGO	CAO	NA2O	K2O	TIO2	MNO	P2O5	TOTAL	LOI
AY1a6	63.795	18.148	3.643	1.620	3.516	4.493	3.368	1.002	0.035	0.191	99.808	1.38
AY2a13	60.810	18.150	5.642	2.275	3.605	3.838	3.587	0.992	0.036	0.190	99.124	1.75
AY3a11	50.335	17.747	7.245	5.574	12.308	3.687	1.238	1.279	0.085	0.238	99.735	8.63

FIG. B10 : Example of major element analysis file

```
AY1a6
 SIO2  63.795 AL2O3  18.148 FE2O3   3.643 MGO   1.620 CAO   3.516 NA2O   4.493
 K2O    3.368 TIO2    1.002 MNO    0.035 P2O5   0.191 LOI   1.38
 NI    15.1 CR    11.5 V   133.1 SC    15.1 CU    14.9 ZN   142.6
 SR   300.1 RB    70.4 ZR   188.2 NB     9.9 BA   532.7 TH    12.3
 LA    20.9 CE    50.9 ND    23.1 SM     5.1 Y    18.9 TIO2CR    1.078 TIO2V    1.045
-1
AY2a13
 SIO2  60.810 AL2O3  18.150 FE2O3   5.642 MGO   2.275 CAO   3.605 NA2O   3.838
 K2O    3.587 TIO2    0.992 MNO    0.036 P2O5   0.190 LOI   1.75
 NI    14.6 CR    10.0 V   124.0 SC    15.5 CU    13.9 ZN    80.8
 SR   314.5 RB    78.4 ZR   187.2 NB     8.9 BA   676.3 TH    13.5
 LA    22.8 CE    49.5 ND    22.9 SM     3.2 Y    21.2 TIO2CR    1.018 TIO2V    1.014
-1
```

FIG. B11 : Example of a norminput file, complete with major and trace element data.

(e) External records CALIB and ELNAME if option PRELOAD:Y is chosen. These records are held in core storage until log-off, and form the necessary input to program VARPLOT, if calibration graphs are to be plotted.

Calibration uses regression to solve for m^i and c^i in the equation

$$X_s^i = m^i R_s^i + c^i$$

Analogous variables in the program are i=J, s=V, X_s^i =P(J,V), R_s^i =R(J,V), m^i =MA(J), c^i =CX(J). It is assumed that precision errors on count ratios are substantially smaller than errors in the standard concentrations, and the regression has therefore been carried out by minimizing the sum of squares of errors in concentrations. This assumption is not strictly valid, but several regression procedures have been tested which have little difference in practice.

For a sample s, the error Δ_s is given by :

$$\Delta_s = mR_s + c - X_s \quad \text{for constant i}$$

so that sum of squares of errors is given by

$$\sum_1^N \Delta_s^2 = (mR_s + c - X_s)^2$$

where N = total number of standards used in ith calibration. At the minimum,

$$\partial\Sigma\Delta_s^2/\partial m = 0 \text{ , and } \partial\Sigma\Delta_s^2/\partial c = 0$$

Therefore $\sum_{s=1}^{N} 2R_s(mR_s+c-X_s)=0$ and $\sum_{s=1}^{N} 2(mR_s+c-X_s)=0$

$$m\Sigma R_s^2 + c\Sigma R_s - \Sigma R_s X_s = 0 \quad \text{and} \quad m\Sigma R_s + Nc - \Sigma X_s = 0$$

substituting into the first equation gives

$$Nm\Sigma R_s^2 + \Sigma X_s \Sigma R_s - m\Sigma R_s \Sigma R_s - N\Sigma R_s X_s = 0$$

and $$m = \frac{N\Sigma R_s X_s - \Sigma X_c \Sigma R_s}{N\Sigma R_s^2 - \Sigma R_s \Sigma R_s}$$

Converting to the variable names in the program gives

$$MA(J) = \frac{STAN(J)\cdot ERP(J) - ER(J)\cdot EP(J)}{STAN(J)\cdot ERR(J) - ER(J)\cdot ER(J)}$$

and, substituting, the value of CX(J).

(iii) CRTRACE (Fig. B12)
Source file: XRFS ; Object file XRFY
Input data: file of XRF data from Cr-tube program 91 (Table B9) with initial sample names and terminal 999.
Output data: One or both of
Count ratio file, comparable to Fig. B6, uncorrected for interferences,

Corrected file, of count ratios corrected for interference of Ca on Sc, Ti on V and La.

Spurious counts for both peak and background are detected if subsequent counts exceed the first by a constant amount (DIFF(J)).

The program is very similar to RATMAJ, but includes interference regressions. It was considered that the method of minimizing errors in one of the variables, as used for the major element calibration regression, was unsatisfactory when errors on the two variables were of the same order, and a method of regression which minimizes errors normal to the eventual line was derived as follows.

Consider a point (x_i, y_i) a short distance Δ_i away from the eventual line of equation $y=mx+c$,

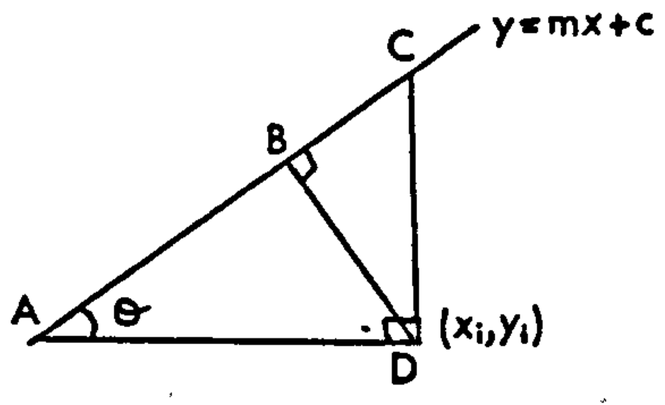

Point A has co-ordinates $(\frac{y_i-c}{m}, y_i)$
Point C has co-ordinates (x_i, mx_i+c)
Therefore,

$$CD = mx_i + c - y_i$$
and $$AD = x_i + (c-y_i)/m$$

$$BD = \Delta_i = CD\cos\theta = AD\sin\theta$$

and since $\sin^2\theta + \cos^2\theta = 1$,

$$\frac{\Delta_i^2}{CD^2} + \frac{\Delta_i^2}{AD^2} = 1$$

and sum of squares of errors

$$\sum_i \Delta_i^2 = \sum_i \frac{CD^2 \cdot AD^2}{CD^2 + AD^2} = \sum_i \frac{(mx_i + c - y_i)^2 \left(x_i + \frac{c-y_i}{m}\right)^2}{(mx_i + c - y_i)^2 + \left(x_i + \frac{c-y_i}{m}\right)^2}$$

and multiplying through by m^2,

$$\sum_i \Delta_i^2 = \sum_i \frac{(mx_i + c - y_i)}{m^2 + 1}$$

For a stationary point, $\partial\Delta_i^2/\partial m = 0$ and $\partial\Delta_i^2/\partial c = 0$

$$\sum_{i=1}^{N} \Delta_i^2 = \frac{\Sigma y_i^2 - 2m\Sigma x_i y_i + 2cm\Sigma x_i - 2c\Sigma y_i + m^2\Sigma x_i^2 + Nc^2}{m^2 + 1}$$

As before, two simultaneous equations are given

$$① \frac{\partial}{\partial c}\Delta_i^2 = \frac{2}{m^2+1}\sum_1^N (mx_i - y_i + c) = 0 \quad \Rightarrow \quad c = \frac{\Sigma y_i - m\Sigma x_i}{N}$$

$$② \frac{\partial}{\partial m}\Delta_i^2 = \frac{2}{m^2+1}\sum_1^N (cx_i - x_i y_i + mx_i^2) - \frac{2m}{(m^2+1)^2}\sum_1^N (y_i - mx_i - c)^2 = 0$$

$$\therefore \quad (m^2+1)\sum_1^N (cx_i - x_i y_i + mx_i^2) = m\sum_1^N (y_i - mx_i - c)^2$$

$$\text{or} \quad m\Sigma y_i^2 + (1-m^2)\Sigma x_i y_i + c(m^2-1)\Sigma x_i - 2cm\Sigma y_i - m\Sigma x_i^2 + Nmc^2 = 0$$

Substituting for c and multiplying through by N,

$$N m \Sigma y_i^2 + N(1-m^2)\Sigma x_i y_i + (m^2-1)(\Sigma x_i \Sigma y_i - m \Sigma x_i \Sigma x_i)$$
$$-2m \Sigma y_i (\Sigma y_i - m \Sigma x_i) - mN \Sigma x_i^2 + m(\Sigma y_i - m \Sigma x_i)^2 = 0$$

$$\therefore m^2(\Sigma y_i \Sigma x_i - N \Sigma x_i y_i) + m[N \Sigma y_i^2 + \Sigma x_i \Sigma x_i - \Sigma y_i \Sigma y_i - N \Sigma x_i^2]$$
$$+ N \Sigma x_i y_i - \Sigma y_i \Sigma x_i = 0$$

In the programs, $\Sigma y_i \Sigma x_i - N \Sigma x_i y_i$ = REA and

$N \Sigma y_i^2 - N \Sigma x_i^2 + (\Sigma x_i)^2 - (\Sigma y_i)^2$ = REB, so that

$$REA m^2 + REB m - REA = 0$$

Two values for m and c are produced, corresponding to a maximum and a minimum in the $\Sigma \Delta_i^2$ - m - c relation. The values producing minimum sum of squares of errors are determined by substitution of the two pairs of m, c values into this relation. The method of regression has been used for interference corrections in CRTRACE and WTRACE, and for the trace element calibration regressions.

By replying 'Y' to the prompt P-B/B?, it is possible to obtain output of count ratios divided by background, i.e. the Anderman-Kemp matrix correction method. This may be run for comparison between the different methods of matrix correction.

(iii) WTRACE (Fig. B13)
Source file: XRFS ; Object file: XRFY
Input data: file of XRF data from W-tube program 91 (Table B10), with initial sample names and terminal 999.
Output data: comparable to CRTRACE.

The program is very similar to CRTRACE, but spurious counts are detected in the same manner as in RATMAJ. Backgrounds are interpolated assuming linearity between two background positions.

(iv) TRACE (Fig. B14)
Source file: XRFS ; Object file: XRFY
Input data: a combination of
(a) File of direct XRF output from pre-sample loader program
(b) Count ratio file (corrected) from CRTRACE or WTRACE or an analogous program, e.g. ODDTRACE
(c) Mass absorption corrected count ratio file, previously output by TRACE
(d) Concentrations of standards in file TRACANAL (Fig. B15)
(e) Calibration gradients and intercepts in file TRACDATA (similar to STDATA)
(f) Major element compositions of samples analysed (and any others) in analysis file format (Fig. B10)
(g) Major element compositions as (f) with LOI
(h) Major element compositions as norminput file (Fig. B11)
(i) As (h) with LOI
(j) Major and trace element compositions in norminput

FIG. B12 : Compiled listing of program CRTRACE

```
1476    EXTERNALROUTINE CRTRACE
1477        DYNAMICROUTINESPEC RSTRG(STRINGNAME S)
1478        DYNAMICROUTINESPEC RTILLSP(STRINGNAME S)
1479        DYNAMICROUTINESPEC DEFINE(STRING (63) S)
1480        DYNAMICROUTINESPEC PROMPT(STRING(15) S)
1481        INTEGER NOSAMS,V,J,A,B,C,D
1482        STRING(220) S,S1,REGRESS
1483        PROMPT('INPUT FILE: ');RSTRG(S)
1484        DEFINE('ST1,'.S)
1485        PROMPT('CTRATIO FILE: ');RSTRG(S1)
1486        IF S1='.NULL' THEN->3
1487        DEFINE('ST2,'.S1)
1488        3:PROMPT('CORRECTED FILE:');RSTRG(S)
1489          DEFINE('ST3,'.S)
1490          PRINTSTRING('REGRESSION FOR INTERFERENCE CORRECTION? (Y OR N)')
1491          NEWLINE;PROMPT('ANSWER: ');RSTRG(REGRESS)
1492          ! THIS REGRESSION ONLY FEASIBLE IF SAMPLES IN FILE INCLUDE
1493             ! INTSG, INTSE, INTSA, INTSBTI, INTSATI.
1494        PROMPT('NO.OF SAMPLES: ');READ(NOSAMS)
1495        BEGIN
1496            STRING(20) ARRAY NS(1:NOSAMS)
1497        REALARRAY CA,TI(1:NOSAMS),CR(1:5,1:NOSAMS),BG(1:6,1:NOSAMS)
1498        CONSISHORTINTEGERARRAY DIFF(1:10)=30,60,200,100,50,25,30,160,30,40
1499          ! FACTORS USED IN DETECTION OF SPURIOUS COUNTS
1500        INTEGERARRAY Z(1:5),INITP,INITB,RAT(1:3)
1501        D=0
1502        SELECTINPUT(1)
1503        CYCLE V=1,1,NOSAMS
1504        RTILLSP(NS(V));CA(V)=0;TI(V)=0
1505          ! READS IN SAMPLE NAMES
1506        CYCLE B=1,1,5;BG(B,V)=0;REPEAT
1507        REPEAT;V=-3
1508        1:CYCLE B=1,1,4
1509          RSTRG(S);IF S='999' THEN->2;REPEAT
1510          ! END OF FILE MARKER
1511          V=V+3
1512        CYCLE J=1,1,5
1513          CYCLE A=1,1,3;RAT(A)=0 ;REPEAT
1514          IF J=1 OR J=2 START
1515          ! READS IN PRESET TIME CA AND TI - NEEDS CHANGING
1516        9:    CYCLE A=1,1,3
1517              READ(B);READ(B)
1518              CYCLE B=1,1,3
1519              READ(C);RAT(B)=RAT(B)+C;READ(C)
1520              REPEAT;REPEAT
1521              IF D=999 THEN->10
1522              CYCLE A=1,1,3
1523              IF J=1 THEN CA(V+A)=RAT(A)/2000000 ELSE TI(V+A)=RAT(A)
1524              REPEAT
1525              CYCLE A=1,1,3;RAT(A)=0;REPEAT
1526              IF J=1 THEN->8
1527              D=999
1528              ->9
1529           10:  CYCLE B=1,1,3
1530              TI(V+B)=(TI(V+B)+2.5*RAT(B))/200000 ; !UNITS COUNTS/MILLISEC//10
1531              BG(6,V+B)=RAT(B)/5000
1532              RAT(B)=0
1533              REPEAT
1534              D=0
1535           8:   FINISH
1536          CYCLE A=1,1,4
1537          READ(Z(J));READ(B);READ(B);READ(B)
1538          CYCLE B=1,1,3
1539          READ(C);RAT(B)=RAT(B)+C
1540          IF A=1 THEN INITP(B)=RAT(B) ELSESTART
1541              IF !C-INITP(B)!>DIFF(J) START
1542                 NEWLINE
1543                 PRINTSTRING('SPURIOUS COUNT FOR ELEMENT ');PRINT(Z(J),2,0)
1544                 PRINTSTRING(', SAMPLE '.NS(V+B))
1545                 FINISH
1546              FINISH
1547          READ(C)
1548          REPEAT;READ(B);READ(B)
1549          CYCLE B=1,1,3
1550          READ(C);RAT(B)=RAT(B)-C
1551          IF A=1 THEN INITB(B)=C ELSESTART
1552              IF !C-INITB(B)!>DIFF(J+5) START
1553                 NEWLINE
1554                 PRINTSTRING('SPURIOUS COUNT FOR BACKGROUND ');PRINT(Z(J),2,0)
1555                 PRINTSTRING(', SAMPLE '.NS(V+B))
1556                 FINISH
1557              FINISH
1558          BG(J,V+B)=BG(J,V+B)+C
1559          READ(C)
1560          REPEAT;REPEAT
1561          CYCLE A=1,1,3
1562          CR(J,V+A)=RAT(A)/40000
1563          BG(J,V+A)=BG(J,V+A)/40000
1564          REPEAT;REPEAT;->1
```

FIG. B12 : continued. Program CRTRACE

```
1565            2:IF S1="*NULL" THEN=24
1566              SELECTOUTPUT(2);SETMARGINS(2,1,130)
1567              SPACES(20)
1568              CYCLE J=1,1,5
1569              PRINT(Z(J),2,0);SPACES(8)
1570              REPEAT
1571              PRINTSTRING("CAKB         TIKB")
1572              NEWLINES(2)
1573              CYCLE V=1,1,NOSAMS
1574              PRINTSTRING(NS(V));SPACES(16-LENGTH(NS(V)))
1575              CYCLE J=1,1,5
1576              PRINT(CR(J,V),2,6);SPACE
1577              REPEAT
1578              SPACES(6);PRINT(CA(V),4,6);SPACE;PRINT(TI(V),4,6)
1579              NEWLINE;REPEAT
1580            4:BEGIN
1581                  LONGREALARRAY MA,CX(1:6),EYY,EX,EY,EXY,EXX(1:3)
1582                  INTEGER NOPOINTS;REAL REB,REA,REC
1583                  IF REGRESS="N" START
1584                     SELECTOUTPUT(99);SELECTINPUT(98)
1585                     MA(1)=.084735; MA(2)=.116606; MA(3)=.007956
1586                     ! INTERFERENCE CORRECTION GRADIENTS DERIVED BY EARLIER
1587                       ! REGRESSION (1=SC, 2=V, 3=LA)
1588                     ->5
1589                     FINISH
1590                  ! REGRESSION AS IN WTRACE
1591                  NOPOINTS=0
1592                  CYCLE C=1,1,3
1593                  EYY(C)=0;EX(C)=0;EY(C)=0;EXY(C)=0;EXX(C)=0
1594                  REPEAT
1595                  CYCLE V=1,1,NOSAMS
1596                  UNLESS NS(V)->("INT").S THEN=26
1597                  IF CHARNO(NS(V),6)="P" THEN=26
1598                  EX(1)=EX(1)+CA(V)
1599                  EX(2)=EX(2)+TI(V)
1600                  EX(3)=EX(3)+TI(V)
1601                  EXX(1)=EXX(1)+CA(V)**2
1602                  EXX(2)=EXX(2)+TI(V)**2
1603                  EXX(3)=EXX(3)+TI(V)**2
1604                  EXY(1)=EXY(1)+CA(V)*CR(1,V)
1605                  EXY(2)=EXY(2)+TI(V)*CR(2,V)
1606                  EXY(3)=EXY(3)+TI(V)*CR(5,V)
1607                  CYCLE C=1,1,3
1608                  IF C=3 THEN A=5 ELSE A=C
1609                  EY(C)=EY(C)+CR(A,V)
1610                  EYY(C)=EYY(C)+CR(A,V)**2
1611                  REPEAT
1612                  NOPOINTS=NOPOINTS+1
1613                6:REPEAT
1614                  CYCLE C=1,1,3
1615                  REB=NOPOINTS*EYY(C)-NOPOINTS*EXX(C)-EX(C)**2-EY(C)**2
1616                  REA=EY(C)*EX(C)-NOPOINTS*EXY(C)
1617                  MA(C)=(-REB+SQRT(REB**2+4*REA**2))/(2*REA)
1618                  MA(C+3)=(-REB-SQRT(REB**2+4*REA**2))/(2*REA)
1619                  CX(C)=(EY(C)-MA(C)*EX(C))/NOPOINTS
1620                  CX(C+3)=(EY(C)-MA(C+3)*EX(C))/NOPOINTS
1621                  REPEAT
1622                  SELECTOUTPUT(99);SELECTINPUT(98)
1623                  CYCLE C=1,1,3
1624                  CYCLE B=0,1,1
1625                  REC="A(C+3+B)**2+1
1626                  REC=(EYY(C)-2*MA(C+3*B)*EXY(C)+2*CX(C+3*B)*MA(C+3*B)*EX(C) C
     C                    -2*CX(C+3*B)*EY(C) C
     C                          +EXX(C)*MA(C+3*B)**2+NOPOINTS*CX(C+3*B)**2)/"EC
1627                IF B=0 THEN REA=REC
1628                  REPEAT
1629                  IF REC<REA THEN MA(C)=MA(C+3) AND CX(C)=CX(C+3)
1630                  IF C=1 THEN S="SC";IF C=2 THEN S="V";IF C=3 THEN S="LA"
1631                  PRINTSTRING("INTERFERENCE CORRECTION FOR "."S."."IS")
1632                  PRINT(MA(C),2,6)
1633                  PRINTSTRING(" COUNT RATIO "."S."." PER UNIT INTEPFERING ELEMENT")
1634                  NEWLINE
1635                PRINTSTRING("INTERCEPT OF CORRECTION IS AT COUNT RATIO ")
1636                  PRINT(CX(C),2,6)
1637                  NEWLINE
1638                  REPEAT
1639               5:NEWLINE; PRINTSTRING("LA CORRECTION? (Y OR N)")
1640                  ! LA CORRECTION PERHAPS NOT NEEDED IF FINE COLLIMATOR USED.
1641                  NEWLINE; PROMPT(": ");RSTRG(REGRESS)
1642                  PROMPT("P-B/B? ");RSTRG(S1)
1643                  ! "Y" FOR ANDERMAN-KEMP CORRECTION
1644                  SELECTOUTPUT(3);SETMARGINS(3,1,130);SPACES(20)
1645                  CYCLE J=1,1,5;PRINT(Z(J),2,3);SPACES(8);REPEAT
1646                  PRINTSTRING("17")
1647                  NEWLINES(2)
1648                  CYCLE V=1,1,NOSAMS
1649                  CR(1,V)=CR(1,V)-"A(1)*CA(V)
1650                  CR(2,V)=CR(2,V)-"A(2)*TI(V)
1651                  IF REGRESS="N" THEN=27
1652                  CR(5,V)=CR(5,V)-"A(3)*TI(V)
```

FIG. B12 : continued. Program CRTRACE

```
1653                7:PRINTSTRING(NS(V));SPACES(16-LENGTH(NS(V)))
1654                  IF S1="Y" THEN TI(V)=TI(V)/PG(6,V)
1655                  CYCLE J=1,1,5
1656                  IF S1="Y" THEN CR(J,V)=CR(J,V)/PG(J,V)
1657                  ! ANDERMAN-KEMP CORRECTION
1658                  PRINT(CR(J,V),2,6);SPACE
1659                  REPEAT
1660                  PRINT(TI(V),4,6)
1661                  NEWLINE
1662                  REPEAT
1663                  END

1664              END

1665        END
```

FIG. B13 : Compiled listing of program WTRACE

```
1666    EXTERNALROUTINE WTRACE
1667        DYNAMICROUTINESPEC RSTRG(STRINGNAME S)
1668        DYNAMICROUTINESPEC RTILLSP(STRINGNAME S)
1669        DYNAMICROUTINESPEC DEFINE(STRING (63) S)
1670        DYNAMICROUTINESPEC PROMPT(STRING(15) S)
1671        INTEGER NOSAMS,V,J,A,B,C,BUNG,INDTIME,THMON
1672        LONGREAL RE1,RE2
1673        STRING(200) S,S1,REGRESS,PB
1674        PROMPT("INPUT FILE: ");RSTRG(S)
1675        DEFINE("ST1,".S)
1676        PROMPT("CTRATIO FILE: ");RSTRG(S1)
1677        IF S1=".NULL" THEN->3
1678        DEFINE("ST2,".S1)
1679        3:PROMPT("CORRECTED FILE:");RSTRG(S)
1680          DEFINE("ST3,".S)
1681          PRINTSTRING("REGRESSION FOR INTERFERENCE CORRECTION? (Y OR N)")
1682          NEWLINE;PROMPT("ANSWER: ");RSTRG(REGRESS)
1683          ! REGRESSION ONLY POSSIBLE IF WIDE RANGE OF INTERFERENCE STANDARDS
1684              ! INCLUDED
1685        PROMPT("NO.OF SAMPLES: ");READ(NOSAMS)
1686        BEGIN
1687            STRING(20) ARRAY NS(1:NOSAMS)
1688            REALARRAY CR(1:13,1:NOSAMS),INITP,INITB,RAT(1:3),TIME(1:13) C
   C              ,BG(1:13,1:NOSAMS)
1689            CONSTREALARRAY DIFF(1:26)=1.3,1.3,.5,.8,1,.8,.8,1,.7,2.3,1.7,2.5,
1690                  15,15,0,20,0,70,0,70,0,0,120,100,35
1691              ! FACTORS USED IN DETECTION OF SPURIOUS COUNTS
1692            INTEGERARRAY Z,MONCOUNT(1:13),THB(1:3)
1693            SELECTINPUT(1)
1694            CYCLE V=1,1,NOSAMS
1695            CYCLE J=1,1,13
1696            BG(J,V)=0
1697            REPEAT
1698            RTILLSP(NS(V))
1699            REPEATV=-3
1700            BUNG=3
1701            !
1702            B1:V=V+BUNG
1703              BUNG=0
1704            1:"STRG(S)
1705              WHILE S->(" ").S CYCLE; REPEAT
1706              IF S="999" THEN->22
1707              !END OF FILE MARKER
1708              IF S="91" THEN->A1
1709              ! 91 - BEGINNING OF CYCLE MARKER
1710              BUNG=BUNG+1
1711              ! LAST 5 LINES COUNT NUMBER OF SAMPLES (BUNG) IN NEW CYCLE
1712              ->1
1713            A1:CYCLE J=1,1,13
1714              TIME(J)=0
1715              REPEAT
1716            !
1717              CYCLE J=1,1,13
1718              ! 13 ELEMENTS
1719              IF J=3 OR J=9 THEN RSTRG(S)
1720              CYCLE A=1,1,BUNG
1721              RAT(A)=0
1722              REPEAT
1723              IF J=1 OR J=2 OR J=9 OR J=11 OR J=13 START
1724                 CYCLE A=1,1,4
1725              ! 4 PEAK-BACKGROUND PAIRS: NI, ZN, CR, SM, TIO2W
1726                 READ(Z(J));READ(B);READ(B);READ(B)
1727                 CYCLE B=1,1,BUNG
1728              ! BUNG SAMPLES
1729                 READ(C);RAT(B)=RAT(B)+C
1730                 IF A=1 THEN INITP(B)=C ELSESTART
1731              ! INITIAL PEAK SET ON FIRST PK/BG PAIR, OTHERWISE SPURIOUS COUNT CHECK
1732                     IF !C-INITP(B)!>DIFF(J)*SQRT(INITP(B)) START
1733                        NEWLINE
1734                        PRINTSTRING("SPURIOUS COUNT FOR ELEMENT ");PRINT(Z(J),2,0)
1735                        PRINTSTRING(", SAMPLE ".NS(V+B))
1736                        FINISH
1737                     FINISH
1738                 READ(C)
1739                 REPEAT
1740                 READ(B);READ(B)
1741                 CYCLE B=1,1,BUNG
1742                 IF J=9 START
1743            ! CR
1744                     READ(C)
1745                     IF A=1 OR A=2 START
1746                        BG(9,V+B)=BG(9,V+B)+2*(6924-6850)*C/(706R-6850)
1747             ! CR- 2 BACKGROUND POSITIONS
1748                     RAT(B)=RAT(B)-2*(6924-6850)*C/(706R-6850)
1749                     IF A=1 THEN INITB(B)=C ELSESTART
1750                        IF !C-INITB(B)!>5 START
1751                           NEWLINE
1752                           PRINTSTRING("SPURIOUS COUNT FOR BACKGROUND 24,")
1753                           PRINTSTRING("SAMPLE ".NS(V+B))
```

FIG. B13 : continued. Program WTRACE

```
1754                              FINISH
1755                           FINISH
1756                        FINISH
1757                     IF A=3 OR A=4 START
1758                        RAT(B)=RAT(B)-2*(7068-6924)*C/(7068-6850)
1759                        BG(9,V+B)=BG(9,V+B)+2*(6924-6850)*C/(7068-6850)
1760                        IF A=3 THEN INITB(B)=C ELSESTART
1761                           IF !C-INITB(B)!>6 START
1762                              NEWLINE
1763                              PRINTSTRING('SPURIOUS COUNT FOR BACKGROUND 24,')
1764                              PRINTSTRING('SAMPLE '.NS(V+B))
1765                              FINISH
1766                           FINISH
1767                        FINISH
1768                     ->C1
1769                     FINISH
1770                  ! IF J ISN'T CR THEN NEXT 9 LINES EXECUTED
1771                     READ(C);RAT(B)=RAT(B)-C
1772                     BG(J,V+B)=BG(J,V+B)+C
1773                     IF A=1 THEN INITB(B)=C ELSESTART
1774                        IF !C-INITB(B)!>DIFF(J+13) START
1775                           NEWLINE
1776                           PRINTSTRING('SPURIOUS COUNT FOR BACKGROUND ')
1777                            PRINT(Z(J),2,0);PRINTSTRING(', SAMPLE '.NS(V+B))
1778                            FINISH
1779                        FINISH
1780               C1:   READ(C)
1781                     REPEAT;REPEAT
1782                     CYCLE B=1,1,BUNG
1783                     CR(J,V+B)=RAT(B)/40000
1784                     BG(J,V+B)=BG(J,V+B)/40000
1785                     REPEAT
1786                     FINISH
1787                  IF J=3 OR J=5 OR J=7 OR J=10 START
1788                  ! TH, SR, ZR, CE - ALL HAVE NO BACKGROUNDS
1789                     CYCLE A=1,1,4
1790                     READ(Z(J));READ(C);READ(MONCOUNT(J));READ(INDTIME)
1791                     TIME(J)=TIME(J)+INDTIME/4
1792                  ! TIME COUNTED FOR EACH ELEMENT AND MONITOR COUNT READ IN.
1793                     CYCLE B=1,1,BUNG
1794                     READ(C);RAT(B)=RAT(B)+C
1795                     IF A=1 THEN INITP(B)=C ELSESTART
1796                        IF !C-INITP(B)!>DIFF(J)*SQRT(INITP(B)) START
1797                           NEWLINE
1798                           PRINTSTRING('SPURIOUS COUNT FOR ELEMENT ');PRINT(Z(J),2,0)
1799                           PRINTSTRING(', SAMPLE '.NS(V+B))
1800                           FINISH
1801                        FINISH
1802                     READ(C)
1803                     REPEAT;REPEAT
1804                     CYCLE B=1,1,BUNG
1805                     CR(J,V+B)=RAT(B)/40000
1806                     REPEAT
1807                     FINISH
1808               IF J=4 START
1809                  ! RB, FIRSTLY A SET OF EXTRA BACKGROUNDS (THB) FOR TH IS READ IN
1810                     READ(C);READ(C)
1811                     CYCLE B=1,1,BUNG
1812                     READ(THB(B))
1813                     READ(THMON)
1814                  ! TIME ON TH BACKGROUND
1815                     REPEAT
1816                     FINISH
1817                  IF J=4 OR J=6 OR J=8 OR J=12 START
1818                  ! RB, Y, NB, ND: 4PK, 4BG WHICH MUST BE USED FOR OTHER ELEMENTS
1819                     CYCLE A=1,1,4
1820                     READ(Z(J));READ(C);READ(MONCOUNT(J));READ(INDTIME)
1821                     TIME(J)=TIME(J)+INDTIME/4
1822                  ! MONITOR COUNTS AND TIME
1823                     CYCLE B=1,1,BUNG
1824                     READ(C);RAT(B)=RAT(B)+C
1825                  IF A=1 THEN INITP(B)=C ELSESTART
1826                     IF !C-INITP(B)!>DIFF(J)*SQRT(INITP(B)) START
1827                        NEWLINE
1828                        PRINTSTRING('SPURIOUS COUNT FOR ELEMENT ');PRINT(Z(J),2,0)
1829                        PRINTSTRING(', SAMPLE '.NS(V+B))
1830                        FINISH
1831                     FINISH
1832               READ(C)
1833               REPEAT
1834               READ(C);READ(C)
1835               CYCLE B=1,1,BUNG
1836               READ(C);BG(J,V+B)=BG(J,V+B)+C
1837               IF A=1 THEN INITB(B)=C ELSESTART
1838                  IF !C-INITB(B)!>DIFF(J+13) START
1839                     NEWLINE
1840                     PRINTSTRING('SPURIOUS COUNT FOR BACKGROUND ')
1841                     PRINT(Z(J),2,0);PRINTSTRING(', SAMPLE '.NS(V+B))
1842                     FINISH
1843                  FINISH
```

FIG. B13 : continued. Program WTRACE

```
1844                READ(C)
1845                REPEAT;REPEAT
1846                CYCLE B=1,1,BUNG
1847                CR(J,V+B)=PAT(B)/40000
1848                BG(J,V+B)=BG(J,V+B)/40000
1849                REPEAT
1850                FINISH
1851              REPEAT
1852              CYCLE P=1,1,BUNG
1853             ! CALCULATIONS OF BACKGROUNDS FOR 3=TH, 4=RB, 5=SR, 6=Y, 7=ZR, 8=NB
1854               ! 10=CE, USING PEAK AND BACKGROUND ANGLES AND BACKGROUND
1855              ! COUNTS, TIMES AND MONITOR COUNTS.
1856            BG(3,V+B)=((.00005*THB(B)+.5*(BG(4,V+B)*MONCOUNT(4)*TIME(3)/(TIME(4) &
   C                 *MONCOUNT(3))))*(2737-2416)*(2860-2737)+(BG(6,V+B)*TIME(3) &
   C                  *MONCOUNT(6)/(TIME(6)*MONCOUNT(3))))/(2860-2416)
1857              RE1=(BG(4,V+B)*(2651-2416)+(2860-2651)*(BG(6,V+B) &
   C                 *MONCOUNT(6)*TIME(4)/(TIME(6)*MONCOUNT(4))))/(2860-2416)
1858              BG(5,V+B)=((BG(4,V+B)*MONCOUNT(4)*TIME(5)/(TIME(4) &
   C                 *MONCOUNT(5)))*(2504-2416)+(2860-2504)*(BG(6,V+B)*TIME(5) &
   C                  *MONCOUNT(6)/(TIME(6)*MONCOUNT(5))))/(2860-2416)
1859              RE2=(BG(6,V+B)*(2368-2090)+(2416-2368)*(BG(8,V+B) &
   C                 *MONCOUNT(8)*TIME(6)/(TIME(8)*MONCOUNT(6))))/(2416-2090)
1860              BG(7,V+B)=((BG(6,V+B)*MONCOUNT(6)*TIME(7)/(TIME(6)* &
   C                  MONCOUNT(7)))*(2245-2090)+(2416-2245)*(BG(8,V+B)*TIME(7)* &
   C                  MONCOUNT(8)/(TIME(8)*MONCOUNT(7))))/(2416-2090)
1861              BG(8,V+B)=((BG(6,V+B)*MONCOUNT(6)*TIME(8)/(TIME(6)* &
   C                  MONCOUNT(8)))*(2130-2090)+(2416-2130)*BG(8,V+5))/(2416-2090)
1862              BG(10,V+B)=BG(12,V+B)*MONCOUNT(12)*TIME(10)/(TIME(12)* &
   C                  MONCOUNT(10))
1863              BG(4,V+B)=RE1;BG(6,V+B)=RE2
1864              ! NEXT 5 LINES SUBTRACT BACKGROUNDS
1865              CYCLE J=3,1,8
1866              CR(J,V+B)=CR(J,V+B)-BG(J,V+B)
1867              REPEAT
1868              CR(10,V+B)=CR(10,V+B)-BG(10,V+B)
1869              CR(12,V+B)=CR(12,V+B)-BG(12,V+B)
1870              REPEAT
1871              ->91
1872            2:IF S1="."NULL" THEN->4
1873              ! NEXT 13 LINES PRINT FILE OF UNCORRECTED COUNT RATIOS.
1874              SELECTOUTPUT(2);SETMARGINS(2,1,130)
1875              SPACES(16)
1876              CYCLE J=1,1,13
1877              IF Z(J)=25 THEN Z(J)=17
1878              PRINT(Z(J),2,0);SPACES(8)
1879              REPEAT
1880              NEWLINES(2)
1881              CYCLE V=1,1,NOSAMS
1882              PRINTSTRING(NS(V));SPACES(12-LENGTH(NS(V)))
1883              CYCLE J=1,1,13
1884              PRINT(CR(J,V),2,6);SPACE
1885              REPEAT
1886              NEWLINE;REPEAT
1887            4:BEGIN
1888                LONGREALARRAY MA,CX(6:13),EYY,EX,EY,EXY,EXX(6:9)
1889                INTEGERARRAY NOP(6:9)
1890                REAL REB,REA,REC
1891                IF REGRESS="N" START
1892                  MA(6)=.359550; MA(7)=.093729
1893                  MA(8)=.024535; MA(9)=.032563
1894                 ! INTERFERENCE CORPECTION GRADIENTS DETERMINED IN A PREVIOUS
1895                  ! REGRESSION: 6=RB ON Y, 7=SR ON ZR, 8=CE ON SM, 9=CE ON NC.
1896                  SELECTOUTPUT(99);SELECTINPUT(98)
1897                  ->5
1898                  FINISH
1899                CYCLE C=6,1,9
1900                EYY(C)=0;EX(C)=0;EY(C)=0;EXY(C)=0;EXX(C)=0;NOP(C)=0
1901                REPEAT
1902                CYCLE V=1,1,NOSAMS
1903                ! CYCLE THROUGH TOTAL NUMBER OF SAMPLES
1904                UNLESS NS(V)->("INT").S THEN->6
1905                ! IF SAMPLE NAME DOESN'T START WITH "INT" THEN EXCLUDE FROM REGRESSION
1906                IF LENGTH(NS(V))<6 THEN->6
1907                ! IF ONLY 5 OR LESS CHARACTERS IN SAMPLE NAME EXCLUDE FROM REGRESSION
1908                IF CHARNO(NS(V),6)="T" THEN->6
1909                IF CHARNO(NS(V),6)="B" THEN->8
1910                ! USE "A" SERIES INTERFERENCE STANDARDS FOR Y, ZR.
1911                CYCLE C=6,1,7
1912                EX(C)=EX(C)+CR(C-2,V)
1913                ! X=RB,SR
1914                EY(C)=EY(C)+CR(C,V)
1915                ! Y=Y, ZR
1916                EXX(C)=EXX(C)+CR(C-2,V)**2
1917                EYY(C)=EYY(C)+CR(C,V)**2
1918                EXY(C)=EXY(C)+CR(C,V)*CR(C-2,V)
1919                NOP(C)=NOP(C)+1
1920                REPEAT
1921                ->6
1922              8:CYCLE C=8,1,9
1923                ! USE B SERIES INTERFERENCE STANDARDS FOR SM, NB
```

FIG. B13 : continued. Program WTRACE

```
1924                EX(C)=EX(C)+CR(10,V)
1925                ! X=CE
1926                EY(C)=EY(C)+CR(C+3,V)
1927               ! Y=SM, ND
1928                EXX(C)=EXX(C)+CR(10,V)**2
1929                EYY(C)=EYY(C)+CR(C+3,V)**2
1930                EXY(C)=EXY(C)+CR(10,V)*CR(C+3,V)
1931                NOP(C)=NOP(C)+1
1932                REPEAT
1933              6:REPEAT
1934                CYCLE C=6,1,9
1935                REB=NOP(C)*EYY(C)-NOP(C)*EXX(C)*EX(C)**2-EY(C)**2
1936                REA=EY(C)*EX(C)-NOP(C)*EXY(C)
1937                MA(C)=(-REB+SQRT(REB**2+4*REA**2))/(2*REA)
1938                MA(C+4)=(-REB-SQRT(REB**2+4*REA**2))/(2*REA)
1939                CX(C)=(EY(C)-MA(C)*EX(C))/NOP(C)
1940                CX(C+4)=(EY(C)-MA(C+4)*EX(C))/NOP(C)
1941                ! LAST 6 LINES - CALCULATION OF 2 GRADIENT-INTERCEPT PAIRS
1942                REPEAT
1943                SELECTOUTPUT(99);SELECTINPUT(98)
1944                CYCLE C=6,1,9
1945                CYCLE B=0,1,1
1946                REC=MA(C+4*B)**2+1
1947                REC=(EYY(C)-2*MA(C+4*B)*EXY(C)+2*CX(C+4*B)*MA(C+4*B)*EX(C) C
   C                   -2*CX(C+4*B)*EY(C) C
   C                         +EXX(C)*MA(C+4*B)**2+NOP(C)*CX(C+4*B)**2)/REC
1948              IF B=0 THEN REA=REC
1949                REPEAT
1950                IF REC<REA THEN MA(C)=MA(C+4) AND CX(C)=CX(C+4)
1951                ! LAST 9 LINES - SELECTION OF M/C PAIR GIVING MINIMUM
1952                IF C=6 THEN S="Y";IF C=7 THEN S="ZR";IF C=8 THEN S="SM"
1953                IF C=9 THEN S="ND"
1954                PRINTSTRING("INTERFERENCE CORRECTION FOR ".S." IS")
1955                PRINT(MA(C),2,6)
1956                PRINTSTRING(" COUNT RATIO ".S." PER UNIT INTERFERING ELEMENT")
1957                NEWLINE
1958               PRINTSTRING("INTERCEPT OF CORRECTION IS AT COUNT RATIO ")
1959                PRINT(CX(C),2,6)
1960                NEWLINE
1961                REPEAT
1962              5:PROMPT("P-B/E? ");RSTRG(PB)
1963                ! ANDERMAN-KEMP CORRECTION
1964                SELECTOUTPUT(3);SETMARGINS(3,1,130);SPACES(13)
1965               ! PRINTING OF FILE OF CORRECTED COUNT RATIOS.
1966                CYCLE J=1,1,13;PRINT(Z(J),2,0);SPACES(5);REPEAT
1967                IF Z(J)=25 THEN Z(J)=17
1968                NEWLINES(2)
1969                CYCLE V=1,1,NOSAMS
1970                CYCLE C=6,1,7
1971                CR(C,V)=CR(C,V)-MA(C)*CR(C-2,V)
1972                REPEAT
1973                CYCLE C=8,1,9
1974                CR(C+3,V)=CR(C+3,V)-MA(C)*CR(10,V)
1975                REPEAT
1976                ! LAST 6 LINES MAKE INTERFERENCE CORRECTIONS
1977                PRINTSTRING(NS(V));SPACES(9-LENGTH(NS(V)))
1978                CYCLE J=1,1,13
1979                IF PB="Y" THEN CR(J,V)=CR(J,V)/BG(J,V)
1980                ! ANDERMAN-KEMP CORRECTION MADE IF REQUIRED
1981                PRINT(CR(J,V),2,6)
1982                REPEAT
1983                NEWLINE
1984                REPEAT
1985                END

1986              END

1987        END

1988    ENDOFFILE
```

FIG. B14 : Compiled listing of program TRACE

```
407     EXTERNALREALFN REALSTR(STRINGNAME S)
408         REAL RE; INTEGER A,B
409         RE=0
410         1:CYCLE A=1,1,LENGTH(S)
411           IF CHARNO(S,A)=*'.' THENEXIT
412           REPEAT
413           IF A=LENGTH(S) AND CHARNO(S,A)#*'.' THEN S=S.*'.0' AND->21
414           IF A=1 THEN S=*'0'.S AND->21
415           CYCLE B=1,1,A-1
416           RE=RE+(CHARNO(S,B)-48)*(10**(A-1-B))
417           REPEAT
418           CYCLE B=A+1,1,LENGTH(S)
419           RE=RE+(CHARNO(S,B)-48)*(10**(A-B))
420           REPEAT
421           RESULT=RE
422           END

423     EXTERNALROUTINE TRACE
424         ROUTINE ANALY(STRING(255)S,LONGREALARRAYNAME MAJ,INTEGER V)
425             INTEGER I
426             STRING(47)S1
427             CYCLE I=1,1,14
428             S->S1.(* *).S
429               IF I>=11 THEN MAJ(I+1,V)=REALSTR(S1) ELSE MAJ(I,V)=REALSTR(S1)
430             REPEAT
431             END

432         DYNAMICINTEGERFNSPEC INTEGSTR(STRINGNAME S)
433         DYNAMICROUTINESPEC PRELOAD(STRING(63) S)
434         DYNAMICROUTINESPEC DEFINE(STRING(63)S)
435         DYNAMICROUTINESPEC PROMPT(STRING(15)S)
436         DYNAMICROUTINESPEC RSTRG(STRINGNAME S)
437         INTEGER NOSAMS,BLOCK,EG,A,ZBG,ZBPVS,NOELS,B,V,NOEL,ZBP,COUNT,T,Y,K
438         INTEGER ANALF,FG
439         INTEGERARRAY STAN(1:20)
440         INTEGER ECOUNTS,ZA
441         LONGREALARRAY ECC,EP,EC,ECP,EPP(1:20),MA,CX(1:2,1:20),REC(1:2)
442         LONGREAL PA,REA,REB
443         INTEGERARRAY STANINIT,STANFINAL(0:20),Z,THETAP,THETA1,THETA2(1:20)
444         STRING(255) CPS,STANSUSED,STNO,OMIT,HEAD,TAIL,MT,STANSPRES,LT
445         STRING(200) S1,S2,S3,S4,ROCK,NSZB,ANSWER,S5,PREL,S6
446         ANALF=0;COUNT=0
447         STANSUSED=**;STANSPRES=**
448         PROMPT(*INPUT FILE: *);RSTRG(S1)
449         IF S1=*.NULL* THEN->21
450         DEFINE(*ST1,*.S1)
451         1:PROMPT(*CRATIO FILE: *);RSTRG(S2)
452           ! INPUT FROM WTRACE OR CRTRACE
453           IF S2=*.NULL* THEN->2
454           DEFINE(*ST2,*.S2)
455         2:PROMPT(*CORRECTED FILE:*);RSTRG(S6)
456            ! MASS ABSORPTION CORRECTED COUNT RATIOS (INPUT OR OUTPUT)
457           IF S6=*.NULL* THEN->A2
458           DEFINE(*ST4,*.S6)
459         A2:PROMPT(*ANALYSIS FILE: *);RSTRG(S3)
460           IF S3=*.NULL* THEN->3
461           DEFINE(*ST3,*.S3)
462         3:PROMPT(*NORMINPUTFILE: *);RSTRG(S5)
463           IF S5=*.NULL* THEN->33
464           DEFINE(*ST9,*.S5)
465         33:DEFINE(*ST5,*.*EGEOG7.TRACANAL*)
466         ! ATOMIC NUMBERS FOR WHICH NAMED STANDARD IS NOT TO BE USED IN CALIBRATION
467           OMIT=*SY3 21,57,39;GSM 57,60,62;PCC1 56,57,28,24;UBN 28,24;JS1 41;*.C
  C                *TAN21 21,57,39;JG1 41,60;GSP1 57,58,60,62;*. C
  C           *INTSBA2 24,60,58;FKN 30,39;GH 30;INTSGA2 60,58;*. C
  C             *INTSBB2 57,21;INTSGB2 57,21;INTSBB3 21;INTSGB3 21;*
468           DEFINE(*ST7,*.*.*TEMP*)
469           IF S2=*.NULL* AND S6=*.NULL* THEN ANSWER=*N* AND->212
470           ! REFERS TO INPUT FROM MU-CORRECTED FILE
471           NEWLINE
472           PRINTSTRING(*DO YOU REQUIRE MASS ABSORPTION CORRECTIONS? (Y OR N)*)
473           NEWLINE
474           PROMPT(*ANSWER: *);RSTRG(ANSWER)
475           IF ANSWER=*N* THEN->212
476           NEWLINE
477           PRINTSTRING(*STATE MAJOR ELEMENT ANALYSIS FILE FOR M.A. CORRECTIONS.*)
478           NEWLINE
479           PROMPT(*: *);RSTRG(S4)
480           DEFINE(*ST8,*.S4)
481         12:PROMPT(*NO. SAMPLES: *);READ(NOSAMS)
482           NEWLINE
483           PRINTSTRING(*STATE NO. OF GROUPS OF STANDARDS*)
484           NEWLINE
485           PROMPT(*: *);READ(BLOCK)
486           IF BLOCK=0 THEN DEFINE(*ST6,*.*EGEOG7.TRACDATA*) AND->24
487           PROMPT(*PRELOAD? *);RSTRG(PREL)
488           DEFINE(*ST6,*.*TRACDATA*)
489           CYCLE A=1,1,BLOCK
490           PRINTSTRING(*STATE POSITION IN SEQUENCE OF SPECIMENS OF FIRST *)
```

FIG. B14 : continued. Program TRACE

```
491         PRINTSTRING('STANDARD OF GROUP ')
492           PRINT(A,1,0);NEWLINE
493           PROMPT(': ');READ(STANINIT(A))
494           PRINTSTRING('STATE POSITION IN SEQUENCE OF SPECIMENS OF FINAL ')
495         PRINTSTRING('STANDARD OF GROUP ')
496           PRINT(A,1,0);NEWLINE
497           PROMPT(': ');READ(STANFINAL(A))
498           REPEAT
499           PRINTSTRING('OMIT='.OMIT);NEWLINE
500           PROMPT('CHANGE OMIT? ');RSTRG(NSZB)
501           IF NSZB='Y' THEN PROMPT('TYPE OMIT: ') AND RSTRG(OMIT)
502         4:EQ=0;ZBPNS=0;Y=0
503         35:BEGIN
504               STRING(10)ARRAY NS(1:(NOSAMS+4)),ELEM(1:20),MAJEL(1:18)
505               CONSTREALARRAY MUFUDGE(1:9)=.908,.928,.987,.992,1.1.008,1.016,
506                     1.024,.918
507               ! FACTORS RELATING TO NON-LINEARITY OF MU WITH WAVELENGTH-CUBED
508               ! THESE RELATE TO NI, ZN, TH, RB, SR, Y, ZR, NB, CU IN ORDER
509             LONGREAL MU2,MU3
510             LONGREALARRAY ECOUNT(1:4),BG1,BG2,P,PK(1:(NOSAMS+4),1:20),
C                  LOI(1:(NOSAMS+4)),MAJ(1:18,1:NOSAMS),MU1(1:9)
511           CONSTREALARRAY COEF1(1:10)=7.08,6.5,48.7,5.88,26.3,5.43,26.7,
512               26.1,48.8,7.9
513             ! OXIDE MU-COEFFICIENTS AT SR KA; ! MAJOR ELEMENT ORDER AS USUAL
514           CONSTREALARRAY COEF2(1:10)=105.6,97,90.5,87.6,340.1,80.5,343.7,
515               364.5,86.9,117.7
516             ! OXIDE COEFFICIENTS AT CRKA
517           CONSTREALARRAY COEF3(1:10)=176.6,162.1,148.9,146.4,553.3,134.3,
518                   558.8,93.4,142.8,196.8
519             ! OXIDE COEFFICIENTS AT TIKA
520             CYCLE V=1,1,NOSAMS
521             LOI(V)=0
522             CYCLE NOEL=1,1,18
523             MAJ(NOEL,V)=0
524             REPEAT;REPEAT
525             MAJEL(1)='SIO2';MAJEL(2)='AL203';MAJEL(3)='FE203'
526             MAJEL(4)='MGO';MAJEL(5)='CAO';MAJEL(6)='NA20';MAJEL(7)='K20'
527             MAJEL(8)='TIO2';MAJEL(9)='MNO';MAJEL(10)='P205';MAJEL(11)=''
528             MAJEL(12)='LOI';MAJEL(13)='V';MAJEL(14)='LA';MAJEL(15)='BA'
529             MAJEL(16)='SC';MAJEL(17)='CU';MAJEL(18)='TIO2CR'
530             ! MAJEL(11) IS TOTAL OXIDES
531             IF S1='.NULL' THEN->24
532             ! UNTIL LABEL 24 REFERS TO PRE-SAMPLE LOADER RUNS
533             CYCLE V=1,1,(NOSAMS+4)
534             CYCLE A=1,1,20
535             BG1(V,A)=0
536             REPEAT;REPEAT
537             SELECTINPUT(1);->5
538           14:Z(NOEL)=ZBG
539             CYCLE B=1,1,4
540             V=(EQ-1)*4+B
541             PK(V,NOEL)=ECOUNT(B)/ECOUNTS
542             REPEAT
543           5:EQ=EQ+1
544             ZBG=0
545             CYCLE B=1,1,4
546             IF Y=1 THEN ROCK=NSZB AND Y=0 ELSE RSTRG(ROCK)
547             WHILE ROCK->(' ').ROCK CYCLE;REPEAT
548             IF ROCK='999' THEN->15
549             V=(EQ-1)*4+B
550             NS(V)<-ROCK
551             REPEAT
552             NSZB='0'
553             READ(B);NOEL=0
554             ->92
555           6:IF NEXTSYMBOL=NL THEN SKIPSYMBOL
556             WHILE NEXTSYMBOL=' ' THEN SKIPSYMBOL
557             IF NEXTITEM<='/' OR NEXTITEM>=':' THEN->14
558           92:READ(ZBP)
559             IF NEXTSYMBOL#' ' OR ZBP>99 THEN->10 ELSE->11
560           10:UNLESS NEXTSYMBOL=10 THEN RSTRG(NSZB)
561             SELECTOUTPUT(7);WRITE(ZBP,1)
562             PRINTSTRING(NSZB) UNLESS NSZB='0'
563             SELECTOUTPUT(99);CLOSESTREAM(7);SELECTINPUT(7)
564             RSTRG(NSZB);Y=1
565             SELECTINPUT(98);CLOSESTREAM(7);SELECTINPUT(1);->14
566           11:READ(K)
567             IF ZBP=ZBG THEN->7
568             IF ZBG=0 THEN->8
569             CYCLE B=1,1,4
570             ECOUNT(B)=ECOUNT(B)/ECOUNTS
571             REPEAT
572             IF ZBG<10 OR ZBG>70 THEN->9
573             Z(NOEL)=ZBG
574             CYCLE B=1,1,4
575             V=(EQ-1)*4+B
576             PK(V,NOEL)=ECOUNT(B)
577             REPEAT
578           8:NOEL=NOEL+1
579             ->13
```

FIG. B14 : continued. Program TRACE

```
580             9:CYCLE B=1,1,4
581               V=(EQ-1)*4+B
582               IF ZBP<10 OR ZBP>70 THEN BG1(V,NOEL)=ECOUNT(B) AND-200
583               BG2(V,NOEL)=ECOUNT(B)
584             9:REPEAT
585             10:ECOUNTS=0
586               CYCLE B=1,1,4
587               ECOUNT(B)=0
588               REPEAT
589             7:ZSG=ZBP
590               CYCLE B=1,1,4
591               READ(COUNT);READ(T)
592               ECOUNT(B)=COUNT/(T/1000)+ECOUNT(B)
593               REPEAT
594               ECOUNTS=ECOUNTS+1
595               ->6
596             15:NOELS=NOEL;NOSAMS=(EQ-1)*4
597               SELECTINPUT(98)
598               NEWLINE
599               PRINTSTRING('LIST PEAK ANGLES USED (WITHOUT DECI*AL POINT)')
600               P*INTSTRING(' IN RESPONSE TO PROMPT OF  ELEMENT NAME')
601               NEWLINE
602               CYCLE NOEL=1,1,NOELS
603             ; IF Z(NOEL)#37 THEN->16
604               ELE*(NOEL)='RB'
605             ; THETA1(NOEL)=2720
606               THETA2(NOEL)=2600
607               PROMPT('RB: ');READ(THETAP(NOEL))
608               ->17
609             16:IF Z(NOEL)#38 THEN->18
610               ELE*(NOEL)='SR'
611               THETA1(NOEL)=2600
612               THETA2(NOEL)=2450
613               PROMPT('SR: ');READ(THETAP(NOEL))
614               ->17
615             18:NEWLINE
616               PRINTSTRING('ATOMIC NUMBE* (IE. E-SET ADDRESS) ')
617               WRITE(Z(NOEL),1);PRINTSTRING(' NOT RECOGNIZED. PLEASE IDENTIFY')
618               NEWLINE
619               PROMPT('ELE*ENT: ');RSTRG(ELE*(NOEL))
620               PROMPT('PEAK ANGLE: ');READ(THETAP(NOEL))
621               IF BG1(1,NOEL)=0 THEN->20
622               PROMPT('1ST BG ANGLE: ');READ(THETA1(NOEL))
623               PROMPT('2ND BG ANGLE: ');READ(THETA2(NOEL))
624               ->17
625             20:PROMPT('BG ANGLE: ');READ(THETA2(NOEL))
626             17:REPEAT
627               CYCLE V=1,1,NOSAMS
628               CYCLE NOEL=1,1,NOELS
629               IF BG1(V,NOEL)=0 THEN->21
630               BG1(V,NOEL)=(THETAP(NOEL)-THETA2(NOEL))*(BG1(V,NOEL)-BG2(V,NOEL))
631               BG2(V,NOEL)=BG1(V,NOEL)/(THETA1(NOEL)-THETA2(NOEL)) +BG2(V,NOEL)
632             21:PK(V,NOEL)=PK(V,NOEL)-BG2(V,NOEL)
633               REPEAT
634               REPEAT
635             24:IF S1='.NULL' OR S2='.NULL' START
636                  IF S2='.NULL' THEN SELECTINPUT(4) AND SETMARGINS(4,1,160) C
  C                    ELSE SELECTINPUT(2) AND SETMARGINS(2,1,160)
637                  ! NEXT 6 LINES READ IN ATOMIC NUMBERS FROM COUNT RATIO FILE INPUT
638                  ! AND COUNT THEM. NOELS= NO.OF ELEMENTS ANALYSED
639                  NOELS=0
640             B21: NOELS=NOELS+1
641                  WHILE NEXTSYMBOL=' ' THEN SKIPSYMBOL
642                  IF NEXTSYMBOL=NL THEN->A21
643                  READ(Z(NOELS));->B21
644             A21: NOELS=NOELS-1
645                  CYCLE V=1,1,NOSAMS
646                  PTILLSP(NS(V))
647                  CYCLE NOEL=1,1,NOELS
648             READ(PK(V,NOEL))
649             REPEAT;REPEAT
650             IF Z(1)=29 START
651                ! W-TUBE TRACES INPUT
652                ELEM(1)='NI';ELE*(2)='ZN';ELEM(3)='TH'
653                ELEM(4)='RB';ELEM(5)='SR';ELE*(6)='Y'
654                ELEM(7)='ZR';ELEM(8)='NB';ELEM(9)='CR';ELEM(10)='CE'
655                ELEM(11)='SM';ELEM(12)='ND';ELEM(13)='TIO2W'
656                ->*+1
657                FINISH
658             IF Z(1)=21 START
659                ! CR-TUBE TRACES INPUT
660                ELE*(1)='SC';ELEM(2)='V';ELEM(3)='CU';ELEM(4)='BA';ELEM(5)='LA'
661                ELEM(6)='TIO2C'
662                CYCLE V=1,1,NOSAMS
663                PK(V,6)=PK(V,6)-.185*PK(V,2)
664                ! TIO2CR CORRECTED FOR BALB3 AND VKA INTERFERENCE
665                PK(V,2)=PK(V,2)*(1+.1156*.185)
666                ! V.COR*ECTED FOR V INTERFERENCE ON TI CR V (THIS LINE COULD
667                          !          BE OMITTED)
668                PK(V,5)=PK(V,5)+.007956*.185*PK(V,2)
```

FIG. B14 : continued. Program TRACE

```
669                 ! LA COPRECTED FOR HAVING REMOVED TOO MUCH IN CRTRACE BECAUSE
670                 ! OF V BACK-INTERFERENCE ON TIME
671                  REPEAT
672                  FINISH;ELSE;START
673                  SELECTINPUT(98);SELECTOUTPUT(99)
674                  NEWLINE;PRINTSTRING('TYPE ELEMENTS IN ORDER');NEWLINE
675                  ! INPUT FROM ANY OTHER COUNT RATIO FILE (EG. HF, EU)
676                  CYCLE NOEL=1,1,NOELS
677                  PROMPT('ELEMENT: ');RSTRG(ELEM(NOEL))
678                  REPEAT
679                  FINISH
680            F41: FINISH
681              IF ANSWER='N' THEN-222
682              ! MATRIX CORRECTION UNTIL LABEL 22
683              SELECTINPUT(8)
684              ! INPUT FROM MAJOR ELEMENT COMPOSITIONS FILE
685            CYCLE V=1,1,NOSAMS
686              ! CYCLES THROUGH ALL SAMPLES.
687              ! STANDARD COMPOSITIONS INSERTED HERE INTO ARRAY MAJ IF
688              ! STANDARD NAME IS IDENTIFIED. ESSENTIAL TO USE CORRECT NAMES. NAME
689              ! IS ADDED TO LIST OF STANDARDS IN INPUT DATA- STANSPRES. 'LOI'
690              ! (11TH VALUE) IS CO2+H2O FROM ABBEY (1977)
691            IF NS(V)->('INTSG').ROCK THEN  C
C                ANALY('73.3 14.04 2.13 0 2.06 3.91 3.9 0 0 0 0 0 0 0 0 ',MAJ,V) AND->E41
692            IF NS(V)='INTSBTI' THEN ANALY('49.07 13.53 10.05 '.C
C                '9.45 10.19 2.85 1 3.92 0 0 0 0 0 0 0 ',MAJ,V) AND->E41
693            IF NS(V)='INTSA' THEN ANALY('61.67 13.92 6.19 '.C
C                '4.62 6.22 3.41 2.46 1 0 0 0 0 0 0 0 ',MAJ,V) AND->E41
694            IF NS(V)='INTSATI'THEN ANALY('60.92 13.74 6.1' .C
C                ' 4.74 6.12 3.37 2.43 2.29 0 0 0 0 0 0 ',MAJ,V) AND->E41
695            IF NS(V)->('INTSB').ROCK THEN ANALY('50.05 13.8 ' .C
C                '10.25 9.64 10.39 2.91 1.02 2 0 0 0 0 0 0 ',MAJ,V) AND->E41
696            IF NS(V)='SY3'THEN ANALY('59.68 11.8 6.47' .C
C                ' 2.64 8.26 4.15 4.24 .15 .33 .54 .87 51 1400 440 ',MAJ,V) C
C                AND STANSPRES=STANSPRES.' ',NS(V) AND->E41
697            IF NS(V)='AGV1' THEN ANALY('59.72 17.22 6.84 ' .C
C                '1.55 5 4.31 2.93 1.05 .1 .5 .83 125 45 1200 ',MAJ,V) C
C                AND STANSPRES=STANSPRES.' ',NS(V) AND->E41
698            IF NS(V)='BCR1'THEN ANALY('54.85 13.68 13.52 ' .C
C                '3.49 6.98 3.29 1.68 2.22 .19 .33 .76 410 25 680 ',MAJ,V) C
C                AND STANSPRES=STANSPRES.' ',NS(V) AND->E41
699            IF NS(V)='G2'THEN ANALY('69.19 15.35 2.67'. C
C                ' .77 1.98 4.06 4.52 .5 .04 .14 .63 34 100 1850 ',MAJ,V) C
C                AND STANSPRES=STANSPRES.' ',NS(V) AND->E41
700            IF NS(V)='GSP1' THEN ANALY('67.31 15.19 4.33 '. C
C                '.96 2.02 2.8 5.53 .56 .04 .28 .69 49 130 1300 ',MAJ,V) C
C                AND STANSPRES=STANSPRES.' ',NS(V) AND->E41
701            IF NS(V)='PCC1'THEN ANALY('42.15 .73 8.28 '. C
C                '43.63 .53 .01 0.0 .01 .12 0.0 4.8 31 0 0 ',MAJ,V) C
C                AND STANSPRES=STANSPRES.' ',NS(V) AND->E41
702            IF NS(V)='BR' THEN ANALY('38.39 10.25 12.9 '. C
C                '13.35 13.87 3.07 1.41 2.61 .2 1.05 3.17 240 80 1050 ',MAJ,V) C
C                AND STANSPRES=STANSPRES.' ',NS(V) AND->E41
703            IF NS(V)='GA'THEN ANALY('69.96 14.51 2.77 '. C
C                '.95 2.45 3.55 4.03 .38 .09 .12 .98 38 38 850 ',MAJ,V) C
C                AND STANSPRES=STANSPRES.' ',NS(V) AND->E41
704            IF NS(V)='GH'THEN ANALY('75.85 12.51 1.36 '. C
C                '.03 .69 3.85 4.76 .08 .05 .01 .6 5 25 22 ',MAJ,V) C
C                AND STANSPRES=STANSPRES.' ',NS(V) AND->E41
705            IF NS(V)='GSN'THEN ANALY('65.98 14.71 3.75 '. C
C                '2.31 2.51 3.78 4.64 .68 .06 .28 1.25 62 90 1400 ',MAJ,V) C
C                AND STANSPRES=STANSPRES.' ',NS(V) AND->E41
706            IF NS(V)='JB1'THEN ANALY('52.62 14.62 9.01 '. C
C                '7.76 9.35 2.79 1.42 1.34 .15 .26 1.19 210 36 490 ',MAJ,V) C
C                AND STANSPRES=STANSPRES.' ',NS(V) AND->E41
707            IF NS(V)='JG1'THEN ANALY('72.36 14.2 2.16 '. C
C                '.76 2.17 3.39 3.96 .27 .06 .09 .62 24 22 460 ',MAJ,V) C
C                AND STANSPRES=STANSPRES.' ',NS(V) AND->E41
708            IF NS(V)='TANZ1'THEN ANALY('62.65 16.52 5.93 '. C
C                '1.89 5.19 4.39 1.23 .59 .11 .14 1.53 99 15 670 ',MAJ,V) C
C                AND STANSPRES=STANSPRES.' ',NS(V) AND->E41
709            IF NS(V)='DRN' THEN ANALY('52.88 17.56 9.69 '. C
C                '4.47 7.09 3 1.73 1.1 .21 .25 2.35 220 0 380 ',MAJ,V) C
C                AND STANSPRES=STANSPRES.' ',NS(V) AND->E41
710            IF NS(V)='UBN' THEN ANALY('39.93 2.97 6.45 '. C
C                '35.4 1.18 .1 .02 .12 .12 .03 11.72 75 0 45 ',MAJ,V) C
C                AND STANSPRES=STANSPRES.' ',NS(V) AND->E41
711            IF NS(V)='PKN' THEN ANALY('65.11 18.64 .09 .'. C
C                '01 .11 2.58 12.83 .02 0.0 .02 .4 5 0 210 ',MAJ,V) C
C                AND STANSPRES=STANSPRES.' ',NS(V) AND->E41
712            IF NS(V)='W1' THEN ANALY('52.72 14.87 11.11 6.63 10.98 2.15'. C
C                ' .64 1.07 .17 .14 .59 240 12 160 ',MAJ,V) AND C
C                STANSPRES=STANSPRES.' ',NS(V) AND->E41
713            IF NS(V)='SY2' THEN ANALY('60.09 12.15 6.29 2.69 8 4.35 4.51'. C
C                ' .15 .32 .44 .92 50 85 460 ',MAJ,V) AND C
C                STANSPRES=STANSPRES.' ',NS(V) AND->E41
714            IF NS(V)='TB' THEN ANALY('60.3 20.55 6.94 1.94 .33 1.31'. C
C                ' 3.85 .93 .05 .1 3.95 105 56 720 ',MAJ,V) AND C
C                STANSPRES=STANSPRES.' ',NS(V) AND->E41
715            !ANALYSES OF STANDARDS FROM ABBEY 1977
```

FIG. B14 : continued. Program TRACE

```
716               COUNT=1
717               IF ANALF=1 THEN->241
71P               ! ANALF=1 => COMPOSITIONS FILE IS IN ANALYSIS FILE FORMAT
719               ! NEXT 8 LINES IDENTIFY FORMAT OF ANALYSIS FILE
72?             E41:WHILE NEXTSYMBOL=' ' THEN SKIPSYMBOL
721               IF NEXTSYMBOL='S' START
722               ! FIRST NON-SPACE CHARACTER IN FILE IS 'S' - COULD BE ANALYSIS FILE
723               !  (SIO2) OR SAMPLE NAME BEGINNING WITH S
724                  CYCLE NOEL=1,1,12
725                  RTILLSP(MAJEL(NOEL))
726                  IF NOEL=1 AND MAJEL(NOEL)#'SIO2' THEN EXIT
727                  REPEAT
728                  IF MAJEL(1)#'SIO2' THEN ROCK=MAJEL(1) AND C
  C                     MAJEL(1)='SIO2' AND ->A41 ELSE ANALF=1
729               ! ANALF=1 IF FIRST ITEM IN FILE IS SIO2
73?               ! NEXT 14 LINES READ IN DATA FROM ANALYSIS FILE INTO ARRAY MAJ
731             41:  RTILLSP(ROCK)
732                  IF ROCK='STOP' START
733                     IF COUNT=0 THEN COUNT=4
734                     ->44
735                     FINISH
736                  IF ROCK#NS(V) START
737                     IF ROCK->(NS(V).'@').HT THEN NS(V)=ROCK AND->46
738                     RSTRG(ROCK)
739                     ->41
74?                  FINISH
741             46:  CYCLE NOEL=1,1,12
742                  READ(MAJ(NOEL,V));REPEAT
743                  ->841
744                  FINISH
745               !
746                 ! NEXT 29 LINES TAKE DATA FROM NORMINPUT FILE
747                 ! PROGRAM OPERATES FASTEST IF SAMPLE ORDER IN NORMINPUT FILE IS
748                 ! SAME AS ORDER OF COUNT RATIOS.
749               C41:RSTRG(ROCK)
7??                 IF ROCK->ROCK.(' .') OR ROCK->ROCK.('.') THEN->A41
751               A41:IF ROCK#NS(V) START
752                     IF ROCK->(NS(V).'@').HT THEN NS(V)=ROCK AND->D41
753                 ! IF @ SYMBOLS USED IN COMPOSITIONS FILE. THEY WILL TRANSFER TO
754                 ! OUTPUT DATA. THEY NEED NOT APPEAR IN COUNT RATIO FILE
755                     CYCLE; RTILLSP(ROCK)
756                     IF ROCK='-1' OR ROCK='END' OR ROCK='-2' THENEXIT
757                     READ(PA)
758                     REPEAT
759                     IF ROCK='-1' OR ROCK='END' THEN->C41
76?                  IF ROCK='-2' START
761                     IF COUNT=0 THEN COUNT=4
762                     ->44
763                     FINISH
764                  FINISH
765             D41:RTILLSP(ROCK)
766                 IF ROCK='-1' THEN->841
767                 IF ROCK ='-2' START
768                    SELECTINPUT(9A);CLOSESTREAM(8);SELECTINPUT(8)
769                    ->841
77?                    FINISH
771                 READ(PA)
772                 CYCLE NOEL=1,1,18
773                 IF ROCK=MAJEL(NOEL) START
774                    MAJ(NOEL,V)=PA
775                    IF NOEL<11 THEN MAJ(11,V)=MAJ(11,V)+PA
776                    ! TOTAL OXIDES CREATED
777                    EXIT
778                    FINISH
779                 REPEAT
78?                 ->241
781             841:IF NS(V)='INTSBB1' THEN MAJ(13,V)=1020 AND MAJ(14,V)=1002
782                 IF NS(V)='INTSGB1' THEN MAJ(13,V)=1050 AND MAJ(14,V)=1017
783                 IF NS(V)='INTSBB2' THEN MAJ(13,V)=420 AND MAJ(14,V)=577
784                 IF NS(V)='INTSGB2' THEN MAJ(13,V)=444 AND MAJ(14,V)=430
785                 IF NS(V)='INTSBB3' THEN MAJ(13,V)=99 AND MAJ(14,V)=136
786                 IF NS(V)='INTSGB3' THEN MAJ(13,V)=100 AND MAJ(14,V)=97
787                 IF NS(V)='INTSBB4' THEN MAJ(13,V)=20.7 AND MAJ(14,V)=28.5
788                 IF NS(V)='INTSGB4' THEN MAJ(13,V)=19.2 AND MAJ(14,V)=18.6
789                 IF NS(V)='INTSBA1' THEN MAJ(15,V)=1313
79?                 IF NS(V)='INTSGA1' THEN MAJ(15,V)=2534
791                 IF NS(V)='INTSBA2' THEN MAJ(15,V)=535
792                 IF NS(V)='INTSGA2' THEN MAJ(15,V)=1054
793                 IF NS(V)='INTSBA3' THEN MAJ(15,V)=107
794                 IF NS(V)='INTSGA3' THEN MAJ(15,V)=250
795                 IF NS(V)='INTSBA4' THEN MAJ(15,V)=25
796                 IF NS(V)='INTSGA4' THEN MAJ(15,V)=50.1
797                 ! V, LA AND BA DATA FOR INTERFERENCE STANDARDS
798                 CYCLE FG=1,1,9
799                 MU1(FG)=0
8??                 REPEAT
8?1                 MU2=0;MU3=0
8?2                 CYCLE NOEL=1,1,10
8?3                 CYCLE FG=1,1,9
8?4                 IF NOEL=1 OR NOEL=5 OR 6<NOEL<10 THEN PA=MUFUDGE(FG) ELSE PA=1
```

FIG. B14 : continued. Program TRACE

```
805             ! 4TH PERIOD OXIDES MULTIPLIED BY MUFUDGE, OTHERS BY 1
806             MU1(FG)=MU1(FG)+MAJ(NOEL,V)*COEF1(NOEL)*PA
807             REPEAT
808             MU2=MU2+MAJ(NOEL,V)*COEF2(NOEL)
809             MU3=MU3+MAJ(NOEL,V)*COEF3(NOEL)
810             ! 12 MASS ABSORPTION COEFFICIENTS CALCULATED PER SAMPLE
811             REPEAT
812             IF MAJ(12,V)=0 START
813             ! IF NO LOI DATA INPUT PROGRAM ASSUMES UNIGNITED SAMPLES
814             ! NEXT 5 LINES ASSUME 100-TOTAL OXIDES  FOR UNIGNITED SAMPLES IS
815                     ! 50 H2O - 50 CO2
816                CYCLE FG=1,1,9
817                MU1(FG)=(MU1(FG)+(100-MAJ(11,V))*1.88)/1000
818                REPEAT
819                MU2=(MU2+(100-MAJ(11,V))*30.9)/1000
820                MU3=(MU3+(100-MAJ(11,V))*52.7)/1000
821                ->43
822                FINISH
823             LOI(V)=MAJ(12,V)
824             IF STANSPRES->HT.(NS(V)).LT START
825                ! IF SAMPLE IS STANDARD THEN LOI QUOTED IS H2O+CO2
826                CYCLE FG=1,1,9
827                MU1(FG)=(MU1(FG)+LOI(V)*1.88)/1000
828                REPEAT
829                MU2=(MU2+LOI(V)*30.9)/1000
830                MU3=(MU3+LOI(V)*52.7)/1000
831                ->43
832                FINISH
833             ! NEXT 5 LINES APPLY TO IGNITED SAMPLES: TOTAL MU IS REDUCED BY
834                ! (100-LOI)/100 AND THEN LOI (H2O+CO2) CONTRIBUTION ADDED.
835             CYCLE FG=1,1,9
836             MU1(FG)=(MU1(FG)*(100-LOI(V))/100+LOI(V)*1.88)/1000
837             REPEAT
838             MU2=(MU2*(100-LOI(V))/100+LOI(V)*30.9)/1000
839             MU3=(MU3*(100-LOI(V))/100+LOI(V)*52.7)/1000
840          43:->40
841          44:SELECTINPUT(98)
842             UNLESS COUNT=4 THEN CLOSESTREAM(8) AND SELECTINPUT(8) C
  C                 AND COUNT=0 AND->E41
843             COUNT=1
844             SELECTOUTPUT(99)
845             NEWLINE
846             PRINTSTRING('ANALYSIS OF '.NS(V).' NOT PRESENT IN FILE '.S$)
847             NEWLINE
848             PRINTSTRING('DO YOU REQUIRE MATRIX CORRECTION TO THIS SAMPLE? (Y OR')
849          PRINTSTRING(' N)')
850             NEWLINE
851             PROMPT('ANSWER: ');RSTRG(ROCK)
852             IF ROCK='N' START
853                CYCLE FG=1,1,9
854                MU1(FG)=1
855                REPEAT
856                MU2=10;MU3=20
857                ->45
858                FINISH
859             PRINTSTRING('TYPE IN MAJOR ELEMENT ANALYSIS IN STANDARD ORDER')
860             NEWLINE
861             PRINTSTRING(', INCLUDING TOTAL OXIDES AND LOSS ON IGNITION (IF ')
862             NEWLINE
863             PRINTSTRING('USED), IN RESPONSE TO PROMPT OF "DATA".')
864             PROMPT('DATA: ')
865             NEWLINE;->46
866          45:IF ROCK='Y' OR ROCK='N' THEN SELECTINPUT(8)
867             SELECTINPUT(96);CLOSESTREAM(8);SELECTINPUT(8)
868          40:CYCLE NOEL=1,1,NOELS
869             ! SELECTS CORRECT COEFFICIENT FOR EACH ELEMENT ANALYSED, AND
870             !     MULTIPLIES THE COUNT RATIO BY IT
871             IF ELEM(NOEL)='TH' THEN PK(V,NOEL)=PK(V,NOEL)*MU1(3) AND->48
872             IF ELEM(NOEL)='DY' THEN PK(V,NOEL)=PK(V,NOEL)*MU1(1) AND->48
873             IF ELEM(NOEL)='HF' THEN PK(V,NOEL)=PK(V,NOEL)*(MU1(1)+MU1(9))C
  C                 /2  AND->48
874             IF ELEM(NOEL)='SC' OR ELEM(NOEL)='V' OR ELEM(NOEL)='LA' OR C
  C                   ELEM(NOEL)='TIO2CR' OR ELEM(NOEL)='TIO2V' C
  C                     THEN PK(V,NOEL)=PK(V,NOEL)*MU3/20 AND->48
875             IF ELEM(NOEL)='CR' OR ELEM(NOEL)='BA' OR ELEM(NOEL)='CE'  C
  C                   OR ELEM(NOEL)='ND' OR ELEM(NOEL)='SM' THEN C
  C                PK(V,NOEL)=PK(V,NOEL)*MU2/10 AND->48
876             IF ELEM(NOEL)='CU' THEN PK(V,NOEL)=PK(V,NOEL)*MU1(9) AND->48
877             PK(V,NOEL)=PK(V,NOEL)*MU1(NOEL)
878          48:REPEAT
879             REPEAT
880             IF S6='.NULL' THEN->22
881             ! PRINTED OF MU-CORRECTED COUNT RATIOS (NB. NOT CORRECTED FOR V/CR, LA/NB)
882             SELECTOUTPUT(4);SETMARGINS(4,1,130);SPACES(13)
883             CYCLE NOEL=1,1,NOELS; PRINT(Z(NOEL),2,3);SPACES(7);REPEAT
884             NEWLINES(2)
885             CYCLE V=1,1,NOSAMS
886             PRINTSTRING(NS(V));SPACES(9-LENGTH(NS(V)))
887             CYCLE NOEL=1,1,NOELS
888             PRINT(PK(V,NOEL),2,6)
```

FIG. B14 : continued. Program TRACE

```
889             REPEAT
890             NEWLINE
891             REPEAT
892           22:CYCLE NOEL=1,1,NOELS
893             ECC(NOEL)=0;EP(NOEL)=0;EC(NOEL)=0;ECP(NOEL)=0;STAN(NOEL)=0;EPP(NOEL)=0
894             REPEAT
895             IF ELEM(1)#"NI" THEN->A22
896             ! INPUT DATA FROM &TRACE SHOULD BE CORRECTED FOR V/CR, LA/NB
897             SELECTOUTPUT(99);SELECTINPUT(98)
898             ! INPUT/OUTPUT REVERTS TO INTERACTIVE TERMINAL
899             BEGIN
900                 LONGREALARRAY MA,CX(8:11),EX,EY,EXY,EXX,EYY(8:9)
901                 REAL REA,REB,REC
902                 INTEGER NOPOINTS,J,B
903                 NEWLINE
904                 PRINTSTRING("REGRESSION FOR NB AND CR CORRECTIONS? (Y OR N)")
905                 NEWLINE
906                 PROMPT("ANSWER: ");RSTRG(HT)
907                 ! REGRESSION ONLY POSSIBLE IF "B" SERIES INTERFERENCE STANDARDS PRESENT
908                 IF HT="N" START
909                     MA(8)=.00001461;MA(9)=.00001407
910                     ->C22
911                     ! CORRECTION GRADIENTS FROM PREVIOUS REGRESSION - 8=NB, 9=CR
912                     FINISH
913                 CYCLE J=8,1,9
914                 EX(J)=0;EY(J)=0;EXY(J)=0;EXX(J)=0;EYY(J)=0
915                 REPEAT
916                 ! REGRESSION PROCEDURE AS IN WTRACE
917                 NOPOINTS=0
918                 CYCLE V=1,1,NOSAMS
919                 UNLESS NS(V)->("INTS").HT THEN->B22
920                 IF LENGTH(NS(V))<6 THEN->B22
921                 UNLESS CHARNO(NS(V),6)="B" THEN->B22
922                 CYCLE J=8,1,9
923                 EX(J)=EX(J)+MAJ(22-J,V)
924                 EY(J)=EY(J)+PK(V,J)
925                 EXY(J)=EXY(J)+PK(V,J)*MAJ(22-J,V)
926                 EXX(J)=EXX(J)+MAJ(22-J,V)**2
927                 EYY(J)=EYY(J)+PK(V,J)**2
928                 REPEAT
929                 NOPOINTS=NOPOINTS+1
930               B22:REPEAT
931                 CYCLE J=8,1,9
932                 REB=NOPOINTS*EYY(J)-NOPOINTS*EXX(J)+EX(J)**2-EY(J)**2
933                 REA=EY(J)*EX(J)-NOPOINTS*EXY(J)
934                 MA(J)=(-REB+SQRT(REB**2+4*REA**2))/(2*REA)
935                 MA(J+2)=(-REB-SQRT(REB**2+4*REA**2))/(2*REA)
936                 CX(J)=(EY(J)-MA(J)*EX(J))/NOPOINTS
937                 CX(J+2)=(EY(J)-MA(J+2)*EX(J))/NOPOINTS
938                 REPEAT
939                 CYCLE J=8,1,9
940                 CYCLE B=0,1,1
941                 REC=MA(J+2*B)**2+1
942                 REC=(EYY(J)-2*MA(J+2*B)*EXY(J)+2*CX(J+2*B)*MA(J+2*B)*EX(J) C
  C                      -2*CX(J+2*B)*EY(J) C
  C                      +EXX(J)*MA(J+2*B)**2+NOPOINTS*CX(J+2*B)**2)/REC
943                 IF B=0 THEN REA=REC
944                 REPEAT
945                 IF REC<REA THEN MA(J)=MA(J+2) AND CX(J)=CX(J+2)
946                 NEWLINE
947                 PRINTSTRING("INTERFERENCE CORRECTION FOR ".ELEM(J)." IS")
948                 PRINT(MA(J),1,8);PRINTSTRING(" COUNT RATIO ".ELEM(J))
949                 NEWLINE; PRINTSTRING("PER UNIT INTERFERING ELEMENT")
950                 NEWLINE
951                 PRINTSTRING("INTERCEPT OF CORRECTION IS AT COUNT RATIO ")
952                 PRINT(CX(J),1,8)
953                 NEWLINE
954                 REPEAT
955               C22:CYCLE V=1,1,NOSAMS
956                 CYCLE J=8,1,9
957                 PK(V,J)=PK(V,J)-MA(J)*MAJ(22-J,V)*(100-LOI(V))/100
958                 ! CORRECTION FOR CR AND NB REDUCED BECAUSE V AND LA REFER TO DRY
959                     ! SAMPLE
960                 REPEAT
961                 PK(V,13)=PK(V,13)-.000082*MAJ(13,V)-.0000088*MAJ(15,V)
962                 ! TIO2W CORRECTED FOR V (13) AND BA (15) INTERFERENCE
963                 REPEAT
964                 END

965             A22:IF BLOCK=0 THEN->26 ELSE->27
966             26:SELECTINPUT(6)
967               ! NO STANDARDS, CALIBRATION TAKEN FROM TRACDATA.
968               CYCLE NOEL=1,1,NOELS
969               READ(Z(NOEL));READ(MA(1,NOEL));READ(CX(1,NOEL))
970               REPEAT
971               ->28
972             27:IF PREL="Y" THEN PRELOAD("")
973               ! NEW CALIBRATION, PROCEDURE AS IN MAJORS
974               CYCLE NOEL=1,1,NOELS
975               ELNAME(NOEL)=ELEM(NOEL)
```

FIG B14 : continued. Program TRACE

```
976             REPEAT
977             SELECTINPUT(5);SET MARGINS(5,1,150)
978             ! INPUT FROM TRACANAL
979             STANSUSED="
980             CYCLE A=1,1,BLOCK
981             CYCLE V=STANINIT(A),1,STANFINAL(A)
982           29:RSTRG(STNO)
983             IF STNO="STOP" THEN->230
984             IF STNO=NS(V) THEN->231
985             RSTRG(STNO);->29
986           31:STANSUSED<-STANSUSED.' '.STNO
987             CYCLE B=1,1,18
988             READ(ZA);READ(PA)
989             ! 18 ATOMIC NUMBER-CONCENTRATION PAIRS PER STANDARD
990             CYCLE NOEL=1,1,NOELS
991             IF Z(NOEL)=ZA THEN P(V,NOEL)=PA AND EXIT
992             REPEAT;REPEAT
993             ! NEXT 38 LINES PROVIDE EXTRA OMISSIONS FROM CALIBRATIONS
994             CYCLE NOEL=1,1,NOELS
995           IF Z(NOEL)=29 OR Z(NOEL)=17  START
996                IF STNO->('INTS').TAIL THEN->A30
997             FINISH
998           IF STNO="SY3" AND Z(NOEL)=62 THEN->C30
999           IF STNO->('INTS').HT START
1000             IF Z(NOEL)=24 OR Z(NOEL)=28 THEN->A30
1001             IF HT="B" OR HT="G" START
1002                IF Z(NOEL)=41 OR Z(NOEL)=62 THEN->A30
1003                FINISH
1004             FINISH
1005           IF STNO="PCC1" OR STNO="UBN" OR STNO="TANZ1" OR STNO="FKN" C
C                 OR STNO="DRN" OR STNO="SY3" START
1006             IF Z(NOEL)=41 OR Z(NOEL)=58 OR Z(NOEL)=60 OR Z(NOEL)=62 C
C                  THEN->A30
1007             FINISH
1008           IF STNO="PCC1" OR STNO="UBN" START
1009             IF Z(NOEL)=39 OR Z(NOEL)=40 THEN->A30
1010             FINISH
1011           IF Z(NOEL)=90 START
1012             IF STNO="PCC1" OR STNO="UBN" OR STNO="GSN" OR STNO="FKN"C
C                OR STNO="TANZ1" OR STNO="DRN" OR STNO="SY3" THEN->A30
1013             FINISH
1014           IF Z(NOEL)=37 START
1015             IF STNO="TANZ1" OR STNO="FKN" OR STNO="INTSGA2" THEN->A30
1016             FINISH
1017           IF STNO->('INTS').HT.('A2') START
1018             IF Z(NOEL)=28 OR Z(NOEL)=41 THEN->A30
1019             FINISH
1020             IF STNO->('INTS').HT.('B2') START
1021                IF Z(NOEL)=38 OR Z(NOEL)=39 THEN->A30
1022                FINISH
1023             IF Z(NOEL)=40 START
1024                IF STNO="FKN" OR STNO="INTSBB2" THEN->A30
1025                FINISH
1026             IF STNO->('INTS').HT.('1') START
1027                UNLESS Z(NOEL)=56 THEN->A30
1028                FINISH
1029          C30:IF OMIT->HEAD.(STNO.' ').TAIL START
1030          B30:  CYCLE ZA=1,1,LENGTH(TAIL)
1031                ZBP=740
1032                IF CHARNO(TAIL,ZA)=';' OR CHARNO(TAIL,ZA)=',' START
1033                   HT=FRO"STRING(TAIL,1,ZA-1)
1034                   IF Z(NOEL)=INTEGSTR(HT) THEN ZBP=750 ANDEXIT
1035                   IF CHARNO(TAIL,ZA)=';' THENEXIT
1036                   TAIL->HEAD.(',').TAIL
1037                   ZBP=730;EXIT
1038                   FINISH
1039                REPEAT
1040                IF ZBP=750 THEN->A30
1041                IF ZBP=730 THEN->B30
1042                FINISH
1043             ! REGRESSION COMPARABLE TO WTRACE
1044             STAN(NOEL)=STAN(NOEL)+1
1045             CALIB(NOEL)_STPC(STAN(NOEL))=P(V,NOEL)
1046             CALIB(NOEL)_STRAT(STAN(NOEL))=PK(V,NOEL)
1047             EP(NOEL)=EP(NOEL)+P(V,NOEL)
1048             EC(NOEL)=EC(NOEL)+PK(V,NOEL)
1049             ECC(NOEL)=ECC(NOEL)+PK(V,NOEL)**2
1050             ECP(NOEL)=ECP(NOEL)+PK(V,NOEL)*P(V,NOEL)
1051             EPP(NOEL)=EPP(NOEL)+P(V,NOEL)**2
1052          A30:REPEAT
1053          30:SELECTINPUT(98);CLOSESTREAM(5);SELECTINPUT(5)
1054             REPEAT;REPEAT
1055             SELECTOUTPUT(6)
1056             CYCLE NOEL=1,1,NOELS
1057             REB=STAN(NOEL)*EPP(NOEL)-STAN(NOEL)*ECC(NOEL)*EC(NOEL)**2-EP(NOEL)**2
1058             REA=EC(NOEL)*EP(NOEL)-STAN(NOEL)*ECP(NOEL)
1059             MA(1,NOEL)=(-REB+SQRT(REB**2+4*REA**2))/(2*REA)
1060             MA(2,NOEL)=(-REB-SQRT(REB**2+4*REA**2))/(2*REA)
1061             CX(1,NOEL)=(EP(NOEL)-MA(1,NOEL)*EC(NOEL))/STAN(NOEL)
1062             CX(2,NOEL)=(EP(NOEL)-MA(2,NOEL)*EC(NOEL))/STAN(NOEL)
```

FIG. B14 : continued. Program TRACE

```
1062              CYCLE ZBP=1,1,2
1064              REC(ZBP)=MA(ZBP,NOEL)**2+1
1065              REC(ZBP)=(EPP(NOEL)-2*MA(ZBP,NOEL)*ECP(NOEL)+2*CX(ZBP,NOEL)*MA C
   C                (ZBP,NOEL)*EC(NOEL)-2*CX(ZBP,NOEL)*EP(NOEL)*ECC(NOEL)*MA(ZBP,NOEL)C
   C                **2*STAN(NOEL)*CX(ZBP,NOEL)**2)/REC(ZBP)
1066              REPEAT
1067            IF REC(2)<REC(1) THEN MA(1,NOEL)=MA(2,NOEL) AND CX(1,NOEL)=CX(2,NOEL)
1068              CYCLE ZBP=1,1,40
1069              IF CALIB(NOEL)_STPC(ZBP)=0 AND CALIB(NOEL)_STRAT(ZBP)=0 C
   C                  THEN CALIB(NOEL)_STPC(ZBP)=.00001
1070              REPEAT
1071              CALIB(NOEL)_CALP=MA(1,NOEL)
1072              CALIB(NOEL)_CALC=CX(1,NOEL)
1073              PRINT(Z(NOEL),2,0)
1074              ! UPDATING TRACDATA
1075              PRINT(MA(1,NOEL),5,7);SPACES(2)
1076              PRINT(CX(1,NOEL),5,7);NEWLINE
1077              REPEAT
1078              NEWLINES(2)
1079              PRINTSTRING(STANSUSED)
1080            28:IF S3="",NULL" THEN->50
1081              SELECTOUTPUT(3);SET MARGINS(3,1,130)
1082              ! PRINTS ANALYSIS FILE, WITH COPY OF TRACDATA AT START
1083              CYCLE NOEL=1,1,NOELS
1084              PRINT(Z(NOEL),2,0);PRINT(MA(1,NOEL),5,7);SPACES(2)
1085              PRINT(CX(1,NOEL),5,7);NEWLINE
1086              REPEAT
1087              NEWLINES(2)
1088              PRINTSTRING(STANSUSED)
1089              NEWLINE; PRINTSTRING(OMIT)
1090              NEWLINES(8)
1091              SPACES(14)
1092              CYCLE NOEL=1,1,NOELS
1093              PRINTSTRING(ELEM(NOEL));SPACES(8-LENGTH(ELEM(NOEL)))
1094              REPEAT
1095              PRINTSTRING("TIO2M")
1096              NEWLINE
1097              CYCLE V=1,1,NOSAMS
1098              NEWLINES(2)
1099              PRINTSTRING(NS(V));SPACES(9-LENGTH(NS(V)))
1100              CYCLE NOEL=1,1,NOELS
1101              IF STANSPRES->HT.(NS(V)).LT START
1102                 PA=MA(1,NOEL)*PK(V,NOEL)*CX(1,NOEL)
1103                 ! CALCULATES ANALYSES OF STANDARDS (WET)
1104                 ->928
1105                 FINISH
1106              PA=(MA(1,NOEL)*PK(V,NOEL)*CX(1,NOEL))*100/(100-LOI(V))
1107              ! CALCULATES ANALYSES; ! IF LOI \ON-ZERO RECALCULATES TO DRY BASIS
1108            828:IF ELEM(NOEL)->("TIO2").HT THEN PRINT(PA,3,3) AND->828
1109              PRINT(PA,5,1)
1110            A28:REPEAT
1111              PRINT(MAJ(8,V),3,3) UNLESS MAJ(8,V)=0
1112              REPEAT
1113            50:IF S5="",NULL" THEN->32
1114              IF S1#"",NULL" OR S2#"",NULL" THEN->34
1115              ! CREATES NORMINPUT FILE FROM ANALYSIS FILE
1116              NEWLINE
1117              PROMPT("NO.OF ELEMENTS:");READ(NOELS)
1118              SELECTINPUT(3)
1119              *STRG(CPS)
1120              CYCLE NOEL=1,1,NOELS
1121              WHILE CPS->(" ").CPS CYCLE;REPEAT
1122              IF NOEL=NOELS THEN ELEM(NOEL)=CPS AND->37
1123            CPS->ELEM(NOEL).(" ").CPS
1124            37:REPEAT
1125              CYCLE V=1,1,NOSAMS
1126            RSTRG(CPS)
1127              CPS->NS(V).(" ").CPS
1128              SELECTOUTPUT(7)
1129              PRINTSTRING(CPS);NEWLINE
1130              SELECTOUTPUT(99);CLOSESTREAM(7);SELECTINPUT(7)
1131              CYCLE NOEL=1,1,NOELS
1132              READ(BG1(V,NOEL))
1133              REPEAT
1134              SELECTINPUT(3);CLOSESTREAM(7)
1135            REPEAT;->36
1136            34:CYCLE V=1,1,NOSAMS
1137              CYCLE NOEL=1,1,NOELS
1138              BG1(V,NOEL)=(PK(V,NOEL)*MA(1,NOEL)*CX(1,NOEL))*100/(100-LOI(V))
1139              REPEAT;REPEAT
1140            36:SELECTOUTPUT(9);SET MARGINS(9,1,130)
1141              ! PRINTS NORMINPUT FILE, OMITTING STANDARDS
1142              CYCLE V=1,1,NOSAMS
1143              IF STANSPRES->HT.(NS(V)).LT THEN->A36
1144              PRINTSTRING(NS(V));PRINTSTRING(",")
1145              NEWLINE
1146              CYCLE NOEL=1,1,10
1147              PRINTSTRING(MAJEL(NOEL)); PRINT(MAJ(NOEL,V),4,3)
1148              SPACE; IF NOEL=5 THEN NEWLINE
1149              REPEAT
```

FIG. B14 : continued. Program TRACE

```
1150              NEWLINE
1151              IF MAJ(12,V)=0 THEN->B36
1152              PRINTSTRING('LOI');PRINT(MAJ(12,V),3,2);SPACE
1153            B36:IF Z(1)=21 THEN->C36
1154              CYCLE NOEL=13,1,17
1155              PRINTSTRING(MAJEL(NOEL));PRINT(MAJ(NOEL,V),5,1);SPACE
1156              REPEAT
1157              NEWLINE
1158              PRINTSTRING(MAJEL(18));PRINT(MAJ(18,V),2,3);SPACE
1159            C36:CYCLE NOEL=1,1,NOELS
1160              IF NOEL=4 OR NOEL=9 THEN NEWLINE
1161              IF ELEM(NOEL)->('TIO2').TAIL THEN PRINTSTRING(ELEM(NOEL)) AND C
   C                  PRINT(BG1(V,NOEL),1,3) AND->D36
1162              PRINTSTRING(ELEM(NOEL));PRINT(BG1(V,NOEL),5,1);SPACE
1163            D36:REPEAT
1164              NEWLINE
1165              IF V=NOSAMS THEN PRINTSTRING('-2') ELSE PRINTSTRING('-1')
1166              NEWLINE
1167            A36:REPEAT
1168            32:END

1169          END
?  UNUSED LABEL     35
```

FIG. B15 : Part of file TRACANAL - trace element standard data

```
G2
56 1850 29 11 57 100 21 4 23 34 58 150 24 9 41 14 28 6 37 170 38 480 39 12 30 85 40 300 17 .5 90 24 60 60 62 7.3
GSP1
56 1300 29 35 57 200 21 8 23 49 58 390 24 13 41 29 28 9 37 250 38 230 39 32 30 98 40 500 17 .66 90 105 60 190 62 27
AGV1
56 1200 29 63 57 45 21 12 23 125 58 63 24 12 41 15 28 17 37 67 38 660 39 26 30 84 40 220 17 1.05 90 6.4 60 39 62 5.9
STOP
```

file previously output by TRACE.

Output data: a combination of

(A) Count ratio file (only possible if (a) above chosen)

(B) Mass absorption corrected count ratio file, as (c) above

(C) Trace element analysis file, comparable to Fig. B10, with only the elements present as atomic numbers in the input count ratios. If (g), (i) or (j) with LOI are used for matrix correction, then all trace element analyses will be multiplied by 100/(100-LOI), i.e. they will be quoted volatile-free. In these cases, the ignited major element analyses (and V and La, if correction to Cr and Nb is required) are reduced by (100-LOI)/100 prior to matrix correction, and the LOI is assumed to be 50% CO2, 50% H2O for its contribution to matrix correction. If input data from WTRACE is to be processed, and the file used for matrix correction does not contain V, La or Ba values, then no correction will be made to the Cr, Nb and TiO2W concentrations, respectively.

(D) Norminput file, similar to Fig. B11, and containing the newly processed trace element data, together with major and Cr-tube trace data, if such were present in the file used for matrix correction.

(E) File TRACDATA, similar to Fig. B9, updated with each new calibration.

(F) External records CALIB and ELNAME, as for MAJORS (ii)(e).

The program is not dissimilar to MAJORS, but is considerably more complex. If input data from WTRACE is used, then interference corrections for V on Cr and La on Nb are made by regressing matrix-corrected count ratios against ppm V and La present in the file used for matrix correction. All regressions carried out in TRACE are by the perpendicular-to-line method.

While there is a large number of possible routes by which data may be run using these programs, for ignited samples the most convenient way to obtain a full analysis is as follows:

(1) RATMAJ and MAJORS, leading to Analysis file with LOI values

(2) CRTRACE and TRACE, leading to norminput file with major elements, LOI and Cr-tube trace elements.

(3) WTRACE and TRACE, leading to a norminput file containing the full analysis, all recalculated volatile-free.

B11 : COMPARISON WITH OTHER XRF METHODS

During the course of this study 35 samples with analyses quoted in Gandy (1973a) were re-analysed using the techniques previously described. Prior to comparison of results, the data of Gandy (1973a) were recalculated to 100%, to provide volatile-free analyses directly comparable with those of the author. Plots of the two values for each sample should ideally yield a 1:1 straight line, but only values for K2O are a reasonable approximation to this. It will be seen that REE and Y compare particularly badly

Fig. B16 : Comparison of analyses of S18-S52 from Table B17 and Gandy (1973a)

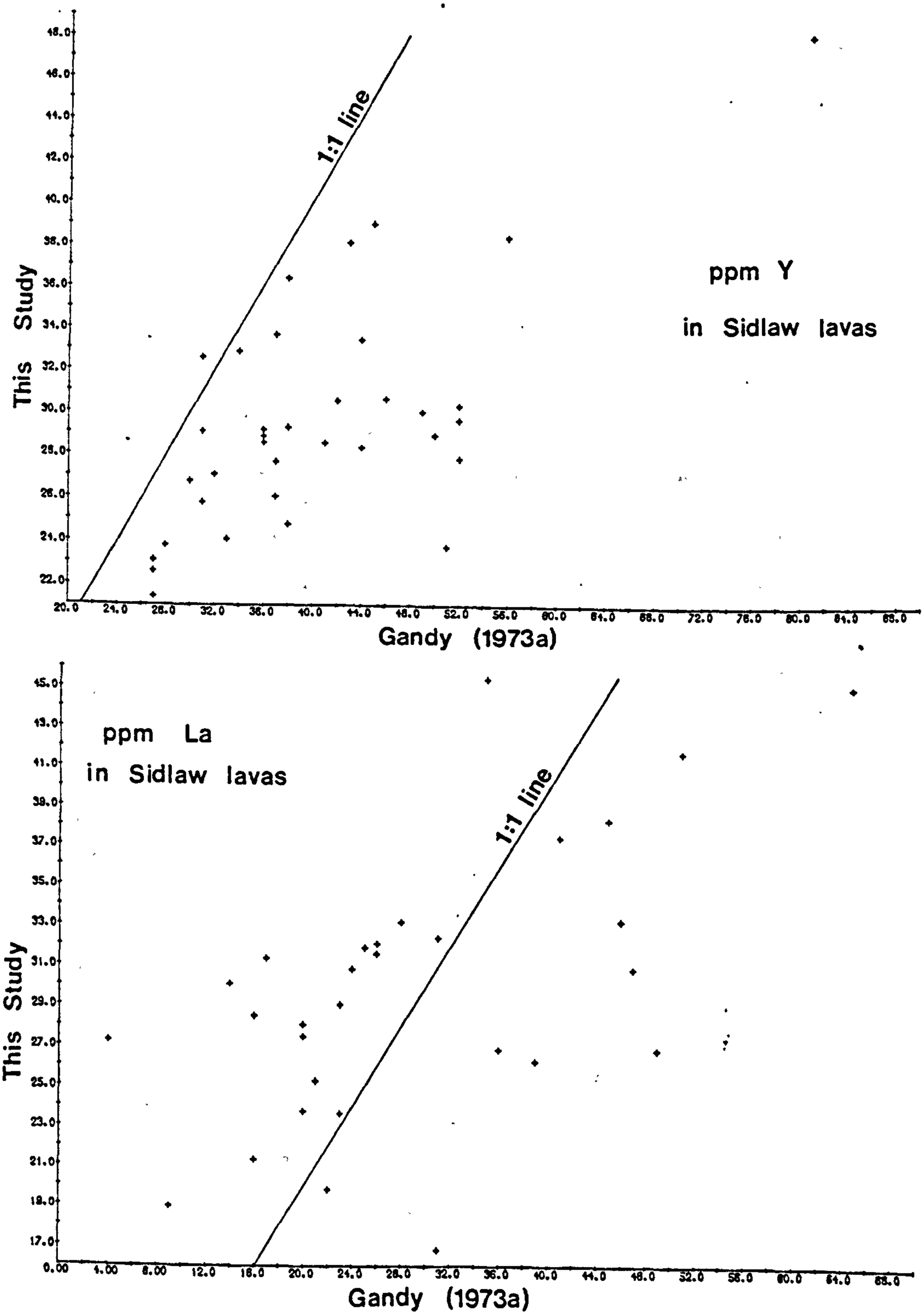

(Fig. B16). It is difficult to suggest reasons for the large discrepancies in many elements, for a comprehensive account of the techniques used is not given in Gandy (1973a). It is suspected that some of the discrepancies in trace elements are caused by use of the Anderman-Kemp method of matrix correction, and the analysis of elements such as Ba, La and Ce on the highly energetic K_α lines. The strong evidence presented in Figs. B1, B3, Tables B15, B16 for the accuracy of the present techniques suggests that the analyses in Gandy (1973a) should be used with extreme caution.

Graham (in preparation) has re-analysed samples from Grenada, West Indies, previously analysed by Arculus (1973) at the University of Durham, and reports very large differences for several major elements. The differences are thought to be at least in part due to the use of an iterative correction procedure for counts made on pressed powder pellets (Holland and Brindle, 1966).

B12 : FUTURE IMPROVEMENTS IN METHOD

A number of modifications may possibly be made to improve the reported techniques in the future.
(i) The use of a monitor in counting for TiK_β and CaK_β in the Cr-tube trace element program.
(ii) Improvements in mass absorption coefficients, and possibly the extension of the calculation to give a coefficient for each analytical wavelength.
(iii) The use of matrix correction for major elements.
(iv) Improvements in knowledge of standard concentrations or in homogeneity of standards.
(v) Use of improved knowledge of the relationship between background intensity and mass absorption coefficient to remove any problems caused by residual background B* (section B5iii).
(vi) Improvements in spectrometer resolution, reducing the magnitude of interference corrections.
(vii) An understanding of the origin of the TiO2W-TiO2 discrepancy (section B9) may lead to changes in the techniques.
(viii) Use of an interference correction for NdL_α, on CeL_β, and possibly the use of an interference correction for CrK_α on the Nd and Ce backgrounds.
(ix) Change in position of Cu background to avoid interference by HfL_α and 2nd order ZrK_α.

Precision and detection limits may easily be improved for all elements by increasing the total counting time. This may be done either by increasing the number of counts which the monitor is required to accumulate, or by increasing the number of peak-background pairs. The former method does not require modification of the computer programs, but if the interval between successive references to the monitor becomes too great then medium term machine drift can become important. It is thought that the low analytical precision quoted for Sm results from this effect, for the time between references to the monitor was here as

long as 18 min. It is believed that this time should be kept to less than about 6 min, and it has been shown that, by increasing substantially the number of peak-background pairs and counting for about 30 min per sample, Hf may be analysed to a precision of ± 0.5 ppm. Precision for Sm, Th and also Ba could therefore be improved by increasing the number of peak-background pairs. Analysis of a number of low concentration elements has been attempted using this method: it is believed that analysis of at least Hf, U, Pr, Cs and possibly Eu may be feasible.

Table B17 : Analyses of samples listed in Table A1 for 10 major and 17 trace elements.

FE203 is total iron as Fe203, LOI is loss on ignition. TI02CR and TI02W are Ti02 determined on trace element pellets as in section B9.

* = negative concentration; this has only occurred for Th (minimum -5 ppm), Sm (-2 ppm), Sc (-0.6 ppm) and Na20 (-0.06 %). With the exception of Th, these are within the precision limits of zero concentration. The negative Th values do not appear to be the result of interference on background, and may have the same origin as the differences in Th content between the samples quoted in Table A2, and between MT45 run for precision (Table B7) and reproducability (Table B3) data.

n.d. = not determined.

TABLE B17

	L1324	L3a1	L4a1	L5a14	L8a1	L9a7	L10a8	L11a8	L12a1
SIO2	64.04	52.86	51.65	64.26	54.57	56.07	59.88	59.36	53.53
AL2O3	16.28	16.40	16.26	16.57	15.67	15.73	17.02	16.95	16.79
FE2O3	4.81	8.65	9.44	4.96	8.58	7.96	5.67	6.93	8.21
MGO	2.62	6.88	4.04	2.21	5.92	4.44	3.62	4.46	4.30
CAO	2.84	7.14	10.75	3.72	6.54	7.11	4.88	1.67	9.36
NA2O	4.50	3.72	3.65	4.20	3.75	3.90	4.83	5.84	3.70
K2O	3.669	2.212	1.901	3.123	2.973	1.948	2.584	2.905	1.987
TIO2	0.739	1.443	1.640	0.706	1.238	1.271	0.941	1.002	1.336
MNO	0.066	0.116	0.128	0.052	0.156	0.083	0.078	0.096	0.120
P2O5	0.233	0.460	0.465	0.208	0.523	0.363	0.340	0.344	0.432
TOTAL	99.82	99.89	99.93	100.00	99.92	99.87	99.83	99.55	99.77
LOI	3.82	2.17	4.55	3.40	1.60	1.71	1.34	2.22	6.17
NI	44.0	164.0	175.5	42.8	100.3	133.7	60.5	73.2	160.1
CR	73.0	370.8	312.6	87.7	275.4	250.3	143.7	160.3	295.3
V	86.1	165.6	168.9	84.4	139.9	163.8	115.6	125.0	168.1
SC	12.2	22.9	24.6	12.5	17.5	20.5	14.6	14.8	23.0
CU	17.9	18.4	23.5	20.4	12.6	44.8	31.6	14.2	32.8
ZN	62.4	85.5	89.2	56.3	89.6	77.3	65.6	77.1	93.7
SR	655.2	1251.4	1064.6	624.4	1333.6	926.3	1065.1	1427.6	961.4
RB	79.2	36.8	25.9	66.8	63.8	36.9	41.0	47.2	22.4
ZR	205.2	193.5	229.9	176.9	211.9	197.6	162.1	161.1	231.1
NB	10.6	15.3	15.8	9.3	13.6	14.3	9.9	10.4	15.4
BA	1913.4	1079.2	804.0	1316.0	1418.1	744.6	1106.1	1430.3	697.4
TH	4.6	5.0	5.8	3.9	7.3	6.1	3.2	2.8	7.5
LA	31.5	34.8	33.3	27.8	44.7	32.3	30.4	33.1	38.7
CE	73.0	79.7	77.9	62.1	99.5	66.5	66.7	69.2	87.7
ND	31.9	37.1	36.9	28.4	43.5	29.8	30.2	31.6	40.8
SM	4.4	5.6	7.8	6.2	9.4	8.4	4.3	7.2	12.8
Y	18.3	21.0	23.3	16.1	17.4	20.8	15.5	15.7	23.1
TIO2CR	0.722	1.517	1.716	0.676	1.167	1.229	1.004	1.044	1.443
TIO2W	0.730	1.531	1.727	0.692	1.196	1.286	0.988	1.042	1.446

	L13a1	L14a8	L18a1	L19a1	L21a7	L22a20	L23a1	L24a7	L25a1
SIO2	57.62	61.05	56.78	51.91	59.55	64.56	48.90	54.27	55.01
AL2O3	16.57	16.70	16.62	16.98	16.31	15.69	17.47	16.10	16.89
FE2O3	7.39	5.92	8.06	7.62	6.23	4.97	9.87	7.58	7.42
MGO	3.63	3.06	3.33	4.62	3.69	1.31	7.19	5.72	4.56
CAO	6.82	4.48	6.79	11.22	5.62	2.74	10.57	7.98	8.47
NA2O	3.68	4.74	3.35	3.39	4.14	5.42	2.70	3.70	3.48
K2O	2.285	2.587	2.624	1.693	2.517	3.019	1.095	2.493	1.958
TIO2	1.345	0.787	1.376	1.692	1.026	0.728	1.535	1.331	1.317
MNO	0.091	0.051	0.089	0.134	0.087	0.053	0.135	0.101	0.081
P2O5	0.430	0.339	0.464	0.491	0.389	0.287	0.395	0.453	0.436
TOTAL	99.86	99.74	99.48	99.75	99.56	99.78	99.85	99.73	99.63
LOI	3.83	1.64	4.16	6.52	1.56	3.09	2.90	3.45	5.89
NI	161.1	48.6	154.3	177.7	76.9	33.6	91.9	164.9	158.3
CR	297.2	90.8	314.1	405.4	158.6	26.2	148.8	304.7	301.3
V	147.6	91.3	153.7	201.5	125.2	58.3	205.0	144.4	152.4
SC	23.4	11.8	24.2	30.7	15.9	10.9	29.6	21.8	22.0
CU	15.8	19.9	24.8	23.4	20.9	10.3	45.5	14.4	18.6
ZN	75.7	61.0	61.4	76.2	62.8	54.7	70.4	87.1	84.3
SR	892.7	1100.1	963.9	1082.1	1037.3	1176.8	1113.6	1022.7	957.5
RB	47.4	41.7	47.8	27.7	40.9	54.5	13.6	48.9	27.4
ZR	230.3	146.4	223.4	238.5	175.4	133.2	160.4	220.8	229.3
NB	15.4	8.9	14.7	18.7	10.9	10.4	5.4	15.0	15.1
BA	757.2	1359.0	985.6	626.5	1150.5	1242.5	694.8	942.1	824.0
TH	8.0	2.9	8.9	6.6	4.2	5.6	*	6.1	6.6
LA	39.4	34.5	40.9	36.9	37.8	39.5	21.1	41.8	39.7
CE	88.6	73.2	91.1	80.1	73.1	71.2	56.3	91.5	86.4
ND	38.8	33.1	43.7	35.9	35.3	32.1	33.2	43.0	38.7
SM	7.6	7.1	7.4	13.3	11.0	2.4	10.8	10.1	8.8
Y	23.6	14.6	21.7	22.0	15.5	14.3	26.5	22.1	22.5
TIO2CR	1.338	0.825	1.326	1.662	1.041	0.744	1.651	1.399	1.385
TIO2W	1.359	0.810	1.349	1.714	1.041	0.739	1.589	1.367	1.385

TABLE B17

	L26@7	L29@13	L30@13	L34@45	L35@21	L38@20	L41@20	L42@19	L43@22
SIO2	54.57	62.45	62.67	53.14	74.77	62.73	57.75	71.76	68.84
AL2O3	15.57	16.37	16.32	17.26	14.60	17.71	17.16	14.43	16.21
FE2O3	7.73	5.31	5.09	9.61	1.14	5.84	5.46	2.28	3.45
MGO	6.61	2.79	3.10	6.36	0.85	3.43	5.43	0.41	0.88
CAO	7.42	3.90	3.26	5.35	0.97	2.20	5.16	4.21	1.99
NA2O	3.48	4.06	4.75	5.39	2.06	4.25	4.14	4.02	4.19
K2O	2.272	3.197	2.930	1.986	5.355	2.224	1.900	2.776	3.540
TIO2	1.335	0.840	0.831	1.227	0.216	0.805	0.984	0.271	0.601
MNO	0.086	0.080	0.077	0.100	0.060	0.033	0.121	0.045	0.062
P2O5	0.486	0.269	0.267	0.407	0.054	0.310	0.344	0.090	0.210
TOTAL	99.56	99.25	99.28	99.53	100.06	99.53	99.46	100.29	99.98
LOI	3.29	2.76	1.86	6.35	2.40	4.34	2.22	4.45	3.77
NI	172.7	40.8	40.4	173.5	8.1	73.6	92.7	13.1	19.1
CR	295.3	65.3	66.2	354.6	5.4	121.6	140.4	13.9	38.9
V	138.7	99.0	100.4	162.7	8.0	109.2	133.1	21.7	60.9
SC	18.2	13.1	12.5	26.3	3.4	14.6	18.5	4.6	8.2
CU	27.5	23.0	22.7	34.7	2.3	10.2	21.8	4.0	8.1
ZN	75.9	63.3	64.8	104.3	41.9	82.3	106.3	17.2	29.4
SR	1200.0	1059.9	1179.5	997.9	264.1	515.4	1024.2	328.8	465.1
RB	45.3	70.5	69.3	44.9	124.0	57.8	32.0	68.6	80.0
ZR	199.4	194.5	196.5	181.2	181.8	153.4	169.3	122.8	188.3
NB	14.4	9.2	9.0	8.9	14.5	8.3	9.5	12.1	12.4
BA	1051.1	1582.0	1302.9	1049.5	1056.6	345.6	932.2	1143.6	1059.9
TH	8.9	9.7	8.1	4.9	12.4	7.2	4.5	10.1	12.0
LA	44.0	35.2	35.1	34.6	35.4	31.6	29.2	28.5	38.0
CE	97.1	73.8	71.4	73.0	73.2	51.2	65.2	54.7	73.7
ND	45.2	33.3	33.0	36.7	30.5	28.9	29.8	24.0	30.2
SM	5.4	4.2	*	6.2	5.7	4.3	2.9	4.0	2.0
Y	22.4	18.9	18.0	20.6	18.8	15.5	18.3	17.6	15.4
TIO2CR	1.282	0.838	0.842	1.248	0.230	0.816	0.979	0.300	0.604
TIO2W	1.317	0.837	0.842	1.279	0.242	0.830	0.993	0.303	0.628

	L44@1	L45@8	L50@45	L51@9	L52@9	L54@22	L55@22	L56@1	L58@1
SIO2	55.33	61.27	59.61	60.30	60.83	56.25	57.26	52.53	53.01
AL2O3	16.21	16.92	15.65	16.48	16.50	15.28	19.05	16.19	16.70
FE2O3	9.71	5.39	6.09	5.92	6.40	5.81	8.37	7.91	8.47
MGO	5.63	3.50	4.84	3.51	4.58	5.00	2.21	7.60	6.74
CAO	5.74	4.37	5.79	5.75	2.82	5.75	1.34	7.44	6.44
NA2O	3.43	4.53	3.58	3.98	4.70	4.37	5.11	3.54	3.79
K2O	1.709	2.634	2.442	2.529	2.239	4.338	4.412	2.689	2.119
TIO2	1.427	0.808	1.031	0.919	0.933	0.885	0.817	1.166	1.608
MNO	0.075	0.068	0.082	0.075	0.062	0.098	0.043	0.130	0.150
P2O5	0.369	0.356	0.390	0.353	0.343	0.593	0.625	0.553	0.466
TOTAL	99.62	99.84	99.51	99.82	99.41	99.38	99.24	99.75	99.50
LOI	1.95	1.35	2.42	2.10	2.49	5.11	2.33	2.71	2.18
NI	181.3	44.7	132.7	81.1	82.9	195.5	14.0	215.6	158.2
CR	338.5	88.9	233.1	166.1	174.3	376.8	6.9	412.9	279.0
V	175.8	95.0	116.0	109.7	118.4	113.9	137.0	160.2	156.1
SC	24.1	12.3	14.3	14.5	15.3	16.6	10.6	18.0	17.7
CU	114.4	25.9	24.6	27.4	23.8	26.6	29.3	38.0	41.1
ZN	77.1	70.3	72.9	72.3	80.4	79.2	151.1	81.8	75.7
SR	726.8	1141.9	927.9	1065.5	1155.8	2236.3	1728.2	1435.0	1040.4
RB	32.7	43.1	40.9	47.6	31.1	57.0	81.0	45.1	22.5
ZR	205.1	149.8	188.5	169.3	172.7	157.3	225.9	192.3	197.4
NB	13.7	9.4	11.3	11.0	11.5	7.4	9.8	10.0	17.4
BA	773.3	1318.0	1105.2	1073.3	1042.4	2998.0	1772.0	1258.9	949.8
TH	4.2	3.4	3.6	6.5	6.8	7.5	15.0	3.1	0.3
LA	26.1	32.8	34.6	36.7	34.3	75.7	80.7	38.6	29.2
CE	62.7	67.8	76.6	76.4	72.2	155.8	183.5	88.2	73.2
ND	28.5	32.2	33.4	33.2	32.2	81.0	87.4	43.7	34.6
SM	10.3	8.0	6.4	6.7	6.5	11.7	11.5	6.8	5.9
Y	20.2	14.1	15.7	15.6	16.7	16.6	17.2	16.7	18.7
TIO2CR	1.277	0.818	1.035	0.942	0.940	0.939	0.845	1.244	1.707
TIO2W	1.371	0.832	1.050	0.944	0.952	0.917	0.839	1.239	1.668

TABLE B17

	L61a47	L63a47	L64a7	L65a7	L67a1	L68a1	L71a1	L73a12	L75a19
SIO2	59.38	54.92	58.10	53.54	53.72	55.56	56.87	50.92	65.97
AL203	16.72	17.25	15.90	15.75	17.34	13.86	16.12	17.55	17.38
FE203	6.24	8.05	7.39	7.40	7.80	7.11	7.27	9.60	3.80
MGO	3.14	3.55	4.25	7.75	6.21	5.12	5.03	4.77	0.78
CAO	7.11	7.42	5.88	6.19	6.65	7.79	6.25	10.35	1.58
NA2O	4.12	4.25	3.83	3.91	4.54	3.74	3.86	3.56	5.49
K2O	2.148	1.979	2.554	3.065	1.997	2.405	2.433	1.236	3.736
TIO2	0.975	1.461	1.020	1.185	1.197	1.087	1.321	1.590	0.838
MNO	0.072	0.073	0.080	0.136	0.100	0.098	0.074	0.108	0.037
P2O5	0.339	0.508	0.425	0.512	0.429	0.456	0.484	0.387	0.263
TOTAL	100.25	99.47	99.41	99.55	99.97	99.22	99.71	100.08	99.86
LOI	4.15	4.55	2.81	2.71	1.48	2.79	3.32	5.18	1.32
NI	96.1	113.9	182.4	210.4	146.4	155.3	162.5	152.8	12.2
CR	169.4	225.7	270.5	320.1	366.0	235.1	273.5	330.0	19.9
V	100.6	223.6	135.7	139.0	145.6	128.1	137.4	200.5	71.5
SC	17.4	18.7	18.3	14.0	21.8	16.6	20.8	34.8	7.8
CU	23.7	12.6	23.5	35.4	15.4	27.7	23.0	58.2	3.9
ZN	70.6	84.6	76.0	76.8	67.0	74.8	76.1	81.6	54.6
SR	1047.0	1184.2	1311.9	1538.1	1201.5	1424.1	1150.6	887.7	1063.9
RB	21.9	23.7	42.5	58.1	28.2	39.5	41.2	18.3	79.0
ZR	165.3	195.6	170.5	181.6	148.9	181.0	214.7	203.3	769.2
NB	10.6	17.6	12.1	11.0	9.7	12.3	17.3	11.4	10.1
BA	1438.8	872.0	1162.3	1770.7	1040.0	1050.0	868.0	581.5	3227.2
TH	3.3	1.3	6.8	*	1.2	6.0	4.7	4.3	1.9
LA	31.5	29.5	43.9	33.4	31.5	43.2	43.9	28.6	38.6
CE	63.6	68.9	86.9	77.6	69.8	93.2	88.8	61.5	79.2
ND	31.4	32.7	39.2	38.2	33.8	41.6	41.1	30.7	38.7
SM	6.4	6.8	7.3	7.8	6.9	7.1	4.8	3.2	7.5
Y	17.2	18.3	16.2	15.7	16.7	19.8	19.0	25.8	21.7
TIO2CR	1.030	1.502	1.034	1.253	1.080	1.059	1.356	1.622	0.892
TIO2W	1.025	1.515	1.045	1.252	1.139	1.102	1.373	1.642	0.871

	L77a19	L79a13	L82a25	L86a13	L87a3	L91a3	L92a19	L95a13	L97a7
SIO2	67.00	63.34	63.90	62.69	61.08	60.33	77.61	62.91	58.33
AL203	16.07	16.95	16.09	16.52	17.21	14.38	12.05	16.44	16.44
FE203	3.46	4.88	5.75	4.96	8.66	7.35	1.33	5.21	6.40
MGO	2.51	2.18	3.43	3.49	2.83	5.77	0.28	3.04	6.38
CAO	1.46	2.62	3.59	3.65	2.93	2.57	0.95	4.09	5.80
NA2O	5.17	5.87	3.52	4.15	1.07	3.65	2.36	3.75	3.34
K2O	3.468	3.239	2.535	2.997	3.994	2.580	5.278	3.423	2.090
TIO2	0.520	0.952	0.787	0.850	1.362	1.137	0.205	0.826	0.790
MNO	0.036	0.070	0.061	0.064	0.065	0.086	0.035	0.056	0.104
P2O5	0.226	0.310	0.240	0.275	0.415	0.346	0.017	0.262	0.281
TOTAL	99.91	100.34	99.91	99.65	99.61	99.20	100.11	100.00	99.96
LOI	2.04	1.60	1.14	2.97	5.83	4.29	1.61	2.93	2.38
NI	45.7	17.0	69.5	39.9	150.2	130.3	4.6	38.5	126.9
CR	86.1	21.0	153.1	66.0	464.9	384.1	4.0	62.7	305.1
V	72.7	118.0	110.1	114.9	133.1	129.2	8.8	110.9	146.3
SC	9.2	11.2	15.4	14.4	24.5	22.5	2.8	14.7	21.6
CU	15.0	20.5	4.7	22.6	26.3	25.9	3.1	19.4	24.8
ZN	59.3	64.3	44.8	67.0	61.5	94.3	22.8	63.0	67.4
SR	1612.1	1130.1	821.1	979.8	309.8	900.7	325.4	906.9	882.2
RB	54.8	71.0	70.0	74.2	117.2	53.1	105.6	74.0	35.6
ZR	114.8	226.8	183.8	202.1	242.6	197.1	203.5	206.4	138.6
NB	6.8	11.1	9.2	9.7	17.2	14.0	12.4	9.9	7.7
BA	1223.4	1274.9	1092.8	1238.5	626.9	951.1	2125.9	1359.0	996.3
TH	3.3	7.9	6.9	7.6	8.7	7.2	7.7	6.5	3.4
LA	23.7	34.9	31.2	36.9	37.5	28.0	43.0	37.0	26.8
CE	50.6	77.3	63.8	75.9	71.1	53.1	85.3	76.8	59.7
ND	24.8	35.7	27.1	34.2	32.9	28.8	35.9	34.3	27.2
SM	5.4	7.0	6.3	6.7	7.6	6.0	6.1	6.4	6.4
Y	9.0	20.4	16.7	18.6	19.3	17.7	16.0	17.7	17.5
TIO2CR	0.562	0.971	0.858	0.855	1.350	1.162	0.228	0.873	0.807
TIO2W	0.557	0.974	0.834	0.866	1.394	1.192	0.240	0.865	0.816

TABLE B17

	L9806	L9919	L10006	L10119	L10213	L11315	L12019	L12113	L12226
SIO2	60.67	73.58	63.00	58.44	63.08	57.11	68.45	60.22	52.69
AL2O3	17.11	13.29	17.22	17.05	16.45	16.22	14.51	16.92	15.91
FE2O3	5.65	3.32	4.83	6.90	5.12	3.45	4.36	5.92	8.33
MGO	2.16	0.64	1.64	4.25	3.37	4.58	2.17	3.57	6.56
CAO	4.00	1.95	2.21	6.13	3.56	5.09	0.47	4.73	8.72
NA2O	5.83	3.32	6.01	3.55	4.32	4.11	4.50	3.94	3.65
K2O	3.158	3.069	3.287	2.022	3.083	5.006	4.620	3.189	2.046
TIO2	0.934	0.607	0.929	0.914	0.783	0.918	0.552	1.057	1.064
MNO	0.069	0.040	0.057	0.069	0.073	0.074	0.068	0.083	0.084
P2O5	0.288	0.231	0.268	0.204	0.240	0.615	0.211	0.315	0.465
TOTAL	99.87	100.04	99.47	99.51	100.07	99.17	99.91	99.95	99.52
LOI	4.07	1.85	2.20	2.11	2.36	2.06	1.35	2.95	3.61
NI	24.1	7.1	12.4	52.5	45.7	96.8	27.1	66.4	184.6
CR	37.0	33.1	14.7	84.8	82.9	114.2	43.3	115.4	320.1
V	98.3	30.9	98.5	138.2	104.5	104.8	60.0	127.8	169.8
SC	12.3	4.2	9.3	19.3	13.7	11.1	10.2	17.7	25.1
CU	14.9	1.9	10.9	20.1	23.9	26.8	7.7	22.8	22.4
ZN	65.6	31.7	63.4	65.6	63.9	78.4	63.4	66.4	72.7
SR	821.3	506.1	1120.6	936.5	792.4	1898.4	520.7	748.0	1766.6
RB	73.4	51.7	71.0	33.2	67.8	148.0	104.2	75.5	20.2
ZR	501.3	617.1	654.7	115.8	186.6	361.3	172.3	219.2	112.5
NB	8.9	8.4	10.8	6.1	8.8	9.2	33.6	10.6	7.2
BA	1912.8	1973.0	2223.9	969.9	1184.7	2107.0	1265.5	870.9	1372.5
TH	3.2	1.0	3.2	2.6	6.1	1.1	13.0	6.2	0.3
LA	36.7	30.8	35.4	16.3	33.7	40.7	28.2	37.3	34.7
CE	76.9	63.5	75.9	40.8	67.2	96.6	56.4	76.8	85.8
ND	35.3	30.6	36.9	21.2	30.1	48.2	26.4	33.1	45.1
SM	5.6	4.2	5.0	4.6	2.6	4.2	3.9	5.5	6.6
Y	21.5	16.5	22.7	17.5	17.8	13.6	26.1	20.9	17.9
TIO2CR	1.004	0.644	0.994	0.963	0.769	0.987	0.623	1.105	1.121
TIO2W	1.002	0.651	0.979	0.951	0.784	0.971	0.611	1.120	1.128

	L12515	L12687	L12813	L12931	L13019	L13185	L13285	L13331	L13726
SIO2	62.95	55.97	61.32	55.79	66.68	64.48	59.32	57.29	53.10
AL2O3	15.49	16.60	16.71	17.25	17.19	15.96	18.32	17.30	16.31
FE2O3	4.09	7.43	5.59	6.60	3.61	4.55	4.99	7.04	7.91
MGO	3.23	4.71	3.00	5.14	2.20	2.55	3.40	3.73	6.04
CAO	3.95	6.24	5.02	6.97	0.63	1.75	5.15	3.83	7.28
NA2O	4.69	4.26	3.86	4.05	5.58	4.20	4.51	6.46	4.34
K2O	4.432	2.990	2.683	2.079	2.742	5.477	2.927	2.382	2.920
TIO2	0.513	1.076	0.896	1.382	0.631	0.700	1.270	1.143	1.065
MNO	0.064	0.077	0.071	0.096	0.052	0.083	0.055	0.102	0.106
P2O5	0.338	0.533	0.277	0.482	0.165	0.223	0.351	0.464	0.472
TOTAL	99.74	99.88	99.52	99.84	99.47	99.98	100.30	99.74	99.55
LOI	1.08	2.06	1.63	2.86	2.17	1.94	2.66	3.39	5.41
NI	66.0	81.0	73.9	133.1	18.1	29.1	57.4	85.0	142.0
CR	66.5	192.8	128.1	207.9	36.3	51.7	108.8	164.0	187.6
V	69.7	124.5	110.8	152.9	51.2	88.8	149.7	135.6	170.2
SC	8.7	15.0	15.6	22.6	6.3	10.5	21.4	15.5	23.1
CU	20.9	20.3	27.7	35.9	4.9	12.1	57.6	24.3	18.3
ZN	55.9	77.0	58.4	86.9	64.6	54.5	58.8	93.4	84.1
SR	1978.2	1559.4	1003.9	1016.3	1197.9	847.1	918.3	2008.7	971.0
RB	68.7	43.1	57.3	27.2	71.7	112.1	64.6	37.1	28.9
ZR	170.2	187.3	187.3	229.0	526.7	213.4	242.9	194.3	126.1
NB	8.1	13.3	9.4	16.4	10.2	12.6	10.5	16.1	6.9
BA	2239.0	1688.3	1058.2	900.9	1929.5	2315.9	1074.8	970.1	1877.1
TH	12.7	2.1	5.6	3.0	3.7	7.9	5.9	1.5	0.2
LA	66.4	39.3	33.5	39.8	38.2	27.2	39.4	37.9	37.4
CE	140.6	87.4	71.4	89.2	81.0	52.8	76.0	76.1	84.5
ND	62.7	42.3	32.1	40.1	42.5	29.2	34.5	37.6	44.9
SM	7.6	5.6	3.6	5.5	6.0	3.9	4.2	4.5	5.9
Y	13.5	16.2	17.8	22.8	22.8	15.8	18.2	17.1	18.4
TIO2CR	0.539	1.102	0.926	1.368	0.638	0.730	1.308	1.128	1.123
TIO2W	0.536	1.095	0.922	1.391	0.645	0.739	1.333	1.166	1.131

TABLE B17

	L140a1	L141a1	L146a7	L148a1	L150a21	L151a1	L152a1	L153a1	L155a7
SIO2	55.34	52.67	54.76	53.50	73.11	53.26	54.99	52.64	53.99
AL203	17.43	16.87	17.04	16.58	14.94	17.26	16.56	16.25	16.59
FE203	6.35	8.70	7.50	7.90	1.39	9.43	8.20	9.38	8.37
MGO	5.83	5.52	5.79	6.92	0.36	4.72	5.55	6.11	4.59
CAO	5.74	6.48	6.66	6.87	0.77	1.96	7.24	8.33	7.86
NA2O	4.41	4.90	3.95	3.85	4.30	5.99	3.72	3.46	4.29
K2O	2.559	1.963	2.257	2.062	4.923	2.622	1.851	1.713	2.160
TIO2	1.296	1.575	1.209	1.464	0.313	1.606	1.435	1.636	1.524
MNO	0.079	0.230	0.067	0.158	0.045	0.069	0.090	0.105	0.122
P2O5	0.466	0.547	0.385	0.512	0.048	0.484	0.393	0.416	0.520
TOTAL	99.49	99.45	99.61	99.82	100.21	99.39	100.03	100.02	100.05
LOI	1.72	2.08	1.69	2.17	1.19	2.14	1.75	1.88	2.12
NI	124.1	99.3	142.2	151.0	6.6	147.8	179.8	184.2	158.2
CR	266.0	222.6	302.1	283.5	6.3	319.6	316.8	322.8	295.5
V	159.0	167.4	151.6	156.5	18.9	97.5	207.0	158.0	175.3
SC	19.5	16.6	19.9	20.1	4.0	23.8	22.9	22.2	20.1
CU	49.1	23.5	32.1	16.6	6.7	32.9	41.5	42.8	30.8
ZN	89.9	91.6	66.0	80.0	34.4	92.9	89.2	81.1	77.7
SR	1326.9	1629.9	984.1	942.8	279.8	1177.8	858.1	924.8	1077.9
RB	37.0	10.3	36.8	37.0	106.4	38.2	40.3	33.5	41.9
ZR	167.3	170.7	186.5	236.6	251.9	215.4	229.0	230.6	248.3
NB	11.8	12.9	13.6	18.6	13.5	19.0	15.9	15.1	18.4
BA	1163.1	1338.4	849.5	796.7	1709.0	1690.8	646.3	651.2	873.6
TH	*	*	2.1	3.6	11.0	3.0	3.7	3.1	1.6
LA	33.1	31.1	34.0	35.4	69.4	45.4	36.5	33.2	35.5
CE	69.4	71.6	74.1	78.9	115.2	90.0	72.0	72.3	82.8
ND	32.2	36.2	33.6	35.2	51.7	41.6	34.1	33.0	38.6
SM	0.6	3.4	7.1	4.1	5.7	6.3	4.3	5.0	8.1
Y	16.4	16.5	20.0	22.0	20.4	23.6	22.3	26.2	20.9
TIO2CR	1.316	1.658	1.149	1.370	0.356	1.667	1.369	1.373	1.377
TIO2W	1.346	1.635	1.172	1.443	0.357	1.651	1.403	1.491	1.458

	L156a19	L157a13	L158a13	GC1a7	GC3a44	GC4a44	GC5a21	GC6a17	GC8a19
SIO2	65.06	60.02	61.58	55.85	61.36	62.91	67.51	65.21	75.16
AL203	16.91	17.52	16.50	16.97	16.23	15.00	16.02	16.27	14.10
FE203	3.97	5.98	5.42	7.77	5.78	5.30	3.37	4.32	0.96
MGO	1.77	3.12	3.21	4.10	3.23	2.83	1.42	2.20	0.29
CAO	1.81	5.30	5.22	5.82	4.78	4.67	2.40	3.19	0.58
NA2O	4.96	3.87	3.73	4.82	3.90	3.21	4.23	4.16	4.46
K2O	3.998	3.011	3.328	2.190	2.687	3.499	3.687	3.250	4.079
TIO2	0.761	0.878	0.858	1.349	0.885	0.840	0.555	0.641	0.169
MNO	0.032	0.055	0.071	0.122	0.080	0.084	0.062	0.059	0.052
P2O5	0.247	0.353	0.270	0.405	0.324	0.294	0.158	0.223	0.047
TOTAL	99.50	100.11	100.19	99.39	99.25	99.64	99.41	99.53	99.90
LOI	1.26	3.95	4.70	1.68	1.68	2.17	2.07	1.75	0.44
NI	14.4	53.1	77.3	74.2	49.3	40.7	15.9	32.2	3.8
CR	35.2	89.0	137.7	136.1	98.3	97.4	29.2	51.5	4.7
V	59.6	117.7	117.3	116.1	105.0	94.4	47.2	72.6	4.5
SC	6.8	15.6	15.7	15.5	13.3	13.2	6.9	7.8	2.1
CU	1.9	19.7	26.9	19.9	22.0	20.6	9.9	15.1	2.7
ZN	58.2	80.9	66.5	84.1	73.8	58.7	56.1	61.7	30.5
SR	939.5	1269.3	857.3	1236.2	1205.8	1253.6	817.2	988.9	182.3
RB	78.2	51.7	70.2	36.9	78.1	55.2	85.6	75.2	110.6
ZR	740.6	190.5	188.4	189.0	248.0	261.0	261.1	177.5	110.3
NB	10.2	8.6	9.9	12.0	11.8	11.4	10.9	10.7	11.4
BA	3260.5	1334.6	944.7	920.9	1272.1	1399.8	1635.3	1309.0	1215.2
TH	0.0	7.4	5.7	1.5	5.0	6.6	6.5	5.7	10.6
LA	34.8	40.2	29.0	30.6	39.0	40.2	37.8	31.3	28.2
CE	77.5	87.3	61.2	69.5	81.5	99.0	76.4	67.3	56.9
ND	37.0	42.4	29.5	31.5	38.3	39.9	33.5	28.6	23.5
SM	3.8	4.3	2.7	6.1	4.8	5.8	4.1	4.5	2.5
Y	20.2	16.7	16.6	21.1	23.1	23.0	19.1	16.3	15.0
TIO2CR	0.802	0.950	0.919	1.210	0.903	0.874	0.571	0.632	0.179
TIO2W	0.808	0.933	0.918	1.259	0.909	0.886	0.571	0.631	0.194

TABLE B17

	GC10a14	GC11a11	GC12a10	GC13a19	GC16a19	GC17a21	GC18a13	GC19a25	GC20a25
SIO2	63.09	53.87	57.91	78.42	70.74	75.59	62.24	59.88	62.58
AL2O3	16.25	16.66	16.77	12.47	15.49	14.07	18.03	15.49	16.76
FE2O3	5.30	8.71	6.78	0.77	2.09	1.34	4.35	6.36	5.06
MGO	2.86	4.37	4.12	0.29	0.44	0.42	2.35	4.53	2.39
CAO	4.57	7.06	5.91	0.57	1.64	0.68	3.45	4.94	3.83
NA2O	3.97	3.80	4.42	5.25	4.58	2.82	5.10	3.90	4.32
K2O	2.723	2.824	2.490	2.445	4.245	4.430	3.058	2.853	3.369
TIO2	0.719	1.512	1.158	0.161	0.318	0.230	0.614	1.246	0.862
MNO	0.065	0.111	0.097	0.027	0.033	0.038	0.056	0.091	0.068
P2O5	0.244	0.462	0.397	0.036	0.115	0.039	0.228	0.413	0.284
TOTAL	99.79	99.37	100.05	100.44	99.69	99.65	99.48	99.49	99.52
LOI	0.87	1.54	0.71	0.84	1.19	1.56	2.13	1.05	1.32
NI	59.7	103.1	61.3	4.4	6.7	5.3	43.5	75.2	25.9
CR	126.9	249.0	114.5	4.7	8.1	7.1	82.3	189.1	41.0
V	85.9	619.9	127.3	4.8	25.3	10.7	71.7	112.0	93.4
SC	11.5	19.7	14.9	2.1	2.4	2.3	9.1	15.9	12.7
CU	23.8	7.6	24.2	4.4	4.7	2.6	11.7	25.2	17.4
ZN	66.6	81.2	84.3	13.6	41.6	26.7	70.6	104.0	66.0
SR	908.5	1069.5	987.9	204.2	598.8	292.3	1118.2	802.0	763.8
RB	56.7	37.1	46.4	52.8	99.9	142.7	55.5	73.1	74.1
ZR	174.3	216.3	192.6	109.5	171.0	173.6	141.6	289.8	199.7
NB	8.8	14.5	11.6	11.0	11.0	10.6	7.7	18.1	11.5
BA	1190.3	1009.7	981.9	926.8	1415.7	1383.2	1489.1	1104.3	1254.4
TH	4.1	2.3	4.7	9.8	8.2	7.8	2.4	10.6	3.3
LA	35.9	29.3	33.5	23.7	29.9	32.7	28.0	50.9	34.3
CE	69.4	69.7	73.9	53.1	64.1	57.7	54.9	100.0	71.9
ND	32.4	34.3	32.4	22.5	26.9	27.4	25.0	41.6	29.4
SM	5.7	6.9	6.6	3.9	4.8	5.9	3.6	6.5	4.3
Y	17.1	21.3	19.7	14.0	15.6	15.6	12.1	21.5	16.5
TIO2CR	0.751	1.594	1.146	0.174	0.324	0.221	0.596	1.096	0.892
TIO2W	0.738	1.556	1.138	0.185	0.339	0.232	0.616	1.058	0.877

	GC23a6	GC24a21	GC25a19	GC26a16	GC28a13	GC29a16	GC30a22	GC31a19	BN1a24
SIO2	64.56	66.89	77.84	59.86	62.69	61.33	66.07	76.24	65.04
AL2O3	16.91	16.63	12.96	16.81	16.25	15.31	15.71	13.55	16.96
FE2O3	4.19	3.34	0.68	6.62	5.27	5.79	3.92	0.84	4.28
MGO	1.83	1.29	0.19	3.55	2.88	3.27	2.00	0.30	1.88
CAO	3.41	2.69	0.40	4.71	4.30	4.99	3.07	0.76	3.24
NA2O	4.46	4.41	4.62	4.23	4.77	3.31	4.32	2.40	4.30
K2O	3.376	3.703	3.611	2.694	2.476	3.551	3.642	6.135	3.525
TIO2	0.729	0.618	0.134	0.351	0.742	0.871	0.604	0.154	0.616
MNO	0.067	0.063	0.041	0.098	0.072	0.081	0.073	0.057	0.076
P2O5	0.277	0.173	0.034	0.366	0.267	0.311	0.185	0.035	0.219
TOTAL	99.80	99.80	100.52	99.88	99.72	99.80	99.59	100.48	100.13
LOI	0.95	0.85	0.51	1.19	1.80	1.34	1.75	1.33	0.80
NI	22.1	14.7	3.8	63.1	59.9	51.8	22.4	5.4	17.0
CR	42.6	24.5	4.3	116.4	118.8	110.4	44.7	4.4	22.8
V	66.2	46.1	3.2	110.2	93.4	104.6	74.0	3.2	74.7
SC	7.5	6.7	1.5	13.3	12.2	13.1	9.7	2.3	8.8
CU	11.1	13.4	4.2	17.9	17.9	22.8	24.5	3.7	34.2
ZN	69.1	56.6	16.7	80.7	71.5	70.3	50.5	27.3	63.4
SR	1090.6	937.8	163.0	1017.8	966.1	1183.3	632.7	252.8	1022.4
RB	75.9	85.4	94.8	59.0	48.0	80.9	91.2	126.3	70.1
ZR	362.8	346.7	101.6	174.8	156.1	243.0	177.1	111.9	165.0
NB	11.8	11.4	8.8	10.9	8.6	11.0	10.6	12.8	11.1
BA	1536.7	1909.1	1211.1	1138.0	1096.6	1544.1	1130.2	1436.5	1370.5
TH	5.5	7.0	6.7	3.2	5.0	6.1	9.1	7.2	5.0
LA	40.0	40.9	18.1	33.6	29.3	37.5	33.6	23.5	33.1
CE	85.7	83.9	40.2	71.9	62.7	84.7	67.0	53.8	67.2
ND	35.8	36.9	19.0	29.6	26.1	38.6	24.9	24.0	30.7
SM	4.7	6.6	3.0	5.3	4.7	8.1	2.9	10.6	2.0
Y	17.2	19.5	11.9	16.9	14.4	21.5	15.3	16.8	16.3
TIO2CR	0.761	0.661	0.139	0.974	0.728	0.888	0.659	0.182	0.646
TIO2W	0.749	0.656	0.154	0.970	0.735	0.891	0.663	0.194	0.651

TABLE B17

	BN2@21	BN3@24	BN4@16	BN5@24	BN6@16	BN7@16	BN8@16	BN9@16	BN10@16
SIO2	62.55	63.78	64.94	65.56	66.58	64.71	64.71	65.21	63.76
AL2O3	16.84	17.01	16.53	16.31	15.58	15.43	16.41	16.58	16.68
FE2O3	5.06	4.48	4.28	4.07	3.82	4.37	4.04	4.69	4.81
MGO	2.73	2.51	2.19	2.20	2.44	2.59	1.97	2.31	2.49
CAO	4.06	4.10	3.54	3.53	3.57	4.17	3.56	3.50	4.07
NA2O	4.50	4.63	4.73	4.34	3.65	4.13	4.79	4.08	4.21
K2O	3.226	2.733	2.965	3.000	3.515	3.074	2.985	2.555	2.884
TIO2	0.774	0.582	0.559	0.351	0.563	0.593	0.576	0.585	0.654
MNO	0.074	0.067	0.076	0.065	0.074	0.058	0.046	0.073	0.080
P2O5	0.291	0.239	0.212	0.196	0.203	0.214	0.204	0.203	0.230
TOTAL	100.10	100.13	100.03	100.03	99.99	100.35	99.29	99.78	99.86
LOI	0.25	0.43	0.65	0.60	0.65	0.48	0.53	1.35	0.50
NI	38.9	34.2	36.4	30.5	39.2	41.7	27.6	31.1	39.8
CR	76.6	56.2	65.3	56.1	68.8	71.2	45.6	51.5	61.1
V	92.8	81.6	77.3	72.9	69.6	85.1	74.2	76.0	84.7
SC	11.4	10.0	9.7	9.3	10.1	10.3	9.0	8.3	10.8
CU	15.8	5.9	6.7	4.3	4.4	74.8	6.9	5.6	31.4
ZN	71.1	66.0	58.4	47.4	60.2	65.2	60.7	66.6	60.3
SR	965.2	1091.2	1008.3	1101.6	1049.0	1101.1	1032.6	1064.1	1091.6
RB	80.5	49.5	54.5	61.0	56.5	53.6	52.0	60.2	58.0
ZR	163.0	130.4	125.2	121.6	131.7	137.9	141.7	142.8	134.3
NB	9.5	6.9	7.6	6.5	7.0	7.2	7.5	7.3	7.9
BA	1179.4	1533.0	1396.6	1350.5	1640.1	1347.1	1340.2	1313.0	1363.1
TH	4.4	2.4	4.0	3.4	0.8	3.2	3.5	4.7	3.5
LA	34.7	27.8	26.2	26.8	26.0	26.2	29.5	26.4	26.8
CE	67.6	59.2	57.6	49.9	54.6	55.8	58.8	52.3	55.8
ND	30.9	26.0	25.8	23.1	24.4	25.4	26.2	24.0	26.0
SM	2.6	3.9	3.0	3.5	2.9	4.8	4.9	4.1	5.1
Y	14.8	13.0	12.0	12.0	11.5	13.0	12.3	12.6	13.2
TIO2CR	0.829	0.642	0.584	0.589	0.599	0.627	0.604	0.565	0.683
TIO2W	0.807	0.623	0.579	0.579	0.586	0.620	0.591	0.570	0.680

	BN11@24	SC1@6	SC2@6	SC3@19	SC4@16	SC5@19	SC6@19	SC7@25	SC8@16
SIO2	63.00	59.86	60.00	71.13	64.91	68.57	76.59	74.79	64.21
AL2O3	16.53	17.80	19.31	15.27	16.15	15.90	12.31	13.11	16.08
FE2O3	4.78	6.40	4.71	3.22	4.35	3.63	1.48	2.25	5.29
MGO	2.77	1.75	1.82	0.80	2.05	1.62	0.65	0.34	1.33
CAO	4.26	0.64	1.47	2.41	4.25	2.81	0.39	0.69	5.29
NA2O	4.55	5.09	6.48	4.46	4.14	4.22	3.53	3.15	4.14
K2O	2.678	6.563	4.431	2.254	2.730	2.275	4.924	5.441	2.551
TIO2	0.610	0.813	1.085	0.429	0.782	0.473	0.180	0.232	0.501
MNO	0.071	0.100	0.049	0.031	0.092	0.040	0.062	0.028	0.085
P2O5	0.216	0.227	0.232	0.117	0.176	0.118	0.018	0.022	0.139
TOTAL	99.47	99.24	99.58	100.13	99.64	99.66	100.14	100.05	99.62
LOI	0.65	1.31	1.51	0.79	1.15	1.25	0.80	0.38	3.62
NI	48.6	19.5	43.6	14.3	32.5	21.7	4.4	4.9	33.5
CR	88.5	7.7	174.6	24.0	86.6	34.3	3.7	4.3	72.3
V	84.8	81.3	98.8	56.2	122.1	82.9	16.9	5.8	76.6
SC	11.6	10.7	18.3	8.2	15.8	9.6	3.7	11.1	10.3
CU	4.6	15.9	17.9	7.2	8.4	11.9	18.5	4.2	7.5
ZN	60.9	47.5	46.9	27.2	56.1	45.2	21.8	58.9	146.9
SR	997.0	324.7	492.6	455.8	485.5	453.9	61.8	91.9	379.4
RB	43.7	191.4	130.0	58.7	78.8	53.3	133.8	146.9	72.6
ZR	130.4	445.2	229.6	108.1	184.5	108.5	166.1	415.7	145.9
NB	7.5	25.2	15.4	5.8	15.0	4.9	20.8	27.3	7.5
BA	1414.2	1497.4	1017.3	492.1	559.4	475.2	721.4	837.9	504.6
TH	3.8	9.6	11.2	6.9	10.3	4.7	16.2	20.1	11.0
LA	22.6	47.7	60.0	30.4	31.6	19.0	31.2	69.0	22.5
CE	52.0	325.7	78.7	45.2	62.9	35.5	156.7	151.4	49.0
ND	23.7	48.3	40.8	21.1	28.1	17.3	35.1	64.7	17.2
SM	3.1	9.3	5.4	3.3	4.0	2.3	7.0	11.9	1.5
Y	11.3	43.3	18.8	9.6	19.5	10.7	27.2	49.1	13.1
TIO2CR	0.625	0.784	1.073	0.429	0.793	0.472	0.174	0.243	0.510
TIO2W	0.626	0.802	1.082	0.439	0.804	0.483	0.185	0.257	0.516

TABLE B17

	SC9a24	SC10a14	SC11a1	SC12a7	SC13a12	SC14a1	SC15a19	SC16a21	MT1a11
SIO2	59.77	61.12	50.94	52.28	52.23	52.08	78.82	76.43	53.31
AL2O3	17.30	15.98	16.61	15.61	16.74	15.88	11.68	12.96	18.11
FE2O3	6.20	6.35	9.71	7.68	10.82	8.39	1.28	2.21	8.66
MGO	3.03	4.73	7.04	7.53	2.74	5.56	0.18	0.66	4.30
CAO	3.51	3.50	8.11	8.79	6.46	7.09	0.59	0.46	6.90
NA2O	5.36	3.65	3.64	3.36	4.42	3.67	2.38	2.55	4.12
K2O	3.290	2.925	1.426	1.924	2.721	1.673	5.243	4.959	1.884
TIO2	0.712	1.015	1.829	1.516	2.097	1.664	0.096	0.198	1.711
MNO	0.038	0.141	0.134	0.235	0.128	0.265	0.029	0.031	0.145
P2O5	0.282	0.254	0.332	0.511	0.807	0.438	0.014	0.039	0.420
TOTAL	99.51	99.67	99.77	99.44	99.15	99.71	100.31	100.49	99.56
LOI	0.97	3.52	1.92	2.03	1.00	2.44	0.62	1.22	1.32
NI	56.8	31.1	98.7	170.3	46.1	223.7	5.0	7.4	26.2
CR	113.2	51.9	197.6	423.0	57.4	433.9	3.9	8.3	9.3
V	109.2	124.2	182.2	187.7	206.6	177.6	6.7	13.2	174.6
SC	15.9	17.5	24.5	30.6	17.5	21.5	3.2	2.9	19.5
CU	15.7	15.2	27.1	36.1	31.6	6.7	20.6	3.1	34.5
ZN	45.9	94.8	75.6	83.7	79.8	91.4	73.4	22.2	72.3
SR	656.8	365.5	577.3	825.0	745.2	758.3	29.3	113.9	634.7
RB	77.6	66.7	24.2	38.7	58.6	18.4	237.8	120.0	43.1
ZR	165.9	208.5	204.3	224.1	377.2	224.2	158.0	112.9	248.1
NB	9.5	14.2	14.6	17.0	29.3	16.8	27.0	19.1	12.8
BA	840.6	816.7	289.0	526.6	596.2	506.2	163.6	444.8	513.5
TH	14.7	11.6	6.3	6.4	12.2	5.5	26.0	23.9	9.5
LA	58.1	40.4	23.6	50.4	80.7	41.9	42.0	37.1	30.3
CE	108.9	82.2	53.5	111.6	172.6	93.2	100.3	74.2	75.1
ND	44.1	35.7	25.3	51.5	72.7	42.6	49.0	27.4	38.6
SM	7.4	9.6	4.6	7.3	12.0	4.6	13.1	3.3	5.3
Y	16.5	21.9	27.0	24.2	35.7	23.3	68.0	15.0	29.3
TIO2CR	0.767	0.940	1.727	1.546	2.169	1.708	0.097	0.217	1.540
TIO2W	0.759	0.958	1.827	1.570	2.187	1.740	0.110	0.224	1.647

	MT2a11	MT3a1	MT4a11	MT5a18	MT6a1	MT7a1	MT8a1	MT9a18	MT10a10
SIO2	52.60	55.34	54.93	61.57	52.56	52.81	53.89	62.16	56.93
AL2O3	16.28	17.85	17.82	17.74	18.36	18.37	18.37	17.91	16.25
FE2O3	8.23	9.42	8.85	6.69	9.79	9.00	8.10	5.20	6.89
MGO	7.79	2.84	3.54	0.99	5.36	5.57	4.03	1.52	6.49
CAO	8.39	5.86	5.90	2.42	3.99	3.53	7.06	2.40	6.54
NA2O	3.25	4.04	4.30	5.08	3.46	4.99	4.26	4.76	3.48
K2O	1.135	1.879	2.280	4.054	3.646	2.599	1.972	4.371	1.474
TIO2	1.500	1.700	1.611	0.700	1.757	1.756	1.728	0.714	1.130
MNO	0.165	0.063	0.076	0.052	0.079	0.120	0.067	0.050	0.131
P2O5	0.271	0.427	0.581	0.403	0.433	0.439	0.440	0.405	0.270
TOTAL	99.61	99.41	99.90	99.70	99.44	99.18	99.92	99.49	99.59
LOI	1.84	0.99	1.10	0.99	2.58	2.74	1.05	1.32	1.60
NI	171.0	24.1	13.8	5.6	22.6	26.7	25.6	5.2	154.4
CR	353.0	7.5	7.0	4.8	7.1	8.5	6.1	5.6	277.9
V	176.5	156.3	124.1	15.2	185.9	188.2	163.7	11.1	142.7
SC	23.7	21.0	15.9	4.7	23.0	21.8	19.8	4.6	19.8
CU	29.9	24.3	25.2	6.8	30.3	11.4	34.9	8.5	26.3
ZN	73.4	58.9	79.5	69.4	88.6	147.4	51.2	80.4	77.0
SR	537.1	653.8	577.3	354.0	459.4	431.3	672.8	337.8	546.4
RB	20.3	43.9	62.4	131.7	52.5	43.0	44.4	134.4	18.1
ZR	176.1	241.6	322.7	642.0	252.9	256.4	253.0	651.2	215.9
NB	10.8	12.4	16.6	29.4	13.8	13.3	12.4	29.7	12.9
BA	311.2	535.9	529.3	836.1	478.6	554.9	344.2	989.0	495.7
TH	2.7	5.5	10.3	23.7	9.0	6.7	6.4	21.4	7.3
LA	17.8	31.7	39.4	69.4	32.9	33.0	33.8	66.2	34.6
CE	43.2	79.6	96.6	146.7	70.8	73.5	77.4	141.6	67.7
ND	20.7	39.4	48.0	60.0	34.4	37.4	35.8	58.5	29.9
SM	2.9	5.3	9.6	10.7	6.7	6.9	11.5	9.6	3.6
Y	24.5	28.4	37.9	39.5	31.2	30.4	30.7	38.0	23.5
TIO2CR	1.539	1.359	1.368	0.697	1.602	1.697	1.450	0.697	1.232
TIO2W	1.596	1.482	1.469	0.708	1.677	1.723	1.559	0.700	1.227

TABLE B17

	MT11a13	MT12a11	MT13a10	MT14a12	MT15a13	MT16a13	MT17a1	MT18a10	MT19a10
SIO2	57.28	56.98	57.72	55.47	58.39	59.93	49.73	56.06	56.20
AL2O3	15.96	16.49	15.95	16.04	16.19	15.78	17.06	16.09	16.36
FE2O3	6.80	6.58	7.29	7.95	6.98	5.61	11.58	7.79	7.17
MGO	6.26	5.54	5.08	5.71	5.08	5.06	5.54	5.09	5.85
CAO	6.07	6.66	6.59	7.20	7.03	5.69	8.72	6.95	6.55
NA2O	3.59	3.83	3.61	3.79	3.61	4.06	3.25	3.46	3.73
K2O	2.070	1.924	1.980	1.523	1.105	0.929	1.359	1.966	1.926
TIO2	1.125	1.292	1.174	1.402	1.126	1.112	1.899	1.380	1.282
MNO	0.114	0.127	0.089	0.140	0.186	0.123	0.159	0.173	0.087
P2O5	0.277	0.300	0.292	0.279	0.248	0.244	0.443	0.319	0.326
TOTAL	99.55	99.72	99.77	99.59	99.94	99.54	99.73	99.26	99.47
LOI	1.13	1.38	1.67	1.38	1.93	1.68	1.76	1.46	1.58
NI	166.6	120.6	163.9	110.4	98.6	92.2	94.2	130.0	167.8
CR	265.5	193.1	287.1	217.3	175.1	157.8	154.2	253.4	239.2
V	129.5	162.1	147.0	159.2	152.1	148.9	184.3	165.1	148.9
SC	18.5	21.7	20.5	22.0	20.0	19.7	24.9	23.0	21.5
CU	31.7	17.4	17.2	24.9	30.8	35.2	21.7	34.8	25.9
ZN	68.4	73.4	67.6	74.2	67.7	72.6	71.8	61.9	81.3
SR	507.6	522.1	512.9	457.2	549.7	669.6	556.2	463.8	585.8
RB	58.2	51.5	55.0	39.0	18.1	33.9	19.2	55.1	46.8
ZR	213.6	227.3	217.1	208.2	222.3	217.2	236.5	264.5	206.2
NB	12.4	14.7	12.7	14.3	12.7	13.4	19.3	15.0	13.5
BA	494.9	406.0	422.4	311.5	437.4	428.7	291.3	380.1	526.1
TH	8.4	10.8	9.6	7.3	13.0	11.5	6.2	10.2	8.9
LA	30.7	33.7	25.9	26.9	33.8	35.2	26.8	30.5	33.6
CE	61.6	70.6	58.7	61.6	72.4	71.4	59.1	65.9	66.2
ND	27.5	30.0	26.0	25.7	29.0	27.1	26.2	29.6	29.9
SM	5.2	3.8	3.9	5.2	6.5	3.1	8.9	9.2	5.3
Y	24.8	23.7	23.9	24.8	23.8	22.6	29.6	27.7	22.5
TIO2CR	1.091	1.388	1.173	1.372	1.240	1.214	1.629	1.446	1.292
TIO2W	1.139	1.397	1.201	1.413	1.202	1.187	1.792	1.452	1.336

	MT20a1	MT21a10	MT22a11	MT23a1	MT24a11	MT25a11	MT26a11	MT27a18	MT29a18
SIO2	52.31	54.97	52.72	53.02	54.30	53.70	52.20	62.06	60.28
AL2O3	16.52	15.85	16.30	17.62	18.70	18.88	17.83	17.88	17.89
FE2O3	9.22	7.01	9.00	8.20	7.87	7.97	8.69	4.94	6.16
MGO	10.81	6.58	6.74	6.56	3.63	3.92	4.79	1.55	2.19
CAO	2.09	7.03	7.51	5.89	6.57	6.52	7.79	3.08	3.21
NA2O	1.80	3.64	3.48	4.34	4.43	4.27	3.74	4.83	4.88
K2O	4.007	2.145	1.782	1.919	2.035	1.973	2.000	4.057	3.731
TIO2	1.933	1.518	1.361	1.707	1.539	1.564	1.647	0.735	0.825
MNO	0.056	0.109	0.100	0.102	0.078	0.113	0.101	0.035	0.085
P2O5	0.440	0.465	0.358	0.386	0.359	0.369	0.435	0.416	0.437
TOTAL	99.19	99.33	99.36	99.85	99.50	99.28	99.21	99.58	99.69
LOI	5.93	1.50	1.64	1.57	1.13	1.38	1.38	1.18	1.09
NI	197.8	208.0	162.0	127.9	29.2	29.7	74.2	7.3	8.7
CR	400.2	343.1	307.3	217.7	8.2	7.4	112.7	7.7	12.2
V	196.8	148.7	174.7	171.4	153.4	145.0	178.2	11.9	27.3
SC	32.0	17.0	22.9	29.8	16.3	16.3	20.7	5.4	7.2
CU	6.1	48.0	14.2	24.4	30.5	16.5	33.5	6.8	9.2
ZN	170.0	80.7	74.1	90.0	75.8	83.3	80.0	58.7	98.2
SR	237.0	816.8	693.7	576.4	739.6	719.4	590.2	396.5	385.8
RB	34.8	43.4	36.1	35.6	46.8	44.1	59.5	133.8	124.3
ZR	242.6	273.4	205.2	232.2	230.5	230.1	302.8	637.2	516.0
NB	18.4	17.1	13.0	14.7	13.0	12.7	15.0	29.0	28.0
BA	333.7	674.4	596.4	367.9	528.3	535.1	440.5	772.0	678.7
TH	5.0	10.6	8.0	3.8	7.7	7.9	14.4	27.1	27.1
LA	26.4	41.5	28.9	24.0	30.8	28.4	34.6	65.9	61.8
CE	54.6	93.4	65.0	59.0	67.1	70.2	78.7	142.0	141.1
ND	24.4	42.0	30.8	28.0	32.9	33.7	39.3	56.0	57.6
SM	4.3	10.0	6.7	5.8	5.9	6.9	8.9	8.0	9.4
Y	23.2	26.7	24.1	27.0	27.9	29.2	32.3	36.4	36.3
TIO2CR	1.576	1.453	1.359	1.586	1.393	1.449	1.445	0.712	0.846
TIO2W	1.737	1.518	1.375	1.682	1.483	1.533	1.538	0.739	0.859

TABLE B17

	MT30a12	MT31a12	MT32a10	MT33a20	MT34a13	MT35a20	MT36a28	MT37a28	MT38a1
SIO2	57.71	56.42	55.45	57.75	59.72	54.51	57.71	57.62	55.81
AL2O3	17.19	17.40	16.15	17.86	16.76	18.45	16.06	15.77	17.02
FE2O3	6.54	7.61	8.07	6.62	6.53	8.08	5.86	7.27	7.07
MGO	3.07	3.81	5.29	3.27	3.81	3.82	5.68	5.71	5.12
CAO	5.87	6.00	6.89	5.67	4.98	6.54	4.87	5.59	7.47
NA2O	4.24	3.96	3.69	3.35	3.42	4.41	4.21	3.90	3.92
K2O	2.642	2.613	2.050	2.630	2.972	1.998	2.310	2.260	1.465
TIO2	1.332	1.341	1.375	1.350	1.136	1.533	1.323	1.298	1.481
MNO	0.144	0.130	0.061	0.089	0.128	0.076	0.080	0.036	0.137
P2O5	0.376	0.381	0.374	0.375	0.294	0.363	0.360	0.347	0.373
TOTAL	99.12	99.66	99.40	99.55	99.75	99.79	99.46	99.80	99.87
LOI	1.06	1.45	1.21	1.32	1.27	1.59	1.31	1.33	1.14
NI	17.9	18.9	175.1	8.6	48.4	27.7	109.5	101.4	88.5
CR	13.2	13.6	308.8	3.7	106.8	7.3	321.0	298.4	121.8
V	164.0	169.0	172.5	137.2	135.8	147.8	140.3	129.8	150.6
SC	19.4	19.6	23.0	16.6	22.2	14.8	21.8	18.7	19.8
CU	9.7	10.7	29.2	11.6	21.2	24.5	17.4	18.5	27.5
ZN	89.4	97.2	82.6	84.7	151.1	98.4	70.6	74.8	69.6
SR	779.4	746.3	721.6	831.6	527.6	636.9	562.6	566.3	736.9
RB	78.5	80.1	52.0	74.5	92.3	44.0	54.8	55.4	15.4
ZR	274.7	276.1	213.7	284.2	266.8	221.6	254.1	248.9	239.7
NB	15.9	16.6	14.4	17.4	15.4	12.0	18.2	16.6	15.4
BA	620.5	631.3	564.0	675.4	692.1	530.5	562.2	573.4	585.7
TH	12.0	13.4	9.1	13.6	16.2	9.9	7.1	8.6	7.3
LA	46.5	48.3	30.3	52.1	39.0	30.7	35.0	37.0	32.1
CE	98.8	102.8	73.1	109.9	85.7	67.7	70.4	73.4	74.7
ND	43.7	44.2	31.9	48.8	40.2	32.0	31.9	33.7	34.2
SM	4.9	6.4	6.2	7.1	7.1	6.3	5.4	5.9	7.4
Y	25.6	25.0	22.8	26.3	28.8	27.5	25.1	24.7	25.8
TIO2CR	1.367	1.398	1.296	1.389	1.066	1.363	1.290	1.216	1.505
TIO2W	1.362	1.406	1.339	1.399	1.090	1.473	1.323	1.269	1.524

	MT39a1	MT40a11	MT41a5	MT42a7	MT43a12	MT44a12	MT45a12	MT46a5	MT47a13
SIO2	55.24	54.56	59.88	53.80	54.99	54.27	54.85	58.34	59.97
AL2O3	16.95	17.29	16.53	15.72	16.18	15.99	15.70	16.98	17.28
FE2O3	7.87	7.08	5.65	7.67	7.61	7.68	8.25	8.22	6.30
MGO	4.96	5.67	4.36	8.64	6.47	6.86	6.80	3.75	3.02
CAO	6.73	7.47	5.23	7.83	7.59	9.36	8.03	3.19	3.47
NA2O	4.15	4.23	3.92	3.37	3.48	3.32	3.34	4.45	4.42
K2O	1.924	1.403	2.548	1.584	2.031	1.342	1.358	3.040	3.376
TIO2	1.529	1.535	0.999	1.303	1.341	1.312	1.285	1.116	1.232
MNO	0.082	0.187	0.063	0.097	0.074	0.146	0.128	0.055	0.077
P2O5	0.370	0.381	0.263	0.363	0.371	0.353	0.349	0.255	0.345
TOTAL	99.81	99.81	99.43	100.38	100.13	99.64	100.10	99.39	99.48
LOI	1.06	0.90	1.14	1.98	1.23	1.29	1.60	2.84	2.23
NI	77.5	84.8	115.2	267.0	141.9	146.2	138.3	72.1	47.8
CR	114.4	126.7	232.0	540.3	318.1	296.1	293.1	165.0	98.2
V	136.3	160.7	123.9	165.9	175.0	175.6	169.2	115.0	140.8
SC	21.0	20.3	19.6	25.5	28.4	24.8	24.8	23.2	24.2
CU	14.8	27.0	19.8	29.9	34.5	20.8	49.8	17.2	17.8
ZN	105.9	71.9	57.7	73.0	73.4	57.7	68.3	43.7	54.4
SR	666.3	699.4	688.1	559.8	562.6	628.7	603.5	401.3	557.3
RB	41.6	14.7	66.3	37.2	54.2	15.3	17.4	103.6	100.6
ZR	234.8	239.2	180.9	228.1	264.6	253.6	248.9	249.4	310.6
NB	15.9	16.0	11.1	11.4	11.9	12.6	12.4	13.9	15.0
BA	537.5	552.7	836.8	435.2	524.4	539.2	541.7	1197.7	898.4
TH	4.2	6.0	7.6	5.4	10.2	7.4	11.5	12.9	17.8
LA	28.1	37.3	29.8	28.8	32.5	32.9	33.4	47.1	45.6
CE	70.0	74.7	57.6	61.9	76.4	76.1	75.2	74.1	88.5
ND	31.7	33.9	26.5	30.9	36.4	34.5	35.2	41.5	41.6
SM	3.5	6.2	5.2	5.3	7.0	5.8	5.3	8.5	9.1
Y	23.9	25.0	17.6	24.6	26.2	25.8	26.0	25.5	22.6
TIO2CR	1.267	1.653	0.969	1.235	1.289	1.335	1.353	1.013	1.125
TIO2W	1.381	1.633	0.980	1.290	1.357	1.373	1.327	1.055	1.173

TABLE B17

	MT48@10	MT49@1	MT50@20	MT51@16	MT52@22	MT53@16	MT54@13	MT55@1	MT56@1
SIO2	59.35	57.87	55.95	64.18	68.10	55.89	60.67	50.34	58.44
AL2O3	17.00	16.87	16.74	16.10	15.33	16.52	18.51	17.13	17.99
FE2O3	7.05	6.01	7.56	5.28	3.18	7.16	6.35	9.59	5.24
MGO	2.48	1.20	5.01	1.21	2.40	5.40	1.95	9.00	4.01
CAO	4.00	10.75	6.95	4.00	2.22	7.43	4.88	8.26	4.88
NA2O	4.66	3.75	3.55	4.26	4.85	3.29	3.17	2.88	5.26
K2O	3.020	2.278	1.928	3.379	3.114	2.037	2.060	1.044	0.827
TIO2	1.284	1.054	1.291	0.977	0.369	1.224	1.420	1.571	2.005
MNO	0.083	0.107	0.117	0.041	0.048	0.079	0.053	0.082	0.078
P2O5	0.290	0.261	0.287	0.279	0.110	0.289	0.294	0.415	0.508
TOTAL	99.21	100.14	99.38	99.74	99.73	99.33	99.36	100.32	99.23
LOI	2.01	5.62	0.74	1.34	1.82	1.53	3.71	8.80	3.55
NI	71.5	71.3	41.3	24.0	30.7	114.2	23.8	205.3	160.3
CR	223.7	194.9	113.6	27.8	43.9	268.0	27.9	487.6	480.7
V	189.6	137.6	145.2	84.9	63.5	165.9	158.1	189.0	203.5
SC	26.8	21.8	23.4	13.4	8.5	25.8	15.7	32.5	35.7
CU	17.7	13.5	28.7	12.2	9.2	26.3	32.0	21.1	35.4
ZN	45.8	53.9	78.1	18.7	40.3	73.2	105.2	76.6	87.5
SR	602.2	641.1	680.1	516.1	383.6	622.5	356.2	443.3	810.3
RB	96.0	59.8	46.6	98.8	72.7	53.8	45.3	22.1	16.8
ZR	314.5	199.6	199.4	273.5	106.5	218.8	292.2	224.7	233.0
NB	15.9	11.6	12.9	16.6	4.8	14.5	15.3	16.0	15.8
BA	1017.3	614.3	550.2	898.1	725.6	583.5	428.1	405.3	381.5
TH	17.5	12.2	11.5	14.8	5.5	7.6	13.3	12.5	4.4
LA	42.2	30.3	29.3	54.7	11.7	34.4	25.5	35.2	26.0
CE	85.4	67.3	61.9	105.4	26.4	71.1	64.1	77.2	69.9
ND	37.3	29.5	29.4	37.8	13.4	31.7	32.3	38.7	36.4
SM	6.8	5.3	7.2	4.5	1.8	6.3	6.0	7.3	5.6
Y	21.5	21.0	25.8	16.3	10.2	24.3	28.8	24.3	27.6
TIO2CR	1.247	1.043	1.148	0.968	0.400	1.274	1.440	1.476	1.977
TIO2W	1.292	1.109	1.238	0.989	0.403	1.272	1.482	1.596	2.105

	MT58@19	MT59@19	MT60@19	S1@12	S2@12	S4@20	S5@11	S6@11	S8@11
SIO2	65.20	65.37	64.60	52.69	52.98	52.11	52.34	54.16	51.76
AL2O3	17.13	17.16	17.47	19.31	18.83	19.21	16.49	17.11	17.03
FE2O3	4.42	4.50	4.86	7.19	8.24	8.63	9.14	8.21	10.92
MGO	1.42	1.17	1.50	5.20	4.71	5.03	6.90	5.12	4.50
CAO	3.06	2.48	0.55	7.90	7.91	7.79	8.63	7.85	7.83
NA2O	3.98	4.15	3.85	4.14	4.22	4.06	3.03	3.57	3.94
K2O	3.525	3.634	5.825	1.191	1.204	1.350	1.038	1.471	1.408
TIO2	0.659	0.676	0.675	1.582	1.507	1.612	1.399	1.625	2.027
MNO	0.047	0.033	0.070	0.153	0.147	0.146	0.139	0.089	0.196
P2O5	0.296	0.299	0.277	0.318	0.307	0.321	0.211	0.286	0.332
TOTAL	99.73	99.48	99.68	99.67	100.06	99.25	99.31	99.49	99.94
LOI	2.01	1.43	1.66	1.55	1.05	1.21	1.56	1.18	0.55
NI	5.8	6.7	7.4	46.6	47.4	45.3	129.9	51.2	20.4
CR	6.1	7.5	7.3	113.9	112.1	29.3	351.3	111.0	33.6
V	45.5	38.5	31.8	174.3	170.7	154.5	156.8	187.8	247.6
SC	9.7	9.6	8.8	27.6	26.6	24.2	24.2	25.0	26.1
CU	10.1	5.2	3.3	21.3	16.8	28.4	24.6	45.0	22.8
ZN	67.5	60.5	51.8	106.2	80.1	64.6	75.5	64.9	84.4
SR	365.9	379.9	119.7	516.2	502.9	626.0	429.2	563.3	325.2
RB	102.4	105.4	105.1	25.3	26.8	32.1	24.5	28.5	31.5
ZR	322.9	320.1	322.4	227.6	225.8	210.6	160.0	212.5	215.9
NB	20.1	19.8	20.2	9.8	5.6	7.7	8.1	14.8	10.9
BA	827.3	815.8	743.8	299.2	316.9	339.2	247.2	367.8	358.7
TH	17.9	15.7	15.1	*	0.0	*	*	3.6	2.6
LA	48.4	46.2	52.4	20.2	23.6	22.8	16.6	23.7	22.0
CE	106.7	105.7	116.5	50.3	53.9	53.4	34.0	48.6	52.6
ND	44.8	44.6	48.1	27.3	28.5	30.2	17.7	25.8	27.0
SM	7.5	7.8	7.8	6.5	7.8	6.0	5.8	7.4	5.5
Y	28.9	29.0	28.0	31.5	32.1	32.2	25.6	31.3	33.3
TIO2CR	0.698	0.659	0.698	1.670	1.646	1.312	1.317	1.374	1.922
TIO2W	0.709	0.697	0.717	1.659	1.602	1.423	1.370	1.608	1.983

TABLE B17

	S9a12	S10a20	S12a12	S13a10	S15a12	S16a11	S17a20	S18a11	S19a11
SIO2	54.40	53.48	56.49	56.69	56.88	53.94	52.88	54.37	52.08
AL203	17.42	17.93	16.37	17.10	17.89	17.97	18.45	16.37	18.99
FE203	10.98	8.40	7.31	7.33	7.08	8.04	8.37	8.43	7.43
MGO	4.25	4.39	5.39	4.10	3.36	4.65	4.85	6.82	5.77
CAO	5.41	7.69	7.46	5.17	6.32	7.63	7.20	7.41	8.68
NA20	3.79	3.95	3.60	4.17	4.40	4.07	4.15	3.61	3.56
K20	1.898	1.945	1.664	2.865	1.791	1.484	1.451	1.387	1.312
TIO2	1.105	1.538	1.217	1.734	1.475	1.579	1.660	1.104	1.400
MNO	0.047	0.082	0.091	0.133	0.094	0.111	0.065	0.107	0.099
P205	0.285	0.363	0.291	0.547	0.361	0.306	0.311	0.291	0.295
TOTAL	99.60	99.77	99.89	99.85	99.65	99.78	99.37	99.30	99.61
LOI	1.50	1.39	1.23	1.19	0.81	0.86	1.37	1.11	1.55
NI	78.1	10.4	80.8	59.0	22.1	28.7	27.8	159.2	46.5
CR	54.6	5.2	113.0	51.3	31.2	24.8	16.9	285.7	76.4
V	141.6	149.7	150.5	129.5	134.9	134.2	150.7	122.3	180.6
SC	21.2	20.9	23.1	19.1	19.2	18.1	22.7	19.9	29.5
CU	27.4	18.5	25.7	62.4	17.3	21.4	16.7	21.4	21.4
ZN	54.5	61.4	69.2	112.9	61.1	93.5	93.2	75.3	68.5
SR	682.6	1197.9	613.4	410.5	559.6	555.9	583.6	647.7	521.9
RB	33.4	32.1	43.0	117.8	42.8	37.0	36.7	28.4	21.1
ZR	215.6	242.1	205.0	540.5	260.1	213.4	204.8	187.3	183.7
NB	11.7	8.3	11.7	24.5	13.6	13.0	12.0	10.6	7.2
BA	516.5	880.3	434.7	459.9	418.2	390.3	368.1	368.4	326.3
TH	4.5	3.2	5.4	22.9	3.8	2.5	4.4	5.2	4.9
LA	31.7	32.3	33.2	58.0	27.9	29.4	23.3	22.3	21.3
CE	58.7	76.7	67.0	130.8	53.6	56.7	56.0	44.3	47.4
ND	26.4	42.6	32.6	57.8	30.0	28.1	25.1	21.8	24.0
SM	4.6	7.3	8.6	8.9	6.0	8.6	5.3	3.4	4.7
Y	20.6	31.0	25.5	47.3	28.0	27.0	25.3	23.8	23.1
TIO2CR	1.156	1.334	1.213	1.756	1.438	1.126	1.195	0.992	1.249
TIO2W	1.154	1.407	1.233	1.781	1.503	1.254	1.380	1.038	1.357

	S20a18	S21a12	S22a20	S23a11	S24a11	S25a12	S26a11	S27a11	S28a12
SIO2	55.48	53.74	54.54	54.48	53.80	53.78	54.19	58.29	54.04
AL203	17.62	16.80	17.87	18.55	17.75	17.60	18.09	17.36	16.53
FE203	8.67	8.54	7.89	7.24	8.44	8.57	8.27	8.08	8.53
MGO	4.38	5.70	4.62	4.11	4.42	4.65	4.49	2.22	6.69
CAO	1.35	7.95	7.33	7.54	7.37	7.70	7.47	4.57	7.98
NA20	4.71	3.62	3.89	4.13	3.97	3.86	3.94	5.18	3.42
K20	5.331	1.542	1.541	1.476	1.457	1.581	1.508	2.206	1.000
TIO2	1.382	1.486	1.522	1.624	1.558	1.675	1.579	1.236	1.176
MNO	0.080	0.118	0.154	0.117	0.156	0.151	0.093	0.100	0.176
P205	0.604	0.346	0.306	0.319	0.304	0.371	0.302	0.647	0.288
TOTAL	99.62	99.85	99.76	99.69	99.24	99.94	99.94	99.38	99.83
LOI	2.17	1.31	1.00	1.12	0.42	0.82	1.16	1.03	1.58
NI	14.3	94.8	31.9	25.9	26.5	46.5	27.0	N.D.	94.4
CR	6.7	127.5	29.2	17.9	20.9	59.5	17.7	N.D.	80.8
V	150.3	175.8	155.5	186.8	161.7	153.5	157.1	30.3	137.7
SC	12.4	22.7	19.8	20.6	20.1	20.3	18.9	11.6	16.6
CU	14.8	51.5	35.0	19.2	18.4	17.3	21.0	9.0	18.7
ZN	112.7	64.0	79.8	85.0	74.0	70.0	83.6	91.3	59.7
SR	326.8	800.6	527.2	558.1	531.9	595.3	545.5	386.6	695.9
RB	68.7	33.9	39.3	35.4	34.2	33.7	38.9	57.7	17.6
ZR	351.0	212.5	210.4	220.3	215.4	255.1	220.1	417.9	200.0
NB	17.7	11.1	13.7	13.9	13.3	16.5	13.4	19.8	11.8
BA	787.0	523.4	392.8	374.6	362.9	414.2	378.7	473.5	431.8
TH	11.0	9.4	8.7	2.7	5.9	6.9	3.8	8.4	8.0
LA	45.5	29.1	28.5	25.9	24.7	31.9	27.4	38.4	32.4
CE	99.8	65.8	62.7	58.0	54.3	59.8	56.2	96.4	63.9
ND	46.0	33.6	28.5	29.3	27.1	33.0	27.6	49.8	33.2
SM	9.3	5.2	4.7	4.8	5.1	6.4	5.8	10.4	6.6
Y	30.7	28.6	28.6	27.7	28.4	30.1	27.9	48.0	23.8
TIO2CR	1.431	1.450	1.410	1.454	1.518	1.473	1.245	1.152	1.190
TIO2W	1.449	1.523	1.482	1.540	1.542	1.562	1.357	1.175	1.204

TABLE B17

	S29a12	S30a11	S31a11	S32a11	S33a11	S34a11	S35a11	S36a11	S37a6
SIO2	53.85	55.53	53.15	53.24	53.89	54.13	55.56	56.01	64.79
AL2O3	17.45	18.05	16.95	17.76	16.91	18.53	16.59	16.57	17.11
FE2O3	8.63	8.94	8.12	8.67	8.02	8.10	8.01	6.80	4.21
MGO	4.20	3.12	6.54	4.32	6.54	4.29	4.97	5.62	1.04
CAO	7.72	6.40	9.28	7.74	8.63	7.63	7.13	6.83	2.81
NA2O	3.99	4.29	3.35	3.92	3.34	4.00	3.64	3.67	5.29
K2O	1.606	1.654	0.625	1.512	1.026	1.436	1.904	1.942	2.925
TIO2	1.680	1.710	1.379	1.723	1.384	1.613	1.391	1.418	0.688
MNO	0.133	0.094	0.140	0.075	0.095	0.092	0.100	0.072	0.045
P2O5	0.374	0.284	0.218	0.388	0.225	0.320	0.334	0.335	0.331
TOTAL	99.63	100.08	99.77	99.46	100.06	100.14	99.64	99.26	99.24
LOI	0.86	0.67	1.61	0.96	1.66	1.25	1.54	1.34	1.28
NI	46.0	15.1	N.D.	43.2	68.5	28.0	120.1	119.7	N.D.
CR	64.8	21.3	N.D.	63.8	231.1	19.7	161.9	164.5	N.D.
V	157.5	107.6	178.7	134.2	166.7	159.2	138.8	141.6	34.4
SC	20.4	18.1	26.8	21.2	24.0	20.9	18.1	17.8	5.5
CU	23.5	13.7	32.9	22.4	26.7	22.5	24.3	26.2	19.0
ZN	77.2	67.0	72.5	53.7	66.8	65.7	83.1	82.0	137.8
SR	597.5	539.1	441.9	622.1	413.3	574.0	717.4	704.9	448.0
RB	34.9	45.8	5.5	35.1	17.1	26.4	45.3	44.2	65.3
ZR	255.1	208.3	165.3	259.0	168.4	228.3	207.1	207.2	434.5
NB	15.3	11.0	8.0	15.1	8.5	12.6	12.5	12.6	17.6
BA	410.4	398.8	247.4	412.6	246.7	373.0	630.6	647.6	719.4
TH	11.8	11.5	7.5	6.2	4.8	3.9	8.1	6.8	10.9
LA	31.6	23.6	16.8	33.2	18.9	27.2	30.0	31.3	41.8
CE	65.6	56.3	34.9	69.5	34.0	56.1	68.2	66.5	86.5
ND	31.3	27.3	18.7	33.4	17.6	27.0	28.5	29.6	37.3
SM	7.2	4.1	4.2	7.6	4.1	4.7	4.3	4.4	4.9
Y	29.7	33.5	25.8	30.4	26.1	29.0	24.8	24.1	30.6
TIO2CR	1.487	1.218	1.457	1.218	1.348	1.595	1.379	1.308	0.739
TIO2W	1.566	1.354	1.475	1.339	1.440	1.634	1.405	1.358	0.737

	S38a16	S39a11	S40a22	S41a22	S42a12	S43a12	S44a5	S45a1	S46a1
SIO2	61.67	54.48	53.92	66.14	54.11	53.65	56.99	52.18	54.98
AL2O3	15.24	15.89	17.35	14.35	17.68	17.80	15.34	17.96	16.52
FE2O3	6.60	7.90	8.27	4.26	7.87	8.58	7.00	8.39	8.26
MGO	3.80	7.19	5.39	1.94	4.09	4.41	7.25	6.16	5.04
CAO	2.20	7.27	6.46	2.06	7.51	7.62	6.24	7.07	7.32
NA2O	4.55	3.52	4.56	4.00	4.24	4.06	3.73	3.99	3.94
K2O	3.658	1.624	1.730	5.956	1.697	1.571	1.846	1.506	1.696
TIO2	1.405	1.299	1.471	0.829	1.679	1.685	1.150	1.625	1.599
MNO	0.048	0.145	0.089	0.071	0.193	0.116	0.128	0.139	0.151
P2O5	0.322	0.283	0.302	0.207	0.377	0.374	0.240	0.341	0.382
TOTAL	99.49	99.60	99.55	99.71	99.45	99.86	99.90	99.36	99.89
LOI	2.43	1.56	1.98	1.47	0.95	0.90	0.75	2.10	1.53
NI	N.D.	N.D.	34.9	5.3	N.D.	38.2	176.3	N.D.	N.D.
CR	N.D.	N.D.	85.7	5.2	N.D.	52.0	366.5	N.D.	N.D.
V	192.0	145.6	172.0	57.2	167.1	154.7	118.7	189.7	151.7
SC	17.1	18.9	23.9	13.7	22.2	19.8	18.2	26.1	20.5
CU	35.0	45.9	35.2	43.2	17.9	20.0	32.4	30.9	37.8
ZN	195.8	72.1	129.2	42.2	75.0	78.3	67.5	154.7	73.6
SR	307.1	494.7	618.3	212.6	587.6	614.0	558.7	560.1	713.1
RB	88.6	39.5	41.1	104.8	36.0	34.3	55.7	33.4	34.6
ZR	261.7	193.8	203.0	532.8	268.8	259.8	200.5	247.1	240.2
NB	13.7	10.1	12.7	22.9	17.3	14.8	10.6	11.1	15.9
BA	996.6	421.0	400.8	695.4	446.1	416.9	468.4	436.8	515.1
TH	10.8	9.3	7.5	16.4	8.4	7.0	10.9	7.0	6.6
LA	37.5	26.2	25.8	45.1	33.3	30.8	26.8	29.0	30.9
CE	76.5	51.3	52.7	96.9	69.6	59.1	55.4	59.7	62.3
ND	35.7	23.8	24.3	40.4	33.5	31.4	25.8	31.5	31.4
SM	6.5	6.7	5.8	8.8	7.9	7.6	3.8	7.0	8.1
Y	29.3	22.6	27.1	38.4	29.2	29.1	21.4	38.1	26.8
TIO2CR	1.426	1.355	1.324	0.809	1.615	1.360	1.069	1.658	1.629
TIO2W	1.427	1.339	1.384	0.834	1.620	1.441	1.112	1.666	1.632

TABLE B17

	S47a11	S48a11	S49a1	S50a11	S51a11	S52a10	OC1a11	OC2a10	OC3a10
SIO2	51.98	52.81	51.58	56.47	52.30	52.23	56.85	55.19	57.04
AL2O3	18.26	19.91	16.19	17.10	18.43	16.41	17.75	17.58	17.51
FE2O3	10.07	8.17	9.41	9.32	9.93	9.59	7.58	7.74	7.46
MGO	4.64	3.43	7.80	2.38	3.95	5.12	3.88	3.66	5.25
CAO	6.96	6.80	8.78	6.45	7.32	8.14	6.13	7.89	3.99
NA2O	4.17	4.68	3.19	4.15	4.27	3.68	3.87	3.79	2.93
K2O	1.478	1.613	1.037	1.946	1.485	1.492	2.329	2.128	3.968
TIO2	1.699	1.799	1.629	1.912	1.731	1.601	1.293	1.535	1.283
MNO	0.105	0.290	0.165	0.076	0.137	0.162	0.087	0.086	0.058
P2O5	0.341	0.395	0.306	0.425	0.346	0.345	0.234	0.333	0.297
TOTAL	99.70	99.89	100.08	100.22	99.90	99.78	100.00	99.93	99.80
LOI	1.39	1.25	1.95	0.91	1.45	1.20	3.19	3.70	3.30
NI	11.9	10.6	169.2	27.2	12.7	63.5	50.5	42.4	58.9
CR	7.3	5.4	374.0	39.7	9.5	152.0	85.0	95.9	109.1
V	146.9	190.8	170.7	166.7	174.0	159.6	179.3	196.1	180.1
SC	16.4	22.1	23.8	21.9	18.5	24.6	27.1	28.8	25.7
CU	20.2	14.6	19.1	29.1	14.9	21.4	11.3	15.5	11.5
ZN	82.1	86.2	77.6	60.0	75.2	79.3	77.0	78.8	298.8
SR	703.8	762.9	625.5	470.4	688.2	507.1	554.7	516.5	417.5
RB	33.5	31.7	20.9	49.4	31.1	39.7	43.9	57.4	63.0
ZR	210.3	247.1	191.0	280.3	214.7	247.1	191.5	302.1	261.8
NB	10.9	11.8	11.8	16.3	10.7	9.9	9.8	14.1	12.3
BA	445.9	450.8	352.0	481.8	435.5	389.8	594.3	542.2	614.0
TH	6.6	5.4	6.4	8.9	8.1	8.1	3.5	9.8	9.3
LA	25.2	32.1	19.8	28.4	28.0	23.7	21.8	32.6	26.5
CE	64.1	76.9	49.5	67.0	60.8	51.4	49.3	74.7	59.7
ND	34.7	40.4	25.8	35.4	33.2	32.4	26.7	37.0	29.4
SM	7.4	7.4	6.4	7.6	7.1	6.6	6.2	8.8	7.8
Y	32.9	36.4	28.9	39.0	32.6	33.7	27.4	36.9	27.9
TIO2CR	1.328	1.858	1.402	1.806	1.641	1.366	1.397	1.635	1.367
TIO2W	1.446	1.860	1.514	1.873	1.681	1.433	1.390	1.629	1.367

	OC4a13	OC5a10	OC7a13	OC8a13	OC9a10	OC10a18	OC11a5	OC12a10	OC13a12
SIO2	59.93	57.96	60.16	61.08	60.78	57.71	57.91	60.05	57.35
AL2O3	17.35	17.30	16.20	16.12	16.45	18.40	17.60	16.42	16.77
FE2O3	6.39	7.31	7.37	6.07	6.04	3.05	7.62	6.98	7.57
MGO	3.28	3.66	3.01	3.25	4.29	1.93	3.95	3.90	2.90
CAO	4.78	4.72	4.39	2.92	2.29	0.92	2.47	4.55	6.38
NA2O	4.42	3.40	4.10	4.49	4.36	5.70	4.13	3.88	4.10
K2O	2.496	4.374	3.122	3.736	4.448	5.199	4.562	3.100	2.475
TIO2	1.175	1.316	1.239	1.198	1.259	1.625	1.545	1.085	1.303
MNO	0.062	0.073	0.114	0.114	0.123	0.073	0.094	0.081	0.094
P2O5	0.289	0.318	0.339	0.337	0.339	0.430	0.415	0.297	0.300
TOTAL	100.18	100.43	100.34	99.32	100.38	103.04	100.28	100.33	99.25
LOI	1.24	3.63	1.08	1.55	2.02	1.51	2.06	2.22	3.81
NI	30.2	64.2	29.6	24.0	27.8	13.2	14.0	24.3	25.4
CR	34.6	136.0	70.2	43.8	66.9	6.3	6.6	32.2	20.2
V	135.1	159.9	123.8	123.2	126.1	127.0	166.8	126.8	141.4
SC	17.4	23.1	17.5	15.2	19.3	16.4	15.9	19.1	18.6
CU	16.0	20.7	22.5	26.5	37.5	25.3	17.3	24.4	24.5
ZN	75.9	119.2	66.4	68.7	116.4	71.0	126.3	69.1	76.5
SR	629.0	381.9	430.8	431.7	300.2	552.5	451.2	765.3	705.5
RB	69.8	85.6	101.8	117.8	126.4	104.4	97.9	72.3	72.0
ZR	272.5	302.2	392.4	403.7	410.2	409.1	387.7	289.7	296.3
NB	14.2	14.4	17.3	16.8	17.3	17.7	16.5	12.1	13.6
BA	829.0	774.8	787.2	775.2	1178.7	1759.3	1261.0	938.9	715.9
TH	12.2	11.2	16.2	16.3	16.4	11.7	13.7	13.3	13.1
LA	31.8	34.3	36.0	40.1	39.4	41.8	36.8	34.6	30.9
CE	70.7	68.8	87.0	90.2	90.7	90.5	86.9	82.5	69.8
ND	34.6	32.5	43.2	42.3	44.4	45.1	43.4	41.2	33.8
SM	6.8	5.3	6.7	7.3	9.0	9.9	9.0	7.2	6.3
Y	29.3	29.5	39.2	40.0	41.5	38.9	36.8	29.6	33.6
TIO2CR	1.241	1.422	1.206	1.189	1.254	1.684	1.645	1.023	1.254
TIO2W	1.233	1.399	1.244	1.179	1.260	1.680	1.608	1.033	1.261

TABLE B17

	OC15a10	OC17a12	OC18a12	OC19a13	OC20a16	OC21a20	OC22a10	OC23a16	OC24a18
SIO2	56.76	53.46	55.08	61.87	61.67	54.08	53.72	58.02	58.21
AL203	16.03	17.42	17.58	17.07	17.24	17.36	16.28	17.86	17.53
FE203	7.60	8.03	7.91	5.89	6.06	7.98	8.26	6.51	6.76
MGO	5.92	5.23	4.25	0.88	2.75	4.67	5.49	4.28	1.21
CAO	6.92	7.85	8.20	5.80	3.91	8.65	8.76	5.71	8.36
NA20	3.62	3.95	3.85	4.36	5.15	3.75	3.38	4.51	4.05
K20	1.709	1.742	1.730	2.676	2.401	1.919	2.363	1.877	2.016
TIO2	1.135	1.301	1.278	0.823	0.753	1.123	1.159	0.980	1.392
MNO	0.134	0.089	0.116	0.098	0.102	0.086	0.119	0.055	0.075
P205	0.286	0.346	0.316	0.377	0.177	0.250	0.349	0.286	0.453
TOTAL	100.11	99.45	100.30	99.86	100.20	100.06	99.88	100.09	100.06
LOI	0.86	1.68	1.22	2.99	1.68	2.75	0.96	1.57	3.80
NI	129.5	67.8	59.3	13.1	31.2	113.6	33.5	42.2	40.3
CR	248.9	63.4	51.2	19.1	45.8	174.0	45.8	64.2	15.7
V	166.0	178.0	182.5	54.8	116.4	170.4	160.2	108.8	150.1
SC	21.4	21.8	20.3	9.6	16.5	23.1	21.5	14.5	18.6
CU	29.2	40.5	41.0	11.0	18.3	23.7	39.8	18.0	13.2
ZN	84.7	74.3	66.9	57.4	67.9	56.8	82.1	71.4	90.5
SR	579.8	784.3	814.0	516.5	547.9	677.4	1785.0	641.0	652.9
RB	38.1	35.0	33.2	66.8	55.7	47.0	41.1	40.9	28.5
ZR	183.5	195.0	184.0	315.7	159.8	156.1	186.0	218.2	272.6
NB	11.9	10.4	9.2	15.7	8.8	8.5	5.2	11.8	18.6
BA	456.9	614.2	632.0	703.9	698.6	563.0	1167.9	488.0	564.2
TH	6.9	4.8	1.4	8.7	4.7	6.9	6.3	4.7	5.7
LA	29.1	25.6	25.3	34.0	20.9	24.9	42.8	20.5	39.3
CE	57.2	62.9	58.2	77.4	42.2	50.0	100.9	51.6	87.9
ND	26.6	32.9	32.7	35.9	20.7	23.4	55.2	25.5	38.8
SM	5.6	7.0	5.2	7.7	6.8	7.8	10.4	5.7	6.2
Y	20.6	25.6	26.0	27.3	18.9	21.4	27.8	22.9	27.4
TIO2CR	1.171	1.314	1.240	0.826	0.745	1.033	1.000	0.965	1.484
TIO2W	1.183	1.351	1.261	0.820	0.748	1.081	1.050	0.982	1.484

	OC25a16	OC26a16	OC27a18	OC28a10	OC30a22	OC31a10	OC32a5	OC33a5	OC35a18
SIO2	61.72	62.24	57.32	58.33	69.11	55.40	69.60	56.51	63.67
AL203	17.43	17.41	17.52	17.74	15.55	17.62	16.36	20.26	16.27
FE203	5.62	5.55	7.26	5.83	3.71	7.06	1.68	4.78	4.74
MGO	2.21	2.26	3.11	4.30	1.26	4.16	0.68	5.77	2.89
CAO	4.72	4.62	5.58	6.70	0.22	8.86	0.52	1.56	3.97
NA20	4.79	4.53	4.37	3.50	3.33	3.53	4.38	5.48	4.27
K20	2.494	2.527	2.812	1.596	5.519	1.850	5.534	3.157	2.677
TIO2	0.770	0.773	1.462	1.255	0.462	1.498	0.513	1.243	0.772
MNO	0.103	0.131	0.174	0.144	0.025	0.147	0.019	0.105	0.053
P205	0.241	0.250	0.505	0.270	0.096	0.333	0.209	0.290	0.192
TOTAL	100.09	100.29	100.10	99.67	99.29	100.45	99.49	99.15	99.51
LOI	0.88	0.98	0.84	1.16	1.63	3.75	1.21	4.32	1.53
NI	11.9	12.6	7.2	55.4	5.1	45.3	5.4	78.6	57.3
CR	9.3	10.1	4.7	59.4	3.6	101.5	10.9	87.9	138.7
V	85.3	86.0	142.2	147.5	10.0	183.3	30.2	158.6	95.1
SC	9.9	10.0	16.8	20.4	8.8	27.6	4.7	21.9	16.6
CU	15.6	13.3	16.5	15.4	3.0	14.8	1.7	2.1	10.3
ZN	60.5	63.7	88.5	68.1	39.0	118.8	17.3	58.7	67.4
SR	588.1	567.0	818.2	750.7	162.7	542.5	282.7	596.8	413.1
RB	61.4	64.1	78.1	19.9	135.3	33.6	115.7	50.3	57.8
ZR	226.0	226.4	371.1	204.7	716.7	294.8	333.4	194.6	164.7
NB	11.9	11.5	14.8	11.6	27.0	13.4	15.5	11.6	17.5
BA	712.3	734.8	947.6	701.2	1145.7	525.8	1710.0	884.2	702.3
TH	8.7	9.3	10.9	5.5	29.8	11.7	6.9	5.2	9.2
LA	28.2	28.7	45.3	20.8	59.3	26.4	28.2	31.0	37.7
CE	61.4	65.0	106.4	53.6	134.2	53.6	65.6	63.2	77.4
ND	29.4	30.3	56.2	27.3	59.6	33.2	30.3	34.6	32.4
SM	6.4	7.2	10.8	3.8	11.5	9.4	4.5	4.5	4.1
Y	24.1	24.7	35.1	28.4	48.7	33.5	21.1	27.8	22.7
TIO2CR	0.713	0.730	1.525	1.306	0.472	1.559	0.570	1.220	0.821
TIO2W	0.725	0.749	1.505	1.308	0.479	1.557	0.573	1.261	0.800

TABLE B17

	OC36@13	OC38@20	OC39@20	OC41@6	OC42@10	OC43@13	OC44@11	OC47@22	OC48@22
SIO2	63.89	55.70	63.10	63.67	53.81	62.06	54.59	54.22	66.35
AL2O3	17.56	18.60	16.70	17.42	17.46	17.52	18.53	17.86	15.83
FE2O3	4.22	8.44	5.08	4.95	9.34	5.18	8.10	8.19	4.29
MGO	1.97	4.01	4.56	1.46	4.33	2.13	2.99	7.41	1.12
CAO	1.25	4.26	1.61	3.72	7.87	3.86	7.85	5.86	1.68
NA2O	6.23	4.18	3.92	4.56	3.59	5.08	4.06	3.82	4.96
K2O	3.145	2.252	3.549	2.386	1.531	2.473	1.677	1.691	4.019
TIO2	0.719	1.217	0.830	0.724	1.213	0.798	1.296	0.884	0.897
MNO	0.062	0.077	0.072	0.100	0.118	0.098	0.113	0.087	0.037
P2O5	0.249	0.335	0.198	0.334	0.219	0.275	0.328	0.205	0.189
TOTAL	99.30	99.07	99.61	99.33	99.49	99.48	99.53	100.23	99.37
LOI	1.88	2.08	2.66	1.01	1.05	1.04	1.98	2.37	1.63
NI	9.7	5.0	38.2	4.6	23.7	17.4	19.1	79.2	8.4
CR	13.2	3.6	120.3	3.1	17.8	24.8	3.9	184.4	6.6
Y	62.3	133.1	106.0	32.7	206.7	79.2	163.0	145.1	57.3
SC	8.4	15.8	19.3	6.4	25.4	9.9	14.9	26.7	10.3
CU	6.1	12.1	19.2	12.9	52.8	17.5	23.5	32.6	7.9
ZN	35.7	168.8	63.8	109.0	74.6	63.7	73.1	78.5	44.9
SR	581.1	473.1	301.2	504.9	719.2	573.8	775.0	541.2	246.6
RB	53.7	37.2	55.9	56.2	29.6	53.4	35.6	43.8	81.7
ZR	280.7	201.7	172.6	257.2	173.1	259.6	207.7	159.5	574.8
NB	12.8	10.0	16.0	15.4	7.9	12.5	11.3	7.6	19.4
BA	1011.2	491.6	847.4	688.3	654.7	704.6	519.2	380.6	761.3
TH	8.4	6.6	8.1	5.4	5.0	10.3	7.1	5.0	19.3
LA	34.8	21.9	34.6	29.6	20.0	32.4	24.4	16.1	40.4
CE	79.6	52.4	69.5	64.8	43.2	72.3	60.9	34.8	91.9
ND	35.9	27.5	27.9	28.4	24.2	36.2	31.0	18.9	41.7
SM	4.5	6.9	6.7	6.9	6.2	6.4	5.2	4.0	7.7
Y	25.4	26.5	23.3	23.1	27.9	29.5	25.0	23.7	40.0
TIO2CR	0.719	1.277	0.832	0.730	1.221	0.804	1.280	0.823	0.950
TIO2W	0.725	1.262	0.835	0.735	1.263	0.806	1.282	0.846	0.929

	OC50@10	OC51@13	OC52@10	OC53@16	OC54@14	OC35@22	OC56@16	OC57@18	OC58@19
SIO2	55.89	60.84	55.76	62.19	64.43	63.73	61.56	62.60	70.70
AL2O3	17.90	18.44	18.15	17.36	16.85	17.41	17.14	16.44	16.03
FE2O3	7.63	4.67	7.07	4.99	4.32	4.32	5.57	5.71	2.82
MGO	3.57	2.30	2.46	2.71	2.39	2.29	2.45	1.86	0.85
CAO	7.20	5.37	7.22	3.99	4.27	2.50	4.56	2.73	0.39
NA2O	4.25	4.47	5.09	4.81	4.31	5.31	4.58	4.62	2.65
K2O	1.474	2.031	2.318	2.143	2.185	2.976	2.394	3.674	5.888
TIO2	1.148	0.904	1.281	0.768	0.568	0.547	0.775	1.151	0.245
MNO	0.085	0.071	0.105	0.063	0.062	0.053	0.091	0.112	0.052
P2O5	0.312	0.316	0.284	0.215	0.180	0.213	0.244	0.409	0.123
TOTAL	99.44	99.41	99.75	99.24	99.56	99.34	99.35	99.30	99.74
LOI	1.15	1.48	2.95	1.33	1.18	1.56	1.17	1.22	1.82
NI	46.1	24.2	28.8	24.7	26.2	13.4	12.1	5.8	16.4
CR	64.2	23.7	26.4	29.2	38.8	22.2	9.8	3.2	25.8
V	136.4	104.5	171.0	91.0	66.0	57.9	74.2	88.8	7.9
SC	18.5	11.2	20.9	12.0	9.9	6.6	10.5	13.5	2.6
CU	33.9	19.9	14.6	10.7	21.3	32.9	15.7	22.5	45.3
ZN	63.2	100.3	47.5	55.7	111.2	59.3	72.4	95.2	45.1
SR	734.8	575.4	607.1	615.7	577.9	494.9	561.6	391.5	169.2
RB	28.8	48.2	61.8	44.1	60.4	46.6	57.2	115.7	128.6
ZR	199.9	230.4	189.2	187.8	169.5	216.3	224.5	409.3	191.8
NB	10.5	9.7	11.0	10.4	7.9	11.3	11.2	17.8	18.4
BA	418.8	540.2	506.4	648.2	677.2	904.1	740.8	827.6	937.3
TH	3.9	7.4	5.4	6.3	7.4	5.6	7.5	15.5	11.1
LA	19.4	24.1	21.3	22.4	22.6	22.9	31.7	42.5	45.1
CE	48.0	53.5	42.5	47.9	43.5	50.9	65.1	96.0	85.0
ND	23.8	24.5	20.3	23.2	20.6	22.6	31.0	46.3	33.1
SM	6.1	3.9	3.8	4.5	4.0	3.5	6.0	8.7	3.8
Y	25.7	19.7	23.3	20.2	14.0	15.4	24.7	38.2	20.3
TIO2CR	1.128	0.973	1.271	0.809	0.553	0.579	0.743	1.195	0.256
TIO2W	1.154	0.958	1.284	0.804	0.565	0.570	0.759	1.174	0.266

TABLE B17

	OC59a19	OC61a16	OC63a18	OC64a20	OC65a16	OC67a16	OC69a5	OC71a22	OC72a22
SIO2	73.27	60.27	61.65	64.97	62.95	65.01	62.64	59.66	53.24
AL2O3	14.53	17.83	18.08	17.22	17.02	15.69	17.55	17.21	17.72
FE2O3	1.58	5.67	5.21	4.40	4.88	4.22	4.61	5.87	8.11
MGO	0.45	2.88	2.45	0.83	2.30	1.35	3.38	3.84	5.33
CAO	0.36	5.24	3.78	3.34	4.14	4.38	2.88	3.80	7.71
NA2O	4.14	4.60	4.23	4.77	4.17	3.89	3.56	4.33	4.03
K2O	4.892	2.277	3.020	3.085	3.153	2.973	4.099	3.201	1.670
TIO2	0.224	0.704	0.685	0.575	0.646	0.638	0.762	1.061	1.224
MNO	0.041	0.085	0.118	0.059	0.055	0.048	0.034	0.093	0.116
P2O5	0.110	0.239	0.442	0.325	0.300	0.290	0.199	0.343	0.347
TOTAL	99.59	99.78	99.65	99.67	99.61	99.49	99.70	99.41	99.50
LOI	0.83	0.94	1.51	1.81	0.95	0.57	2.31	1.62	1.01
NI	10.6	29.2	4.4	5.3	18.9	18.8	24.5	49.9	81.9
CR	21.5	40.1	3.6	6.1	26.6	28.1	20.7	75.8	124.9
V	4.8	114.4	26.2	30.5	75.9	71.0	97.5	102.5	141.7
SC	2.0	13.4	7.5	6.3	10.1	9.3	11.6	15.1	16.9
CU	4.1	25.5	4.3	3.8	17.5	17.1	17.1	35.2	50.1
ZN	37.6	57.5	118.8	55.3	70.7	55.6	56.8	64.7	63.6
SR	254.2	876.9	592.0	354.8	514.4	548.1	330.1	509.5	647.0
RB	100.0	55.6	55.8	73.0	101.4	94.7	73.8	73.1	38.6
ZR	170.8	175.4	325.8	274.9	343.7	334.0	183.4	270.9	211.4
NB	17.2	9.2	13.6	14.0	11.2	10.3	9.3	13.3	9.2
BA	1144.4	989.9	596.9	687.9	751.2	751.1	637.6	648.1	458.3
TH	8.2	10.1	6.2	6.2	13.2	14.2	8.9	12.0	5.3
LA	36.4	28.3	37.6	34.5	32.6	32.8	27.2	34.7	25.1
CE	74.0	58.7	87.8	67.8	68.3	67.4	55.1	70.4	58.4
ND	27.5	27.6	41.3	37.0	28.8	27.2	23.8	28.5	29.0
SM	4.7	5.7	6.6	5.1	3.7	4.4	4.2	6.8	7.3
Y	16.1	18.7	28.8	32.4	16.9	16.0	18.9	23.1	24.4
TIO2CR	0.244	0.728	0.738	0.655	0.697	0.694	0.797	0.937	1.152
TIO2W	0.252	0.730	0.733	0.679	0.689	0.673	0.794	1.008	1.192

	OC73a11	OC74a12	OC75a12	OC76a1	OC77a10	OC78a12	OC79a12	OC80a20	OC81a12
SIO2	55.03	53.23	52.70	53.60	58.14	54.55	52.79	57.84	52.13
AL2O3	17.30	16.73	16.64	16.70	16.26	18.09	17.23	18.24	17.91
FE2O3	7.46	8.71	8.84	7.65	6.20	7.46	8.56	6.81	7.81
MGO	5.01	5.84	5.91	6.49	4.83	4.94	5.47	2.29	6.59
CAO	6.47	8.21	8.76	8.29	6.62	7.72	8.96	6.13	6.32
NA2O	3.90	3.43	3.43	3.54	3.81	3.65	3.49	4.40	4.77
K2O	2.470	1.670	1.127	1.489	2.301	1.505	1.334	2.036	1.436
TIO2	1.208	1.480	1.581	1.362	1.016	1.019	1.646	1.190	1.512
MNO	0.057	0.089	0.093	0.092	0.071	0.139	0.140	0.130	0.231
P2O5	0.390	0.367	0.248	0.322	0.285	0.247	0.303	0.442	0.357
TOTAL	99.30	99.76	99.33	99.53	99.53	99.32	99.92	99.51	99.06
LOI	3.42	2.10	1.62	2.38	1.10	0.85	1.05	1.24	2.77
NI	76.9	116.9	62.4	146.4	111.2	74.0	55.0	6.9	99.0
CR	83.8	155.6	141.6	239.6	178.1	104.0	131.3	4.3	134.6
V	163.6	201.1	186.6	157.9	149.9	147.0	215.7	121.2	221.8
SC	21.6	25.7	24.5	24.1	18.3	18.7	26.3	14.1	25.3
CU	42.0	42.6	19.9	18.8	52.2	39.2	30.8	12.2	18.4
ZN	109.1	82.5	61.3	72.4	53.7	59.6	78.5	56.0	123.8
SR	638.1	536.1	609.8	661.7	823.2	631.0	685.9	595.0	926.6
RB	50.3	44.4	20.9	24.9	55.2	30.4	25.7	48.0	26.1
ZR	249.5	232.3	160.4	205.5	211.4	169.5	193.9	262.6	229.8
NB	9.4	11.3	6.5	10.1	9.9	7.3	7.7	14.0	11.2
BA	582.1	432.4	433.0	544.9	735.3	407.5	496.7	532.0	472.0
TH	5.7	7.0	3.3	0.5	5.4	*	3.2	6.4	5.7
LA	33.4	27.4	17.0	22.7	29.3	21.2	23.9	32.9	28.0
CE	78.1	61.4	38.9	50.8	64.5	47.7	57.6	72.7	64.9
ND	39.2	32.0	24.9	26.4	32.3	24.4	31.5	35.0	33.8
SM	6.4	8.0	7.2	7.2	10.5	5.4	9.3	5.0	5.2
Y	27.4	28.5	29.2	24.9	20.4	21.6	30.7	30.5	29.2
TIO2CR	1.333	1.598	1.370	1.280	1.040	1.047	1.748	1.252	1.622
TIO2W	1.319	1.581	1.472	1.336	1.025	1.040	1.746	1.236	1.604

TABLE B17

	OC82a12	OC83a10	OC84a10	OC85a10	OC86a38	OC87a38	OC88a38	OC88Aa34	OC88Da34
SIO2	54.73	55.75	55.50	52.22	55.20	61.34	61.39	53.94	52.78
AL2O3	18.15	17.18	17.34	17.76	18.27	17.78	17.61	16.77	15.90
FE2O3	7.85	7.68	7.51	8.63	8.08	5.24	5.69	13.41	10.58
MGO	4.32	4.54	4.80	5.23	3.71	2.16	2.42	6.78	7.67
CAO	8.32	7.26	7.17	8.87	6.61	2.53	2.46	3.46	3.29
NA2O	3.68	3.89	3.63	3.76	4.38	4.87	4.43	2.75	1.32
K2O	1.343	1.700	1.667	1.350	1.624	4.128	4.339	3.784	6.048
TIO2	1.353	1.306	1.325	1.201	1.428	0.775	0.779	1.438	1.589
MNO	0.154	0.131	0.127	0.161	0.094	0.058	0.073	0.122	0.159
P2O5	0.283	0.288	0.291	0.292	0.359	0.399	0.403	0.619	0.338
TOTAL	100.17	99.72	99.36	99.49	99.75	99.28	99.60	100.07	99.68
LOI	0.74	0.78	0.76	1.06	0.76	1.17	1.37	3.62	5.76
NI	52.0	63.2	61.9	103.0	19.2	6.7	5.9	9.1	15.9
CR	28.4	91.5	84.6	221.7	26.2	6.4	6.4	3.7	16.4
V	186.7	150.2	137.9	190.7	117.1	46.9	43.4	109.4	153.2
SC	26.5	20.3	19.1	25.9	16.0	6.7	6.5	19.0	28.0
CU	90.2	29.5	27.3	29.7	17.4	8.7	6.6	13.9	23.8
ZN	75.0	65.0	68.1	67.0	63.8	81.2	66.4	122.2	103.7
SR	626.8	521.1	540.8	565.6	627.8	382.2	425.6	371.5	99.1
RB	31.3	42.1	43.1	29.9	34.0	51.6	68.9	25.7	68.5
ZR	186.9	199.2	199.9	188.4	249.3	307.3	298.5	70.0	154.4
NB	9.7	12.3	11.6	7.0	12.7	15.3	15.1	10.4	8.9
BA	389.7	400.4	412.4	421.5	425.1	638.5	1041.6	384.8	432.2
TH	4.4	5.8	6.5	4.0	4.7	6.6	6.4	2.8	5.1
LA	23.3	24.8	26.4	22.1	26.0	35.7	37.0	28.2	39.7
CE	55.2	55.2	55.2	48.6	65.2	77.0	78.5	61.0	77.9
ND	26.1	28.1	25.5	25.3	30.4	34.1	37.0	29.5	35.3
SM	4.7	6.4	5.6	7.2	7.4	6.6	5.9	3.8	3.6
Y	24.8	27.8	26.2	25.1	31.2	28.4	27.8	15.8	15.3
TIO2CR	1.404	1.301	1.186	1.204	1.184	0.814	0.771	1.389	1.594
TIO2W	1.422	1.324	1.261	1.210	1.266	0.815	0.777	1.409	1.601

	OC88Ea34	OC89a13	OC90a1	OC91a12	OC92a12	OC93a13	OC94a13	OC95a20	OC96a1
SIO2	53.67	64.75	52.84	52.30	52.40	53.79	59.20	56.63	52.36
AL2O3	18.42	17.88	16.23	16.09	18.75	15.72	15.55	18.22	15.77
FE2O3	8.66	2.54	8.46	7.25	7.23	6.49	6.83	7.79	8.36
MGO	6.90	1.02	6.92	6.84	3.23	4.83	3.74	2.81	8.19
CAO	0.83	3.97	9.90	10.66	9.88	5.08	7.03	5.91	7.73
NA2O	3.69	4.68	3.35	3.16	4.47	3.37	3.13	4.54	3.14
K2O	4.964	3.604	1.135	1.680	1.618	2.691	2.737	1.936	1.829
TIO2	1.929	0.901	1.249	1.242	1.572	1.075	1.068	1.240	1.405
MNO	0.102	0.026	0.086	0.100	0.096	0.072	0.081	0.118	0.149
P2O5	0.217	0.283	0.234	0.294	0.300	0.291	0.291	0.439	0.370
TOTAL	99.38	99.67	100.41	99.61	99.53	99.41	99.65	99.64	99.31
LOI	3.92	1.73	2.75	3.53	3.10	1.39	2.76	1.13	2.53
NI	15.1	9.4	210.3	296.3	40.6	90.1	88.5	5.9	207.2
CR	15.5	9.8	408.7	506.9	33.3	134.4	152.9	3.2	432.6
V	179.9	102.9	166.5	183.5	199.6	112.4	110.4	111.6	166.3
SC	30.4	11.0	25.9	26.2	21.9	17.1	18.6	14.5	24.0
CU	13.1	7.9	32.3	37.2	28.2	36.5	25.6	10.6	25.7
ZN	144.8	17.8	73.4	93.4	126.7	55.9	61.3	62.4	73.5
SR	193.7	480.9	597.4	674.1	709.3	734.7	561.3	614.9	544.0
RB	64.9	90.7	16.8	33.6	39.5	79.6	83.2	45.2	46.4
ZR	186.0	221.3	169.1	227.6	208.6	243.5	250.3	257.8	266.4
NB	11.5	12.8	7.7	7.6	7.6	13.3	14.0	13.4	9.3
BA	926.1	789.1	330.4	518.5	446.0	796.0	724.9	511.0	516.9
TH	0.5	8.0	4.3	5.9	3.7	11.2	9.6	4.8	6.0
LA	71.5	30.8	18.6	22.4	20.2	41.7	39.6	27.6	27.1
CE	124.4	65.0	37.6	49.8	47.8	88.5	82.3	67.7	57.6
ND	44.9	27.5	18.2	28.3	26.9	38.8	36.6	33.0	30.6
SM	5.1	4.8	4.2	3.7	6.7	11.0	8.6	7.8	6.6
Y	11.5	17.3	22.7	24.3	29.6	23.4	25.3	29.8	27.8
TIO2CR	1.811	1.004	1.298	1.288	1.514	0.856	0.893	1.160	1.345
TIO2W	1.859	0.981	1.330	1.294	1.567	0.931	0.936	1.190	1.435

TABLE B17

	OC97a20	OC98a13	OC99a20	OC100a11	OC101a1	OC102a11	OC103a13	OC104a11	OC105a1
SIO2	57.30	60.55	57.25	56.35	54.73	50.84	55.55	53.57	55.80
AL2O3	18.08	15.87	17.93	16.78	16.70	17.51	15.73	16.47	18.41
FE2O3	7.54	5.79	7.41	7.29	7.64	10.45	6.72	8.10	7.04
MGO	2.46	4.52	2.50	5.13	5.73	5.24	7.10	6.83	4.71
CAO	5.53	5.21	5.37	7.17	8.14	8.09	7.25	7.64	4.01
NA2O	4.76	3.90	4.99	4.09	3.70	3.69	3.66	3.91	4.31
K2O	1.786	1.973	1.906	1.186	0.911	1.032	1.916	1.183	3.005
TIO2	1.127	1.045	1.113	1.238	1.304	1.510	1.158	1.384	1.560
MNO	0.154	0.158	0.140	0.098	0.109	0.080	0.085	0.112	0.052
P2O5	0.609	0.358	0.597	0.251	0.281	0.241	0.306	0.309	0.365
TOTAL	99.34	99.37	99.20	99.59	99.25	99.68	99.48	99.51	99.27
LOI	0.95	1.49	0.59	0.39	1.07	1.60	0.97	1.41	1.90
NI	5.1	79.2	4.0	56.1	99.2	183.4	192.5	171.5	23.4
CR	4.2	144.7	4.0	130.2	134.9	330.3	397.8	245.0	7.9
V	57.1	108.4	61.7	136.0	154.7	198.9	154.4	137.2	164.0
SC	10.7	12.9	10.1	20.0	22.7	29.9	22.6	19.1	20.5
CU	7.1	22.9	7.5	25.7	35.1	49.3	27.7	18.2	15.2
ZN	83.5	70.7	79.3	66.2	69.7	57.9	71.1	77.4	119.6
SR	632.5	849.9	607.4	558.1	610.4	440.9	550.3	551.6	536.9
RB	36.4	19.0	41.3	25.3	7.7	20.7	52.8	17.1	48.8
ZR	285.7	245.4	279.4	161.7	183.4	160.5	236.1	192.8	239.5
NB	14.6	15.1	13.9	8.7	11.3	6.7	9.0	11.5	13.1
BA	500.8	959.2	485.3	334.6	371.3	285.7	512.1	409.8	461.4
TH	1.0	8.3	5.7	1.1	3.8	2.6	4.8	0.0	7.0
LA	32.6	45.5	33.1	17.6	22.3	18.2	24.5	23.9	30.9
CE	76.5	87.8	78.4	40.1	47.8	36.7	54.8	50.6	64.0
ND	38.8	37.0	39.5	20.4	23.1	20.1	27.9	23.9	30.4
SM	6.6	5.8	8.6	4.7	6.4	5.0	6.5	4.5	4.8
Y	34.5	20.2	33.0	21.3	24.1	27.4	23.2	25.4	27.5
TIO2CR	1.066	1.123	1.139	1.125	1.340	1.574	1.184	1.399	1.539
TIO2W	1.075	1.099	1.133	1.157	1.341	1.595	1.224	1.400	1.564

	OC106a13	OC107a22	OC108a13	OC109a13	OC110a12	OC111a22	OC112a12	OC113a11	OC115a11
SIO2	61.47	55.73	58.03	61.56	53.33	74.81	55.90	52.84	53.80
AL2O3	17.28	18.52	17.61	17.27	18.58	14.56	18.71	18.54	15.81
FE2O3	5.10	7.02	6.62	5.48	7.69	1.22	7.43	9.41	6.79
MGO	2.94	4.62	2.93	2.32	5.18	0.38	2.76	3.51	7.20
CAO	4.53	4.38	6.19	4.71	8.85	0.91	6.90	7.49	8.26
NA2O	4.29	3.18	4.36	4.13	3.62	2.40	4.55	3.99	3.71
K2O	2.351	4.454	2.035	2.516	1.011	5.077	1.644	1.598	1.415
TIO2	0.996	1.266	1.358	1.013	1.163	0.128	1.542	1.669	1.277
MNO	0.115	0.075	0.101	0.099	0.132	0.042	0.110	0.074	0.125
P2O5	0.267	0.253	0.251	0.232	0.161	0.047	0.338	0.344	0.273
TOTAL	99.34	99.48	99.47	99.43	99.72	100.57	99.88	99.57	99.66
LOI	1.15	3.71	0.98	0.84	0.64	2.01	0.59	1.19	1.17
NI	22.2	14.8	12.1	7.7	23.3	4.2	14.3	17.8	219.3
CR	22.9	11.5	7.9	6.6	43.8	3.7	14.0	7.9	513.2
V	107.4	182.8	162.3	115.4	196.6	2.7	162.0	165.9	179.4
SC	13.5	21.7	17.0	12.6	26.3	1.2	16.9	19.5	29.5
CU	19.2	16.0	20.4	9.8	18.3	3.4	24.6	16.0	20.3
ZN	65.2	83.5	69.3	67.8	67.6	23.5	67.1	81.7	62.6
SR	623.2	500.2	656.3	579.9	657.9	101.5	541.6	665.4	542.6
RB	59.2	52.6	53.2	74.5	18.6	126.8	41.2	32.6	29.3
ZR	222.4	172.9	194.2	231.7	117.1	114.7	244.2	226.4	186.3
NB	12.5	9.4	13.4	13.6	6.7	20.3	11.4	16.0	8.4
BA	644.9	619.3	594.7	640.2	269.2	1009.5	399.8	408.0	399.3
TH	10.4	8.3	7.3	13.1	2.1	12.0	5.4	5.9	3.8
LA	34.6	31.1	25.7	36.5	12.3	23.4	26.0	28.0	21.3
CE	79.3	60.8	61.9	73.7	31.1	54.7	61.3	57.1	44.6
ND	34.9	30.2	28.4	30.2	17.4	24.4	30.7	30.0	22.8
SM	5.7	6.4	6.0	4.8	4.0	5.2	8.0	7.6	6.9
Y	24.9	23.0	25.8	24.3	22.8	26.5	32.2	30.4	23.6
TIO2CR	1.011	1.294	1.335	1.014	1.210	0.146	1.483	1.594	1.273
TIO2W	1.000	1.350	1.374	1.025	1.298	0.159	1.535	1.678	1.294

TABLE B17

	OC116a4	OC117a19	OC118a11	OC119a11	OC120a12	OC121a12	OC122a9	OC123a9	OC124a9
SIO2	54.00	79.18	51.97	51.10	57.15	56.13	60.27	59.86	60.15
AL2O3	16.86	13.89	17.19	17.03	17.53	17.41	16.55	16.44	16.52
FE2O3	7.57	0.82	7.75	9.32	6.58	6.59	6.16	6.18	6.12
MGO	6.25	0.20	7.67	6.50	4.71	4.99	3.33	3.88	3.55
CAO	7.80	0.85	7.86	7.64	6.50	6.81	5.68	6.16	5.89
NA2O	3.95	0.17	3.83	4.02	4.33	4.02	3.94	4.32	4.11
K2O	1.398	4.725	1.019	1.124	1.798	1.741	2.259	1.468	2.114
TIO2	1.413	0.130	1.657	1.601	1.096	1.113	1.047	1.061	1.058
MNO	0.142	0.069	0.132	0.103	0.120	0.120	0.072	0.145	0.113
P2O5	0.334	0.054	0.300	0.296	0.284	0.283	0.257	0.250	0.257
TOTAL	99.71	100.10	99.39	99.32	100.11	99.21	99.57	99.76	99.89
LOI	1.04	3.56	1.92	1.46	1.18	1.01	1.10	1.06	0.88
NI	153.5	8.6	126.7	138.8	81.4	93.2	33.5	30.3	30.9
CR	249.7	3.7	333.0	342.4	154.4	170.7	92.8	66.6	68.9
V	146.7	10.6	188.1	193.2	143.5	149.7	125.2	124.7	123.3
SC	19.9	0.9	31.2	32.1	21.4	21.7	19.0	16.9	17.8
CU	39.3	48.3	16.0	26.5	32.3	31.5	19.4	17.2	17.5
ZN	61.2	5.4	89.7	75.6	72.5	72.0	65.9	66.6	63.7
SR	584.3	258.2	547.4	572.9	709.8	719.2	586.5	657.1	607.2
RB	23.5	92.6	17.2	18.9	41.8	37.0	54.9	29.7	60.2
ZR	208.0	109.6	189.7	184.0	191.3	186.2	226.2	224.7	224.2
NB	11.7	18.2	9.4	10.6	11.5	11.1	13.9	14.6	14.0
BA	455.8	656.3	250.4	285.3	559.5	542.3	564.6	586.9	552.4
TH	1.6	13.0	0.9	1.7	4.1	6.1	11.0	10.0	12.8
LA	29.1	37.0	17.4	19.2	26.6	24.7	35.1	37.4	35.9
CE	58.3	72.8	42.2	41.5	54.6	50.3	73.2	72.1	75.2
ND	26.7	26.2	23.7	22.7	26.6	25.4	30.7	29.6	33.1
SM	5.8	4.5	6.9	5.7	5.1	6.0	0.9	6.4	6.0
Y	25.6	17.0	26.5	30.5	24.2	23.0	21.9	23.1	23.4
TIO2CR	1.457	0.148	1.463	1.603	1.132	1.120	1.078	1.152	1.083
TIO2W	1.463	0.158	1.574	1.660	1.136	1.130	1.076	1.116	1.092

	OC126a19	OC127a22	OC128a19	OC129a1	OC130a18	OC131a10	OC132a1	OC133a1	OC134a9
SIO2	75.59	61.93	78.86	55.32	59.03	59.99	55.10	57.12	60.26
AL2O3	13.43	17.61	12.02	17.43	17.97	16.18	16.36	15.91	16.92
FE2O3	1.75	4.50	0.76	6.78	6.55	6.82	7.72	7.18	5.83
MGO	0.30	0.91	0.16	5.30	2.57	2.83	6.35	5.84	3.91
CAO	0.29	6.35	0.45	7.15	4.46	5.16	7.10	6.71	5.25
NA2O	5.61	4.73	4.57	4.24	4.58	4.13	3.92	3.65	3.97
K2O	3.067	2.431	3.128	1.570	2.431	2.440	1.467	1.674	2.189
TIO2	0.120	1.045	0.109	1.389	1.275	1.225	1.303	1.078	1.076
MNO	0.028	0.056	0.038	0.089	0.110	0.061	0.089	0.115	0.063
P2O5	0.047	0.252	0.044	0.258	0.297	0.391	0.244	0.245	0.261
TOTAL	100.24	99.82	100.14	99.52	99.26	99.22	99.66	99.53	99.73
LOI	0.63	2.95	0.51	1.09	1.41	0.79	1.04	0.82	1.22
NI	4.9	53.7	3.6	102.5	7.3	93.4	115.1	126.8	31.2
CR	4.2	94.2	3.9	265.5	2.9	113.4	254.9	248.6	89.9
V	2.3	114.8	7.5	147.4	138.0	144.3	137.0	125.3	131.3
SC	0.8	20.9	0.6	23.0	15.6	18.3	22.6	19.1	20.8
CU	31.8	33.1	4.7	22.0	8.6	18.5	25.5	21.8	18.8
ZN	26.3	31.9	13.4	64.1	68.1	73.3	67.5	66.6	72.1
SR	141.2	474.0	128.2	510.3	644.5	744.8	493.0	482.8	505.1
RB	39.3	78.1	65.6	39.8	62.3	55.5	36.5	45.2	63.1
ZR	105.1	199.1	93.8	197.4	230.6	231.1	195.7	209.1	228.0
NB	19.7	10.6	16.7	11.9	14.3	14.8	11.3	14.7	14.2
BA	852.8	520.8	791.0	355.8	618.2	844.4	337.4	389.2	579.4
TH	13.2	10.2	10.4	8.2	9.8	8.6	7.0	10.6	9.2
LA	22.8	25.4	19.0	25.4	30.5	45.0	25.5	31.3	37.5
CE	53.0	56.5	43.1	57.2	69.0	97.7	53.0	65.7	74.0
ND	23.6	25.1	20.9	25.1	31.7	37.1	23.0	26.7	31.2
SM	4.9	7.8	4.4	7.5	8.2	6.9	6.0	6.0	4.3
Y	21.9	20.0	21.3	25.2	25.6	20.3	24.3	24.2	21.6
TIO2CR	0.133	0.945	0.117	1.154	1.339	1.274	1.119	1.014	1.095
TIO2W	0.144	1.016	0.136	1.253	1.368	1.259	1.205	1.059	1.109

TABLE B17

	OC135a9	OC136a9	OC137a22	OC138a9	OC139a22	OC140a12	OC141a22	OC143a22	OC145a13
SIO2	59.38	59.03	54.95	59.35	54.97	52.80	58.45	56.94	59.44
AL2O3	16.94	16.60	17.31	16.68	17.31	17.94	16.50	17.23	16.19
FE2O3	6.20	6.38	7.41	6.78	7.80	8.97	6.53	7.06	6.11
MGO	3.41	3.62	4.65	3.66	4.37	4.95	4.22	4.16	4.75
CAO	5.96	6.05	8.06	5.41	7.94	7.66	5.81	6.04	6.02
NA2O	4.06	4.26	3.97	3.79	3.94	4.16	4.17	4.49	3.94
K2O	2.178	2.189	1.431	2.229	1.373	1.233	2.204	1.962	1.595
TIO2	1.155	1.153	1.491	1.149	1.410	1.593	1.142	1.309	1.119
MNO	0.104	0.080	0.142	0.053	0.130	0.149	0.091	0.121	0.157
P2O5	0.278	0.272	0.302	0.274	0.267	0.281	0.268	0.297	0.231
TOTAL	99.67	99.64	99.70	99.37	99.50	99.72	99.38	99.61	99.54
LOI	1.04	0.98	0.66	1.14	0.56	0.61	0.96	1.07	1.19
NI	32.9	43.3	41.7	34.9	29.6	29.4	46.4	40.7	60.3
CR	51.6	83.4	109.9	53.3	69.2	28.0	96.4	36.2	78.2
V	132.0	116.3	158.1	99.5	139.3	178.1	112.9	125.0	121.4
SC	18.3	18.3	23.4	18.4	19.4	21.7	17.5	17.9	16.2
CU	21.5	19.7	29.5	18.5	26.8	20.9	23.3	25.5	32.6
ZN	59.2	65.3	60.7	72.5	61.1	39.0	64.7	65.2	90.2
SR	611.8	590.0	611.1	617.1	567.1	617.7	610.0	584.6	640.2
RB	60.7	60.4	32.0	63.5	33.5	25.0	60.5	50.2	23.2
ZR	236.2	229.4	206.5	232.7	193.6	208.5	220.0	219.9	208.9
NB	14.3	15.0	11.2	14.2	10.2	11.1	13.4	13.0	14.2
BA	575.8	558.8	398.8	575.3	409.5	356.6	619.7	517.8	584.4
TH	9.5	11.3	4.2	12.2	5.8	1.5	10.3	6.2	14.0
LA	35.2	32.5	23.4	32.4	22.0	22.5	32.3	29.1	36.5
CE	76.3	72.3	51.4	67.9	51.0	31.5	70.6	62.0	78.8
ND	31.4	30.4	25.7	28.5	24.8	26.9	29.3	28.9	32.3
SM	6.0	6.5	5.7	6.8	5.9	6.8	6.2	8.5	4.3
Y	23.8	25.7	26.8	25.5	27.8	30.2	24.5	25.2	22.1
TIO2CR	1.139	1.028	1.516	0.921	1.296	1.389	1.065	1.173	1.149
TIO2W	1.162	1.078	1.551	0.968	1.355	1.470	1.119	1.221	1.149

	OC146a19	OC147a18	OC148a11	OC149a11	OC150a22	OC152a12	OC153a10	PE1a1	PE3a11
SIO2	70.74	59.11	54.76	55.04	54.54	50.59	56.74	50.13	53.83
AL2O3	14.61	17.88	17.38	16.90	18.11	14.62	15.56	16.95	19.07
FE2O3	2.82	6.20	7.79	7.47	8.40	9.16	7.25	10.84	3.90
MGO	1.07	2.90	4.41	5.29	3.36	10.82	6.65	2.79	0.48
CAO	2.16	4.72	8.13	7.91	6.09	9.20	6.61	11.95	13.93
NA2O	4.22	4.78	3.86	3.65	4.17	2.60	3.63	4.10	5.20
K2O	3.134	2.356	1.344	1.655	2.387	1.093	1.808	1.105	1.799
TIO2	0.346	1.278	1.428	1.503	1.664	1.145	1.100	1.847	1.583
MNO	0.029	0.160	0.095	0.109	0.067	0.135	0.105	0.159	0.172
P2O5	0.135	0.300	0.264	0.332	0.578	0.298	0.276	0.387	0.345
TOTAL	99.27	99.69	99.45	99.76	99.36	99.66	99.73	100.25	100.31
LOI	0.78	1.00	0.89	1.15	1.01	1.08	0.86	6.75	7.95
NI	8.0	7.1	31.3	110.8	14.1	241.8	164.0	176.1	6.0
CR	8.3	3.7	80.8	215.1	7.9	659.8	333.5	320.5	5.5
V	17.1	132.6	156.9	168.7	125.1	188.0	124.7	255.7	138.3
SC	2.6	15.3	20.3	22.2	15.2	30.8	18.9	28.5	16.6
CU	6.6	9.1	24.4	31.8	31.9	44.6	35.5	20.8	32.6
ZN	32.9	88.3	60.8	69.0	71.8	57.4	66.0	83.4	87.3
SR	387.6	657.5	598.9	641.2	591.5	552.3	573.4	626.3	517.5
RB	79.4	59.8	29.6	30.4	65.3	23.1	42.0	20.6	36.1
ZR	214.2	228.6	189.1	211.6	325.5	152.5	187.9	245.8	246.1
NB	9.9	14.2	10.0	14.4	17.9	7.6	11.7	7.9	11.6
BA	581.2	615.6	399.4	460.8	551.5	398.1	583.6	274.2	335.1
TH	11.8	10.6	3.1	5.8	9.9	5.7	7.7	8.9	9.4
LA	24.5	31.5	21.3	27.7	43.0	21.7	27.2	16.6	22.6
CE	53.2	69.4	49.4	59.8	92.2	47.1	60.8	46.0	61.0
ND	21.9	32.7	24.9	28.2	46.2	26.1	25.7	27.2	33.2
SM	2.2	6.1	7.4	7.5	10.1	2.2	3.0	6.9	5.8
Y	14.3	25.7	26.6	25.7	37.8	23.4	20.7	30.3	35.5
TIO2CR	0.298	1.304	1.251	1.502	1.355	1.164	1.014	1.857	1.692
TIO2W	0.368	1.298	1.340	1.509	1.466	1.184	1.034	1.922	1.706

TABLE B17

	PE3A@11	PE4@19	PE5@20	PE6@1	PE8@11	PE9@11	PE10@20	PE11@12	PE12@29
SIO2	55.17	73.01	49.74	53.02	56.04	54.93	56.28	50.63	67.36
AL2O3	18.15	15.28	18.62	16.32	16.85	17.75	18.54	19.13	17.08
FE2O3	9.28	1.74	10.81	8.76	8.65	7.68	8.71	8.52	3.50
MGO	3.29	0.33	5.91	6.36	4.25	5.01	2.24	3.53	0.64
CAO	6.43	1.86	7.99	7.97	7.76	7.66	4.53	9.88	2.78
NA2O	4.53	3.55	3.91	3.48	3.44	3.43	5.33	4.12	4.02
K2O	1.371	4.051	0.936	0.810	0.965	1.125	2.155	1.652	4.120
TIO2	1.637	0.190	2.081	1.520	1.263	1.187	1.185	1.448	0.484
MNO	0.109	0.072	0.138	0.094	0.060	0.159	0.076	0.210	0.063
P2O5	0.340	0.090	0.334	0.257	0.206	0.184	0.466	0.471	0.221
TOTAL	100.30	100.15	100.45	99.79	99.47	100.12	99.51	100.08	100.27
LOI	1.76	2.89	2.62	1.67	1.85	3.78	2.86	6.92	2.29
NI	7.5	7.5	20.0	81.9	117.7	124.7	5.0	42.1	4.4
CR	4.6	4.2	11.4	281.5	265.3	312.0	3.9	57.8	3.7
V	121.4	0.9	184.0	180.9	194.4	179.5	100.5	207.9	10.7
SC	15.0	1.1	24.8	30.6	33.1	36.4	12.5	26.5	5.3
CU	12.4	9.2	13.7	9.9	23.7	28.0	16.5	13.7	3.7
ZN	100.2	20.0	107.2	80.7	177.0	195.9	89.3	364.1	60.1
SR	535.6	218.8	733.1	489.2	472.5	467.4	468.8	340.2	251.2
RB	31.9	99.7	15.2	9.3	20.1	21.1	42.5	52.4	121.8
ZR	231.1	269.9	208.4	192.2	150.3	143.9	269.3	431.2	427.6
NB	11.3	17.4	8.1	9.3	7.2	6.6	12.8	17.4	27.8
BA	359.7	731.7	327.0	262.8	254.5	336.2	536.5	256.7	855.0
TH	7.7	14.1	5.1	7.1	3.7	6.4	9.9	17.7	16.8
LA	22.3	46.5	19.9	16.6	13.3	17.4	34.0	37.6	52.8
CE	53.7	93.6	46.0	38.7	31.9	32.6	70.8	94.3	107.8
ND	29.0	35.9	28.1	22.2	16.3	17.8	37.7	47.8	45.5
SM	5.5	5.2	6.6	6.2	4.0	3.6	7.3	9.5	6.9
Y	33.6	25.9	35.8	28.8	23.6	25.2	32.6	50.0	37.2
TIO2CR	1.513	0.214	1.803	1.535	1.314	1.244	1.187	2.084	0.462
TIO2W	1.591	0.217	1.884	1.597	1.335	1.243	1.197	2.075	0.462

	PE13@11	PE14@5	PE15@5	PE16@5	PE17@12	PE18@13	PE19@29	PE20@29	PE21@6
SIO2	57.55	55.16	56.98	59.69	53.21	60.68	69.27	62.17	56.73
AL2O3	16.86	17.26	15.91	15.47	16.07	18.07	16.58	18.22	18.88
FE2O3	8.92	4.17	7.05	5.39	10.30	5.81	2.80	5.52	8.70
MGO	4.94	3.15	7.46	5.18	4.19	1.81	0.68	0.53	4.38
CAO	6.85	13.84	6.62	8.74	5.64	1.67	1.49	6.40	2.30
NA2O	3.32	3.50	3.37	3.21	6.05	9.43	5.00	4.00	5.89
K2O	0.378	1.599	1.587	1.632	1.836	1.653	3.858	2.177	1.690
TIO2	1.164	1.041	0.997	0.770	1.639	1.162	0.344	0.800	1.085
MNO	0.058	0.158	0.092	0.085	0.124	0.073	0.038	0.061	0.050
P2O5	0.188	0.208	0.181	0.201	0.522	0.378	0.154	0.339	0.252
TOTAL	100.23	100.08	100.25	100.37	99.79	99.74	100.21	100.22	99.95
LOI	3.92	8.21	2.61	3.91	4.25	1.45	0.88	4.38	4.31
NI	102.5	159.9	166.2	245.5	139.8	11.2	5.1	5.1	31.0
CR	290.6	449.4	380.6	424.8	330.7	12.2	4.4	4.7	19.1
V	156.4	158.3	131.2	120.0	176.6	108.3	11.6	83.3	133.4
SC	33.6	25.8	20.2	18.8	29.9	13.5	2.5	8.7	17.0
CU	53.8	19.2	20.4	30.3	26.3	14.5	1.7	7.9	37.4
ZN	79.8	105.9	68.5	101.4	94.5	106.0	65.5	45.2	83.4
SR	419.7	464.7	445.3	534.2	847.4	313.9	396.4	731.1	269.1
RB	5.0	42.9	43.7	25.9	34.5	21.4	86.0	51.0	44.8
ZR	137.6	165.3	152.2	156.1	353.0	313.7	351.7	302.5	254.7
NB	6.1	9.6	9.5	12.9	15.1	23.3	11.7	10.4	15.5
BA	236.1	371.3	422.6	574.2	794.4	235.0	1505.6	899.3	321.5
TH	5.5	6.9	7.9	6.4	12.4	16.8	11.8	8.7	11.4
LA	12.9	21.6	21.1	24.0	44.0	38.0	45.9	36.0	38.1
CE	24.7	44.9	40.7	48.6	103.3	81.6	94.6	80.4	74.6
ND	14.7	21.7	17.6	21.3	55.2	37.8	42.5	38.1	30.3
SM	3.9	2.2	3.9	6.3	14.5	8.5	5.5	5.4	5.8
Y	19.7	21.7	20.8	15.7	43.9	32.7	25.3	23.6	24.3
TIO2CR	1.142	1.061	0.942	0.833	1.880	1.225	0.372	0.858	1.072
TIO2W	1.183	1.102	0.991	0.825	1.858	1.203	0.367	0.853	1.102

TABLE B17

	PE22820	PE23820	PE2487	PE25822	PE26813	PE27822	PE28822	PE29822	PE31822
SIO2	55.95	55.12	56.34	75.64	56.92	74.53	74.59	59.88	75.84
AL203	16.98	17.23	18.26	14.61	16.27	14.69	15.06	17.87	14.22
FE203	10.38	9.65	7.66	0.56	7.75	1.03	1.76	7.13	0.98
MGO	5.08	3.47	6.04	0.27	6.42	0.27	0.20	2.74	0.15
CAO	3.31	5.78	3.99	0.46	6.33	0.69	0.12	3.75	0.10
NA20	3.85	4.67	4.81	4.37	3.40	4.64	4.72	5.01	4.02
K20	2.343	2.102	1.051	4.230	1.633	4.187	3.612	1.945	4.515
TIO2	1.733	1.743	1.205	0.103	1.283	0.111	0.048	0.857	0.089
MNO	0.095	0.123	0.113	0.030	0.097	0.086	0.045	0.119	0.019
P205	0.296	0.311	0.157	0.045	0.222	0.048	0.055	0.478	0.039
TOTAL	100.02	100.20	99.63	100.32	100.32	100.28	100.21	99.79	99.95
LOI	2.54	1.18	3.06	0.99	1.06	0.30	0.89	1.79	0.35
NI	24.9	22.6	32.8	4.1	119.1	3.9	3.9	4.4	3.8
CR	36.3	30.8	121.8	3.3	281.1	3.7	3.0	3.9	3.0
V	172.6	188.2	191.5	1.8	139.2	2.3	2.3	26.6	4.1
SC	29.4	25.1	33.4	1.7	22.8	1.9	*	7.6	1.1
CU	13.8	16.9	28.4	2.8	19.9	3.2	3.1	6.0	3.1
ZN	149.0	95.7	78.0	30.0	67.6	59.4	61.1	119.1	15.3
SR	277.0	449.4	714.4	93.4	412.6	154.7	103.6	440.7	180.8
RB	59.4	62.0	18.5	95.1	49.2	94.9	90.6	45.8	98.8
ZR	218.0	233.6	145.9	91.6	210.9	100.4	96.5	267.5	66.0
NB	12.0	13.6	8.2	16.5	9.6	15.6	15.6	11.0	18.0
BA	478.6	403.4	638.9	1359.1	371.7	1647.2	927.0	574.6	959.2
TH	8.1	9.4	5.5	10.3	7.0	9.1	10.1	6.7	7.9
LA	23.1	28.2	16.1	19.7	21.9	27.2	26.5	29.2	14.5
CE	49.1	61.5	26.8	48.8	45.6	56.0	57.7	60.8	32.8
ND	24.7	32.2	15.7	22.3	23.5	24.9	24.5	33.1	17.7
SM	7.0	7.6	4.3	4.9	6.2	5.0	5.3	5.8	4.7
Y	34.9	37.3	26.3	23.2	27.1	23.2	7.0	33.1	25.7
TIO2CR	1.513	1.556	1.197	0.106	1.171	0.120	0.049	0.896	0.093
TIO2W	1.590	1.611	1.194	0.120	1.223	0.129	0.064	0.898	0.115

	PE32828	PE33820	PE34819	PE36819	PE37845	PE38829	PE39829	PE40849	PE41810
SIO2	47.94	55.12	80.24	79.81	49.56	63.53	64.88	50.94	57.87
AL203	18.09	18.53	14.64	15.83	17.32	17.39	17.32	17.09	16.29
FE203	10.55	6.96	1.00	0.81	10.08	5.39	4.60	9.37	6.66
MGO	2.71	4.85	0.25	0.19	6.07	1.09	1.23	5.81	6.38
CAO	13.91	7.61	1.87	0.06	9.90	3.46	2.15	8.39	7.43
NA20	3.57	3.81	0.08	*	3.63	4.46	5.62	4.22	3.37
K20	1.197	1.398	2.562	3.855	1.648	2.694	3.022	1.664	0.940
TIO2	1.768	1.610	0.029	0.029	1.623	0.659	0.510	1.516	0.871
MNO	0.147	0.067	0.040	0.059	0.148	0.061	0.033	0.135	0.133
P205	0.487	0.353	0.045	0.065	0.523	0.348	0.271	0.330	0.184
TOTAL	100.37	100.30	100.75	100.65	100.50	100.09	99.64	99.47	100.13
LOI	8.67	5.03	4.76	3.45	3.47	4.40	1.02	7.21	1.83
NI	122.5	31.0	5.3	5.1	195.4	5.7	4.9	110.8	106.6
CR	271.9	94.3	3.1	3.0	340.8	6.5	4.6	339.3	190.5
V	212.2	204.4	1.6	2.4	178.7	27.7	17.0	202.4	150.9
SC	31.4	32.3	0.6	0.1	22.6	8.1	4.5	30.6	22.0
CU	14.1	33.5	2.3	3.0	32.8	4.9	3.9	11.8	18.0
ZN	202.4	191.9	65.3	64.5	85.7	90.9	64.1	100.1	66.1
SR	678.6	624.6	323.2	372.1	817.7	309.8	790.1	684.4	718.7
RB	23.2	24.7	90.7	121.8	33.7	80.1	64.6	27.3	24.8
ZR	234.9	241.2	40.8	44.3	239.9	273.9	355.0	228.0	163.1
NB	14.9	13.5	24.2	26.2	9.5	14.5	11.7	7.4	11.0
BA	432.5	397.9	69.7	168.0	531.0	511.0	1264.2	705.5	552.3
TH	8.5	6.8	7.8	9.8	9.1	8.0	7.6	3.0	6.7
LA	26.7	29.6	11.3	12.1	34.2	33.5	42.2	32.9	24.0
CE	63.9	64.9	27.0	30.1	80.8	69.8	89.9	74.5	51.2
ND	32.3	33.2	12.7	14.8	45.8	33.8	43.9	37.1	21.8
SM	8.1	5.7	2.5	3.7	12.4	6.2	4.2	8.2	3.8
Y	29.5	27.8	5.3	4.9	31.4	36.6	28.0	26.7	20.8
TIO2CR	1.775	1.641	0.031	0.030	1.667	0.658	0.487	1.528	0.977
TIO2W	1.867	1.685	0.050	0.045	1.669	0.671	0.489	1.548	0.947

TABLE B17

	PE4286	PE4411	PE4620	PE4881	PE5119	AY186	AY213	AY311	AY485
SIO2	62.89	51.73	70.01	53.51	71.43	63.80	60.81	50.33	57.18
AL2O3	18.09	17.44	15.21	17.76	15.61	18.15	18.15	17.75	15.57
FE2O3	5.19	9.46	3.42	8.19	2.76	3.64	5.64	7.25	6.81
MGO	1.13	5.14	0.65	5.40	0.64	1.62	2.28	5.57	6.75
CAO	4.51	9.90	2.81	8.94	1.97	3.52	3.61	12.31	7.31
NA2O	3.96	2.83	3.30	3.16	4.42	4.49	3.84	3.69	3.25
K2O	3.096	1.486	3.491	0.788	3.115	3.368	3.587	1.238	1.704
TIO2	0.715	1.389	0.510	1.106	0.310	1.002	0.992	1.279	0.996
MNO	0.052	0.055	0.120	0.071	0.018	0.035	0.036	0.085	0.092
P2O5	0.285	0.233	0.140	0.168	0.127	0.191	0.190	0.238	0.210
TOTAL	99.91	99.65	99.66	99.09	99.80	99.81	99.12	99.74	99.87
LOI	2.82	9.55	2.14	3.31	0.75	1.38	1.75	8.63	1.33
NI	7.4	117.5	34.0	93.3	7.2	15.1	14.6	197.0	164.9
CR	7.3	320.9	98.2	280.6	8.3	11.5	10.0	394.0	326.7
V	38.3	179.1	61.7	201.6	19.1	133.1	124.0	191.3	130.1
SC	6.2	27.8	10.5	36.3	2.6	15.1	15.5	30.2	20.2
CU	7.8	33.4	14.5	16.8	6.9	14.9	13.9	155.4	40.6
ZN	86.0	56.2	34.4	66.2	31.0	142.6	80.8	143.6	65.9
SR	645.1	457.8	264.5	404.2	602.2	330.1	314.5	485.6	517.0
RB	96.3	52.9	93.0	13.4	66.8	70.4	78.4	13.8	41.6
ZR	258.0	193.6	175.3	135.5	173.2	138.2	187.2	170.7	173.6
NB	13.3	7.6	11.8	7.2	11.3	9.9	8.9	6.4	9.9
BA	897.5	357.7	1037.8	318.4	1249.9	532.7	676.3	492.9	453.7
TH	7.6	5.0	13.4	6.1	13.3	12.3	13.5	10.0	0.5
LA	31.8	16.2	30.8	13.1	26.9	20.9	22.8	19.5	23.3
CE	69.6	37.1	59.2	31.3	55.2	50.9	49.5	41.8	43.2
ND	33.0	20.4	24.4	16.2	22.3	23.1	22.9	22.5	20.5
SM	7.1	5.5	2.6	4.3	4.4	5.1	3.2	3.3	4.1
Y	24.7	24.1	16.1	23.0	13.1	18.9	21.2	21.1	18.8
TIO2CR	0.777	1.433	0.550	1.234	0.339	1.078	1.018	1.375	1.041
TIO2W	0.768	1.438	0.534	1.210	0.333	1.045	1.014	1.380	1.049

	AY510	AY611	AY720	AY811	AY96	AY1028	AY1185	AY1213	AY135
SIO2	56.50	53.11	56.57	56.37	62.98	57.47	57.08	65.03	56.78
AL2O3	17.08	17.76	17.20	16.56	18.93	16.79	17.16	16.29	16.53
FE2O3	7.61	9.02	8.39	7.80	2.82	7.09	8.43	4.02	7.71
MGO	3.78	7.78	3.31	4.82	0.25	4.39	5.20	1.35	4.78
CAO	8.30	2.87	6.07	6.09	2.34	7.01	5.74	5.58	6.50
NA2O	3.62	5.13	4.10	4.14	8.80	3.61	3.56	3.76	3.91
K2O	1.738	1.648	2.000	1.845	2.098	1.756	0.982	2.388	1.711
TIO2	1.103	1.503	1.576	1.302	0.829	1.189	1.189	0.796	1.163
MNO	0.051	0.064	0.088	0.042	0.020	0.109	0.077	0.097	0.095
P2O5	0.179	0.277	0.292	0.295	0.196	0.245	0.243	0.169	0.235
TOTAL	99.96	99.15	99.60	99.27	99.27	99.66	99.65	99.49	99.42
LOI	4.88	4.20	0.97	1.36	1.27	1.73	4.37	0.64	0.98
NI	78.3	185.2	11.1	96.3	10.9	107.2	105.4	55.2	103.2
CR	189.2	269.0	19.8	154.8	30.4	205.6	207.1	161.3	190.5
V	172.9	193.9	166.7	139.7	34.5	146.1	160.8	108.1	129.5
SC	29.8	29.1	26.4	20.6	11.5	22.9	24.3	18.1	20.5
CU	20.5	92.2	27.9	24.2	6.4	13.6	26.5	12.2	34.5
ZN	200.7	363.9	80.3	40.2	10.0	70.2	508.7	40.7	62.7
SR	382.8	201.9	447.1	443.7	247.8	454.8	348.7	499.8	446.7
RB	47.2	43.4	58.2	49.7	25.1	51.0	21.3	73.7	52.3
ZR	157.1	214.1	254.9	231.7	163.9	211.8	207.8	160.5	205.5
NB	8.2	11.9	11.4	13.1	10.0	9.5	9.2	7.6	8.5
BA	332.1	319.6	485.0	428.7	521.6	431.4	255.7	667.5	433.8
TH	3.0	0.5	10.8	10.9	9.2	8.3	9.8	9.6	9.2
LA	18.4	21.2	23.6	24.7	12.0	19.5	20.2	21.2	22.1
CE	34.4	45.7	52.9	53.8	32.6	43.0	45.3	41.5	44.2
ND	18.1	22.4	27.8	26.0	19.9	21.3	22.0	20.0	22.3
SM	1.7	3.1	5.7	4.9	3.5	4.2	2.8	3.1	4.2
Y	20.9	25.4	33.5	28.1	16.1	26.7	27.9	18.3	26.1
TIO2CR	1.141	1.414	1.451	1.231	0.884	1.181	1.288	0.844	1.086
TIO2W	1.164	1.452	1.535	1.256	0.855	1.194	1.262	0.827	1.144

TABLE B17

	AY14a13	AY15a5	AY16a10	AY17a12	AY18a5	AY19a13	AY19Aa10	AY20a10	AY21a22
SIO2	60.32	60.53	55.42	56.19	56.30	59.91	55.31	55.54	55.70
AL203	16.99	17.28	16.85	16.95	18.14	15.47	17.31	17.15	16.92
FE203	5.45	5.09	7.83	7.63	6.08	5.82	7.16	7.48	7.98
MGO	3.96	5.24	5.05	4.73	6.59	4.75	5.26	5.08	6.96
CAO	5.39	3.66	7.18	7.08	4.12	5.70	6.91	7.11	5.03
NA2O	4.11	4.58	3.91	3.88	4.71	3.60	4.11	4.14	3.68
K2O	2.251	1.956	1.517	1.676	1.723	2.160	1.660	1.580	1.453
TIO2	0.829	0.858	1.269	1.262	0.903	0.811	1.264	1.291	1.116
MNO	0.115	0.128	0.106	0.145	0.165	0.111	0.049	0.086	0.056
P2O5	0.169	0.175	0.263	0.266	0.182	0.169	0.267	0.260	0.199
TOTAL	99.57	99.50	99.39	99.80	98.92	99.49	99.30	99.73	99.09
LOI	1.10	3.77	1.05	1.12	3.13	0.99	1.27	0.91	4.81
NI	96.9	99.0	82.1	79.1	95.9	92.7	72.5	75.8	66.6
CR	182.5	191.9	175.3	180.2	190.6	156.4	172.4	176.9	168.5
V	115.8	138.3	180.6	159.5	150.9	110.0	153.6	151.3	195.0
SC	19.4	23.3	24.6	24.6	23.4	18.0	25.0	24.6	33.3
CU	19.1	30.5	26.7	44.1	22.6	22.0	34.8	34.9	35.3
ZN	55.1	163.2	134.8	58.0	1000.1	51.9	56.1	60.9	549.7
SR	483.8	368.0	521.1	507.8	400.3	495.0	496.7	488.4	316.3
RB	61.0	52.4	24.1	40.0	18.6	59.9	42.8	42.0	29.0
ZR	168.0	174.2	206.1	204.8	180.1	153.0	203.3	211.5	163.0
NB	7.1	7.2	8.7	9.1	6.7	6.5	9.7	9.4	8.2
BA	669.6	416.1	462.4	440.0	571.3	682.8	458.2	437.8	403.6
TH	9.0	10.2	3.9	4.6	7.2	4.4	0.0	3.3	8.1
LA	22.0	20.0	21.4	24.1	26.3	17.3	20.0	21.8	17.8
CE	39.0	43.6	49.2	50.2	53.8	42.3	47.7	49.5	38.0
ND	18.3	19.2	24.6	25.1	25.4	18.9	23.6	24.1	18.7
SM	3.5	2.9	3.6	6.6	5.0	2.1	5.2	2.9	2.9
Y	19.2	18.9	27.8	26.3	20.9	19.0	26.3	28.4	26.7
TIO2CR	0.850	0.854	1.223	1.235	1.011	0.838	1.140	1.164	1.222
TIO2W	0.864	0.884	1.264	1.295	0.970	0.833	1.189	1.249	1.215

	AY22a13	AY23a5	AY24a10	AY25a10	AY26a11	AY27a10	AY28a5	AY30a1	AY31a11
SIO2	59.73	58.26	55.20	53.31	56.58	55.48	61.37	52.10	52.82
AL203	16.55	17.61	17.02	17.94	17.43	17.62	16.57	17.13	17.83
FE203	6.38	5.96	7.60	8.45	10.03	6.93	6.75	8.66	8.58
MGO	3.59	4.04	5.55	5.46	5.36	5.48	3.39	3.31	5.64
CAO	5.41	5.66	6.99	6.64	2.05	7.14	2.65	11.76	7.18
NA2O	4.06	4.16	3.95	4.01	3.89	4.10	4.53	3.17	4.37
K2O	2.055	2.082	1.640	1.549	2.560	1.539	2.634	1.567	1.499
TIO2	1.094	1.172	1.257	1.621	1.199	1.264	1.427	1.183	1.622
MNO	0.063	0.066	0.068	0.058	0.025	0.067	0.054	0.041	0.120
P2O5	0.248	0.269	0.261	0.283	0.199	0.264	0.279	0.260	0.250
TOTAL	99.18	99.27	99.53	99.33	99.32	99.89	99.64	99.20	99.92
LOI	1.12	1.94	1.21	1.53	3.35	1.12	2.06	8.93	4.68
NI	100.5	96.9	78.5	65.4	59.7	90.7	7.3	187.9	93.9
CR	213.7	221.6	175.9	187.7	169.1	182.3	6.2	325.0	182.0
V	131.2	142.1	147.8	201.5	174.1	177.5	180.6	327.4	203.1
SC	23.4	24.5	24.3	31.4	33.4	27.0	24.8	26.1	34.1
CU	21.4	14.3	29.9	37.7	9.0	23.3	7.5	11.7	18.1
ZN	135.1	430.7	55.8	115.6	262.8	133.1	125.6	76.8	65.5
SR	428.4	443.5	491.1	503.8	209.7	516.8	229.9	390.4	373.3
RB	64.7	54.8	39.5	35.0	31.5	27.4	58.5	26.4	28.1
ZR	210.8	225.8	200.9	214.3	163.5	211.1	245.2	165.3	184.1
NB	10.1	12.2	11.7	9.9	9.5	11.1	14.7	8.6	9.2
BA	432.5	437.5	457.5	407.6	347.0	454.6	457.1	471.4	304.1
TH	8.8	8.3	4.2	4.1	5.1	8.0	8.8	7.7	7.0
LA	22.7	22.8	22.2	20.3	15.5	22.8	28.2	14.3	15.6
CE	47.3	48.9	47.6	44.3	31.6	48.1	61.3	36.4	38.1
ND	22.8	24.5	23.3	23.9	16.6	24.3	30.2	18.2	21.4
SM	4.3	4.9	4.5	5.1	4.2	4.7	6.1	6.8	5.8
Y	22.0	26.8	25.3	28.8	22.7	25.4	29.9	24.2	30.4
TIO2CR	1.055	1.151	1.103	1.522	1.186	1.329	1.489	1.284	1.541
TIO2W	1.090	1.171	1.173	1.575	1.201	1.337	1.481	1.291	1.613

TABLE B17

	AY32@10	AY33@22	AY34@22	AY35@13	AY37@10	AY38@12	AY40@6	AY41@1	C1@31
SIO2	57.04	57.41	68.21	57.05	55.16	52.16	59.59	54.24	64.81
AL203	17.74	17.93	16.19	16.81	18.43	18.01	17.47	18.43	15.64
FE203	6.47	7.46	3.37	6.89	8.60	8.17	5.07	8.45	5.08
MGO	5.78	5.51	1.26	4.68	4.92	3.54	2.83	4.86	3.36
CAO	4.84	3.72	1.59	7.51	3.65	10.41	2.88	3.80	1.89
NA2O	4.31	4.09	4.50	3.41	4.53	3.71	3.59	5.01	2.65
K2O	1.740	1.517	3.824	1.846	1.905	1.387	5.921	3.293	5.084
TIO2	1.208	1.296	0.484	1.102	1.684	1.460	0.695	1.340	0.813
MNO	0.093	0.012	0.026	0.071	0.078	0.125	0.045	0.139	0.024
P2O5	0.196	0.259	0.191	0.186	0.270	0.241	0.269	0.202	0.272
TOTAL	99.42	99.20	99.64	99.56	99.22	99.20	99.35	99.77	99.63
LOI	2.81	3.42	1.22	1.48	2.95	5.14	3.57	2.92	2.26
NI	88.9	30.5	6.3	81.0	15.2	17.8	18.1	47.9	53.5
CR	245.1	42.6	5.6	215.9	51.2	59.3	20.6	10.8	69.2
V	171.7	174.1	13.1	147.1	218.9	132.3	73.8	144.8	77.4
SC	31.5	25.8	4.7	23.3	37.6	29.8	8.3	23.6	12.3
CU	19.6	27.8	0.9	28.3	17.8	23.9	8.3	14.8	24.5
ZN	62.6	419.8	116.2	59.9	77.7	52.3	80.2	81.4	80.3
SR	319.5	304.8	236.8	404.9	338.1	494.3	186.9	1428.5	217.9
RB	58.5	42.7	73.4	58.9	45.6	35.1	157.5	78.5	162.6
ZR	244.3	247.6	298.0	212.3	277.2	225.5	232.7	153.6	278.3
NB	9.3	10.3	14.9	8.9	10.4	7.5	10.1	6.0	16.0
BA	288.2	422.0	915.0	425.2	680.5	329.6	1460.7	804.8	700.7
TH	12.7	10.8	12.3	11.6	9.4	10.1	10.1	6.6	28.0
LA	20.7	22.1	34.9	19.6	21.6	18.6	22.4	16.5	49.3
CE	47.1	48.3	73.7	42.7	49.8	45.7	46.6	35.3	103.1
ND	24.8	24.2	34.1	21.2	25.7	23.6	22.5	21.0	38.8
SM	5.4	5.3	6.0	5.4	7.5	4.6	4.1	3.6	5.9
Y	30.0	28.6	28.7	27.1	32.0	32.2	21.7	24.1	19.6
TIO2CR	1.204	1.294	0.527	1.079	1.656	1.292	0.767	1.130	0.777
TIO2W	1.248	1.390	0.527	1.106	1.723	1.385	0.754	1.175	0.786

	C2@33	C5@31	C7@30	C8@30	C9@33	C10@31	C11@31	C12@30	C13@30
SIO2	63.14	61.74	62.20	62.39	62.85	61.85	61.54	60.88	61.74
AL203	16.34	16.18	15.97	15.93	15.94	16.23	16.21	16.07	15.83
FE203	5.25	5.30	4.88	5.10	5.05	5.41	5.27	5.43	5.55
MGO	3.76	3.11	2.93	2.34	3.25	3.21	3.35	3.42	2.81
CAO	2.75	4.64	5.47	5.43	5.01	4.06	5.12	5.36	4.77
NA2O	3.68	3.67	3.62	3.50	4.20	3.52	3.71	3.71	3.75
K2O	3.847	3.466	3.369	3.631	2.356	3.581	3.507	3.413	3.621
TIO2	0.931	1.052	1.045	0.917	0.929	1.091	1.081	1.068	1.025
MNO	0.061	0.056	0.070	0.081	0.100	0.055	0.109	0.116	0.069
P2O5	0.317	0.353	0.348	0.338	0.341	0.388	0.391	0.374	0.368
TOTAL	100.08	99.57	99.97	99.66	100.02	99.39	100.30	99.84	99.54
LOI	2.10	3.42	1.70	3.62	2.14	2.31	1.60	1.26	3.51
NI	75.7	57.3	51.4	57.0	49.7	50.1	49.4	45.5	49.1
CR	135.9	93.6	75.8	94.9	81.7	80.2	80.5	67.2	77.2
V	103.5	109.9	94.5	89.1	85.9	104.7	98.3	101.3	96.7
SC	14.9	16.1	12.7	13.7	11.3	16.1	14.2	13.7	13.4
CU	38.5	23.9	21.8	22.0	27.0	16.1	21.5	21.3	20.0
ZN	88.7	116.1	65.4	68.5	62.4	81.3	75.5	66.3	71.5
SR	397.7	354.7	494.9	556.0	1025.3	459.8	535.1	573.7	543.6
RB	140.5	146.1	146.8	140.2	55.4	140.5	142.2	137.4	147.1
ZR	290.8	302.3	297.3	281.2	284.8	315.1	318.2	319.5	306.3
NB	16.3	17.2	14.2	13.5	13.3	18.0	17.6	16.7	15.8
BA	766.8	638.2	695.9	731.3	1097.4	736.0	764.5	745.3	798.9
TH	23.6	28.4	23.3	24.9	23.6	23.0	23.1	25.0	22.3
LA	55.8	55.7	56.0	59.1	65.2	39.0	51.5	63.6	60.2
CE	118.6	117.2	112.6	121.5	127.7	122.1	126.3	131.9	119.5
ND	42.9	44.9	43.1	46.3	47.3	47.9	47.6	48.9	46.5
SM	6.1	7.3	7.1	6.0	3.9	8.2	7.3	6.1	8.3
Y	20.2	22.0	22.1	20.3	19.7	23.0	24.1	24.0	22.1
TIO2CR	0.951	1.088	1.010	0.899	0.950	1.049	1.052	1.040	0.977
TIO2W	0.952	1.072	1.033	0.909	0.929	1.076	1.039	1.038	0.997

TABLE B17

	C15a33	C16a14	C17a31	C18a32	C19a30	C21a31	C22a33	C23a22	C27a30
SIO2	63.27	63.45	62.23	62.08	62.28	63.61	61.22	70.43	62.01
AL2O3	15.93	15.94	16.11	16.15	16.51	15.88	15.73	15.37	15.88
FE2O3	4.91	4.92	5.17	5.50	3.34	4.89	4.74	2.23	5.65
MGO	3.31	3.04	2.37	3.10	2.19	2.42	3.52	0.60	3.21
CAO	4.61	4.73	5.25	4.89	7.00	4.83	1.70	0.45	3.39
NA2O	4.07	3.38	3.59	3.34	3.78	5.34	3.13	4.08	3.82
K2O	2.541	3.257	3.661	3.266	3.492	3.896	7.527	6.152	3.900
TIO2	0.907	0.863	1.006	1.031	1.021	0.874	0.886	0.369	0.926
MNO	0.065	0.067	0.063	0.086	0.098	0.073	0.031	0.025	0.075
P2O5	0.323	0.290	0.346	0.339	0.338	0.294	0.317	0.072	0.333
TOTAL	99.94	99.93	99.78	99.97	100.06	100.10	99.81	99.77	99.20
LOI	1.78	2.59	3.46	1.67	3.52	4.48	2.94	0.96	2.46
NI	46.3	49.4	56.1	48.1	58.3	38.1	47.9	5.7	53.3
CR	80.0	96.6	95.9	83.1	104.7	105.9	84.0	3.2	105.9
V	86.5	92.0	108.8	101.5	102.9	96.0	91.7	17.8	93.5
SC	10.8	11.8	14.6	13.2	15.8	14.3	14.1	4.5	14.9
CU	21.4	18.2	17.3	23.9	31.1	23.8	11.0	4.9	6.2
ZN	59.9	65.5	71.5	64.4	114.2	57.9	84.5	49.9	142.7
SR	810.3	632.5	645.5	614.1	529.6	579.3	134.4	155.2	385.5
RB	74.5	88.8	145.2	75.1	151.5	158.5	171.2	185.9	146.6
ZR	282.8	280.5	307.1	308.3	298.9	277.2	280.3	419.0	276.9
NB	14.6	13.3	16.3	15.9	16.2	13.2	14.7	18.0	14.3
BA	1073.0	1021.2	747.6	868.2	687.6	789.3	733.6	831.1	695.3
TH	25.4	24.9	25.2	23.7	28.4	20.9	23.2	33.0	18.5
LA	66.2	57.1	57.4	55.0	55.7	55.4	64.1	110.9	57.9
CE	119.0	112.2	119.9	121.7	117.4	109.7	130.0	198.7	119.9
ND	44.8	43.5	47.1	46.5	45.1	41.6	46.2	62.7	45.7
SM	8.0	7.3	6.7	6.4	7.6	5.2	7.6	8.5	5.1
Y	20.8	19.6	22.1	22.1	22.5	20.0	16.4	19.3	20.6
TIO2CR	0.916	0.891	1.061	1.029	1.037	0.893	0.962	0.404	0.884
TIO2W	0.906	0.891	1.058	1.021	1.035	0.908	0.960	0.399	0.881

	C28a22	C29a32	C30a33	C31a31	C33a33	C34a32	C35a40	C36a31	C37a33
SIO2	69.98	62.45	65.37	63.37	65.95	62.68	63.67	63.46	64.63
AL2O3	15.21	16.18	15.74	16.01	15.83	15.20	16.58	16.34	15.84
FE2O3	3.19	5.26	4.31	4.94	4.03	5.66	4.19	4.78	4.72
MGO	1.66	2.54	2.17	2.88	2.42	3.68	1.66	2.92	2.80
CAO	1.70	4.09	3.92	3.47	4.20	1.58	2.66	3.30	3.14
NA2O	1.91	3.69	3.46	3.32	4.41	2.89	1.89	3.81	3.61
K2O	5.372	4.130	3.576	4.597	1.720	5.889	8.041	4.123	3.714
TIO2	0.419	0.975	0.818	0.847	0.696	0.918	0.792	0.887	0.885
MNO	0.049	0.065	0.052	0.045	0.053	0.042	0.059	0.044	0.044
P2O5	0.149	0.334	0.297	0.297	0.241	0.328	0.204	0.297	0.318
TOTAL	99.64	99.72	99.71	99.77	99.55	99.86	99.74	99.94	99.70
LOI	3.21	3.17	2.09	2.90	2.52	3.26	4.35	2.62	2.08
NI	13.4	61.4	52.6	56.7	31.9	41.8	15.4	39.5	62.4
CR	29.3	105.2	99.8	100.2	62.0	59.4	16.0	81.4	108.1
V	50.4	98.0	85.1	87.3	70.9	98.6	73.5	95.8	89.0
SC	7.8	14.6	12.8	13.0	8.8	14.0	9.3	14.4	13.4
CU	7.1	16.6	20.8	15.4	21.0	17.5	3.9	11.4	24.5
ZN	65.4	108.9	120.0	116.8	60.2	256.5	74.0	145.9	99.1
SR	127.5	358.1	447.9	340.6	958.4	136.1	146.0	328.4	425.0
RB	242.8	152.9	151.9	160.7	65.6	156.8	269.2	145.4	163.1
ZR	199.5	299.6	261.9	271.7	227.9	296.2	385.9	262.4	276.5
NB	12.3	16.6	13.5	13.9	11.8	13.9	17.8	13.7	13.9
BA	804.9	658.6	697.0	666.6	1634.8	804.6	1205.3	747.0	668.4
TH	27.9	20.3	24.9	24.1	17.2	19.8	30.2	19.5	22.4
LA	56.3	57.3	55.6	53.7	65.1	35.8	77.8	52.9	55.7
CE	111.6	119.8	114.4	115.6	102.9	115.5	149.8	106.3	118.6
ND	44.2	44.0	43.1	42.0	40.9	45.5	56.1	40.6	44.9
SM	6.3	5.5	7.1	7.5	7.8	7.6	7.2	5.3	6.3
Y	19.6	21.2	17.0	20.1	16.3	20.1	24.7	20.7	18.1
TIO2CR	0.517	1.006	0.862	0.875	0.748	0.953	0.841	0.935	0.934
TIO2W	0.496	1.000	0.848	0.884	0.727	0.945	0.853	0.932	0.929

TABLE B17

	C38@32	C40@22	C41@19	C43@32	C44@31	C45@30	C46@33	C47@22	C48@22
SIO2	61.68	68.42	78.31	63.15	63.28	63.56	63.85	65.59	61.72
AL2O3	16.02	14.85	12.48	16.09	15.58	15.58	15.79	15.57	15.58
FE2O3	5.90	3.41	0.62	5.13	4.94	4.78	4.75	3.95	5.41
MGO	3.93	2.29	0.13	3.78	3.77	3.51	3.50	2.67	3.88
CAO	4.28	1.78	0.13	3.48	4.00	4.32	3.62	2.78	4.13
NA2O	3.50	3.82	3.65	3.44	3.44	3.26	3.37	3.75	3.88
K2O	3.215	4.340	4.857	3.400	3.659	3.498	3.728	4.246	3.525
TIO2	1.009	0.636	0.133	0.907	0.857	0.852	0.830	0.756	0.946
MNO	0.085	0.063	0.001	0.091	0.084	0.076	0.074	0.064	0.098
P2O5	0.372	0.248	0.025	0.301	0.304	0.302	0.294	0.275	0.354
TOTAL	99.99	99.85	100.34	99.78	99.93	99.75	99.72	99.65	99.52
LOI	1.99	1.71	2.69	0.65	1.48	1.27	1.65	2.89	1.11
NI	72.8	40.9	4.3	74.7	76.2	55.5	68.1	44.8	68.1
CR	106.4	70.5	4.5	134.0	131.5	107.0	113.3	69.9	125.6
V	107.6	67.0	3.1	103.7	92.1	98.1	89.4	76.5	95.0
SC	13.7	9.6	0.6	14.5	13.2	11.5	12.3	10.8	13.9
CU	31.8	18.2	3.5	19.6	24.1	25.9	19.5	23.9	26.5
ZN	74.5	65.2	83.3	127.5	84.2	65.3	71.4	69.7	76.2
SR	689.2	241.1	61.7	530.4	502.0	457.6	486.1	360.0	482.5
RB	85.3	200.7	195.5	137.6	147.8	137.1	133.3	175.8	141.1
ZR	298.7	187.2	128.6	260.8	265.2	256.3	263.9	247.0	257.0
NB	15.7	17.2	20.6	13.7	13.8	14.4	14.3	16.3	15.0
BA	754.8	566.3	130.0	896.3	872.5	745.5	819.8	780.9	714.5
TH	17.5	29.2	39.6	21.8	21.1	23.7	23.2	25.4	19.8
LA	59.7	57.4	45.2	57.9	56.6	52.2	50.7	57.4	53.6
CE	126.3	110.5	92.6	115.7	111.6	109.5	107.7	119.1	110.8
ND	48.5	43.1	34.4	43.2	43.6	40.7	42.5	45.9	43.5
SM	6.0	5.4	5.3	6.0	5.6	7.0	5.0	4.6	7.7
Y	21.5	21.3	20.0	19.5	19.5	19.8	18.4	20.7	21.8
TIO2CR	1.051	0.714	0.137	0.902	0.853	0.860	0.833	0.799	0.972
TIO2W	1.036	0.711	0.150	0.912	0.858	0.854	0.824	0.817	0.949

	C49@4	C50@14	C51@14	C52@22	C54@33	C55@40	C57@40	C58@22	C59@29
SIO2	64.24	62.34	62.57	67.58	64.89	66.01	66.69	63.90	69.45
AL2O3	15.81	15.76	15.70	15.39	15.79	15.53	15.79	16.11	15.33
FE2O3	4.39	5.08	5.02	3.46	4.36	4.37	5.24	4.47	2.75
MGO	2.62	3.54	3.38	2.31	2.79	2.17	1.21	2.83	2.13
CAO	3.20	4.62	4.31	2.37	4.35	2.65	0.77	2.32	1.12
NA2O	4.00	3.63	3.70	3.65	4.79	2.34	3.64	3.92	3.34
K2O	4.380	3.372	3.600	4.371	1.504	5.828	5.516	4.805	5.301
TIO2	0.794	0.901	0.899	0.647	0.837	0.710	0.770	0.809	0.482
MNO	0.085	0.098	0.087	0.068	0.076	0.052	0.048	0.077	0.036
P2O5	0.270	0.288	0.296	0.226	0.276	0.257	0.196	0.301	0.174
TOTAL	99.77	99.63	99.55	100.07	99.65	99.90	99.87	99.55	100.10
LOI	0.56	0.27	0.38	1.41	3.19	3.57	1.57	1.63	1.75
NI	39.3	62.9	67.8	36.3	34.4	59.8	13.9	29.6	27.6
CR	66.8	116.6	118.9	59.7	63.9	85.4	14.7	49.8	50.9
V	75.0	87.5	90.9	57.9	80.2	74.5	63.3	84.3	45.7
SC	10.8	12.3	12.1	8.2	10.3	10.4	7.5	9.5	6.3
CU	19.8	29.6	26.2	21.6	19.6	12.3	9.1	18.6	9.3
ZN	77.3	69.5	69.9	50.8	62.6	132.3	115.1	74.7	68.0
SR	440.7	497.8	468.4	421.0	839.6	207.4	279.1	566.0	238.9
RB	185.7	110.9	152.0	188.4	58.9	191.4	203.3	166.0	256.9
ZR	295.2	266.0	277.0	214.6	282.2	259.0	385.9	330.6	203.1
NB	16.5	12.7	13.8	15.5	14.7	15.7	17.9	15.5	11.5
BA	799.0	743.0	715.5	717.3	738.2	733.3	1183.3	1153.5	707.7
TH	25.7	22.3	21.3	27.0	23.3	24.9	31.5	20.0	27.4
LA	58.4	53.3	56.2	55.1	60.0	55.6	59.6	66.9	50.1
CE	116.2	106.9	115.2	107.0	115.7	113.1	142.7	138.1	95.6
ND	44.1	41.3	42.8	41.4	40.2	43.0	51.8	51.3	36.2
SM	7.5	7.3	7.8	4.6	5.9	6.9	8.9	8.2	5.2
Y	22.0	19.4	19.3	20.3	20.3	19.5	23.5	20.8	13.7
TIO2CR	0.790	0.939	0.916	0.634	0.871	0.762	0.828	0.778	0.514
TIO2W	0.803	0.945	0.904	0.635	0.863	0.749	0.823	0.788	0.535

TABLE B17

	C60@33	C61@32	C62@22	C64@25	SA1@48	SA2@48	SA5@48	SA6@1	SA7@48
SIO2	63.41	65.85	64.21	61.63	57.28	55.10	57.00	54.61	55.75
AL2O3	16.43	16.09	15.30	16.14	16.28	15.86	16.92	15.92	16.71
FE2O3	4.57	4.02	4.42	4.88	6.58	7.57	6.97	8.66	7.58
MGO	3.38	2.67	2.94	3.72	5.74	5.70	6.50	9.67	6.71
CAO	1.29	1.13	3.50	4.53	5.89	4.53	5.46	4.25	5.26
NA2O	4.17	4.07	3.73	3.52	3.54	3.45	3.33	2.80	3.42
K2O	4.747	4.343	4.032	3.736	2.080	2.016	1.736	1.842	2.157
TIO2	0.869	0.882	0.807	0.915	1.291	1.377	1.022	1.247	1.306
MNO	0.079	0.053	0.080	0.085	0.069	0.040	0.040	0.038	0.071
P2O5	0.339	0.321	0.292	0.351	0.424	0.434	0.193	0.304	0.343
TOTAL	99.28	99.43	99.32	99.61	100.18	99.07	99.17	99.33	99.31
LOI	2.29	2.48	0.52	1.33	2.77	2.57	2.99	3.56	3.32
NI	69.5	34.3	52.6	92.8	188.0	171.9	190.2	286.0	198.3
CR	118.4	68.9	91.5	108.0	379.2	330.4	354.5	519.6	402.8
V	91.3	77.4	72.3	90.4	122.1	118.7	123.3	150.1	121.5
SC	13.0	11.8	10.0	12.4	21.6	25.3	26.4	28.1	23.1
CU	4.0	7.7	21.6	66.6	17.7	18.8	25.1	26.0	14.4
ZN	89.8	105.3	65.9	95.1	111.6	138.0	268.7	124.9	169.3
SR	511.5	384.7	463.3	645.9	522.9	498.9	473.1	642.2	532.9
RB	144.3	151.2	183.2	130.5	55.0	53.3	47.9	49.9	53.0
ZR	262.6	294.8	248.6	283.0	281.4	292.8	173.0	219.7	261.3
NB	12.9	13.9	15.5	13.9	18.3	20.0	8.0	13.0	14.4
BA	969.5	739.6	695.4	981.5	540.9	481.2	400.9	464.4	519.3
TH	15.7	23.3	24.6	16.2	5.8	2.9	4.1	5.8	6.8
LA	56.7	52.4	53.0	57.9	37.7	38.9	20.5	34.8	33.3
CE	111.7	112.4	112.4	117.9	80.5	79.6	45.0	57.3	65.6
ND	44.4	44.1	42.2	46.0	35.8	36.1	21.4	28.5	30.1
SM	4.6	6.6	7.2	7.2	4.3	5.8	4.5	6.0	5.5
Y	17.1	18.6	20.4	20.6	27.8	30.3	19.7	24.7	24.1
TIO2CR	0.932	0.924	0.778	0.929	1.242	1.279	0.977	1.093	1.246
TIO2W	0.919	0.915	0.788	0.939	1.286	1.340	1.024	1.165	1.307

	SA8@1	SA9@48	SA10@1	SA11@1	SA12@44	SA13@6	SA14@1	SA15@6	SA16@6
SIO2	56.07	53.95	54.63	54.78	64.84	67.63	60.66	64.98	59.15
AL2O3	16.40	15.55	15.31	16.93	17.23	17.53	15.81	17.15	20.25
FE2O3	5.79	9.13	7.10	7.85	4.91	5.29	6.21	4.76	6.09
MGO	2.99	7.31	4.24	6.04	2.70	1.41	5.08	3.93	6.69
CAO	10.55	7.05	11.35	7.74	0.94	0.53	5.82	1.06	3.22
NA2O	3.49	3.21	2.87	2.86	4.50	4.10	3.03	5.03	2.20
K2O	2.095	1.615	2.217	2.210	3.399	2.243	1.667	1.685	0.764
TIO2	1.291	1.196	1.113	1.139	0.761	0.733	0.940	0.756	0.940
MNO	0.133	0.119	0.125	0.072	0.074	0.045	0.079	0.050	0.029
P2O5	0.423	0.361	0.288	0.240	0.179	0.162	0.198	0.166	0.207
TOTAL	99.23	99.49	99.25	99.85	99.52	99.68	99.49	99.57	99.54
LOI	6.83	6.82	9.51	9.60	3.00	2.80	3.58	2.99	8.03
NI	171.3	241.1	278.1	277.2	27.2	30.2	203.0	22.6	61.4
CR	379.2	378.5	459.9	552.7	39.5	75.5	439.6	39.8	69.1
V	118.9	114.7	146.2	182.1	84.5	93.9	123.0	71.1	121.5
SC	21.1	22.0	22.9	26.3	12.6	15.9	23.9	14.3	19.8
CU	23.1	135.5	24.9	15.2	7.4	14.2	21.5	14.7	6.6
ZN	80.6	92.4	64.5	105.5	89.9	37.7	63.1	64.1	157.0
SR	459.7	317.0	771.7	392.7	135.8	354.5	429.0	370.7	115.4
RB	53.6	20.7	52.4	42.0	66.8	44.6	44.6	44.2	21.9
ZR	284.2	234.7	204.4	186.5	187.5	177.8	161.9	194.9	184.7
NB	19.7	15.0	15.1	9.4	10.0	8.7	8.0	9.8	11.3
BA	463.7	345.7	519.0	416.2	826.3	147.6	425.2	514.4	95.3
TH	6.3	8.6	3.3	4.8	1.9	5.0	2.4	5.9	8.9
LA	37.4	27.2	28.3	28.6	30.2	21.6	23.0	21.7	17.1
CE	76.0	58.6	65.6	50.1	53.2	74.5	41.2	46.7	43.1
ND	37.8	26.8	31.8	26.2	34.4	21.5	20.4	21.2	21.6
SM	4.7	4.1	6.7	5.4	6.0	3.1	4.4	3.0	3.6
Y	28.9	29.8	21.9	23.3	44.7	16.1	19.8	21.7	18.2
TIO2CR	1.326	1.202	1.149	1.140	0.748	0.719	0.864	0.769	0.984
TIO2W	1.351	1.219	1.160	1.129	0.761	0.722	0.910	0.761	0.977

TABLE B17

	SA17@51	SA18@13	SA19@48	SA20@1	SA21@6	NI1@22	NI2@44	NI3@44	NI5@16
SIO2	60.62	63.52	58.68	53.75	71.76	62.99	69.60	67.61	66.64
AL2O3	16.53	17.71	16.69	16.83	13.53	15.80	15.78	15.88	15.48
FE2O3	5.98	5.27	6.71	7.59	3.96	5.81	2.92	3.69	3.81
MGO	2.86	2.58	6.34	7.96	1.00	0.77	0.57	0.85	3.36
CAO	7.31	3.49	1.07	7.33	2.65	0.76	2.38	2.80	2.53
NA2O	3.35	4.36	5.04	3.24	4.93	1.00	3.62	3.77	3.63
K2O	1.851	1.837	3.444	1.397	1.194	10.713	4.187	3.881	3.278
TIO2	0.860	0.786	0.894	1.159	0.417	0.741	0.451	0.526	0.555
MNO	0.110	0.056	0.087	0.094	0.083	0.023	0.008	0.020	0.058
P2O5	0.295	0.185	0.188	0.260	0.117	0.423	0.155	0.193	0.159
TOTAL	99.77	99.79	99.13	99.61	99.83	100.03	99.67	99.22	99.50
LOI	7.29	4.30	3.48	2.59	3.98	1.29	1.04	1.33	1.85
NI	83.0	32.2	174.5	259.1	34.3	58.9	21.9	26.0	44.8
CR	225.0	63.0	335.0	518.8	50.3	227.4	54.4	73.6	85.9
V	114.2	104.0	134.5	161.4	47.8	107.8	53.8	64.4	78.5
SC	18.3	17.3	21.0	26.7	7.7	13.7	6.5	9.8	10.8
CU	15.1	11.6	38.3	9.9	14.9	51.5	12.1	9.2	18.2
ZN	80.4	71.1	167.7	80.2	35.0	13.5	17.2	17.6	60.8
SR	675.9	281.9	354.7	719.7	148.5	608.8	616.6	824.8	307.2
RB	55.7	46.1	66.4	33.2	34.8	130.4	99.0	92.5	90.9
ZR	261.3	156.2	173.0	171.5	149.7	280.9	143.3	135.2	178.5
NB	12.5	10.6	8.9	9.3	10.0	11.9	7.8	8.2	11.5
BA	680.1	491.5	1244.0	588.0	182.9	1644.7	1324.0	1455.1	707.2
TH	12.0	8.2	1.9	0.9	8.9	14.7	10.1	8.6	14.2
LA	39.8	17.7	20.3	25.8	25.9	55.4	23.7	28.8	27.1
CE	87.7	36.8	55.8	55.8	51.0	128.5	50.9	53.6	58.5
ND	39.7	18.7	24.4	28.4	20.9	57.7	21.8	24.1	25.0
SM	6.8	2.9	3.8	4.9	3.0	10.2	2.8	3.0	0.4
Y	24.1	18.3	20.2	25.9	12.6	20.9	11.6	11.0	16.1
TIO2CR	0.897	0.783	0.919	1.128	0.441	0.744	0.453	0.509	0.569
TIO2W	0.900	0.779	0.927	1.134	0.440	0.766	0.463	0.522	0.581

	NI6@16	NI8@16	NI10@5	NI11@13	NI12@19	NI13@20	AR1@13	AR2@1	AR3@19
SIO2	66.54	67.96	65.89	59.36	67.18	64.96	67.95	53.33	63.95
AL2O3	15.44	15.84	16.65	16.50	15.82	15.64	15.30	16.34	15.24
FE2O3	3.78	3.31	4.74	6.01	3.83	4.27	3.31	7.07	4.04
MGO	2.75	1.76	2.58	4.24	2.07	1.87	1.05	7.99	1.42
CAO	3.48	2.29	1.25	6.27	3.43	4.82	1.86	6.25	5.83
NA2O	3.91	4.78	5.25	3.08	3.41	3.44	4.83	2.96	5.48
K2O	2.920	3.042	1.725	2.555	3.675	2.727	3.671	3.841	3.363
TIO2	0.540	0.548	0.837	1.015	0.530	0.631	0.554	1.371	0.510
MNO	0.060	0.063	0.051	0.099	0.037	0.069	0.033	0.069	0.055
P2O5	0.159	0.147	0.291	0.325	0.152	0.242	0.193	0.719	0.264
TOTAL	99.59	99.73	99.27	99.46	100.13	99.67	99.75	99.95	100.13
LOI	1.26	1.45	2.44	1.37	1.46	1.30	1.29	5.60	4.64
NI	47.6	14.3	5.0	58.5	53.8	19.4	20.8	238.6	43.8
CR	89.8	18.5	4.7	78.7	115.8	9.5	73.0	339.7	68.7
V	73.0	64.3	100.5	135.5	78.4	93.8	56.8	147.2	61.1
SC	11.7	8.1	9.5	17.4	12.1	11.4	9.7	21.8	10.1
CU	23.0	7.4	2.4	26.9	18.5	9.8	11.3	14.7	22.8
ZN	54.9	81.9	79.1	64.2	52.8	50.3	26.7	160.1	30.5
SR	344.8	363.9	726.0	620.8	366.5	453.2	735.3	1260.8	704.6
RB	89.9	96.2	48.2	59.4	83.5	58.2	74.9	113.7	56.5
ZR	177.6	171.8	241.1	188.6	159.4	177.4	175.1	258.9	208.2
NB	11.7	12.0	14.3	10.2	9.4	9.4	10.0	12.8	12.9
BA	721.8	1004.5	741.0	814.6	893.5	752.4	1481.5	1893.3	1516.4
TH	14.3	10.7	11.7	9.8	12.5	9.9	11.3	8.3	16.4
LA	29.7	26.7	50.2	31.0	31.7	29.0	40.3	46.9	45.5
CE	60.1	55.6	91.2	71.2	65.0	53.5	72.6	117.8	105.4
ND	22.5	24.0	37.7	29.8	24.9	26.2	31.1	54.5	44.8
SM	1.6	5.0	6.5	7.2	2.3	4.5	3.5	6.1	2.2
Y	16.0	16.1	20.1	17.6	13.1	13.2	14.3	18.0	15.3
TIO2CR	0.565	0.581	0.833	1.035	0.558	0.673	0.587	1.376	0.561
TIO2W	0.559	0.569	0.853	1.030	0.555	0.655	0.576	1.386	0.536

TABLE B17

	AR5@19	AR6@44	AR7@19	AR8@13	AR9@13	AR10@13	AR11@22	NG1@11	NG2@12
SIO2	66.96	66.79	67.25	63.19	67.71	58.77	69.28	53.87	59.18
AL2O3	15.55	16.38	16.42	16.44	15.80	15.76	14.29	16.31	16.35
FE2O3	4.43	3.75	3.50	4.80	3.50	5.58	4.39	8.73	7.68
MGO	2.05	2.22	1.36	3.21	1.63	1.42	1.03	5.70	2.68
CAO	1.56	1.12	1.49	1.96	2.05	1.74	2.55	7.38	4.41
NA2O	4.46	6.13	5.14	5.16	4.68	2.30	3.78	3.51	4.28
K2O	3.665	2.373	3.489	3.778	3.313	10.777	3.458	2.028	2.718
TIO2	0.654	0.565	0.548	0.655	0.542	0.795	0.758	1.689	1.604
MNO	0.053	0.058	0.033	0.066	0.041	0.056	0.084	0.102	0.101
P2O5	0.242	0.212	0.167	0.265	0.220	0.304	0.152	0.495	0.505
TOTAL	99.62	99.58	99.40	99.52	99.49	99.49	99.78	99.81	99.52
LOI	1.44	1.36	1.04	2.47	1.44	2.69	0.47	1.22	1.35
NI	42.7	42.5	24.7	50.7	29.7	27.6	6.3	90.1	29.3
CR	121.1	92.4	17.7	74.0	81.0	114.6	6.0	157.3	42.6
V	89.8	79.9	59.7	84.2	95.4	50.1	42.2	135.5	132.0
SC	12.7	9.7	8.6	12.4	9.8	11.1	11.7	20.5	20.0
CU	18.0	10.2	12.0	23.7	17.7	12.3	12.0	24.7	14.3
ZN	37.0	56.3	30.8	68.6	32.4	25.8	49.8	84.3	80.3
SR	832.0	749.6	914.3	782.6	798.1	159.5	153.9	625.0	499.1
RB	76.6	47.6	71.2	58.2	67.3	113.8	96.4	50.3	76.4
ZR	228.1	146.4	141.7	205.4	162.3	204.3	373.7	309.2	372.4
NB	12.2	8.1	8.8	10.2	9.7	11.2	19.0	20.6	24.6
BA	1713.4	1075.5	1889.0	2209.6	1914.9	3637.3	917.6	689.5	880.7
TH	20.1	10.2	4.8	9.7	7.5	1.7	14.3	12.1	16.5
LA	45.3	26.8	23.0	36.5	31.7	18.7	43.2	52.0	67.4
CE	99.5	59.6	48.4	82.5	65.4	46.1	88.3	116.7	132.2
ND	43.9	26.9	23.7	34.9	30.4	23.9	40.6	50.1	63.8
SM	5.8	5.3	5.0	6.0	5.4	9.1	9.2	10.2	10.8
Y	18.8	12.6	13.6	18.6	13.1	20.6	50.1	37.1	44.0
TIO2CR	0.673	0.588	0.575	0.657	0.527	0.861	0.725	1.404	1.422
TIO2W	0.667	0.588	0.569	0.667	0.537	0.882	0.734	1.547	1.534

	NG3@22	SH1@52	SH2@52	SH3@52	SH4@11	SH5@21	SH6@21	SH7@13	SH8@13
SIO2	64.94	69.27	65.46	66.79	52.51	67.27	66.78	59.62	59.78
AL2O3	15.78	14.43	14.33	13.91	14.97	16.27	16.59	14.92	14.97
FE2O3	4.59	5.23	7.06	7.03	13.21	4.03	3.98	9.77	8.63
MGO	0.83	0.32	1.24	1.21	3.97	0.35	0.21	3.12	2.74
CAO	4.79	0.23	1.25	0.66	7.74	0.24	0.22	3.46	4.08
NA2O	2.71	4.89	4.43	3.16	3.47	4.59	4.26	3.96	3.33
K2O	5.404	4.197	3.845	5.204	1.517	5.458	7.137	2.470	3.550
TIO2	0.732	0.535	1.133	1.097	1.855	0.447	0.461	1.601	1.558
MNO	0.083	0.063	0.163	0.175	0.284	0.020	0.029	0.318	0.353
P2O5	0.246	0.103	0.307	0.300	0.286	0.085	0.087	0.343	0.457
TOTAL	100.09	99.27	99.21	99.54	99.81	99.75	99.75	99.57	99.45
LOI	3.72	0.67	1.42	1.43	0.58	0.70	0.73	1.57	1.30
NI	16.1	3.7	4.4	5.6	11.8	5.8	4.9	4.5	18.1
CR	35.4	2.9	4.5	4.0	8.0	3.9	2.4	2.0	10.5
V	81.2	4.5	39.0	36.7	360.3	14.7	13.4	183.2	131.0
SC	11.3	11.9	15.3	15.5	38.5	10.3	12.6	28.9	23.2
CU	6.7	2.3	4.3	9.0	14.0	1.7	2.1	14.5	17.7
ZN	44.8	86.4	324.7	283.1	111.8	44.2	14.5	381.4	317.2
SR	310.2	162.7	256.3	224.1	434.5	164.5	169.7	322.3	476.9
RB	214.2	108.7	90.1	123.0	30.5	140.7	172.3	59.0	93.5
ZR	307.8	406.0	422.9	408.7	182.1	696.6	702.3	280.6	278.3
NB	18.9	23.0	24.2	23.3	13.3	20.5	20.2	15.2	17.7
BA	1117.8	1647.1	1767.0	2798.2	904.3	1044.9	1234.8	778.9	1410.6
TH	26.5	8.7	8.8	6.0	9.8	13.2	13.7	6.6	7.4
LA	64.9	51.6	59.8	42.0	29.0	18.1	46.3	34.4	47.0
CE	128.0	108.6	117.5	89.0	59.6	45.6	89.7	75.5	91.3
ND	48.0	48.5	53.4	47.1	27.8	19.7	40.3	34.6	42.8
SM	6.8	6.2	8.1	9.2	5.9	3.2	5.6	5.5	6.6
Y	22.1	46.0	48.2	49.7	31.4	30.3	35.3	35.9	38.6
TIO2CR	0.723	0.570	1.158	1.115	1.927	0.440	0.449	1.657	1.594
TIO2W	0.758	0.569	1.175	1.130	1.944	0.460	0.466	1.656	1.592

TABLE B17

	SH9a13	SH10a5	SH11a19	SH12a52	SH13a52	SH14a19	SH15a11	SH16a20	SH17a21
SIO2	59.22	60.87	78.02	69.20	70.00	61.91	55.54	54.26	74.42
AL203	14.98	15.14	11.43	14.15	14.37	15.83	16.58	16.93	13.51
FE203	8.83	8.01	2.10	5.56	4.83	5.15	8.96	8.55	2.18
MGO	3.00	2.28	0.18	0.20	0.23	0.52	4.29	4.06	0.14
CAO	4.42	2.32	0.05	0.32	0.25	3.66	3.35	8.40	0.22
NA2O	3.49	5.95	0.12	4.63	3.37	3.28	5.32	2.77	1.10
K2O	3.080	2.539	8.573	4.591	5.769	7.802	3.670	2.305	8.233
TIO2	1.549	1.526	0.091	0.775	0.535	0.942	1.381	1.423	0.177
MNO	0.203	0.216	*	0.083	0.148	0.081	0.066	0.143	0.038
P2O5	0.441	0.535	0.010	0.163	0.104	0.250	0.353	0.367	0.017
TOTAL	99.20	99.38	100.57	99.59	99.61	99.42	99.51	99.81	100.03
LOI	1.40	1.27	0.58	0.68	0.74	2.77	0.91	0.93	0.75
NI	13.7	3.4	5.0	4.8	5.2	7.4	18.8	41.3	4.6
CR	10.5	3.2	4.1	5.5	3.6	6.9	6.6	24.5	4.8
V	126.8	84.6	4.4	11.1	5.7	33.6	186.5	211.9	1.0
SC	22.8	20.8	*	12.7	13.0	14.1	20.0	23.6	0.3
CU	18.3	3.2	5.0	3.6	3.2	5.7	15.0	36.3	1.3
ZN	249.0	421.3	24.3	42.6	17.3	23.2	39.2	71.6	18.8
SR	431.2	403.0	24.0	174.1	115.9	278.3	363.8	667.3	75.9
RB	77.7	55.6	245.1	144.9	144.6	142.0	155.2	47.0	153.6
ZR	276.6	287.5	331.9	487.8	403.0	441.0	240.9	218.3	406.0
NB	17.5	17.6	26.9	25.2	22.1	26.3	17.0	17.3	37.7
BA	1035.5	1620.9	1457.7	1707.4	2557.4	2542.1	1310.0	1806.8	790.2
TH	6.7	3.1	18.2	12.0	4.2	4.8	5.3	4.2	17.6
LA	45.3	48.1	12.4	45.9	56.0	71.3	37.1	43.4	82.1
CE	94.3	98.8	37.6	124.6	137.5	142.1	74.5	90.1	171.3
ND	43.5	47.5	15.4	44.6	54.2	52.6	33.7	39.1	59.1
SM	8.1	7.4	3.3	7.7	7.2	10.7	7.6	8.3	10.7
Y	38.1	41.3	48.4	41.8	38.7	41.3	27.0	30.6	44.2
TIO2CR	1.539	1.521	0.103	0.789	0.555	0.896	1.344	1.411	0.182
TIO2W	1.564	1.531	0.114	0.789	0.571	0.914	1.335	1.443	0.195

	SH18a20	SH19a20	SH20a19	SH22a20	SH23a12	SH24a11	SH25a11	SH27a11	SH28a19
SIO2	52.69	53.04	67.50	51.91	50.01	51.41	49.86	58.11	72.27
AL203	17.02	16.91	15.33	16.45	18.92	17.35	16.29	15.59	13.33
FE203	12.75	11.69	5.05	10.93	8.07	11.18	10.38	8.32	4.30
MGO	3.91	5.77	0.42	4.12	7.61	3.84	8.52	4.65	0.23
CAO	4.74	4.99	0.54	5.44	10.28	5.66	9.60	5.00	0.06
NA2O	3.73	3.55	4.93	3.30	2.81	3.14	2.93	3.90	2.99
K2O	1.980	1.014	4.734	4.746	0.593	4.023	0.571	2.548	6.684
TIO2	1.947	1.748	0.534	1.784	0.811	1.900	1.038	0.929	0.314
MNO	0.254	0.213	0.078	0.166	0.113	0.155	0.251	0.533	0.037
P2O5	0.401	0.308	0.113	0.434	0.104	0.459	0.135	0.157	0.019
TOTAL	99.42	99.24	99.22	99.28	99.32	99.12	99.57	99.74	100.22
LOI	2.73	3.08	0.89	1.95	2.18	2.73	2.75	1.71	0.51
NI	49.7	66.9	3.4	19.2	143.1	22.2	195.3	73.4	6.0
CR	44.9	101.8	2.6	4.4	239.3	4.1	351.2	155.6	3.0
V	263.3	251.4	5.0	234.0	143.2	255.7	203.0	159.3	2.4
SC	27.2	36.5	15.1	22.3	25.7	27.6	31.6	28.9	0.5
CU	7.7	5.3	1.1	34.7	25.8	44.6	36.5	16.3	3.2
ZN	246.6	291.1	370.5	102.7	67.1	139.6	170.0	473.1	62.0
SR	633.6	462.0	281.9	721.0	468.2	576.9	308.4	318.2	33.9
RB	59.7	26.4	108.6	93.3	16.5	91.3	33.1	80.4	221.5
ZR	228.1	173.1	588.5	270.0	68.7	275.1	108.7	202.5	393.0
NB	17.2	12.3	21.4	18.6	5.0	19.5	8.8	18.2	34.6
BA	1198.1	792.2	3185.3	1690.2	331.3	2015.3	141.3	769.6	421.2
TH	0.5	2.8	4.3	5.2	0.4	3.5	*	11.4	13.2
LA	35.0	24.0	63.3	49.0	5.4	48.1	10.3	33.0	70.6
CE	67.5	48.4	129.1	97.3	15.2	100.1	12.1	61.4	165.7
ND	33.1	23.6	58.4	44.9	8.3	46.4	8.3	26.2	54.8
SM	7.4	4.7	9.2	8.1	2.6	9.8	3.6	2.3	10.0
Y	32.9	30.0	40.3	34.6	15.4	34.1	23.1	31.2	47.0
TIO2CR	1.787	1.590	0.570	1.549	0.783	1.771	1.029	0.992	0.337
TIO2W	1.861	1.648	0.581	1.693	0.804	1.810	1.047	0.994	0.342

TABLE B17

	SH29a4	SH30a10	SH31a11	SH32a11	SH33a19	SH34a19	SH35a19	SH36a11	SH37a11
SIO2	56.50	56.86	54.02	57.25	76.20	74.90	66.57	51.28	51.73
AL2O3	15.73	15.65	18.82	15.70	12.91	12.76	15.89	17.45	15.69
FE2O3	8.19	8.32	10.41	7.78	1.76	2.69	4.39	9.42	10.37
MGO	5.20	5.09	2.88	5.36	0.11	0.08	0.84	5.80	6.75
CAO	7.52	7.20	2.50	8.17	0.10	0.05	1.05	8.97	7.48
NA2O	3.21	3.09	6.44	2.97	3.64	1.75	6.12	3.53	4.26
K2O	2.011	2.121	1.959	1.549	5.130	3.130	3.589	1.144	1.303
TIO2	0.973	0.994	1.075	0.767	0.166	0.186	0.571	1.600	1.452
MNO	0.129	0.138	0.568	0.206	0.011	0.028	0.171	0.393	0.232
P2O5	0.155	0.161	0.167	0.090	0.018	0.015	0.152	0.292	0.270
TOTAL	99.62	99.62	98.83	99.34	100.04	100.59	99.33	99.89	99.53
LOI	0.49	0.33	2.12	1.59	0.65	0.43	1.41	1.42	4.67
NI	67.0	69.2	146.6	136.5	4.7	4.2	3.8	59.4	110.0
CR	151.9	152.5	228.4	341.3	3.4	3.2	3.5	61.8	211.2
V	123.5	137.5	172.1	161.8	1.3	0.2	8.4	245.6	211.5
SC	23.3	24.5	38.4	32.9	*	*	11.4	34.6	32.1
CU	12.4	11.5	30.9	14.4	7.5	9.9	1.3	67.4	13.2
ZN	84.3	96.3	1246.5	111.1	60.0	29.2	1235.3	577.5	402.1
SR	411.1	396.1	750.5	256.7	69.2	38.9	139.1	466.3	403.5
RB	72.8	63.5	95.3	49.0	159.2	222.8	76.7	23.1	48.8
ZR	170.4	186.3	123.0	99.2	344.0	851.2	515.8	167.7	156.2
NB	18.0	18.4	11.4	9.3	38.8	28.2	22.6	11.5	12.3
BA	747.5	759.6	1106.6	398.0	630.9	710.2	845.1	714.5	453.6
TH	9.9	10.1	3.5	5.3	22.8	17.4	14.3	0.7	1.4
LA	31.1	32.3	21.0	18.5	69.6	36.8	94.4	22.7	23.0
CE	57.5	65.5	40.4	34.4	116.7	80.5	179.1	52.5	47.5
ND	23.7	26.2	18.2	13.7	53.1	33.0	67.3	27.0	23.9
SM	5.8	4.1	*	3.3	9.7	3.5	7.2	3.9	3.3
Y	29.5	31.6	25.3	26.1	56.4	46.2	42.6	28.7	25.0
TIO2CR	0.811	0.953	0.888	0.775	0.184	0.192	0.600	1.668	1.328
TIO2W	0.868	0.977	0.943	0.799	0.193	0.207	0.596	1.681	1.368

	SH38a1	SH39a12	SH40a52	SH41a52	OR1a12	OR2a12	OR3a12	OR4a12	OR5a22
SIO2	50.89	53.61	63.36	64.36	50.47	52.23	48.20	51.44	49.98
AL2O3	15.65	16.07	14.69	14.57	20.28	19.23	16.26	19.86	15.74
FE2O3	12.55	9.04	6.97	6.84	7.11	6.97	8.57	7.15	10.48
MGO	4.82	5.84	1.96	1.98	1.51	5.04	9.84	4.45	9.71
CAO	7.11	6.45	2.49	2.07	10.75	7.79	9.79	7.49	8.02
NA2O	5.10	3.68	4.70	4.51	3.04	5.20	3.44	5.37	2.83
K2O	1.123	2.599	3.576	3.925	4.089	1.545	1.492	1.556	1.179
TIO2	1.495	1.226	1.240	1.203	1.421	1.167	1.255	1.241	1.232
MNO	0.315	0.603	0.234	0.172	0.076	0.132	0.127	0.133	0.091
P2O5	0.267	0.236	0.320	0.307	0.779	0.709	0.560	0.734	0.191
TOTAL	99.32	99.35	99.54	99.93	99.53	100.01	99.55	99.42	99.47
LOI	2.87	2.02	0.95	1.21	7.07	2.92	1.61	3.42	3.15
NI	60.8	43.1	9.3	9.2	46.4	53.5	196.8	32.3	264.3
CR	43.3	50.5	10.1	10.8	48.6	72.5	284.0	17.1	408.5
V	222.3	211.7	99.0	97.0	170.5	150.5	198.7	166.7	186.1
SC	32.3	35.0	19.3	17.4	23.4	23.4	29.3	19.8	31.1
CU	10.4	52.5	17.5	8.5	10.5	40.1	50.0	44.6	61.2
ZN	667.9	861.5	517.2	237.1	141.0	55.6	51.5	49.6	73.6
SR	479.8	527.2	541.9	485.7	1165.5	1316.7	1178.9	1266.0	330.7
RB	45.0	80.3	100.3	107.5	98.2	14.6	25.9	19.5	29.5
ZR	153.9	192.0	282.1	297.3	166.4	208.8	148.8	195.7	96.2
NB	12.4	11.8	16.6	16.2	57.8	32.5	43.3	42.2	15.3
BA	557.2	1139.0	1389.4	1569.0	2741.7	1952.7	1471.2	2395.9	523.6
TH	2.2	2.4	7.1	6.7	2.4	2.0	6.6	*	*
LA	20.5	24.9	40.5	39.1	61.9	51.0	66.6	56.1	14.8
CE	41.8	55.9	88.1	85.1	119.0	112.3	112.8	102.4	23.5
ND	21.0	26.2	40.8	39.7	48.7	49.9	42.2	45.1	10.4
SM	3.2	3.8	9.0	8.2	4.8	6.5	7.3	5.7	4.4
Y	26.7	29.7	34.6	32.7	24.6	23.0	25.6	24.0	22.5
TIO2CR	1.411	1.268	1.177	1.171	1.572	1.248	1.359	1.280	1.148
TIO2W	1.454	1.262	1.199	1.185	1.545	1.215	1.324	1.287	1.210

TABLE B17

	OR6@22	OR7@11	OR8@11
SIO2	49.81	49.67	49.23
AL2O3	14.76	15.02	16.68
FE2O3	11.41	11.32	9.24
MGO	6.00	7.73	6.76
CAO	5.80	10.12	10.63
NA2O	1.90	2.83	3.05
K2O	6.427	1.302	2.854
TIO2	2.445	1.348	1.268
MNO	0.082	0.147	0.077
P2O5	0.483	0.235	0.224
TOTAL	99.13	99.72	100.01
LOI	5.80	3.98	8.84
NI	38.3	93.3	104.0
CR	47.8	189.6	269.7
V	326.1	217.8	270.5
SC	34.9	33.6	45.4
CU	131.0	136.1	79.1
ZN	106.1	63.2	59.0
SR	384.8	351.6	349.6
RB	154.8	25.5	63.1
ZR	214.1	103.8	99.5
NB	52.7	17.3	16.7
BA	2967.2	824.9	577.6
TH	*	*	1.0
LA	35.7	16.8	19.0
CE	73.5	33.4	34.5
ND	34.6	16.3	16.4
SM	8.7	4.6	4.0
Y	42.2	26.8	24.2
TIO2CR	2.733	1.216	1.302
TIO2W	2.773	1.292	1.320

APPENDIX C : ELECTRON MICROPROBE TECHNIQUES

All mineral analyses were performed on the Cambridge Instruments electron probe microanalyzer of the Grant Institute of Geology. A wavelength dispersive system (WDS) was used for silicate and apatite analyses, and for the analysis of Zr and Nb in oxide minerals. Most oxide minerals were analyzed using a Link Systems energy dispersive system (EDS), however.

C1 : WAVELENGTH DISPERSIVE SYSTEM

All analyses were performed using a gun potential of 20 kV. A nominal probe current of 30 nA was used for the major elements, but to provide higher count rates for the minor elements a 60 nA current was used. The current was frequently monitored using a Faraday cage. Beam diameter was about 1μm. Analytical conditions, standards used and approximate precision are given in Table C1. A vaccuum-deposited carbon film provided a conductive coating, and standards and samples were coated simultaneously. Samples were stored in a dessicator prior to analysis. In general, counting times were divided into a number of 10 or 20 s counts to allow detection of any changes in count rate due to volatilization, burning or pulse height depression. Volatilization was only observed for K, and this element was therefore analysed first for all minerals. Deep burning of the specimen was only encountered during the analysis of apatite on basal sections: this was readily overcome by restricting analysis to prism sections.

Dead time correction and conversion to apparent concentrations were carried out using the computer program APPCONC, written by D.J. Humphries. Apparent concentrations used were in general calculated relative to averages of standard counts measured before and after each set of analyses, but on rare occasions refer to only one set of standards, where significant drift in standard count rates occurred. Corrections for matrix absorption, atomic number and enhancement (ZAF) were made using the iterative computer program PROBE, written by D.J. Humphries, based on the program of Duncumb and Jones (1969).

C2 : ENERGY DISPERSIVE SYSTEM

An EDS method with a nominal 6 nA probe current was used for some of the oxide minerals. 100 s livetimes were used on a Si(Li) detector: precision is a little worse than for WDS analyses. Apparent concentrations were calculated relative to a cobalt metal standard, and full calibration is only necessary at infrequent intervals. These calculations and ZAF corrections were made on an on-line Data General computer, using a program written by Statham (1975).

TABLE C1 : Analytical conditions used in wavelength dispersive electron microprobe analysis.

Element & line	Crystal	Background offset $2\theta^{o}$	Peak time	Background time	Typical conc^{n}. $\pm 2\sigma$	Standard
Si K_α	RAP	+1.5	40	20	55±0.3%	Wollastonite
Al K_α	RAP	+1.5	40	20	30±0.15%	Synthetic Corundum
Fe K_α	LiF	±2.0	40	20	11±0.16%	Metal
Mg K_α	RAP	+1.5	40	20	30±0.2%	Synthetic Periclase
Ca K_α	PE	±2.0	40	20	13±0.1%	Wollastonite
Na K_α	RAP	+1.5	pl 50 px 30	20	5±0.1%	Jadeite
K K_α	PE	±1.75	pl 50 px 30	20	0.2±0.015%	Orthoclase
Ti K_α	LiF	±2.0	40	20	0.3±0.04%	Rutile or metal
Mn K_α	LiF	±2.0	20	20	0.2±0.06	Metal
Cr K_α	LiF	±2.0	20	20	0.35±0.06%	Metal
Ni K_α	LiF	±2.0	100	80	600±180 ppm	Metal
Zr L_{α_1}	PE	±1.0	160	160	1420±140 ppm	Metal
Nb L_{α_1}	PE	±1.0	320	320	150±80 ppm	Metal
Sr L_{α_1}	PE	+1.0	100	80	1350±160 ppm	Celestite
Ba L_{α_1}	Qz	±2.0	100	120	450±200 ppm	Barytes
P K_α	PE	±2.0	80	80	42±0.16%	Apatite
La L_{α_1}	Qz	+1.0	100	80	1120±230 ppm	Synthetic Standards: Drake and Weill, (1972)
Ce L_{α_1}	Qz	±1.0	80	80	1130±300 ppm	
Nd L_{α_1}	Qz	+1.0	80	80	470±270 ppm	
Sm L_{α_1}	Qz	+0.75	100	80	300±220 ppm	
Y L_{α_1}	PE	±2.0	100	80	410±120 ppm	

Table C2 : Average core compositions of O.R.S. mineral phases.
Average analyses for each mineral type in a rock have been computed using the program MEANFILE (Appendix D), and tabulated using the program MINTAB, written by A.M. Graham.

Analysis numbers (first line) are referred to in the text of the thesis; the analysis name is the rock in which the mineral was analysed. N.B. two analyses are frequently given for the same rock in the same table; these may refer to phenocryst and xenocryst compositions, for example, or most commonly to coexisting ortho- and clinopyroxene.

The number in parentheses is the number of individual analyses incorporated in the average.

Tables are in the order olivine - pyroxene - plagioclase - amphibole - biotite - spinel - ilmenite - apatite. FEO refers to total iron as FeO; Fe203 in spinels has been recalculated assuming R304.

The low totals for many analyses are mainly due to the non-analysis of minor elements, in particular H20, F and Cl, but also including elements such as Zn and V in oxide minerals, and Ba in biotites. The minor elements analysed for these minerals are quoted in Table C4.

AVERAGE CORE COMPOSITIONS OF O.R.S. OLIVINES

TABLE C2

	1	2	3	4
	MT45	OC72	OC152	OR3
	(5)	(4)	(5)	(3)
SIO2	40.37	36.28	39.42	39.39
TIO2	0.00	0.02	0.03	0.00
AL2O3	0.05	0.05	0.06	0.04
CR2O3	0.05	0.00	0.05	0.01
FEO	14.45	34.70	17.38	16.17
MNO	0.21	0.66	0.30	0.31
MGO	45.72	29.03	42.79	44.66
NIO	0.26	0.07	0.22	0.20
CAO	0.16	0.13	0.16	0.23
TOTAL	101.28	100.93	100.41	101.00
MOLE PERCENT ENDMEMBERS				
FO	84.9	59.9	81.4	83.1
FA	15.1	40.1	18.6	16.9

AVERAGE CORE COMPOSITIONS OF O.R.S. PYROXENES

TABLE C2

	1	2	3	4	5	6	7	8
	L26	L73	L51	L113*	L113	L68*	L79	L50
	(3)	(3)	(5)	(2)	(3)	(2)	(4)	(4)
SIO2	50.65	50.19	51.91	53.33	51.91	52.32	51.59	50.63
TIO2	0.70	0.77	0.46	0.28	0.56	0.61	0.77	0.71
AL2O3	3.73	4.72	2.40	0.64	2.94	1.32	2.65	4.10
CR2O3	0.00	0.71	0.32	0.01	0.02	0.02	0.06	0.68
FEO	6.40	5.60	5.94	6.28	6.24	6.53	7.93	5.09
MNO	0.16	0.15	0.16	0.21	0.13	0.22	0.23	0.10
MGO	15.12	15.83	17.04	15.58	15.89	15.92	15.14	16.32
CAO	21.76	20.63	19.57	21.47	20.06	20.91	20.80	20.40
NA2O	0.39	0.49	0.41	0.57	0.53	0.42	0.44	0.59
K2O	0.00	0.00	0.02	0.03	0.05	0.02	0.01	0.03
TOTAL	98.91	99.08	98.24	98.38	98.33	98.28	99.64	98.65
MOLE PERCENT ENDMEMBERS								
EN	44.0	46.8	49.5	45.1	47.0	46.0	43.8	48.2
FS	10.4	9.3	9.7	10.2	10.3	10.6	12.9	8.4
WO	45.5	43.9	40.8	44.7	42.7	43.4	43.3	43.3

	9	10	11	12	13	14	15	16
	L50*	L121	L128	L146	GC1	GC25	GC26*	GC29
	(1)	(2)	(3)	(4)	(5)	(4)	(2)	(3)
SIO2	53.36	51.26	51.17	50.54	50.99	51.48	53.31	51.96
TIO2	0.25	0.74	0.78	0.95	0.99	0.80	0.27	0.63
AL2O3	0.39	2.22	2.15	3.97	1.99	3.31	0.38	2.60
CR2O3	0.00	0.15	0.14	0.44	0.06	0.15	0.02	0.04
FEO	7.43	9.55	9.20	6.30	8.38	7.67	10.08	7.72
MNO	0.19	0.21	0.19	0.16	0.27	0.19	0.30	0.26
MGO	15.76	14.79	15.05	15.39	15.34	15.37	14.51	15.18
CAO	20.97	19.54	19.57	21.12	20.00	20.44	20.62	20.69
NA2O	0.40	0.53	0.51	0.42	0.49	0.39	0.37	0.44
K2O	0.03	0.03	0.00	0.01	0.00	0.00	0.00	0.01
TOTAL	98.79	99.03	98.78	99.30	98.51	99.83	99.87	99.53
MOLE PERCENT ENDMEMBERS								
EN	45.0	43.3	43.9	45.1	44.6	44.7	41.5	44.2
FS	11.9	15.7	15.1	10.4	13.7	12.5	16.2	12.6
WO	43.1	41.1	41.0	44.5	41.8	42.8	42.4	43.2

	17	18	19	20	21	22	23	24
	BN2	MT45	MT10	MT10	MT42	S44	S12	S13
	(4)	(7)	(3)	(1)	(8)	(5)	(5)	(4)
SIO2	51.54	51.62	54.73	52.10	51.67	55.11	52.48	51.35
TIO2	0.46	0.75	0.29	0.74	0.80	0.25	0.67	1.05
AL2O3	2.49	3.05	1.65	2.38	2.96	1.52	2.13	1.83
CR2O3	0.06	0.41	0.35	0.69	0.40	0.42	0.26	0.06
FEO	9.63	5.67	11.36	6.30	5.86	10.32	7.72	9.67
MNO	0.26	0.12	0.23	0.13	0.10	0.21	0.22	0.26
MGO	13.90	16.17	29.18	16.67	16.17	30.60	17.48	15.07
CAO	20.43	21.51	1.97	20.10	21.43	1.75	18.44	19.43
NA2O	0.63	0.28	0.00	0.37	0.29	0.00	0.32	0.38
TOTAL	99.40	99.59	99.77	99.49	99.70	100.19	99.73	99.30
MOLE PERCENT ENDMEMBERS								
EN	40.9	46.5	78.9	48.1	46.4	81.3	49.9	43.6
FS	15.9	9.1	17.2	10.2	9.4	15.4	12.3	16.0
WO	43.2	44.4	3.8	41.7	44.2	3.3	37.8	40.4

* = Augite forming reaction rim to quartz ?phenocrysts

AVERAGE CORE COMPOSITIONS OF O.R.S. PYROXENES — TABLE C2

	25	26	27	28	29	30	31	32
	S52	S52	S28	S41	OC22	OC13	OC17	OC27
	(3)	(3)	(5)	(5)	(6)	(5)	(7)	(1)
SIO2	52.69	51.59	51.77	51.63	50.90	50.32	50.51	49.72
TIO2	0.47	0.52	0.75	0.73	0.80	0.82	0.91	1.01
AL2O3	1.81	1.91	2.42	1.35	3.14	2.47	2.53	4.00
CR2O3	0.01	0.03	0.24	0.00	0.00	0.00	0.04	0.00
FEO	19.52	9.70	7.57	11.78	7.25	11.80	11.39	8.04
MNO	0.43	0.29	0.20	0.39	0.24	0.39	0.32	0.21
MGO	23.39	16.04	16.98	13.71	15.78	13.98	15.07	14.85
CAO	1.99	18.48	18.45	19.44	20.17	18.70	17.38	20.35
NA2O	0.00	0.38	0.37	0.36	0.47	0.52	0.54	0.45
K2O	0.00	0.00	0.00	0.01	0.00	0.00	0.00	0.00
TOTAL	100.32	99.35	98.78	99.39	98.75	99.01	98.70	98.63
MOLE PERCENT ENDMEMBERS								
EN	65.4	46.1	49.2	40.0	45.9	41.1	44.4	43.7
FS	30.6	15.7	12.3	19.3	11.8	19.4	18.8	13.3
WO	4.0	38.2	38.4	40.7	42.2	39.5	36.8	43.0

	33	34	35	36	37	38	39	40
	OC15	OC15	OC23	OC7	OC25	OC43	OC98	OC98
	(4)	(4)	(4)	(6)	(5)	(3)	(5)	(3)
SIO2	50.72	54.40	50.73	50.87	51.74	50.39	54.07	51.28
TIO2	0.75	0.23	0.79	0.68	0.47	0.83	0.36	0.72
AL2O3	3.71	2.09	2.91	2.10	1.94	3.64	1.29	2.36
CR2O3	0.47	0.17	0.11	0.19	0.00	0.03	0.15	0.27
FEO	6.55	11.71	9.43	12.93	9.09	9.11	13.82	9.35
MNO	0.16	0.22	0.26	0.42	0.42	0.35	0.32	0.27
MGO	16.12	29.39	14.67	13.23	14.79	14.30	27.59	15.94
CAO	20.04	1.36	19.38	18.14	20.29	19.85	1.97	18.33
NA2O	0.39	0.05	0.50	0.55	0.44	0.53	0.00	0.55
K2O	0.00	0.00	0.00	0.01	0.01	0.00	0.00	0.01
TOTAL	98.94	99.73	99.00	99.13	99.19	99.04	99.59	99.07
MOLE PERCENT ENDMEMBERS								
EN	47.1	79.2	43.1	39.5	42.9	42.5	75.1	46.4
FS	10.8	17.8	15.5	21.6	14.8	15.2	21.1	15.3
WO	42.1	3.0	41.4	38.9	42.3	42.4	3.8	38.3

	41	42	43	44	45	46	47	48
	OC67	OC67	OC72	OC123	OC123	OC85	OC54	OC84
	(3)	(4)	(4)	(4)	(5)	(2)	(7)	(3)
SIO2	51.43	53.55	51.02	52.24	55.48	49.33	51.44	55.48
TIO2	0.43	0.13	1.13	0.58	0.18	1.15	0.38	0.19
AL2O3	2.59	0.43	2.42	2.50	2.05	6.34	2.08	1.89
CR2O3	0.05	0.01	0.28	0.25	0.66	0.06	0.15	0.44
FEO	8.70	19.70	8.12	6.33	9.47	6.53	9.20	10.27
MNO	0.34	0.80	0.24	0.18	0.24	0.14	0.34	0.18
MGO	14.41	23.90	15.00	16.50	30.82	15.24	14.61	30.26
CAO	20.78	1.12	20.48	20.42	1.32	19.49	20.52	1.60
NA2O	0.45	0.00	0.45	0.33	0.00	0.59	0.54	0.00
K2O	0.01	0.00	0.00	0.00	0.00	0.00	0.00	0.00
TOTAL	99.20	99.65	99.16	99.42	100.23	98.87	99.27	100.32
MOLE PERCENT ENDMEMBERS								
EN	42.1	66.8	43.8	47.5	83.1	46.3	42.3	81.4
FS	14.3	30.9	13.3	10.3	14.3	11.1	15.0	15.5
WO	43.6	2.3	42.9	42.2	2.6	42.6	42.7	3.1

AVERAGE CORE COMPOSITIONS OF O.R.S. PYROXENES

TABLE C2

	49	50	51	52	53	54	55	56
	OC84	OC93	OC93	OC103	OC103	OC108	OC108	OC152
	(5)	(6)	(4)	(3)	(5)	(4)	(2)	(5)
SIO2	51.04	51.56	53.65	55.90	52.01	53.51	51.91	50.51
TIO2	0.82	0.80	0.44	0.15	0.63	0.40	0.74	0.89
AL2O3	3.69	2.18	1.30	1.67	3.63	2.81	2.76	3.86
CR2O3	0.44	0.16	0.09	0.37	0.59	0.05	0.02	0.47
FEO	7.81	8.57	17.32	8.87	6.24	14.99	8.72	5.93
MNO	0.18	0.20	0.38	0.19	0.18	0.30	0.27	0.15
MGO	15.72	15.98	25.11	30.90	17.15	27.06	15.05	15.67
CAO	19.25	19.43	1.83	1.89	18.94	1.43	20.42	21.55
NA2O	0.49	0.35	0.00	0.00	0.47	0.00	0.42	0.30
K2O	0.00	0.00	0.00	0.00	0.00	0.00	0.00	0.00
TOTAL	99.44	99.25	100.12	99.95	99.85	100.54	100.30	99.33
MOLE PERCENT ENDMEMBERS								
EN	46.3	46.0	69.5	83.0	50.1	74.1	43.5	45.4
FS	12.9	13.8	26.9	13.4	10.2	23.0	14.1	9.7
WO	40.8	40.2	3.6	3.6	39.7	2.8	42.4	44.9

	57	58	59	60	61	62	63	64
	OC131	OC140*	OC140	PE16	PE24	PE25	PE26	PE15
	(3)	(2)	(1)	(6)	(4)	(5)	(3)	(4)
SIO2	51.90	53.07	52.06	55.58	51.92	54.34	51.78	55.01
TIO2	0.80	0.39	0.93	0.18	0.50	0.31	0.86	0.23
AL2O3	2.15	0.71	1.80	1.44	2.77	2.26	2.14	1.74
CR2O3	0.40	0.03	0.03	0.30	0.64	0.37	0.38	0.33
FEO	7.87	19.68	9.80	9.48	5.18	11.93	7.45	11.26
MNO	0.23	0.61	0.35	0.21	0.14	0.23	0.22	0.25
MGO	16.45	22.68	14.94	30.82	16.77	28.74	16.02	29.21
CAO	19.24	2.24	19.48	1.60	20.78	1.75	20.05	1.82
NA2O	0.38	0.00	0.44	0.06	0.34	0.11	0.36	0.06
K2O	0.01	0.00	0.02	0.00	0.00	0.02	0.01	0.00
TOTAL	99.44	99.41	99.87	99.67	99.05	100.07	99.28	99.91
MOLE PERCENT ENDMEMBERS								
EN	47.4	64.2	43.4	82.7	48.4	78.3	46.3	79.3
FS	12.7	31.3	16.0	14.3	8.4	18.2	12.1	17.1
WO	39.9	4.6	40.7	3.1	43.2	3.4	41.6	3.6

	65	66	67	68	69	70	71	72
	PE41	PE41	AY4	AY13	AY27	AY12	AY12	AY35
	(7)	(4)	(5)	(3)	(5)	(3)	(2)	(5)
SIO2	52.80	55.45	55.06	53.44	52.23	54.28	52.34	51.89
TIO2	0.41	0.23	0.25	0.28	0.62	0.27	0.49	0.35
AL2O3	1.98	1.21	1.59	1.27	2.23	1.45	2.13	1.63
CR2O3	0.45	0.16	0.30	0.20	0.55	0.23	0.31	0.11
FEO	5.99	11.20	10.78	15.71	6.83	13.10	7.33	23.18
MNO	0.16	0.29	0.25	0.34	0.20	0.30	0.24	0.50
MGO	17.20	29.69	29.39	25.90	17.05	27.86	16.81	20.54
CAO	20.35	1.76	1.96	1.96	19.09	2.05	19.27	1.69
NA2O	0.27	0.00	0.00	0.00	0.36	0.00	0.31	0.00
K2O	0.00	0.00	0.00	0.00	0.02	0.00	0.00	0.00
TOTAL	99.62	100.00	99.58	99.11	99.19	99.54	99.22	99.89
MOLE PERCENT ENDMEMBERS								
EN	48.9	79.7	79.8	71.7	49.3	76.0	48.3	59.1
FS	9.3	16.9	16.4	24.4	11.1	20.0	11.8	37.4
WO	41.6	3.4	3.8	3.9	39.6	4.0	39.8	3.5

* = ?xenocryst

AVERAGE CORE COMPOSITIONS OF O.R.S. PYROXENES

TABLE C2

	73	74	75	76	77	78	79	80
	AY35	AY38	C54	C54	C51	C51	C33	C33
	(3)	(6)	(6)	(4)	(4)	(6)	(7)	(5)
SIO2	51.53	51.41	52.87	51.21	53.23	51.63	52.82	51.00
TIO2	0.55	0.90	0.34	0.70	0.39	0.63	0.37	0.78
AL2O3	1.53	2.02	1.18	1.85	1.29	2.24	1.25	2.07
CR2O3	0.01	0.04	0.06	0.07	0.03	0.08	0.06	0.15
FEO	12.21	11.74	20.24	10.44	17.84	8.93	20.12	11.34
MNO	0.35	0.33	0.50	0.29	0.43	0.24	0.49	0.30
MGO	13.69	14.88	23.00	14.20	24.94	15.04	22.99	14.20
CAO	19.06	17.73	1.49	19.68	1.58	19.98	1.61	18.73
NA2O	0.37	0.38	0.07	0.47	0.06	0.47	0.03	0.46
TOTAL	99.31	99.44	99.76	98.91	99.79	99.24	99.74	99.04
MOLE PERCENT ENDMEMBERS								
EN	40.0	43.5	64.9	41.5	69.1	43.7	64.9	41.7
FS	20.0	19.3	32.0	17.1	27.7	14.6	31.9	18.7
WO	40.0	37.2	3.0	41.3	3.1	41.7	3.3	39.6

	81	82	83	84	85	86	87	88
	C62	C62	C7	C7	C48	C58	OR3	SH23
	(3)	(2)	(5)	(5)	(4)	(5)	(4)	(5)
SIO2	53.94	53.52	51.02	53.15	52.20	52.17	49.43	51.78
TIO2	0.19	0.12	0.87	0.41	0.41	0.38	1.37	0.39
AL2O3	0.52	0.56	2.27	1.25	1.33	1.56	5.71	3.68
CR2O3	0.02	0.01	0.07	0.02	0.02	0.01	0.18	0.77
FEO	19.75	7.95	10.10	17.88	8.88	8.24	6.46	6.05
MNO	0.52	0.35	0.31	0.44	0.32	0.52	0.18	0.17
MGO	24.02	13.99	14.80	24.75	14.58	14.72	14.06	17.18
CAO	1.08	22.90	19.31	1.77	20.97	20.99	21.95	19.11
NA2O	0.03	0.53	0.45	0.06	0.43	0.51	0.63	0.32
K2O	0.00	0.00	0.01	0.00	0.01	0.01	0.00	0.00
TOTAL	100.18	99.93	99.21	99.73	99.15	99.12	99.98	99.45
MOLE PERCENT ENDMEMBERS								
EN	66.9	40.1	43.1	68.6	42.1	42.8	42.0	50.1
FS	30.9	12.8	16.5	27.8	14.4	13.4	10.8	9.9
WO	2.2	47.1	40.4	3.5	43.5	43.8	47.2	40.0

	89	90
	SH9	SH30
	(5)	(1)
SIO2	51.41	51.31
TIO2	0.75	0.24
AL2O3	1.52	0.82
CR2O3	0.01	0.00
FEO	12.91	13.06
MNO	0.48	0.49
MGO	14.25	13.11
CAO	17.78	18.87
NA2O	0.32	0.33
K2O	0.01	0.00
TOTAL	99.44	98.23
MOLE PERCENT ENDMEMBERS		
EN	41.6	38.6
FS	21.1	21.5
WO	37.3	39.9

AVERAGE CORE COMPOSITIONS OF O.R.S. PLAGIOCLASE

TABLE C2

	1	2	3	4	5	6	7	8
	L73	L68*	L95	L50	L50*	L121	L128	GC3
	(3)	(3)	(3)	(2)	(3)	(4)	(5)	(4)
SIO2	51.35	63.01	55.76	56.31	60.40	55.88	56.59	54.01
TIO2	0.09	0.14	0.07	0.05	0.02	0.10	0.11	0.03
AL2O3	29.48	20.84	27.36	26.55	23.91	26.75	26.10	27.71
CR2O3	0.00	0.00	0.02	0.01	0.00	0.00	0.00	0.01
FEO	0.48	0.34	0.47	0.41	0.20	0.61	0.66	0.49
MNO	0.00	0.00	0.05	0.00	0.00	0.00	0.02	0.00
MGO	0.16	0.03	0.09	0.07	0.03	0.10	0.15	0.06
CAO	13.33	3.21	10.37	9.42	6.26	9.67	9.16	10.77
NA2O	3.86	6.25	5.32	5.79	7.00	5.54	5.92	4.76
K2O	0.21	4.69	0.47	0.56	1.26	0.55	0.63	0.72
TOTAL	98.95	98.51	99.98	99.18	99.10	99.22	99.35	98.56
MOLE PERCENT ENDMEMBERS								
AB	33.9	56.3	46.8	51.0	62.0	49.3	52.0	42.6
AN	64.9	16.0	50.4	45.8	30.7	47.5	44.4	53.2
OR	1.2	27.8	2.8	3.2	7.4	3.2	3.7	4.2

	9	10	11	12	13	14	15	16
	GC6	GC26	GC29	GC30	BN2	BN3	BN7	MT4
	(3)	(1)	(5)	(5)	(3)	(3)	(4)	(4)
SIO2	60.31	54.57	53.93	56.62	53.78	55.14	56.45	52.28
TIO2	0.03	0.04	0.02	0.01	0.05	0.03	0.03	0.05
AL2O3	24.14	27.78	28.47	26.56	28.50	27.47	26.90	29.03
FEO	0.00	0.56	0.45	0.29	0.67	0.38	0.34	0.56
MGO	0.07	0.06	0.06	0.04	0.21	0.07	0.06	0.11
CAO	5.63	11.01	11.53	9.20	10.61	10.23	9.33	12.60
NA2O	7.81	4.93	4.71	5.98	4.71	5.59	6.00	4.17
K2O	0.69	0.44	0.30	0.44	0.44	0.29	0.33	0.28
TOTAL	98.69	99.38	99.47	99.14	98.97	99.19	99.44	99.09
MOLE PERCENT ENDMEMBERS								
AB	68.7	43.6	41.8	52.7	43.4	48.9	52.8	36.8
AN	27.3	53.8	56.5	44.8	54.0	49.5	45.3	61.5
OR	4.0	2.6	1.7	2.6	2.6	1.6	1.9	1.6

	17	18	19	20	21	22	23	24
	MT45	MT10	S44	S33	S8	S12	S13	S52
	(4)	(3)	(5)	(4)	(5)	(4)	(3)	(5)
SIO2	50.67	53.62	54.41	52.02	52.93	54.14	56.28	54.22
TIO2	0.07	0.07	0.06	0.06	0.15	0.09	0.14	0.10
AL2O3	29.92	28.44	27.86	29.80	28.54	28.40	26.65	28.16
FEO	0.69	0.51	0.55	0.33	0.68	0.55	0.48	0.70
MGO	0.15	0.19	0.12	0.17	0.19	0.18	0.09	0.19
CAO	14.09	11.87	11.30	13.36	11.84	11.61	9.64	11.13
NA2O	3.36	4.59	5.01	3.64	4.45	4.73	5.64	4.85
K2O	0.20	0.30	0.34	0.16	0.32	0.66	1.35	0.76
TOTAL	99.15	99.59	99.66	99.74	99.09	100.35	100.27	100.11
MOLE PERCENT ENDMEMBERS								
AB	29.8	40.4	43.7	33.9	39.7	40.9	47.6	42.2
AN	69.0	57.8	54.4	65.2	58.4	55.4	44.9	53.5
OR	1.2	1.8	1.9	1.0	1.9	3.7	7.5	4.3

* = xenocryst

AVERAGE CORE COMPOSITIONS OF O.R.S. PLAGIOCLASE — TABLE C2

	25	26	27	28	29	30	31	32
	S28	S41	S50	OC22	OC13	OC17	OC27	OC15
	(3)	(1)	(5)	(2)	(4)	(5)	(3)	(2)
SIO2	53.30	69.03	52.08	53.51	57.67	55.51	55.13	52.47
TIO2	0.05	0.00	0.05	0.06	0.08	0.10	0.09	0.07
AL2O3	27.70	19.28	28.66	27.82	25.37	26.50	26.91	28.34
FEO	0.56	0.01	0.49	0.71	0.53	0.62	0.65	0.73
MGO	0.16	0.00	0.10	0.07	0.06	0.09	0.08	0.25
CAO	11.82	0.36	12.67	11.30	8.17	9.83	9.88	12.15
NA2O	4.65	11.41	4.17	4.57	6.24	5.50	5.43	4.40
K2O	0.31	0.04	0.23	0.41	0.93	0.64	0.61	0.29
TOTAL	98.55	100.13	98.45	98.46	99.06	98.78	98.78	98.71
MOLE PERCENT ENDMEMBERS								
AB	40.9	98.1	36.8	41.2	54.9	48.4	48.1	39.0
AN	57.3	1.7	61.8	56.4	39.7	47.8	48.4	59.4
OR	1.8	0.2	1.3	2.4	5.4	3.7	3.5	1.7

	33	34	35	36	37	38	39	40
	OC15*	OC23	OC7	OC25	OC2	OC43	OC88A	OC88B
	(1)	(2)	(4)	(3)	(4)	(4)	(3)	(7)
SIO2	56.12	53.77	56.75	58.16	55.83	55.11	55.47	53.15
TIO2	0.08	0.06	0.11	0.06	0.11	0.05	0.03	0.03
AL2O3	26.49	28.15	26.37	25.47	26.33	27.19	27.49	29.12
FEO	0.91	0.46	0.40	0.38	0.51	0.45	0.37	0.43
MGO	0.08	0.08	0.05	0.05	0.09	0.05	0.03	0.16
CAO	9.38	11.23	9.29	8.22	9.75	10.09	10.17	12.92
NA2O	5.90	4.92	5.81	6.51	5.58	5.48	5.63	3.73
K2O	0.70	0.24	0.76	0.55	0.65	0.32	0.28	0.23
TOTAL	99.66	98.91	99.54	99.40	98.85	98.75	99.48	99.76
MOLE PERCENT ENDMEMBERS								
AB	51.1	43.6	50.8	57.0	49.0	48.6	49.2	33.8
AN	44.9	55.0	44.8	39.8	47.3	49.5	49.2	64.8
OR	4.0	1.4	4.4	3.2	3.8	1.9	1.6	1.4

	41	42	43	44	45	46	47	48
	OC98	OC67	OC72	OC123	OC86	OC54	OC84	OC93
	(4)	(7)	(6)	(1)	(6)	(6)	(5)	(5)
SIO2	56.30	52.14	55.86	53.11	53.41	55.39	53.81	54.71
TIO2	0.10	0.03	0.09	0.07	0.04	0.02	0.08	0.08
AL2O3	25.76	29.34	26.66	27.92	27.98	27.94	28.78	27.73
FEO	0.94	0.53	0.33	0.85	0.38	0.39	0.47	0.66
MGO	0.12	0.08	0.04	0.15	0.08	0.04	0.09	0.09
CAO	9.11	12.49	9.79	12.05	11.64	10.45	11.64	10.63
NA2O	5.90	4.26	5.86	4.45	4.71	5.38	4.69	5.17
K2O	0.63	0.20	0.35	0.30	0.26	0.32	0.34	0.52
TOTAL	98.89	99.08	98.99	98.91	98.49	99.93	99.91	99.60
MOLE PERCENT ENDMEMBERS								
AB	52.0	37.7	51.0	39.3	41.7	47.3	41.4	45.4
AN	44.3	61.1	47.0	58.9	56.8	50.8	56.7	51.6
OR	3.7	1.2	2.0	1.8	1.5	1.8	2.0	3.0

* = Groundmass composition

AVERAGE CORE COMPOSITIONS OF O.R.S. PLAGIOCLASE

TABLE C2

	49	50	51	52	53	54	55	56
	OC103	OC108	OC128	OC152	OC131	OC140	PE16	PE26
	(4)	(4)	(5)	(5)	(3)	(6)	(4)	(4)
SIO2	53.90	52.72	64.54	50.30	54.38	51.81	53.74	53.35
TIO2	0.08	0.06	0.01	0.05	0.07	0.06	0.06	0.07
AL2O3	28.43	29.53	21.80	30.03	27.40	29.52	27.89	28.73
FEO	0.59	0.49	0.15	0.82	0.65	0.52	0.41	0.44
MGO	0.16	0.07	0.00	0.08	0.16	0.07	0.17	0.11
CAO	11.70	12.56	3.05	13.99	11.03	12.98	11.55	11.86
NA2O	4.60	4.17	9.06	3.45	5.04	4.04	4.72	4.63
K2O	0.38	0.22	0.98	0.25	0.43	0.25	0.35	0.32
TOTAL	99.83	99.84	99.60	99.01	99.17	99.27	98.90	99.53
MOLE PERCENT ENDMEMBERS								
AB	40.6	37.1	79.5	30.5	44.1	35.5	41.6	40.6
AN	57.2	61.6	14.8	68.0	53.4	63.0	56.3	57.5
OR	2.2	1.3	5.7	1.5	2.5	1.5	2.0	1.9

	57	58	59	60	61	62	63	64
	PE12	PE15	PE19	PE3A	PE8	PE41	AY4	AY13
	(2)	(5)	(3)	(4)	(6)	(6)	(2)	(5)
SIO2	56.81	52.94	60.39	54.68	52.14	53.23	53.42	55.03
TIO2	0.02	0.03	0.00	0.05	0.07	0.05	0.07	0.11
AL2O3	26.50	28.63	23.84	27.75	29.46	28.58	28.25	26.99
FEO	0.27	0.48	0.17	0.43	0.42	0.58	0.61	0.53
MGO	0.03	0.15	0.01	0.05	0.18	0.17	0.30	0.11
CAO	9.06	12.00	5.79	10.48	12.96	12.10	12.08	10.65
NA2O	6.06	4.44	7.84	5.29	4.02	4.49	4.57	5.42
K2O	0.42	0.29	0.61	0.32	0.20	0.29	0.29	0.41
TOTAL	99.19	98.97	98.65	99.05	99.46	99.50	99.60	99.24
MOLE PERCENT ENDMEMBERS								
AB	53.4	39.4	68.5	46.8	35.5	39.5	40.0	46.8
AN	44.1	58.9	27.9	51.3	63.3	58.8	58.4	50.9
OR	2.4	1.7	3.5	1.8	1.2	1.7	1.7	2.3

	65	66	67	68	69	70	71	72
	AY27	AY12	AY35	AY38	C54	C51	C33	C62
	(6)	(5)	(4)	(3)	(4)	(6)	(8)	(5)
SIO2	54.87	54.17	56.01	50.46	56.07	55.85	55.27	57.01
TIO2	0.09	0.07	0.07	0.05	0.06	0.04	0.06	0.05
AL2O3	27.34	28.29	27.13	30.77	25.92	26.90	26.99	26.43
FEO	0.49	0.50	0.40	0.42	0.54	0.44	0.54	0.27
MGO	0.12	0.14	0.08	0.14	0.09	0.03	0.07	0.02
CAO	10.80	11.05	9.96	14.15	9.49	9.38	10.11	8.83
NA2O	5.24	4.90	5.46	3.19	5.52	5.99	5.50	7.18
K2O	0.42	0.42	0.56	0.21	0.80	0.23	0.61	0.25
TOTAL	99.36	99.55	99.67	99.39	98.50	98.85	99.15	100.04
MOLE PERCENT ENDMEMBERS								
AB	45.6	43.4	48.2	28.6	48.9	52.9	47.9	58.7
AN	52.0	54.1	48.6	70.1	46.5	45.8	48.6	39.9
OR	2.4	2.4	3.3	1.3	4.7	1.3	3.5	1.4

AVERAGE CORE COMPOSITIONS OF O.R.S. PLAGIOCLASE

TABLE C2

	73	74	75	76	77	78	79	80
	C52	C7	C48	C58	OR3	SH23	SH9	SH30
	(4)	(5)	(4)	(4)	(2)	(4)	(4)	(6)
SIO2	58.47	56.05	59.05	57.27	47.43	51.01	56.69	51.88
TIO2	0.03	0.09	0.07	0.05	0.03	0.02	0.08	0.07
AL2O3	25.56	26.63	25.14	25.91	32.59	30.27	26.01	29.39
FEO	0.30	0.55	0.42	0.37	0.42	0.35	0.65	0.61
MGO	0.03	0.08	0.06	0.05	0.06	0.21	0.10	0.10
CAO	7.95	9.54	9.35	8.24	16.55	14.04	9.25	12.85
NA2O	7.64	5.60	5.14	6.16	2.09	3.44	5.91	3.93
K2O	0.47	0.77	0.27	0.79	0.15	0.09	0.52	0.30
TOTAL	100.45	99.32	99.52	98.84	99.31	99.44	99.20	99.13
MOLE PERCENT ENDMEMBERS								
AB	61.9	49.2	49.0	54.9	18.4	30.6	52.0	35.0
AN	35.6	46.3	49.3	40.5	80.7	68.9	45.0	63.3
OR	2.5	4.4	1.7	4.6	0.9	0.5	3.0	1.7

AVERAGE CORE COMPOSITIONS OF O.R.S. AMPHIBOLES

	1	2	3	4	5	6	7	8
	GC3	GC29	GC30	BN2	BN3	BN3*	BN7	BN7*
	(3)	(3)	(4)	(1)	(3)	(1)	(3)	(1)
SIO2	41.76	42.44	46.65	41.82	43.58	53.25	43.28	52.27
TIO2	2.39	3.60	1.97	2.00	2.85	0.18	2.64	0.27
AL2O3	10.97	11.27	7.31	12.36	10.06	2.93	10.71	3.66
CR2O3	0.04	0.01	0.02	0.02	0.03	0.05	0.03	0.07
FEO	11.65	11.14	11.99	13.90	11.21	10.08	11.16	12.60
MNO	0.12	0.11	0.31	0.17	0.13	0.83	0.14	0.67
MGO	14.16	14.23	14.87	12.62	14.60	16.60	14.73	14.73
NIO	0.00	0.03	0.03	0.00	0.00	0.00	0.00	0.00
CAO	11.19	11.25	11.18	10.93	11.40	12.55	11.17	12.03
NA2O	2.48	2.47	1.75	2.45	2.19	0.40	2.42	0.50
K2O	0.71	0.89	0.67	0.63	0.59	0.07	0.68	0.28
TOTAL	95.48	97.46	96.74	96.91	96.66	96.94	96.97	97.09

	9	10	11	12	13
	S41	OC23	OC25	OC67	C62
	(2)	(3)	(2)	(5)	(1)
SIO2	49.05	40.45	41.24	42.26	53.99
TIO2	1.08	3.17	3.31	2.72	0.25
AL2O3	2.59	13.38	12.15	11.53	1.88
CR2O3	0.00	0.05	0.01	0.05	0.00
FEO	20.11	11.84	11.25	11.50	7.37
MNO	0.55	0.17	0.18	0.16	0.33
MGO	10.35	13.40	14.25	14.09	19.48
CAO	8.14	10.92	11.03	11.15	11.63
NA2O	4.02	2.68	2.83	2.18	0.28
K2O	0.97	0.50	0.59	0.85	0.04
TOTAL	96.88	96.56	96.85	96.51	95.26

* = Actinolitic amphibole pseudomorphing clinopyroxene

AVERAGE CORE COMPOSITIONS OF O.R.S. BIOTITES

TABLE C2

	1	2	3	4	5	6	7	8
	L113	L139	BN3	OC72	OC128	PE29	PE4	PE12
	(3)	(3)	(2)	(3)	(3)	(1)	(2)	(2)
SIO2	39.17	36.33	36.42	37.27	36.04	32.84	35.22	38.07
TIO2	6.37	4.59	4.17	5.63	4.10	2.69	4.11	4.73
AL2O3	12.00	14.29	13.54	12.80	14.57	16.04	15.71	13.60
CR2O3	0.01	0.00	0.01	0.00	0.00	0.03	0.02	0.01
FEO	6.67	13.11	16.53	16.10	18.97	27.34	20.71	11.62
MNO	0.06	0.09	0.36	0.07	0.67	0.33	0.35	0.26
MGO	20.41	16.11	12.99	13.91	12.29	5.27	9.08	16.68
CAO	0.03	0.05	0.60	0.00	0.00	0.12	0.01	0.03
NA2O	0.76	0.79	0.08	0.27	0.65	0.75	0.56	0.52
K2O	8.92	8.28	8.87	9.27	8.63	7.57	8.37	9.09
TOTAL	94.40	93.66	93.57	95.34	95.93	93.04	94.13	94.61

	9	10	11	12	13	14
	PE19	C62	C52	C48	C58	C65
	(2)	(3)	(1)	(1)	(3)	(3)
SIO2	37.01	38.81	37.87	37.34	37.04	37.78
TIO2	4.29	4.84	5.29	6.23	6.35	4.84
AL2O3	14.83	12.04	12.70	12.93	13.46	14.28
CR2O3	0.00	0.02	0.04	0.04	0.02	0.05
FEO	11.09	11.66	10.76	14.11	11.42	12.23
MNO	0.24	0.09	0.10	0.18	0.07	0.09
MGO	17.23	17.24	17.59	15.04	16.42	15.88
CAO	0.01	0.00	0.00	0.00	0.01	0.02
NA2O	0.93	0.13	0.32	0.24	0.82	0.59
K2O	8.63	9.43	9.40	9.02	8.76	8.75
TOTAL	94.27	94.26	94.08	95.13	94.37	94.52

AVERAGE CORE COMPOSITIONS OF O.R.S. SPINELS

TABLE C2

	1	2	3	4	5	6	7	8
	L51	L68	L68	L79	L95	L121	L128	L146
	(3)	(2)	(1)	(1)	(1)	(2)	(3)	(2)
SIO2	0.45	0.53	0.50	0.13	0.59	1.62	0.93	0.13
TIO2	15.73	7.54	5.50	12.66	12.05	10.20	13.55	7.03
AL2O3	1.01	0.90	1.37	2.38	2.10	0.70	1.33	1.52
CR2O3	0.49	0.94	0.00	0.04	0.25	1.61	1.39	0.75
FE2O3	32.77	48.34	52.63	37.94	39.14	39.84	34.18	51.25
FEO	43.55	36.06	35.73	40.44	41.84	37.83	39.07	35.13
MNO	0.49	0.20	0.00	0.28	0.09	2.08	3.93	0.19
MGO	0.15	0.34	0.00	0.30	0.08	0.09	0.07	1.03
CAO	0.20	0.27	0.00	0.05	0.05	0.23	0.18	0.10
NA2O	0.04	0.04	0.00	0.06	0.00	0.13	0.00	0.00
K2O	0.07	0.06	0.00	0.05	0.03	0.07	0.04	0.04
TOTAL	94.95	95.22	95.72	94.34	96.22	94.38	94.67	97.18

	9	10	11	12	13	14	15	16
	GC29	GC30	BN3	BN7	S13	OC22	OC27	OC15
	(4)	(2)	(2)	(1)	(2)	(2)	(1)	(1)
SIO2	0.00	0.00	0.62	0.43	0.41	0.05	0.33	0.14
TIO2	9.79	4.19	0.37	5.01	18.01	3.31	13.77	7.96
AL2O3	2.09	1.51	0.21	0.16	2.39	1.05	2.92	0.87
CR2O3	0.56	0.38	0.42	0.23	1.30	0.13	0.01	1.00
FE2O3	45.39	57.87	66.31	56.59	27.62	59.89	35.81	49.63
FEO	39.44	34.41	30.48	35.43	44.61	32.38	40.07	36.26
MNO	0.05	0.40	1.56	0.10	2.53	0.11	3.47	0.31
MGO	0.13	0.00	0.09	0.05	0.00	0.71	0.07	0.80
ZNO	0.00	0.00	0.00	0.00	0.96	0.00	0.00	0.00
CAO	0.03	0.00	0.09	0.10	0.00	0.04	0.00	0.05
TOTAL	97.48	98.78	100.14	98.07	97.83	97.68	96.46	97.02

	17	18	19	20	21	22	23	24
	OC23	OC7	OC43	OC88A	OC98	OC67	OC72	OC54
	(2)	(1)	(5)	(2)	(4)	(3)	(3)	(3)
SIO2	0.85	0.35	0.00	0.00	0.00	0.00	0.00	0.39
TIO2	14.97	20.07	14.44	9.73	15.20	9.70	9.22	12.34
AL2O3	1.81	2.23	0.98	1.63	2.00	2.29	1.56	1.33
CR2O3	0.36	0.06	0.05	0.00	1.40	0.00	0.25	0.22
FE2O3	32.62	22.82	37.67	45.81	32.60	45.85	47.79	40.94
FEO	42.37	43.64	36.77	37.15	41.16	36.93	38.04	39.08
MNO	1.62	4.94	5.22	0.39	2.50	0.61	0.15	1.43
MGO	0.08	0.04	0.07	0.96	0.08	0.85	0.56	0.48
ZNO	0.00	0.00	0.06	0.00	0.06	0.20	0.00	1.20
CAO	0.26	0.07	1.08	0.00	0.14	0.34	0.08	0.04
TOTAL	95.52	94.24	96.34	95.68	95.15	96.77	97.67	97.45

AVERAGE CORE COMPOSITIONS OF O.R.S. SPINELS

	25	26	27	28	29
	OC128	OC152	PE3A	C7	C48
	(5)	(6)	(5)	(1)	(1)
SIO2	0.46	0.31	1.60	0.00	0.00
TIO2	2.30	8.66	10.44	14.13	0.93
AL2O3	2.70	2.90	1.29	1.31	0.00
CR2O3	0.00	5.41	0.03	0.51	0.79
FE2O3	57.87	43.26	41.37	35.47	64.50
FEO	30.52	34.37	41.14	42.25	31.06
MNO	1.84	0.45	0.10	0.00	0.00
MGO	0.36	2.92	0.00	0.00	0.00
ZNO	0.05	0.05	0.75	0.39	0.00
CAO	0.00	0.07	0.13	0.00	0.00
TOTAL	96.21	98.60	96.85	93.95	97.28

AVERAGE CORE COMPOSITIONS OF O.R.S. ILMENITES

TABLE C2

	1	2	3	4	5	6	7	8
	L51	L113	L79	L146	S13	OC22	OC72	OC54
	(1)	(2)	(1)	(1)	(1)	(1)	(3)	(1)
SIO2	0.21	0.21	0.02	0.10	0.31	0.00	0.00	0.38
TIO2	49.75	37.57	47.09	45.47	48.42	39.55	49.30	43.51
AL2O3	0.35	0.60	0.45	0.12	0.00	0.11	0.07	0.28
CR2O3	0.13	0.00	0.00	0.11	0.16	0.05	0.00	0.00
FEO	43.63	50.12	48.18	45.05	48.01	53.83	47.68	49.12
MNO	0.34	0.47	0.34	0.55	0.58	0.57	0.81	0.70
MGO	0.72	4.09	0.47	3.78	2.11	2.65	1.29	0.68
CAO	0.34	0.35	0.09	0.09	0.00	0.04	0.16	0.13
NA2O	0.06	0.06	0.00	0.00	0.00	0.00	0.00	0.00
K2O	0.06	0.06	0.03	0.04	0.00	0.00	0.00	0.00
TOTAL	95.60	93.84	96.59	95.31	99.59	96.81	99.31	94.80

	9	10	11	12	13	14	15	16
	OC128	OC152	C54	C51	C52	C52	C7	C48
	(1)	(1)	(2)	(1)	(1)	(1)	(3)	(3)
SIO2	0.34	0.00	0.81	0.00	0.00	0.04	0.00	0.00
TIO2	34.02	46.92	46.29	45.22	45.98	48.05	48.39	45.38
AL2O3	1.28	0.00	0.23	0.08	0.04	0.03	0.13	0.00
CR2O3	0.00	0.42	0.29	0.21	0.05	0.05	0.11	0.12
FEO	55.42	43.80	46.85	50.91	50.23	44.98	47.48	49.34
MNO	2.30	0.52	0.45	2.18	2.06	4.77	0.66	2.98
MGO	0.00	5.48	3.17	0.19	0.15	0.15	1.12	0.15
ZNO	0.00	0.00	0.00	0.00	0.00	0.00	0.17	0.10
CAO	0.00	0.00	0.07	0.00	0.00	0.03	0.00	0.16
TOTAL	93.36	97.14	98.17	98.79	98.51	98.10	98.06	98.23

	17
	C65
	(1)
TIO2	38.87
AL2O3	0.48
CR2O3	0.29
FEO	53.95
MNO	0.33
MGO	0.60
ZNO	0.31
TOTAL	94.83

AVERAGE CORE COMPOSITIONS OF O.R.S. APATITE

TABLE C2

	L113	L139	GC3	BN3	OC88A	C7	C51
	(2)	(4)	(3)	(2)	(3)	(2)	(2)
CaO	53.61	54.41	54.68	54.86	54.63	54.43	54.69
P_2O_5	40.81	41.91	41.10	41.44	41.66	41.59	41.10
Total*	94.42	96.32	95.78	96.30	96.29	96.02	95.79
La	780	1090	877	1090	813	1650	1720
Ce	1570	1925	1737	1855	1283	3290	3825
Nd	950	1115	1107	1045	873	1635	1960
Sm	340	360	377	365	303	355	420
Y	185	173	390	275	390	635	560
Sr	1710	2258	1673	1740	940	675	300

* = Total does not include trace elements, or Si, Fe, F, Cl etc. (undetermined)

O.R.S. GARNET COMPOSITIONS

	1	2	3	4	5	6	7
	1PE28	1PE28	2PE28	2PE28	3PE28	4PE28	4PE28
	(R)	(C)	(C)	(R)		(C)	(R)
SIO2	36.31	36.61	36.96	36.45	37.09	36.95	36.60
TIO2	0.10	0.04	0.19	0.16	0.25	0.26	0.03
AL2O3	20.39	20.35	20.18	20.52	20.16	20.28	20.41
FEO	35.16	34.72	35.17	35.64	35.07	35.06	35.99
MNO	5.87	6.67	3.20	4.43	2.86	2.89	5.61
MGO	1.33	1.26	1.29	2.18	1.42	1.46	1.13
CAO	0.49	0.41	3.42	0.30	3.79	3.75	0.41
K2O	0.01	0.01	0.01	0.01	0.01	0.01	0.01
TOTAL	99.66	100.06	100.42	99.69	100.65	100.66	100.18
PYR	6.2	6.0	5.5	9.7	6.0	6.1	5.2
ALM	92.1	92.6	84.0	89.3	82.6	82.6	93.4
GRO	1.6	1.4	10.5	1.0	11.4	11.3	1.4

CORE-RIM PAIRS OF STRAITON PYROXENES

	1	2	3	4	5	6	7	8
	2AY35	2AY35	5AY35	5AY35	3AY35	3AY35	5AY38	5AY38
	(C)	(R)	(C)	(R)	(C)	(R)	(C)	(R)
SIO2	51.87	53.66	52.06	52.31	51.43	52.03	51.56	51.88
TIO2	0.27	0.54	0.26	0.31	0.53	0.77	0.83	0.95
AL2O3	1.25	0.98	1.02	0.89	1.68	1.62	1.79	2.04
CR2O3	0.04	0.08	0.07	0.02	0.03	0.14	0.02	0.13
FEO	23.31	16.06	24.02	23.44	12.07	9.29	12.91	10.00
MNO	0.48	0.35	0.56	0.55	0.36	0.22	0.36	0.31
MGO	20.93	25.57	20.29	20.58	13.61	16.19	14.32	15.50
CAO	1.50	2.11	1.63	1.64	19.42	18.26	17.27	18.78
NA2O	0.00	0.00	0.00	0.00	0.37	0.27	0.45	0.33
K2O	0.00	0.00	0.00	0.00	0.00	0.00	0.00	0.00
TOTAL	99.65	99.36	99.92	99.75	99.51	98.78	99.52	99.93
MOLE PERCENT ENDMEMBERS								
EN	59.7	70.8	58.1	58.9	39.6	46.9	42.1	44.8
FS	37.3	25.0	38.6	37.7	19.7	15.1	21.3	16.2
WO	3.1	4.2	3.3	3.4	40.6	38.0	36.5	39.0

TABLE C3 : Electron microprobe analyses of phenocrysts showing important zoning. (see sections 6.1, 6.2).

(C) refers to core analysis, (R) to rim.

TABLE C4 : Average electron microprobe analyses (ppm.) for trace elements in minerals of Table C2. * = not detected.

PYROXENE ^{o}= orthopyroxene, ^{c}= clinopyroxene.

	5	12	18	19	20	21	22	27	80	83	84	87
	L113	L146	MT45	MT10^{o}	MT10^{c}	MT42	S44	S28	C33	C7^{c}	C7^{o}	OR3
Ni			398	630	730	443	808	203		*	258	238
Zr	*	*							*	?200	*	

PLAGIOCLASE ^{x}= xenocryst

	4	5	10	11	14	16	17	18	19	20	25
	L50	L50^{x}	GC26	GC29	BN3	MT4	MT45	MT10	S44	S33	S28
Sr	2425	1440	3160	3306	3635	1510	1400	1247	1342	1110	1220
Ba			400	438							

	52	66	67	68	71	74	77	78	79	80
	OC152	AY12	AY38	AY35	C33	C7	OR3	SH23	SH9	SH30
Sr	1290	1087	817	990	1390	1417	2270	750	1187	1012

AMPHIBOLE

		Sr	Ba	Zr
2	GC29	1530	920	*

BIOTITE

	1	2	4	5
	L113	L139	OC72	OC128
Ba	2965	10280	1020	6565
Sr	420	*	190	145
Zr	140		140	140

ILMENITE

	1	2	4	5	10	15	17
	L51	L113	L146	S13	OC152	C7	C65
Zr	2050	2065	1610	1370	2400	1940	720
Nb				190			
Ni						690	

SPINEL

	8	9	26	28
	L146	GC29	OC152	C7
Zr	*	*	140	*
Ni				480

APPENDIX D : DATA HANDLING COMPUTER PROGRAMS

The large quantity of analytical data generated in the course of this research required the use of a comprehensive package of data handling programs. The majority of the programs used have been written by the author in IMP (ERCC, 1974) and all take as input the norminput file output of the XRF data processing programs or the 'punchfile' output of the PROBE program (Appendix C), which are in a similar free format (Fig. B11). The programs written are summarized briefly here: more comprehensive program documentation is available at the Grant Institute.

D1 : ABSTRACT

Source file : ATOMS ; Object file : ATOMY

This is a manipulative program allowing the rapid extraction of groups of related analyses from the input file, and the creation of an output file containing the selected analyses in the same format. Analysis groups output may be determined by a particular group of characters in the analysis title e.g. 'PLG', or '@11' or by specifying the silica range required in the output analyses.

D2 : MEANFILE

Source file : ATOMS ; Object file : ATOMY

This program calculates arithmetic means of groups of analyses in the input data, and outputs the means as a file in norminput format. The groups of analyses averaged are chosen through having identical analysis titles, or through being all the same mineral type from the same rock. For example, PXC10C23@16, PXC30C23@16, PXC5<C>0C23@16 would be included in an average PXC90C23@16, but not PLG10C23@16 or PXC10C23@36. Rim analyses (those containing the sequence <R>) may be included in the mean if so required. All analyses quoted in Table C2 were generated using this program, not including <R> compositions in the average.

D3 : RATCALC

Source file : ANALTABS ; Object file : ANALTABY

This program calculates mean, median, range, quartiles and interquartile mean for element/oxide concentrations and ratios. Output is to the interactive terminal. Quartiles quoted in Chapter 9 were generated using this program.

D4 : ANALTAB

Source file : ANALTABS ; Object file : ANALTABY

This program generated Table B17; negative input is replaced by an asterisk and input of 0.00001 is interpreted as not determined 'n.d.'.

D5 : ATOM

Source file : ATOMS ; Object file : ATOMY

This program recalculates mineral analyses as atomic constituents; minerals are identified by the presence of one of OLI, PXO, PXC, AMP, BIO, GNT, PLG, KSP, SPI, ILM as the first three letters in the analysis title. Spinels and ilmenites have ferric iron recalculated on an R304 and R203 basis, respectively. In addition to file or line printer

output, the atomic constituents may be retained in core storage after termination of the program by use of the option PRELOAD. These may then be used as input for VARPLOT (section D7).

D6 : NORMS
Source file : NORMS ; Object file : NORMY
This program calculates the CIPW norms of input analyses using a user-selected iron oxidation ratio. Norms are not recast to 100% and should have the same total as the input analysis oxides. Output may again be retained in core storage, as for ATOM.

D7 : VARPLOT
Source files : GRAPHS, PLOTS ; Object files : GRAPHY, PLOTY

This program has been used to create all the variation diagrams presented in this thesis. It may create a wide variety of variation diagrams using the input analyses, and many arithmetic combinations of these including logs and reciprocals. It may also use data on atomic or normative constituents of the input, previously created in core storage using ATOM or NORMS. If this facility is used, then the input to VARPLOT should contain the same samples in the same order as was used in the input for ATOM or NORMS. A range of triangular diagrams, including the pyroxene quadrilateral, may also be plotted.

Symbols on graphs may correspond to differences in initial lettering in the sample names. For example, the file required to produce Table B17 could be used to generate different symbols for all L-samples, all GC-samples etc. Alternatively, symbols may correspond to the number following the '@' symbol in the sample name. While this is frequently described as a 'phenocryst assemblage' in the text, any division may be used, and the 'phenocryst assemblages' corresponding to the 52 numbers currently permissable are given in Table D1. If the required name is not present, it is possible to allocate a temporary name to a number by use of the facility CHANGE ASSEMB. Symbol keys may be placed on graphs at user-specified positions and arrowed lines may be drawn between bulk rock-groundmass pairs, or between core-rim pairs for phenocryst mineral compositions.

The program is mainly located in the source file PLOTS, but uses routines from the file GRAPHS, and uses the basic plotting routines of the ERCC Graphpack (ERCC, 1977).

TABLE D1 : "Phenocryst Assemblages" corresponding to the number after the '@' symbol in rock names.

1 Ol	27 Cpx+Pl
2 Opx	28 Ol+Opx+Pl
3 Cpx	29 "Trachyte"
4 Pl	30 Coarse granular Opx+Cpx+Pl
5 Opx+Pl	31 Fine granular Opx+Cpx+Pl
6 Opx+Pl+Hb	32 Hyalopilitic Opx+Cpx+Pl
7 Ol+Cpx	33 Vitrophyric Opx+Cpx+Pl
8 Opx+Cpx	34 Cumulate
9 Ol+Opx+Cpx	35 (a default code)
10 Ol+Opx+Cpx+Pl	36 Xenocryst
11 Ol+Pl	37 Groundmass
12 Ol+Cpx+Pl	38 Ol+Hb+Pl
13 Opx+Cpx+Pl	39 Wehrlite
14 Opx+Cpx+Pl+Bi	40 "Mica-felsite"
15 Cpx+Hb+Bi	41 Harzburgite
16 Cpx+Opx+Pl+Hb	42 Websterite
17 Pl+Bi	43 Dunite
18 "Trachyandesite"	44 Opx+Pl+Hb+Bi
19 Acid Lava	45 Ol+Cpx+Hb+Pl
20 Aphyric Lava	46 Ol+Opx+Cpx+Hb
21 Ignimbrite	47 Ol+Hb
22 Intrusive Rock	48 Ol+Opx
23 Groundmass	49 Ol+Opx+Pl+Hb
24 Opx+Cpx+Pl+Hb+Bi	50 Opx+Hb
25 Hornfelsed Lava	51 Ol+Cpx+Pl+Bi
26 Ol+Cpx+Bi	52 Pl+Kspar+Opx+Cpx